Journal of Thoracic Disease

Volume 6 Number 12 December 2014 Pages 1654-1891; E246-E312

Vol 6, No 12 December 2014 ISSN 2072-1439

JOURNAL of THORACIC DISEASE

www.jthoracdis.com

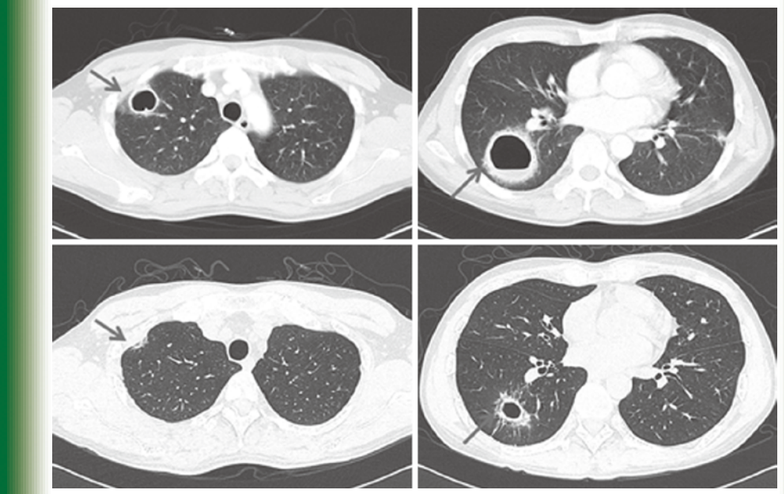

Published by

The Official Publication of

Indexed in PubMed, SCI

Aims and Scope

The *Journal of Thoracic Disease* (JTD, J Thorac Dis, pISSN: 2072-1439; eISSN: 2077-6624) was founded in Dec 2009, indexed in Pubmed/Pubmed Central in Dec 2011, and Science Citation Index (SCI) on Feb 4, 2013. It is published quarterly (Dec 2009- Dec 2011), bimonthly (Jan 2012- Dec 2013), and monthly (Jan 2014-), and openly distributed worldwide. JTD publishes manuscripts that describe new findings in the field to provide current, practical information on the diagnosis and treatment of conditions related to thoracic disease (lung disease, cardiac disease, breast disease and esophagus disease). Original articles are considered most important and will be processed for rapid review by the members of Editorial Board. Clinical trial notes, Cancer genetics reports, Epidemiology notes and Technical notes are also published. Case reports implying new findings that have significant clinical impact are carefully processed for possible publication. Review articles are published in principle at the Editor's request. There is no fee involved throughout the publication process. The acceptance of the article is based on the merit of quality of the manuscripts. All the submission and reviewing are conducted electronically so that rapid review is assured.

The Official Publication of:

- Guangzhou Institute of Respiratory Disease (GIRD)
- China State Key Laboratory of Respiratory Disease
- First Affiliated Hospital of Guangzhou Medical University
- Society for Thoracic Disease (STD)

Endorsed by:

- International COPD Coalition (ICC)

Editorial Correspondence

HK office:
Daoyuan Wang.
Pioneer Bioscience Publishing Company
Room 604, 6/F Hollywood Center, 77-91 Queen's road, Sheung Wan, Hong Kong.

Guangzhou office:
Guangqiao Zeng, MD
Guangzhou Institute of Respiratory Disease & The First Affiliated Hospital of Guangzhou Medical University.
No. 151, Yanjiang Rd, Guangzhou 510120, China.

Email: jtd@thepbpc.org
www.jthoracdis.com

Note to NIH Grantees

Pursuant to NIH mandate, Pioneer Bioscience Publishing Company will post the accepted version of contributions authored by NIH grant-holders to PubMed Central upon acceptance. This accepted version will be made publicly available 2 months after publication. For further information, see www.thepbpc.org

Conflict of Interest Policy for Editors

The full policy and the Editors' disclosure statements are available online at: www.jthoracdis.com

Disclaimer

The Publisher and Editors cannot be held responsible for errors or any consequences arising from the use of information contained in this journal; the views and opinions expressed do not necessarily reflect those of the Publisher and Editors, neither does the publication of advertisements constitute any endorsement by the Publisher and Editors of the products advertised.

Cover image:

Computed tomography (CT) findings of a 43-year-old man. (See P1762 in this issue).

For submission instructions, subscription and all other information visit www.jthoracdis.com

Table of Contents

Editorial

Original Article

Brief Report

Visualized Surgery

GCTAB Column

Review Article

Statistic Corner

Meet the Professor

Opinion

Case Report

Letter to the Editor

ICC COLUMN: The Voice of the Patient

News

Between You and Me

Erratum

Editorial

The next challenge for VATS lobectomy surgeons

Antonio E. Martin-Ucar

Department of Thoracic Surgery, University Hospitals Nottingham NHS Trust, Nottingham, UK

Correspondence to: Antonio E. Martin-Ucar. Consultant, Thoracic Surgeon, Department of Thoracic Surgery, University Hospitals Nottingham NHS Trust, Nottingham, UK. Email: lungsout@yahoo.com.

Submitted Oct 22, 2014. Accepted for publication Oct 27, 2014.
doi: 10.3978/j.issn.2072-1439.2014.11.41
View this article at: http://dx.doi.org/10.3978/j.issn.2072-1439.2014.11.41

Dr. Xu stimulating manuscript (1) shows the progress made in VAT surgery over recent years. The series of patients undergoing bronchial sleeve resections via VATS represent another new challenge for thoracic surgeons in the search for improved outcomes.

Now it is finally accepted the role of bronchial sleeve resections as a beneficial alternative to pneumonectomy whenever technically possible and the argument VATS *vs.* open lobectomy approaches conclusion due to the recent widespread adoption of the different VATS approaches by surgeons worldwide, the authors present the next step of evolution in the indications for VATS surgery.

As with any less common indication for a surgical technique the manuscript touches on important factors to ensure safe and successful implementation of surgical techniques. Experience by the surgeon in both VATS lung resection and in open airway reconstructions is vital to perform these procedures safely and efficiently by VATS.

The authors mention two important technical points specific to these operations: complete circumferential excision of the bronchus (avoiding "wedge" bronchoplasty) and the change from an interrupted into a continuous suture for the anastomosis. While it is tempting for the inexperienced surgeon to maintain some continuity between the two bronchial ends thinking it will facilitate the anastomosis, only when confidence grows and complete sleeves are performed one realizes that the anastomosis is constructed easier if the ends are fully free and separated and it will also improve the anastomotic result with avoidance of possible early stenosis and angulation of the bronchoplasty. Many surgeons, normally following experiences in transplant techniques, made a transition from interrupted to continuous anastomoses in their open airways reconstructions that makes the procedure simpler, faster and less likely to create winding of the sutures. This is clearly magnified in a VATS approach as the surgical field is restricted.

The authors so far had avoided vascular reconstructions with their VATS approach, although other selected groups have reported their experiences. I am sure their step-by-step introduction of VATS techniques with their large experience will soon be performing them. Indeed these are the keys for efficient introduction of VATS bronchial sleeves by more surgeons: progressive experience in open sleeves and VATS lobectomy, careful consideration to the steps to be taken during the operation and once these skills are achieved the individual experience will be the determinant of progress. In my opinion it is of paramount importance, however, to learn (even small details) from surgeons performing the operations, be in the form of formal training, visits or by non-edited videos of procedures. The experiences of pioneer surgeons should not be discarded because of individual limits. "Is there anyone so wise as to learn by the experience of others?" Voltaire dixit.

Acknowledgements

Disclosure: The author declares no conflict of interest.

References

1. Xu X, Chen H, Yin W, et al. Thoracoscopic half carina resection and bronchial sleeve resection for central lung cancer. Surg Innov 2014;21:481-6.

Cite this article as: Martin-Ucar AE. The next challenge for VATS lobectomy surgeons. J Thorac Dis 2014;6(12):1654. doi: 10.3978/j.issn.2072-1439.2014.11.41

Editorial

Spontaneous esophageal rupture as the underlying cause of pneumothorax: early recognition is crucial

George Garas[1], Paul Zarogoulidis[2], Alkiviadis Efthymiou[3], Thanos Athanasiou[1], Kosmas Tsakiridis[4], Sofia Mpaka[5], Emmanouil Zacharakis[1]

[1]Department of Surgery and Cancer, St. Mary's Hospital, Imperial College London, London, UK; [2]Pulmonary Department-Oncology Unit, "G. Papanikolaou" General Hospital, Aristotle University of Thessaloniki, Thessaloniki, Greece; [3]Department of Gastroenterology, "Saint Luke" Private Hospital, Thessaloniki, Panorama, Greece; [4]Department of Cardiothoracic Surgery, "Saint Luke" Private Hospital, Panorama, Thessaloniki, Greece; [5]Department of Oncology, "Interbalkan" European Medical Center, Thessaloniki, Greece

Correspondence to: Paul Zarogoulidis. Pulmonary Department-Oncology Unit, "G. Papanikolaou" General Hospital, Aristotle University of Thessaloniki, Thessaloniki, Greece. Email: pzarog@hotmail.com.

Abstract: Boerhaave's syndrome (BS), also known as "spontaneous rupture of the esophagus", constitutes an emergency that requires early diagnosis if death or serious morbidity are to be prevented. First described in 1724, BS is thought to be more common than once thought. Its true incidence remains unknown. Mortality ranges between 20-40% with timely treatment but this rises to virtually 100% if treatment is delayed by more than 48 hours. This is unfortunately a common occurrence due to delayed diagnosis. The commonest precipitating factor is vomiting but BS can be truly "spontaneous". The classical clinical presentation described consists of vomiting, chest pain, and subcutaneous emphysema. However, and contrary to popular belief, this triad is actually uncommon accounting for the frequently delayed diagnosis. A less recognised presenting feature of BS is with pneumothorax due to associated rupture of the parietal pleura. Pneumothorax has been shown to be present in more than 20% of cases of BS-sometimes with a coexistent pleural effusion (hydropneumothorax). This article aims to raise awareness about pneumothorax as the sole initial presenting feature of BS and alert clinicians to consider BS in the differential diagnosis of any patient with respiratory symptoms and a recent history of vomiting.

Keywords: Boerhaave's syndrome (BS); esophagus; perforation; pneumothorax; hydropneumothorax

Submitted Oct 17, 2014. Accepted for publication Oct 22, 2014.
doi: 10.3978/j.issn.2072-1439.2014.12.04
View this article at: http://dx.doi.org/10.3978/j.issn.2072-1439.2014.12.04

Boerhaave's syndrome (BS), also known as "spontaneous rupture of the esophagus" constitutes a life-threatening condition. The adjective "spontaneous" does not imply absence of a precipitating factor, but instead the fact that the rupture is not a consequence of direct trauma (usually caused by instrumentation or a foreign body). The commonest precipitating factor associated with BS is vomiting although other precipitants have been described such as straining, lifting or even laughing (1). BS contrasts with Mallory-Weiss syndrome where the tear is confined to the mucosa and commonly associated with hematemesis. In BS, the tear is transmural leading to esophageal perforation. Hematemesis is rarely present (2).

From a historical viewpoint, BS was first described by the Dutch physician, Hermann Boerhaave in 1724. It was a post-mortem diagnosis for the Grand Admiral of The Netherlands, Jan van Wassenaer, who died 18 hours after developing excruciating chest pain following vomiting. On autopsy, the tear was identified in the distal esophagus and undigested food seen in the left pleural cavity (1,3).

The true incidence of BS in the general population is unknown. However, it is thought to be more common than once thought as many cases of BS are diagnosed post-mortem resulting in under-reporting and thus an underestimate both with regards to its incidence and mortality (3).

The classical clinical presentation of BS traditionally taught at medical school and described in textbooks is Mackler's triad. This consists of vomiting, chest pain, and subcutaneous emphysema (4). However, and contrary to popular belief, this triad is actually uncommon. Characteristically, in a series of 14 patients eventually diagnosed with BS, only one presented with this triad (5). As such, reliance on those clinical features can be misleading. As a matter of fact, the symptoms associated with BS are more often than not, non-specific, resulting in delayed diagnosis.

The pathophysiology of BS involves a sudden rise in intraluminal esophageal pressure forcing the gastric contents against a tight cricopharyngeus muscle. This is most commonly the result of retching or vomiting, although as previously discussed, these may be completely absent (3). In addition to the situations described earlier, BS can be truly "spontaneous" with no apparent predisposing factor. Cases of BS have been described in patients during bending over, watching television or even during their sleep (6).

The perforation in BS has a predilection for the left lateral aspect of the distal esophagus (90% of cases) (7,8). There are several anatomical reasons to explain this. These include thinning of the muscle in the distal esophagus, weakening of its wall as a result of vessels and nerves entering it, lack of supporting neighboring structures and the fact that at the left diaphragmatic crus, the esophagus makes an anterior angulation (5).

Once the esophagus perforates, a number of events follow. All of these events pose an imminent threat to life. Their exact effect depends on where in the esophagus the perforation has occurred. Since the distal left lateral aspect is the most frequently affected site, signs and symptoms relate to this site in 75-90% of cases (2).

As the esophagus ruptures, the parietal pleura can either rupture with it or alternatively, become breached at a later stage secondary to the enzymatic effect of the gastric contents. In either case, a pleural breach will lead to a pneumothorax or hydropneumothorax depending on whether air only or air with fluid have leaked from the esophagus into the pleural cavity (2).

Other conditions that can lead to BS include pneumomediastinum, mediastinitis, abscess formation and septic shock. These are all a direct result of the esophageal and/or gastric contents spilling into the mediastinum. If the perforation is sealed, the patient may appear deceivingly well with no (or few) signs of systemic inflammatory response syndrome before they suddenly decompensate. Hence, none of the aforementioned features may be present in the initial setting and there may even be absence of any preceding history of vomiting or retching to complicate things further (3). As such, pneumothorax may be the sole initial presenting feature of BS.

It is of paramount importance for clinicians of all specialties to appreciate this, i.e., that BS can masquerade as "spontaneous" pneumothorax with no other "classical" features. Rarely, this can be a tension pneumothorax (2,9). As already stated, Mackler's triad is uncommon (5), and vomiting or retching are not always present (3). This clouds the clinical picture and makes the timely diagnosis of BS unlikely (3).

Diagnostic delay carries a very high risk of death. Similar to other acute esophageal disorders, the mortality of BS is exceedingly high and rises steeply with time (10). It is reported to be in the order of 25% if treatment is started within 24 hours, but reaches almost 100% at 48 hours (7,8). These exceedingly high mortality figures illustrate the critical importance of timely diagnosis of BS. Any diagnostic delay is very likely to lead to patient death.

Clinically, BS should always be considered in cases of pneumothorax or chest pain if early diagnosis is not to be missed. As the Harvard physician Soma Weiss who described the eponymous Mallory-Weiss syndrome said, "A diagnosis is easy, as long as you think of it". When a patient is misdiagnosed, appropriate treatment is delayed, and in the case of BS, death becomes almost a certainty (2).

It is therefore crucial that the diagnosis of BS is rapidly made even before the patient leaves the emergency department. Like with all cases in clinical medicine, history taking followed by physical examination are mandated. Although history alone will sometimes give away the diagnosis, more often than not, this is not the case. Radiological investigations most commonly provide the diagnosis in BS but clinical suspicion is essential so as to request these in time and look for the relevant signs (2).

The first radiological investigation to be requested is a simple chest radiograph. A chest radiograph is likely to show the presence of pneumomediastinum or pneumothorax (or hydropneumothorax if a concomitant pleural effusion is present) most commonly on the left (3). The presence of pneumomediastinum with a preceding history of vomiting or retching followed by acute chest pain is virtually pathognomonic of BS. However, pneumomediastinum may take more than an hour to develop and is not present in 10-12% of cases (3). It is thus imperative for clinicians to be aware of this percentage of false-negative results on chest radiograph. This will prevent false reassurance and

diagnostic delay.

In the presence of clinical suspicion for BS, a contrast swallow study is mandated. This is irrespective of whether or not the chest radiograph has revealed any positive findings. A water-soluble contrast medium such as gastrografin is recommended. This is not only likely to confirm the diagnosis by showing the extravasation of contrast into the mediastinum and/or pleural cavity (although 15-25% false-negative results have been reported for this examination, too) (11,12), but will also delineate the anatomical site of the perforation and thus guide the surgeon in their attempt to close the defect (11). Surgery, as part of a multidisciplinary approach, constitutes the "gold standard" treatment of this otherwise fatal syndrome if it is diagnosed within 24 hours (13). Various techniques and technologies are available in modern esophageal surgery but these are beyond the scope of this article (14,15). Beyond 24 hours, the prognosis significantly worsens and conservative treatment is usually advocated with surgery reserved for patients with a septic profile (9). Other investigations for BS include CT with or without oral contrast and needle thoracentesis if a pleural effusion exists. In the latter, biochemical and cytological examination of the pleural fluid can give the diagnosis by revealing the presence of salivary amylase and undigested food contents respectively (11,16).

In this editorial, we are hoping to raise the awareness about BS and how important it is for every clinician to have this diagnosis at the back of their mind when consulting a patient with the primary complaint of acute dyspnea, chest pain, or where a pneumothorax has already been diagnosed; even in the absence of a "typical history" for BS. The pneumothorax may only represent the "tip of the iceberg" and has been shown to be present in more than 20% of cases of BS-sometimes with a coexistent pleural effusion (hydropneumothorax) (17).

Thus, when encountering a patient with a pneumothorax, it is paramount to directly ask on history taking for predisposing factors for BS (such as vomiting or retching) and take a detailed pain history, look for signs of sepsis on clinical examination and observations, feel for surgical emphysema and request the appropriate imaging modalities in a timely manner. The clinician needs to look for the relevant imaging signs described earlier but also appreciate that false-negative results can occur.

The esophagus is an unforgiving organ (18,19). As it originates in the neck, extends through the thorax and terminates in the abdomen, it bears no respect for the arbitrary boundaries that exist between specialties (20). All clinicians, no matter what specialty they belong to, need to be aware that BS is probably more common than generally thought and of the different ways it can present. This includes pneumothorax as the sole initial presenting feature. Early clinical suspicion will lead to timely diagnosis and maximize the survival chances for the patient.

Acknowledgements

Disclosure: The authors declare no conflicts of interest.

References

1. Janjua KJ. Boerhaave's syndrome. Postgrad Med J 1997;73:265-70.
2. Onyeka WO, Booth SJ. Boerhaave's syndrome presenting as tension pneumothorax. J Accid Emerg Med 1999;16:235-6.
3. Henderson JA, Péloquin AJ. Boerhaave revisited: spontaneous esophageal perforation as a diagnostic masquerader. Am J Med 1989;86:559-67.
4. Mackler SA. Spontaneous rupture of the esophagus; an experimental and clinical study. Surg Gynecol Obstet 1952;95:345-56.
5. Jagminas L, Silverman RA. Boerhaave's syndrome presenting with abdominal pain and right hydropneumothorax. Am J Emerg Med 1996;14:53-6.
6. Marston EL, Valk HL. Spontaneous perforation of the esophagus: review of the literature and report of a case. Ann Intern Med 1959;51:590-607.
7. Abbott OA, Mansour KA, Logan WD Jr, et al. Atraumatic so-called "spontaneous" rupture of the esophagus. A review of 47 personal cases with comments on a new method of surgical therapy. J Thorac Cardiovasc Surg 1970;59:67-83.
8. Goldstein LA, Thompson WR. Esophageal perforations: a 15 year experience. Am J Surg 1982;143:495-503.
9. Venø S, Eckardt J. Boerhaave's syndrome and tension pneumothorax secondary to Norovirus induced forceful emesis. J Thorac Dis 2013;5:E38-40.
10. Garas G, Wou C, Sawyer J, et al. Acute oesophageal necrosis syndrome. BMJ Case Rep 2011;2011:bcr1020103423.
11. Drury M, Anderson W, Heffner JE. Diagnostic value of pleural fluid cytology in occult Boerhaave's syndrome. Chest 1992;102:976-8.
12. Suzuki M, Sato N, Matsuda J, et al. A case of rapid diagnosis of Boerhaave syndrome by thoracic drainage. J

Emerg Med 2012;43:e419-23.
13. Shaker H, Elsayed H, Whittle I, et al. The influence of the 'golden 24-h rule' on the prognosis of oesophageal perforation in the modern era. Eur J Cardiothorac Surg 2010;38:216-22.
14. Garas G, Kayani B, Tolley N, et al. Is there a role for intraoperative recurrent laryngeal nerve monitoring during high mediastinal lymph node dissection in three-stage oesophagectomy for oesophageal cancer? Int J Surg 2013;11:370-3.
15. Kayani B, Garas G, Arshad M, et al. Is hand-sewn anastomosis superior to stapled anastomosis following oesophagectomy? Int J Surg 2014;12:7-15.
16. Demetriou GA, Nair MS. Biliary contents in the chest drain tube: a finding not to ignore. BMJ Case Rep 2013;2013:bcr2013009849.
17. Ghanem N, Altehoefer C, Springer O, et al. Radiological findings in Boerhaave's syndrome. Emerg Radiol 2003;10:8-13.
18. Hennessy TP, Cuschieri A. Surgery of the oesophagus. Balliere Tindall 1986;56:667-72.
19. Kayani B, Zacharakis E, Ahmed K, et al. Lymph node metastases and prognosis in oesophageal carcinoma--a systematic review. Eur J Surg Oncol 2011;37:747-53.
20. Lewis TM, Zacharakis E, Hoare J, et al. Gastrointestinal images: complete tubular duplication of the oesophagus in an adult. J Gastrointest Surg 2010;14:1340-2.

Cite this article as: Garas G, Zarogoulidis P, Efthymiou A, Athanasiou T, Tsakiridis K, Mpaka S, Zacharakis E. Spontaneous esophageal rupture as the underlying cause of pneumothorax: early recognition is crucial. J Thorac Dis 2014;6(12):1655-1658. doi: 10.3978/j.issn.2072-1439.2014.12.04

Editorial

Big data and clinical research: perspective from a clinician

Zhongheng Zhang

Department of Critical Care Medicine, Jinhua Municipal Central Hospital, Jinhua Hospital of Zhejiang University, Jinhua 321000, China
Correspondence to: Zhongheng Zhang, MMed. 351#, Mingyue Street, Jinhua 321000, China. Email: zh_zhang1984@hotmail.com.

Submitted Oct 11, 2014. Accepted for publication Nov 13, 2014.
doi: 10.3978/j.issn.2072-1439.2014.12.12
View this article at: http://dx.doi.org/10.3978/j.issn.2072-1439.2014.12.12

Introduction

The 21st century is an era of information technology and people faces information explosion with large amount of data. The term big data has been defined in Wikepedia as: big data is the term for a collection of data sets so large and complex that it becomes difficult to process using on-hand database management tools or traditional data processing applications. In all areas of disciplines, such a big data may help to explore underlying mechanisms of varieties of phenomenon, and further facilitate decision-making. For example, in the 2012 USA presidential election, data-driven decision-making played a huge role in helping Obama win (1). In biomedical field, big data also begin to show its important role. Medical decision-making is becoming more and more dependent on data analysis, rather than conventional experience and intuition (2).

The present paper will focus on how to do clinical research by using big data. Firstly, I will review some basic concepts of clinical research and some characteristics of big data. Next, I will take some examples to illustrate how to address clinical uncertainty via data mining. The aim of the article is to provide more insights into clinical research based on big data in the hope that more people will take initiatives to conduct further investigations into clinical big data. I cannot list all detailed technical issues in this article, for which I will provide more references. Interested investigators may take these references as tutorials to guide them through the difficult journal of data exploration.

Bewilderedness in the current clinical research

It is well known that clinical research can be generally categorized into interventional and observational studies. The former is an experimental study that certain interventions will be given to participants. The most commonly performed randomized controlled trial (RCT) belongs to this kind of study. RCT usually has strict inclusion and exclusion criteria for participants. The procedure of randomization is employed to balance potential confounding factors between treatment and control arms. RCTs and/or systematic review involving high quality RCTs are the gold standard for clinical guidelines. However, with more and more RCTs being conducted, its limitations have arisen. In the area of sepsis and critical care medicine, we have compared the results obtained from RCTs and observational studies, and found that interventional effects obtained from these two types of study were quite different (3,4). Biological efficacy, a measurement of effect size under strict experimental condition, can be obtained by RCT. However, this biological efficacy may be attenuated or even not take place at real world setting. In this circumstance the biological efficacy cannot be translated into clinical efficacy (5). Clinical effectiveness is the most relevant to clinicians. The next question goes to why biological efficacy cannot be translated to clinical effectiveness. The plausible explanation is that RCTs are usually conducted with strict experimental design. There is a long list of inclusion and exclusion criteria. The participants are highly selected to exclude potential confounders. The protocol of intervention is also strictly defined with respect to timing, dosing and sequence of procedure. However, in reality, the condition as defined in RCTs cannot be fulfilled. Patients are usually complicated by comorbidities such as renal dysfunction, hypertension, and congestive heart failure. The timing of drug administration may be delayed due to admission at busy hours. As a result, it is probably that we treat our patients based on knowledge derived from a minority of highly selected patients. That is to say, the conclusion from RCTs may not be generalizable to "real world" patients.

Although there is no solution to above-mentioned

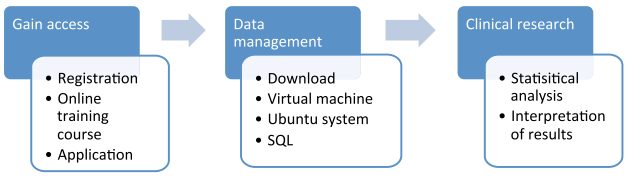

Figure 1 Flow chart of exploring MIMIC-II database. SQL, structural query language; MIMIC-II, multiparameter intelligent monitoring in intensive care II.

Figure 2 Certificate of completion of the training cause "protecting human research participants". NIH, provided by National Institute of Health.

limitations of current clinical research, big data may provide some insights into future direction of clinical trials (6,7). Wang and colleagues have proposed that big-data clinical trial (BCT) may become a mainstay type of clinical research and complement RCT in an important way (8,9). Big data in clinical study refers to the information collected using electronic database. These data come from daily routine clinical practice without modification or screening with strict inclusion and exclusion criteria, therefore retaining its real-world features (10). The advantage of BCT is that the result directly reflects clinical effectiveness. Big data in medical or epidemiological research generally consists electronic medical record system, administrative registry for chronic and infectious diseases and medical insurance system (11). As clinicians, our research may focused on EMR system which consists information on demographics, laboratory findings, microbiology data, medical order, procedures, surgery and clinical outcomes (12). However, big data is not a panacea without limitations. BCT is a kind of observational study in nature and has inherent limitations of its kind. For example, the observed and un-observed baseline characteristics cannot be well balanced. The conclusion may not be generalizable to other institutions if data were collected from single center. Such limitation can be addressed with advanced statistical method such as random effects model and bootstrap estimation of coefficient.

How to do clinical research with big data: an example from multiparameter intelligent monitoring in intensive care II (MIMIC-II)

This section will take MIMIC-II as an example to illustrate how to incorporate big data into clinical research (13). The flow chart of analysis is shown in *Figure 1*.

MIMIC-IIis an open access database comprising clinical data of ICU patients from Beth Israel Deaconess Medical Center (http://physionet.org/mimic2/). The database is consistently updating with current version of 2.6 that contains >30,000 ICU patients from 2001 to 2008 (14). MIMIC-II consists clinical data and high resolution waveform.

Gaining access to MIMIC-II

The investigator should register a username via on the website, and then apply for the access to database. An online training course named "protecting human research participants" should be completed and a certification number will be assigned to individual investigator (*Figure 2*). With this certification number, one is qualified to apply for the access to database. After a couple of days, the whole database is accessible to you and data analysis can be performed according to one's interests.

Conceiving clinical research ideas

With such a huge amount of clinical data, the next question is how to conceive clinical research ideas. Firstly, I would like to enumerate several types of clinical research by using big data (*Table 1*). The first one involves exploration of risk factors, for which high resolution data are usually required for confounding controls. Multivariable models, stratification and propensity score analysis are useful tool for such kind of analysis. The second involves assessment of effectiveness of interventions. Similarly, this type of study requires high-resolution data to control for confounding factors. Bias associated with selective treatment may play an important role and should be considered in study design. The third involves prediction model building, which aims to fit a model for future prediction. The forth type is

Table 1 Types of clinical studies by using big data

Types of studies	Examples (research question)	Requirement for clinical data†	Note
Risk factor evaluation (independency)	Is urine output on ICU entry associated with mortality outcome?	High resolution (other risk factors should be provided)	Multivariable model, stratified analysis and propensity score analysis can be employed
Effectiveness of intervention	Will PiCCO monitoring improve outcome of patients with septic shock?	High resolution (including a large number of confounding factors)	Intervention may be given for patients with different conditions. These conditions should be controlled to avoid "selective treatment"
Prediction model	Prediction model for ICU delirium	Moderate resolution (general description of risk factors)	The predictive value of whole model is stressed, rather than a single risk factor
Epidemiological study	The incidence and prevalence of catheter-related blood stream infection in ICU	Low resolution	A simple description is enough and no risk factor adjustment is required
Implementation and efficacy of healthcare policy	Is the policy of screening and controlling hypertension effective in lowering cardiovascular event rate?	Low resolution	No complex clinical data are required

†, resolution of clinical data refers to the intensity of data recording. For example, the study on urine output requires it be recorded on hourly basis. The resolution is higher for hourly urine output than daily urine output. For risk factor analysis, every covariate should be completely recorded. Otherwise, the resolution is not enough if some covariates are missing in the dataset.

assessment of cost-effectiveness of health policy.

Another key issue is how to conceive research ideas that can be addressed with database. There are two approaches: one is to perform data mining according to your research question, and the other is to adapt your research question to the database. Sometimes these two approaches may be used simultaneously. In a study investigating the association of lactate and clinical outcome (15), we planed to explore lactate measured on ICU entry at the outset. However, after data mining we found that lactate was usually measured repeatedly and decision was made to explore the trend of lactate (lactate clearance). The study protocol was adapted accordingly.

To conceive research idea based on your data is another way. One can perform statistical description for a dataset, by using traditional central tendency (mean, median) and discrete tendency (full range, 95% confidence interval). Graphical demonstration may be particularly helpful. For example, contour plot may help to explore associations between three variables; histogram can be used to explore distribution of a variable. However, someone may contend that a peek at dataset before drafting a study protocol may introduce bias (e.g., the problem of multiple testing and selective reporting are of this kind). That is to say, twenty times statistical testing for association will result in one with $P<0.05$ among independently generated random variables. I acknowledge this limitation, but such study can still be used as hypothesis generating and provide rationale for further explorations.

Another type of study is to investigate simple and easily obtainable parameters. By using such parameters, your study and ideas can be addressed by using varieties of database. Our study group has previously performed association study involving urine output and mortality (16). Because urine output is an essential but easily obtainable variable, it should be recorded in all kinds of ICUs. There is no reason to omit this recording, just like all other vital signs. We were confident at the outset that urine output must be carefully recorded in MIMIC-II, and the study was expected to conduct smoothly. Such simple variables included temperature, electrolytes and heart rate. In another study we investigated the association of ionized calcium and mortality (17). However, studies involving simple variables are usually criticized as being lack of novelty, and this may be the most important reason to reject our paper.

Figure 3 Dual flow chart of data management and statistical analysis by using STATA.

Data extraction

There is a small version of the MIMIC-II that can be accessed via query builder (https://mimic2app.csail.mit.edu/querybuilder/). A limited number of rows can be exported from this version, and thus it is primarily used for testing structural query language (SQL). I found that it is useful for preliminary exploration of the data. I was doing research on brain natriuretic peptide (BNP) when I first encounter the MIMIC-II (18,19), the first idea come to my mind is to use this big data to establish a linkage between BNP and clinical outcome. However, when I started to explore the database I found that the information on BNP was scarce. In the end I realized that the payment for medical insurance in USA is closely monitored and not every one was indicated to have BNP measured (e.g., BNP is only covered by insurance when it is used to determine the cause of respiratory distress in emergency department). Query builder can be accessed via windows operating system that is convenient for most Chinese users, whereas the whole database can only be extracted via virtual machine on Ubuntu operating system.

Access to the whole MIMIC-II database requires the users to have some basic knowledge on virtual machine and Ubuntu operating system. The downloaded package compressed file with suffix ".tar", taking disc space of 30 G. The file can be directly imported into the virtual box (Oracle). After entering username and password, one gains access to the Ubuntu operating system. The username and password are mimic2 and 2CIMIM_2v6, respectively. Pgadmin is the most popular and feature rich open Source administration and development platform for PostgreSQL, it will be opened to extract data under Ubuntu operating system.

Some investigators may want to export data for further analysis under Windows system. Data transferring between different operating systems can be performed via email. The file extracted has suffix of .cvs, which can be imported into Stata statistical package. Other statistical software such as SAS and SPSS also support this format.

Data processing using Stata

The author is more familiar with Stata statistical package in data processing, and the following section will introduce some steps in data processing with Stata.

Data processing using Stata is consisted of data management and statistical analysis. In my experience around 80% time and energy are spent on data management. This step included several aspects: (I) to generate new variables, for example, one wants to transform continuous variable age into binary variable (e.g., old *vs.* young); (II) variable checking, the sum module can check for some senseless values (e.g., age =200); (III) to transform string variable into numerical variable, or vise versa; (IV) combination of dataset. Different types of variable are stored in different relational tables. They should be combined into one dataset for the purpose of statistical analysis. Stata provided very useful modules such as merge and append for this purpose. Statistical analysis in based on correctly performed data management.

One advantage of Stata is its ability to record complete process of data analysis. Data analysis can be performed in three ways: windows pull-down menu, command input in command window and do-file. I suggest that data analysis be performed by using do-file, because it is able to record the whole process of how data is managed and analyzed. This will facilitate replication of analysis and made revisions. Furthermore, cooperation among researchers also requires do-file. The other two methods (e.g., windows pull-down menu and command input in command window) are mainly used to test a stata syntax or to facilitate draw graphs with complex options.

A complete dual flow chart of data analysis using stata is shown in *Figure 3*. I suggest split data analysis into two parts: data management and statistical analysis. The left column shows data management that will make changes to the dataset in memory. Dataset generated by using do-file will be stored in memory with suffix of ".dta". The right column simply performs statistical analysis and will not significantly change the dataset.

Using structural query language (SQL) to extract data

An important step in preparing data for analysis is data extraction by using SQL. Efficient use of SQL will save a lot of time and disc space. Some tasks previously mentioned during data management can be performed at the step of data extraction. For example, one intends to restrict data analysis to adult population. This can be performed by using stata command "if", or using SQL "where" clause. I prefer to use stata for data management because it tracks the process of data management. However, it is at the discretion of investigator.

A simple SQL syntax can be written as: Select *variable name* from *table name* where *conditions*, where variable name refers to variables contained in relational tables. The asterisk "*" can replace the variable name if all variables are expected to be extracted. The table name refers to the name of the relational table. The conditions are a set of expressions used to select observations fulfilling certain criteria. For example, the expression "age >65" can be used if your target population is old people. For complex SQL syntax, readers can see other textbooks on SQL such as the language of SQL: How to Access Data in Relational Databases edited by Larry Rockoff and SQL Cookbook by Anthony Molinaro.

Conclusions

The exploration of big data is a process of trial and error. Someone may feel that it is a task of distress, but I feel it is a hard way filled with success and surprise. The secret of human disease may lurk under the vast ocean of big data, waiting us to decode and understand them. The article is not intended to serve as a step-by-step guidance on using big data but to inspire people who are interested in doing exploration on it. In China, it is possible to establish our own high quality big data because we have the largest population in the world.

Acknowledgements

Disclosure: The author declares no conflict of interest.

References

1. Scherer M. Inside the Secret World of the Data Crunchers Who Helped Obama Win. Available online: http://swampland.time.com/2012/11/07/inside-the-secret-world-of-quants-and-data-crunchers-who-helped-obama-win/
2. Margolis R, Derr L, Dunn M, et al. The National Institutes of Health's Big Data to Knowledge (BD2K) initiative: capitalizing on biomedical big data. J Am Med Inform Assoc 2014;21:957-8.
3. Zhang Z, Ni H, Xu X. Do the observational studies using propensity score analysis agree with randomized controlled trials in the area of sepsis? J Crit Care 2014;29:886.e9-15.
4. Zhang Z, Ni H, Xu X. Observational studies using propensity score analysis underestimated the effect sizes in critical care medicine. J Clin Epidemiol 2014;67:932-9.
5. Nallamothu BK, Hayward RA, Bates ER. Beyond the randomized clinical trial: the role of effectiveness studies in evaluating cardiovascular therapies. Circulation 2008;118:1294-303.
6. Schneeweiss S. Learning from big health care data. N Engl J Med 2014;370:2161-3.
7. Psaty BM, Breckenridge AM. Mini-Sentinel and regulatory science--big data rendered fit and functional. N Engl J Med 2014;370:2165-7.
8. Wang SD. Opportunities and challenges of clinical research in the big-data era: from RCT to BCT. J Thorac Dis 2013;5:721-3.
9. Wang SD, Shen Y. Redefining big-data clinical trial (BCT). Ann Transl Med 2014;2:96.
10. Albert RK. "Lies, damned lies ..." and observational studies in comparative effectiveness research. Am J Respir Crit Care Med 2013;187:1173-7.
11. Cooke CR, Iwashyna TJ. Using existing data to address important clinical questions in critical care. Crit Care Med 2013;41:886-96.
12. Peters SG, Buntrock JD. Big data and the electronic health record. J Ambul Care Manage 2014;37:206-10.
13. Saeed M, Villarroel M, Reisner AT, et al. Multiparameter Intelligent Monitoring in Intensive Care II: a public-access intensive care unit database. Crit Care Med 2011;39:952-60.
14. Scott DJ, Lee J, Silva I, et al. Accessing the public MIMIC-II intensive care relational database for clinical research. BMC Med Inform Decis Mak 2013;13:9.
15. Zhang Z, Chen K, Ni H, et al. Predictive value of lactate in unselected critically ill patients: an analysis using fractional polynomials. J Thorac Dis 2014;6:995-1003.
16. Zhang Z, Xu X, Ni H, et al. Urine output on ICU entry is associated with hospital mortality in unselected critically ill patients. J Nephrol 2014;27:65-71.
17. Zhang Z, Xu X, Ni H, et al. Predictive value of ionized calcium in critically ill patients: an analysis of a large

clinical database MIMIC II. PLoS One 2014;9:e95204.
18. Zhang Z, Zhang Z, Xue Y, et al. Prognostic value of B-type natriuretic peptide (BNP) and its potential role in guiding fluid therapy in critically ill septic patients. Scand J Trauma Resusc Emerg Med 2012;20:86.
19. Zhang Z, Ni H, Lu B, et al. Changes in brain natriuretic peptide are correlated with changes in global end-diastolic volume index. J Thorac Dis 2013;5:156-60.

Cite this article as: Zhang Z. Big data and clinical research: perspective from a clinician. J Thorac Dis 2014;6(12):1659-1664. doi: 10.3978/j.issn.2072-1439.2014.12.12

Editorial

Endobronchial ultrasound-guided transbronchial needle aspiration: a maturing technique

Jianjun Zhang, Yangang Ren

China Medical University, Shenyang 110001, China

Correspondence to: Professor Yangang Ren. China Medical University, 77 Puhe Road, North New District, Shenyang 110001, China. Email: broren@163.com.

Submitted Nov 02, 2014. Accepted for publication Dec 06, 2014.

doi: 10.3978/j.issn.2072-1439.2014.12.35

View this article at: http://dx.doi.org/10.3978/j.issn.2072-1439.2014.12.35

Accurate, quick pathological identification of a pulmonary or mediastinal mass is one of most challenging issues in thoracic oncology. This is particularly important when it comes to operable lung cancers in which a pre-surgical evaluation of mediastinal lymph node involvement is widely recognized as indispensible. For this purpose, mediastinoscopy was an accepted gold standard with 80% sensitivity and 100% specificity in the screening (1). Unfortunately, considerable invasiveness and the need for general anesthesia associated with mediastinoscopy limit the accessibility of this procedure to N2-3 lymph nodes; moreover, repetitive mediastinoscopy is hardly feasible owing to the formation of dense adhesions.

Endobronchial ultrasound (EBUS) is a procedure in which a miniature ultrasound probe is advanced into the airway lumen via fiberoptic bronchoscopy for real-time scanning, thus enabling study of histological characteristics as well as ultrasound imaging of the adjacent anatomy. In recent years, a novel EBUS-based technique, EBUS-guided transbronchial needle aspiration (EBUS-TBNA) has emerged (2), which can achieve precise aspiration biopsy of the peribronchial pulmonary lesions. In a number of studies, EBUS-TBNA has been shown to yield excellent diagnostic performance for central-type lung cancers without bronchial invasion, presurgical staging of mediastinal lymph nodes, and unexplained hilar or mediastinal masses (1,3,4). For example, the sensitivity of EBUS-TBNA is 85% to 95% and the specificity may be up to 100% in the staging of mediastinal lymph nodes and diagnosis of lung cancer (1,3). The real-time imaging with EBUS-TBNA enables accurate puncture that is difficult with mediastinoscopy, making it possible to biopsy a suspected lesion surrounding but not yet protruding into the bronchi; this is particularly relevant for central-type lung cancers without airway invasion. In addition, EBUS-TBNA is associated with satisfactory safety of puncture (5). The complications are infrequent, and mainly include cough, bleeding, and hypoxemia, which can be readily corrected by application of local anesthesia, clotting agents, reduction of manipulation time, and enhanced oxygen inhalation. The use of EBUS with guide-sheath (EBUS-GS) or electromagnetic navigation may further improve the diagnosis rate of peripheral lung lesions (6,7). Conceivably, samples obtained with needle aspiration under ultrasound guiding may not suffice in size for a confirmatory pathological study. For this concern, rapid on-site evaluation (ROSE) has been used in TBNA of adenopathies and peripheral lesions; although, its significance in sampling centrally located lesions has not been validated. Several studies noted that ROSE of transbronchial aspirates by a cytopathologist during bronchoscopy may minimize the chance of inadequate biopsy and increase TBNA yield (8,9). However, for experienced endoscopic ultrasound specialists, ROSE seems to have no effect on the diagnosis rate with transesophageal-guided needle aspiration (10,11). Even when no cytological examination was performed on site, a diagnosis rate over 90% for mediastinal lymph nodes with EBUS-TBNA has been reported (12). The necessity and indications for rapid on-site evaluation in cases that undergo EBUS-TBNA require further clinical observation. In certain occasions, though, the harvested specimen does turn out to be insufficient owing to low tissue content and mechanical rupture, and it may be difficult to accurately and reliably distinguish between adenocarcinoma and squamous cell carcinoma based on morphology alone, especially in poorly

differentiated tumors. In such cases, immunohistochemical markers should be helpful to differentiate between adenocarcinoma and squamous cell carcinoma. Terry *et al.* (13) showed that combinations of biomarkers including TTF-1, p63, CK7, CK5/6, Napsin A, and mucicarmine can be fairly efficient for differential diagnosis between the two types of cancers.

At present, the commonly used needle aspiration techniques in the field of thoracic disease include classical TBNA, transesophageal endoscopic ultrasound-guided fine needle aspiration (EUS-FNA), and transthoracic needle aspiration (TNA) (5,14-16). Transesophageal EUS-FNA allows examining lymph nodes of the aorta, pulmonary artery (group 5), around the esophagus (group 8), and pulmonary ligament (group 9), which are not accessible with EBUS-TBNA. Combination of EBUS-TBNA and transesophageal EUS-FNA can achieve complete mediastinal staging, and access any lymph-node station that cannot be accomplished by either alone. And the diagnostic sensitivity, has been reported to be 93-94% (17). In comparison, classical TBNA relies on chest computed tomography to locate the site for a blind puncture to sample the mediastinal tumor and lymph nodes, which is difficult to manipulate, far less accurate and successful, and hardly precedes mediastinoscopy in terms of its scope of application.

In addition, progress in EBUS has been made with respect to lung cancer treatment. EBUS can be used to implant radiation particles for local radiotherapy in lung cancer patients who are not candidates for surgery, and has shown satisfactory effects (18). Repeated EBUS-TBNA for patients has made a difference in the re-evaluation of hilar and mediastinal tumors and lymph nodes after neoadjuvant chemotherapy, which is an important aspect in determining the treatment response (19). However, the use of EBUS-TBNA for mediastinal re-staging after combination chemotherapy is not ideal; its diagnostic sensitivity was only 76% and the negative predictive value was 20% (19). Therefore, most researchers believe that the negative results of EBUS-TBNA should be confirmed by mediastinoscopy, surgical lymph node sampling, or clinical follow-up to compensate for the limitations of the technique (20). Subsequent studies have found a negative predictive value of 78% for EBUS-TBNA in mediastinal restaging after combination chemotherapy, and cases with negative results do not require further surgery for re-staging (21). Studies on large samples are needed to further investigate the negative predictive value of EBUS-TBNA for mediastinal restaging after combination chemotherapy.

With respect to its use in other chest disorders, EBUS-TBNA showed diagnostic sensitivity of 91% for patients with clinically suspected lymphoma (22); the diagnostic rate achieved with EBUS-TBNA for sarcoidosis was 83-94% (23). EBUS can also be useful for unexplained recurrent hemoptysis (24) and drainage of mediastinal bronchogenic cysts (25). One study that focused on the learning curve for EBUS indicated that only ten training sessions were required to master the major know-how of this procedure (26,27).

In summary, EBUS-TBNA demonstrates high sensitivity and accuracy in diagnosis of lung cancers, mediastinal tumors and metastasis. Compared with many other investigational modalities, EBUS-TBNA is minimally invasive, safe, and cost-effective. This maturing technique adds to the armamentarium for management of thoracic diseases.

Acknowledgements

Disclosure: The authors declare no conflict of interest.

References

1. Gompelmann D, Eberhardt R, Herth FJ. Endobronchial ultrasound. Endosc Ultrasound 2012;1:69-74.
2. Herth FJ. Endobronchial ultrasound: first choice for the mediastinum. Endosc Ultrasound 2013;2:179-80.
3. Ømark Petersen H, Eckardt J, Hakami A, et al. The value of mediastinal staging with endobronchial ultrasound-guided transbronchial needle aspiration in patients with lung cancer. Eur J Cardiothorac Surg 2009;36:465-8.
4. Zhang Y, Wang KP. Evolution of transbronchial needle aspiration - a hybrid method. J Thorac Dis 2013;5:234-9.
5. Zaric B, Stojsic V, Sarcev T, et al. Advanced bronchoscopic techniques in diagnosis and staging of lung cancer. J Thorac Dis 2013;5 Suppl 4:S359-70.
6. Schuhmann M, Eberhardt R, Herth FJ. Endobronchial ultrasound for peripheral lesions: a review. Endosc Ultrasound 2013;2:3-6.
7. Chee A, Stather DR, Maceachern P, et al. Diagnostic utility of peripheral endobronchial ultrasound with electromagnetic navigation bronchoscopy in peripheral lung nodules. Respirology 2013;18:784-9.
8. Tofts RP, Lee PM, Sung AW. Interventional pulmonology approaches in the diagnosis and treatment of early stage non small cell lung cancer. Transl Lung Cancer Res

2013;2:316-31.
9. Chin R Jr, McCain TW, Lucia MA, et al. Transbronchial needle aspiration in diagnosing and staging lung cancer: how many aspirates are needed? Am J Respir Crit Care Med 2002;166:377-81.
10. Cermak TS, Wang B, DeBrito P, et al. Does on-site adequacy evaluation reduce the nondiagnostic rate in endoscopic ultrasound-guided fine-needle aspiration of pancreatic lesions? Cancer Cytopathol 2012 Oct;120:319-25. PubMed
11. Dietrich CF, Jenssen C. Endoscopic ultrasound-guided sampling in gastroenterology: European society of gastrointestinal endoscopy technical guidelines. Endosc Ultrasound 2013;2:117-22.
12. Shimizu K, Okita R, Nakata M. Clinical significance of the tumor microenvironment in non-small cell lung cancer. Ann Transl Med 2013;1:20.
13. Terry J, Leung S, Laskin J, et al. Optimal immunohistochemical markers for distinguishing lung adenocarcinomas from squamous cell carcinomas in small tumor samples. Am J Surg Pathol 2010;34:1805-11.
14. Krishna SG, Ghouri YA, Suzuki R, et al. Uterine cervical cancer metastases to mediastinal lymph nodes diagnosed by endoscopic ultrasound-guided fine needle aspiration. Endosc Ultrasound 2013;2:219-21.
15. Costache MI, Iordache S, Karstensen JG, et al. Endoscopic ultrasound-guided fine needle aspiration: from the past to the future. Endosc Ultrasound 2013;2:77-85.
16. Ioncica AM, Bektas M, Suzuki R, et al. Role of EUS-FNA in Recurrent Lung Cancer: Maximum Results with Minimum (minimally invasive) Effort. Endosc Ultrasound 2013;2:102-4.
17. Wallace MB, Pascual JM, Raimondo M, et al. Minimally invasive endoscopic staging of suspected lung cancer. JAMA 2008;299:540-6.
18. Harley DP, Krimsky WS, Sarkar S, et al. Fiducial marker placement using endobronchial ultrasound and navigational bronchoscopy for stereotactic radiosurgery: an alternative strategy. Ann Thorac Surg 2010;89:368-73; discussion 373-4.
19. Herth FJ, Annema JT, Eberhardt R, et al. Endobronchial ultrasound with transbronchial needle aspiration for restaging the mediastinum in lung cancer. J Clin Oncol 2008;26:3346-50.
20. Almeida FA. Bronchoscopy and endobronchial ultrasound for diagnosis and staging of lung cancer. Cleve Clin J Med 2012;79 Electronic Suppl 1:eS11-6.
21. Szlubowski A, Herth FJ, Soja J, et al. Endobronchial ultrasound-guided needle aspiration in non-small-cell lung cancer restaging verified by the transcervical bilateral extended mediastinal lymphadenectomy--a prospective study. Eur J Cardiothorac Surg 2010;37:1180-4.
22. Kennedy MP, Jimenez CA, Bruzzi JF, et al. Endobronchial ultrasound-guided transbronchial needle aspiration in the diagnosis of lymphoma. Thorax 2008;63:360-5.
23. Chatterjee DK, Wolfe T, Lee J, et al. Convergence of nanotechnology with radiation therapy-insights and implications for clinical translation. Transl Cancer Res 2013;2:256-68.
24. Patil S, Ayachit R. Unexplained intermittent hemoptysis with normal chest radiograph necessitates bronchoscopy'-mucoepidermoid carcinoma of lung: Case report. J Transl Intern Med 2014;2:40-4.
25. Galluccio G, Lucantoni G. Mediastinal bronchogenic cyst's recurrence treated with EBUS-FNA with a long-term follow-up. Eur J Cardiothorac Surg 2006;29:627-9; discussion 629.
26. Groth SS, Whitson BA, D'Cunha J, et al. Endobronchial ultrasound-guided fine-needle aspiration of mediastinal lymph nodes: a single institution's early learning curve. Ann Thorac Surg 2008;86:1104-9; discussion 1109-10.
27. Ge N, Sun S. Endoscopic ultrasound: An all in one technique vibrates virtually around the whole internal medical field. J Transl Intern Med 2014;2:104-6.

Cite this article as: Zhang J, Ren Y. Endobronchial ultrasound-guided transbronchial needle aspiration: a maturing technique. J Thorac Dis 2014;6(12):1665-1667. doi: 10.3978/j.issn.2072-1439.2014.12.35

Original Article

The lung cancer epidemic in Spanish women: an analysis of mortality rates over a 37-year period

Jose Luis López-Campos[1,2], Miguel Ruiz-Ramos[3], Carmen Calero[1,2]

[1]Unidad Médico-Quirúrgica de Enfermedades Respiratorias. Instituto de Biomedicina de Sevilla (IBiS), Hospital Universitario Virgen del Rocio/ Universidad de Sevilla, Spain; [2]CIBER de Enfermedades Respiratorias (CIBERES). Instituto de Salud Carlos III, Madrid, Spain; [3]Consejería de Salud y Bienestar Social de Andalucía, Seville, Spain

Correspondence to: Jose Luis López-Campos, MD. Hospital Universitario Virgen del Rocio, Avda. Manuel Siurot, 41013 Seville, Spain. Email: lcampos@separ.es.

Background: Lung cancer continues to be the leading cause of cancer-related mortality in the European Union (EU) and deaths from lung cancer have been projected to escalate to epidemic proportions amongst females over the next years. We examined lung cancer mortality rates in men and women from Andalusia (Spain) over a 37-year period [1975-2012].

Methods: Longitudinal epidemiological study analyzing lung cancer mortality trends in males and females. Data on lung cancer mortality in Andalusia for the period 1975-2012 were obtained from the official cause-of-death publications of the Institute of Statistics of Andalusia. For each sex, age-standardized (European standard population) mortality rates (ASR) from lung cancer were calculated for all ages and truncated at 30-64, 65-74, and >75 years using the direct method. Standardized rate trends by age and sex were estimated by joinpoint regression analysis.

Results: In men, the ASR steadily increased through the period 1993-1995, reaching a peak of 145.72 deaths/100,000 people. Subsequently, lung cancer deaths decreased to a rate of 125.47 in the 2011-2012 period. A moderate increase was seen in women until the late 1990s and early 2000s. Thereafter, a very notable rise was observed in females for all age groups, the only exception being older subjects. The sex differences decreased from 8.6:1 in the 1975-1977 period to 6.8:1 in the 2011-2012 period.

Conclusions: Lung cancer mortality rates decreased significantly in Andalusian men from 1975 to 2012. More importantly, we demonstrate for the first time the beginning of the lung cancer epidemics in Andalusian women as previously predicted for this area.

Keywords: Lung cancer; mortality; males; females; epidemics

Submitted Feb 04, 2014. Accepted for publication Aug 14, 2014.
doi: 10.3978/j.issn.2072-1439.2014.10.28
View this article at: http://dx.doi.org/10.3978/j.issn.2072-1439.2014.10.28

Introduction

Lung cancer continues to be the leading cause of cancer-related death in the European Union (EU). An estimated 334,800 European people died of lung cancer in 2006, representing 19.7% of all cancer deaths (1). In the EU as a whole, mortality from lung cancer in men reached a peak of 53.3/100,000 in the late 1980s but declined thereafter to reach 44.0/100,000 in the early 2000s. In contrast, lung cancer mortality tended to rise in women from 9.0 to 11.4/100,000 over the same calendar period (2) and it has been hypothesized that deaths from lung cancer in females will escalate to epidemic proportions over the next years (3).

The trends of lung cancer mortality in Spain are similar to those observed in the EU as a whole. Starting in the nineties, age-specific death rates in males decreased for each age group under 85 years old. However, a statistically significant annual increase of 6.3% in truncated mortality rates has been observed in women since 1992 (4). Consequently, lung cancer age-standardized mortality rates

for females doubled from 5.6 in 1980 to 11.3 in 2005 in all regions of the country (5) and are also projected to increase over the next years (6).

Lung cancer mortality trends have been thoroughly examined in Andalusia (7-9), the second largest Spanish region with a surface area of 87,268 km² and over 8 million inhabitants. In the mid-nineties, there has been a convergence in lung cancer deaths for Andalusian men and women (8) with a decrease in the male-to-female mortality ratio (9). However, previous series describing mortality trends until the year 2000 did not observe the projected epidemic rise of lung cancer deaths in women (8).

The present study extends the comparison of lung cancer mortality rates in Andalusian men and women over a longer period of time [1975-2012]; herein, the projected epidemic in female lung mortality rates is being demonstrated for the first time in Andalusia. These enhanced data will improve the utility and quality of cancer surveillance activities and are the key to improving cancer prevention strategies.

Methods

Data on lung cancer mortality in Andalusia for the period 1975-2012 were obtained from the official cause-of-death publications of the Institute of Statistics of Andalusia. Population estimates referred to the population as of July 1 of each year based on official census information. Lung cancer corresponds to codes 162 in the International Classification of Diseases (ICD) 8th and 9th revisions (1975-1979 and 1980-1998, respectively) and C33-C34 in the 10th revision [1999-2012]. For each sex, age-standardized (European standard population) mortality rates (ASR) from lung cancer were calculated for all ages and truncated at 30-64, 65-74, and >75 years using the direct method. The results were expressed as rates per 100,000 person-years.

The standardized rate trends by age and sex were estimated by joinpoint regression analysis (10). Specifically, we used joinpoint regression analysis to identify the changes in the slope of mortality trends. We selected the best fitting points (the "joinpoints") where the rate changed significantly. This approach has two major advantages. First, it allows the precise identification of significant trend changes. Second, it provides a framework for estimating the increase or decrease occurring in each time interval using the percentage of annual change (PAC). We used the Surveillance Epidemiology and End Results (SEER) Stat software (Joinpoint Regression Program, Version 4.0.4., Statistical Research and Applications Branch, National Cancer Institute, Bethesda, MD, USA, 2011) for calculations. We also fitted segmented Poisson regression models to estimate the changes of trends over time. Standardized rates were used as the dependent variable, whereas the year of death was entered in the model as the independent variable (11). In all analyses, a two-tailed P value <0.05 was considered statistically significant.

Results

In men, the ASR steadily increased through the period 1993-1995, reaching a peak of 145.72 deaths/100,000 people. Subsequently, lung cancer deaths decreased to a rate of 125.47 in the 2011-2012 period. Truncated rates at 30-64, 65-74, and >75 years showed similar patterns, although less evident amongst older age groups (*Figure 1*, *Table 1*). Joinpoint regression analysis unambiguously identified the inflexion points at which there was a significant change in the trends (i.e., a striking rise was observed until 1993 which was followed by a decrease thereafter; *Figure 1*, *Table 2*).

However, opposite trends in lung cancer death rates were observed in women. A moderate increase was seen until the late 1990s and early 2000s. Thereafter, a very notable rise was observed for all age groups, albeit to lesser extent in the 65-74 years age group and without clear trends in older age groups (*Figure 1*, *Table 1*). Joinpoint regression analysis successfully identified the timing and extent of mortality increase (*Figure 1*, *Table 2*).

The combined analysis of mortality rates in men and women showed a specular pattern with a marked reduction in sex difference (from 8.6:1 for the period 1975-1977 to 6.8:1 for the period 2011-2012) which became more evident as of the late 1990s.

Discussion

Vital statistics of lung cancer provide valuable information on the occurrence of lung cancer because the highly aggressive nature of the disease makes its incidence and mortality rates nearly identical (12). The present study shows that lung cancer mortality rates decreased significantly in Andalusian men from 1975 to 2012. More importantly, we show for the first time the beginning of the lung cancer epidemics in Andalusian women as previously predicted for this area (8).

Our results should be interpreted in light of the evolving smoking patterns in our area. As of 1993, tobacco consumption in Andalusia has been constantly decreasing

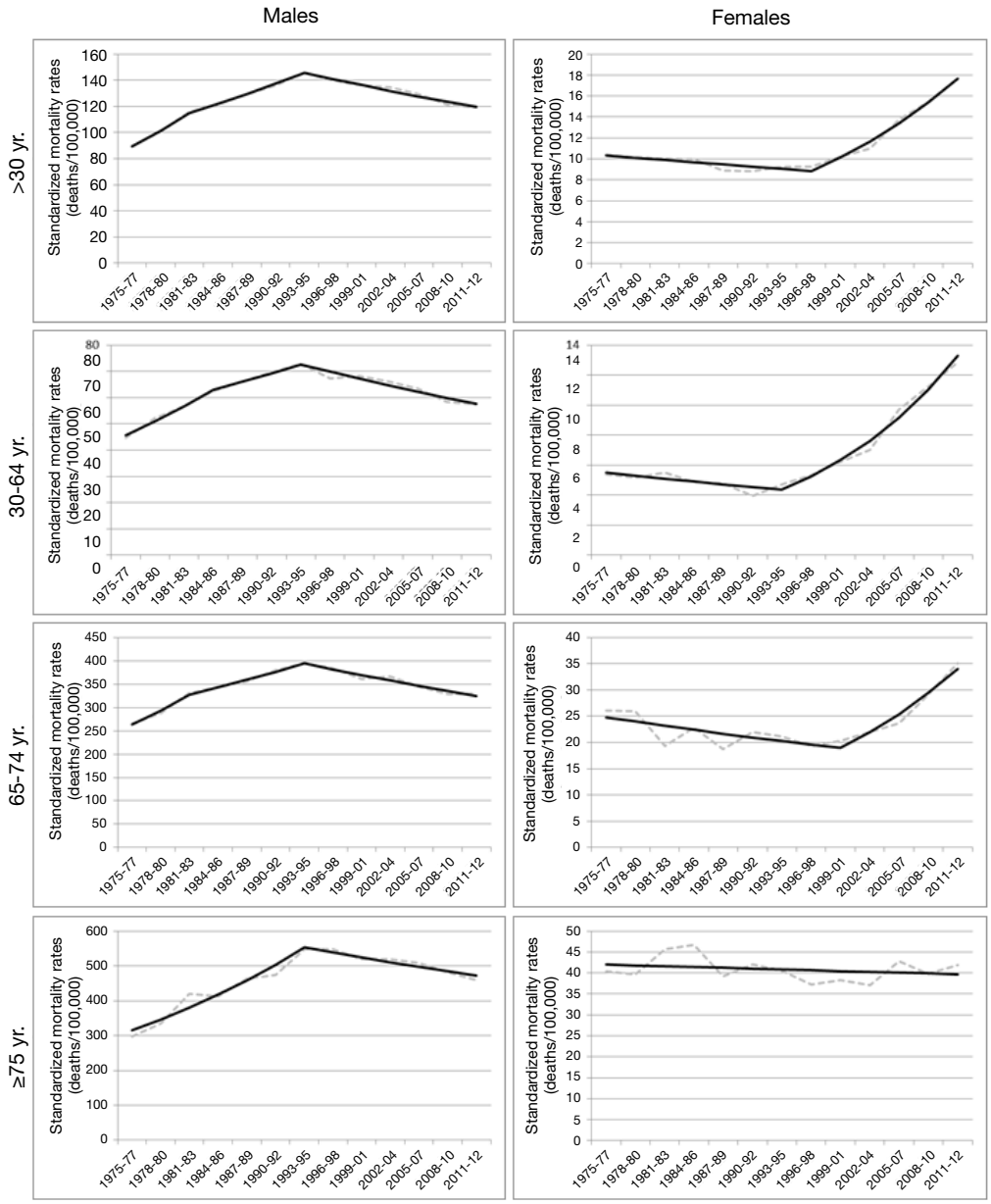

Figure 1 Age-standardized mortality and joinpoint regression trends of lung cancer deaths in Andalusia, 1975-2012. Solid lines represent the joinpoint regression lines, whereas dashed lines indicate age-standardized mortality.

in most—but not all—of the age groups (6). In particular, teen smoking patterns do not show marked sex differences in Spain. Interestingly, the results of the 2006 Spanish National Health Survey have shown for the first time that the smoking prevalence was significantly higher in females than in males aged between 16 and 24 years. The last 2011/2012 Spanish National Health Survey confirmed the declining trend regarding sex differences in smoking, with a prevalence of 27.9% in males and of 20.2% in females aged ≥15 years (13).

The lung cancer mortality data used in our study were based on death certificates. Obviously, the accuracy of our findings substantially depends on the quality of cause-of-death information in death certificates, especially for older age groups. Because death certification in Andalusia is performed according to international standards and is subjected to quality controls, we are reasonably confident that our data are internally valid (14). Previous studies have supported the validity of death certification for the most

Table 1 Age-standardized mortality trends from lung cancer in Andalusia, 1975-2012

Period	Deaths		Crude		ASR		ASR 30-64		ASR 65-74		ASR ≥75	
	Males	Females	Males	Females	Males	Females	Males	Females	Males	Females	Males	Females
1975-1977	3,335	515	82.54	11.26	89.52	10.39	44.71	5.39	265.55	26.13	296.78	40.39
1978-1980	3,981	538	95.47	11.43	101.08	10.16	52.18	5.19	288.30	25.97	335.72	39.61
1981-1983	4,868	557	112.16	11.43	115.97	10.04	56.78	5.51	330.83	19.36	420.63	45.73
1984-1986	5,487	608	120.12	11.93	121.51	9.99	62.49	4.86	343.30	22.78	412.15	46.69
1987-1989	6,220	563	130.15	10.60	129.52	8.91	66.14	4.79	355.22	18.71	463.45	39.14
1990-1992	6,899	599	137.75	10.80	136.11	8.85	69.58	3.96	379.82	22.00	474.74	42.01
1993-1995	7,852	656	146.94	11.12	145.72	9.25	72.87	4.71	394.76	21.19	547.66	40.48
1996-1998	8,004	685	140.89	10.95	140.02	9.28	67.35	5.32	384.20	19.39	548.42	37.18
1999-2001	8,200	783	137.20	11.93	135.92	10.22	68.20	6.24	361.51	20.35	519.96	38.33
2002-2004	8,644	871	137.60	12.66	134.64	10.98	66.06	7.03	365.68	22.03	518.97	37.03
2005-2007	8,777	1,129	133.00	15.65	129.14	13.76	63.45	9.72	344.14	23.67	508.31	42.80
2008-2010	8,768	1,292	126.82	17.13	121.34	15.44	58.38	11.24	329.10	29.12	481.77	39.79
2011-2012	5,974	1,015	125.47	19.58	119.10	17.64	57.36	12.89	329.88	35.04	460.23	41.84

ASR, age-standardized mortality rates.

Table 2 Trend changes according to joinpoint regression analysis

Groups	Period	PAC	Period 1	PAC	Period 2	PAC	Period 3	PAC
Males								
ASR	1975-1977; 2011-2012	1.27	1975-1977; 1981-1983	13.5*	1981-1983; 1993-1995	6.1*	1993-1995; 2011-2012	–3.2*
ASR 30-64	1975-1977; 2011-2012	0.99	1975-1977; 1984-1986	11.3*	1984-1986; 1993-1995	4.8	1993-1995; 2011-2012	–3.8*
ASR 65-74	1975-1977; 2011-2012	1.13	1975-1977; 1984-1986	11.6*	1984-1986; 1993-1995	4.8*	1993-1995; 2011-2012	–3.2*
ASR ≥75	1975-1977; 2011-2012	2.12	1975-1977; 1993-1995	9.8*	1993-1995; 2011-1912	–2.6*		
Females								
ASR	1975-1977; 2011-2012	4.76*	1975-1977; 1999-2001	–2.2*	1999-2001; 2011-2012	14.8*		
ASR 30-64	1975-1977; 2011-2012	9.03*	1975-1977; 1993-1995	–3.8	1993-1995; 2011-2012	20.3*		
ASR 65-74	1975-1977; 2011-2012	2.4	1975-1977; 1999-2001	–3.3*	1999-2001; 2011-2012	15.8*		
ASR ≥75	1975-1977; 2011-2012	–0.47						

*, P<0.05. PAC, percentage of annual change; ASR, age-standardized mortality rates.

common malignancies occurring in Spain (15). Despite a modest risk of underreporting cancer deaths, certificates are generally considered a valid source for population-based cancer registries (15).

In most EU countries, there has been an increase in deaths from lung cancer in female subjects (3). However, more favorable trends in young women over recent years have been observed (16), suggesting that effective tobacco control measures have been implemented when the outbreak was recognized (17). Unfortunately, the Spanish national and regional anti-tobacco regulations have not been able to impede the expected lung cancer epidemics amongst Andalusian women. Accordingly, factors other than smoking may also influence the incidence of lung cancer in women. Although there have been reports suggesting the onset of lung cancer epidemics in Spain (5), to our knowledge, the outbreak occurring in Andalusia has not been previously reported (8). A previous study has shown that lung cancer mortality increased significantly in Andalusian women aged between 35 and 64 years, although the mortality rates remained very low until the year 2000 (8). Thereafter, there was a steady and substantial increase that can be explained by the growth of tobacco use during the last decades (18). Collectively, the current data extend our previous findings up to the year 2012 and unequivocally demonstrate that a lung cancer epidemic swept through the female Andalusian population.

Cancer mortality trends in 33 European countries between 1970 and 2009 have been recently analyzed and the projected EU rates for the year 2015 estimated according to the World Health Organization data (3). The authors demonstrated that lung cancer death rates for women have been increasing up to recent years in most European countries, although a few notable exceptions exist (Eastern EU nations). Our current findings in Andalusia corroborate the occurrence of an unfavorable mortality trend in lung cancer mortality observed in women living in Southern Europe.

Evidence-based strategies for prevention are eagerly required to reverse the rising trend of lung cancer mortality. Besides anti-tobacco policy measures, low-dose computed tomography may be useful to detect early stages of lung cancer (19). Further studies are needed to examine the usefulness of lung cancer screening programs from the perspectives of cost-effectiveness and survival benefit.

In summary, there are two principal findings in this study. First, we have shown that lung cancer mortality rates decreased significantly in Andalusian men from 1975 to 2012. Second, we demonstrate the beginning of the lung cancer epidemics in Andalusian women as previously predicted for this area. Local anti-tobacco regulations have not demonstrated an effect in reversing the predicted mortality increase. Our results suggest imposing more effective tobacco use control policies and designing region-specific programs to reduce lung cancer mortality risks.

Acknowledgments

The authors gratefully acknowledge Enzo Emanuele (Living Research S.A.S., Robbio, Italy) for his excellent editorial assistance.
Disclosure: The authors declare no conflict of interest.

References

1. Ferlay J, Autier P, Boniol M, et al. Estimates of the cancer incidence and mortality in Europe in 2006. Ann Oncol 2007;18:581-92.
2. La Vecchia C, Bosetti C, Lucchini F, et al. Cancer mortality in Europe, 2000-2004, and an overview of trends since 1975. Ann Oncol 2010;21:1323-60.
3. Bosetti C, Malvezzi M, Rosso T, et al. Lung cancer mortality in European women: trends and predictions. Lung Cancer 2012;78:171-8.
4. Cayuela A, Rodríguez-Domínguez S, et al. Lung cancer mortality trends in Spain between 1980 and 2005. Arch Bronconeumol 2008;44:70-4.
5. Cayuela A, Rodríguez-Domínguez S, López-Campos JL, et al. Lung cancer mortality trends by geographical area in Spanish women, 1980-2005. Int J Tuberc Lung Dis 2008;12:453-7.
6. Cayuela A, Rodríguez-Dominguez S, López-Campos JL, et al. Lung cancer mortality in Spain: estimating the future burden to the year 2028. Int J Tuberc Lung Dis 2011;15:1117-21.
7. Ruiz Ramos M, Viciana Fernández F, Canto Casasola V, et al. Evolution of mortality due to lung cancer in Andalusia between 1975 and 1977. Aten Primaria 2000;25:220-5.
8. Cayuela A, Rodríguez-Domínguez S, López-Campos JL, et al. Joinpoint regression analysis of lung cancer mortality, Andalusia 1975-2000. Ann Oncol 2004;15:793-6.
9. Cayuela A, Rodríguez-Domínguez S, Jara-Palomares L, et al. Gender differences in lung cancer mortality trends in Andalusia 1975-2008: a joinpoint regression analysis. Med Oncol 2012;29:1593-8.
10. Kim HJ, Fay MP, Feuer EJ, et al. Permutation tests for

joinpoint regression with applications to cancer rates. Stat Med 2000;19:335-51.
11. National Cancer Institute. Surveillance Research Cancer Control and Population Sciences. Joinpoint Regression Program. Available online: http://surveillance.cancer.gov/joinpoint/
12. Malvezzi M, Bosetti C, Rosso T, et al. Lung cancer mortality in European men: trends and predictions. Lung Cancer 2013;80:138-45.
13. Instituto Nacional de Estadística. Encuesta Nacional de Salud 2011 – 2012. Last accessed: 04/07/2013. Available online: http://www.msssi.gob.es/estadEstudios/estadisticas/encuestaNacional/encuestaNac2011/NotaTecnica2011-12.pdf
14. Glasser JH. The quality and utility of death certificate data. Am J Public Health 1981;71:231-3.
15. Cáffaro Rovira M, Garau Llinás I, Cabeza Irigoyen E, et al. Validity of death certificates for cancer in Mallorca. Gac Sanit 1995;9:166-73.
16. Didkowska J, Manczuk M, McNeill A, et al. Lung cancer mortality at ages 35-54 in the European Union: ecological study of evolving tobacco epidemics. BMJ 2005;331:189-91.
17. Levi F, Lucchini F, Negri E, et al. Continuing declines in cancer mortality in the European Union. Ann Oncol 2007;18:593-5.
18. Solano-Reina S, De Granda-Orive JI, Jiménez-Ruiz CA. Smoking cessation: an essential component in the treatment of lung cancer patients. Arch Bronconeumol 2011;47:477.
19. Infante M, Cavuto S, Lutman FR, et al. A randomized study of lung cancer screening with spiral computed tomography: three-year results from the DANTE trial. Am J Respir Crit Care Med 2009;180:445-53.

Cite this article as: López-Campos JL, Ruiz-Ramos M, Calero C. The lung cancer epidemic in Spanish women: an analysis of mortality rates over a 37-year period. J Thorac Dis 2014;6(12):1668-1673. doi: 10.3978/j.issn.2072-1439.2014.10.28

Original Article

Treatment of giant emphysamous bulla with endobronchial valves in patients with chronic obstructive pulmonary disease: a case series

Qing Tian, Yang An, Bin-Bin Xiao, Liang-An Chen

Department of Respiratory Diseases, Chinese PLA General Hospital, Beijing 100853, China

Correspondence to: Liang-An Chen, MD, PhD. Department of Respiratory Diseases, Chinese PLA General Hospital, Fuxing Road No.28, Beijing 100853, China. Email: chenla301@hotmail.com.

Background: Giant emphysamtous bulla (GEB) can negatively affect the pulmonary functions of chronic obstructive pulmonary diseases (COPD) patients, including decreased forced expiratory volume in 1 s (FEV_1) and increased functional residual capacity (FRC). The aim of this study was to evaluate the efficacy of endobronchial valve (EBV) to treat bullae and to find efficacy predictors of successful treatment.

Methods: Five COPD patients with giant bulla were treated using EBVs. Before the EBV deployment, collateral ventilation (CV) between the targeted and adjacent lobes was evaluated with Chartis system.

Results: In the two patients with negative CV, the mean value of FEV_1 increased from 27.1±11.4% of predicted value before EBV treatment to 32.8±12.0% (P>0.05) at 1 month after EBV treatment, than to 31.7±24.5% (P>0.05) at 6 months after EBV treatment. Only one patient, whose bulla occupied the whole right middle lung, displayed sustained improvement of FEV_1 at 6 months after EBV treatment. In the three patients with positive CV, the mean value of FEV_1 decreased from 28.8±19.0% of predicted value before EBV treatment to 24.8±12.6% (P>0.05) at 1 month after EBV treatment, than to 22.1±10.8% (P>0.05) at 6 months after EBV treatment.

Conclusions: EBV is an effective measure to treat highly selected COPD patients with giant bulla. Although, EBV treatment can achieve transient improvement of lung function at patients with CV negative bulla, long-term benefit was merely observed at the patient with a bulla at right middle lobe (RML).

Keywords: Endobronchial valve (EBV); bulla; chronic obstructive pulmonary diseases (COPD); collateral ventilation (CV)

Submitted May 26, 2014. Accepted for publication Aug 18, 2014.

doi: 10.3978/j.issn.2072-1439.2014.11.07

View this article at: http://dx.doi.org/10.3978/j.issn.2072-1439.2014.11.07

Introduction

A bulla is an air-filled space in the lung with a diameter greater than one centimeter. While the volume of a bulla excesses one-third of a hemithorax, it is considered as a giant emphysematous bulla. Although bullae can appear in healthy persons or patients with relatively rare hereditary diseases, the most bullae are associated with COPD and emphysema. Giant emphysematous bulla can result in detrimental effects on lung function of COPD patients, such as decreased forced expiratory volume in 1 s (FEV_1), increased total lung capacity (TLC) and functional residual capacity (FRC), and a reduction of diffusing capacity of the lung for carbon monoxide (DLCO) (1,2).

For the medical measures are not effective to treat giant emphysematous bulla, surgical intervention is recommended to eliminate the bullous lesions. The surgical approaches include bullectomy, lobectomy and pneumonectomy which may improve lung function and quality of life in selected patients (3,4). Although several less invasive approaches were attempted to treat giant emphysematous bulla, their efficacy is in debate at present (5-7). Recently, Dr. Santini and colleagues from Italy have reported successful endobronchial treatment of giant emphysematous bulla with one-way valves [Endobronchial

valve (EBV), Zephyr®, Pulmonx, Inc., Palo Alto, Calif., USA] (8). In this study, we present our primary experiences of treatment of giant emphysematous bulla using EBV, and analyze the factors influencing the efficacy of the treatment.

Methods

Study design

This study is conducted by experienced pulmonologists in the Chinese PLA general hospital. It is a retrospective study to investigate the efficacy and safety of EBV treatment of giant emphysematous bulla. The research ethics committee of the hospital approved this study, and all the patients rendered informed consent.

Patient selection

The candidates of EBV treatment should have severe or worse airflow limitation according to the GOLD guideline. At these patients, medical therapy and rehabilitation have reached a platform to relieve the symptoms of dyspnea and to improve the exercise tolerance. The candidates should have giant emphysematous bulla displayed on the chest CT. The giant emphysematous bulla can be an isolated large bulla with relatively well conserved lung tissue in adjacent lobe(s) or multiply bullae in different lobes.

Lung function

Lung function tests were performed before and after EBV deployment. FEV_1 and RV of all patients were measured using the spirometer and body plethysmography (MasterScreen Gold Standard; Jaeger, Wurzburg, Germany).

Imaging

The patients received HRCT in the department of radiology of our hospital using a multidetector system (Somatom Definition, Siemens Medical Solution, Forchheim, Germany). The reconstructions were performed by the radiologist (Dr. Nie YK), who has >20 years of experience in thoracic CT. The coronal reconstructions were made in one patient (patient 1) to evaluate the volume change of bullae after the EBV treatment.

Collateral ventilation (CV) evaluation

CV between target lobe and adjacent lobes was evaluated using Chartis® system (Pulmonx, Inc., Redwood, Calif., USA). The Chartis system consists of two parts. A balloon catheter was used to occlude the target lobe and transduce the airflow from the lobe to the console through the central lumen of the catheter. The one-way valve and sensors are integrated in the console, in which the airflow and pressure can be measured and displayed simultaneously and dynamically. The reduction of airflow from the target lobe occluded indicates that the CV between target lobe and adjacent lobe(s) was negative.

EBV deployment

The Zephyr® EBV prevents the airflow from entering the target lobe during inspiration and allows the airflow out of the lobe during expiration. The target bronchus was verified to be within Zephyr® EBV size range using sizing gauge located at the proximal end of the delivery housing. Before the placement of EBV, it would be confirmed that the minimum depth mark was distal to carina of target bronchus.

Statistical analysis

The mean value and standard deviation of FEV_1 before the EBV treatment were compared with the data after the treatment using *t*-test. A P value <0.05 was regarded as statistically significant. SAS statistical software was used.

Results

Subject characteristics

From Oct 2011 to Jan 2013, we have treated five COPD patients with giant emphysematous bulla using EBV. The clinical data of these patients were retrieved retrospectively (*Table 1*). All the five EBV-treated patients were male, and the age ranged from 51 to 70 years (mean 63.0 years). All patients were at stage II or III of COPD. *Figures 1-5*, which displayed the CT images before and after the EBV treatment and Chartis images, are numbered sequentially according to the order of patients 1 to 5.

CV status

The patient 1 had an isolated giant bulla in the right lower lobe (RLL) (*Figure 1A*). While assessing the CV with

Table 1 Patient characteristics

Characteristics	Pt. 1	Pt. 2	Pt. 3	Pt. 4	Pt. 5
Age	66	70	65	51	63
Sex	M	M	M	M	M
PaO_2 (mmHg)	67.9	66.4	71.2	63.1	55.5
$PaCO_2$ (mmHg)	56.8	56.1	33.8	48.5	59.2
FEV_1 (L/s)	0.51	1.15	1.07	0.37	0.87
FEV_1 (%)	19.1	48.5	35.1	10.7	27.2
FVC (L)	1.60	1.79*	2.63	0.83	2.77
FVC (%)	47.2	54.7*	66.8	19.3	67.7
TLC (L)	8.09	3.94*	8.38	NA**	7.11
TLC (%)	134.3	74.6*	124.3	NA**	102.9
RV (L)	6.16	1.74*	5.37	NA**	4.08
RV (%)	259.7	102.4*	217.7	NA**	166.6
DLCO (%)	23.4	74.5	46.2	NA**	20.9
6MWT (m)	120	370	330	50	180
Location of bulla	RLL	RLL	RML	LUL	LLL

*, Helium dilution method; **, the data was absent because of the patient 4 cannot tolerate the closed environment of body plethysmography. Pt., patient; M, male; FVC, forced vital capacity; FEV_1, forced expiratory volume in 1 s; TLC, total lung capacity; RV, residual volume; DLCO, diffusion capacity of carbon monoxide; 6MWT, 6-min walking testing; LLL, left lower lobe, RLL, right lower lobe; RUL, right upper lobe; RML, right middle lobe; LUL, left upper lobe.

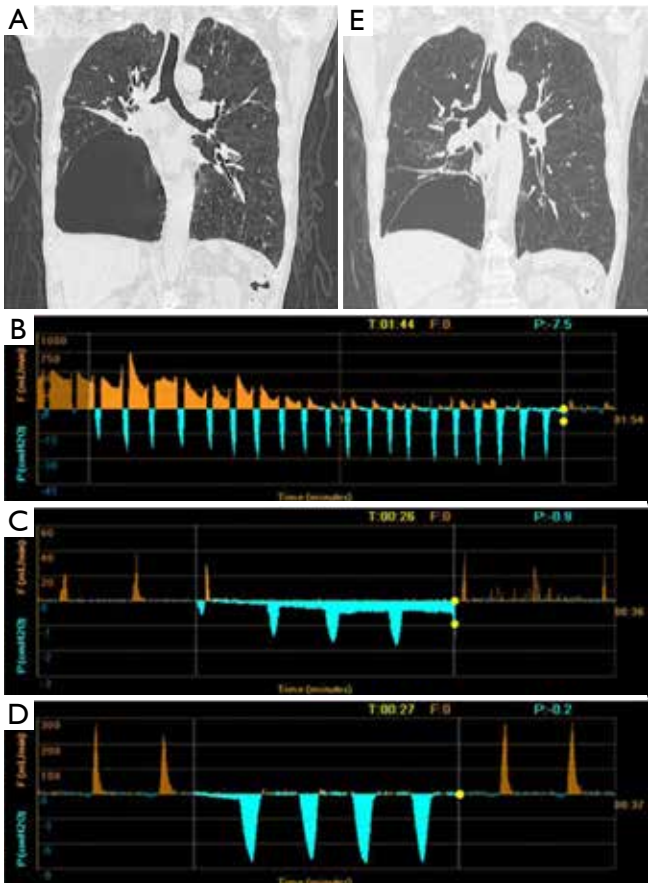

Figure 1 Chest CT and Chartis result of patient 1. (A) A bulla in the RLL and atelectasis of right RML; (B) drop of airflow to zero indicated CV is negative at RUL; (C) Chartis test showed low flow at RML; (D) Chartis test showed low flow at RLL; (E) the volume of bulla reduced and the atelectasis of RML disappeared. RLL, right lower lobe; RML, right middle lobe; CV, collateral ventilation; RUL, right upper lobe.

Chartis system, the patient 1 displayed decrease of flow at right upper lobe (RUL) (*Figure 1B*) and low flow at both right middle lobe (RML) (*Figure 1C*) and RLL (*Figure 1D*). The patient 2 had multiple bullae in the RLL and RUL (*Figure 2A*), and the Chartis test was positive both at RUL (*Figure 2B*) and RLL (*Figure 2C*) on the patient 2. An isolated giant bulla was located in the RML on the patient 3 (*Figure 3A*). For the RLL of patient number 3 cannot be occluded totally by the balloon of Chartis system, the Chartis test only showed decrease of flow at RUL (*Figure 3B*) and low flow at the targeted RML (*Figure 3C*) on the patient 3. On the patient 4, who has a bulla in the left upper lobe (LUL) (*Figure 4A*), although air flow of LUL showed continued decline, it cannot return to zero ever after 10 minutes (*Figure 4B*). So the Chartis test of LLL of patient 4 is typical positive (*Figure 4C*). On the patient 5 with a bulla in the left lower lobe (LLL) (*Figure 5A*), the Chartis test showed constant air flow at LUL (*Figure 5B*) and low flow at the targeted LLL (*Figure 5C*).

EBV treatment summary

The procedure was performed in all the seven patients under local anaesthetics (1% tetrracaine solution, <5 mL). Low dose of glucocorticoid was prescribed before EBV treatment. All the valves were delivered to the targeted lobes successfully. Five EBV 4.0 and five EBV 5.5 valves were used in these patients, and the median number of valves was 2 valves (range, 1 to 3 valves) per patient. In the patient 3, only one valve was inserted in the airway of RML corresponding to the bulla. No patient experienced respiratory failure during and after the procedure.

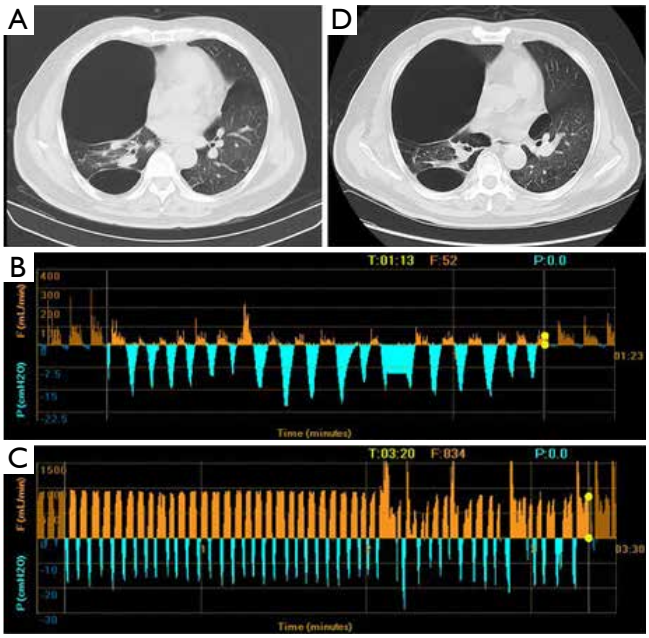

Figure 2 CT imaging and Chartis result of patient 2. (A) A bulla in RUL and severe destruction of lung tissue of RUL; (B) Chartis test showed low flow at RUL; (C) CV was positive as measured by Chartis system at RLL; (D) chest CT did not show reduction of bulla volume at RUL. RUL, right upper lobe; CV, collateral ventilation; RLL, right lower lobe.

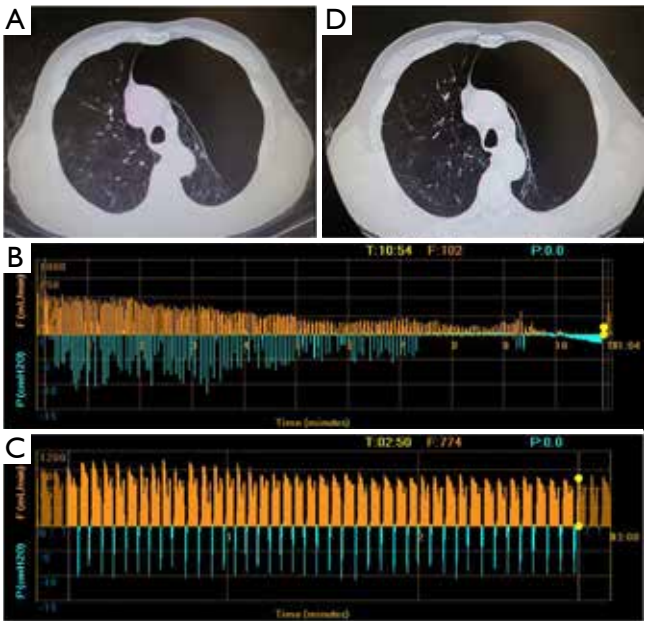

Figure 4 Chest CT and CV status of patient 4. (A) A bulla occupied the apical part of left semi-thoracic cave; (B) the airflow cannot drop to zero even after more than 10 minutes with LUL occluded; (C) the Chartis assessment showed sustained air flow while LLL was occluded; (D) the volume of LUL remained unchanged after EBV deployment. CV, collateral ventilation; LUL, left upper lobe; LLL, left lower lobe; EBV, endobronchial valve.

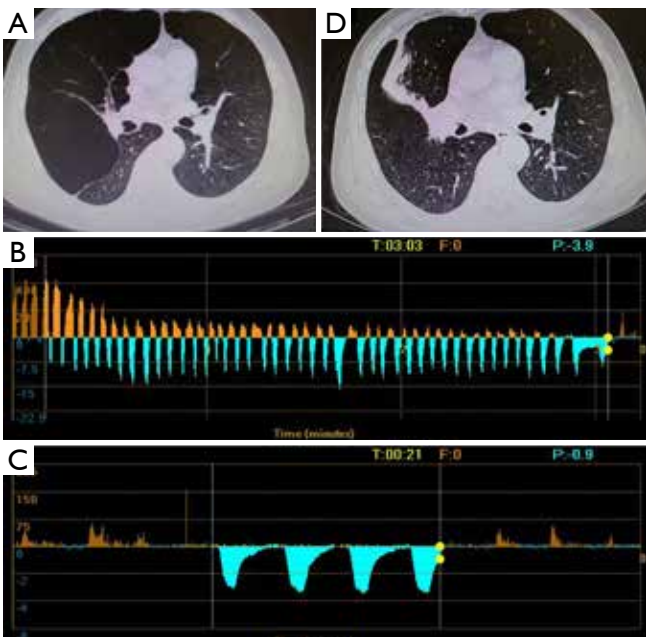

Figure 3 Chest CT and Chartis results of patient 3. (A) A bulla located in the RML; (B) CV is negative at RUL; (C) the Chartis assessment showed low flow at RML; (D) the bulla vanished after EBV treatment. RML, right middle lobe; CV, collateral ventilation; RUL, right upper lobe.

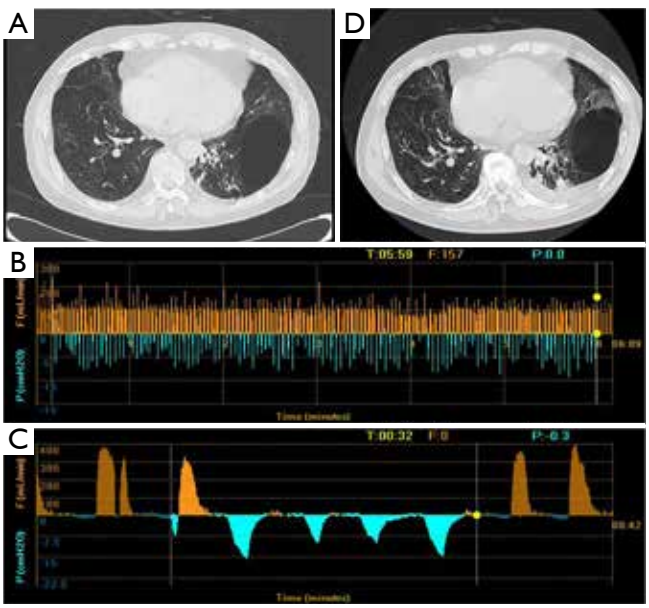

Figure 5 Clinical features of patient 5. (A) CT scan showed a bulla at the position of LLL; (B) the Chartis assessment showed the presence of CV at LUL; (C) low flow at LLL; (D) the volume of the bulla did not change after the EBV placement. CV, collateral ventilation; LLL, left lower lobe; LUL, left upper lobe; EBV, endobronchial valve.

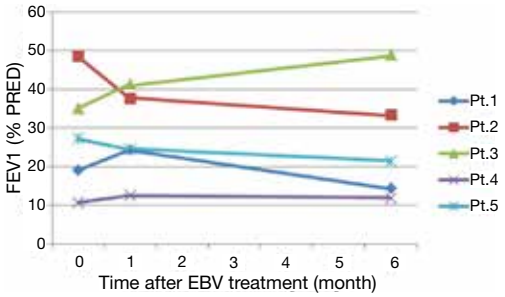

Figure 6 FEV_1 before and after EBV treatment. At 6 months after the treatment, FEV_1 went back to the level before the procedure in most of the patients, except in the patient 3, whose FEV_1 increased from 35.1% to 49.0% of predicted value. FEV_1, forced expiratory volume in 1 s; EBV, endobronchial valve.

Follow-up

Lung function tests

In the two patients with negative CV, the mean value of FEV_1 increased from 27.1±11.4% of predicted value before EBV treatment to 32.8±12.0% (P>0.05) at 1 month after EBV treatment, than to 31.7±24.5% (P>0.05) at 6 months after EBV treatment. Although the patient 1 experienced improvement of FEV_1 1 month after EBV treatment, FEV_1 dropped to the level even lower than it before the treatment. Only the FEV_1 of patient 3 improved continuously after the procedure (*Figure 6*). However, in the three patients with positive CV, the mean value of FEV_1 decreased from 28.8±19.0% of predicted value before EBV treatment to 24.8±12.6% (P>0.05) at 1 month after EBV treatment, than to 22.1±10.8% (P>0.05) at 6 months after EBV treatment. The FEV_1 of two CV positive patients (patients 2 and 5) displayed continuous decrease at 1 and 6 months after EBV treatment. The FEV_1 of patient 4 did not have significant change after the EBV treatment.

Chest imaging

On patient 1, the volume of the bullae and the corresponding LLL decreased at 6 months after EBV treatment (*Figure 1A,E*). The volume of bullae did not change after EBV treatment on patient 2 (*Figure 2A,D*), 4 (*Figure 4A,D*) and 5 (*Figure 5A,D*). The bulla in the RML vanished, and atelectasis of RML happened at 6 months after EBV deployment on patient 3 (*Figure 3A,D*).

Discussion

At present, the limited data showed that the incidence of giant pulmonary bullae was not high (0.21 per 100,000 per year, Iceland) (9). Bullectomy was regarded as a safe and effective measure to improve pulmonary function of COPD patients. Persistent air leak is still a major complication of bullectomy. Although additional pleurodesis (10,11) and diverse reinforcement techniques (12,13) were used to prevent persistent air leak or recurrence of pneumothorax, these techniques were not available for most of patients who received bullectomy. The COPD patients with giant bulla were excluded from the largest clinical trial of EBV to treatment of COPD (EBV for emphysema palliation trail, VENT) (14), but one recent paper reported the efficacy of EBV treatment of giant bullae (8). Santini *et al.* have treated nine patients with giant emphysematous bullae using EBVs, and their preliminary data suggested the efficacy and feasibility of EBV to improve the lung function and quality of life. For that study, which has not rendered the detailed datum of lung function and chest CT of all the treated patients, did not perform subgroup analysis, the indicators of EBV treatment efficacy cannot be evaluated. At the same time, the Chartis system was not used to evaluate CV on those patients.

In our study, we have used Chartis system to measure CV of targeted lobes. And we compared the CV status and chest CT between patients with improvement of lung function and those without. As displayed in *Table 2*, the CV-negative patients (patients 1 and 3) showed improvement of lung function and reduced bulla volume at 1 month after the EBV treatment. However, the improved FEV_1 of the patient 1 fell below the baseline before EBV treatment at 6 months after the treatment. Only FEV_1 of patient 3 showed sustained improvement from 1 to 6 months after the EBV treatment. Two CV positive patients experienced deteriorated lung function, and one CV positive patient did not have significant change of lung function at six months after the EBV treatment.

Lung function of patient 1 experienced transient improvement at 1 month and deterioration at 6 months after EBV treatment. At patient 1, there is still some area of well-conserved lung parenchyma at treated RLL. But, at patient 3, the giant bulla occupied the whole RML, and only negligible lung parenchyma was conserved. The quantity of well-conserved lung parenchyma is an important factor to be considered before ELVR, for lung parenchyma is significantly valuable at severe COPD patients. At these patients, the improvement of lung function from any technique may be offset because of the sacrifice of the lung parenchyma.

Table 2 Clinical data of the treated patients

Patient number	FEV_1 before EBV placement (%)	FEV_1 1 month after EBV placement (%)	Change of FEV_1 (%)	FEV_1 6 months after EBV placement (%)	Change of FEV_1 (%)	CV status	Ateclectasis	Volume reduction of bulla
1	19.1	24.3	+5.0	14.4	–4.7	–	+	+
2	48.5	37.6	–10.9	33.3	–15.2	+	–	–
3	35.1	41.3	+6.2	49.0	+13.9	–	+	+
4	10.7	12.5	+1.8	11.8	+1.1	+	–	–
5	27.2	24.4	–2.8	21.3	–5.9	+	–	–

FEV_1, forced expiratory volume in 1 s; EBV, endobronchial valve; CV, collateral ventilation.

While using the Chartis system to evaluate CV status of targeted lobe of EBV treatment, the CV status of patient with giant bulla displayed three patterns. For the bullae are under-ventilated as illustrated by previous studies (15,16), CV test will display low flow in the corresponding lobe of giant bulla. Low flow in the corresponding lobe of giant bulla and decrease of flow in the adjacent lobe(s) indicated CV is negative in the corresponding lobe of giant bulla. While low flow in the corresponding lobe of giant bulla and continuous flow in the adjacent lobe(s) suggested CV is positive. However, if the parenchyma of surrounding lung tissue and adjacent lobe are destructed severely by chronic inflammation, the bulla will communicate with adjacent lobe(s). Obviously, in this situation, continuous flow appears in both the corresponding lobe of giant bulla and adjacent lobe(s), CV is positive in the corresponding lobe of giant bulla.

Inevitably, there are several limitations in this study. Firstly, the patient population is too small to make statistics analysis. Secondly, at present, for the volume of bulla cannot be calculated precisely, it is difficult to set a cutoff value of ratio of bulla volume to conserved lung volume under which ELVR should be denied.

In conclusion, EBV is an effective measure to treat highly selected COPD patients with giant bulla. Although, EBV treatment can achieve transient improvement of lung function at patients with CV negative bulla, long-term benefit was merely observed at the patient with a bulla at RML. In the future, randomized clinical trials should be performed to verify the safety and effectiveness in larger COPD population with giant bulla. Despite the treatment of giant bulla at RML displayed good result in one patient, more patients with giant bulla at RML should be included in future investigation. Furthermore, efforts should be paid to develop novel mini-invasive ways to treat giant bulla, which have CV with neighbor lobes, via bronchoscopy. For example, if we can occlude the CV passage of one bulla, the COPD patient may benefit from EBV placement at the anatomical airway of the corresponding lobe of the bulla.

Acknowledgements

Authors' contributions: TQ designed this research and finished this paper. QF collected clinical data of some patients. CL participated in the design of this research and performed most procedures of EBV deployment. AY collected and managed the data of patients. XB did follow-up work of treated patients.

Disclosure: The authors declare no conflict of interest.

References

1. Wade JF 3rd, Mortenson R, Irvin CG. Physiologic evaluation of bullous emphysema. Chest 1991;100:1151-4.
2. Nickoladze GD. Functional results of surgery for bullous emphysema. Chest 1992;101:119-22.
3. Palla A, Desideri M, Rossi G, et al. Elective surgery for giant bullous emphysema: a 5-year clinical and functional follow-up. Chest 2005;128:2043-50.
4. Schipper PH, Meyers BF, Battafarano RJ, et al. Outcomes after resection of giant emphysematous bullae. Ann Thorac Surg 2004;78:976-82.
5. Venn GE, Williams PR, Goldstraw P. Intracavity drainage for bullous, emphysematous lung disease: experience with the Brompton technique. Thorax 1988;43:998-1002.
6. Takizawa H, Kondo K, Sakiyama S, et al. Computed tomography-guided drainage for large pulmonary bullae. Interact Cardiovasc Thorac Surg 2004;3:283-5.
7. Bhattacharyya P, Sarkar D, Nag S, et al. Transbronchial decompression of emphysematous bullae: a new

therapeutic approach. Eur Respir J 2007;29:1003-6.
8. Santini M, Fiorelli A, Vicidomini G, et al. Endobronchial treatment of giant emphysematous bullae with one-way valves: a new approach for surgically unfit patients. Eur J Cardiothorac Surg 2011;40:1425-31.
9. Gunnarsson SI, Johannesson KB, Gudjonsdottir M, et al. Incidence and outcomes of surgical resection for giant pulmonary bullae--a population-based study. Scand J Surg 2012;101:166-9.
10. Dubois L, Malthaner RA. Video-assisted thoracoscopic bullectomy and talc poudrage for spontaneous pneumothoraces: effect on short-term lung function. J Thorac Cardiovasc Surg 2010;140:1272-5.
11. Nakanishi K. Comparison of cryoprecipitate with commercial fibrinogen in bullectomy. Asian Cardiovasc Thorac Ann 2010;18:27-32.
12. Saito T, Kaneda H, Konobu T, et al. The covering with forceps-assisted polymeric biodegradable sheet and endostapling method: a simplified technique for wide coverage and reinforcement of staple-line in video-assisted thoracoscopic bullectomy for spontaneous pneumothorax. Interact Cardiovasc Thorac Surg 2011;12:103-5.
13. Sakamoto K, Takei H, Nishii T, et al. Staple line coverage with absorbable mesh after thoracoscopic bullectomy for spontaneous pneumothorax. Surg Endosc 2004;18:478-81.
14. Sciurba FC, Ernst A, Herth FJ, et al. A randomized study of endobronchial valves for advanced emphysema. N Engl J Med 2010;363:1233-44.
15. Morgan MD, Strickland B. Computed tomography in the assessment of bullous lung disease. Br J Dis Chest 1984;78:10-25.
16. Suga K, Iwanaga H, Tokuda O, et al. Intrabullous ventilation in pulmonary emphysema: assessment with dynamic xenon-133 gas SPECT. Nucl Med Commun 2012;33:371-8.

Cite this article as: Tian Q, An Y, Xiao BB, Chen LA. Treatment of giant emphysamtous bulla with endobronchial valves in patients with chronic obstructive pulmonary disease: a case series. J Thorac Dis 2014;6(12):1674-1680. doi: 10.3978/j.issn.2072-1439.2014.11.07

Original Article

Effect of a neutrophil elastase inhibitor on ventilator-induced lung injury in rats

Do-Hyung Kim[1]*, Jae Ho Chung[2]*, Bong Soo Son[1], Yeon Ji Kim[1], Sang Gwon Lee[1]

[1]Department of Thoracic and Cardiovascular Surgery, Pusan National University Yangsan Hospital, Pusan, Korea; [2]Division of Pulmonology, Department of Internal Medicine, International St. Mary's Hospital, Catholic Kwandong University College of Medicine, Incheon, Korea

*These authors contributed equally to this work.

Correspondence to: Sang Gwon Lee, MD. Department of Thoracic and Cardiovascular Surgery, Pusan National University Yangsan Hospital, Beomeori, Mulgeum-eup, Yangsan 626-770, Korea. Email: lsgwon@gmail.com.

Objective: We hypothesized that pretreatment with sivelestat therapy could attenuate ventilator-induced lung injury (VILI) and lung inflammation in a rat model.

Methods: The neutrophil elastase inhibitor was administered intraperitoneally 30 min before and at the initiation of ventilation. The rats were categorized as (I) sham group; (II) VILI group; (III) sivelestat group; (IV) early sivelestat group. Wet-to-dry weight ratio, bronchoalveolar lavage fluid (BALF) neutrophil and protein, tissue malondialdehyde (MDA) and histologic VILI scores were investigated.

Results: The ratio of wet-to-dry weight, BALF neutrophil and protein, tissue MDA and VILI scores were significantly increased in the VILI group compared to the sham group [3.85±0.32 *vs.* 9.05±1.02, P<0.001; (0.89±0.93)×10^4 *vs.* (7.67±1.41)×10^4 cells/mL, P<0.001; 2.34±0.47 *vs.* 23.01±3.96 mg/mL, P<0.001; 14.43±1.01 *vs.* 36.56±5.45 nmol/mg protein, P<0.001; 3.78±0.67 *vs.* 7.00±1.41, P<0.001]. This increase was attenuated in the early sivelestat group compared with the sivelestat group [wet-to-dry ratio: 6.76±2.01 *vs.* 7.39±0.32, P=0.032; BALF neutrophil: (5.56±1.13)×10^4 *vs.* (3.89±1.05)×10^4 cells/mL, P=0.021; BALF protein: 15.57±2.32 *vs.* 18.38±2.00 mg/mL, P=0.024; tissue MDA: 29.16±3.01 *vs.* 26.31±2.58, P=0.049; VILI scores: 6.33±1.41 *vs.* 5.00±0.50, P=0.024].

Conclusions: Pretreatment with a neutrophil elastase inhibitor attenuates VILI in a rat model.

Keywords: Ventilator-induced lung injury (VILI); neutrophil elastase

Submitted Jun 07, 2014. Accepted for publication Aug 14, 2014.
doi: 10.3978/j.issn.2072-1439.2014.11.10
View this article at: http://dx.doi.org/10.3978/j.issn.2072-1439.2014.11.10

Introduction

Mechanical ventilation (MV) can initiate as well as exacerbate lung injury, which is referred to as ventilator-induced lung injury (VILI). As well as causing lung injury, it can also decrease the functioning of other organs and contribute to mortality (1). VILI can lead to remote organ dysfunction and multiple organ failure (2).

Multifactorial etiologies of VILI, from either direct or indirect injury to the lung, have been postulated (3). Diffuse alveolar damage and initial vascular leak with a neutrophil-predominant inflammatory response are the key features of VILI (4). High-tidal-volume (VT) MV has been proved to induce the activation of proinflammatory cytokines, and thus lead to VILI (5). MV with high tidal volumes and pressure can lead to increased alveolar-capillary permeability accompanied by the release of pro-inflammatory mediators by the lung cells in response to mechanical stretch. These stimuli trigger detachment of endothelial cells from the basement membrane and synthesis of extracellular matrix components (6). Injurious MV also promotes alveolar coagulopathy and fibrin deposition within the airways (7). Additionally, the generation of reactive oxygen species (ROS) during VILI causes direct cellular injury and triggers ROS-sensitive, aberrant activation of cellular mechanisms leading to severe inflammation, resulting in rapid transcription of pro-inflammatory

cytokines and chemokines (8). Neutrophils accumulate in the microvasculature of injured lungs, releasing various cytokines, chemokines and proteases. Among these proteins, the activity of neutrophil elastase is increased in patients with adult respiratory distress syndrome (9).

Neutrophil elastase, located downstream in the humoral mediator network, contributes to the development of vascular endothelial injury in concert with other mediators, which leads to increased permeability, vasodilation, and activation of the coagulation cascade (10). Furthermore, this pulmonary pro-inflammatory response is not confined to the lungs and extends into the systemic circulation, contributing to the development of systemic inflammatory response syndrome (SIRS) and multiple organ dysfunction syndrome (MODS) (11). Modulating this imbalance between pro- and anti-inflammatory mediators in the lung could be used as a therapeutic approach.

Sivelestat {ONO-5046; sodium N-[2-[4-(2,2-dimethylpropionyloxy) phenylsulfonylaminobenzoyl] aminoacetate tetrahydrate]} is a specific inhibitor of neutrophil elastase, discovered and characterized by Ono Pharmaceutical Co. Ltd. in Japan (12). Investigators have reported that the neutrophil elastase inhibitor sivelestat plays protective roles in the lung with ischemia-reperfusion injury (13), and lipopolysaccharide-induced injury (14).

Recently, it has been reported that post-operative sivelestat administration after transthoracic esophagectomy improved the pathophysiological condition of SIRS and the post-operative clinical course even in patients without complications, as well as the deterioration of the PaO_2 (arterial oxygen tension)/FiO_2 (inspired oxygen fractional concentration) ratio in the post-operative period following esophagectomy (15), and surgery for congenital heart disease with pulmonary hypertension (16). However, its prophylactic effect on VILI is unknown. Sakashita showed that neutrophil elastase inhibitor, given 30 min before ventilation, suppressed subsequent neutrophilic inflammation, attenuating the histopathological degree of lung damage, lowering neutrophil accumulation and lung water content, induced by VILI with high tidal volume ventilation in the C57/BL6 mice model (17).

We hypothesized that pretreatment with neutrophil elastase inhibitor (sivelestat) would decrease ventilator-induced microvascular permeability, recruitment of neutrophils and oxidative injury. To test this hypothesis, we ventilated with high tidal volume and examined the effects of sivelestat in preventing acute lung injury (ALI) induced by VILI in a rat model and examined its effect on lung injury and compared ALI parameters with those resulting from prophylactic sivelestat and routine sivelestat. This study explored the role of the protective effect of sivelestat in lung injury induced by VILI in a rat model and to provide theoretical basis for clinical treatment.

Methods

Animal preparation

Eight-week-old Sparague-Dawley rat weighing 200-300 g were used. All animals received humane care, in compliance with the "Principles of Laboratory Animal Care" formulated by the National Society for Medical Research and the "Guide for the Care and Use of Laboratory Animals" prepared by the Institute of Laboratory Animal Resources and published by the National Institutes of Health. Our protocol and experimental methods were approved by the Animal Care and Use Committee of the Laboratory Animal Service of the University of Pusan University School of Medicine. All surgery was performed under ketamine anesthesia and all efforts were made to minimize suffering.

Experimental groups

Anesthetized rats received MV with a high tidal volume (20 mL/kg) for 3 h. The neutrophil elastase inhibitor (sivelestat, 100 mg/kg) was administered intraperitoneally (i.p.) 30 min before and at the initiation of ventilation. The rats were categorized as (I) sham group: injected with saline (10 mg/kg body, i.p.) at the time of ventilation start; (II) VILI group; (III) sivelestat group: sivelestat (100 mg/kg body, i.p.) at the initiation of ventilation; (IV) early sivelestat group: sivelestat (100 mg/kg body, i.p.) 30 min before ventilation and at the initiation of ventilation.

Rats subjected to sham, VILI, sivelestat and early sivelestat group were injected with an identical volume of placebo-control solution or sivelestat. In each group, underwent measurements for lung water content, bronchoalveolar lavage fluid (BALF) neutrophil and BALF protein, MDA, hematoxylin and eosin (H&E) stain.

Murine model of VILI

We used our established mouse model of VILI as previously described (18). Rats were anesthetized i.p. with ketamine (100 mg/kg; Eurovet Animal Health BV, Bladel, the Netherland). After inserting a 22-gauge ventilation cannula

into the trachea, the rats were placed in the supine position on a warming device and then connected to a ventilator. The VILI model was defined as a high VT of 20 mL/kg, a respiratory rate of 60 breaths per min and MV maintained for 3 h at an inspiratory oxygen fraction of 0.21. The ventilator was a model 683 from Harvard Apparatus Co. (Harvard Apparatus, Holliston, MA, USA). Sham group, the rats were injected with saline (10 mg/kg body, i.p.) at the time of ventilation start. Sivelestat pretreated VILI group were injected with sivelestat (100 mg/kg body, i.p.) 30 min before ventilation and sivelestat treated VILI group were sivelestat (100 mg/kg body, i.p.) at the time of ventilation start.

Lung water content

Lung water content related to lung injury was measured using the lung wet-to-dry weight ratio as described (19). The left lower lungs were weighed immediately after removal (wet weight) and again after drying in an oven at 60 ℃ for 72 h (dry weight). The lung wet-to-dry weight ratio was calculated as the ratio of wet weight to dry weight. Lung wet-to-dry weight ratio was used as an index of pulmonary edema formation.

Bronchoalveolar lavage fluid (BALF) protein levels

After MV for 3 h, the right lung was used for bronchoalveolar lavage via slow intratracheal injection of two sequential 1-mL aliquots of sterile normal NaCl. Bronchoalveolar lavage was performed twice using 1 mL of saline. Total cell counts were determined using standard hematological procedures in 40-μL aliquots of each sample. The remaining fluid was centrifuged at 1,500 rpm for 10 min (at 4 ℃) and the supernatant was stored at –80 ℃ until analysis. The protein quantification method using bicinchoninic acid was developed by Smith *et al*. (20). The Lowry assay (21) and this assay are of similar sensitivity, but this assay is stable under alkali conditions and can be carried out as a one-step process compared to the two steps needed in the Lowry assay. Total protein concentration in the BALF was determined with the WelProtTM Protein Assay Kit (Welgene, Daegu, Korea) according to the manufacturer's instructions.

Bronchoalveolar lavage fluid (BALF) neutrophil counts

BALF was obtained from the right lung and cell counts were determined using a hemocytometer (Beckman Coulter, Fullerton, CA, USA). Differential counts were performed on cytospin preparations stained with a modified Giemsa stain, Diff-Quick (Dade Behring AG, Düdingen, Switzerland).

Malondialdehyde (MDA) assay

Oxidative injury from VILI was determined by measuring the tissue concentration of MDA, a marker of lipid peroxidation in lung tissue. MDA, which is an end product of lipid peroxidation, was estimated using the Oxiselect TBARS assay kit containing thiobarbituric acid-reactive substances (Cell Biolabs, San Diego, CA, USA) according to the manufacturer's instructions. The MDA concentration was calculated using the absorbance coefficient of the MDA-TBA complex (absorbance coefficient $\varepsilon=1.56^5$ $cm^{-1}\cdot M^{-1}$) and is expressed as nanomoles per milligram of protein (nmol/mg protein).

Histopathological grading of VILI

For histological examination, the right upper lobe of the lung was fixed in 10% neutral-buffered formalin, embedded in paraffin, and sectioned at 4 μm thickness. After deparaffinization and dehydration, the sections were stained with H&E for microscopic examination.

The lungs were reviewed from five non-overlapping fields by a single pathologist (Korea CFC Pathology Laboratory, Jin Kyu Park) blinded to the therapeutic category of the rat. A modified VILI histological scoring system was applied as described (22). Lung injury was scored on a scale of 0-4 using the average score of the following items: (I) alveolar capillary congestion; (II) hemorrhage; (III) infiltration of neutrophils into the airspace or the vessel wall and thickness of the alveolar wall; and (IV) alveolar wall thickness/hyaline membrane formation.

A score of 0 represented normal findings and scores of 1, 2, 3 and 4 represented mild (<25% lung involvement), moderate (25-50% lung involvement), severe (50-75% lung involvement) and very severe (>75% lung involvement) lung involvement, respectively. The overall score was based on the sum of all scores.

Statistical analysis

Data are expressed as means ± standard deviation (SD). When data were not normally distributed according to a Kolmogorov-Smirnov test, we used Wilcoxon signed-rank test. Differences among groups were analyzed using a one-

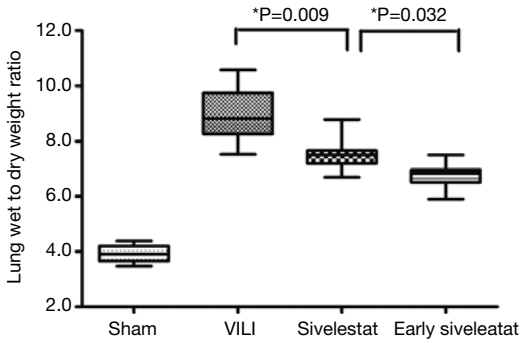

Figure 1 Assessment of lung water content in ventilator-induced lung injury. Wet-to-dry weight ratio of lungs was measured in which whole lungs by dividing wet weight by dry weight (n=10 per group).

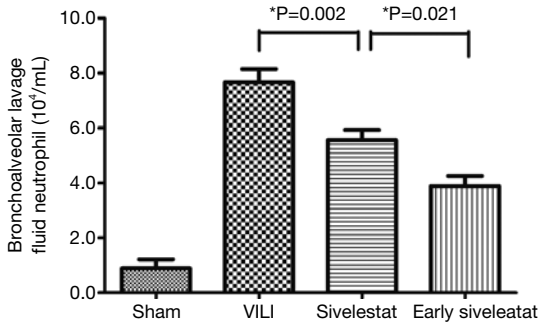

Figure 2 Assessment of bronchoalveolar lavage fluid neutrophil count (10^4/mL) (n=10 per group).

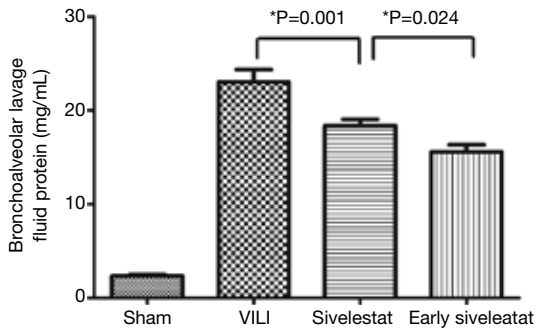

Figure 3 Assessment of bronchoalveolar lavage fluid protein concentration (mg/mL) (n=10 per group).

way analysis of variance or the Kruskal-Wallis test. When differences were statistically significant, individual results were compared using the Bonferroni test. The Kruskal-Wallis test was used for the analysis of VILI score. A P value of <0.05 was considered to indicate significance. Statistical analyses were performed using SPSS for Windows (version 20.0; SPSS Inc.; Chicago, IL, USA).

Results

Sivelestat decreases lung edema induced by VILI

The ratio of wet-to-dry weight, a parameter of lung edema, was significantly increased in the VILI group (*Figure 1*; 9.05±1.02, P<0.001). This increase was significantly attenuated in the Early sivelestat group (6.76±2.01) compared with the Sivelestat group (7.39±0.32, P=0.036). These data indicate that early administration of sivelestat inhibited lung edema induced by high VT ventilation.

Effect of sivelestat on BALF parameters (alveolar-capillary leak due to VILI)

In the VILI group, the BALF neutrophil counts (*Figure 2*), and protein concentration (*Figure 3*) were significantly increased. BALF neutrophil [$(0.89\pm0.93)\times10^4$ *vs.* $(7.67\pm1.41)\times10^4$ cells/mL, respectively; P<0.001] and protein (2.34±0.47 *vs.* 23.01±3.96 mg/mL, respectively; P<0.001) levels were significantly higher in the VILI group compared to the sham group. The early sivelestat group exhibited reduced increases in protein concentration (18.38±2.00 *vs.* 15.57±2.32 mg/mL, respectively; P=0.024), neutrophil count [$(5.56\pm1.13)\times10^4$ *vs.* $(3.89\pm1.05)\times10^4$ cells/mL, respectively; P=0.021) in BALF compared to the sivelestat group. These findings suggest that early sivelestat administration inhibits the subsequent development of VILI, including neutrophil accumulation.

Effect of sivelestat on lung lipid peroxidation

The concentration of MDA, an indicator of the degree of lipid peroxidation, was increased to a significantly lesser extent in the early sivelestat group (*Figure 4*). Tissue MDA was significantly higher in the VILI group than the Sham group MDA (14.43±1.01 *vs.* 36.56±5.45 nmol/mg protein, respectively; P=0.001). The early sivelestat group exhibited a reduced increase in MDA concentration (29.16±3.01 *vs.* 26.31±2.58 nmol/mg protein, respectively; P=0.049) compared with the Sivelestat group. These findings suggest that sivelestat inhibits the subsequent development of VILI, including lipid peroxidation.

Histological assessment of lung injury

H&E-stained lung sections of each experimental group are shown in *Figure 5*: sham group (A), VILI group (B), sivelestat group (C) and early sivelestat group (D). The images are representative histological lung tissue sections (magnification, ×100, H&E stain). Perivascular and interstitial edema, inflammatory cell infiltration, intra-alveolar hemorrhage, and hyaline membrane formation or wall thickness of lung architecture were detected in the lungs of the VILI animals. The lungs of the early sivelestat-treated animals showed minor signs of pulmonary edema and cell influx. *Figure 6* shows the histopathological grades of VILI using the scoring system. The VILI scores were significantly increased in the VILI group compared with the sham group (*Table 1*, 3.78±0.67 and 7.00±1.41, respectively, P<0.001). The scores in the Early sivelestat group were significantly lower than those in the Sivelestat group (6.33±1.41 and 5.00±0.50, respectively, P=0.023). Early administration of sivelestat successfully reduced the histopathological severity of lung injury.

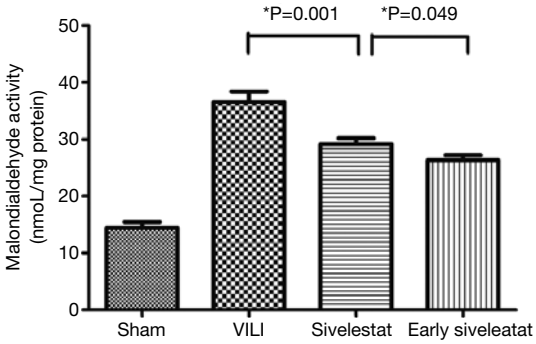

Figure 4 Assessment of malondialdehyde activity (nmol/mg protein) (n=10 per group).

Discussion

We have shown that pretreatment with sivelestat attenuates the physiological, biochemical, and histological deterioration in the high-VT-induced VILI rat model. Sivelestat attenuated the pulmonary edema, as shown by

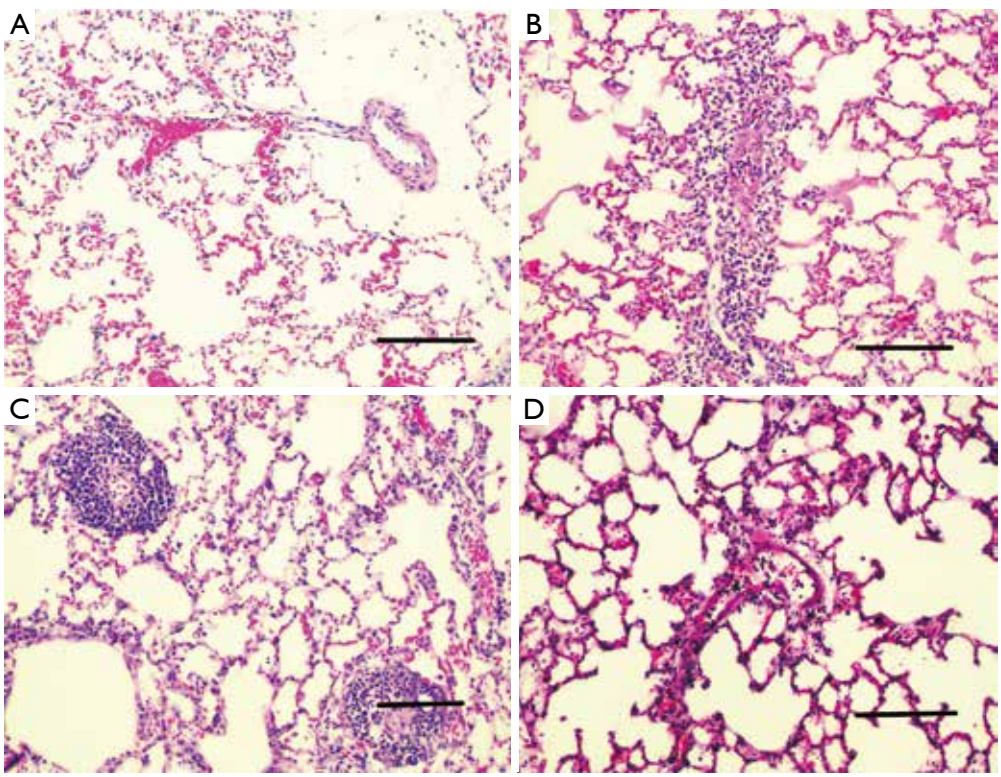

Figure 5 Hematoxylin and eosin-stained lung sections of each experimental groups (magnification, ×100, scale bars represent 200 μm). (A) Sham group; (B) VILI group; (C) sivelestat group; and (D) early sivelestat group.

the amelioration of the increased wet/dry-weight ratio and BALF protein levels. The protective effect of sivelestat may be due, in part, to protection of the pulmonary endothelium from the elastase released by neutrophils. This indicates that the drug also attenuated the accumulation of neutrophils in the lung.

MV causes the activation of macrophages, which promotes the migration of neutrophils from blood vessels into the alveolar space and discharge of neutrophil elastase and oxidants. Alveolar-capillary membranes are subsequently damaged and activated neutrophils induce an increase in lung vascular permeability that causes protein-rich lung edema (23). Neutrophil elastase is a protease that can degrade key structural elements of connective tissue, such as elastin, collagen, and proteoglycan (24). Neutrophil elastase has been implicated in the increase in permeability in both vascular endothelial (25) and alveolar epithelial (26) cells that are involved in lung edema. Additionally, it has been reported that sivelestat indirectly reduces neutrophil sequestration by suppressing the release of neutrophil chemotactic factors (IL-8) (13), inflammatory cytokines (IL-6, TNF-α) (12), and other adhesion-promoting molecules (P-selectin, intercellular adhesion molecule-1) (27). These findings have strengthened the notion that MV can lead to the infiltration of neutrophils, and that neutrophils become targets of neutrophil elastase during the pathogenesis of VILI. Previous studies reported that sivelestat reduced lung injury associated with SIRS in humans and decreased endotoxin-induced lung injury in animal models (28). Neutrophil elastase is known to play a central role in the pathophysiology of ALI, not only by causing direct tissue injury but also by amplifying the inflammatory response. Sivelestat improved the arterial oxygen tension to the inspired oxygen fraction (PaO_2/FiO_2) and decreased the length of stay in the intensive care unit and days on a ventilator for patients with ALI and acute respiratory distress syndrome (ARDS) (29). Moreover, treatment of ARDS with sivelestat reduced serum cytokine levels (30). Several animal studies have shown neutrophil elastase inhibition to be effective (13,31-34). However, sivelestat has not been shown to suppress the release of cytokines associated with VILI, and no reliable, conclusive clinical study has yet been conducted (35). In the present study, we pretreated animals with neutrophil elastase inhibitor and ventilated them with injurious VT. By contrast with lung injuries in previous studies, induced by intraperitoneal endotoxin, ischemia-reperfusion, and thrombin (13,31-34), we induced lung injury by high VT ventilation that continued to injure the lungs during ventilation compared to previous studies.

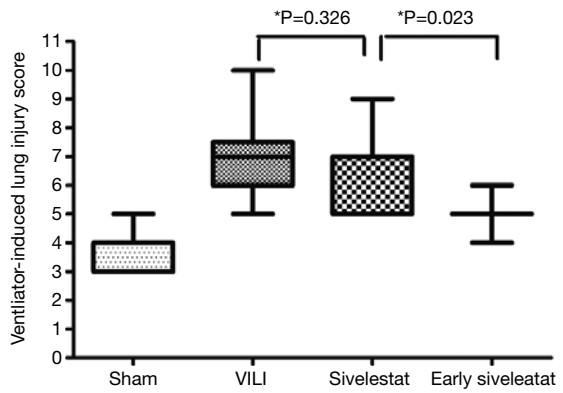

Figure 6 Ventilator-induced lung injury (VILI) scores between experimental groups. VILI scores are based on leukocyte infiltration, exudative oedema, hemorrhage and alveolar wall thickness (n=10 per group).

Table 1 Ventilator-induced lung injury (VILI) score in each experimental groups

Group	Alveolar congestion	Hemorrhage	Neutrophil infiltration	Alveolar wall thickness	Total score
Sham	2.78±0.97	0.44±0.53	0.33±0.50	0.22±0.44	3.78±0.67
VILI	3.44±0.88	1.00±0.71	1.22±0.44	1.33±1.58	7.00±1.41[a]
Sivelestat	3.78±0.44	1.00±0.71	0.67±0.71	0.89±0.93	6.33±1.41[b]
Early sivelestat	3.44±0.88	0.56±0.53	0.89±0.33	0.11±0.33	5.00±0.50[c]

Data are presented as mean ± standard deviation. Acute lung injury was scored in each sample according to the following four items: alveolar congestion, hemorrhage, infiltration or aggregation of neutrophils in airspace or the vessel wall, and thickness of the alveolar wall. A score of 0 represented normal findings and scores of 1, 2, 3 and 4 represented mild (<25%), moderate (25-50%), severe (50-75%) and very severe (>75%) lung involvement, respectively. The overall score was based on the sum of all scores. [a], P<0.001 between sham and VILI; [b], P=0.326 between VILI and sivelestat; [c], P=0.023 between sivelestat and early sivelestat.

Lipid peroxidation is a well-defined mechanism of cellular damage in animals and plants. Lipid peroxides are unstable indicators of oxidative stress in cells that decompose to form more complex and reactive compounds such as MDA and 4-hydroxynonenal, natural bi-products of lipid peroxidation. Oxidative modification of lipids can be induced *in vitro* by a wide array of pro-oxidant agents and occurs *in vivo* during aging and in certain disease conditions. Measuring the end products of lipid peroxidation is one of the most widely accepted assays of oxidative damage. These aldehydic secondary products of lipid peroxidation are generally accepted markers of oxidative stress. Recent reports have shown that oxygen radicals released from neutrophils might contribute to the development of acute edematous lung injury in isolated rabbit lungs (36) and antioxidants attenuated ALI in isolated perfused rat lungs (37). Our findings showed that the concentration of MDA, an indicator of the degree of lipid peroxidation, was increased to a significantly lesser extent in the Early sivelestat group. Therefore, the antioxidant role of sivelestat is anticipated to prevent the development of ALI in our experimental system.

A Japanese phase III trial demonstrated that sivelestat was effective for patients with ALI associated with SIRS, showing increased pulmonary oxygenation ability, a decrease in the duration of MV, and a shortened stay in the intensive care unit (ICU) (13). It has been reported recently that post-operative sivelestat administration after transthoracic esophagectomy improved the pathophysiological condition of SIRS and the postoperative clinical course even in patients without complications, as well as the deterioration of the PaO_2/FiO_2 ratio in the postoperative period following esophagectomy (15), surgery for congenital heart disease with pulmonary hypertension (16). However, its prophylactic effect on VILI is still unknown. In accordance of Sakashita *et al*. study (17), our study showed that prophylactic sivelestat attenuate VILI. Additionally, our study showed that prophylactic sivelestat administration attenuate VILI more effectively, compared to conventional sivelestat administration. This interesting finding showed that the timing of sivelestat treatment is important. To our knowledge, this is the first study on the optimal timing for the administration of sivelestat.

Although the Japanese research showed elastase inhibition to be beneficial in the pulmonary function of ALI/ARDS patients (38), the STRIVE study did not show that sivelestat was efficacious in a broad spectrum of ALI/ARDS cases (35). The population under study may encompass too broad a range of pathogenetic mechanisms to detect the effectiveness of treatment for specific conditions. This difference in sampling precision may account for the discrepancy in the findings of the STRIVE study and the Japanese report. In several experimental models of SIRS and ARDS, pretreatment with cytokine receptor antagonists or their specific antibodies (39) prevents lung injury. However, these agents have not been demonstrated to be effective in preventing ARDS in clinical trials (40). This discrepancy between experimental and clinical results may be related to the time course of intervention, because the clinical treatment of ARDS usually occurs after the development of SIRS and ARDS. Our study have limitation, we did not measure neutrophil elastase activiy, so inhibition of neutrophil elastase by sivelestat in treatment rats were not shown. Further investigation is required to clarify which patients can benefit from sivelestat and to determine the most effective use of neutrophil elastase inhibitors in the clinical treatment of VILI.

Conclusions

In conclusion, the present study showed that neutrophil elastase might play an important role in the progression of VILI. The mechanisms underlying the effect of neutrophil elastase on lung injury are an increased neutrophil elastase activity, resulting in an increase in pulmonary vascular permeability. Our results indicate that pretreatment with sivelestat can prevent the progression of lung injury caused by neutrophil elastase, although further clinical studies are needed to confirm the results reported in our experimental rat model.

Acknowledgements

This study was supported by the Research Institute for Convergence of Biomedical Science and Technology, Pusan National University Yangsan Hospital.

Authors' contributions: All authors contributed conception, analysis, interpretation, revising, and final approval of the manuscript. Do-Hyung Kim and Jae Ho Chung equally served as co-first authors and had full access to all of the data in the study. Sang Gwon Lee took responsibility for the integrity of the data. Yeon Ji Kim carried out experiment and Bong Soo Son provided study management.

Disclosure: The authors declare no conflict of interest.

References

1. MacCallum NS, Evans TW. Epidemiology of acute lung injury. Curr Opin Crit Care 2005;11:43-9.
2. Amato MB, Barbas CS, Medeiros DM, et al. Effect of a protective-ventilation strategy on mortality in the acute respiratory distress syndrome. N Engl J Med 1998;338:347-54.
3. Dos Santos CC, Slutsky AS. Invited review: mechanisms of ventilator-induced lung injury: a perspective. J Appl Physiol (1985) 2000;89:1645-55.
4. Ware LB, Matthay MA. The acute respiratory distress syndrome. N Engl J Med 2000;342:1334-49.
5. Pinhu L, Whitehead T, Evans T, et al. Ventilator-associated lung injury. Lancet 2003;361:332-40.
6. Al-Jamal R, Ludwig MS. Changes in proteoglycans and lung tissue mechanics during excessive mechanical ventilation in rats. Am J Physiol Lung Cell Mol Physiol 2001;281:L1078-87.
7. Choi G, Wolthuis EK, Bresser P, et al. Mechanical ventilation with lower tidal volumes and positive end-expiratory pressure prevents alveolar coagulation in patients without lung injury. Anesthesiology 2006;105:689-95.
8. Papaiahgari S, Yerrapureddy A, Reddy SR, et al. Genetic and pharmacologic evidence links oxidative stress to ventilator-induced lung injury in mice. Am J Respir Crit Care Med 2007;176:1222-35.
9. Rocker GM, Wiseman MS, Pearson D, et al. Diagnostic criteria for adult respiratory distress syndrome: time for reappraisal. Lancet 1989;1:120-3.
10. Russell JA. Management of sepsis. N Engl J Med 2006;355:1699-713.
11. Ferring M, Vincent JL. Is outcome from ARDS related to the severity of respiratory failure? Eur Respir J 1997;10:1297-300.
12. Kawabata K, Suzuki M, Sugitani M, et al. ONO-5046, a novel inhibitor of human neutrophil elastase. Biochem Biophys Res Commun 1991;177:814-20.
13. Takayama M, Ishibashi M, Ishii H, et al. Effects of neutrophil elastase inhibitor (ONO-5046) on lung injury after intestinal ischemia-reperfusion. J Appl Physiol 2001;91:1800-7.
14. Inoue Y, Seiyama A, Tanaka H, et al. Protective effects of a selective neutrophil elastase inhibitor (sivelestat) on lipopolysaccharide-induced acute dysfunction of the pulmonary microcirculation. Crit Care Med 2005;33:1814-22.
15. Suda K, Kitagawa Y, Ozawa S, et al. Neutrophil elastase inhibitor improves postoperative clinical courses after thoracic esophagectomy. Dis Esophagus 2007;20:478-86.
16. Nomura N, Asano M, Saito T, et al. Sivelestat attenuates lung injury in surgery for congenital heart disease with pulmonary hypertension. Ann Thorac Surg 2013;96:2184-91.
17. Sakashita A, Nishimura Y, Nishiuma T, et al. Neutrophil elastase inhibitor (sivelestat) attenuates subsequent ventilator-induced lung injury in mice. Eur J Pharmacol 2007;571:62-71.
18. Li LF, Huang CC, Lin HC, et al. Unfractionated heparin and enoxaparin reduce high-stretch ventilation augmented lung injury: a prospective, controlled animal experiment. Crit Care 2009;13:R108.
19. Quinn DA, Moufarrej RK, Volokhov A, et al. Interactions of lung stretch, hyperoxia, and MIP-2 production in ventilator-induced lung injury. J Appl Physiol 2002;93:517-25.
20. Smith PK, Krohn RI, Hermanson GT, et al. Measurement of protein using bicinchoninic acid. Anal Biochem 1985;150:76-85.
21. Lowry OH, Rosebrough NJ, Farr AL, et al. Protein measurement with the Folin phenol reagent. J Biol Chem 1951;193:265-75.
22. Belperio JA, Keane MP, Burdick MD, et al. Critical role for CXCR2 and CXCR2 ligands during the pathogenesis of ventilator-induced lung injury. J Clin Invest 2002;110:1703-16.
23. Dreyfuss D, Saumon G. Ventilator-induced lung injury: lessons from experimental studies. Am J Respir Crit Care Med 1998;157:294-323.
24. Campbell EJ, Campbell MA. Pericellular proteolysis by neutrophils in the presence of proteinase inhibitors: effects of substrate opsonization. J Cell Biol 1988;106:667-76.
25. Suttorp N, Nolte A, Wilke A, et al. Human neutrophil elastase increases permeability of cultured pulmonary endothelial cell monolayers. Int J Microcirc Clin Exp 1993;13:187-203.
26. Peterson MW, Walter ME, Nygaard SD. Effect of neutrophil mediators on epithelial permeability. Am J Respir Cell Mol Biol 1995;13:719-27.
27. Doerschuk CM, Quinlan WM, Doyle NA, et al. The role of P-selectin and ICAM-1 in acute lung injury as determined using blocking antibodies and mutant mice. J Immunol 1996;157:4609-14.
28. Sakamaki F, Ishizaka A, Urano T, et al. Effect of a specific neutrophil elastase inhibitor, ONO-5046, on endotoxin-

induced acute lung injury. Am J Respir Crit Care Med 1996;153:391-7.
29. Kawabata K, Hagio T, Matsuoka S. The role of neutrophil elastase in acute lung injury. Eur J Pharmacol 2002;451:1-10.
30. Okayama N, Kakihana Y, Setoguchi D, et al. Clinical effects of a neutrophil elastase inhibitor, sivelestat, in patients with acute respiratory distress syndrome. J Anesth 2006;20:6-10.
31. Kubo K, Kobayashi T, Hayano T, et al. Effects of ONO-5046, a specific neutrophil elastase inhibitor, on endotoxin-induced lung injury in sheep. J Appl Physiol 1994;77:1333-40.
32. Nishina K, Mikawa K, Takao Y, et al. ONO-5046, an elastase inhibitor, attenuates endotoxin-induced acute lung injury in rabbits. Anesth Analg 1997;84:1097-103.
33. Miyazaki Y, Inoue T, Kyi M, et al. Effects of a neutrophil elastase inhibitor (ONO-5046) on acute pulmonary injury induced by tumor necrosis factor alpha (TNFalpha) and activated neutrophils in isolated perfused rabbit lungs. Am J Respir Crit Care Med 1998;157:89-94.
34. Tomizawa N, Ohwada S, Ohya T, et al. The effects of a neutrophil elastase inhibitor (ONO-5046.Na) and neutrophil depletion using a granulotrap (G-1) column on lung reperfusion injury in dogs. J Heart Lung Transplant 1999;18:637-45.
35. Zeiher BG, Artigas A, Vincent JL, et al. Neutrophil elastase inhibition in acute lung injury: results of the STRIVE study. Crit Care Med 2004;32:1695-702.
36. Shasby DM, Vanbenthuysen KM, Tate RM, et al. Granulocytes mediate acute edematous lung injury in rabbits and in isolated rabbit lungs perfused with phorbol myristate acetate: role of oxygen radicals. Am Rev Respir Dis 1982;125:443-7.
37. McDonald RJ, Berger EM, Repine JE. Neutrophil-derived oxygen metabolites stimulate thromboxane release, pulmonary artery pressure increases, and weight gains in isolated perfused rat lungs. Am Rev Respir Dis 1987;135:957-9.
38. Tamakuma S, Ogawa M, Aikawa N, et al. Relationship between neutrophil elastase and acute lung injury in humans. Pulm Pharmacol Ther 2004;17:271-9.
39. Caty MG, Guice KS, Oldham KT, et al. Evidence for tumor necrosis factor-induced pulmonary microvascular injury after intestinal ischemia-reperfusion injury. Ann Surg 1990;212:694-700.
40. Kollef MH, Schuster DP. The acute respiratory distress syndrome. N Engl J Med 1995;332:27-37.

Cite this article as: Kim DH, Chung JH, Son BS, Kim YJ, Lee SG. Effect of a neutrophil elastase inhibitor on ventilator-induced lung injury in rats. J Thorac Dis 2014;6(12):1681-1689. doi: 10.3978/j.issn.2072-1439.2014.11.10

Original Article

Cost and effectiveness of video-assisted thoracoscopic surgery for clinical stage I non-small cell lung cancer: a population-based analysis

Hsin-Yuan Fang[1,2*], Fei-Yuan Hsiao[3,4,5*], Hsu-Chih Huang[6*], Yu-Sen Lin[1*], Chih-Yi Chen[1#], Shwn-Huey Shieh[7], Pin-Ru Chen[1], Chein-Kuang Chen[1], Chun-Ru Chien[2,8]

[1]Department of Chest Surgery, China Medical University Hospital, Taichung, Taiwan; [2]School of Medicine, College of Medicine, China Medical University, Taichung, Taiwan; [3]Graduate Institute of Clinical Pharmacy, College of Medicine, [4]School of Pharmacy, College of Medicine, National Taiwan University, Taipei, Taiwan; [5]Department of Pharmacy, National Taiwan University Hospital, Taipei, Taiwan; [6]Division of Trauma, Emergency Surgery, and Critical Care, China Medical University Hospital, Taichung, Taiwan; [7]Department of Health Services Administration, College of Health Care, China Medical University, Taichung, Taiwan; [8]Department of Radiation Oncology, China Medical University Hospital, Taichung, Taiwan

*These authors contributed equally to this work; #This author is currently in Chung Shan Medical University.

Correspondence to: Chun-Ru Chien, MD, PhD. School of Medicine, College of Medicine, China Medical University, No. 91 Hsueh-Shih Road, North District, Taichung 40402, Taiwan. Email: d16181@mail.cmu.edu.tw.

Background: Video-assisted thoracoscopic surgery (VATS) is a minimally invasive alternative to conventional surgery (CS). We aimed to estimate the short-term cost-effectiveness of VATS *vs.* CS for clinical stage I non-small cell lung cancer (NSCLC-c-stage-I) patients from the payer's perspective (National Health Insurance).

Methods: We identified NSCLC-c-stage-I patients diagnosed and received surgery within 2007-2009 through a comprehensive population-based database containing cancer and death registries, and reimbursement data. The duration of interest was 1 year. We included potential confounding covariables through literature searching and our own experience, and used a propensity score to construct a 1:1 population for adjustment.

Results: Our study population constituted 966 patients. The mean hospital stay [days, standard deviation (SD)] were 14.4 [7] and 16.1 (7.7) for VATS and CS respectively (P=0.002). The mean cost (2013 USD) and survival (year) was $22,316 *vs.* $21,976 and 0.98 *vs.* 0.974 for VATS *vs.* CS. The probability for VATS to be cost-effective (i.e., positive net benefit) was 0.49 & 0.56 at willingness-to-pay (WTP) 50,000 & 100,000 USD/life-year, respectively.

Conclusions: We provide the first empirical evidence that when compared to CS, VATS was potentially cost-effective in the short term (1 year) within the common WTP levels in Taiwan.

Keywords: Cost-effectiveness analysis; video-assisted thoracoscopic surgery (VATS); clinical stage I non-small cell lung cancer (NSCLC-c-stage-I)

Submitted Jul 21, 2014. Accepted for publication Sep 25, 2014.
doi: 10.3978/j.issn.2072-1439.2014.10.27
View this article at: http://dx.doi.org/10.3978/j.issn.2072-1439.2014.10.27

Introduction

Surgery is the cornerstone of curative treatment for early stage non-small cell lung cancer (NSCLC) (1). Lobectomy is the usual approach but the role of sublobectomy is also debated (1,2). Video-assisted thoracoscopic surgery (VATS) is a minimally invasive alternative to open thoracotomy and may lead to better survival outcome (1,3). Due to its minimally invasive nature, VATS is also associated with less surgical trauma, less use of narcotics, and fewer complications (4,5).

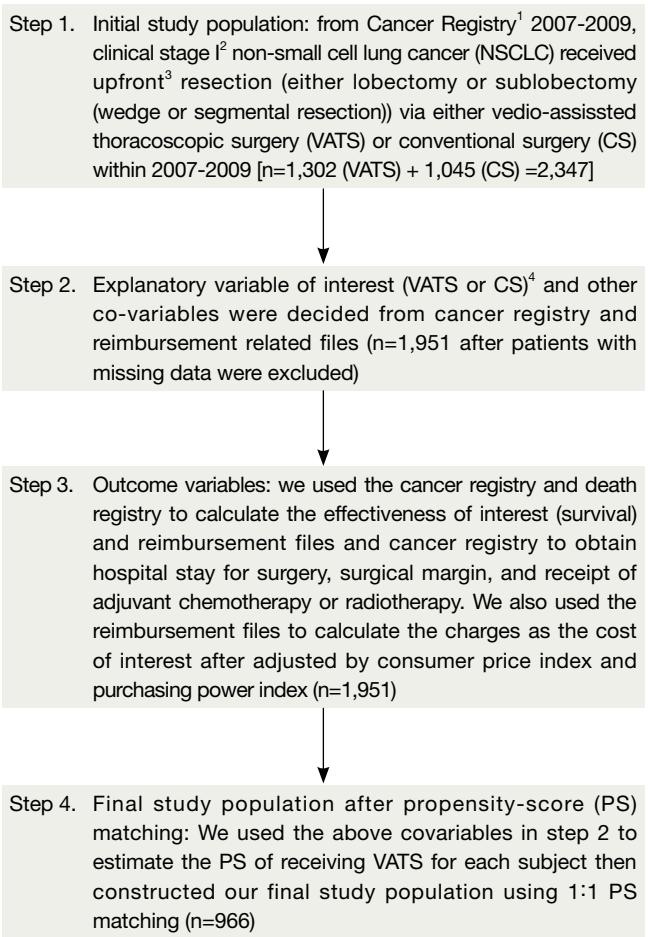

Figure 1 Study flow chart. [1], we only included those treated (class 1-2) by any single institution to ensure data consistency; [2], 6thAmerican Joint Committee on Cancer staging; [3], those who received neoadjuvant therapy were excluded; [4], for each institute, we excluded those cases received CS before 1st VATS case to ensure accessibility to VATS.

However, VATS is associated with a higher initial cost and may be overall more costly (6,7). Cost-effectiveness is an important issue nowadays (8). In an era when affordable cancer care is a worldwide issue, the cost-effectiveness of VATS should also be considered because this consideration will possibly affect patients' access to cancer treatment (9).

To our knowledge, the cost-effectiveness (regarding cost per life year saved) of VATS has not been reported in the literature except our previous preliminary report (10). Therefore, the aim of our study is to compare the cost and effectiveness of VATS *vs.* conventional surgery (CS) for clinical stage I NSCLC via this updated population-based propensity score (PS) matched analysis.

Materials and methods

Data source

The Collaboration Center of Health Information Application (CCHIA) database is a set of databases with complete information regarding cancer and death registration, and reimbursement data from National Health Insurance (NHI) for the whole Taiwanese population. The cancer registry within CCHIA provides details regarding individual demographics, tumor histology, cancer primary sites, stage of disease, and primary surgical, radiation, and systemic therapy. NHI is a single compulsory payer with universal coverage in Taiwan and provides a comprehensive services package "All medically necessary services are covered. The package covers inpatient, outpatient, dental services, traditional Chinese medicine, and maintains a very long list of nearly 20,000 items of prescription drugs". NHI's reimbursement data files at the CCHIA provide information regarding the income of the insured, details of treatment received, and the characteristics of health care providers.

Study population and study design

Our study flow chart is depicted in *Figure 1*. Our target populations were clinical stage I NSCLC patients received either VATS or CS within 2007-2009. In brief, the date of admission for surgery was used as the index date. We set the duration of interest as one year within the index date. We then decided the explanatory variable of interest (VATS *vs.* CS) based on the reimbursement coding. We also collected other covariables for the adjustment of potential non-randomized treatment selection and cost and effectiveness data from the CCHIA (see next sub-section "other explanatory covariables"). Finally, we constructed a PS matched sample based on PS estimated through the above covariables to compare the cost and effectiveness of VATS *vs.* CS within the duration of interest. In PS analysis, we modeled the use of VATS (*vs.* CS) as the dependent variable and the covariables as independent variables, and used non-conditional logistic regression to model the probability of receiving VATS as commonly used in the literatures (11,12). We then used the logit of the probability as the PS, as commonly used in the literature (12). This study had been approved by Research Ethics Committee in our institute [CMUH103-REC-005].

Other explanatory covariables

Firstly, we searched the literature regarding potential factors

that might influence the cost of VATS. We used the following balanced search filters regarding costs or economics in the PubMed "['costs and cost analysis' (MeSH) OR costs (Title/Abstract) OR cost effective* (Title/Abstract)] OR [cost* (Title/Abstract) OR 'costs and cost analysis' (MeSH:noexp) OR cost benefit analysis* (Title/Abstract) OR cost-benefit analysis (MeSH) OR health care costs (MeSH:noexp)]" as in the literatures (13,14). We combined the above keywords with "(cancer) AND (VATS OR thoracoscopic)" and found that social economic status (SES), surgeons' case load, and tumor location might influence the cost after VATS (15-17). Secondly, we collected other factors that were not reported in the literature but that might affect the cost of VATS based on our clinical and research experiences. In this regard, we also included patient demographic factors (age, gender, and residency region), patient characteristics (comorbidity), disease characteristics (histology and pathological stage), treatment pattern (surgical type), and health service provider characteristics (treating hospital preference) based on our clinical experiences and prior NHI and CCHIA related studies (18-24). Age was classified as ≥65 years old or not. Patient residency was classified as northern Taiwan or elsewhere. SES was classified as high (income greater than minimal wage) or not. Histology was classified as adenocarcinoma or others. Pathological stage was classified as early or advanced (beyond stage I). Tumor location was classified as lower *vs.* upper/middle. Surgical type was classified as lobectomy or sublobectomy. Surgeons' case load was classified as high *vs.* low (split at the median in our study sample). Treating hospital preference was classified as high (at least half of their patients were treated by VATS) or low.

Cost and effectiveness assessment

We included the following issues in effectiveness assessment: hospital stay for surgery, pathological stage, surgical margin, receipt of adjuvant chemotherapy or radiotherapy, survival within duration of interest, and overall survival. We obtained survival status according to the death registry, hospital stay from reimbursement files, and the other issues from cancer registry. The cost and cost-effectiveness were conducted from a Taiwan NHI perspective (i.e., charges to NHI). The cost was limited to the duration of interest then converted to 2013 USD by purchasing the power parity and consumer price indexes. The cost within our duration of interest was further broken down into four quarters (i.e., every 3 months) to illustrate the cost in different disease phrases. We then applied various thresholds of willingness-to-pay (WTP) to calculate the net benefit (NB) when VATS was compared to CS by applying the following equation (25):

NB = effectiveness * WTP – cost.

WTP refers to the amount of money the payer is willing to pay for an outcome. The commonly cited WTP threshold [50,000-100,000 USD/life year (LY)] means that the payer is generally willing to pay 50,000-100,000 USD to gain a year of life and this was considered a threshold to decide whether an intervention was cost-effective or not (26,27). This WTP range also covers the World Health Organization (WHO) criteria (3 times gross domestic product per capita) regarding cost-effectiveness in Taiwan [around 58,042 (19,347.329*3)] (28). When the incremental NB (INB) of an intervention is positive at a specific WTP level, this means that this intervention is associated with a positive net monetary gain, so it is also cost-effective at this specific WTP level.

Statistical analysis

Tabulation and standardized difference were used to assess the balance of covariates between PS-matched groups. We used a stratified log-rank test to compare the survival of VATS versus CS for the entire follow-up period (censored on 1 January 2012) (12). Other outcomes between VATS and CS were compared with McNemar test or paired *t*-test (12). We used the paired *t*-test to evaluate the statistical significance of the INB, and then constructed the cost-effectiveness acceptability curve (CEAcC) (25). SAS 9.3 (SAS Institute, Cary, NC, USA) was used for all the analysis.

Results

Identification of the study cases (Figure 1, Table 1)

As revealed in *Figure 1*, 2,347 clinical stage I NSCLC patients treated with either VATS or CS were identified as the initial study population. After exclusion of those with missing data and matching by PS, the final study population included 966 patients. The characteristics of these patients are described in *Table 1*. A good balance of covariables and small standardized differences (<0.1) were seen for all covariables.

Cost and effectiveness

The mean hospital stay (in days, with standard deviation (SD)) were 14.4 [7] and 16.1 (7.7) for VATS and CS respectively (P=0.002). The distribution regarding

Table 1 Patient characteristics of the propensity-score matched final study population

Covariables	VATS number	(%, rounded)	CS number	(%, rounded)	Standardized difference (rounded)
Age					0.01
<65 y/o	233	[48]	235	[49]	
≥65 y/o	250	[52]	248	[51]	
Gender					0.06
Male	254	[53]	240	[50]	
Female	229	[47]	243	[50]	
Residency					0.02
North	241	[50]	245	[51]	
Non-north	242	[50]	238	[49]	
Social-economic status					0.01
High	253	[52]	251	[52]	
Low	230	[48]	232	[48]	
Comorbidity					0.03
Without	170	[35]	176	[36]	
With	313	[65]	307	[64]	
Histology					0.05
Adenocarcinoma	365	[76]	375	[78]	
Non-adenocarcinoma	118	[24]	108	[22]	
Stage					0.03
Early	407	[84]	401	[83]	
Advanced	76	[16]	82	[17]	
Location					0.01
Upper/middle	316	[65]	318	[66]	
Lower	167	[35]	165	[34]	
Surgery					0.07
Lobectomy	424	[88]	412	[85]	
Sublobectomy	59	[12]	71	[15]	
Hospital preference					0.05
High	243	[50]	231	[48]	
Low	240	[50]	252	[52]	
Surgeon case load					0.06
High	241	[50]	255	[53]	
Low	242	[50]	228	[47]	

CS, conventional surgery; VATS, video-assisted thoracoscopic surgery; y/o, years old.

surgical margin and receipt of adjuvant chemotherapy or radiotherapy were similar between VATS and CS without statistical significance. For the entire follow-up period, the survival rate of VATS was better than CS (2 years: 92% *vs.* 90%, P=0.8), but was not of statistical significance. The Kaplan-Meier survival curve is depicted in *Figure 2*. The mean cost (2013 USD) and survival (year) within one year after surgery were higher for VATS versus CS ($22,316 *vs.* $21,976; 0.98 *vs.* 0.974). Given the above incremental cost $340 (=22,316 – 21,976) and incremental effectiveness 0.06 (=0.98 – 0.974) LY, the net benefit if WTP equals $50,000/LY would be negative $40 (=0.006*50,000 – 340) but positive $260 (=0.006*100,000 – 340) if WTP equals $100,000/LY. The incremental cost-effectiveness ratio (ICER) when VATS was compared to CS was 56,667 (=340/0.006) (USD/LY). The above results were also tabulated in *Table 2*. Although VATS is associated with higher initial cost (in the 1st quarter after surgery), the difference

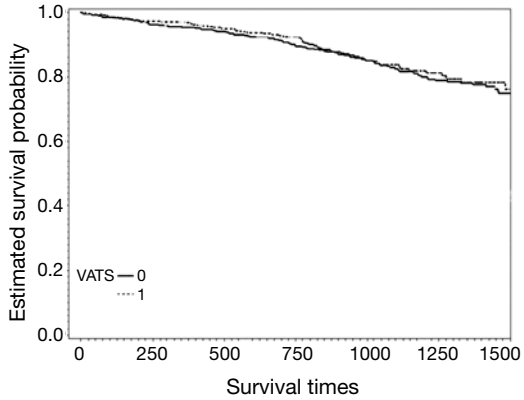

Figure 2 Kaplan-Meier survival curve (in days). Video-assisted thoracoscopic surgery (VATS =1 in dotted line) *vs.* conventional surgery (VATS =0 in solid line); P=0.8.

Table 2 Cost-effectiveness analysis results*

Outcomes	VATS	CS
Cost (2013 USD)	22,316	21,976
Effectiveness (lift-year)	0.980	0.974
Incremental cost	340	Reference
Incremental effectiveness	0.006	Reference
ICER	56,667	Reference
INB (at WTP 50,000)	–40	Reference
INB (at WTP 100,000)	260	Reference

CS, conventional surgery; ICER, incremental cost-effectiveness ratio; INB, incremental net benefit; VATS, video-assisted thoracoscopic surgery; WTP, willingness-to-pay (unit: USD/life-year); *, cost round at integral; life-year rounded at 3rd decimal.

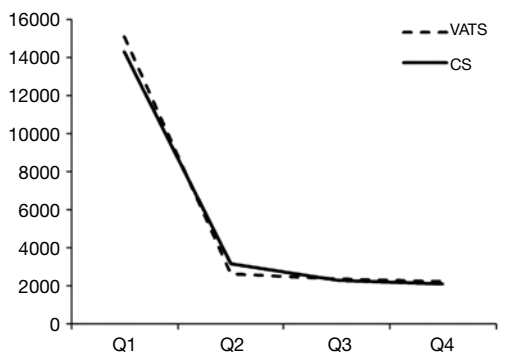

Figure 3 Time trend of cost. Vertical axis: 2013 USD; transverse axis: 1st-4th quarter after surgery; video-assisted thoracoscopic surgery (in dotted line) *vs.* conventional surgery (in solid line).

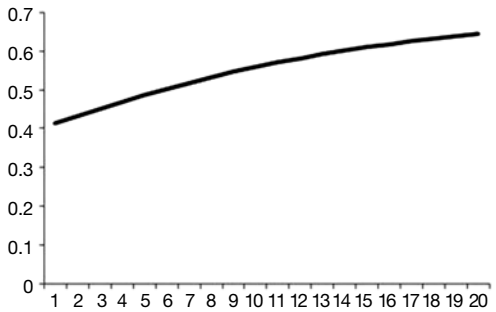

Figure 4 Cost-effectiveness acceptability curve. Vertical axis: probability of video-assisted thoracoscopic surgery to be cost-effective; Transverse axis: willingness-to-pay (unit: 10,000 US dollars/life-year).

is not obvious in the end of follow-up (*Figure 3*). When we changed the WTP level, the corresponding probability of VATS to be cost-effective (i.e., positive net benefit) as estimated by paired *t*-test was shown in *Figure 4*. For example, the probability was 0.49 & 0.56 at WTP 50,000 & 100,000, respectively.

Discussion

In this population-based propensity-score matched cost-effectiveness analysis, we provide the first empirical evidence that VATS is potentially cost-effective versus CS in the short-term (1 year) within the common WTP levels from a payer's perspective since our estimated ICER ($56,667 USD/LY) was below either the common criteria ($100,000 USD/LY) or the WHO criteria ($58,042 USD/LY).

Our results were compatible with the literatures in that VATS provides better survival (1,3). The higher cost for VATS might partly be due to the higher operation fee for VATS *vs.* CS (dereferences in operation fee: $399 for VATS lobectomy *vs.* CS lobectomy whereas $224 for VATS sublobectomy *vs.* CS sublobectomy, both in USD 2013). Our estimated cost within 1 year after surgery was also higher for VATS as ever reported by other study (8), although conflict results had also been reported (7,15,29-31). Our updated estimates were also in line with our previous preliminary estimates but were more representative now given the much larger sample size (10).

Although the interpretation of our results is that VATS is potentially cost-effective within the common WTP levels in the short term, we could not specify to specific VATS due to data limitation. For example, we could not define whether VATS was complete or assisted (32). There were also some

other limitations in our study. Firstly, there is always concern in potential unobserved confounding bias although we had performed comprehensive literature searching and used our own clinical and research experiences to include potential confounders we suspected. Secondly, although the long term outcome of early stage NSCLC was quite good, whether our duration of interest (1 year) was long enough to fully capture the cost-effectiveness of VATS versus CS might deserve further studies although longer follow-up might make VATS more favorable given the slightly improved survival and similar cost in the end of our follow-up period (as revealed in *Figures 2,3*).

Conclusions

In this population-based propensity-score matched cost-effectiveness analysis, we provide the first empirical evidence that when compared to CS, VATS was potentially cost-effective in the short term (1 year) within the common willingness-to-pay levels from a payer's perspective in Taiwan. Further studies would be helpful to see the long term results and whether the same results could be obtained in other health care systems.

Acknowledgements

The data analyzed in this study was provided by the Collaboration Centre for Health Information Application (CCHIA), Ministry of Health and Welfare, Executive Yuan, Taiwan. The author would like to thank the funding agencies [the Ministry of Health and Welfare (MOHW104-TD-B-111-03)] for their financial support. The corresponding author would like to thank Dr. Ya-Chen Tina Shih for her mentoring.

Funding: This work was supported by the Health and welfare surcharge of tobacco products, China Medical University Hospital Cancer Research Center of Excellence, Taiwan [MOHW104-TD-B-111-03].

Authors' contributions: The authors—and not the funding bodies or CCHIA—had full control of in the study design, in the collection, analysis and interpretation of data; in the writing of the manuscript; and in the decision to submit the manuscript for publication. All authors have contributed significantly, and that all authors are in agreement with the content of the manuscript. C.R.C participated in the concept and design, analysis and interpretation of data, and drafting of the manuscript. H.Y.F, F.Y.H, H.C.H and Y.S.L participated in the concept and design, interpretation of data, and drafting of the manuscript. C.Y.C, S.H.S, P.R.C and C.K.C participated in the concept and design, and interpretation of data. All authors have approved the manuscript as submitted.

Disclosure: The authors declare no conflict of interest.

References

1. Vansteenkiste J, De Ruysscher D, Eberhardt WE, et al. Early and locally advanced non-small-cell lung cancer (NSCLC): ESMO Clinical Practice Guidelines for diagnosis, treatment and follow-up. Ann Oncol 2013;24 Suppl 6:vi89-98.
2. Fan J, Wang L, Jiang GN, et al. Sublobectomy versus lobectomy for stage I non-small-cell lung cancer, a meta-analysis of published studies. Ann Surg Oncol 2012;19:661-8.
3. Li Z, Liu H, Li L. Video-assisted thoracoscopic surgery versus open lobectomy for stage I lung cancer: A meta-analysis of long-term outcomes. Exp Ther Med 2012;3:886-892.
4. Chen HW, Du M. Video-assisted thoracic surgery for lung carcinoma. J Thorac Dis 2013;5:912-3.
5. Fang HY, Chen CY, Wang YC, et al. Consistently lower narcotics consumption after video-assisted thoracoscopic surgery for early stage non-small cell lung cancer when compared to open surgery: a one-year follow-up study. Eur J Cardiothorac Surg 2013;43:783-6.
6. Van Schil P. Cost analysis of video-assisted thoracic surgery versus thoracotomy: critical review. Eur Respir J 2003;22:735-8.
7. Piwkowski C, Gabryel P, Gałęcki B, et al. High costs as a slow down factor of thoracoscopic lobectomy development in Poland - an institutional experience. Wideochir Inne Tech Malo Inwazyjne 2013;8:334-41.
8. Abbott DE, Sutton JM, Edwards MJ. Making the case for cost-effectiveness research. J Surg Oncol 2014;109:509-15.
9. Chalkidou K, Marquez P, Dhillon PK, et al. Evidence-informed frameworks for cost-effective cancer care and prevention in low, middle, and high-income countries. Lancet Oncol 2014 ;15:e119-31.
10. Chien CR, Wang PH, Shih YCT. Cost-effectiveness analysis of video-assisted thoracic surgery vs. open surgery for patients with newly diagnosed stage I nonsmall cell lung cancer. ISPOR 17th Annual International Meeting, Washington DC, USA; 2012 Jun 2-6. Value Health 2012;15:A77.
11. Rosenbaum PR. Basic Tools of Multivariate Matching.

In: Rosenbaum PR. eds. Design of Observational Studies. Springer Series in Statistics, Springer, 2010:163-85.
12. Austin PC, Chiu M, Ko DT, et al. Propensity score matching for estimating treatment effect. In: Faries DE, Leon AC, Haro JM, et al. eds. Analysis of Observational Health Care Data Using SAS. USA: SAS Institute, Cary, NC, 2010:51-84.
13. Glanville J, Paisley S. Identifying economic evaluations for health technology assessment. Int J Technol Assess Health Care 2010;26:436-40.
14. Smieliauskas F, Chien CR, Shen C, et al. Cost-effectiveness analyses of targeted oral anti-cancer drugs: a systematic review. Pharmacoeconomics 2014;32:651-80.
15. Swanson SJ, Meyers BF, Gunnarsson CL, et al. Video-assisted thoracoscopic lobectomy is less costly and morbid than open lobectomy: a retrospective multiinstitutional database analysis. Ann Thorac Surg 2012;93:1027-32.
16. Cho S, Do YW, Lee EB. Comparison of costs for video-assisted thoracic surgery lobectomy and open lobectomy for non-small cell lung cancer. Surg Endosc 2011;25:1054-61.
17. Gopaldas RR, Bakaeen FG, Dao TK, et al. Video-assisted thoracoscopic versus open thoracotomy lobectomy in a cohort of 13,619 patients. Ann Thorac Surg 2010;89:1563-70.
18. Lin CC, Hsia TC, Chien CR. 3rd line Erlotinib for lung cancer in Asia may be as cost-effective as in the Western world. Lung Cancer 2012;76:499-500.
19. Chien CR, Su SY, Cohen L, et al. Use of Chinese medicine among survivors of nasopharyngeal carcinoma in Taiwan: a population-based study. Integr Cancer Ther 2012;11:221-31.
20. Hsia TC, Tu CY, Chen HJ, et al. Effectiveness of intensity-modulated radiotherapy for lung cancer. Clin Oncol (R Coll Radiol) 2013;25:447-8.
21. Chien CR, Shih YC. Use of personalized decision analysis in decision making for Palliative vs. surgical management of the oldest-old patients with localized skin cancer in a culturally sensitive environment: a case study of a 96-year-old male Taiwanese patient. J Pain Symptom Manage 2013;45:792-7.
22. Chien CR, Lin HW, Yang CH, et al. High case volume of radiation oncologists is associated with better survival of nasopharyngeal carcinoma patients treated with radiotherapy: a multifactorial cohort analysis. Clin Otolaryngol 2011;36:558-65.
23. Chien CR, Hsia TC, Chen CY. Cost-effectiveness of chemotherapy combined with thoracic radiotherapy versus chemotherapy alone for limited stage small cell lung cancer: A population-based propensity-score matched analysis. Thoracic Cancer 2014;5:530-6.
24. Ke TW, Liao YM, Chiang HC, et al. Effectiveness of neoadjuvant concurrent chemoradiotherapy versus up-front proctectomy in clinical stage II-III rectal cancer: A population-based study. Asia Pac J Clin Oncol 2014. [Epub ahead of print].
25. Hoch JS, Briggs AH, Willan AR. Something old, something new, something borrowed, something blue: a framework for the marriage of health econometrics and cost-effectiveness analysis. Health Econ 2002;11:415-30.
26. Konski A. Economic analysis of health care interventions. Semin Radiat Oncol 2008;18:168-74.
27. Shih YC, Halpern MT. Economic evaluations of medical care interventions for cancer patients: how, why, and what does it mean? CA Cancer J Clin 2008;58:231-44.
28. Available online: http://www.who.int/choice/costs/CER_thresholds/en/
29. Farjah F, Backhus LM, Varghese TK, et al. Ninety-day costs of video-assisted thoracic surgery versus open lobectomy for lung cancer. Ann Thorac Surg 2014;98:191-6.
30. Lacin T, Swanson S. Current costs of video-assisted thoracic surgery (VATS) lobectomy. J Thorac Dis 2013;5 Suppl 3:S190-3.
31. Ramos R, Masuet C, Gossot D. Lobectomy for early-stage lung carcinoma: a cost analysis of full thoracoscopy versus posterolateral thoracotomy. Surg Endosc 2012;26:431-7.
32. He J, Shao W, Cao C, et al. Long-term outcome and cost-effectiveness of complete versus assisted video-assisted thoracic surgery for non-small cell lung cancer. J Surg Oncol 2011;104:162-8.

Cite this article as: Fang HY, Hsiao FY, Huang HC, Lin YS, Chen CY, Shieh SH, Chen PR, Chen CK, Chien CR. Cost and effectiveness of video-assisted thoracoscopic surgery for clinical stage I non-small cell lung cancer: a population-based analysis. J Thorac Dis 2014;6(12):1690-1696. doi: 10.3978/j.issn.2072-1439.2014.10.27

Original Article

Predictive risk factors for lymph node metastasis in patients with small size non-small cell lung cancer

Feichao Bao, Ping Yuan, Xiaoshuai Yuan, Xiayi Lv, Zhitian Wang, Jian Hu

Department of Thoracic Surgery, First Hospital, College of Medicine, Zhejiang University, Hangzhou 310003, China

Correspondence to: Jian Hu, MD, PhD. Department of Thoracic Surgery, First Hospital, College of Medicine, Zhejiang University, No. 79, Qingchun Road, Hangzhou 310003, China. Email: hujian.medzju@gmail.com.

Background: Accurate clinical staging of non-small cell lung cancer (NSCLC) is essential for developing an optimal treatment strategy. This study aimed to determine the predictive risk factors for lymph node metastasis, including both N1 and N2 metastases, in clinical T1aN0 NSCLC patients.

Methods: We retrospectively evaluated clinical T1aN0M0 NSCLC patients who showed no radiologic evidence of lymph node metastasis, and who had undergone surgical pulmonary resection with systematic mediastinal node dissection or sampling at the First Affiliated Hospital of Zhejiang University between January 2011 and June 2013. Univariate and multivariate logistic regression analyses were performed to identify predictive factors for node metastasis.

Results: Pathologically positive lymph nodes were found in 16.2% (51/315) of the patients. Positive N1 nodes were found in 12.4% (39/315) of the patients, and positive N2 nodes were identified in 13.0% (41/315) of the patients. Some 9.2% (29/315) of the patients had both positive N1 and N2 nodes, and 3.8% (12/315) of the patients had nodal skip metastasis. Variables of preoperative radiographic tumor size, non-upper lobe located tumors, high carcinoembryonic antigen (CEA) levels and micropapillary predominant adenocarcinoma (AC) were identified as predictors for positive N1 or N2 node multivariate analysis.

Conclusions: Pathologically positive lymph nodes were common in small size NSCLC patients with clinical negative lymph nodes. Therefore, preoperative staging should be performed more thoroughly to increase accuracy, especially for patients who have the larger size, non-upper lobe located, high CEA level or micropapillary predominant ACs.

Keywords: Non-small cell lung cancer (NSCLC); lymph node metastasis; sublobar resections

Submitted Jul 10, 2014. Accepted for publication Sep 24, 2014.

doi: 10.3978/j.issn.2072-1439.2014.11.05

View this article at: http://dx.doi.org/10.3978/j.issn.2072-1439.2014.11.05

Introduction

Lung cancer is the leading cause of cancer-related death worldwide, with a 5-year survival rate of 16% (1). With the widespread use of low-dose computed tomography, more small size (2 cm or less) non-small cell lung cancers (NSCLC) are being discovered (2). It is important to accurately stage NSCLC before treatment, as the treatment varies by stages. As for pT1aN0 NSCLC patients, lobectomies are recommended, as suggested by a randomized control trial performed by the Lung Cancer Study Group in 1995 (3). However, recent studies have indicated that for T1aN0M0 NSCLC patients, segmentectomy is as effective as lobectomy (4). For patients with T1aN1 NSCLC, the choice of treatment is controversial, as a recent multicenter phase III study favored neoadjuvant chemotherapy rather than surgery alone (5). However, for patients with T1aN2 NSCLC, it is clearly beneficial to take neoadjuvant chemotherapy (6).

Many sophisticated examination methods are being used for the accurate nodal staging of lung cancer patients. These methods include both non-invasive and invasive examination procedures such as integrated fluorodeoxyglucose positron emission tomography/computed tomography (PET-CT), endobronchial

ultrasound-guided transbronchial needle aspiration (EBUS-TBNA), endoscopic ultrasound-guided fine-needle aspiration (EUS-FNA) and mediastinoscopy (7). As for small size NSCLC patients, the frequencies for positive N1 and N2 are 5% and 4-10%, respectively, which are quite low (8-11). Therefore, this study aimed to determine the predictive risk factors for lymph node metastasis (including both N1 and N2 metastases) in clinical T1aN0 NSCLC patients.

Patients and methods

Patients

We retrospectively evaluated cT1aN0M0 NSCLC patients who showed no radiologic evidence of lymph node metastasis, and who underwent surgical pulmonary resections with systematic mediastinal node dissections or sampling at the First Affiliated Hospital of Zhejiang University between January 2011 and June 2013. Patients who received preoperative chemotherapy and/or radiation therapy were excluded from this study.

All of the participating patients underwent preoperative staging with contrast-enhanced CT scans. Mediastinal lymph nodes were considered to be positive by CT-scan criteria if their short axis was 1 cm wide or more. Additional diagnostic examinations [including brain magnetic resonance imaging (MRI) or CT, pulmonary function analysis, abdominal ultrasonography, bronchoscopy and bone scanning] were performed before each surgery, as was routine. However, no invasive examinations for mediastinal staging such as mediastinoscopy, EBUS-TBNA or EUS-FNA were used preoperatively.

We reviewed the medical records of each patient for demographic and clinical data. These data included age, sex, smoking status, preoperative serum carcinoembryonic antigen (CEA) level (<5 or ≥5 ng/mL), tumor lobe distribution (upper, middle or lower lobes), tumor location (central or peripheral), tumor size on preoperative radiologic findings, tumor histology [adenocarcinoma (AC), squamous-cell carcinoma or other cell types], symptoms at presentation, and node staging according to pathologic reports. Tumor locations were assessed with bronchoscopy. If the bronchoscopy showed a visible lesion, the location was defined as central. If no visible lesion was found, the location was defined as peripheral. Tumor staging was based on AJCC 7th edition of TNM staging, and the subtype of AC was determined according to the IASLC/ATS/ERS classification (12).

This study was approved by the institutional review board of the First Affiliated Hospital of Zhejiang University. As this was a retrospective analysis, the need to obtain written informed consent from each patient was waived.

Statistical analysis

Univariate analyses and multivariate logistic regression analyses were performed to identify predictors for positive N1 and N2 nodes. Fisher's exact test and Pearson's chi-squared test were used for the univariate analyses. A stepwise selection method was used to build logistic regression models. In the multivariate analyses, categorical variables (sex, tumor location, lobe distribution of tumor, smoking history, symptoms of presentation and tumor histology) and continuous variables (age, preoperative serum CEA level and tumor size on preoperative radiologic findings) were assessed to identify independent predictors. A probability value less than 0.05 was considered statistically significant. All analyses were performed using IBM SPSS 20.0 (IBM Co., Chicago, IL, USA).

Results

Patient characteristics

This study included 315 patients who had clinical T1aN0 non-small lung cancer between January 2011 and June 2013. The patient characteristics are shown in *Table 1*. There were 148 men (47.0%) and 167 women (53.0%). The median age was 59.4 years (range from 32 to 82 years). Some 218 patients (69.2%) were never smokers, and 97 patients (30.8%) were current or former smokers. Centrally located tumors were found in 32 (10.2%) of the patients. The histology of tumors consisted of AC in 281 (89.2%), squamous cell carcinoma (SQC) in 30 (9.5%) and other cell types in four (1.3%) of the patients.

Pathologically positive lymph nodes were found in 16.2% (51/315) of the patients. Positive N1 nodes were found in 12.4% (39/315), and positive N2 nodes were identified in 13.0% (41/315) of the patients. Some 9.2% (29/315) of the patients had both positive N1 and N2 nodes, and 3.8% (12/315) had nodal skip metastasis. Pathological N1 stage was identified in 3.2% (10/315) of the patients, and pathological N2 stage was found in 13.0% (41/315).

Table 1 Patients characteristics

Characteristics	No. of patients	Percentage
Sex		
Male	148	47.0
Female	167	53.0
Age		
<59	153	48.6
≥59	162	51.4
Smoking status		0.0
Never	218	69.2
Current or former	97	30.8
Symptom		
Absent	225	71.4
Present	80	25.4
Tumor size		
≤1 cm	60	19.0
1-2 cm	255	81.0
Tumor location		
Central	32	10.2
Peripheral	283	89.8
Lobe distribution		
LLL	14	4.4
LUL	36	11.4
RLL	26	8.3
RML	18	5.7
RUL	63	20.0
Histology		
AC	281	89.2
SQC	30	9.5
Others	4	1.3

LLL, left lower lobe; LUL, left upper lobe; RLL, right lower lobes; RML, right middle lobes; RUL, right upper lobes; AC, adenocarcinoma; SQC, squamous cell carcinoma.

Table 2 Univariate analysis of positive N1 nodes

Variables	Negative N1 node (%)	Positive N1 node (%)	P value
Sex			
Male	125 (84.5)	23 (15.5)	
Female	151 (90.4)	16 (9.6)	0.109
Age			
<59	142 (86.3)	21 (13.7)	
≥59	144 (88.9)	18 (11.1)	0.623
Smoking status			
Never	197 (90.4)	21 (9.6)	
Current or former	81 (81.4)	18 (18.6)	0.032
Symptom			
Absent	210 (89.4)	25 (10.6)	
Present	66 (82.5)	14 (17.5)	0.108
Tumor size			
≤1 cm	60 (100)	0 (0)	
1-2 cm	216 (84.7)	39 (15.3)	<0.001
Tumor location			
Central	20 (62.5)	12 (37.5)	
Peripheral	256 (90.5)	27 (9.5)	<0.001
Lobe distribution			
UL	186 (93.5)	13 (6.5)	
Non-UL	90 (77.6)	26 (22.4)	<0.001
Histology			
AC	252 (89.7)	29 (10.3)	
Non-AC	24 (70.6)	10 (29.4)	0.001
MPA	16 (66.7)	8 (33.3)	0.004
CEA			
<5	231 (80.9)	23 (9.1)	
≥5	46 (74.2)	16 (25.8)	<0.001

UL, upper lobes; AC, adenocarcinoma; MPA, micropapillary adenocarcinoma; CEA, carcinoembryonic antigen.

Univariate analysis of predictive factors for nodal metastasis

As shown in *Table 2*, the univariate analysis identified the following variables as significant predictive factors for positive N1 nodes: current or former smoker (P=0.032), centrally located tumor (P<0.001), non-AC (P=0.001), micropapillary adenocarcinoma (MPA) (P=0.004), tumor size (P<0.001), non-upper lobe located tumor (P<0.001) and preoperative serum CEA level of 5 ng/mL or more (P=0.001). Symptoms at presentation, age and sex were not identified as significant predictive factors. As for positive N2 nodes, tumor size (P=0.010), MPA (P<0.001), non-upper lobe located tumors (P=0.006) and a preoperative serum CEA level of 5 ng/mL or more (P<0.001) were identified as significant predictors (*Table 3*).

Multivariate analysis of predictive factor for nodal metastasis

The multivariate analysis revealed the following four

Table 3 Univariate analysis of positive N2 nodes

Variables	Negative N2 node (%)	Positive N2 node (%)	P value
Sex			
Male	127 (85.8)	21 (14.2)	
Female	147 (88.0)	20 (12.0)	0.561
Age			
<59	128 (83.7)	25 (16.3)	
≥59	146 (91.0)	16 (9.0)	0.088
Smoking status			
Never	193 (88.5)	25 (11.5)	
Current or former	81 (83.5)	16 (16.5)	0.221
Symptom			
Absent	206 (77.7)	29 (12.3)	
Present	68 (85.0)	12 (15.0)	0.541
Tumor size			
≤1 cm	58 (96.7)	2 (3.3)	
1-2 cm	216 (84.7)	39 (15.3)	0.010
Tumor location			
Central	26 (81.2)	6 (18.8)	
Peripheral	248 (87.6)	35 (12.4)	0.459
Lobe distribution			
UL	181 (91.0)	18 (9.0)	
Non-UL	92 (80.0)	23 (20.0)	0.006
Histology			
AC	244 (86.8)	37 (13.2)	
Non-AC	30 (88.2)	4 (11.8)	0.818
MPA	14 (58.3)	10 (41.7)	<0.001
CEA			
<5	230 (80.9)	23 (9.1)	
≥5	44 (71.0)	18 (29.0)	<0.001

UL, upper lobes; AC, adenocarcinoma; MPA, micropapillary adenocarcinoma; CEA, carcinoembryonic antigen.

significant predictors for node metastasis: tumor size on preoperative radiologic findings [odds ratio (OR) =4.597; 95% confidence interval (CI): 1.427-14.815; P=0.011), non-upper lobe located tumors (OR =2.758; 95% CI: 1.345-5.656; P=0.006), preoperative serum CEA level (OR =1.195; 95% CI: 1.072-1.331; P=0.001) and MPA (OR =3.875; 95% CI: 1.374-10.933; P=0.010) (*Table 4*).

The predictive factors of positive N1 nodes by multivariate analysis were tumor size on preoperative radiologic findings (OR =7.524; 95% CI: 1.608-35.211; P=0.010), non-upper lobe located tumors (OR =3.343; 95% CI: 1.412-7.916; P=0.006), preoperative serum CEA level (OR =1.205; 95% CI: 1.076-1.349; P=0.001) and MPA (OR =3.955; 95% CI: 1.280-12.221; P=0.017) (*Table 4*).

The predictive factors of positive N2 nodes according to multivariate analysis were tumor size on preoperative radiologic findings (OR =4.284; 95% CI: 1.276-14.382; P=0.019), non-upper lobe located tumors (OR =2.577; 95% CI: 1.204-5.516; P=0.015), preoperative serum CEA level (OR =1.099; 95% CI: 1.030-1.173; P=0.004) and MPA (OR =4.038; 95% CI: 1.481-11.010; P=0.006) (*Table 4*).

Discussion

In this study, we identified tumor size (according to preoperative radiologic findings), non-upper lobe located tumors, preoperative serum CEA level and MPA as the four statistically significant predictors of both positive N1 and N2 nodes.

Precise assessment of lymph node metastasis is important for deciding the optimal treatment for patients with operable NSCLC. The survival rate is similar in patients with small NSCLC treated with segmentectomy and those treated with lobectomy (4,13). However, in theory, segmentectomy candidates should be node negative. Therefore, predicting pathological lymph node

Table 4 Multivariate analysis of positive node

Variables	Positive node		Positive N1 node		Positive N2 node	
	OR (95% CI)	P value	OR (95% CI)	P value	OR (95% CI)	P value
Size	4.597 (1.427-14.815)	0.011	7.524 (1.608-35.211)	0.010	4.284 (1.276-14.382)	0.019
Non-UL	2.758 (1.345-5.656)	0.006	3.343 (1.412-7.916)	0.006	2.577 (1.204-5.516)	0.015
CEA	1.195 (1.072-1.331)	0.001	1.205 (1.076-1.349)	0.001	1.099 (1.030-1.173)	0.004
MPA	3.875 (1.374-10.933)	0.010	3.955 (1.280-12.221)	0.017	4.038 (1.481-11.010)	0.006

UL, upper lobes; CEA, carcinoembryonic antigen; MPA, micropapillary adenocarcinoma; OR, odds ratio; CI, confidence interval.

metastasis in patients with clinical T1aN0 lung cancer is of clinical significance for selecting optimal segmentectomy candidates. The prevalence of lymph node metastasis in patients with tumors of 2 cm is approximately 4-10%, which is quite low (8-10). In this study, the incidence of pathological N1 and N2 stages were 3.2% and 13%, respectively, which was consistent with previous studies (8-10). Radiological tumor size is a risk factor for nodal metastasis in clinical node-negative NSCLC patients (8,14-16). However, for tumors of 2 cm or less, the role of tumor size in predicting nodal metastasis remains controversial. Zhang and colleagues reported that the incidence of N1 and N2 metastasis for tumors of 1 cm or less and of 1 to 2 cm were 3.8% (2/51) and 7.4% (14/190), respectively. Large tumor size is commonly associated with aggressive node stage, but no statistical significance for this association was found in this study (9). However, Farjah (17) recently reported that for tumors of 1 cm or less and of 1 to 2 cm, with clinical node negative disease measured by the mean of positron emission tomography (PET), the frequencies of N2 metastases were 25% (8/32) and 4.3% (10/232), respectively. This result indicated that tumors of smaller size with clinical node-negative disease had a high prevalence of pathological N2 metastasis. In our study, large radiographic tumor size was one of the significant predictive factors for node metastasis.

According to our results, lobe distribution of tumors was not a significant predictor for nodal involvement. However, the distributions did suggest that non-upper lobe located tumors had a tendency toward higher incidence of lymph node metastasis (9,14,18). We speculate that a difference in nodal involvement exists between the upper lobe located tumors and the non-upper located tumors. Our data revealed that the incidences of positive N1 and N2 were different between the upper located group and non-upper located group. Both the univariate and multivariate logistic regression analyses identified tumor location as a significant predictor for nodal metastasis. According to present knowledge, the differential in nodal metastases between the upper located and non-upper located tumors may be caused by the different nodal spread patterns in the two types of locations (11).

Serum CEA level was associated with the post-operative pathological stage and prognosis (14,16,18,19). Inoue (19) reported that compared to patients with normal preoperative serum CEA levels and with NSCLC tumors of 2 cm or less in diameter, the 5-year mortality rate for patients with higher CEA levels (≥5 ng/mL) was significantly worse (92.1% *vs.* 77.6%; P<0.01). In addition, increased CEA level was associated with a much higher rate of lymph node metastasis with small size NSCLC (29.2% *vs.* 10.3%; P=0.02). Koike and colleagues reported that preoperative serum CEA level was a predictor for mediastinal nodal metastasis in clinical stage IA NSCLC patients (14). In our study, preoperative serum CEA level was determined to be a significant predictor of lymph node metastasis. This finding indicates that an elevated CEA level is associated with increased lymph node metastasis, might explain the worse prognoses of NSCLC patients with higher CEA levels. Care should thus be taken against lymph node metastasis in patients with high CEA levels.

In 2011, the IASLC/ATS/ERS added micropapillary predominant AC as a new subtype of lung AC (12). Micropapillary predominant AC is of great significance because of its poor prognosis and its higher likelihood of metastasis (20,21). Roh (20) reported that 62.5% (10/16) of patients with a micropapillary component and 21.1% (4/19) of patients with other subtypes of lung AC showed nodal micrometastasis (P=0.014). This finding suggested that a micropapillary component may be a manifestation of aggressive behavior, as shown by frequent nodal micrometastasis. Warth and colleagues (22) reported similar results, finding that 76% of micropapillary-predominant ACs were node positive. In addition, the overall survival rate was much worse for cases of micropapillary predominant AC than for cases of other subtypes. In our study, micropapillary predominant ACs had a much higher prevalence of both N1 and N2 nodes metastasis, and all of the patients with this condition had positive N1 nodes. This result might encourage surgeons to conduct more systematic lymph node dissections for patients with micropapillary predominant ACs. However, sublobar resections such as segmentectomies should be avoided.

We acknowledge that this study had some limitations. First, it was a retrospective study. Second, PET-CT was performed on only a small number of patients because of its unaffordable cost in China. Thus, a prospective, randomized trial needs to be conducted in which PET-CT is performed routinely.

In conclusion, we retrospectively analyzed 315 patients with clinical T1aN0M0 NSCLC who had undergone surgical pulmonary resection and systematic lymph node dissection or sampling at our center. Among these 315 patients, pathologically positive lymph nodes were found in 16.2% (51/315). The results indicate that preoperative staging should be performed more thoroughly to increase accuracy,

especially for patients who have larger size, non-upper lobe located, high CEA level and micropapillary predominant ACs. A prospective, randomized trial with routine PET-CT is warranted to validate our findings.

Acknowledgements

Disclosure: The authors declare no conflict of interest.

References

1. Siegel R, Naishadham D, Jemal A. Cancer statistics, 2013. CA Cancer J Clin 2013;63:11-30.
2. National Lung Screening Trial Research Team, Church TR, Black WC, et al. Results of initial low-dose computed tomographic screening for lung cancer. N Engl J Med 2013;368:1980-91.
3. Ginsberg RJ, Rubinstein LV. Randomized trial of lobectomy versus limited resection for T1 N0 non-small cell lung cancer. Lung Cancer Study Group. Ann Thorac Surg 1995;60:615-22; discussion 622-3.
4. Carr SR, Schuchert MJ, Pennathur A, et al. Impact of tumor size on outcomes after anatomic lung resection for stage 1A non-small cell lung cancer based on the current staging system. J Thorac Cardiovasc Surg 2012;143:390-7.
5. Scagliotti GV, Pastorino U, Vansteenkiste JF, et al. Randomized phase III study of surgery alone or surgery plus preoperative cisplatin and gemcitabine in stages IB to IIIA non-small-cell lung cancer. J Clin Oncol 2012;30:172-8.
6. Tieu BH, Sanborn RE, Thomas CR Jr. Neoadjuvant therapy for resectable non-small cell lung cancer with mediastinal lymph node involvement. Thorac Surg Clin 2008;18:403-15.
7. Lee BE, Kletsman E, Rutledge JR, et al. Utility of endobronchial ultrasound-guided mediastinal lymph node biopsy in patients with non-small cell lung cancer. J Thorac Cardiovasc Surg 2012;143:585-90.
8. Cho S, Song IH, Yang HC, et al. Predictive factors for node metastasis in patients with clinical stage I non-small cell lung cancer. Ann Thorac Surg 2013;96:239-45.
9. Zhang Y, Sun Y, Shen L, et al. Predictive factors of lymph node status in small peripheral non-small cell lung cancers: tumor histology is more reliable. Ann Surg Oncol 2013;20:1949-54.
10. Watanabe S, Oda M, Tsunezuka Y, et al. Peripheral small-sized (2 cm or less) non-small cell lung cancer with mediastinal lymph node metastasis; clinicopathologic features and patterns of nodal spread. Eur J Cardiothorac Surg 2002;22:995-9.
11. Fukui T, Katayama T, Ito S, et al. Clinicopathological features of small-sized non-small cell lung cancer with mediastinal lymph node metastasis. Lung Cancer 2009;66:309-13.
12. Travis WD, Brambilla E, Noguchi M, et al. International association for the study of lung cancer/american thoracic society/european respiratory society international multidisciplinary classification of lung adenocarcinoma. J Thorac Oncol 2011;6:244-85.
13. El-Sherif A, Gooding WE, Santos R, et al. Outcomes of sublobar resection versus lobectomy for stage I non-small cell lung cancer: a 13-year analysis. Ann Thorac Surg 2006;82:408-15; discussion 415-6.
14. Koike T, Koike T, Yamato Y, et al. Predictive risk factors for mediastinal lymph node metastasis in clinical stage IA non-small-cell lung cancer patients. J Thorac Oncol 2012;7:1246-51.
15. Asamura H, Nakayama H, Kondo H, et al. Lymph node involvement, recurrence, and prognosis in resected small, peripheral, non-small-cell lung carcinomas: are these carcinomas candidates for video-assisted lobectomy? J Thorac Cardiovasc Surg 1996;111:1125-34.
16. Tsutani Y, Miyata Y, Nakayama H, et al. Prediction of pathologic node-negative clinical stage IA lung adenocarcinoma for optimal candidates undergoing sublobar resection. J Thorac Cardiovasc Surg 2012;144:1365-71.
17. Farjah F, Lou F, Sima C, et al. A prediction model for pathologic N2 disease in lung cancer patients with a negative mediastinum by positron emission tomography. J Thorac Oncol 2013;8:1170-80.
18. Zhang Y, Sun Y, Xiang J, et al. A prediction model for N2 disease in T1 non-small cell lung cancer. J Thorac Cardiovasc Surg 2012;144:1360-4.
19. Inoue M, Minami M, Shiono H, et al. Clinicopathologic study of resected, peripheral, small-sized, non-small cell lung cancer tumors of 2 cm or less in diameter: pleural invasion and increase of serum carcinoembryonic antigen level as predictors of nodal involvement. J Thorac Cardiovasc Surg 2006;131:988-93.
20. Roh MS, Lee JI, Choi PJ, et al. Relationship between micropapillary component and micrometastasis in the regional lymph nodes of patients with stage I lung adenocarcinoma. Histopathology 2004;45:580-6.
21. Russell PA, Wainer Z, Wright GM, et al. Does lung adenocarcinoma subtype predict patient survival?: A clinicopathologic study based on the new International

Association for the Study of Lung Cancer/American Thoracic Society/European Respiratory Society international multidisciplinary lung adenocarcinoma classification. J Thorac Oncol 2011;6:1496-504.
22. Warth A, Muley T, Meister M, et al. The novel histologic International Association for the Study of Lung Cancer/American Thoracic Society/European Respiratory Society classification system of lung adenocarcinoma is a stage-independent predictor of survival. J Clin Oncol 2012;30:1438-46.

Cite this article as: Bao F, Yuan P, Yuan X, Lv X, Wang Z, Hu J. Predictive risk factors for lymph node metastasis in patients with small size non-small cell lung cancer. J Thorac Dis 2014;6(12):1697-1703. doi: 10.3978/j.issn.2072-1439.2014.11.05

Original Article

The protective effects of glutamine in a rat model of ventilator-induced lung injury

Chin-Ming Chen[1,2], Kuo-Chen Cheng[3,4], Chien-Feng Li[5], Haibo Zhang[6]

[1]Department of Recreation and Healthcare Management, Chia Nan University of Pharmacy & Science, Tainan, Taiwan; [2]Department of Critical Care Medicine, Chi-Mei Medical Center and Chang Jung Christian University, Tainan, Taiwan; [3]Section of Respiratory Care, Department of Internal Medicine, Chi-Mei Medical Center, Tainan, Taiwan; [4]Department of Safety Health and Environment Engineering, Chung Hwa University of Medical Technology, Tainan, Taiwan; [5]Department of Pathology, Chi Mei Medical Center, Tainan, Taiwan; [6]Keenan Research Center for Biomedical Science of St. Michael's Hospital, University of Toronto, Toronto, ON, Canada

Correspondence to: Haibo Zhang. Room 619, 209 Victoria Street, Toronto, ON, M5B 1W8, Canada. Email: Zhangh@smh.ca.

Background: The mortality rate of patients with acute respiratory distress syndrome (ARDS) is still high despite the use of protective ventilatory strategies. We sought to examine the pharmacological effects of glutamine (GLN) in a two-hit model of endotoxin-induced inflammation followed by ventilator-induced lung injury (VILI). We hypothesized that the administration of GLN ameliorates the VILI.

Methods: Sprague-Dawley rats were anesthetized and given lipopolysaccharide (LPS) intratracheally as a first hit to induce lung inflammation, followed 24 h later by a second hit of mechanical ventilation (MV) with either low tidal volume (6 mL/kg) with 5 cmH_2O of positive end-expiratory pressure (PEEP) or high tidal volume (22 mL/kg) with zero PEEP for 4 h. GLN or lactated Ringer's solution as the placebo was administered intravenously 15 min prior to MV.

Results: In the LPS-challenged rats ventilated with high tidal volume, the treatment with GLN improved lung injury indices, lung mechanics and cytokine responses compared with the placebo group.

Conclusions: The administration of GLN given immediately prior to MV may be beneficial in the context of reducing VILI.

Keywords: Acute respiratory distress syndrome (ARDS); mechanical ventilation (MV); glutamine (GLN); cytokines

Submitted Jul 20, 2014. Accepted for publication Sep 24, 2014.
doi: 10.3978/j.issn.2072-1439.2014.11.06
View this article at: http://dx.doi.org/10.3978/j.issn.2072-1439.2014.11.06

Introduction

Acute respiratory distress syndrome (ARDS) is a leading cause of death in critically ill patients (1,2). ARDS is characterized by leukocyte recruitment and increased permeability in the pulmonary capillaries and epithelial barrier resulting in lung edema and tissue hypoxia. Almost all patients with ARDS require mechanical ventilation (MV) for life support (2). However, the utilization of MV may cause alveolar overdistension or shear forces generated during the repetitive opening and closing of the lung units, resulting in atelectasis that leads to ventilator-induced lung injury (VILI) (2). The VILI is frequently associated with multiple distal organ dysfunction as a result of biotrauma (3). The activation of nuclear factor (NF)-κB with the subsequent gene transcription of inflammatory mediators has been previously documented in the context of VILI (4,5). Although the use of low tidal volume has been shown to improve the clinical outcome of certain populations of patients with ARDS, the overall mortality rate of patients with ARDS is still high (6). Furthermore, the application of MV tends towards less "controlled" in the ICU than in the operating room because more patients receiving ventilation are conscious during their ICU stay, making designated low tidal volume ventilation challenging (7-9). There is, therefore, a need to identify therapeutic approaches

in addition to the use of protective MV strategies in the management of ARDS.

Glutamine (GLN) is a conditional essential amino acid that serves as an important energy source for cell proliferation (10). GLN is an essential component for numerous metabolic functions including acid-base homeostasis, gluconeogenesis, nitrogen transport and the synthesis of proteins and nucleic acids (11). GLN has been demonstrated to protect the lung from injury in animal models of ischemia-reperfusion injury, endotoxemia, hyperoxia, smoke inhalation and sepsis (12-17). GLN has been shown to exert immunomodulating properties that attenuate the production of cytokines and chemokines in response to oxidative stress (18) and in animal models of endotoxin-induced lung injury (16,19,20). The beneficial effects of GLN are believed to be associated with the attenuation of NF-κB nuclear translocation or activation, the enhancement of heat shock protein expression (12,21), and the precursor property for glutathione (GSH) synthesis (16,22,23). However, the effects of treatment with GLN are inconclusive in critically ill patients (11,24-27), which might be due to the complicated underlying diseases and the timing of the therapeutic intervention. Because physicians know exactly when MV is applied at bedside, we thus test the hypothesis that the administration of GLN is beneficial to the attenuation of VILI via its anti-inflammatory effects when administered at the onset of MV following acute lung injury.

Materials and methods

Animal preparation

This study was carried out in strict accordance with the recommendations in the Guide for the Care and Use of Laboratory Animals of the National Institutes of Health. The protocol was approved by the Animal Care and Use Committee of Chi-Mei Hospital (Permit Number: CMHFR10212). All surgery was performed under general anesthesia, and all efforts were made to minimize suffering. Male Sprague-Dawley rats (300-400 g) were anesthetized by the intraperitoneal injection of urethane (2 mg/kg, Sigma, St. Louis, MO, USA). Endotoxin (Escherichia coli O55:B5, Sigma) was administered intratracheally at 0.1 mg/kg. The animals were allowed to recover from anesthesia and returned to their cages with access to food and water for 24 h.

The animals were then anesthetized by the intraperitoneal injection of urethane. An intravenous cannula was inserted and kept in the tail vein for the maintenance of anesthesia by a continuous infusion of ketamine (15 mg/kg/h), xylazine (3 mg/kg/h), and pancuronium (0.35 mg/kg/h) and infusion of lactated Ringer's solution. A tracheostomy was performed, and a 14-gauge cannula (Angiocath IV, 2.1×48 mm, Becton Dickinson Infusion Therapy Systems, Sandy, UT) was inserted into the trachea. The rats were ventilated with a Servo 300 ventilator (Siemens, Sweden) using a tidal volume (Vt) of 6 mL/kg, positive end-expiratory pressure (PEEP) of 5 cmH_2O, and respiratory rate of 50 breaths/min with a fraction of inspired oxygen (FiO_2) of 0.4. The right carotid artery was cannulated (Angiocath IV Catheter; 24-gauge) to monitor the mean arterial pressure (MAP) and to collect samples for blood gas measurements.

The animals were stabilized for 30 min after the surgical preparation and assigned to receive MV for 4 h randomly at either low or high Vt. The low Vt groups were ventilated with a Vt of 6 mL/kg and PEEP of 5 cmH_2O at a rate of 45-55 breaths/min. The high Vt groups were ventilated with a Vt of 22 mL/kg and zero PEEP at a respiratory rate of 16-18 breaths/min. The FiO_2 remained as 0.4. GLN (20% Dipeptiven, Fresenius Kabi, Germany) containing 20 g of N(2)-L-alanyl-L-glutamine at a bolus of 0.75 g/kg (3.75 mL/kg) or lactated Ringer's solution as placebo, was administered i.v. in a blind fashion 15 min prior to the randomization of the MV strategies.

Additional groups of naive control and LPS alone without ventilation served as time-matched controls (*Figure 1*). Thus, six groups of ten animals each were studied: naive control animals without LPS and ventilator (Naive), LPS-challenged animals receiving no MV (Control), LPS-challenged animals receiving MV at low Vt (LV), LPS-challenged animals receiving MV at high Vt (HV), LPS-challenged animals receiving MV at low Vt and treated with GLN (LVG), and LPS-challenged animals receiving MV at high Vt and treated with GLN (HVG).

Measurements

Lung elastance was calculated hourly using the formula of (Plateau Pressure—PEEP)/Vt during the study. Blood gases were measured at the beginning of the randomization and hourly thereafter.

The rats were sacrificed by sodium pentobarbital overdose. The lungs were excised via a midline sternotomy, and the static pressure-volume curves were constructed by the manual injection of 0.5 to 1 cm^3 aliquots of air in a stepwise manner starting at atmospheric pressure and continuing until achieving an airway pressure of 30 cmH_2O.

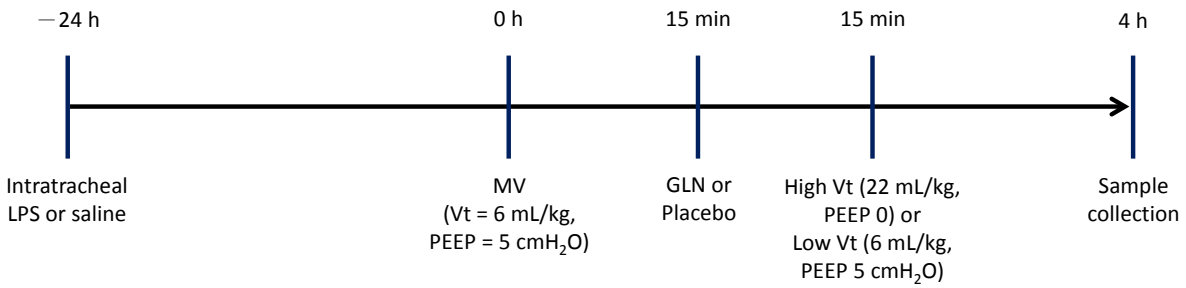

Figure 1 Experimental design. MV, mechanical ventilation; GLN, glutamine.

This procedure was followed by deflation using a similar stepwise approach. Volumes were maintained at each step of air inflation or deflation for 6 seconds.

The left lung was lavaged (bronchoalveolar lavage, BAL) for the assessment of cell differentiation and measurement of cytokines. The right upper lungs were used to measure the wet-to-dry (W/D) lung weight ratio. The measurement of cytokines (IL-1β, IL-6, IL-10, CXCL1 and TNF-α) in the plasma and BAL fluid was performed in a blinded fashion by technicians using rat-specific DuoSet ELISA kits (R & D Systems, Minneapolis, MN, USA).

The rest of the right lungs were used for the histological analysis and assessment of lung injury. The lung injury score was evaluated by a pathologist (CFL) who was blinded to the experimental groups, based on the methods described previously, including neutrophil counts in the alveoli and interstitial space, hyaline membrane, proteinaceous debris filling the airspaces, and alveolar septal thickening (28). Five regions in each lung histology slide were examined. The resulting injury score was represented by a continuous value between zero and one.

Statistical analysis

Data are reported as the means ± standard error and were analyzed by SPSS 13.0 (SPSS Inc. Chicago, IL, USA) using one-way analysis of variance, followed by Bonferroni's multiple comparisons. Two-sided analysis was performed and the significance level was considered to be $P<0.05$.

Results

The mean body weight (355, 351, 359, 363, 357 and 357 g in the Naive, Control, LV, HV, LVG and HVG group, respectively) and length (25.8, 25.7, 26.0, 26.4, 25.9 and 25.8 cm, respectively) was similar in all animals studied. The hemodynamics, including MAP and heart rate, were also similar at baseline and did not differ in all animals during the study (*Table 1*). The amount of fluid infused was identical (≈2.5 mL lactated Ringer's solution) in all rats during the study.

The values of blood gas were similar at baseline in all animals, but the oxygen indices, including PaO_2 and SaO_2, were significantly lower in the HV group at 120 min and onwards (respectively, 149.1±7.6 mmHg and 97.7±0.3% at 120 min, 118.7±11.1 mmHg and 92.6±1.8% at 180 min, 102.1±10.8 mmHg and 89.6±2.0% at 240 min), compared with the other groups (All $P<0.001$) (*Figure 2A,B*).

The lung elastance levels were similar at baseline but increased significantly in the HV group compared with the other groups at 60 min after randomization (*Figure 2C*). Similarly, the static pressure-volume curves showed the worst compliance in the HV group compared with the other groups at the end of the study (*Figure 2D*).

The representative lung histology showed aggravated alveolar collapse and perivascular and peribronchial edema associated with neutrophil infiltration in the HV group. The administration of GLN significantly attenuated the lung injury (*Figure 3*).

The lung W/D ratio and the lung injury score were significantly higher in the HV group than in the other groups (all $P<0.001$) (*Table 2*). The treatment with GLN resulted in a significant reduction in lung injury after MV with a high Vt (*Table 2*).

The total cell count in BAL fluid was somewhat higher in the HV group [$(2.5\pm0.5)\times10^7$/mL], but the difference was not significant compared with the HVG group [$(2.3\pm0.2)\times10^7$/mL, $P=0.290$] and LV group [$(1.9\pm0.2)\times10^7$/mL, $P=0.088$] (*Table 2*). The total cell count was significantly lower in the LVG [$(1.6\pm0.1)\times10^7$/mL, $P=0.011$] and naive ($0.2\pm0.1\times10^7$/mL, $P<0.001$) groups than in the HV group (*Table 2*). The neutrophil count was significantly higher in the HV group than in the other groups (all $P<0.001$) (*Table 2*).

Table 1 Hemodynamics and blood gas analysis (n=10 per group)

Variables	Baseline	60 min	120 min	180 min	240 min
Heart rate (min^{-1})					
LV	406.1±7.9	418.2±7.7	408.1±7.3	403.1±7.6	394.3±7.1
HV	403.6±6.5	414.6±7.3	415.4±6.7	402.0±6.1	395.2±9.9
LVG	411.2±13.3	420.2±11.3	414.3±10.0	403.2±8.2	401.5±8.6
HVG	411.0±4.2	416.2±4.1	415.1±5.5	404.7±2.9	399.0±4.3
MAP (mmHg)					
LV	106.2±2.9	104.2±1.4	102.2±1.6	96.9±1.9	97.1±2.3
HV	103.1±2.2	105.4±1.6	104.2±2.4	100.4±1.5	100.0±2.3
LVG	101.9±1.6	101.5±1.6	100.5±1.4	98.1±1.6	98.1±1.9
HVG	102.4±2.1	104.7±1.9	100.5±2.2	97.3±2.1	99.4±1.9
pH					
LV	7.36±0.06	7.41±0.04	7.41±0.04	7.41±0.04	7.41±0.07
HV	7.39±0.04	7.36±0.03	7.39±0.03	7.41±0.05	7.40±0.04
LVG	7.38±0.06	7.40±0.03	7.40±0.04	7.43±0.03	7.43±0.04
HVG	7.39±0.02	7.39±0.03	7.40±0.04	7.42±0.04	7.41±0.04
$PaCO_2$ (mmHg)					
LV	42.0±1.2	41.2±1.1	40.2±1.2	40.3±1.1	36.7±0.6
HV	42.1±0.8	42.0±0.4	42.9±0.7	38.2±0.7	37.0±0.8
LVG	41.7±1.1	40.1±1.1	40.8±0.7	39.1±0.6	38.9±1.0
HVG	41.6±1.1	42.4±0.8	42.2±0.8	40.0±0.9	39.2±0.7
HCO_3^- (meq/L)					
LV	25.6±0.7	25.6±0.6	24.8±0.7	24.8±0.2	22.5±1.2
HV	25.3±0.4	26.4±0.5	25.7±0.7	24.3±0.7	23.5±1.0
LVG	24.0±0.5	24.5±0.6	24.9±0.6	24.8±0.8	24.3±0.8
HVG	24.3±0.5	25.2±0.4	25.1±0.7	24.8±0.9	24.0±1.1

LV, LPS + low Vt; HV, LPS + high Vt; LVG, LPS + low Vt + glutamine; HVG, LPS + high Vt + glutamine; LPS, lipopolysaccharide.

The plasma levels of IL-1β, IL-6 and IL-10 were higher in the HV group than in the other groups (*Figure 4*). The levels of IL-1β, IL-6, CXCL1 and TNF-α in the BAL fluids were higher in the HV group than in the other groups (*Figure 5*).

Discussion

In the present study, we demonstrated that the administration of GLN protected the lung from the two-hit injury by the attenuation of inflammatory responses, including neutrophil infiltration and cytokine storm. The animals treated with GLN showed better lung mechanics and lung morphology under high Vt MV compared with the placebo group. These results suggest a beneficial effect of the administration of GLN in the context of VILI.

Inflammation and oxidative stress play important roles in the pathogenesis of VILI (3). The release of TNF-α, IL-1β, IL-6 and the CXC chemokine family is associated with neutrophil recruitment (29) and correlated with the severity and mortality of ARDS (30). CXCL1, the homolog of human IL-8 in rats, plays a pivotal role as a chemotactic factor for neutrophil infiltration (31). IL-8 has been shown to be released by lung epithelial cells in response to mechanical stress (32). Previous studies reported that the administration of GLN can reduce IL-1β, IL-8 and TNF-α in LPS-induced lung injury (19), diminish IL-6 in abdominal sepsis (33,34), and inhibit IL-6, IL-8 and TNF-α production in human monocytes stimulated with LPS (35). The anti-inflammatory effects of GLN observed in other

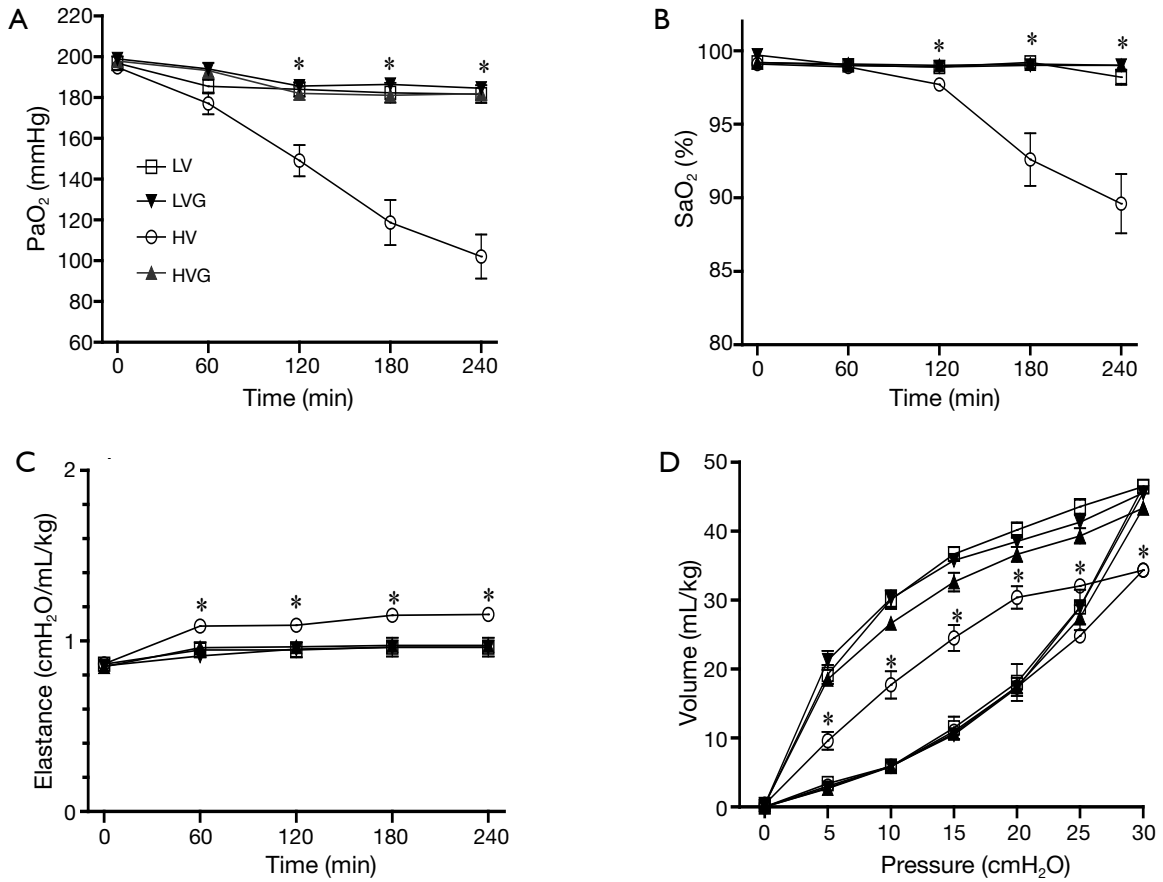

Figure 2 Arterial PaO_2 (A), SaO_2 (B) and lung elastance (C) during 4-h mechanical ventilation after randomization. Static compliance (D) curves at the end of the 4-h mechanical ventilation. *, P<0.05 HV *vs.* other groups. LV, LPS + low Vt; HV, LPS + high Vt; LVG, LPS + low Vt + glutamine; HVG, LPS + high Vt + glutamine; LPS, lipopolysaccharide.

models used in previous studies were confirmed in our model of VILI in the present study.

Neutrophil activation is largely responsible for not only the production of cytokines and chemokines but also oxidative bursts and release of proteolytic enzymes, all contributing to lung injury (6,36,37). In particular, intracellular oxidative stress leads to vascular barrier disruption and pulmonary edema (38,39). Our results observed in the ARDS/VILI model are consistent with those demonstrated in other models, in which the administration of GLN led to significantly reduced neutrophil recruitment in the lung (33,40). The two most important mechanisms by which GLN is protective include its antioxidant effect through the preservation of GSH and the induction of heat shock protein 70 via the O-linked glycosylation-dependent activation of hexosamine biosynthesis (41,42). This heat shock protein is known to enhance cell survival and attenuate the systemic inflammatory response in the setting of lung injury (43). In particular, the enhanced levels of tissue GSH and heat shock proteins may be partially responsible for the attenuated cytokine responses (44) and activation of NF-κB (23,45).

The importance of GLN may have been overlooked in ARDS. Patients with critical illness have been reported to be at high risk of GLN depletion, which might contribute to the development of ARDS (46). In fact, GLN deficiency may have caused failure of the host defense mechanism, delayed wound healing, increased epithelial permeability and bacterial translocation (22). In addition, GLN–enriched parenteral nutrition has been shown to augment glucose use (47) and decrease insulin resistance (48). In experimental models, GLN supplementation was protective against lung injury induced by ischemia-reperfusion, endotoxins, hyperoxia, smoke inhalation and sepsis (12-17).

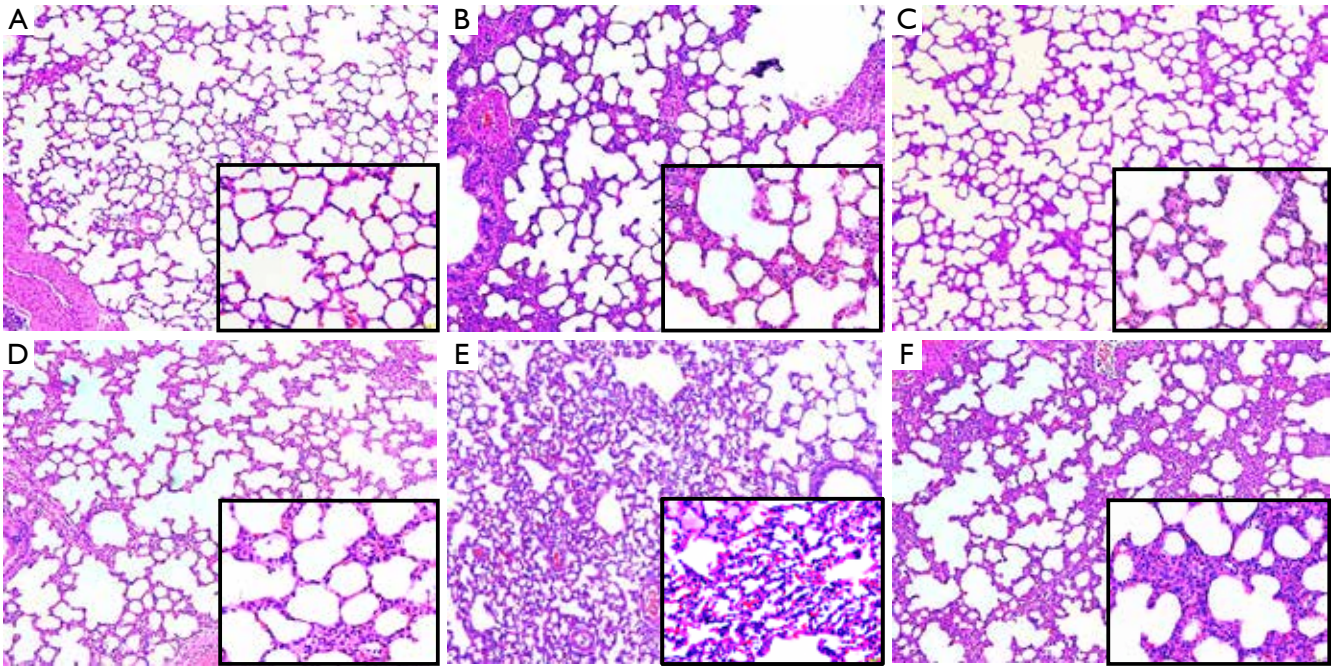

Figure 3 Representative lung histology slides (original magnification 100×/400×). (A) Naive: naive control; (B) control: LPS alone; (C) LV: LPS + low Vt; (D) HV: LPS + Vt; (E) LVG: LPS + low Vt + glutamine; and (F) HVG: LPS + high Vt + glutamine. LPS, lipopolysaccharide.

Table 2 Cell counts in lung lavage fluids, lung wet-to-dry ratio and lung injury score

Group	Total cells (×10^7/mL)	Neutrophils (%)	Lung W/D ratio	Lung injury scores
Naive	0.2±0.1*	0*	4.3±0.3	0.03±0.03*
Control	1.3±0.1†	70.7±1.1	4.5±0.2	0.50±0.02†
LV	1.9±0.2	74.1±0.9	4.6±0.1	0.51±0.06†
HV	2.5±0.5	80.2±0.7	6.1±0.3*	0.84±0.05
LVG	1.6±0.1†	74.5±1.0	4.6±0.1	0.49±0.04†
HVG	2.3±0.2	74.4±1.2	4.7±0.1	0.63±0.07

*, P<0.05 *vs.* other groups; †, P<0.05 *vs.* HV. Naive, naive control; Control, LPS alone; LV, LPS + low Vt; HV, LPS + high Vt; LVG, LPS + low Vt + glutamine; HVG, LPS + high Vt + glutamine; LPS, lipopolysaccharide.

In clinical settings, a recent trial and a meta-analysis did not show significant beneficial effects in critically ill patients treated with GLN (24,25). However, several randomized, controlled clinical trials have reported that supplementation with GLN may reduce the occurrence of infections, length of the hospital stay and mortality rate in critically ill patients (11,26) and may improve the survival rate in burn patients with a Gram-negative bacterial infection (27). Current guidance on nutritional support by the European Societies of Parenteral and Enteral Nutrition recommends GLN supplementation at the grade A level for critically ill patients (49).

In the context of VILI, we employed the two-hit model to reproduce the clinical features of ARDS. Our model used in the present study is different from previous studies testing the effects of GLN in single injury models (16,33,40). For example, (I) we used a relatively low dose of LPS to prime the lung followed by MV to induce VILI, as observed in clinical situations of ARDS. The previous studies used a single hit with either a high dose of LPS or severe sepsis to study the effects of GLN in infection (16,33). Therefore, our study focused on the effects of GLN on

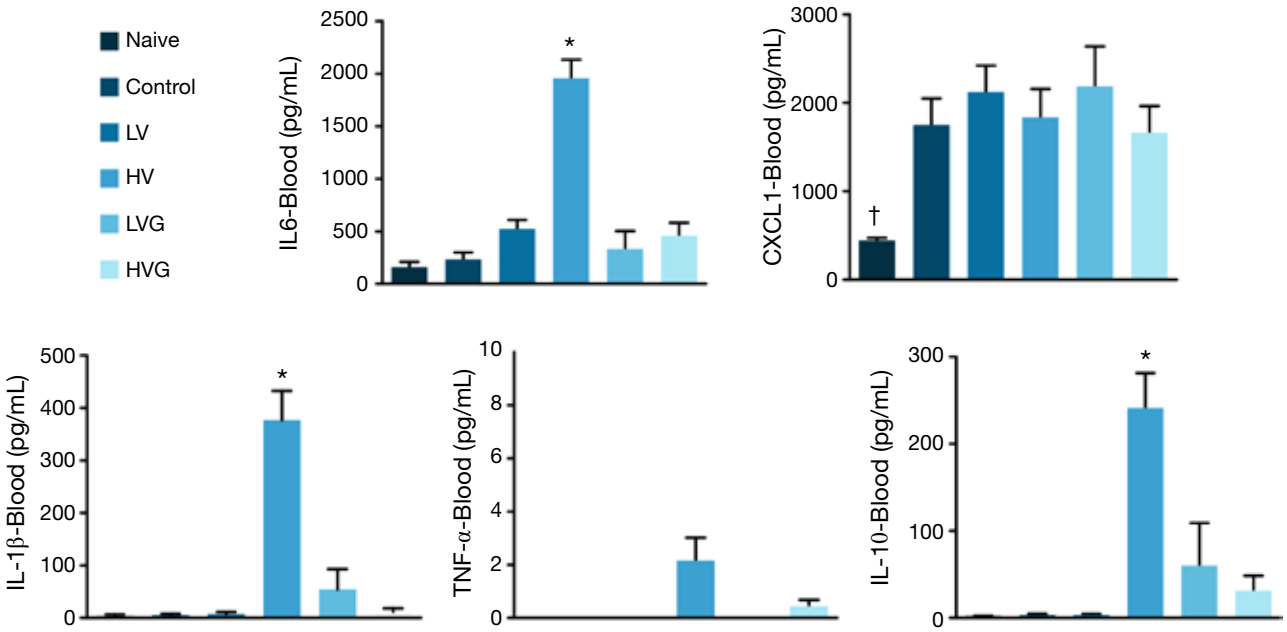

Figure 4 Cytokine levels in the plasma (n=5 for each group). *, P<0.05 HV *vs.* other groups; †, P<0.05 naive *vs.* other groups. Naive, naive control; Control, LPS alone; LV, LPS + low Vt; HV, LPS + high Vt; LVG, LPS + low Vt + glutamine; HVG, LPS + high Vt + glutamine; LPS, lipopolysaccharide.

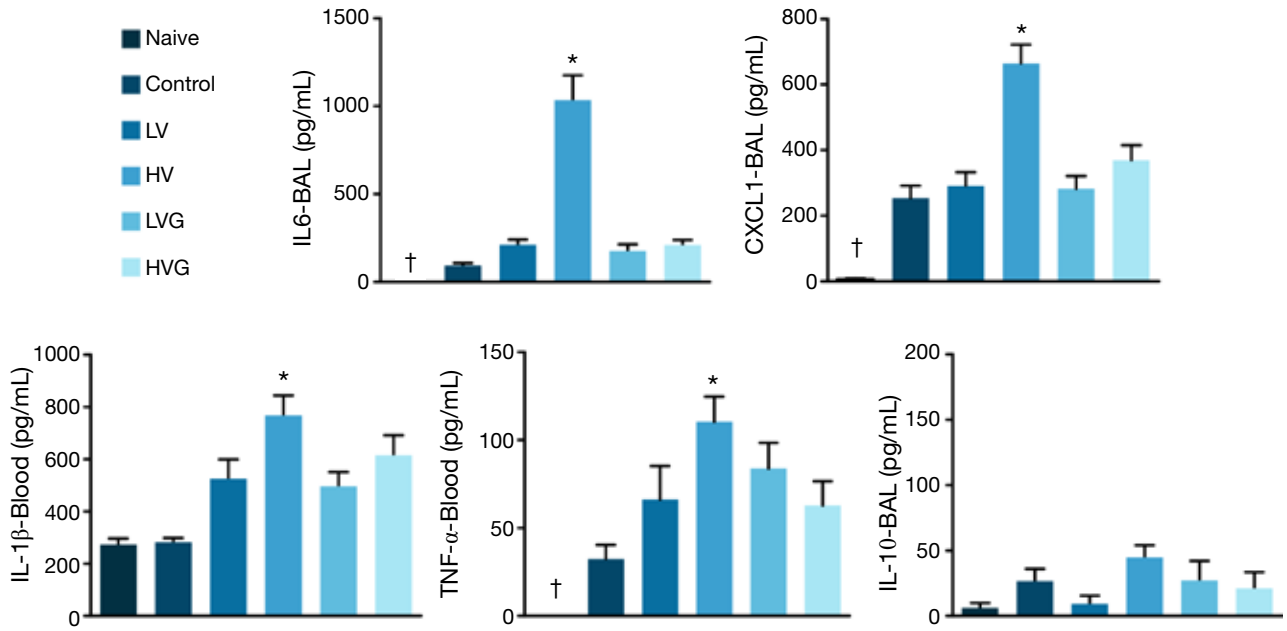

Figure 5 Cytokine levels in the BAL (n=8-10 for each group). *, P<0.05 HV *vs.* other groups; †, P<0.05 naive *vs.* other groups. Naive, naive control; Control, LPS alone; LV, LPS + low Vt; HV, LPS + high Vt; LVG, LPS + low Vt + glutamine; HVG, LPS + high Vt + glutamine; LPS, lipopolysaccharide.

VILI. (II) We administered GLN after LPS instillation, but GLN was given as a pre-treatment prior to LPS induction in a previous study (19). Our model addressed the effects of GLN after an inflammatory response has been established. (III) We administered GLN 30 min before the randomization of the MV strategies in the attempt to attenuate VILI, which is appropriate as the exact time when MV would be applied at bedside is known. This treatment approach would be very relevant to bedside management for ARDS/VILI.

In summary, the beneficial effects of GLN in our study can be explained by several potential mechanisms: (I) the attenuation of neutrophil infiltration in the lung, which is a significant factor in the pathogenesis of ARDS; (II) the reduction of biotrauma, including the cytokine responses (21,34); (III) the preservation of tissue GSH levels that maintain tissue antioxidant capacity by the administration of GLN (16,23,45); and (IV) the up-regulation of heat shock protein 70 following the treatment with GLN (12).

A major limitation of the study is that we were unable to measure the plasma levels of GLN and oxidative stress. Other investigators have previously demonstrated that intracellular GLN depletion in muscle occurred early and remained low during ICU stay (50) and that the low plasma level of GLN was associated with the high mortality (51). Therefore, the beneficial effects of GLN might have been overlooked in the context of VILI. Further research in the field is required to confirm our findings for a potential novel therapeutic target in VILI. The other limitation is that we used only one dose of GLN (0.75 mg/kg), which was similar to the dose used in most previous studies (12-14,16,19). Because the possibility that multiple doses, continuous infusion and/or the enteral route could yield better histological results is not fully excluded, the sensitivity and specificity of the effect cannot be ascertained.

Conclusions

In the present study, we demonstrate that the treatment with GLN administered immediately prior to MV may be beneficial in reducing VILI during ARDS.

Acknowledgements

Authors' contributions: Conceived and designed the experiments: CMC and HZ. Performed the experiments: CMC. Analyzed the data: CMC, KCC and CFL. Contributed reagents/materials/analysis tools: CMC and KCC. Wrote the paper: CMC and HZ.

Disclosure: The authors declare no conflict of interest.

References

1. Ware LB, Matthay MA. The acute respiratory distress syndrome. N Engl J Med 2000;342:1334-49.
2. Rubenfeld GD, Caldwell E, Peabody E, et al. Incidence and outcomes of acute lung injury. N Engl J Med 2005;353:1685-93.
3. Tremblay L, Valenza F, Ribeiro SP, et al. Injurious ventilatory strategies increase cytokines and c-fos m-RNA expression in an isolated rat lung model. J Clin Invest 1997;99:944-52.
4. Held HD, Boettcher S, Hamann L, et al. Ventilation-induced chemokine and cytokine release is associated with activation of nuclear factor-kappaB and is blocked by steroids. Am J Respir Crit Care Med 2001;163:711-6.
5. Ding N, Wang F, Xiao H, et al. Mechanical ventilation enhances HMGB1 expression in an LPS-induced lung injury model. PLoS One 2013;8:e74633.
6. Ventilation with lower tidal volumes as compared with traditional tidal volumes for acute lung injury and the acute respiratory distress syndrome. The Acute Respiratory Distress Syndrome Network. N Engl J Med 2000;342:1301-8.
7. Strøm T, Martinussen T, Toft P. A protocol of no sedation for critically ill patients receiving mechanical ventilation: a randomised trial. Lancet 2010;375:475-80.
8. Ferguson ND. Low tidal volumes for all? JAMA 2012;308:1689-90.
9. Gajic O, Dara SI, Mendez JL, et al. Ventilator-associated lung injury in patients without acute lung injury at the onset of mechanical ventilation. Crit Care Med 2004;32:1817-24.
10. Castell L. Glutamine supplementation in vitro and in vivo, in exercise and in immunodepression. Sports Med 2003;33:323-45.
11. Oliveira GP, Dias CM, Pelosi P, et al. Understanding the mechanisms of glutamine action in critically ill patients. An Acad Bras Cienc 2010;82:417-30.
12. Singleton KD, Serkova N, Beckey VE, et al. Glutamine attenuates lung injury and improves survival after sepsis: role of enhanced heat shock protein expression. Crit Care Med 2005;33:1206-13.
13. Singleton KD, Serkova N, Banerjee A, et al. Glutamine attenuates endotoxin-induced lung metabolic dysfunction: potential role of enhanced heat shock protein 70. Nutrition

2005;21:214-23.
14. Perng WC, Huang KL, Li MH, et al. Glutamine attenuates hyperoxia-induced acute lung injury in mice. Clin Exp Pharmacol Physiol 2010;37:56-61.
15. Peng CK, Huang KL, Wu CP, et al. Glutamine protects ischemia-reperfusion induced acute lung injury in isolated rat lungs. Pulm Pharmacol Ther 2011;24:153-61.
16. Zhang F, Wang X, Pan L, et al. Glutamine attenuates lipopolysaccharide-induced acute lung injury. Nutrition 2009;25:692-8.
17. Li W, Qiu X, Wang J, et al. The therapeutic efficacy of glutamine for rats with smoking inhalation injury. Int Immunopharmacol 2013;16:248-53.
18. Coëffier M, Miralles-Barrachina O, Le Pessot F, et al. Influence of glutamine on cytokine production by human gut in vitro. Cytokine 2001;13:148-54.
19. Liu JC, Wang HT, Wang W. Protective effects of alanyl-glutamine on acute lung injury induced by lipopolysaccharide in rats. Zhong Nan Da Xue Xue Bao Yi Xue Ban 2008;33:1095-100.
20. Hou YC, Pai MH, Chiu WC, et al. Effects of dietary glutamine supplementation on lung injury induced by lipopolysaccharide administration. Am J Physiol Lung Cell Mol Physiol 2009;296:L288-95.
21. Singleton KD, Beckey VE, Wischmeyer PE. Glutamine prevents activation of NF-kappaB and stress kinase pathways, attenuates inflammatory cytokine release, and prevents acute respiratory distress syndrome (ARDS) following sepsis. Shock 2005;24:583-9.
22. Wernerman J. Clinical use of glutamine supplementation. J Nutr 2008;138:2040S-2044S.
23. Zhang F, Wang X, Wang W, et al. Glutamine reduces TNF-alpha by enhancing glutathione synthesis in lipopolysaccharide-stimulated alveolar epithelial cells of rats. Inflammation 2008;31:344-50.
24. Bollhalder L, Pfeil AM, Tomonaga Y, et al. A systematic literature review and meta-analysis of randomized clinical trials of parenteral glutamine supplementation. Clin Nutr 2013;32:213-23.
25. Andrews PJ, Avenell A, Noble DW, et al. Randomised trial of glutamine, selenium, or both, to supplement parenteral nutrition for critically ill patients. BMJ 2011;342:d1542.
26. Wischmeyer PE. Glutamine: role in critical illness and ongoing clinical trials. Curr Opin Gastroenterol 2008;24:190-7.
27. Lin JJ, Chung XJ, Yang CY, et al. A meta-analysis of trials using the intention to treat principle for glutamine supplementation in critically ill patients with burn. Burns 2013;39:565-70.
28. Matute-Bello G, Downey G, Moore BB, et al. An official American Thoracic Society workshop report: features and measurements of experimental acute lung injury in animals. Am J Respir Cell Mol Biol 2011;44:725-38.
29. Williams AE, Chambers RC. The mercurial nature of neutrophils: still an enigma in ARDS? Am J Physiol Lung Cell Mol Physiol 2014;306:L217-30.
30. Moldoveanu B, Otmishi P, Jani P, et al. Inflammatory mechanisms in the lung. J Inflamm Res 2009;2:1-11.
31. Levitt JE, Gould MK, Ware LB, et al. The pathogenetic and prognostic value of biologic markers in acute lung injury. J Intensive Care Med 2009;24:151-67.
32. Vlahakis NE, Schroeder MA, Limper AH, et al. Stretch induces cytokine release by alveolar epithelial cells in vitro. Am J Physiol 1999;277:L167-73.
33. Oliveira GP, Oliveira MB, Santos RS, et al. Intravenous glutamine decreases lung and distal organ injury in an experimental model of abdominal sepsis. Crit Care 2009;13:R74.
34. Yeh CL, Hsu CS, Yeh SL, et al. Dietary glutamine supplementation modulates Th1/Th2 cytokine and interleukin-6 expressions in septic mice. Cytokine 2005;31:329-34.
35. Raspé C, Czeslick E, Weimann A, et al. Glutamine and alanine-induced differential expression of intracellular IL-6, IL-8, and TNF-α in LPS-stimulated monocytes in human whole-blood. Cytokine 2013;62:52-7.
36. Grommes J, Soehnlein O. Contribution of neutrophils to acute lung injury. Mol Med 2011;17:293-307.
37. Zhang H, Downey GP, Suter PM, et al. Conventional mechanical ventilation is associated with bronchoalveolar lavage-induced activation of polymorphonuclear leukocytes: a possible mechanism to explain the systemic consequences of ventilator-induced lung injury in patients with ARDS. Anesthesiology 2002;97:1426-33.
38. Davidovich N, DiPaolo BC, Lawrence GG, et al. Cyclic stretch-induced oxidative stress increases pulmonary alveolar epithelial permeability. Am J Respir Cell Mol Biol 2013;49:156-64.
39. Reddy SP, Hassoun PM, Brower R. Redox imbalance and ventilator-induced lung injury. Antioxid Redox Signal 2007;9:2003-12.
40. Murphy CG, Chen G, Winter DC, et al. Glutamine preconditioning protects against tourniquet-induced local and distant organ injury in a rodent ischemia-reperfusion model. Acta Orthop 2007;78:559-66.
41. Hamiel CR, Pinto S, Hau A, et al. Glutamine enhances

heat shock protein 70 expression via increased hexosamine biosynthetic pathway activity. Am J Physiol Cell Physiol 2009;297:C1509-19.
42. Singleton KD, Wischmeyer PE. Glutamine induces heat shock protein expression via O-glycosylation and phosphorylation of HSF-1 and Sp1. JPEN J Parenter Enteral Nutr 2008;32:371-6.
43. Wheeler DS, Wong HR. Heat shock response and acute lung injury. Free Radic Biol Med 2007;42:1-14.
44. Ribeiro SP, Villar J, Downey GP, et al. Effects of the stress response in septic rats and LPS-stimulated alveolar macrophages: evidence for TNF-alpha posttranslational regulation. Am J Respir Crit Care Med 1996;154:1843-50.
45. Belmonte L, Coëffier M, Le Pessot F, et al. Effects of glutamine supplementation on gut barrier, glutathione content and acute phase response in malnourished rats during inflammatory shock. World J Gastroenterol 2007;13:2833-40.
46. Planas M, Schwartz S, Arbós MA, et al. Plasma glutamine levels in septic patients. JPEN J Parenter Enteral Nutr 1993;17:299-300.
47. Déchelotte P, Hasselmann M, Cynober L, et al. L-alanyl-L-glutamine dipeptide-supplemented total parenteral nutrition reduces infectious complications and glucose intolerance in critically ill patients: the French controlled, randomized, double-blind, multicenter study. Crit Care Med 2006;34:598-604.
48. Bakalar B, Duska F, Pachl J, et al. Parenterally administered dipeptide alanyl-glutamine prevents worsening of insulin sensitivity in multiple-trauma patients. Crit Care Med 2006;34:381-6.
49. Singer P, Berger MM, Van den Berghe G, et al. ESPEN Guidelines on Parenteral Nutrition: intensive care. Clin Nutr 2009;28:387-400.
50. Rotstein OD. Modeling the two-hit hypothesis for evaluating strategies to prevent organ injury after shock/resuscitation. J Trauma 2003;54:S203-6.
51. Oudemans-van Straaten HM, Bosman RJ, Treskes M, et al. Plasma glutamine depletion and patient outcome in acute ICU admissions. Intensive Care Med 2001;27:84-90.

Cite this article as: Chen CM, Cheng KC, Li CF, Zhang H. The protective effects of glutamine in a rat model of ventilator-induced lung injury. J Thorac Dis 2014;6(12):1704-1713. doi: 10.3978/j.issn.2072-1439.2014.11.06

Original Article

Lung cancer staging: the value of PET depends on the clinical setting

Frank C. Detterbeck[1], Santiago Figueroa Almanzar[2]

[1]Department of Surgery, Division of Thoracic Surgery, Yale University School of Medicine, New Haven, CT 06520-8062, USA; [2]General University Hospital of Valencia, Avda, Tres Cruces 2, Valencia 46014, Spain

Correspondence to: Frank C. Detterbeck, MD. Department of Surgery, Division of Thoracic Surgery, Yale University School of Medicine, PO Box 208062, New Haven, CT 06520-8062, USA. Email: frank.detterbeck@yale.edu; Santiago Figueroa Almanzar, MD. Clinical University Hospital of Valencia, Avda, Blasco Ibañez 17, Valencia 46010, Spain. Email: santiago.figueroa@me.com.

Background: Although positron emission tomography (PET) imaging is widely recommended in the evaluation of patients with lung cancer, randomized controlled trials (RCTs) assessing this have demonstrated inconsistent results. We asked whether differences in the clinical context and endpoints could explain these discrepancies.

Methods: We used realist synthesis methods to analyze how contextual differences among RCTs affected the results. We focused on RCTs to minimize confounding yet permit evaluation of differences by comparing across studies.

Results: This analysis suggests that the impact of PET depends on the clinical setting. PET is of greatest benefit in identifying M1 disease in patients with a high chance of such involvement and when little traditional imaging [e.g., abdominal/pelvis computed tomography (CT) and bone scan] is used. Identification of N2,3 involvement by PET prior to resection is seen primarily when there is at least a moderate probability of such and the rate of invasive staging is high. The rate of N2 disease not identified preoperatively appears to increase if PET is used to avoid invasive mediastinal staging in clinical settings in which the risk of N2,3 involvement is moderately high. There is both a potential benefit in avoiding stage-inappropriate resection as well as a risk of missed (stage-appropriate) resection if PET findings are not evaluated carefully.

Conclusions: A blanket recommendation for PET may be too simplistic without considering nuances of the clinical setting.

Keywords: Non-small cell lung cancer; positron emission tomography (PET); staging

Submitted Jun 28, 2014. Accepted for publication Sep 23, 2014.
doi: 10.3978/j.issn.2072-1439.2014.11.16
View this article at: http://dx.doi.org/10.3978/j.issn.2072-1439.2014.11.16

Introduction

Positron emission tomography (PET)—more recently PET with integrated computed tomography (PET/CT)—has become a cornerstone in evaluating patients with lung cancer. This paper focuses on the impact of PET in the pretreatment evaluation of patients with suspected lung cancer. One can look at specific components of this process, such as diagnosis or identification of nodal or distant metastases, but the clinical value is determined by the overall impact of PET on the accuracy of pre-treatment patient evaluation (i.e., definition of disease extent).

Randomized controlled trials (RCTs) assessing the value of PET in patients with known or suspected lung cancer have yielded somewhat inconsistent results. The RCTs suggest that upfront PET is similarly efficient compared to traditional staging (1) and that adding PET to traditional staging does (2) or does not (3) identify more metastases, and does (1,4,5) or does not (3) reduce the number of so-called "futile" thoracotomies. PET does (1) or does not (2,4,5) reduce the rate of invasive mediastinal staging. Furthermore, PET does not seem to affect the overall

survival of patients (2,5).

The inconsistent RCT results leave the exact value of PET unclear. There are significant differences in the design of these trials, the patients included, and the outcomes assessed. This paper explores the results and differences between these trials in order to achieve a better understanding of the role of PET and factors that influence this in patients with lung cancer.

Methods

We chose a realist synthesis method as most appropriate to develop an understanding of factors influencing the impact of PET (what works, for whom, in which setting, why and how?) (6-8). The realist method considers that implementation of an intervention may yield slightly different results depending on the context. This approach combines theoretical understanding and available data to reach a deeper understanding of how an intervention produces the observed outcomes, with a focus on explaining the relationship between the context in which the intervention is applied, the mechanisms by which it works and the outcomes which are produced. This review was conducted following the RAMESES publication standards for realist syntheses (*Figure S1*) (7).

Preliminary scoping of the literature used the recent extensive systematic review conducted for the ACCP Lung Cancer Guidelines (9). We limited the focus to RCT because the impact of PET *vs*. traditional staging is not confounded, yet allows analysis of contextual factors by comparing across studies.

We performed a MEDLINE search [1990-2013] for English language papers assessing the utility of PET or PET/CT in the pre-treatment evaluation of patients with known or suspected lung cancer in a RCT (details available on request). We excluded studies of PET for chemotherapy response, RT treatment planning or restaging after induction therapy. We did not attempt to identify unpublished studies. There was no funding support and no involvement of other people or organizations.

We found five RCTs, involving 1,362 patients (*Table S1*) (1-5,10). Data was abstracted regarding study design, end-points, PET technology, scan interpretation, patient characteristics, and details of pre-enrollment and post-enrollment further studies. Slight discrepancies were noted between two papers reporting on one study; data from the later publication was chosen after communication with the authors (2,10).

The selected studies used various denominators and endpoints, including detection of mediastinal or distant metastases, early recurrence and appropriateness of resection. To enhance comparability, we abstracted raw data and calculated outcomes consistently across the studies on an intent-to-treat basis, for all enrolled eligible patients.

We calculated results according to parameters that could be affected by PET (i.e., whether PET identifies more patients with benign disease, N2,3 or M1 involvement preoperatively *vs*. intra-operatively or within 1 year). We excluded endpoints which PET is unlikely to impact (e.g., "unresectability" or T4) although we show these results when reported. We excluded outcomes such as unrelated death within 1 year, because it seems inappropriate to expect PET to predict unrelated events.

We defined stage-inappropriate resection as surgery for patients with benign lesions or with N2,3 or M1 involvement (although we acknowledge that exceptions exist and sometimes surgery may be considered appropriate). The Viney *et al*.'s study (3) results are presented as if N2 involvement was a contraindication for surgery (contrary to the study authors' policy) in order to be consistent with the general view and with the other studies. Avoidance of inappropriate surgery is important, but so is inappropriately missed resection due to falsely interpreted preoperative staging. Because this was not explicitly reported, we estimated the risk of missed stage-appropriate resection from the incidence of positive PET results subsequently shown to be false-positives.

We assigned a qualitative assessment in each study to patient characteristics and the extent of pre- or post-enrollment but preoperative testing for N2,3 or M1 disease in order to facilitate evaluation of how these factors influenced the study outcomes (a quantitative assessment was not possible). Because of heterogeneity in patient and study design characteristics, a formal meta-analysis or calculation of summary statistics across all studies is not appropriate.

Results

Study characteristics

End-points

The primary outcome in the PLUS and Fischer studies was "futile thoracotomies", defined as preoperatively unrecognized benign disease, N2,3 or M1 involvement, or recurrence or any death within one year (related or not) (4,5).

Viney *et al*. also lists the thoracotomy rate as the primary endpoint, but effectively it is the identification of distant metastases (those with suspected N2 involvement underwent thoracotomy nevertheless) (3). The Maziak study assessed the percentage correctly and incorrectly upstaged, as well as incorrect understaging (but not correct downstaging) by PET/CT *vs*. traditional staging (2). Herder assessed whether PET as the first test reduced the number of tests/procedures to finalize staging and define operability, with secondary endpoints of work-up duration, morbidity and costs (1).

Patient characteristics

The RCTs all enrolled patients deemed potential candidates for surgical resection (*Table 1*), but according to varying criteria. Some studies (1,4) included many patients with significant weight loss—generally considered a marker of distant metastasis. Some studies (4,5) included many patients with clinical evidence of mediastinal node involvement. Merging such features yields a qualitative assessment of the risk of advanced disease, which varies markedly (*Table 1*).

In most studies, the vast majority of patients had lung cancer—either as demonstrated by subsequent work-up or mandated by biopsy prior to study entry. Only the Herder study included many patients (47%) who did not have lung cancer (1).

Patient entry into the RCTs varied markedly: from being referred by a general practitioner (GP) on the basis of a chest radiograph (CXR) alone (1), to a prerequisite of biopsy proof, specialist evaluation and extensive traditional imaging (3). A qualitative assessment of the extent of pre-enrollment evaluation can be assigned (see the last column in *Table 1*).

Thoroughness of preoperative staging

The extensiveness of staging procedures to rule out mediastinal and distant metastases differ markedly between the studies (*Table 2*). The value of PET may be different if all or few patients undergo further testing for N2,3 or M1 disease. The extent of further testing was generally similar between the PET and traditional work-up arms with 2 exceptions. In the Herder study mediastinoscopies were done less often in the PET arm (13% *vs*. 34%) (1). The Maziak study mandated liver/adrenal CT and bone scans only in the traditional arm (2).

Potential factors influencing the impact of PET include scanner technology, interpretation quality, and the extent of confirmation of abnormal findings. These factors also varied between studies (*Table 2*). The thoroughness of the PET interpretation is patterned according to a proposed scale (11). In most studies only a few institutions performed PET scans for all participating sites. This concentrated experience may affect the quality of the interpretation. Only in the Maziak study was PET performed in a more disseminated fashion. The thoroughness of the PET and of preoperative testing for N2,3/M1 disease is qualitatively summarized in the last three columns of *Table 2*.

Outcomes

Preoperative identification of benign disease

The RCTs demonstrate little difference for PET *vs*. traditional evaluation in identifying benign disease preoperatively *vs*. intraoperatively (*Table 3*), but most studies included few patients with benign disease. PET identified more benign disease preoperatively only in the Herder study, which involved patients referred by the GP for potential lung cancer resection based on only a CXR (1). However, this observation is weakened by the fact that there were also more patients overall in the PET arm with benign disease (19% *vs*. 13%) despite randomization (1).

These results suggest that if the diagnosis of lung cancer is fairly certain, either due to a biopsy result or evaluation by a specialist, there is little benefit to PET to identify benign lesions. However, PET can be helpful to evaluate the primary lesion when there is little specialist involvement and limited diagnostic evaluation.

Preoperative identification of mediastinal node involvement

In a RCT the total number of patients with N2,3 involvement should be similar, but PET might identify N2,3 disease more often preoperatively rather than intra- or post-operatively. These results are summarized in *Table S2* and *Figure 1*. While PET seems beneficial in the Fisher and PLUS studies (4,5), the opposite was true in the Herder study (1). The Viney study provided no data for the traditional staging arm (3). The Maziak study observed fewer patients with intraoperative identification of N2 involvement in the PET arm, but with no corresponding increase of preoperatively identified N2 disease by PET (2,10). Therefore, the imbalance in the overall number of patients with N2 disease between the arms (despite randomization) seems to account for the lower rate of intraoperative discovery of N2, rather than PET imaging.

Comparing studies suggests that PET is beneficial in

Table 1 Patient characteristics at study entry

Study	N	Referred by	% biopsy proven	Pre-enrollment studies	PS ≥2 (%)	>5% weight loss (%)	Eligibility	Clinical stage at entry[a] (%)				Risk of advanced stage[b]	Extent of pre-enrollment evaluation
								I	II	III	IV		
Fisher	189	Pulm[c]	–	CT ×2, Bronch	1	–	Oper	28	6	62	4	+++	Moderate
Plus	188	GP	52	Local routine	–	15	cI-III	65	5	29	1	+++	Minimal
Herder	465	GP	–	CXR	4	31	Oper	(38)[d]		(20)[d]	(16)[d]	++++	Minimal
Maziak	337	Specialist	100	CT	4	–	cI-IIIa	78	12	10	0	++	Moderate
Viney	183	T Surg	98	CT ×2, (Bn)[e], Br	7	10	cI, II	92	8	0	0	+	Good

Bn, bone scan; Br, brain scan [either computed tomography (CT) or magnetic resonance imaging (MRI)]; Bronch, fiberoptic bronchoscopy; CT, chest CT; CT ×2, chest and upper abdomen CT; CXR, chest radiograph; GP, general practitioner; Oper, patient deemed candidates for resection (i.e., "operable"); Pulm, Pulmonologist; PS, performance status; T Surg, thoracic surgeon. [a], as reported in study (the low rate of stage IV in some studies appears in conflict with the proportion of patients with significant weight loss); [b], risk based on presence of clinical markers of advanced disease (>5% weight loss, performance status ≥2); [c], specialists who practice both pulmonary medicine and medical oncology for lung cancer; [d], final clinical stage after completion of all post-enrollment studies (not the stage at enrollment); [e], done selectively if symptoms or signs of bone metastases.

Table 2 Post-enrollment conduct of study

Study	Extent of work-up (%)[a]				PET technique	Thoroughness of PET read	Confirmation of suspicious PET findings		Thoroughness of preoperative staging		Quality/thoroughness of PET assessment
	Invasive MLN st.	Brain CT/MRI	Bone scan	Liver, adrenal			N2,3	M1	N2,3	M1	
Fisher	94	0[b]	–	(100)[c]	PET/CT	High	All	Loose	High	Low	Good
Plus	69	4	27	47	PET + CT	Good	Most	Most	Mod	Low	Good
Herder	24[d]	High[e]	High[e]	High[e]	PET[f]	Fair	–	–	Low	High	Fair
Maziak	50	100	100[g]	100[g]	PET/CT	High	All	All	Mod	High	High
Viney	5	(100)[c]	(Few)[c]	(100)[c]	PET[h]	Fair	All	All	Low	High	Good

CT, computed tomography; F/U, follow-up; MLN st., mediastinal lymph node staging (i.e., mediastinoscopy, endobronchial ultrasound and aspiration); MRI, magnetic resonance imaging; PET, positron emission tomography; PET/CT, integrated PET/CT scanner; PET + CT, PET scan with visual correlation with a separate CT. [a], in both arms equally unless indicated; [b], except 1 patient in PET arm; [c], done pre-enrollment; [d], mediastinoscopy done significantly less often in PET arm (13% *vs*. 34%); [e], not specified but patients underwent and average of 7.9 additional tests (equal in both arms); [f], PET read in isolation without correlation with a CT; [g], in conventional work-up arm; [h], CT scan available but was not used during PET interpretation; PET reader knew that the mediastinum was deemed normal on all CT scans.

Table 3 Study endpoints-benign disease

Study	Referred by	% biopsy proven	Pre-enrollment studies	% with lung cancer of all enrolled	Extent of Pre-enrollment evaluation	% benign				Impact of PET on identifying benign Dx
						Preop		Intraop		
						Trad	PET	Trad	PET	
Herder	GP	–	CXR	53	Minimal	12	18	1	1	(↑)[a]
Plus	GP	52	Local routine	93	Low	2	3	7	2	(↑)[a]
Fisher	Pulm[b]	–	CT ×2, Bronch	99	Moderate	–	–	3	0	–
Maziak	Specialist	100	CT	100	Moderate	NA	NA	NA	NA	–
Viney	T Surg	98	CT ×2, (Bn)[c], Br	99	Good	NA	2	NA	2	–

Note: all results calculated on intent to treat basis for entire cohort (arm) in each study. Bn, bone scan; Br, brain scan [either computed tomography (CT) or magnetic resonance imaging (MRI)]; Bronch, fiberoptic bronchoscopy; CT, chest CT; CT ×2, chest and upper abdomen CT; CXR, chest radiograph; Dx, diagnosis; GP, general practitioner; intraop, intraoperatively identified; NA, not applicable; PET, positron emission tomography; preop, preoperatively identified; Pulm, pulmonologist; T Surg, thoracic surgeon; Trad, traditional evaluation arm. [a], The "benefit" of PET in pre- *vs*. intra-operative identification of benign disease is largely due to an discrepancy in the overall incidence of benign disease despite randomization; [b], specialists who practice both pulmonary medicine and medical oncology for lung cancer; [c], done selectively if there were symptoms or signs of bone metastases.

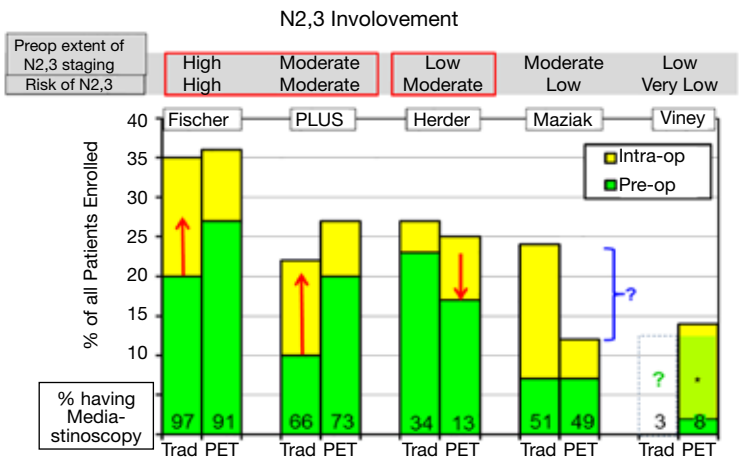

Figure 1 Rate of N2,3 involvement. Rate of N2,3 node involvement diagnosed pre- and intra-operatively. Upwards red arrows indicate a benefit to PET, downward red arrow indicates a detriment. Values represent the percent of all patients enrolled in the respective study arm. Intraop, intraoperatively; preop, preoperatively; Trad, traditional.

preoperatively identifying N2,3 involvement when the risk is high and there is a high rate of invasive staging. PET seems to help identify N2,3 disease even when almost all patients undergo mediastinoscopy-perhaps by directing attention to suspicious nodes. When PET is used to decrease the rate of invasive staging, it appears that the risk of intraoperative discovery of N2 involvement is increased, at least in a patient cohort with a moderate incidence of mediastinal nodal disease. When the risk of N2.3 disease is low, PET has little impact on preoperative identification of nodal involvement.

Preoperative identification of distant metastases

Does PET identify more patients with distant metastases preoperatively and reduce the number found to have M1 disease or recurrence within 1 year? This was seen in the Fisher and PLUS studies but not clearly so in the others (*Table S3*, *Figure 2*) (1-5).

An unexplained difference between the randomized arms exists in the Maziak study in the number of patients with M1 disease (identified at any time) (2). The discrepancy is in the opposite direction as for N2,3 involvement; however, these differences are not explained by postulating that

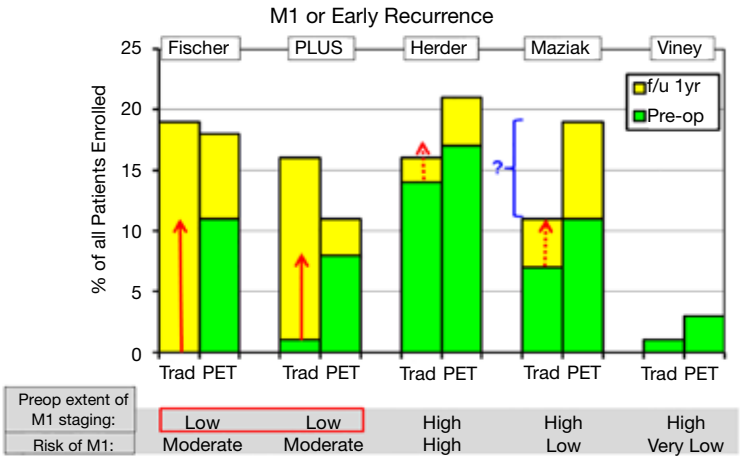

Figure 2 Rate of M1 disease or early recurrence. Rate of M1 disease diagnosed pre-operatively and the rate of early recurrence (within 1 year). Upwards solid red arrows indicate a benefit to PET, dashed red arrows indicate a trend towards a benefit. f/u, follow-up; preop, preoperatively; Trad, traditional; yr, year.

preoperative identification of M1 disease would obviate the need to identify N2,3 involvement. Furthermore, the incidence of M1 disease is higher than expected from the patients' characteristics. The reason for these findings is unclear.

Thus the RCTs suggest that PET helps identify M1 disease preoperatively when the risk is at least moderate and the thoroughness of searching for M1 disease without PET is low. However, PET has little additional impact if the risk of advanced disease is low or when extensive investigation for M1 disease is already being done.

Avoidance of stage-inappropriate resection

Table S4 summarizes the rate of pre- *vs.* intra-/post-operative identification of N2,3/M1 involvement. *Figure 3* shows the rate of stage-inappropriate resection (defined as surgery for something other than stage I, II NSCLC). PET was beneficial by this assessment in the Fischer and PLUS studies and to a lesser extent in the Maziak trial (2,4,5). In the Fischer and PLUS studies PET lowered the overall rates of surgery, but the other studies found no difference. The discrepancy in the Maziak study between a similar overall rate of surgery, yet fewer stage-inappropriate resections with PET, appears to be due to unequal overall rates of N2,3 and M1 involvement between the arms (which should be similar in a randomized study).

The potential of PET to reduce stage–inappropriate surgery is seen in patients with a high risk of advanced cancer and with relatively little investigation for this without PET. PET has little impact when the risk of M1 disease is low or the rate of traditional investigation is high.

Missed stage-appropriate resection

A balanced assessment requires that the rate of missed stage-appropriate resection is assessed. Unfortunately, none of the RCTs addressed this directly. The potential for missed resection can be estimated from the rate of PET findings suggesting N2,3/M1 disease subsequently found to be false positive. This assessment suggests this risk is not minor, although the rate varies markedly (from 1% to 42%) (*Table S4*).

Discussion

The literature on PET for lung cancer staging has progressed from dramatic anecdotal PET images of metastases (not necessarily otherwise undetected) to series comparing PET to historical studies and finally RCTs. Clinical guidelines recommended PET in the evaluation of most lung cancer patients (9,12-14).

However, the RCT results are not consistent with respect to the identification of metastasis, the rate of so-called "futile" thoracotomies and the need to perform invasive mediastinal staging. However, the RCT have differed in terms of the patients included, the endpoints and the context of the studies. We hoped to clarify how details of the design and conduct of the RCTs affected the results. The realist method is specifically designed to explore differences in context to develop a deeper understanding of what works, for whom, in which setting, why and how (6-8).

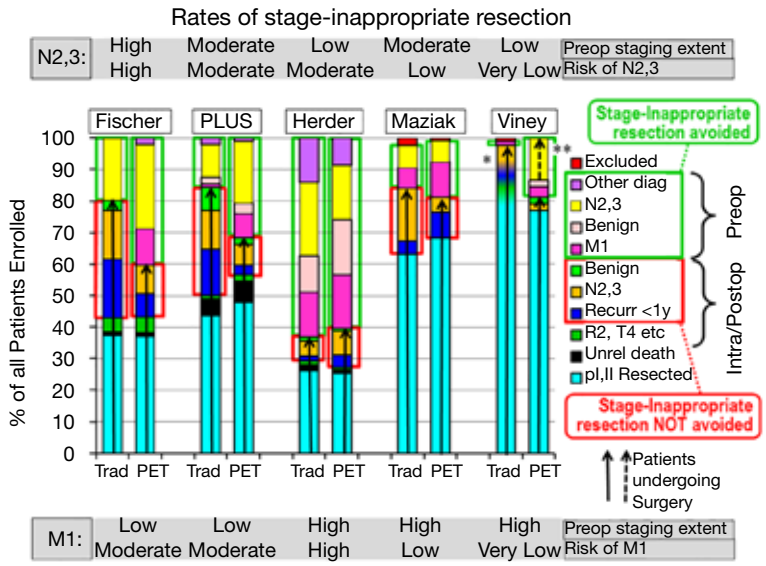

Figure 3 Rate of inappropriate resection. Rate of inappropriate resection avoided or not avoided for all evaluable patients. Black arrows (solid and dashed) indicate the percent of patients operated. *, this study reported several categories of patients together; **, in this study 12% underwent stage-inappropriate resection (for N2,3 positive disease), but if mediastinoscopy had been done for suspicious nodes (assuming 80% sensitivity) then 3% would have undergone stage-inappropriate resection. The dashed black arrow represents these patients, who were operated in this study but would not have been if a more standard policy of investigation of suspicious N2,3 nodes and avoidance of surgery in N2,3 positive patients had been followed. Diag, diagnoses; intraop, intraoperatively; preop, preoperatively; postop, postoperatively (i.e., within 1 year); Recurr, recurrence; Trad, traditional; Unrel, unrelated; yr, year.

Analyzing the reported data relative to consistent specific endpoints allows the RCTs to be compared (*Table 4*). This analysis suggests several conclusions. First, the benefit of PET to identify benign disease is moderate after evaluation by a generalist and limited investigation but low after a specialist's evaluation and more extensive pre-enrollment testing.

Second, the benefit of PET in detecting N2,3 or M1 disease is low if the clinical evaluation and chest CT suggest a low risk of metastasis. PET is of little value for identification of N2,3 disease if the rate of invasive staging is low—and it may be detrimental if it is used to lower the rate of invasive mediastinal staging. However, in cohorts with at least moderate a risk of N2,3 involvement, PET appears to be of benefit even if invasive staging is done in most patients (perhaps by directing attention to suspicious nodes).

Finally, PET is of value in identifying M1 disease if the risk is at least moderate and little traditional imaging is done. If the patient undergoes extensive traditional imaging, there is little additional impact of PET in identifying M1 disease.

Taking everything together, PET is useful if there is at least a moderate risk of metastases (N2,3 or M1), the extent of traditional imaging is low, and the rate of invasive staging is high (*Figure 4*). In these settings PET appears to reduce the rate of stage-inappropriate resection. However, with initial evaluation by a specialist and extensive traditional imaging the impact of adding PET is low. PET does not appear to obviate the need for invasive nodal staging. Furthermore, the rate of potentially misleading false-positive PET results is substantial, suggesting a potential detriment if confirmation of positive PET findings (i.e., mediastinal or distant metastases) is not undertaken diligently.

We avoided the endpoint "futile thoracotomy" because we perceive this to be biased and not conducive to an objective scientific assessment. "Futile" has a strong negative connotation, and is one-sided, ignoring the converse risk of a missed stage-appropriate, potentially curative resection (Considering only the stage-inappropriate resection mandates that all surgery be avoided because then no stage-inappropriate resection will occur). Furthermore, counting unrelated (random, unpredictable) deaths as "futile" resections seems inappropriate as an outcome to assess pre-treatment evaluation. Finally, the majority of lung cancer resections are performed by thoracoscopy, not thoracotomy in cutting-edge thoracic surgical units.

Table 4 Key conclusions

Outcome	Benefit of PET	Little impact of PET	Detriment of PET
Preoperative identification of benign disease	Suspicion by generalist with limited preoperative evaluation	Clinical diagnosis by specialist or biopsy proven	
Preoperative identification of N2,3 disease	High risk of N2,3disease and high rate of invasive staging	Low risk of N2,3 disease Limited invasive mediastinal staging	Using PET to lower the rate of invasive biopsy of N2,3 nodes
Preoperative identification of M1 disease	Moderate to high risk of M1 and limited preoperative investigation	Low risk of M1 disease Extensive traditional imaging for M1	
Avoidance of stage-inappropriate surgery	High risk of N2,3 or M1 and limited preoperative investigation	Low risk of N2,3 or M1 disease Extensive traditional investigation	Possible if there is limited confirmation of PET results[a]

[a], detriment due to a risk of missed stage-appropriate surgery.

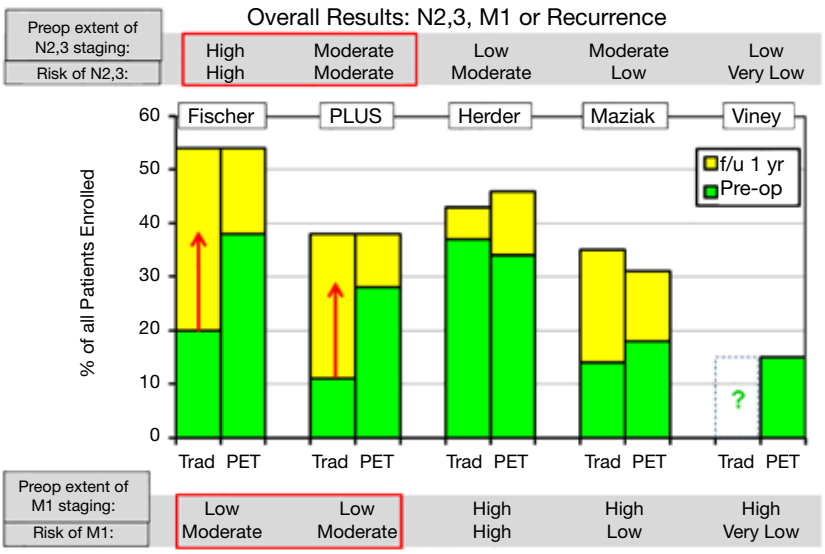

Figure 4 Overall results—rate of N2,3/M1 disease or recurrence. Overall results—rate of either N2,3 or M1 disease diagnosed pre-operatively *vs.* the rate of N2,3 involvement diagnosed intra-operatively or early recurrence (within 1 year). Upwards solid red arrows indicate a benefit to PET. f/u, follow-up; pre-op, preoperatively; Trad, traditional; yr, year.

The quality of the PET imaging and interpretation in the RCTs appears to have been good. We did not find that differences in technical details had an impact (*Table 2*). The use of PET/CT *vs.* stand-alone PET does not alter the findings, suggesting that the setting in which PET is implemented may have a greater impact that the technology itself. Furthermore, PET/CT is not universally available: in the US about half of PET imaging involves stand-alone PET. In the RCTs PET imaging was relatively centralized, whereas in the US PET is performed at many smaller institutions and using mobile scanners. What effect this has on the accuracy of interpretation of the PET scans is unknown.

A difficulty in this analysis are discrepancies in the Maziak study between the randomized arms in the overall rate of N2,3 and M1 disease. There is no discernible explanation for this. These discrepancies drive some of the face-value conclusions of the study, namely that PET identifies more patients with metastases; without this imbalance it is unclear whether this result would hold up.

Outcomes studies suggest PET has an impact in lung cancer, primarily by identifying distant metastases in cIII patients (15-17). Other studies suggest little impact in stage cI patients (15,18). PET detected N2,3 or M1 involvement in 7% of the subset of cI patients in the ACoSOG study, but at a price of falsely suggesting N2,3/M1 disease in 14% (18).

This study also found that while PET could reduce the rate of biopsy for benign lesions from 21% to 11%, this would cause missed (or delayed) resection in 13% of cancers (18). Finally, many studies have consistently reported that ~25% of patients with central or cII or cIII tumors by CT harbor N2,3 involvement despite a PET that is negative in the mediastinum (10,19-24). Thus, other (non-RCT) studies corroborate a significant benefit with PET in some clinical settings but also a potential detriment when the false negative and false positive rates of PET in particular clinical settings are not recognized and the PET results are not appropriately confirmed.

Conclusions

This analysis suggests that while PET can be useful, it depends on many factors. PET appears to be of benefit when the chance of N2,3 or M1 involvement is moderate or high, when the extent of traditional imaging (abdominal/pelvis CT, bone scan) is low, and when the rate of invasive mediastinal staging is high. The impact of PET is low in other settings. If PET is used to avoid invasive mediastinal staging in clinical settings in which the risk of N2,3 involvement is moderately high, PET can lead to lower preoperative and higher intraoperative detection rates of N2 disease. Finally, the data suggests a significant risk of missed curative-intent treatment if positive PET findings are not interpreted carefully. Accurate evaluation is a complex interplay of various clinical aspects (symptoms), risk of metastases, extent of imaging, confirmation of suspicious findings, the thoroughness of intra-operative assessment and of follow-up.

The overriding conclusion of this analysis of RCTs comparing PET to traditional evaluation of lung cancer patients is that the results are dependent on the clinical setting. A blanket recommendation for PET may be too simplistic—various clinical aspects affect the value of PET. A more judicious use of PET may lower costs without negatively impacting the accuracy of evaluation of patients with lung cancer.

Acknowledgements

Disclosure: The authors declare no conflict of interest.

References

1. Herder GJ, Kramer H, Hoekstra OS, et al. Traditional versus up-front [18F] fluorodeoxyglucose-positron emission tomography staging of non-small-cell lung cancer: a Dutch cooperative randomized study. J Clin Oncol 2006;24:1800-6.
2. Maziak DE, Darling GE, Inculet RI, et al. Positron Emission Tomography in Staging Early Lung Cancer. Ann Intern Med 2009;151:221-8.
3. Viney RC, Boyer MJ, King MT, et al. Randomized controlled trial of the role of positron emission tomography in the management of stage I and II non-small-cell lung cancer. J Clin Oncol 2004;22:2357-62.
4. van Tinteren H, Hoekstra OS, Smit EF, et al. Effectiveness of positron emission tomography in the preoperative assessment of patients with suspected non-small-cell lung cancer: the PLUS multicentre randomised trial. Lancet 2002;359:1388-93.
5. Fischer B, Lassen U, Mortensen J, et al. Preoperative Staging of Lung Cancer with Combined PET-CT. N Engl J Med 2009;361:32-9.
6. Wong G, Greenhalgh T, Westhorp G, et al. Realist methods in medical education research: what are they and what can they contribute? Medical Education 2012;46:89-96.
7. Wong G, Greenhalgh T, Westhorp G, et al. RAMESES publication standards: realist syntheses. BMC Med 2013;11:21.
8. Pawson R, Greenhalgh T, Gill H, et al. Realist review-a new method of systematic review designed for complex policy interventions. J Health Serv Res Policy 2005;10:21-34.
9. Silvestri GA, AV Gonzalez, Jantz M, et al. Methods for staging non-small cell lung cancer: Diagnosis and management of lung cancer, 3rd ed: American College of Chest Physicians evidence-based clinical practice guidelines. Chest 2013;143:e211S-50S.
10. Darling GE, Maziak D, Inculet R, et al. Positron Emission Tomography-Computed Tomography Compared with Invasive Mediastinal Staging in Non-small Cell Lung Cancer-Results of mediastinal staging in the early lung positron emission tomograpy trial. J Thorac Oncol 2011;6:1367-72.
11. Detterbeck F, Puchalski J, Rubinowitz A, et al. Classification of the thoroughness of mediastinal staging of lung cancer. Chest 2010;137:436-42.
12. Silvestri GA, Gould MK, Margolis ML, et al. Non-invasive staging of non-small cell lung cancer: ACCP evidenced-based clinical practice guidelines (2nd Edition). Chest 2007;132:178S-201S.

13. Crinò L, Weder W, van Meerbeeck J, et al. Early stage and locally advanced (non-metastatic) non-small-cell lung cancer: ESMO Clinical Practice Guidelines for diagnosis, treatment and follow-up. Ann Oncol 2010;21:v103-v115.
14. Ettinger DS, Akerley W, Borghaei H, et al. Non-small cell lung cancer. J Natl Compr Canc Netw 2012;10:1236-71.
15. Morgensztern D, Goodgame B, Baggstrom M, et al. The effect of FDG-PET on the stage distribution of non-small cell lung cancer. J Thorac Oncol 2008;3:135-9.
16. Morgensztern D, Waqar S, Subramanian J, et al. Improving survival for stage IV non-small cell lung cancer: a surveillance, epidemiology, and end results survey from 1990 to 2005. J Thorac Oncol 2009;4:1524-9.
17. Morgensztern D, Ng SH, Gao F, et al. Trends in stage distribution for patients with non-small cell lung cancer: a National Cancer Database survey. J Thorac Oncol 2010;5:29-33.
18. Kozower BD, Meyers BF, Reed CE, et al. Does Positron Emission Tomography Prevent Nontherapeutic Pulmonary Resections for Clinical Stage IA Lung Cancer? Ann Thorac Surg 2008;85:1166-9.
19. Gould MK, Kuschner WG, Rydzak CE, et al. Test performance of positron emission tomography and computed tomography for mediastinal staging in patients with non-small-cell lung cancer: a meta-analysis. Ann Intern Med 2003;139:879-92.
20. Pozo-Rodríguez F, Martín de Nicolás JL, Sánchez-Nistal MA, et al. Accuracy of Helical Computed Tomography and [18F] Fluorodeoxyglucose Positron Emission Tomography for Identifying Lymph Node Mediastinal Metastases in Potentially Resectable Non-Small-Cell Lung Cancer. J Clin Oncol 2005;23:8348-56.
21. Serra M, Cirera L, Rami-Porta R, et al. Routine positron tomography (PET) and selective mediastinoscopy is as good as routine mediastinoscopy to rule out N2 disease in non-small cell lung cancer (NSCLC). J Clin Oncol 2006;2006:24.
22. Verhagen AFT, Bootsma GP, Tjan-Heijnen VCG, et al. FDG-PET in staging lung cancer: How does it change the algorithm? Lung Cancer 2004;44:175-81.
23. Cerfolio RJ, Bryant AS, Ojha B, et al. Improving the inaccuracies of clinical staging of patients with NSCLC: a prospective trial. Ann Thorac Surg 2005;80:1207-13; discussion 1213-4.
24. Dietlein M, Weber K, Gandjour A, et al. Cost-effectiveness of FDG-PET for the management of potentially operable non-small cell lung cancer; priority for a PET-based strategy after nodal-negative CT results. Eur J Nucl Med 2000;27:1598-609.

Cite this article as: Detterbeck FC, Figueroa Almanzar S. Lung cancer staging: the value of PET depends on the clinical setting. J Thorac Dis 2014;6(12):1714-1723. doi: 10.3978/j.issn.2072-1439.2014.11.16

Title			
√	1	Mention realist review or synthesis	
Abstract			
√	2	Brief description of background, objectives, search, methods of selection, appraisal, analysis and synthesis or sources, main results and implications for practice	
Introduction			
√	3	Rationale for Review	Why is this needed, likely to be useful
√	4	Objectives and focus	State objectives or question, justify focus
Methods			
NA	5	Changes in Review Process	Describe and justify changes that were made
√	6	Why realist synthesis?	Why is realist synthesis appropriate for the study?
√	7	Scoping the literature	Describe, justify initial process of scoping literature
√	8	Searching Processes	Provide rationale for iterative searching, sources accessed, dates
√	9	Selection, Appraisal	Describe inclusion, exclusion judgments
√	10	Data extraction	What was extracted and why?
√	11	Analysis and Synthesis	What constructs were analyzed, how?
Results			
*	12	Flow diagram	Numbers of papers, reasons for exclusion etc.
√	13	Characteristics	Describe characteristics of papers selected
√	14	Main Findings	Key findings with specific focus on theory building and testing
Discussion			
√	15	Summary of findings	Summarize relative to focus, objective
√	16	Strengths/limitations	Include S/L of process followed, need for future studies
√	17	Compare to literature	Compare to existing literature, other reviews
√	18	Conclusion/recommendations	List implications and recommendations for policy or practice
√	19	Funding	Describe any funding sources, role of organizations
*, Available on request; NA, not applicable.			

Figure S1 RAMSES checklist.

Table S1 Setting of study

Study	N	Region	Accrual years	Primary question	Primary outcome measure	PET technique	No. of PET scanners	No. of centers participating
Fisher	189	Denmark	2002-2007	Preop eval accuracy	"Futile" thoracotomy[a]	PET/CT	1	3
Plus	188	Netherlands	1998-1999	Preop eval accuracy	"Futile" thoracotomy[a]	PET + CT	1	9
Herder	465	Netherlands	1999-2001	Role of upfront PET	Number of tests needed	PET[b]	2	22
Maziak	337	Canada	2004-2007	Preop eval accuracy	Detection of IIIb, IV	PET/CT	5	8
Viney	183	Australia	1999-2000	Preop eval accuracy for stage I,II	Detection of IIIb, IV[c]	PET[d]	1	6

CT, computed tomography; PET, positron emission tomography; PET/CT, integrated PET/CT scanner; PET + CT, PET scan with visual correlation with a separate CT; Preop eval, preoperative evaluation. [a], futile thoracotomy defined as thoracotomy despite unrecognized N2,3 or M1 involvement, thoracotomy for benign disease, recurrence within 1 year, or any death within 1 year regardless of the cause; [b], PET read without CT scan available for comparison; [c], the explicit endpoint was the rate of thoracotomy, but effectively the endpoint is identification of distant metastases because patients with suspected mediastinal involvement underwent thoracotomy nevertheless; [d], CT scan available but was not used during PET interpretation; PET reader knew that the mediastinum was deemed normal on all CT scans.

Table S2 Study endpoints-N2,3 involvement

Study	% N2,3 anytime		% N2-3 preop		% N2-3 intraop		% other[a] intraop		Impact of PET on N2,3	Prevalence of cN2,3 disease	Extent of preop N2,3 staging
	Trad	PET	Trad	PET	Trad	PET	Trad	PET			
Fischer	35	36	20	27	15	9	4	5	↑↑	High	High
Plus	22	27	10	20	12	7	1	2	↑↑	Moderate	Moderate
Herder[b]	27	25	23	17	4	8	1	1	↓↓	Moderate	Low[b]
Maziak	24	12	7	7	17	5	–	–	(↑)[c]	Low	Moderate
Viney	–	14	–	12[d]	–	2[d]	–	–	–	Minimal	Low

Note: all results calculated on intent to treat basis for entire cohort (arm) in each study. Intraop, intraoperatively identified; PET, positron emission tomography; preop, preoperatively identified; Trad, traditional evaluation arm. [a], e.g., unresectability, T4, SCLC; metastastic extrathoracic cancer; [b], mediastinoscopy done significantly less often in PET arm (13% *vs*. 34%); [c], a higher rate of intra-operative identification of N2,3 disease in the conventional w/u arm appears to be due to an discrepancy in the overall prevalence of N2,3 disease despite randomization; [d], in the study 2% had preoperatively identified nodes and 12% intraoperatively identified nodes, because the local policy was to ignore suspicious N2,3 nodes and proceed with resection; if mediastinoscopy had been done for suspicious nodes (assuming 80% sensitivity) then 12% would have been identified preoperatively and 2% would have been identified intraoperatively.

Table S3 Study endpoints-distant disease or early recurrence

Study	% M1 anytime		Death (not cancer) within 1 yr		% M1 diagnosed preop		% M1/recur diagnosed within 1 yr		Impact of PET on M1	Risk of advanced stage[a]	Extent of preop M1 staging
	Trad	PET	Trad	PET	Trad	PET	Trad	PET			
Fischer	19	18	1	1	0	11	19	7	↑↑↑↑	+++	Low
Plus	16	12	5	6	1	8	15	3	↑↑↑	+++	Low
Herder	16	21	4	2	14	17	2	4	↑	++++	High
Maziak	11	20	–	–	7	11	4	8	(=)[b]	++	High
Viney	–	–	–	–	1	3	–	–	(=)[c]	+	High

Note: all results calculated on intent to treat basis for entire cohort (arm) in each study. PET, positron emission tomography; preop, preoperatively identified; recur, recurrence; Trad, traditional evaluation arm; yr, year. [a], risk based on presence of clinical markers of advanced disease (>5% weight loss, performance status ≥2); [b], differences in pre- *vs*. intra/post-operative identification of M1 disease or recurrence are conflicting and appear to be due to a discrepancy in the overall prevalence of M1 disease/recurrence despite randomization; [c], impact is not fully able to be assessed because data on early recurrence was not reported.

Table S4 Study endpoints-appropriateness of resection

Study	% undergoing surgery		% stage-inappropriate resection[a]		At risk for missed surgery[b]		Impact of PET on stage-appropriate resection	Impact of PET on N2,3	Impact of PET on M1	Any N2,3/M1 preop		Any N2,3/M1 intraop or in 1 yr	
	Trad	PET	Trad	PET	Trad	PET				Trad	PET	Trad	PET
Fischer	80	61	42	22	–	–	↑↑↑	↑↑	↑↑↑↑	20	38	34	16
Plus	81	65	33	15	–	42	↑↑↑	↑↑↑	↑↑↑	11	28	27	10
Herder	38	41	6	10	1	1	↓	↓↓	↑	37	34	6	12
Maziak	78	81	27	16	1	5	(↑↑)[c]	(↑)[c]	(=)[c]	14	19	21	13
Viney	98	96	–	3[d]	–	10	–	–	=	1	15	–	2

Note: all results calculated on intent to treat basis for entire cohort (arm) in each study. It is assumed that preoperatively identified N2,3 or M1 disease is inappropriate to resect (although there are exceptions to this treatment policy). Intraop, intraoperatively identified; PET, positron emission tomography; preop, preoperatively identified; Trad, traditional evaluation arm. [a], resection but N2,3, M1disease or recurrence in <1 year; [b], imaging that falsely suggested benign disease, N2,3 or M1 disease (which could have led to a stage inappropriate lack of resection if further work-up had not been pursued); [c], due to discrepancies in the overall number of N2,3 patients per arm and M1 patients per arm despite randomization; [d], in the study 12% underwent stage-inappropriate resection (for N2,3 positive disease), but if mediastinoscopy had been done for suspicious nodes (assuming 80% sensitivity) then 3% would have undergone stage-inappropriate resection.

Original Article

Five-year epidemiological survey of valvular heart disease: changes in morbidity, etiological spectrum and management in a cardiovascular center of Southern China

Fang-Zhou Liu[1*], Yu-Mei Xue[1*], Hong-Tao Liao[1*], Xian-Zhang Zhan[1], Hui-Ming Guo[1], Huan-Lei Huang[1], Xian-Hong Fang[1], Wei Wei[1], Fang Rao[1,2], Hai Deng[1], Yang Liu[1], Wei-Dong Lin[1], Shu-Lin Wu[1]

[1]Guangdong Cardiovascular Institute, Guangdong Province Key Laboratory of Structural Heart Disease, [2]Research Center of Medical Science, Guangdong General Hospital, Guangdong Academy of Medical Sciences, Guangzhou 510080, China

*These authors contributed equally to this work.

Correspondence to: Shu-Lin Wu. Department of Cardiovascular, Guangdong Cardiovascular Institute, No. 96 Dongchuan Road, Guangzhou 510080, China. Email: drwushulin@163.com.

Objective: The objective of the present study is to analyze the epidemiological profile of patients with abnormal valvular structure and function and highlight the etiological spectrum and management of valvular heart disease (VHD) in a single cardiovascular center of Southern China in five years.

Methods: The retrospective study included 19,428 consecutive patients (9,441 men and 9,987 women with a mean age of 52.03±20.50 years) with abnormal valvular structure and function who were screened by transthoracic echocardiography (TTE) or transesophageal echocardiography (TEE) at the in-patient department of Guangdong General Hospital from January 2009 to December 2013. Data on baseline characteristics, potential etiology, treatment strategies and discharge outcomes were collected from electronic medical records.

Results: There were 13,549 (69.7%) patients with relatively definite etiology for VHD. VHD was rheumatic in 7,197 (37.0%) patients, congenital in 2,697 (13.9%), degenerative in 2,241 (11.5%), ischemic in 2,460 (12.7%). The prevalence decreased significantly in rheumatic VHD from 2009 to 2013 (from 42.8% to 32.8%, P<0.001), but increased markedly in congenital VHD (from 9.0% to 12.3%, P<0.001), ischemic VHD (from 9.2% to 11.3%, P=0.003) and degenerative VHD (from 8.8% to 14.5%, P<0.001). Meantime, the prevalence of ischemic VHD increased after the age of 45, similar to that of degenerative VHD. From 2009 to 2013, the proportion of patients with VHD undergoing open cardiac valvular surgery decreased (from 49.5% to 44.3%, P<0.001) and that of patients treated with general medication increased (from 49.2% to 54.1%, P<0.001). However, there was markedly increment in video-assisted thoracoscopic surgery (VATS) from 2009 to 2013 (from 0.3% to 4.4%, P<0.001). Increasing tendencies were showed in aortic mechanical valve replacement (from 32.1% to 34.5%, P=0.001) and double mechanical valve replacement (from 20.9% to 22.3%, P=0.035), especially in mitral valvuloplasty (from 8.5% to 15.7%, P<0.001). However, the proportion of patients undergoing bioprosthetic valve replacement decreased from 2009 to 2013 (from 26.3% to 15.5%, P<0.001).

Conclusions: Despite a significant shift from rheumatic towards degenerative etiology from 2009 to 2013, rheumatic VHD remains the leading etiology in Southern China, with a significant increase in the prevalence of ischemic, congenital and degenerative VHD. General medication and cardiac valvular surgery remain the main treatment options. The proportion of VATS increased markedly from 2009 to 2013, and mechanical valve replacement and mitral valvuloplasty showed an increasing tendency.

Keywords: Epidemiological; valvular heart disease (VHD); etiology; cardiac valvular surgery

Submitted Jul 31, 2014. Accepted for publication Oct 15, 2014.
doi: 10.3978/j.issn.2072-1439.2014.11.21
View this article at: http://dx.doi.org/10.3978/j.issn.2072-1439.2014.11.21

Background

Valvular heart disease (VHD) is a common condition in clinical practice that is strongly associated with heart dysfunction and death. The prevalence of VHD is 2.5% in developed countries (1). In the last three decades, the etiology of VHD has changed in parallel with socio-economic development and an increasing aging population. In developing countries, rheumatic heart disease remains the primary cause of VHD (2). Echocardiography is one of the most effective methods for the assessment of valvular structure and function, and it is widely applied for VHD screening in clinical practice. It can provide helpful information regarding the etiology of valvular disorders. The objective of the present study is to analyze the epidemiological profile of patients with abnormal valvular structure and function and highlight the etiological spectrum and management of VHD in a single cardiovascular center of Southern China.

Methods

Patient population and criteria

The present retrospective study included 19,428 consecutive patients with abnormal valvular structure and function who were screened by transthoracic echocardiography (TTE) or transesophageal echocardiography (TEE) at the in-patient department of Guangdong General Hospital between January 2009 and December 2013. Data on baseline characteristics, potential etiology, treatment strategies and discharge outcomes were collected from electronic medical records. Under standard echocardiographic criteria (3), rheumatic VHD was diagnosed on the basis of a medical history of acute rheumatic fever and/or precordial abnormalities, including the presence of a cardiac murmur. Degenerative VHD was defined according to the echocardiographic criteria for calcific valve disease, and ischemic VHD was identified based on a medical history of ischemic heart disease. Autoimmune-mediated VHD was confirmed with a medical history of autoimmune disease. Regarding infective VHD, the Duke classification allows for standardization of its diagnosis.

Statistical methods

All continuous variables were expressed as the mean ± standard deviation. Categorical variables were expressed as percentages or ratios. Patient characteristics were compared across different years using the chi-square test for categorical variables and analysis of variance (ANOVA) for continuous variables. For highly skewed variables, presented as median and first and third quartiles, the Kruskal-Wallis nonparametric test was used. Trends in the different years were assessed using the Cochran-Armitage test. A two-tailed P value <0.05 was considered to indicate statistical significance. All statistical analyses were performed using SAS for Windows version 9.2 (Cary, NC, USA).

Results

Baseline characteristics

The survey included 19,428 patients (9,441 men and 9,987 women with a mean age of 52.03±20.50 years) hospitalized in Guangdong General Hospital. Of these, 25.5% patients had atrial fibrillation (AF), 19.7% had hypertension, and 9.5% had diabetes mellitus. Baseline characteristics are summarized in *Table 1*. A relatively definitive etiology for VHD was identified in 13,549 (69.7%) patients by analyzing clinical data, patient characteristics and echocardiographic information. VHD was rheumatic in 7,197 (37.0%) patients, congenital in 2,697 (13.9%), degenerative in 2,241 (11.5%), ischemic in 2,460 (12.7%), infective in 611 (3.1%), and autoimmune-mediated in 138 (0.7%). The 5-year in-hospital mortality was 577 (3.0%) patients.

General medication was administered in 9,866 (50.8%) patients. A total of 299 (1.5%) patients underwent interventional balloon valvuloplasty. Of 9,263 (47.7%) patients who underwent cardiac valvular surgery, 472 (2.4%) received video-assisted thoracoscopic surgery (VATS) and 8,791 (45.2%) underwent classic open cardiac valvular surgery (*Table 2*). Coronary artery bypass graft (CABG) was performed simultaneously in 492 (2.5%) patients. The Cox maze procedure for AF ablation was performed in 947 (4.9%) patients. Tricuspid and mitral valvuloplasties were performed in 4,883 (25.1%) and 1,103 (5.7%) patients, respectively. Mitral, aortic and double valve replacements were performed in 5,331 (27.4%), 3,680 (18.9%) and 2,264 (11.7%) patients, respectively, and 5.29% of the implanted valves were bioprotheses.

Shifts in the prevalence of different etiologies from 2009 to 2013

Further analysis of the baseline characteristics in different years revealed a shift in the distribution of etiologies for VHD from 2009 to 2013 (*Figure 1*), with significant decrease in the prevalence of rheumatic VHD (from 42.8% to 32.8%, P<0.001) and infective VHD (from 3.5% to 2.2%,

Table 1 Baseline characteristics of patients with VHD from 2009 to 2013

Characteristics	2009 (N=2,960)	2010 (N=3,330)	2011 (N=3,861)	2012 (N=4,159)	2013 (N=5,118)	P value[#]
Mean age (yrs)	52.84±18.08	51.83±19.19	51.29±22.00	51.82±21.30	51.83±21.40	0.048*
Male, N (%)	1,394 (47.1)	1,616 (48.5)	1,873 (48.5)	2,130 (51.2)	2,428 (47.4)	0.404
Medical history, N (%)						
AF	905 (31.0)	860 (26.0)	958 (25.0)	1,073 (26.0)	1,151 (23.0)	<0.001
Hypertension	598 (20.0)	422 (13.0)	797 (21.0)	866 (21.0)	1,135 (22.0)	0.039
Diabetes	262 (8.9)	297 (8.9)	377 (9.8)	414 (10.0)	499 (9.7)	0.195
Etiological analysis, N (%)						
Rheumatic	1,268 (42.8)	1,421 (42.7)	1,402 (36.3)	1,405 (33.8)	1,680 (32.8)	<0.001
Congenital	267 (9.0)	307 (9.2)	457 (11.8)	598 (14.3)	628 (12.3)	<0.001
Degenerative	261 (8.8)	339 (10.2)	517 (13.4)	564 (13.6)	744 (14.5)	<0.001
Ischemic	272 (9.2)	283 (8.5)	353 (9.1)	387 (9.3)	579 (11.3)	<0.001
Infective	104 (3.5)	124 (3.7)	123 (3.2)	142 (3.4)	113 (2.2)	<0.001
Autoimmune	30 (1.0)	15 (0.5)	30 (0.8)	39 (0.9)	36 (0.7)	0.828
Undefined	758 (25.6)	844 (25.3)	982 (25.4)	1,053 (25.3)	1,320 (25.8)	0.813
In-hospital mortality	80 (2.7)	114 (3.4)	115 (3.0)	133 (3.2)	135 (2.6)	0.474

VHD, valvular heart disease; AF, atrial fibrillation. [#], trends across different years; *, comparison for different years by ANOVA test.

Table 2 Managements in patients with VHD from 2009 to 2013

Treatment	2009 (N=2,960)	2010 (N=3,330)	2011 (N=3,861)	2012 (N=4,159)	2013 (N=5,118)	P value[#]
General medication, N (%)	1,455 (49.2)	1,552 (46.6)	1,970 (51.0)	2,121 (51.0)	2,768 (54.1)	<0.001
Intervention, N (%)	39 (1.3)	56 (1.7)	65 (1.7)	58 (1.4)	81 (1.6)	0.778
Cardiac surgery, N (%)	1,466 (49.5)	1,722 (51.7)	1,826 (47.3)	1,980 (47.6)	2,269 (44.3)	<0.001
Open surgery, N (%)	1,456 (49.2)	1,705 (51.2)	1,760 (45.6)	1,828 (44.0)	2,042 (39.9)	<0.001
VATS, N (%)	10 (0.3)	17 (0.5)	66 (1.7)	152 (3.7)	227 (4.4)	<0.001
Simultaneous CABG, N (%)	87 (2.9)	100 (3.0)	87 (2.3)	115 (2.8)	103 (2.0)	0.007
Cox maze procedure, N (%)	192 (6.5)	216(6.5)	216 (5.6)	148 (3.6)	175 (3.4)	<0.001

VHD, valvular heart disease; VATS, video-assisted thoracoscopic surgery; CABG, coronary artery bypass graft; [#], trends across different years.

P<0.001), and an increase in congenital VHD (from 9.0% to 12.3%, P<0.001), ischemic VHD (from 9.2% to 11.3%, P=0.003) and degenerative VHD (from 8.8% to 14.5%, P<0.001). The prevalence of autoimmune-mediated VHD remained stable from 2009 to 2013, with a slight fluctuation from 1.0% to 0.7% (P=0.158).

Distribution of etiologies for VHD among different age groups

Patients were divided into groups according to age, and the prevalence of each VHD type was analyzed in the different groups (*Figure 2*). Congenital VHD accounted for 85.8% of all patients younger than 15 years of age and its prevalence decreased with age. Degenerative and ischemic etiologies were rarely present in the <35 group. The prevalence of rheumatic VHD increased progressively before the age of 35 (from 7.7% to 73.6%), and then reached a plateau (from 71.8% to 73.6%) in the 35-45 and 45-55 groups, subsequently decreasing after the age of 55 (from 71.8% to 2.9%). The prevalence of ischemic VHD increased after the age of 45, similar to that of degenerative VHD, which increasingly predominant after the age of 65 (from 28.5% to 73.2%).

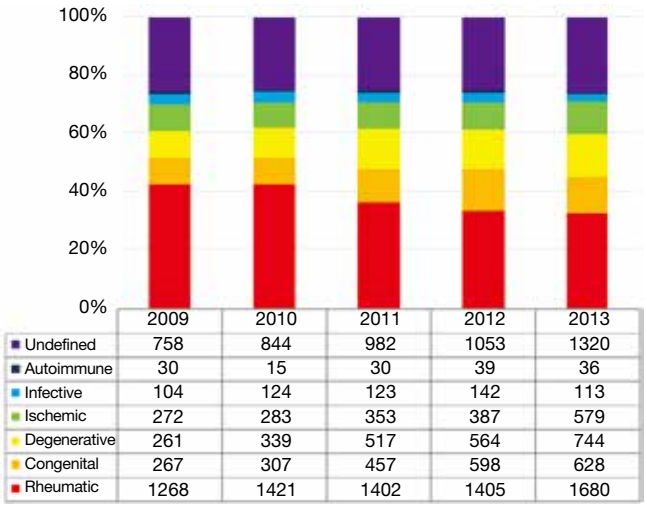

	2009	2010	2011	2012	2013
Undefined	758	844	982	1053	1320
Autoimmune	30	15	30	39	36
Infective	104	124	123	142	113
Ischemic	272	283	353	387	579
Degenerative	261	339	517	564	744
Congenital	267	307	457	598	628
Rheumatic	1268	1421	1402	1405	1680

Figure 1 Distribution of etiologies for VHD according different years in patient of Southern China. A relatively definitive etiology for VHD was identified in 13,549 (69.7%) patients. There were significant decrease in the prevalence of rheumatic VHD (from 42.8% to 32.8%, P<0.001) and infective VHD (from 3.5% to 2.2%, P<0.001), and an increase in congenital VHD (from 9.0% to 12.3%, P<0.001), ischemic VHD (from 9.2% to 11.3%, P=0.003) and degenerative VHD (from 8.8% to 14.5%, P<0.001). The prevalence of autoimmune-mediated VHD remained stable from 2009 to 2013, with a slight fluctuation from 1.0% to 0.7% (P=0.158). VHD, valvular heart disease.

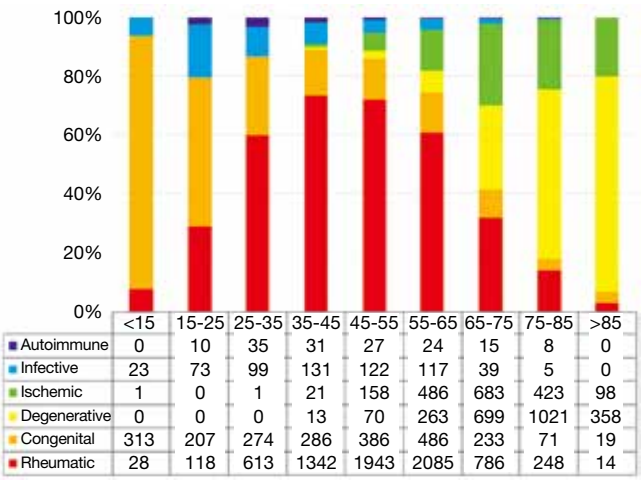

	<15	15-25	25-35	35-45	45-55	55-65	65-75	75-85	>85
Autoimmune	0	10	35	31	27	24	15	8	0
Infective	23	73	99	131	122	117	39	5	0
Ischemic	1	0	1	21	158	486	683	423	98
Degenerative	0	0	0	13	70	263	699	1021	358
Congenital	313	207	274	286	386	486	233	71	19
Rheumatic	28	118	613	1342	1943	2085	786	248	14

Figure 2 Distribution of etiologies for VHD according different age in patient of Southern China. Congenital VHD accounted for 85.8% of all patients younger than 15 years of age and its prevalence decreased with age. Degenerative and ischemic etiologies were rarely present in the <35 group. The prevalence of rheumatic VHD increased progressively before the age of 35 (from 7.7% to 73.6%), and then reached a plateau (from 71.8% to 73.6%) in the 35-45 and 45-55 groups, subsequently decreasing after the age of 55 (from 71.8% to 2.9%). The prevalence of ischemic VHD increased after the age of 45, similar to that of degenerative VHD, which increasingly predominant after the age of 65 (from 28.5% to 73.2%). VHD, valvular heart disease.

Changes in the management of VHD from 2009 to 2013

From 2009 to 2013, the proportion of patients with VHD undergoing open cardiac valvular surgery decreased (from 49.5% to 44.3%, P<0.001) and that of patients treated with general medication increased (from 49.2% to 54.1%, P<0.001). The number of patients treated by VATS increased significantly in this period (from 0.3% to 4.4%, P<0.001). As alternative methods to open cardiac valvular surgery, interventional balloon valvuloplasty and VATS were performed in patients with mild/moderate VHD. In-hospital mortality decreased progressively from 2009 to 2013. Further analysis of the methods of cardiac valvular surgery showed an increasing tendency in aortic mechanical valve replacement (from 32.1% to 34.5%, P=0.001) and double mechanical valve replacement (from 20.9% to 22.3%, P=0.035), especially in mitral valvuloplasty (MVP) (from 8.5% to 15.7%, P<0.001). However, the proportion of patients undergoing bioprosthetic valve replacement decreased from 2009 to 2013 (from 26.3% to 15.5%, P<0.001).

Discussion

Main findings

The main findings of the present study were as follows: (I) although the prevalence of rheumatic VHD decreased significantly from 2009 to 2013, it remained the leading etiology for VHD in Southern China, especially in VHD patients aged 35 to 55 years; (II) from 2009 to 2013, the prevalence of degenerative and ischemic VHD increased significantly whereas that of rheumatic VHD decreased. The prevalence of degenerative VHD increasingly predominant after the age of 65; (III) cardiac valvular surgery was the main treatment for VHD besides general medication. The proportion of patients undergoing VATS increased significantly from 2009 to 2013. Mechanical valve replacement (in particular aortic valve and double valve replacement) and mitral valvuloplasty showed a significant increasing tendency during this period.

Potential reasons for shifts in morbidity and etiological spectrum of VHD

These findings might be mainly relevant considering the socioeconomic development and improvements in quality of life, as well as an increasing aging population. In developing countries, a rheumatic etiology of VHD is prevalent (2), whereas in developed countries, degenerative VHD predominates and is found in 63% of patients (4). The prevalence of rheumatic VHD was reported at 72% in 2006-2007 in a South African center (5). In a recent survey in Turkey that included 1,300 patients hospitalized in 42 centers in 2009, rheumatic VHD accounted for 46% of all VHD patients with mean age of 57 (6). However, rheumatic VHD as second cause of VHD was present in only 22% of patients according to an European epidemiological survey (7). Risk factors for rheumatic etiology are largely associated with a sustained incidence of acute rheumatic fever and socioeconomic status, including the influence of famine, overcrowding, an unhealthy living environment, other communicable diseases, and even war (8). Due to the superior social and economic status and favorable living environment found in Guangdong compared to the rest of China, the prevalence of rheumatic VHD is decreasing progressively, although it is still present in 32.8% of patients, especially in those aged 35 to 55 years.

The surgical databases of developed countries show an increasing burden of VHD in Europe (9), the United States (10) and Canada (11), which is correlated with the predominance of an aging population and degenerative etiology. In the Euro Heart Survey, degenerative etiology was the leading cause of VHD in 63% of patients instead of rheumatic VHD (12). With the improvement of economic conditions and quality of life as well as average lifespan in Guangdong province, the prevalence of degenerative VHD increased from 8.8% in 2009 to 14.5% in 2013, and showed a marked increase after the age of 65. A similar tendency was observed in ischemic VHD, which increased from 9.2% to 11.3%, and in patients older than 45. The shift from rheumatic towards degenerative etiology accounts for the sustained prevalence of VHD and changes in patients' characteristics; however, this shift is mainly observed in developed countries and relatively rich developing countries such as China.

Possible causes for changes in the management of VHD

VHD patients are usually elderly and often present with a high operative risk or relative/absolute contraindications for cardiac surgery, especially considering the aging population and an increasing prevalence of degenerative VHD. Therefore, most patients are ineligible for open cardiac valvular surgery. In contrast, VATS is associated with less trauma, a faster postoperative recovery and better tolerance than classic open cardiac valvular surgery. Consequently, VATS is being widely popularized in clinical practice. Currently, patients choose general medication and VATS over open cardiac valvular surgery. The baseline characteristics showed a significant shift from bioprosthetic valves to mechanical valves from 2009 to 2013. Although long-term anticoagulant treatment and elderly patients at high risk of bleeding might restrict mechanical valve implantation, increasing mechanical valves were still implanted from 2009 to 2013, especially aortic and double valves. By contrast, the limited valvular lifespan and possibility of re-operation could be associated with the decrease in bioprosthetic valve implantation from 2009 to 2013 (13). Furthermore, the high cost of repeat operations increases the economic burden for patients. In the present study, valvuloplasty mainly included the mitral and tricuspid valves, and mitral valve valvuloplasty was performed at an increasing rate from 2009 to 2013. According to the 2014 AHA/ACC guidelines for the management of patients with VHD, MVP is recommended with IIa class in asymptomatic patients with chronic severe primary mitral regurgitation with preserved left ventricular function (14). The shift of MVP is consistent with the current guidelines (*Table 3*).

The prevalence of valvular interventional therapy did not change significantly between 2009 and 2013. Although transcatheter aortic valve implantation (TAVI) and percutaneous edge-to-edge repair as new interventional techniques have expanded the range of valvular interventions, their application is confined to patients who are ineligible or at high risk for cardiac surgery and who were likely to be denied cardiac surgery (15,16). However, the development of interventional techniques will likely result in an expansion in the indications for valvular interventional therapy.

Limitations

The main limitation of the present study is that the findings are mostly based on a regional single center database. Therefore, regional multicenter epidemiological surveys are needed to reduce selection bias and confirm these findings.

Conclusions

Despite a significant shift from rheumatic towards degenerative etiology from 2009 to 2013, rheumatic VHD

Table 3 Characteristics of cardiac valvular surgery method from 2009 to 2013

Cardiac valvular surgery method	2009 (N=1,466)	2010 (N=1,722)	2011 (N=1,826)	2012 (N=1,980)	2013 (N=2,269)	P value[#]
Valvuloplasty, N (%)	990 (67.5)	1,187 (68.9)	1,186 (65.0)	1,214 (61.3)	1,586 (69.9)	0.921
Mitral valve, N (%)	125 (8.5)	186 (10.8)	198 (10.8)	237 (12.0)	357 (15.7)	<0.001
Aortic valve, N (%)	26 (1.8)	26 (1.5)	30 (1.6)	28 (1.4)	47 (2.1)	0.450
Tricuspid valve, N (%)	834 (56.9)	971 (56.4)	955 (52.3)	946 (47.8)	1,177 (51.9)	<0.001
Pulmonary valve, N (%)	5 (0.3)	4 (0.2)	3 (0.2)	3 (0.2)	5 (0.2)	0.498
Mechanical valve replacement, N (%)	1,172 (79.9)	1,265 (73.5)	1,434 (78.5)	1,576 (79.6)	1,831 (80.7)	0.002
Mitral valve, N (%)	700 (47.7)	769 (44.7)	864 (47.3)	913 (46.1)	1,037 (45.7)	0.524
Aortic valve, N (%)	471 (32.1)	491 (28.5)	564 (30.9)	659 (33.3)	783 (34.5)	0.001
Double valve, N (%)	307 (20.9)	314 (18.2)	370 (20.3)	411 (20.8)	506 (22.3)	0.035
Tricuspid valve, N (%)	1 (0.1)	5 (0.3)	6 (0.3)	4 (0.2)	10 (0.2)	0.096
Pulmonary valve, N (%)	0 (0)	0 (0)	0 (0)	0 (0)	1 (0)	0.317
Bioprosthetic valve replacement, N (%)	385 (26.3)	478 (27.8)	332 (18.2)	387 (19.5)	351 (15.5)	<0.001
Mitral valve, N (%)	214 (14.6)	257 (14.9)	162 (8.9)	189 (9.5)	179 (7.9)	<0.001
Aortic valve, N (%)	128 (8.7)	175 (10.2)	131 (7.2)	151 (7.6)	127 (5.6)	<0.001
Double valve, N (%)	66 (4.5)	100 (5.8)	64 (3.5)	67 (3.4)	59 (2.6)	<0.001
Tricuspid valve, N (%)	42 (2.9)	45 (2.6)	37 (2.0)	47 (2.4)	42 (1.9)	0.047
Pulmonary valve, N (%)	1 (0.1)	1 (0.1)	2 (0.1)	0 (0)	3 (0.1)	0.671

[#], trends across different years.

remains the leading etiology in Southern China, with a significant increase in the prevalence of ischemic, congenital and degenerative VHD. General medication and cardiac valvular surgery remain the main treatment options. The proportion of VATS increased markedly from 2009 to 2013, and mechanical valve replacement and mitral valvuloplasty showed an increasing tendency.

Acknowledgements

Funding: The article was funded by National Nature Science Foundation of China (No. 81370295), Twelfth Five-Year Plan-National Key Technology Support Program (No. 2011BAI11B13), and Science and Technology Planning Project of Guangdong Province (No. 2012B031800316, 2012B061800047, 2012B031800317).
Disclosure: The authors declare no conflict of interest.

References

1. Nkomo VT, Gardin JM, Skelton TN, et al. Burden of valvular heart diseases: a population-based study. Lancet 2006;368:1005-11.
2. Marijon E, Ou P, Celermajer DS, et al. Prevalence of rheumatic heart disease detected by echocardiographic screening. N Engl J Med 2007;357:470-6.
3. Valvular stenosis and valvular regurgitation. In: Otto CM. eds. Textbook of Clinical Echocardiography. Philadelphia: Elsevier Saunders, 2004:281-328.
4. Iung B, Baron G, Butchart EG, et al. A prospective survey of patients with valvular heart disease in Europe: The Euro Heart Survey on Valvular Heart Disease. Eur Heart J 2003;24:1231-43.
5. Sliwa K, Carrington M, Mayosi BM, et al. Incidence and characteristics of newly diagnosed rheumatic heart disease in urban African adults: insights from the heart of Soweto study. Eur Heart J 2010;31:719-27.
6. Demirbağ R, Sade LE, Aydın M, et al. The Turkish registry of heart valve disease. Turk Kardiyol Dern Ars 2013;41:1-10.
7. Iung B, Vahanian A. Epidemiology of acquired valvular heart disease. Can J Cardiol 2014;30:962-70.
8. Essop MR, Nkomo VT. Rheumatic and nonrheumatic valvular heart disease: epidemiology, management, and prevention in Africa. Circulation 2005;112:3584-91.
9. Bridgewater B, Gummert J, Walton P, et al. eds. Fourth EACTS adult cardiac surgical database report 2010. Henly-on-Thames, UK: Dendrite Clinical Systems Ltd.,

2010:2010.
10. The US Society of Thoracic Surgeons National Database. Available online: http://www.sts.org/sites/default/files/documents/4thHarvestExecutiveSummary.pdf
11. Hassan A, Newman AM, Gong Y, et al. Use of valve surgery in Canada. Can J Cardiol 2004;20:149-54.
12. Iung B, Baron G, Tornos P, et al. Valvular heart disease in the community: a European experience. Curr Probl Cardiol 2007;32:609-61.
13. Jamieson WR, Burr LH, Miyagishima RT, et al. Re-operation for bioprosthetic aortic structural failure - risk assessment. Eur J Cardiothorac Surg 2003;24:873-8.
14. Nishimura RA, Otto CM, Bonow RO, et al. 2014 AHA/ACC guideline for the management of patients with valvular heart disease: a report of the American College of Cardiology/American Heart Association Task Force on Practice Guidelines. J Am Coll Cardiol 2014;63:e57-185.
15. Grant SW, Devbhandari MP, Grayson AD, et al. What is the impact of providing a transcatheter aortic valve implantation service on conventional aortic valve surgical activity: patient risk factors and outcomes in the first 2 years. Heart 2010;96:1633-7.
16. Malaisrie SC, Tuday E, Lapin B, et al. Transcatheter aortic valve implantation decreases the rate of unoperated aortic stenosis. Eur J Cardiothorac Surg 2011;40:43-8.

Cite this article as: Liu FZ, Xue YM, Liao HT, Zhan XZ, Guo HM, Huang HL, Fang XH, Wei W, Rao F, Deng H, Liu Y, Lin WD, Wu SL. Five-year epidemiological survey of valvular heart disease: changes in morbidity, etiological spectrum and management in a cardiovascular center of Southern China. J Thorac Dis 2014;6(12):1724-1730. doi: 10.3978/j.issn.2072-1439.2014.11.21

Original Article

Rapid pleurodesis is an outpatient alternative in patients with malignant pleural effusions: a prospective randomized controlled trial

Serkan Özkul, Akif Turna, Ahmet Demirkaya, Burcu Aksoy, Kamil Kaynak

Department of Thoracic Surgery, Istanbul University, Cerrahpasa Medical School, Istanbul, Turkey

Correspondence to: Akif Turna, MD, PhD, FETCS. Bilginler Sok, No: 12/1, Sahrayicedid, Istanbul, Turkey. Email: akif.turna@gmail.com.

Background: Chemical pleurodesis can be palliative for recurrent, symptomatic pleural effusions in patients who are not candidate for a thoracic surgical procedure. We hypothesized that effective pleurodesis could be accomplished with a rapid method of pleurodesis as effective as the standard method.

Methods: A prospective randomized 'non-inferiority' trial was conducted in 96 patients with malignant pleural effusion (MPE) who are not potentially curable and/or not amenable to any other surgical intervention. They were randomly allocated to group 1 (rapid pleurodesis) and to group 2 (standard protocol). In group 1, following complete fluid evacuation, talc slurry was instilled into the pleural space. This was accomplished within 2 h of thoracic catheter insertion, unless the drained fluid was more than 1,500 mL. After clamping the tube for 30 min, the pleural space was drained for 1 h, after which the thoracic catheter was removed. In group 2, talc-slurry was administered when the daily drainage was lower than 300 mL/day.

Results: No-complication developed due to talc-slurry in two groups. Complete or partial response was achieved in 35 (87.5%) and 33 (84.6%) patients in group 1 and group 2 respectively (P=0.670). The mean drainage time was 40.7 and 165.2 h in group 1 and group 2 respectively (P<0.001).

Conclusions: Rapid pleurodesis with talc slurry is safe and effective and it can be performed in an outpatient basis.

Keywords: Pleurodesis; talc; malignant pleural effusion (MPE); slurry

Submitted May 19, 2014. Accepted for publication Oct 15, 2014.

doi: 10.3978/j.issn.2072-1439.2014.11.31

View this article at: http://dx.doi.org/10.3978/j.issn.2072-1439.2014.11.31

Introduction

The management of patients with malignant and/or recurrent pleural effusions is cumbersome and can present important diagnostic and therapeutic challenges (1,2).

Pleural effusion causing symptoms such as chest pain and dyspnea is a common problem that causes significant morbidity and can negatively affect quality of life of patients for their remaining months. Despite management of underlying malignancy with chemo/radiotherapy, malignant pleural effusions (MPE) may persist or recur and necessitate palliative interventions in order to control or alleviate the symptoms. Several palliative treatment options are available including therapeutic thoracentesis, tube thoracostomy, chemical pleurodesis, video thoracoscopic pleurodesis and pleuroperitoneal shunt (2,3).

Pleurodesis is performed to inflame the visceral and parietal pleura to fuse the pleura together obliterating the potential pleural space. Pleurodesis with sclerosing agents has a high success rate but requires hospitalization for up to 6 days until chest tubes can be removed (4). It is generally considered standard treatment for recurrent MPE. Asbestos-free talc has been established as the most effective agent for pleurodesis (4). However, various factors have impact on the success of pleurodesis include initial drainage time, chest drain diameter, management of the chest drain (suction, no suction), etc. (5). Success and length of stay of the patients (5-7 days) are of utmost importance since patients with MPE are usually critically ill and/or moribund. In these patients with an expected survival of only 8 months, the aim of a palliative intervention should be reliable alleviation of dyspnea, improving quality of life, shortening hospital

stay as much as possible and keeping the duration of chest tube drainage as short as possible. Traditional catheter drainage of MPE includes tube insertion, daily observation and pleurodesis if daily drainage is <200-400 mL and re-expansion of the lung is provided. However, this approach may lead to very long hospitalization time with limited success of the procedure. We investigated the value and effectiveness of a rapid and pleurodesis method using talc in patients with potentially recurrent pleural effusion. Our secondary hypothesis was whether rapid pleurodesis would decrease the length of hospitalization or not.

Materials and methods

A prospective, randomised method was utilized to compare standard method of pleurodesis with the proposed new rapid pleurodesis process in patients with symptomatic MPE. This is the 'non-inferiority' trial of 'rapid-pleurodesis' that is to prove that 'rapid-pleurodesis' methodology is equally effective to standard procedures with a number of advantages. The institutional review board for human studies has approved the treatment protocols. Type-I (α) error and type-II (β) error were set to 5%. Our non-inferiority margin was 40% difference with a δ0 value of 10%. With a one-sided alternative, we needed to include 40 patients in each arm.

From April 2011 to December 2012, 96 symptomatic patients who had 'potentially' recurrent histologically and/or cytologically proven MPE were evaluated. The patients whose lungs did not expand (n=8), patients with endobronchial lesions (n=3), and ones who are suitable for curative therapy were excluded from the randomization. Of those, 79 patients were amenable to be analyzed (36 patients were allocated in each group). There were 37 men, 42 women. The mean age was 58.8 years (range, 25 to 92 years; standard deviation, 16.32 years). Randomization was performed according to an internet based-random number generator. We also aimed to analyze the effect of rapid pleurodesis on hospital stay as secondary goal of the study. A total of 40 patients were randomized into the rapid-pleurodesis arm whereas 39 patients had standard drainage and pleurodesis (control group).

Thoracic drainage and pleurodesis: using local anesthesia (bupivacaine) and intramuscular preemptive analgesia (ketorolac), a small-bore (12F) thoracic catheter was inserted into the pleural space in the posterior axillary line. Study group (group 1): pleural space was drained using valve system connected to the thoracic catheter. One liter of pleural fluid was drained every 8 h until all 'drainable' fluid was removed. Pleural space drainage was subsequently evaluated using chest radiographs obtained 2 h after the first drainage and the one taken after the last drainage. Pleurodesis with 4 gr. talc (Steritalc; Novatech; La Ciotat; France) slurry was initiated only after obtaining radiographic evidence of the complete evacuation of the fluid and no-trapped lung. In control group (group 2), controlled drainage was done limited to 1 lt at once and maximum 1.5 lt of fluid was drained per day. Chest radiograph was taken in 2 h. Daily follow-up was performed. Pleurodesis with 4 gr talc slurry was initiated only after obtaining radiographic evidence of the complete evacuation of the fluid, if the daily drainage <300 mL. The tube was clamped for 30 min in all patients (group 1 and group 2). Catheter was withdrawn 1 h after the talc-slurry drainage. Pleural fluid LDH, protein, pH, glucose, pleural fluid amylase, cholesterol, arterial blood partial gas pressure, cytopathological, bacteriological analyses were performed in almost all patients. Informed consent was obtained from all patients before their participation in the study. The Institutional Review Board approved the study before its commencement. The randomized trial was in accordance with the 2001 checklist of the Consolidated Standards of Reporting Trials (CONSORT) Statement. The CONSORT recommended flow diagram of patients is shown in *Figure 1*. Patients were followed up with plain chest radiographs at 1, 2, 3 and 6 months (if the patient was alive) after pleurodesis. Responses were classified as: (I) complete (no clinical or radiological recurrence of pleural effusion); (II) partial (small amount of fluid re-accumulation in the chest radiograph, but no symptoms); (III) failure (reaccumulation of fluid causing symptoms or needing thoracentesis) (6). The assessment of success was performed by an investigator blinded to allocation.

The mean follow-up of patients was 5.3 months (range, 1 to 18 months). SPSS 15.0 statistical software program was used in data analysis. Student *t*-test, paired *t*-test, covariance analysis, Fisher exact test were carried out. The difference was deemed significant when $P<0.05$.

Results

The causes of pleural effusions are shown in *Table 1*. Demographic and primary disease characteristics are summarized in *Table 1*. The majority of patients had breast cancer, lung cancer or mesothelioma.

No-complication developed due to talc-slurry in

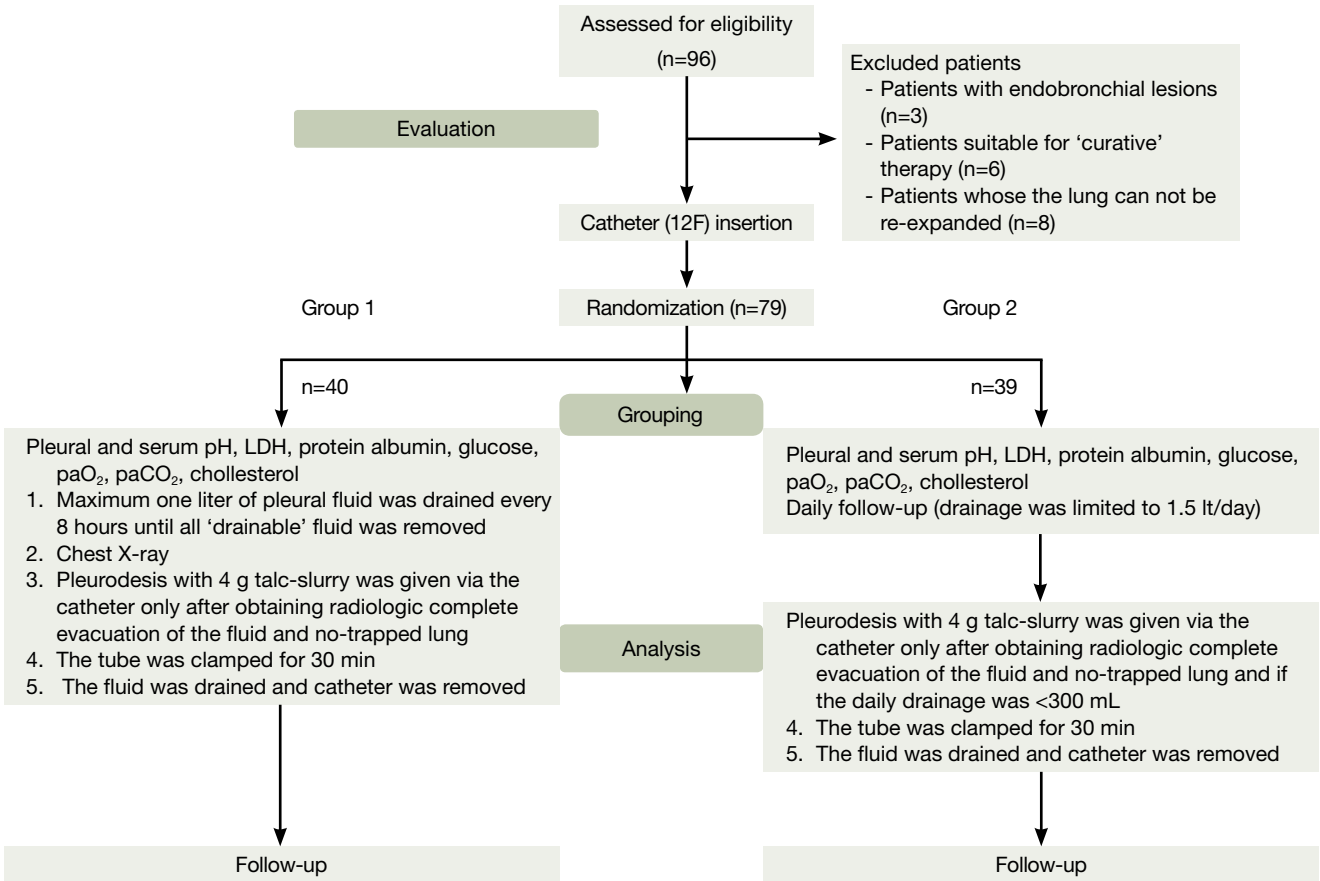

Figure 1 Consort 2010 diagram of the study.

Table 1 Patient characteristics

Characteristics	Group 1 (n=40)	Group 2 (n=39)	P value
Age (years) [mean ± standard deviation]	61.0±17.8 [30-91]	56.0±12.2 [25-92]	0.530
Male/female	16/24	21/18	0.03
Primary site (n)			0.21
Lung	11	9	
Over	4	3	
Gastrointestinal system	3	0	
Urogenital	1	3	
Breast	4	2	
Mesothelioma	2	2	
Esophagus	1	3	
Pancreas	1	3	
Lymphoma	1	4	
Hepatocellular	3	3	
Others	9	7	
Follow-up period (months)	5.75±6.21 (0.1-18)	3.25±6.40 (0.1-18)	0.641

Table 2 Potential surrogate markers for success in all patients

Parameter	Success (mean ± standard deviation)	Recurrence (mean ± standard deviation)	P value
Age	59.4±8.3	62.2±9.9	0.8
Pleural fluid LDH (IU/mL)	330.0±19.0	433.1±21.9	0.3
Pleural fluid albumin (mg/dL)	5.8±1.3	6.3±2.1	0.9
Pleural fluid glucose (mg/dL)	83.0±12.4	76.5±9.4	0.8
PaO_2 (mmHg)	73.0±6.1	71.0±14.7	0.9
$PaCO_2$ (mmHg)	36.9±4.0	37.2±5.0	1
Pleural fluid pH	7.36±0.08	7.42±0.16	0.9

two groups. Four patients (4.8%) developed sub-febrile fever with an elevated white-blood-cell count requiring antibiotics within 48 h of the pleurodesis. Complete or partial response was achieved in 35 (87.5%) and 33 (84.6%) patients in group 1 and group 2 respectively (P=0.670). The mean total drainage was 2,703 mL in group 1, whereas it was 4,329 mL in group 2 (P=0.016). The mean drainage time was 40.7 and 165.2 h in group 1 and group 2 respectively (P<0.001).

The mean length of stay was 2.2 in group 1, whereas it was 9.0 days in group 2 (P<0.001). In rapid-pleurodesis group, the procedure was completed in less than 24 h in 32 out of 40 patients (80.0%). We found no predictive factor indicating success in all patients (*Table 2*).

Discussion

Malignant and/or recurrent pleural effusions are associated with significant morbidity.

The key point to achieve successful pleurodesis is the ability to fully drain the pleural space and to re-expand the lung. Prompt clinical evaluation followed by aggressive treatment often results in successful palliation (1). Treatment response for MPE is highly variable (2). We have developed a new method of rapid pleurodesis, which worked effectively in patients with short survival expectations. The selection of pleurodesis agents stays debatable. Talc is more effective, but is allied with more unfavorable effects. Talc pleurodesis is followed by systemic and pulmonary inflammation (5,7). Spiegler published a rapid pleurodesis series with considerable success, shorter hospital stay and possibly lower cost (8). They found that, chemical pleurodesis can be accomplished with good results in the majority of patients (complete obliteration: 48%, partial response: 31%) with bleomycin in less 1 day.

Yildirim *et al.* preferred to use oxytetracycline for rapid pleurodesis (9). They utilized a very similar rapid pleurodesis methodology. Differently, we drained all pleural fluid before talc-slurry implementation. They advocated oxytetracycline since it was well tolerated by the patients without major side effects (9). In our series, we did not observe any serious side effect possibly attributable to talc. Janssen *et al.* reported that, large-particle size (22.5 μm) talc for pleurodesis is safer and not associated with the development of acute respiratory distress syndrome (10). We used the same particle-size and brand talc. We found that, rapid pleurodesis protocol with talc is safe and effective. It also led to shorter hospital stay and possibly low-hospital cost. It is reasonable to suggest that, fast and effective pleurodesis may have caused less hospital-related morbidity. In the study, the pleural fluid was aspirated manually at 8 h intervals to keep both pleura in close apposition before instillation of talc. The main purpose was to increase the contact duration and surface area of both pleura for increasing the chemical pleuritis in the shortest possible interval.

Reddy and colleagues reported that rapid pleurodesis could be achieved safely and effectively (successful rate: 92%) by combining thoracoscopy and talc poudrage with simultaneous tunneled pleural catheter in patients with symptomatic MPE (11). We did not use tunnelled catheter and thoracoscopy and we utilized talc-slurry which has been proved to be equally effective (12). In our study, 80.6% of patients could be treated less than 24 hours. This means that, rapid pleurodesis can lead to fast palliation without the need for hospitalization (i.e., in an outpatient setting) in most patients. Since the rapid pleurodesis is possible without a need for general anesthesia with a high success rate, we did not perform videothoracoscopic talc implementation in any of our patients.

There are a number of limitations in this study. Firstly, patients with small loculations were not treated in a

specific manner (i.e., not tailored). We did not carry out cost analysis. The number of patients is relatively low. We aimed a total of 80 patients. Despite the fact that we analyzed 79 patients (not 80 patients as the statistical analysis suggested), the primary (the safety and effectiveness of rapid-pleurodesis) goal has been reached in the study. We also did not record and analyze the quality of life of the patients. However, it is plausible to speculate that, rapid pleurodesis could have provided acceptable quality of life since it is effective and shortens hospital stay comparing the standard plerurodesis group.

The findings of the current study showed that the new recommended method of 8 h aspiration intervals and immediate implementation of talc-slurry resulted in reduced days of drainage and hospitalization days (it can be done in outpatient basis) rendering no more morbidity than the standard procedure. Prolonged drainage and hospitalization seems unnecessary if the fluid is completely drained and the lung is re-expanded. Rapid and effective drainage and pleurodesis may lead to better comfort and prognosis in these usually low-performance patients. Further studies are needed to confirm this finding obtained by this rapid pleurodesis method.

Acknowledgements

Authors' contributions: Serkan Özkul carried out the trial, Akif Turna designed and carried out the trial, Ahmet Demirkaya collected and analyzed data with Serkan Özkul and Burcu Aksoy. Burcu Aksoy collected and analyzed with Serkan Özkul and Ahmet Demirkaya. Kamil Kaynak supervised the study.

Disclosure: The authors declare no conflict of interest.

Cite this article as: Özkul S, Turna A, Demirkaya A, Aksoy B, Kaynak K. Rapid pleurodesis is an outpatient alternative in patients with malignant pleural effusions: a prospective randomized controlled trial. J Thorac Dis 2014;6(12):1731-1735. doi: 10.3978/j.issn.2072-1439.2014.11.31

References

1. Belani CP, Pajeau TS, Bennett CL. Treating malignant pleural effusions cost consciously. Chest 1998;113:78S-85S.
2. Putnam JB Jr. Malignant pleural effusions. Surg Clin North Am 2002;82:867-83.
3. Antony VB, Loddenkemper R, Astoul P, et al. Management of malignant pleural effusions. Eur Respir J 2001;18:402-19.
4. Antunes G, Neville E, Duffy J, et al. BTS guidelines for the management of malignant pleural effusions. Thorax 2003;58:ii29-38.
5. Sahn SA. Malignant pleural effusions. In: Shields TW, Locicero J, Reed CE, et al. eds. General Thoracic Surgery. 7th edition. Philadelphia, PA: Lippincott Williams & Wilkins, 2009:875-83.
6. Rodriguez-Panadero F, Antony VB. Pleurodesis: state of the art. Eur Respir J 1997;10:1648-54.
7. West SD, Davies RJ, Lee YC. Pleurodesis for malignant pleural effusions: current controversies and variations in practices. Curr Opin Pulm Med 2004;10:305-10.
8. Spiegler PA, Hurewitz AN, Groth ML. Rapid pleurodesis for malignant pleural effusions. Chest 2003;123:1895-8.
9. Yildirim E, Dural K, Yazkan R, et al. Rapid pleurodesis in symptomatic malignant pleural effusion. Eur J Cardiothorac Surg 2005;27:19-22.
10. Janssen JP, Collier G, Astoul P, et al. Safety of pleurodesis with talc poudrage in malignant pleural effusion: a prospective cohort study. Lancet 2007;369:1535-9.
11. Reddy C, Ernst A, Lamb C, et al. Rapid pleurodesis for malignant pleural effusions: a pilot study. Chest 2011;139:1419-23.
12. Dresler CM, Olak J, Herndon JE 2nd, et al. Phase III intergroup study of talc poudrage vs talc slurry sclerosis for malignant pleural effusion. Chest 2005;127:909-15.

Original Article

Overnight fluid shifts in subjects with and without obstructive sleep apnea

Ning Ding[1]*, Wei Lin[2]*, Xi-Long Zhang[1], Wen-Xiao Ding[1], Bing Gu[3], Bu-Qing Ni[4], Wei Zhang[4], Shi-Jiang Zhang[4], Hong Wang[1]

[1]Department of Respiratory Medicine, [2]Department of Geriatric Medicine, [3]Department of Laboratory Medicine, [4]Department of Cardiothoracic Surgery, The First Affiliated Hospital of Nanjing Medical University, Nanjing 210029, China

*These authors contributed equally to this work.

Correspondence to: Hong Wang, MD, PhD. Department of Respiratory Medicine, The First Affiliated Hospital of Nanjing Medical University, 300 Guangzhou Road, Nanjing 210029, China. Email: drhongwang@163.com.

Objective: To investigate the characteristics of baseline body fluid content and overnight fluid shifts between non-obstructive sleep apnea (non-OSA) and obstructive sleep apnea (OSA) subjects.

Methods: A case-controlled study was performed between February 2013 and January 2014, with 36 (18 OSA and 18 non-OSA) outpatients enrolled in this study. Polysomnographic parameters and results of body fluid were compared between the two groups.

Results: There were no differences in age, weight, and body mass index (BMI) between groups. Compared with the non-OSA group, OSA group had significantly higher neck circumference (NC) and fluid volume shift in the legs. OSA patients had higher left and right leg fluid indices than non-OSA subjects. There were significant correlations between apnoea-hypopnoea index and baseline fluid indices in both legs as well as the reduction in overnight change in both legs fluid volume. The increase in NC was also significantly correlated with the reduction in overnight change in both legs fluid volume, but not with the change in head and neck fluid volume. There were significant correlations between change in NC and increased fluid shifts in head and neck volume.

Conclusions: OSA patients had a higher baseline fluid content in both legs as compared with non-OSA subjects, which may be the basic factor with regards to fluid shifts in OSA patients. The increase in head and neck fluid shift volume did not directly correlate with the severity of OSA.

Keywords: Obstructive sleep apnea (OSA); fluid shift; body composition analysis

Submitted Apr 29, 2014. Accepted for publication Oct 15, 2014.
doi: 10.3978/j.issn.2072-1439.2014.11.19
View this article at: http://dx.doi.org/10.3978/j.issn.2072-1439.2014.11.19

Introduction

Obstructive sleep apnea (OSA) is caused by repetitive occlusion of the upper airway during sleep. A number of factors contribute to upper airway obstruction in OSA patients. The prevalence of OSA increases with increasing body mass index (BMI) and neck circumference (NC) (1,2). However, only one-third of the variability in sleep apnea severity is attributable to these two indices of obesity (3,4). Therefore, factors other than obesity must play a role in the pathogenesis of OSA (5).

Previous studies have shown that fluid accumulates in the legs due to gravity during the daytime, and is redistributed when with supine positioning at night (6). A portion of the shifted fluid accumulates in the neck, and narrows the upper airway, predisposing the patient to OSA (3,7).

Some self-controlled studies have found that the fluid shifts from the legs to the neck existed in healthy subjects (5), OSA patients (7), and heart failure patients (8). However, the characteristics of baseline body fluid content and nocturnal fluid shift between non-OSA and OSA patients remain unclear.

We speculate that OSA patients have more fluid shifts

from the legs to the neck as compared with healthy control subjects, which increase the severity of OSA. We designed this study to test our hypothesis. In this study, we measured baseline body fluids distribution and nocturnal fluid shifts by bioelectrical impedance analysis (InBody 720 system, Biospace Co., Ltd., Korea).

Methods

Subjects

This case-controlled study was performed at the Sleep Medicine Center of The First Affiliated Hospital with Nanjing Medical University. Thirty-six outpatients were enrolled in this study between February 2013 and January 2014.

OSA group inclusion criteria were as follows: age from 18 to 70 years, and an apnea-hypopnea index (AHI) ≥5/hour according to the results of polysomnography (PSG). Age and BMI-matched subjects without OSA (AHI <5) were recruited for the control group. Exclusion criteria for both groups were: (I) a history of stroke or clinical signs of peripheral or central nervous system disorders; (II) previously known heart failure, coronary heart disease, or myocardial infarction; (III) chronic obstructive pulmonary disease or history of asthma; (IV) a history of allergy to a local anesthetic; and (V) pregnancy.

This protocol was approved by the Clinical Study Ethics Committee of The First Affiliated Hospital of Nanjing Medical University. All subjects provided written informed consent prior to study participation.

Polysomnography (PSG)

An evaluation of daytime sleepiness based on the Epworth Sleepiness Scale (ESS) score was calculated prior to the sleep study, which was performed by unattended overnight PSG (Embla S4500 System, USA) as described previously (9). PSG was monitored using five electroencephalographic channels (F4-M1, C4-M1, O2-M1, E12-M2, and E2-M2) and a submental electromyogram. Nasal airflow was measured by continuously recording nasal pressure, snoring, pulse oximetry, and body position, as well as chest and abdominal effort. Analyses were performed by two physicians who specialized in sleep medicine, but were not directly involved in this study.

We used the 2012 standard of the American Academy of Sleep Medicine for scoring sleep apnea events (10): obstructive apnea: complete cessation of airflow with continued paradoxical chest and abdominal excursion for ≥10 s; hypopnea: reduction of airflow >50% baseline lasting ≥10 s and associated with ≥4% desaturation. The AHI was defined as the number of apneas and hypopneas per hour of sleep. A patient with an AHI ≥5/hour was considered to have OSA.

Body fluid analysis

The human body is composed of water, protein, fat, and minerals. These compositions have different bioelectrical impedance. Water and fat content in each part of the body can be detected by bioelectrical impedance analysis. As a user-friendly, safe, simple, and non-invasive technology, bioelectrical impedance analysis can be performed quickly and repeated at short time intervals (11).

Two body fluid analyses were performed using the InBody 720 system (Biospace) for each enrolled subject. The first measurement (pre-sleep, baseline data) was carried out between 21:00 and 22:00 o'clock and the second measurement (post-sleep) was performed when the subject awakened. In order to improve the accuracy of measurement results, fasting was required 3 hours before fluid analyses. The patients were required to empty their bladders, remove their coats and footwear, and stand on the equipment. Subjects were asked to hold the detection handles while breathing calmly. Data would be automatically generated in one minute. The parameters consisted of weight, BMI, NC, left arm fluid index, right arm fluid index, trunk fluid index, left leg fluid index, and right leg fluid index. Fluid shift volume (Δ, mL) for each part of the body was calculated with the formula: (pre-sleep fluid index - post-sleep fluid index) × body weight (kg) ×1,000. Since the fluid index on the head and neck can not be directly detected, we calculated the fluid shift volume by the difference between the other five parts (the total decrease in fluid volume from the legs equals the total increase of fluid volume of the trunk, arms, and head and neck). The formula used for calculation was: Δ left leg + Δ right leg – Δ left arm – Δ right arm – Δ trunk.

Statistical analysis

Statistical analyses were performed using SPSS statistical software (SPSS, Inc., Chicago, IL, USA). Data were expressed as the mean ± standard deviation for normally distributed and as median (interquartile range) for nonnormally distributed, and counts (percentages) for qualitative data. Parameters compared between OSA and non-OSA subjects using the

Table 1 Baseline characteristics between OSA and non-OSA subjects

Characteristics	OSA	non-OSA	T	P
Male, n (%)	17 (94.4)	17 (94.4)	χ^2=0.000	1.000
Age (year)	47.67±9.99	49.28±7.18	–0.556	0.582
Weight (kg)	79.02±6.74	76.13±5.92	1.367	0.181
BMI (kg/m^2)	26.52±1.73	26.24±1.78	0.490	0.628
NC (cm)	38.42±1.74	37.90±1.29	1.012	0.319
Sleep time (min)	412.33±37.05	411.22±38.53	0.088	0.930
ESS score	10.78±4.41	4.56±2.55	5.180	<0.001
AHI, h^{-1}	42.00±20.19	2.06±1.51	8.371	<0.001
ODI, h^{-1}	32.61±18.50	1.11±1.23	7.208	<0.001
Mean SpO_2 (%)	93.89±2,87	97.89±0.68	–5.760	<0.001
Minimal SpO_2 (%)	72.94±8.86	91.33±3.11	–8.309	<0.001

OSA, obstructive sleep apnea; BMI, body mass index; NC, neck circumference; ESS, Epworth Sleepiness Scale; AHI, apnea-hypopnea index; ODI, oxygen desaturation index.

Table 2 Comparisons of fluid volume change between OSA and non-OSA subjects

Characteristics	OSA	non-OSA	Z	P
Change in weight (kg)	–0.250 (–0.175, –0.325)	–0.200 (–0.200, –0.100)	1.829	0.079
Change in BMI (kg/m^2)	–0.010 (0.000, –0.020)	–0.010 (–0.010, –0.000)	1.148	0.279
Change in NC (cm)	+0.600 (0.200, 1.225)	+0.250 (–0.100, 0.325)	–2.825	0.004
Δ left arm (mL)	+79.50 (–19.65, 161.55)	+0.000 (–148.50, 78.53)	–0.794	0.443
Δ right arm (mL)	+80.25 (–19.45, 155.75)	+67.25 (–78.18, 97.18)	–1.140	0.265
Δ trunk (mL)	+79.65 (0.000, 156.00)	+0.000 (–78.20, 96.80)	–1.665	0.097
Δ left leg (mL)	–160.50 (–252.83, –77.80)	–80.45 (–181.50, 109.75)	2.184	0.029
Δ right leg (mL)	–272.35 (334.20, –214.23)	–136.50 (–164.50, 0.000)	3.928	<0.001
Δ head and neck (mL)[#]	+241.20 (138.65, 346.90)	+64.70 (–171.75, 302.60)	–1.614	0.111

OSA, obstructive sleep apnea; BMI, body mass index; NC, neck circumference. Δ fluid shift volume: +, increase fluid volume; –, decrease fluid volume; [#], calculation of Δ head and neck: Δ left leg + Δ right leg – Δ left arm – Δ right arm – Δ trunk.

independent *t*-test for normally distributed data or Mann-Whitney U test for nonnormally distributed data. Pearson correlation analysis was used to analyze the relationship between sleep parameters [AHI, oxygen desaturation index (ODI), mean and minimal SpO_2] and body composition parameters (change in NC, baseline fluid index, fluid shift volumes) adjusted by age, gender and BMI.

Results

Each group had 18 subjects (17 male and 1 female). The average age was 47.67±9.99 years in the OSA group and 49.28±7.18 in the non-OSA group. There were no differences in age, weight, and BMI between groups (*Table 1*).

The changes of fluid volume between two groups are shown in *Table 2*. There were no significant differences between groups with regards to changes in weight and BMI (all P>0.05). OSA patients had a significant increase in NC than non-OSA subjects (P<0.01). There were no significant differences between OSA and non-OSA subjects in fluid volume changes in the arms, trunk and head and neck (all P>0.05). As compared with non-OSA subjects, OSA patients had remarkably reduced fluid volume in both legs.

By comparing of the fluid indices between the two groups, we found that OSA patients had higher left and right legs fluid volume indices than that in non-OSA

Table 3 Comparisons of baseline fluid indices between OSA and non-OSA subjects

Baseline fluid indices	OSA	non-OSA	*t*	P
Left arm fluid index	0.377±0.004	0.374±0.004	1.902	0.066
Right arm fluid index	0.377±0.004	0.375±0.004	1.629	1.112
Trunk fluid index	0.377±0.007	0.374±0.006	1.260	0.216
Left leg fluid index	0.380±0.006	0.375±0.006	2.118	0.042
Right leg fluid index	0.382±0.007	0.377±0.006	2.472	0.019

OSA, obstructive sleep apnea.

Table 4 Correlations between PSG parameters and baseline fluid indices

Variables	Left arm fluid index	Right arm fluid index	Trunk fluid index	Left leg fluid index	Right leg fluid index
AHI	0.465**	0.361*	0.343*	0.500**	0.553**
ODI	0.379*	0.251	0.223	0.410**	0.451**
Mean SpO_2	−0.413**	−0.298	−0.338	−0.439**	−0.527**
Minimal SpO_2	−0.391*	−0.329	−0.318	−0.436**	−0.535**

Note: the values in the table are Pearson correlation coefficient(r) adjusted by age, gender and body mass index; *, P<0.05; **, P<0.01. PSG, polysomnography; AHI, apnea-hypopnea index; ODI, oxygen desaturation index.

Table 5 Correlations between PSG parameters and changes in body compositions parameters

Variables	Change in NC	Δ left arm	Δ right arm	Δ trunk	Δ left leg	Δ right leg	Δ head and neck
AHI	0.696**	0.263	0.307	0.348*	−0.525**	−0.780**	0.333
ODI	0.634**	0.188	0.266	0.342*	−0.490*	−0.690**	0.324
Mean SpO_2	−0.577**	−0.161	−0.279	−0.133	0.433*	0.711**	−0.398*
Minimal SpO_2	−0.518**	−0.216	−0.240	−0.204	0.426**	0.771**	−0.391*

Δ fluid shift volume; the values in the table are Pearson correlation coefficient(r) adjusted by age, gender and body mass index; *, P<0.05; **, P<0.01. PSG, polysomnography; NC, neck circumference; AHI, apnea-hypopnea index; ODI, oxygen desaturation index.

subjects (both P<0.05). Detailed information is shown in *Table 3*.

Table 4 showed the correlations between PSG parameters and baseline fluid index. There were significant correlations between AHI and left arm fluid index (r=0.500, P<0.01) and right leg fluid index (r=0.553, P<0.01). There were inverse relationships found between mean and minimal SpO_2 and left arm fluid index (r=−0.413, P<0.01; r=0.391, P<0.05) left leg fluid index (r=0.439, P<0.01; r=0.436, P<0.01) and right leg fluid index (r=0.527, P<0.01; r=0.535, P<0.01).

Relationships between PSG parameters and change in body composition parameters are shown in *Table 5*. AHI correlated significantly with an increase in NC (r=0.696, P<0.01), increase in fluid volume in the trunk (r=0.348, P<0.05), and decrease in fluid volume in both legs (r=0.525, P<0.01; r=0.780, P<0.01). However, there was no significant correlation between AHI and change in fluid volume in the head and neck (r=0.333, P>0.05). The significant correlation between the change in NC and the increase fluid shift volume in head and neck was found (r=0.493, P<0.01; *Figure 1*): the more fluid shift volume in the head and neck, and the greater the increase in NC.

Discussion

Although the key pathology of OSA is repetitive collapse of the upper airway during sleep, the cause of upper airway collapse remains unclear. It is well known that obesity, male gender, age, upper airway anatomic abnormalities and genetic factors are the risk factors for OSA. Recent

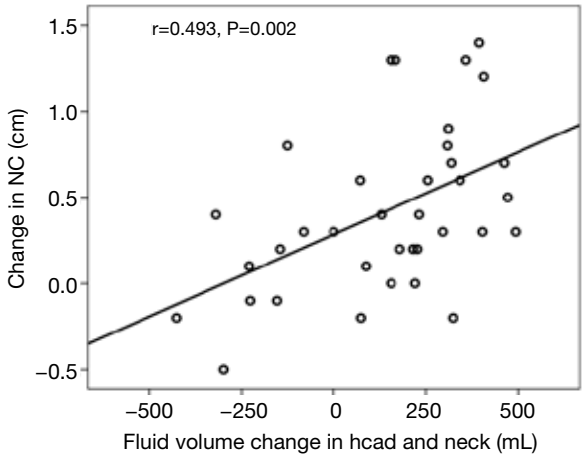

Figure 1 Correlation between overnight change in fluid volume in the head and neck and change in NC. NC, neck circumference.

studies have shown that fluid shifts from the legs to the neck may play an important role in upper airway collapse. The researchers found that fluid displacement from the legs by inflation of anti-shock trousers increased NC, narrowed the pharynx, and increased its collapsibility in awake healthy subjects (3,7,12). They speculated that rostral fluid displacement into the neck contributed to the pathogenesis of OSA. The same team then found that nocturnal rostral fluid shifts contribute to the pathogenesis of both OSA and CSA in patients with heart failure, and that the magnitude of the fluid shifts was directly related to the severity of the sleep apnea (5,8).

Our study provided several novel findings on the pathogenesis of OSA, and suggested new approaches to its prevention and therapy. We accurately analyzed fluid shifts in each part of body and found that OSA patients had more fluid shifts from the legs (especially the right leg) to the neck (increasing in NC, $P<0.05$) than non-OSA subjects (*Table 2*).

In order to clarify why OSA patients had more fluid shifts than the control subjects, we analyzed baseline fluid index, which indicates the "water content" in each part of the body. We found that OSA patients had a higher baseline fluid index in both left and right legs compared with non-OSA subjects (*Table 3*). Although White *et al*. (13) investigated the fluid shift in men with and without OSA, he did not find a difference in leg fluid volume between the two groups. Our results suggest that OSA patients may have mild edema which does not affect normal physiological function in daily life, but lead to more nocturnal fluid shifts. According to this hypothesis, during the day, more fluid accumulates in the intravascular and interstitial spaces of the legs due to gravity, and redistributes rostrally when supine at night, again due to gravity. Some of this fluid may accumulate in the neck, increasing tissue pressure and causing the upper airway to narrow, predisposing to OSA (3,6,7,12).

We also found the direct evidence that an increase in fluid volume in head and neck leads to an increase in NC (*Figure 1*). AHI significantly correlated with change in NC, but not with fluid volume change in the head and neck (*Table 5*). Thus, it can be seen that fluid shifts accumulating in the head and neck is not closely related to OSA. The occurrence of OSA depends on where the fluid accumulates. The tendency is for more fluid accumulation in the peripharyngeal tissues, but not the craniofacial subcutaneous soft tissue, and is thus easier to cause upper airway collapse and OSA.

Kasai and Bucca found that diuretic therapy reduced AHI, overnight shifts in leg fluid volume and an increase in NC (14,15). Compression stockings, which prevent daytime leg fluid accumulation and reduce overnight rostral fluid shifts, reduced the AHI in patients with chronic venous insufficiency and OSA (16). Here, we observed that OSA patients had more baseline fluid retention. Considering the present information, we suggest that body composition analysis should be provided for OSA patients, and followed by diuretic therapy with more baseline fluid retention.

There are several potential limitations in this study. First, a previous study documented that fluid displacement into the peripharyngeal soft tissues leads to increased airflow resistance of the pharynx (3,13); however, we did not measure airflow resistance of the pharynx. Second, it is well known that continuous positive airway pressure (CPAP) treatment contributes to the reduction of AHI. However, a recent study documented that the reduction in AHI, as a response to CPAP treatment, correlated with the degree of decrease in NC overnight. Whether the effect of preventing fluid accumulation in the neck is due to preventing fluid shifts from the legs or not remains unclear. Further investigation is needed.

Conclusions

In summary, OSA patients had more baseline fluid content in both legs compared with non-OSA subjects, which may be the basic factor for the increase in fluid shift seen from the legs to the neck during sleep in OSA patients. Since the increase of fluid shift volume in the head and neck did not

directly correlate with OSA severity, it has been suggested that the destination of the fluid shifts and accumulation is important in the development of sleep apnea.

Acknowledgements

The authors thank head nurse Xi Dai (Department of Geriatric Medicine) for her assistance in measuring body composition.
Funding: This study was supported by Jiangsu Provincial Department of Education (No. CXLX12_0557) and Jiangsu Provincial Special Program of Medical Science (No. BL2012012).
Disclosure: The authors declare no conflict of interest.

References

1. Sakakibara H, Tong M, Matsushita K, et al. Cephalometric abnormalities in non-obese and obese patients with obstructive sleep apnoea. Eur Respir J 1999;13:403-10.
2. Hoffstein V, Szalai JP. Predictive value of clinical features in diagnosing obstructive sleep apnea. Sleep 1993;16:118-22.
3. Chiu KL, Ryan CM, Shiota S, et al. Fluid shift by lower body positive pressure increases pharyngeal resistance in healthy subjects. Am J Respir Crit Care Med 2006;174:1378-83.
4. Dempsey JA, Skatrud JB, Jacques AJ, et al. Anatomic determinants of sleep-disordered breathing across the spectrum of clinical and nonclinical male subjects. Chest 2002;122:840-51.
5. Redolfi S, Yumino D, Ruttanaumpawan P, et al. Relationship between overnight rostral fluid shift and Obstructive Sleep Apnea in nonobese men. Am J Respir Crit Care Med 2009;179:241-6.
6. White LH, Bradley TD. Role of nocturnal rostral fluid shift in the pathogenesis of obstructive and central sleep apnoea. J Physiol 2013;591:1179-93.
7. Su MC, Chiu KL, Ruttanaumpawan P, et al. Lower body positive pressure increases upper airway collapsibility in healthy subjects. Respir Physiol Neurobiol 2008;161:306-12.
8. Yumino D, Redolfi S, Ruttanaumpawan P, et al. Nocturnal rostral fluid shift: a unifying concept for the pathogenesis of obstructive and central sleep apnea in men with heart failure. Circulation 2010;121:1598-605.
9. Ding N, Ni BQ, Zhang XL, et al. Prevalence and Risk Factors of Sleep Disordered Breathing in Patients with Rheumatic valvular Heart Disease. J Clin Sleep Med 2013;9:781-7.
10. Berry RB, Budhiraja R, Gottlieb DJ, et al. Rules for scoring respiratory events in sleep: update of the 2007 AASM Manual for the Scoring of Sleep and Associated Events. Deliberations of the Sleep Apnea Definitions Task Force of the American Academy of Sleep Medicine. J Clin Sleep Med 2012;8:597-619.
11. Tajiri Y, Kato T, Nakayama H, et al. Reduction of skeletal muscle, especially in lower limbs, in Japanese type 2 diabetic patients with insulin resistance and cardiovascular risk factors. Metab Syndr Relat Disord 2010;8:137-42.
12. Shiota S, Ryan CM, Chiu KL, et al. Alterations in upper airway cross-sectional area in response to lower body positive pressure in healthy subjects. Thorax 2007;62:868-72.
13. White LH, Motwani S, Kasai T, et al. Effect of rostral fluid shift on pharyngeal resistance in men with and without obstructive sleep apnea. Respir Physiol Neurobiol 2014;192:17-22.
14. Kasai T, Bradley TD, Friedman O, et al. Effect of intensified diuretic therapy on overnight rostral fluid shift and obstructive sleep apnoea in patients with uncontrolled hypertension. J Hypertens 2014;32:673-80.
15. Bucca CB, Brussino L, Battisti A, et al. Diuretics in obstructive sleep apnea with diastolic heart failure. Chest 2007;132:440-6.
16. Redolfi S, Arnulf I, Pottier M, et al. Attenuation of obstructive sleep apnea by compression stockings in subjects with venous insufficiency. Am J Respir Crit Care Med 2011;184:1062-6.

Cite this article as: Ding N, Lin W, Zhang XL, Ding WX, Gu B, Ni BQ, Zhang W, Zhang SJ, Wang H. Overnight fluid shifts in subjects with and without obstructive sleep apnea. J Thorac Dis 2014;6(12):1736-1741. doi: 10.3978/j.issn.2072-1439.2014.11.19

Original Article

The changes of vaccinia related kinase 1 in grafted heart after rat heart transplantation

Shiguo Qian[1,2*], Xuechao Yang[1*], Kunpeng Wu[1], Qiangsheng Lv[2], Yuanyuan Zhang[2], Jiahong Dai[2], Cheng Chen[2], Jiahai Shi[1]

[1]Department of Cardiothoracic Surgery, Affiliated Hospital of Nantong University, Nantong 226001, China; [2]Department of Cardiothoracic Surgery, People's Hospital of Binhai County, Yancheng 224500, China

*These authors contributed equally to this work.

Correspondence to: Jiahai Shi. Department of Cardiothoracic Surgery, Affiliated Hospital of Nantong University, Nantong 226001, China. Email: happysjh167@163.com.

Objective: To assess the expression and significance of vaccinia-related kinase 1 (VRK1) after rat heart transplantation.

Materials and methods: Lewis and Wistar rats weighing 250 to 300 g were used as donors and recipients. Allografts were from Wistar transplanted into Lewis, and isografts were transplanted from Lewis into Lewis. Grafts were harvested at 1, 3, 5, and 7 days after transplantation. We performed Western Blot of heart tissues after cardiac transplantation. To analyze VRK1 express between the isografts and allografts for immunohistochemical staining. At 5th day after heart transplantation use related cytokines VRK1 for immunohistochemical. We used double immunofluorescent staining on transverse cryosections of graft tissues by co-labeling with different markers, including those for VRK1, activate caspase-3, α-actinin, VCAM-1, CD4.

Results: Compared with rare expression in syngeneic Lewis rat hearts, VRK1 protein level in allogeneic hearts were detected at various survival times after heterotopic heart transplantation, which observably expressed on day 5 postoperative. In addition, we examined the expression of activate caspase-3 in allogeneic hearts, which has a similar expression with VRK1. Immunohistochemical and immunofluorescent method displayed that VRK1 was widely expressed in cytoplasm of cardiac tissue and activate caspase-3 was also expressed in cardiomyocytes. However, the VRK1 wasn't express in inflammation.

Conclusions: The VRK1 expression has increased after heart transplantation in allograft and isograft, and VRK1 may play a significant role in myocardial apoptosis after heterotopic heart transplantation in rats.

Keywords: Vaccinia-related kinase 1 (VRK1); apoptosis; heterotopic heart transplantation; rat

Submitted Sep 11, 2014. Accepted for publication Oct 22, 2014.
doi: 10.3978/j.issn.2072-1439.2014.11.17
View this article at: http://dx.doi.org/10.3978/j.issn.2072-1439.2014.11.17

Introduction

Since the first successful heart transplantation by Christian Barnard in 1967, there have been over 60,000 heart transplants performed worldwide (1). Cardiac transplantation is a significantly used therapy for end-stage heart failure. Allogeneic graft survival is affected by acute chronic and rejection due to incomplete histocompatibility (2,3). The main reasons of allograft failure after heart transplantation are intractable acute rejection, primary graft dysfunction, and coronary graft disease (4). Improved cardiac function and myocardial cell survival after heart transplantation are significant to allograft. Many recent studies aimed to prolong allograft survival, thus improve the effectiveness of the heart transplantation (5).

The vaccinia-related kinases (VRKs) branched off early from the family of casein kinase (CK) I and compose a relatively uncharacterized family of the kinome (6). The VRKs were discovered due to their close sequence relation

to the vaccinia virus B1R serine/threonine kinase (6). B1R is an early protein essential for viral replication (7). There are three members in VRKs family. However, these three kinases differ significantly in their regulatory domains, which are located at the C-terminus in the case of VRK1 and VRK2, and at the N-terminus in VRK3 (8).

It is well known that several Ser/Thr kinases called cyclin-dependent kinases (CDKs) play an important role in cell regulation by reversibly phosphorylating key molecules controlling cell cycle progression (9). Several cell protection mechanisms are based on the ability of the p53 protein to regulate the progression of the cell cycle, the induction of apoptosis, or replicative senescence (7). VRK1 is highly expressed in tumor cells with high proliferation rates (8). It has reported that VRK1 as the first step in a new pathway regulating p53 activity during cell proliferation and anti-apoptosis (7).

All data showed that VRK1 can regulate cell proliferation in many tumors and resist cell apoptosis. Thus, we examined whether cardiomyocytes of heterotopic heart transplantation express VRK1, VRK1 regulates the apoptosis of cardiomyocytes in our model. These evidences indicate that the VRK1 expression has increased after heart transplantation in allograft and isograft, and VRK1 may play a significant role of myocardial apoptosis after heterotopic heart transplantation in rats.

Materials and methods

Animals and heterotopic heart transplantation

Wistar (n=20) and Lewis rats (n=60) with an average body weight of 280 g (range, 250-300 g) were used as donors and recipients. In this study, we use a common technique for heterotopic cervical heart transplantation in rats, which shortens operation time, leading to a high average survival rate of receptor. Hearts from Wistar rats (n=20) were heterotopically transplanted into Lewis rats (n=20). Additional syngeneic hearts were transplanted from Lewis to Lewis (n=40). All animals were operated under anesthesia with chloral hydrate. After surgery, animals were maintained under the same comfortable conditions and fed the same food and water without any antibiotic. Grafts were harvested respectively at postoperative days (POD) 1, 3, 5, and 7. Technically successful transplantation is defined as the forceful beat of the transplant heart. The cardiac grafts rejection was considered complete by cessation of impulse. All surgical interventions and postoperative animal care were performed in accordance with the National Institutes of Health Guide-lines for the Care and Use of Laboratory Animals (National Research Council, 1996, USA) and were approved by the Chinese National Committee to the Use of Experimental Animals for Medical Purposes, Jiangsu Branch. All procedures were performed on animals in an unconscious state. All efforts were made to minimize the number of animals used and their suffering.

Western blot analysis

Western blot was prepared from allogeneic and syngeneic cardiac tissue at each time point after operation (n=5 for each time point). To obtain samples for western blot, the cardiac tissue were excised and snap frozen at –80 ℃ until use. Total protein was isolated from approximately 0.1 g of cardiac tissue at indicated time points. To prepare lysates, frozen heart samples were minced with eye scissors in ice. Total heart tissue protein were then homogenized in lysis buffer containing 1% NP-40, pH 7.5, 5 mmol/L EDTA, 50 mmol/L Tris, 1% SDS, 1% Triton X-100, 1% sodium deoxycholate, 10 mg/mL aprotinin, 1 mmol/L PMSF, and 1 mg/mL leupeptin, then micro centrifuge at 10,000 rpm and 4 ℃ for 20 min to collect the supernatant. After protein concentrations were determined with a Bio-Rad protein assay (Bio-Rad, Hercules, CA, USA), the resulting supernatant was subjected to with SDS-polyacrylamide gel electrophoresis (PAGE). Proteins were transferred to polyvinylidine diflouride filter (PVDF) membranes (Millipore) by a transfer apparatus at 350 mA for 2.5 h. The membranes were blocked with 5% nonfat milk in Tris-buffered saline with Tween (TBST) at room temperature (RT) for 2 h. The filters were immediately rinsed three times in TBST and then incubated overnight with primary antibodies at 4 ℃. Finally, the horseradish peroxidase-conjugated secondary antibody was added to filters for an additional 2 h, and the proteins were examined with an enhanced chemiluminescence detection system (ECL, Pierce Company, USA).

Immunohistochemistry

The syngeneic and allogeneic rats were deeply anesthetized and perfused through the AA with 500 mL of 0.9% saline, followed by 4% paraformaldehyde at different survival time points (n=5 for each time point). After the perfusion, the

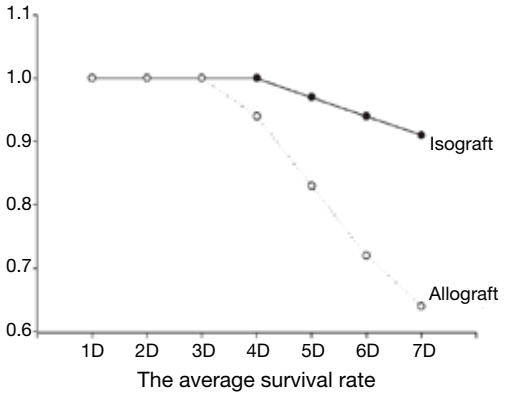

Figure 1 The average survival rate of heterotopic heart transplantation. Compared with the isograft, allograft showed no significant difference in average survival rate. (92.5% *vs.* 88.5%, P>0.05).

hearts of the allogeneic and syngeneic rats were removed and post-fixed in 4% paraformaldehyde for 4 h. The hearts were then subsequently steeped in 20% sucrose for three days and followed by 30% sucrose for another 3 days. Next, the hearts were embedded in OCT (opti-mum cutting temperature compound) compound for cryosectioning. The tissue was cut into 7-μm-thick sections and stored in a freezer at –20 ℃. The sections were removed from the icebox, kept in an oven at 37 ℃ for 2 h, and washed three in 0.01 M PBS for 5 min. All of the sections were blocked with 10% goat serum with 1% (w/v) bovine serum albumin (BSA) and 0.3% Triton X-100 at RT for 2 h and was incubated overnight at 4 ℃ with anti-VRK1 antibody (anti-mouse, 1:50; Abgent), then by incubation in a biotinylated secondary antibody (Vector Laboratories, Burlin-game, CA, USA). Immunostaining was visualized with DAB (Diaminobenzidine, Vector Laboratories). Images were collected under a light microscope (40×) using a DFC 300 FX camera (Leica, DM 5000B; Leica CTR 5000; Germany). Same exposure time and light intensity were applied to all photographs.

Double immunofluorescent staining

The sections were removed from the icebox, kept in an oven at 37 ℃ for 2 h, and washed three in 0.01 M PBS (phosphate buffer solution) for 5 min. To avoid unspecific staining, the sections were blocked with 10% goat serum [3% (w/v) BSA and 0.05% Tween 20 and 0.1% Triton X-100] at RT for 2 h in order to avoid unspecific staining. Then the slides were incubated with polyclonal antibody specific for VRK1 (Santa Cruz, 1:50) and different markers as follows: active caspase-3 (Santa Cruz, 1:100), α-actinin (a marker of heart, Sigma, 1:100), VCAM-1 (a maker of rejection), CD4 (a maker of T cell) overnight at 4 ℃. After was washing in PBS for three times, each time 15 min, a mixture of 4',6-diamidino-2-phenylindole (DAPI) and Fluorescein isothiocyanate- (FITC-) and Cy3-conjugated secondary antibodies were added in a dark room and incubated for 2 h at 4 ℃. Images were collected by Leica fluorescence microscope (Germany). Same exposure time and light intensity were applied to all photographs.

Statistical analysis

All of the data were analyzed with the Stata 7.0 statistical software. All values were expressed as the mean ± SEM. The significance of differences between the experimental groups was determined by a one-way analysis of variance (ANOVA) followed by the Tukey's post hoc multiple comparison tests. P value of less than 0.05 was considered to be statistically significant. Each experiment consisted of at least five replicates per condition.

Results

The average survival rate

The forceful beat of the transplant heart after 72 h was defined as technically successful transplantation. The average survival rate of heterotopic syngeneic heart transplantation is about 92.5%, and 88.5% in allograft (*Figure 1*), which showed no significant difference in syngeneic and allogeneic rats (92.5% *vs.* 88.5%, P>0.05).

The expression of VRK1 in allograft and isograft

To examine the expression pattern of VRK1, western blot analysis and immunohistochemistry experiments were performed on the allograft and isograft at various time points. The VRK1 expression level was low in syngeneic cardiac tissue, but in allografts high expressions of VRK1 is increased observably after operation (*Figure 2*). Heart tissues expression of VRK1 both in allograft and isograft were increased quite markedly after POD5 (P<0.05) (*Figure 3*). In addition, the immunohistochemistry experiments also demonstrated that VRK1 staining was extensively expressed in the cardiomyocytes after heart transplantation

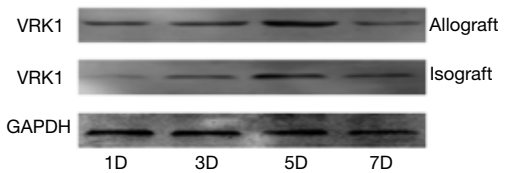

Figure 2 Western blot analysis shows that the protein expression of VRK1 in allografts and isografts. The VRK1 expression had increased after heart transplantation. GAPDH was used as an internal control. VRK1, vaccinia-related kinase 1.

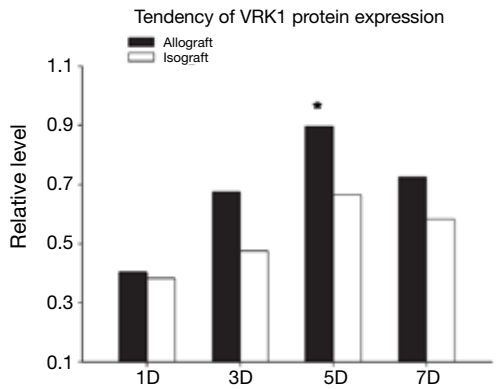

Figure 3 The tendency of VRK1 level expression in allografts and isografts. The bar chart below demonstrates the ratio of VRK1 relative to GAPDH expression for each time point. The data are represented as the mean ± SEM (n=5; *, P<0.05). VRK1, vaccinia-related kinase 1.

(*Figure 4*). Compared with the syngeneic cardiac graft, the stainings of VRK1-positive cells were increased observably after operation in allografts (*Figure 5*). These data indicated that VRK1 protein level had a temporary change after heart transplantation.

The co-localization of VRK1 and α-actinin

To further confirm the cell types expressing VRK1 in grafted cardiac tissues, double labeling immunofluorescent staining was performed. In the isograft tissues, the expression of VRK1 was low in cytoplasm of cardiomyocytes at POD5 (*Figure 6*). However, in the allograft tissue enhanced VRK1 immunocompetence was found in cytoplasm around the cardiomyocytes at POD5 (*Figure 6*). VRK1 expression was significantly increased in cardiomyocytes (P<0.05) at POD5 compared with the isograft group. To identify the proportion of myocardium-positive cells expressing VRK1, a minimum of 200 phenotype-specific marker positive cells were counted between the isograft and allograft groups (*Figure 7*).

The relationship of VRK1 and inflammatory cells

Besides, we examined the relationship between VRK1 with inflammatory cells, aiming to exclude whether the immune response is responsible for VRK1. Double labeling immunofluorescent staining was performed with the following cell-specific markers: VCAM-1, CD4 (*Figure 6*). In the allograft tissues, the co-localization of VRK1 with CD4 was not observed at POD 5. The result of co-localization between VRK1 and VCAM-1 could not be observed (*Figure 6*). The results indicate that VRK1 don't involving in immune rejection induced inflammatory cells infiltration after heart transplantation.

The co-localization of VRK1 and active-caspace-3

To understand whether VRK1 regulates the apoptosis of cardiomyocytes after allograft in murine, we examined the relationship between VRK1 and active caspase-3 after heart transplantation. Western blot analysis showed that the constitutive active caspase-3 level was low at POD1 in allograft, but increased at POD3 and reached a peak at POD5 (P<0.05) (*Figure 8*). The double labeling immunofluorescent staining was performed with the following cell-specific markers: VRK1, DAPI, active caspase-3 to assess the preliminary correlations between VRK1 and active caspase-3 in the allograft at POD5. Markedly, the co-localization of the two molecules increased more significantly in allograft (*Figure 9*).

Discussion

Since the first abdominal heterotopic heart transplantation in the mouse was built in 1973 by Corry *et al*. (10), then Matsuura and colleagues published the cervical heterotopic heart transplantation in the mouse in 1991 (11) and many modified techniques for heterotopic cervical heart transplantation in rats (12-15). Heart transplantation remains the chief method for patients with incurable cardiac diseases (16). As we all known, after heterotopic heart transplantation it exist many pathologic changes: polymorphonuclear leukocyte (PMN)-mediated tissue damage, macrophage infiltrates, cardiac hypertrophy and so on (17,18). In addition, increasing evidence has intensively

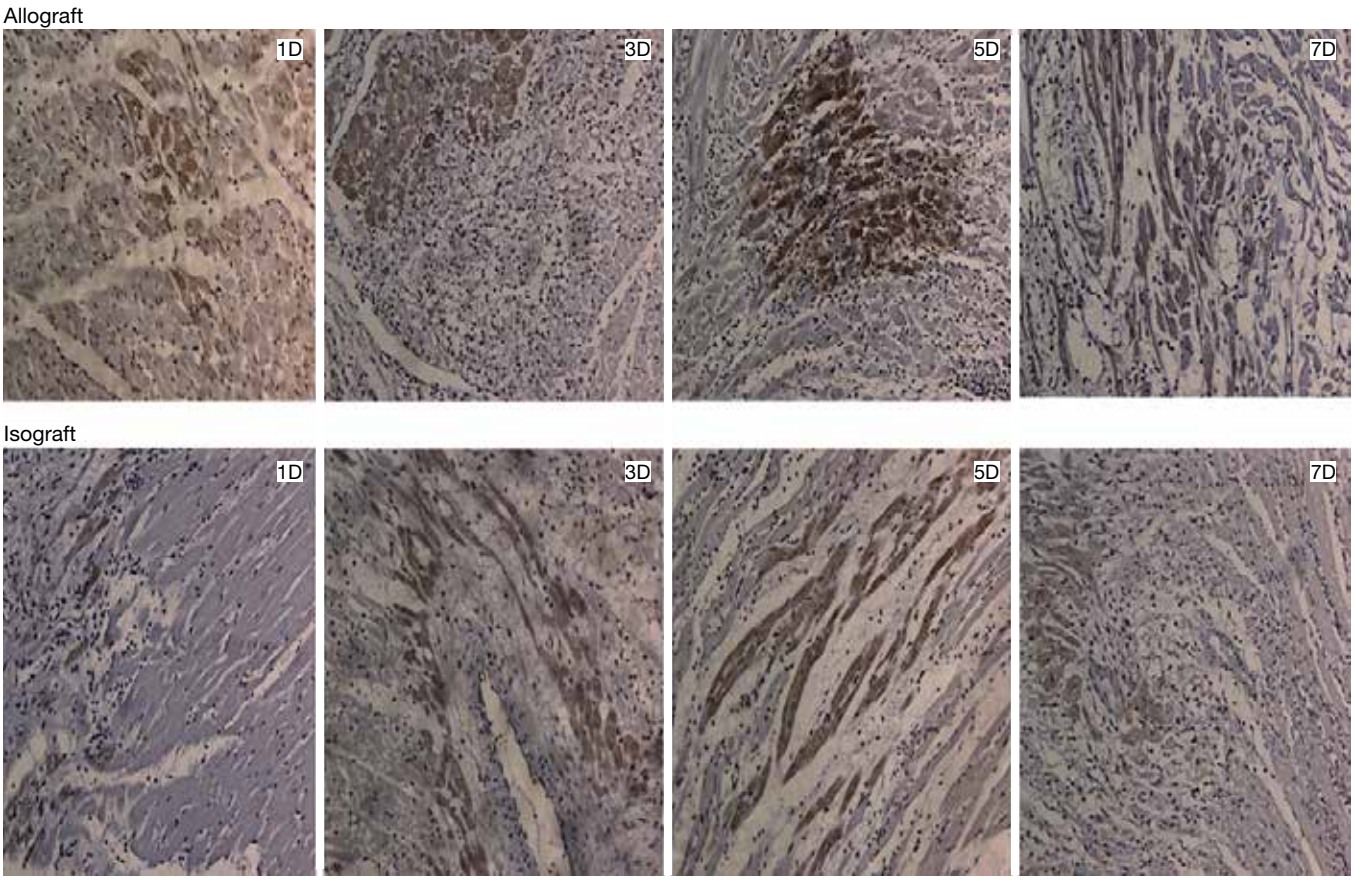

Figure 4 Immunohistochemical staining of VRK1 in allogeneic and syngeneic cardiac tissue. In the isogeneic transplanted heart, positive VRK1 staining was relatively low, however, in allogeneic transplanted heart the stainings of VRK1-positive cells were increased around the cardiomyocytes, especially at POD5. (Original magnification ×40). VRK1, vaccinia-related kinase 1; POD, postoperative days.

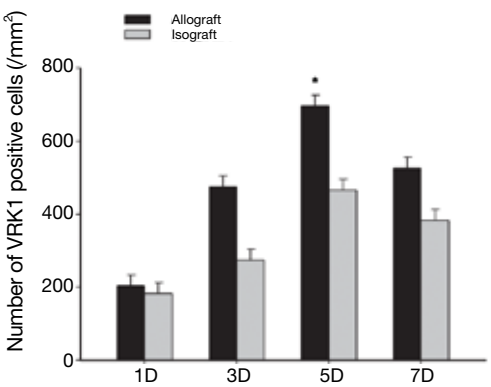

Figure 5 Compared with the syngeneic cardiac graft, the stainings of VRK1-positive cells were increased observably after operation in allografts. Quantitative analysis of VRK1 positive cells after heart transplantation. The VRK1 protein has maximal protein expression at day 5. The data are represented as the mean ± SEM (n=5; *, P<0.05). VRK1, vaccinia-related kinase 1.

demonstrating the existence of apoptosis in cardiac tissue samples (19,20). Many researches have showed that cardiomyocytes apoptosis is popular in allograft (21,22), however, there is not a satisfactory method to ameliorate apoptosis.

In the human kinome, the *VRK* gene family is deemed a novel branch from the lineage which led to the group of CK. The human VRK proteins were originally identified by their homology with the B1R kinase of vaccinia virus, an early protein required for viral DNA synthesis and replication (23). VRK1 in proliferating tissues is highly expressed, such as tumor cell lines, and during the hematopoietic proliferative phase in murine embryo midgestation (23).

Susana and Pedro conclude that VRK1 is an up stream regulator of p53 that be longs to a new signaling pathway (24). Regulation of p53 levels plays a major role in determining

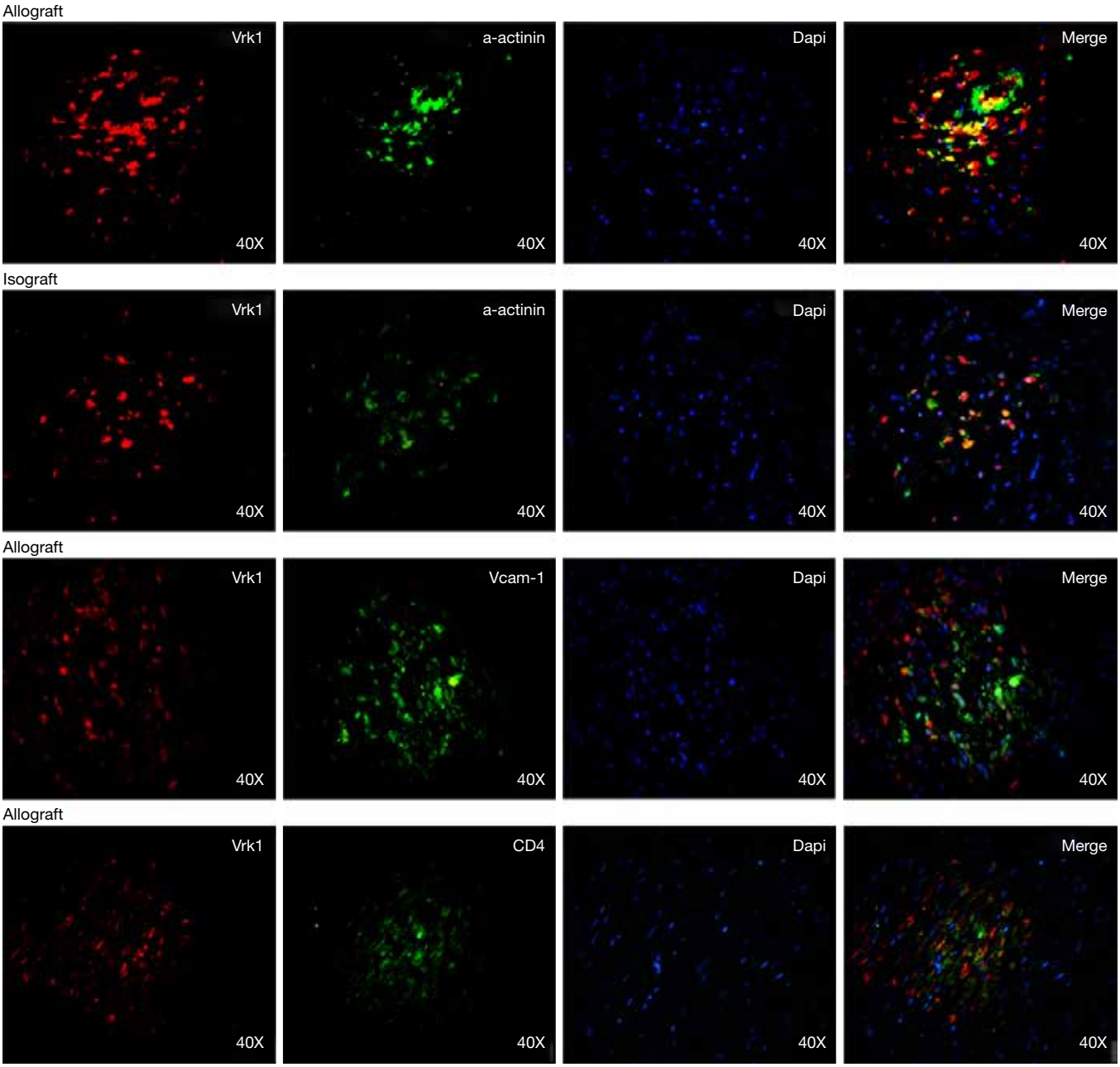

Figure 6 Association of VRK1 with α-actinin, and inflammatory cells after heart transplantation. (A,B) The co-localization of VRK1 with α-actinin was observed at POD5; (C) the co-localization of VRK1 with VCAM-1 was not observed at the 5 d in the transplanted heart after operation; (D) the result of co-localization between VRK1 and CD4 could not be observed. (Original magnification ×40). VRK1, vaccinia-related kinase 1; POD, postoperative days.

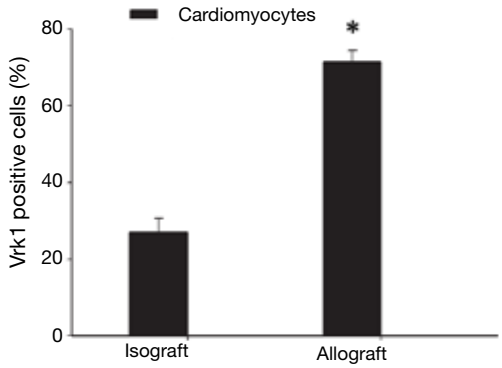

Figure 7 Quantitative analysis of cardiomyocytes positive cells expressing VRK1 (%) in the isograft and allograft group. *, indicate significant difference at P<0.05 compared with isograft-controlled group. Error bars are represented as the mean ± SEM (n=5; *, P<0.05). VRK1, vaccinia-related kinase 1.

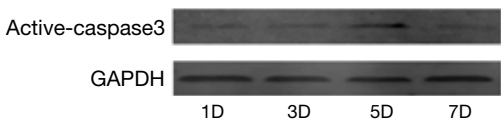

Figure 8 Western blot analysis shows that the protein expression of active caspase-3 in allografts. The active caspase-3 expression had increased after heart transplantation. The changes of active caspase-3 expression were similar to VRK1. VRK1, vaccinia-related kinase 1.

the fate of a cell and its susceptibility to tumor development (7,25). These evidences showed that VRK1 can regulate cell proliferation in many tumors and resist cell apoptosis. However, the expression and significance of VRK1 after rat heart transplantation in domestic and international was not reported.

Therefore, whether VRK1 could regulate the cardiac cells from apoptosis in grafted heart remains an unknown question. According to the western blot, the expression of VRK1 is obviously expressed in allogeneic transplanted heart (*Figures 2,3*). But in isogeneic transplanted heart, the expression of VRK1 protein level was low (*Figures 2,3*). To determine the cellular localization of VRK1 in isogeneic and allogenic transplanted heart, we performed immunohistochemistry experiments with anti-VRK12 mouse monoclonal antibody. In the isogeneic transplanted heart, positive VRK1 staining was relatively low, however, in allogeneic transplanted heart the stainings of VRK1-positive cells were increased around the cardiomyocytes, especially at POD5 (*Figures 4,5*). These data indicated that VRK1 protein level had a temporary change after heart transplantation both in allogeneic and isogeneic transplanted heart.

In order to research the significance of VRK1 in cardiomyocytes after heart transplantation, we examined the relationship of VRK1 and inflammatory cells. In the

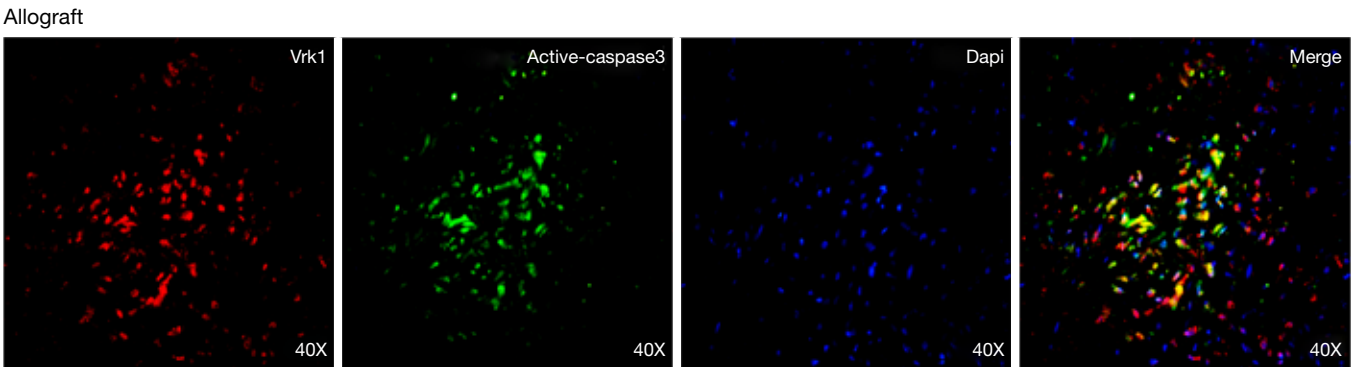

Figure 9 Association of active caspase-3 with VRK1 after heart transplantation. The co-localization of VRK1 with activated caspase-3 was observed at POD5. Representative photomicrographs that illustrate the VRK1 regulate the cardiomyocytes apoptosis after heart transplantation at POD5. (Original magnification ×40). VRK1, vaccinia-related kinase 1; POD, postoperative days.

allograft tissues, the co-localization of VRK1 with CD4 was not observed at POD5. The result of co-localization between VRK1 and VCAM-1 could not be observed (*Figure 6*). The results indicate that VRK1 don't involving in immune rejection induced inflammatory cells infiltration after heart transplantation. To understand whether VRK1 regulates the apoptosis of cardiomyocytes after allograft in murine, we examined the relationship between VRK1 and active caspase-3 after heart transplantation. The result showed that active caspase-3 has a similar expression pattern with VRK1 (*Figures 8*,*9*). We propose VRK1 may regulate the cardiomyocytes apoptosis after heterotopic heart transplantation in murine.

Taken all, we showed that VRK1 expression in cardiomyocytes at allograft was higher than isograft cardiac tissue. VRK1 may serve as a novel therapeutic target for protecting ardiomyocytes after heart transplantation in human.

Acknowledgements

This work was supported by the National Natural Scientific Foundation of China Grant (No.31300902), the "Top Six Types of Talents" Financial Assistance of Jiangsu Province Grant (WS-059) and the Science Foundation of Nantong City Grant (K2010055).
Disclosure: The authors declare no conflict of interest.

References

1. Burch M, Aurora P. Current status of paediatric heart, lung, and heart-lung transplantation. Arch Dis Child 2004;89:386-9.
2. Thom T, Haase N, Rosamond W, et al. Heart disease and stroke statistics--2006 update: a report from the American Heart Association Statistics Committee and Stroke Statistics Subcommittee. Circulation 2006;113:e85-151.
3. Taylor DO, Edwards LB, Mohacsi PJ, et al. The registry of the International Society for Heart and Lung Transplantation: twentieth official adult heart transplant report--2003. J Heart Lung Transplant 2003;22:616-24.
4. John R, Chen JM, Weinberg A, et al. Long-term survival after cardiac retransplantation: a twenty-year single-center experience. J Thorac Cardiovasc Surg 1999;117:543-55.
5. Shi J, Qian S, Meng X, et al. Reliability of intramyocardial electrogram for the noninvasive diagnosis of acute allograft rejection after heart transplantation in rats. J Thorac Dis 2014;6:126-33.
6. Klerkx EP, Lazo PA, Askjaer P. Emerging biological functions of the vaccinia-related kinase (VRK) family. Histol Histopathol 2009;24:749-59.
7. Vega FM, Sevilla A, Lazo PA. p53 Stabilization and accumulation induced by human vaccinia-related kinase 1.Mol Cell Biol. 2004;24:10366-80.
8. Sevilla A, Santos CR, Barcia R, et al. c-Jun phosphorylation by the human vaccinia-related kinase 1 (VRK1) and its cooperation with the N-terminal kinase of c-Jun (JNK). Oncogene 2004;23:8950-8.
9. Nezu J, Oku A, Jones MH, et al. Identification of two novel human putative serine/threonine kinases, VRK1 and VRK2, with structural similarity to vaccinia virus B1R kinase. Genomics 1997;45:327-31.
10. Corry RJ, Winn HJ, Russell PS. Primarily vascularized allografts of hearts in mice. The role of H-2D, H-2K, and non-H-2 antigens in rejection. Transplantation 1973;16:343-50.
11. Matsuura A, Abe T, Yasuura K. Simplified mouse cervical heart transplantation using a cuff technique. Transplantation 1991;51:896-8.
12. Vespignani R, Ruzza A, Czer LS, et al. High definition optical system for microsurgical heterotopic heart transplantation in rats. Transplant Proc 2012;44:1404-6.
13. Huang X, Chen D, Chen L. A modified model of cervical heterotopic cardiac transplantation for chronic rejection research. Zhongguo Xiu Fu Chong Jian Wai Ke Za Zhi. 2008;22:1508-10.
14. Yoshida Y, Hatayama N, Seki K. Study on the preservation with CO (PCO = 200-2,000 hPa), resuscitation, and heterotopic transplantation of an isolated rat heart. Cell Transplant 2009;18:535-40.
15. Ma Y, Wang G. Comparison of 2 heterotopic heart transplant techniques in rats: cervical and abdominal heart. Exp Clin Transplant 2011;9:128-33.
16. Wu W, Qiu Q, Wang H, et al. Nrf2 is crucial to graft survival in a rodent model of heart transplantation. Oxid Med Cell Longev 2013;2013:919313.
17. El-Sawy T, Miura M, Fairchild R. Early T cell response to allografts occurring prior to alloantigen priming up-regulates innate-mediated inflammation and graft necrosis. Am J Pathol 2004;165:147-57.
18. Qian Z, Wasowska BA, Behrens E, et al. C6 produced by macrophages contributes to cardiac allograft rejection. Am J Pathol 1999;155:1293-302.
19. Shaw SM, Critchley WR, Puchalka CM, et al. Brain natriuretic peptide induces CD8+ T cell death via a caspase 3 associated pathway--implications following heart transplantation. Transpl Immunol 2012;26:119-22.

20. Sánchez-Lázaro IJ, Almenar-Bonet L, Romero-Pelechano A, et al. Serum markers of apoptosis in the early period of heart transplantation. Biomarkers 2012;17:254-60.
21. Cristóbal C, Segovia J, Alonso-Pulpón LA, et al. Apoptosis and acute cellular rejection in human heart transplants. Rev Esp Cardiol 2010;63:1061-9.
22. Du JF, Shen XF, Ji XQ, et al. Apoptosis of peripheral T cells in rodent cardiac allograft recipients induced by donor-specific transfusion with impaired inducible costimulator/B7 homologous protein allorecognition. Transplant Proc 2013;45:564-8.
23. Sevilla A, Santos CR, Vega FM, et al. Human vaccinia-related kinase 1 (VRK1) activates the ATF2 transcriptional activity by novel phosphorylation on Thr-73 and Ser-62 and cooperates with JNK. J Biol Chem 2004;279:27458-65.
24. Lopez-Borges S, Lazo PA. The human vaccinia-related kinase 1 (VRK1) phosphorylates threonine-18 within the mdm-2 binding site of the p53 tumour suppressor protein. Oncogene 2000;19:3656-64.
25. Valbuena A, Vega FM, Blanco S, et al. p53 downregulates its activating vaccinia-related kinase 1, forming a new autoregulatory loop. Mol Cell Biol 2006;26:4782-93.

Cite this article as: Qian S, Yang X, Wu K, Lv Q, Zhang Y, Dai J, Chen C, Shi J. The changes of vaccinia related kinase 1 in grafted heart after rat heart transplantation. J Thorac Dis 2014;6(12):1742-1750. doi: 10.3978/j.issn.2072-1439.2014.11.17

Original Article

Uniportal video assisted thoracoscopic lobectomy: primary experience from an Eastern center

Mingxiang Feng[1*], Yaxing Shen[1*], Hao Wang[1], Lijie Tan[1], Xuping Mao[2], Yi Liu[1], Qun Wang[1]

[1]Department of Thoracic Surgery, Zhongshan Hospital of Fudan University, Shanghai 200032, China; [2]Department of Surgery, Danyang People's Hospital of Jiangsu Province, Danyang 212300, China

*These authors contributed equally to the work.

Correspondence to: Lijie Tan, MD. Department of Thoracic Surgery, Zhongshan Hospital of Fudan University, 180 Fenglin Road, Shanghai 200032, China. Email: Tan.lijie@zs-hospital.sh.cn; Xuping Mao, MD. Department of Surgery, Danyang People's Hospital of Jiangsu Province, Danyang 212300, China. Email: Mxp_dy@sina.com

Background: Uniportal video-assisted thoracoscopic surgery (VATS) lobectomy is an emerging technique for the surgical resection of non-small cell lung cancer (NSCLC). Besides its wide debates on safety and efficacy throughout the world, there were few report on uniportal VATS from the Eastern countries. In this article, we summarized our primary experience on uniportal VATS lobectomy in an Eastern center.

Methods: From October 2013 till February 2014, 54 consecutive uniportal VATS lobectomy were performed in the Department of Thoracic Surgery, Zhongshan Hospital of Fudan University. Patients' clinical features and operative details were recorded. Post-operatively, the morbidity and mortality were recorded to analyze the safety and efficacy of uniportal VATS lobectomy for NSCLCs.

Results: Among the 54 planned uniportal VATS lobectomy, there was one conversion to mini-thoracotomy due to lymph node sticking. Extra ports were required in two patients. The uniportal VATS lobectomy was achieved in 51 out of 54 patients (94.4%). The average operation duration was 122.2±37.5 min (90-160 min). The average volume of estimated blood loss during the operation was 88.8±47.1 mL (50-200 mL). The mean chest tube duration and hospital stay were 3.2±1.9 days and 4.6±2.0 days, respectively. There was no postoperative mortality in this study. Two patients suffered from prolonged air leakage (5 and 7 days), and one atrial fibrillation was observed in this cohort.

Conclusions: Based on our primary experience, uniportal VATS lobectomy is a safe and effective procedure for the surgical resection of NSCLCs. The surgical refinements and instrumental improvements would facilitate the technique. Further studies based on larger population are required to determine its benefits towards patients with NSCLCs.

Keywords: Lobectomy; minimally invasive surgery; non-small-cell-lung carcinoma (NSCLC)

Submitted Oct 02, 2014. Accepted for publication Nov 04, 2014.
doi: 10.3978/j.issn.2072-1439.2014.11.20
View this article at: http://dx.doi.org/10.3978/j.issn.2072-1439.2014.11.20

Introduction

The safety and feasibility of video-assisted thoracic surgery (VATS) procedure was well proved since its first application in the early 90s (1,2). While the number of VATS was increasing, a less invasive surgery using decreased number of trocars was demanded. Bases on the accumulated surgical experience and the technical innovation, uniportal VATS was pioneered in some experienced hands from the western countries (3).

Since the first report on uniportal thoracic surgery by Rocco in 2004 (4), the topics on pneumothorax, pleural biopsy, and lung wedge resection using uniportal VATS have shown promising results (5-7). In 2011, Gonzalez-Rivas *et al.* reported their experience of uniportal thoracoscopic lobectomy, the first worldwide published study on major lung resection (8). But there were few articles about uniportal thoracoscopic major lung resection, and less was

Table 1 Clinical features

Demographics	Uniportal VATS (n=51)
Age (years)	51.3±5.3
Sex (male; female)	32; 19
Histology (SC; AD)[a]	9; 42
BMI	24.1±3.6
Location (upper; middle; lower)	28; 2; 21
Operation duration (min)	122.2±37.5
Blood loss (mL)	88.8±47.1
Number of harvested lymph nodes	14.9±3.8
Length of stay (day)	4.6±2.0
Morbidity	3 (5.88%)
Mortality	0 (0%)

VATS, video-assisted thoracoscopic surgery; [a]SC, squamous carcinoma; AD, adenocarcinoma; BMI, body mass index.

Figure 1 The position of the surgeon and the scopist during uniportal video-assisted thoracoscopic surgery (VATS).

known if its application in eastern centers would benefit on patients as well.

Based on our primary experience from uniportal VATS biopsy, we summarize our primary experience on uniportal VATS lobectomy, and evaluate the safety and efficacy of this demanding procedure in this single center.

Materials and methods

The study was approved by the institutional review board and the ethics committee of Zhongshan Hospital of Fudan University. Pre-operative examination including EKG, pulmonary function, chest CT scan, bronchoscope, and brain MRI were administered to exclude the candidates for curative surgery for NSCLC patients.

The inclusion criteria for uniportal VATS lobectomy were as follows:

(I) Patients with clinically staged T1-3N0M0 tumors;
(II) Patients without previous history of cancer;
(III) Patients without previous history of chest surgery;
(IV) Patients with an ASA score of I-II.

The exclusion criteria for uniportal VATS lobectomy were as follows:

(I) Patients with preexisting tuberculosis/asthma/interstitial lung disease;
(II) Patients with cardiac, hepatic or renal dysfunction;
(III) Patients underwent neo-adjuvant therapy.

Clinical features including age, sex, comorbidity, BMI, operation duration, estimated volume of blood loss, morbidity and mortality were recorded in the database (*Table 1*).

Anesthesia and analgesia

All patients received a combination of epidural and general anesthesia, and were provided with patient-controlled analgesia (PCA) postoperatively. After intravenous induction, each patient was intubated with a double -lumen endotracheal tube to accomplish single lung ventilation. During the operation, patients' vital signs were followed every five minutes throughout the operation. All patients were extubated at the end of surgery and transferred to the ward.

Surgical technique

Patients were placed in lateral decubitus position, with the surgeon and the assistant standing on the abdominal side. The assistant stood at the foot-stool (*Figure 1*). The entire procedure was performed under the screen observation.

A 3.5 cm incision was made in the anterior axillary line 4th intercostal space (*Figure 2*) for upper lobe resection and 5th intercostal space for middle and inferior lobe resection. A soft plastic wound protector was applied to the incision without rib-spreading procedure. A 10-mm 30 degree thoracoscope was positioned in the superior side of the incision during the lobectomy. The designed surgical

Figure 2 The incision for uniportal VATS LUL lobectomy. VATS, video-assisted thoracoscopic surgery; LUL, left upper lobe.

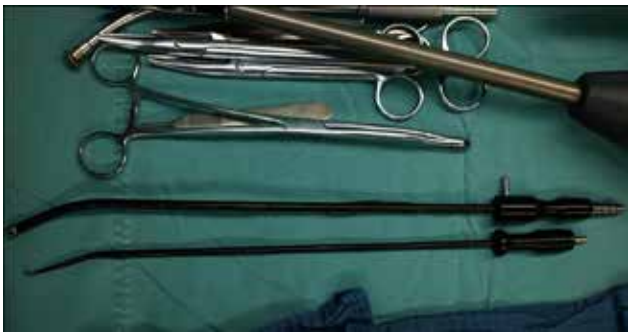

Figure 3 The designed surgical instruments for uniportal VATS. VATS, video-assisted thoracoscopic surgery.

Figure 4 The dissection order of the uniportal VATS left-upper lobectomy. The apical branch of pulmonary artery, and the superior pulmonary vein and the left upper bronchus were dissected in order. VATS, video-assisted thoracoscopic surgery.

Figure 5 Uniportal VATS LUL lobectomy (9).
Available online: http://www.asvide.com/articles/393

instruments (*Figure 3*), in together with the harmonic shear (Ethicon Endo-Surgery Inc, Cincinnati, OH, USA) or hook electro-cautery were applied during the procedure.

The bronchus, vein and artery were divided and dissected separately using an endo-linear stapler (Covidien, Mansfield, MA, USA or Ethicon Endo-Surgery Inc, Cincinnati, OH, USA) or ligated by using hem-o-locks (Weck Surgical, Teleflex, Limerick, USA) before dissection. In the cases of lower or middle lobe lesions, the dissection order was vein, artery and bronchus, and in the cases of upper lobe lesions, and the dissection order would be changed to artery, vein and bronchus (*Figures 4,5*). The specimen was taken out in the specimen bag (Ethicon Endo-Surgery Inc, Cincinnati, OH, USA). Conventionally, systemic mediastinal lymph node dissection was followed after the removal of the target lung. A 28-Fr chest tube was inserted at the end of the operation, and the chest tube would be removed in the cases there was no air leakage and the volume of drainage was less than 200 mL per day 24 hours post-operatively.

Statistical analysis

Clinical data for all patients were collected from the clinical database of our institution by trained surgical coordinators. All data collected was tabulated using Microsoft Excel for

further analysis. Statistical analysis was undertaken using SPSS software (SPSS, Inc, Chicago, Ill, version 17.0, USA).

Results

Between October 2013 and February 2014, a total of 54 uniportal VATS lobectomies were attempted in Zhongshan Hospital of Fudan University. Among these cases, there were 51 patients (94.4%) underwent uniportal resection were completed without conversion to multiple incisions or open thoracotomy: an extra port was added for one left upper lobectomy to place the endo-linear stapler through the upper pulmonary vein. One patient with chronic obstructive pulmonary disease (COPD) was converted to four ports approach due to technique difficulty. One patient was converted to mini-thoracotomy to due lymph node sticking to the pulmonary artery. Pathological diagnosis confirmed the lymph node without tumor metastasis.

Of the 51 cases of uniportal lobectomy, the average operation duration was 122.2±37.5 min (90-160 min). Upper lobe resection cost shorter duration than middle or low lobe resection (90.7±41.6 *vs.* 150.7±34.5 min; P=0.031). The average volume of estimated blood loss was 88.8±47.1 mL (50-200 mL). None of all the 51 patients required blood transfusion. The average number of harvested lymph nodes was 14.9±3.8 [7-23].

Prolonged stay in intensive care unit (ICU) was not recorded among the patients underwent uniportal VATS lobectomy. The median chest tube duration was 2.2 days, ranging from 2 to 9 days. There were eight patients required non-steroidal anti- inflammatory drugs (NSAID) after the removal of epidural analgesia, and five patients continued NSAIDs administration one month after discharge.

Three patients developed complications, including two prolonged air leakages lasting more than 5 days and one atrial fibrillation. There was no perioperative death in this cohort. After the removal of chest tube, all patients were discharged following the confirmation of lung re-expansion by chest X rays. The average length of stay in hospital was 4.6±2.0 days, ranged from 3-10 days.

Discussion

In this study, we retrospectively reviewed the data on uniportal VATS lobectomy in our center. Based on the surgical refinements on the technique and instruments, the uniportal VATS lobectomy showed safety and feasibility in the surgical resection of lung cancer. The results from our single center indicated that uniportal VATS would be an alternative beside conventional VATS lobectomy.

Since introduced in early 1990s, VATS has developed over 20 years from a simple procedure to more complicated operations including lobectomy and esophagectomy. In 2004, Rocco reported the first worldwide uniportal thoracoscopic wedge resection (4). Since then, several articles have confirmed the safety and feasibility of uniportal operation in simple procedure. Undoubtfully, patients would benefit from a surgery with less traumatic manipulations (10-12). Especially when it came to the major operations: Gonzalez-Rivas *et al.* reported their experience of uniportal lobectomy, which was the world's first report on uniportal major lung resection. Since then, Gonzalez-Rivas *et al.* have published serial research relating to uniportal segmentectomy, pneumonectomy, and sleeve lobectomy (8,13,14). The previous experience from the Western medical centers encouraged our attempt on uniportal VATS lobectomy.

Based on the western experience, technical refinements were introduced to the uniportal surgery in our medical center. Firstly, the assistant surgeon stood at the foot-stool, and the shoulder of the assistant was kept in adduction with extended arms throughout the procedure, it would result in better ergonomics in compared with the posture that the shoulder was kept in abduction with both arms flexed (15). Secondly, a wound protector was applied to the incision to avoid iatrogenic contamination to the thoracoscope so that the continuity was assured throughout the uniportal surgery. Thirdly, new surgical instruments were invented to facilitate the uniportal surgery. As the key step of uniportal VATS was to make the angle for the separate dissection of pulmonary root (8), a tiny suction stick with angle was invented to allow more instruments through one single incision. In this report, improved surgical techniques decreased the operative time to an average of 162 min, which was slightly longer in compared with Gonzalez-Rivas's previous report (16).

Different from the previous report on VATS lobectomy, shorter operation duration was recorded in this cohort when the VATS upper lobectomy was performed (17). In three-hole VATS lobectomy, the upper lobectomy was technically more difficult in compared with the lower lobe dissection. Especially when performing the dissection along the apical branch of pulmonary artery, the iatrogenic injury to the artery was not uncommon and would lead to lethal bleeding during the operation (18). On the contrary, in uniportal

VATS lobectomy, the mobilization of apical branch was the first step in dealing with the hilum structure. Located at the 4th intercostal space, the incision was close to the superior border of the superior pulmonary vein, which improved the exposure of apical branch and facilitated the following dissection. In the lower lobectomy, the mobilization of inferior vein would require the assistant surgeon to push the diaphragm and pericardium so that the surgeon could retract the lower lobe. The duration was therefore longer in lower lobe lobectomy in uniportal surgery.

Mediastinal lymph node dissection is another key step of the operation. Though there is debate on the choice of mediastinal lymph node dissection or sampling, we always performed mediastinal lymph node dissection. According to NCCN guidelines, more than three mediastinal lymph node stations were harvested in this cohort. The most difficult part of mediastinal lymph node dissection is the left subcarinal lymph node dissection, which is located deep and hard to be exposed. For left lower lobe (LLL) dissection, we usually dissected the subcarinal lymph node before we cut the left low lobe bronchus. And for left upper lobe dissection, a good method was introduced by Wang (19): a tape was retracted anterior, which was placed through the plane between the left bronchus and the left inferior vein. With this method, subcarinal lymph node dissection became easier in uniportal VATS.

The experience on multi-incision VATS was described as an important step prior to the uniportal surgery (7,20,21). Technically, it would be easier to switch from two ports to single port than from three or four ports to single port (21). However, for those who are familiar with four-port VATS lobectomy, switching from four ports to three ports and then double-port, and sequentially to single port might be time consuming. Meanwhile, in the cases safety would be compromised, additional ports or conversion to open thoracotomy should be considered without hesitation. That explains why the conversion rate was higher in our study than others. On the other hand, the morbidity and mortality rate were close to the previous reports (16).

Previous study convinced that uniportal surgery was associated with less postoperative pain (22). Similar findings were observed in this study, there was very low incidence of NSAID consumption at one month following the operation. As was reported in previous literatures (11), there were 53% routine VATS patients required medications for pain relief, including 26% NSAIDs and 27% narcotics. In this study, the results were promising even when it was not a comparative study on post-operative pain. Further clinical study based on larger population is required to answer this question.

The main limitation of this study was its retrospective design and relatively small sample size. As the number of uniportal VATS was increasing, further studies based on higher evidence level were required to confirm more findings, both surgically and oncologically.

Conclusions

Uniportal VATS lobectomy is safe and feasible. Operative instrument improvement can make uniportal surgery easier. With caution, surgeon can change from four ports to single port.

Acknowledgements

Disclosure: The authors declare no conflict of interest.

References

1. McKenna RJ Jr, Houck W, Fuller CB. Video-assisted thoracic surgery lobectomy: experience with 1,100 cases. Ann Thorac Surg 2006;81:421-5; discussion 425-6.
2. Swanson SJ, Herndon JE 2nd, D'Amico TA, et al. Video-assisted thoracic surgery lobectomy: report of CALGB 39802--a prospective, multi-institution feasibility study. J Clin Oncol 2007;25:4993-7.
3. Ng CS, Rocco G, Wong RH, et al. Uniportal and single-incision video-assisted thoracic surgery: the state of the art. Interact Cardiovasc Thorac Surg 2014;19:661-6.
4. Rocco G, Martin-Ucar A, Passera E. Uniportal VATS wedge pulmonary resections. Ann Thorac Surg 2004;77:726-8.
5. Alar T, Ozcelik C. Single-incision thoracoscopic surgery of pleural effusions for diagnosis and treatment. Surg Endosc 2013;27:4333-6.
6. Berlanga LA, Gigirey O. Uniportal video-assisted thoracic surgery for primary spontaneous pneumothorax using a single-incision laparoscopic surgery port: a feasible and safe procedure. Surg Endosc 2011;25:2044-7.
7. Rocco G, La Rocca A, La Manna C, et al. Uniportal video-assisted thoracoscopic surgery pericardial window. J Thorac Cardiovasc Surg 2006;131:921-2.
8. Gonzalez-Rivas D, Fieira E, Mendez L, et al. Single-port video-assisted thoracoscopic anatomic segmentectomy and right upper lobectomy. Eur J Cardiothorac Surg 2012;42:e169-71.

9. Feng M, Shen Y, Wang H, et al. Uniportal VATS LUL lobectomy. Asvide 2014;1:359. Available online: http://www.asvide.com/articles/393
10. Andreetti C, Menna C, Ibrahim M, et al. Postoperative pain control: videothoracoscopic versus conservative mini-thoracotomic approach†. Eur J Cardiothorac Surg 2014;46:907-12.
11. Nicastri DG, Wisnivesky JP, Litle VR, et al. Thoracoscopic lobectomy: report on safety, discharge independence, pain, and chemotherapy tolerance. J Thorac Cardiovasc Surg 2008;135:642-7.
12. Salati M, Brunelli A, Xiumè F, et al. Uniportal video-assisted thoracic surgery for primary spontaneous pneumothorax: clinical and economic analysis in comparison to the traditional approach. Interact Cardiovasc Thorac Surg 2008;7:63-6.
13. Gonzalez-Rivas D, Fernandez R, Fieira E, et al. Uniportal video-assisted thoracoscopic bronchial sleeve lobectomy: first report. J Thorac Cardiovasc Surg 2013;145:1676-7.
14. Gonzalez-Rivas D, Delgado M, Fieira E, et al. Uniportal video-assisted thoracoscopic pneumonectomy. J Thorac Dis 2013;5 Suppl 3:S246-52.
15. Shen Y, Feng M, Tan L, et al. Thoracoscopic esophagectomy in prone versus decubitus position: ergonomic evaluation from a randomized and controlled study. Ann Thorac Surg 2014;98:1072-8.
16. Gonzalez-Rivas D, Paradela M, Fernandez R, et al. Uniportal video-assisted thoracoscopic lobectomy: two years of experience. Ann Thorac Surg 2013;95:426-32.
17. Gonzalez-Rivas D, Fernandez R, de la Torre M, et al. Thoracoscopic lobectomy through a single incision. Multimed Man Cardiothorac Surg 2012;2012:mms007.
18. Gonzalez-Rivas D, Delgado M, Fieira E, et al. Single-port video-assisted thoracoscopic lobectomy with pulmonary artery reconstruction. Interact Cardiovasc Thorac Surg 2013;17:889-91.
19. Wang BY, Tu CC, Liu CY, et al. Single-incision thoracoscopic lobectomy and segmentectomy with radical lymph node dissection. Ann Thorac Surg 2013;96:977-82.
20. Tam JK, Lim KS. Total muscle-sparing uniportal video-assisted thoracoscopic surgery lobectomy. Ann Thorac Surg 2013;96:1982-6.
21. Gonzalez D, de la Torre M, Paradela M, et al. Video-assisted thoracic surgery lobectomy: 3-year initial experience with 200 cases. Eur J Cardiothorac Surg 2011;40:e21-8.
22. Jutley RS, Khalil MW, Rocco G. Uniportal vs standard three-port VATS technique for spontaneous pneumothorax: comparison of post-operative pain and residual paraesthesia. Eur J Cardiothorac Surg 2005;28:43-6.

Cite this article as: Feng M, Shen Y, Wang H, Tan L, Mao X, Liu Y, Wang Q. Uniportal video assisted thoracoscopic lobectomy: primary experience from an Eastern center. J Thorac Dis 2014;6(12):1751-1756. doi: 10.3978/j.issn.2072-1439.2014.11.20

Original Article

Differences in the clinical and radiological characteristics of lung-involved toxocariasis between toxocariasis with eosinophilia and those without eosinophilia

Bo Mi Park, Sang Ok Jeong, Hee Sun Park, Sung Soo Jung, Sun Young Kim, Ju Ock Kim, Jeong Eun Lee

Department of Internal Medicine, Chungnam National University College of Medicine, Daejeon 301-721, Korea

Correspondence to: Jeong Eun Lee, MD, PhD. Department of Internal Medicine, Chungnam National University College of Medicine, 282 Munhwa-ro, Jung-gu, Daejeon 301-721, Korea. Email: vov-x@hanmail.net.

Background: Previously, most studies did not discuss about the characteristics of lung-involved toxocariasis without eosinophilia. However, the patients are not always accompanied by eosinophilia, so it is necessary to learn about the clinical and radiologic features that may predict pulmonary toxocariasis without eosinophilia. In addition, we also want to check the differences in characteristics between the two groups based on the presence of eosinophilia.

Methods: We investigated patients from October 2009 to February 2014 with antibody against Toxocara positive using enzyme-linked immunosorbent assay (ELISA), abnormal chest X-ray, and computed tomography (CT) findings. This retrospective study included patients diagnosed as toxocariasis with pulmonary involvement, using the results of laboratory findings, symptoms, and CT at the time of diagnosis.

Results: Out of 88 patients, 78% were male and 22% were female; and the mean age was 51 years. The mean eosinophil fraction in peripheral blood was 11.8%. The most common chest CT findings of patients with eosinophilia were nodules plus ground glass opacity (GGO) pattern, and nodules were found in patients with no eosinophilia. Pure GGO was the most common predominant subtype in GGO lesions of patients with eosinophilia. In terms of anatomical distribution, random distribution was seen more in patients with eosinophilia than those without eosinophilia, with statistically significance (P=0.042). In patients who underwent additional CT scans, 44% of those with eosinophilia had migrating lesions and had significant differences from patients without eosinophilia (P=0.008).

Conclusions: There were no significant differences in lesion characteristics with the exception of random anatomic distribution between patients with and without eosinophilia. However, there was a significant difference between the fixation and migration of the lesion in patients with and without eosinophilia.

Keywords: Computed tomography (CT); eosinophilia; lung disease; *Toxocara canis* (*T. canis*); toxocariasis

Submitted Aug 27, 2014. Accepted for publication Nov 13, 2014.
doi: 10.3978/j.issn.2072-1439.2014.12.24
View this article at: http://dx.doi.org/10.3978/j.issn.2072-1439.2014.12.24

Introduction

In the past, majority of the people in Korea were infected with parasites. But today, parasite infection rates have decreased. In 1971, 84.3% of the people were tested positive for parasite eggs, but by 1997, it had decreased to 2.4% (1). However, as the socio-economic status in Korea has improved and family structures have transformed into two-generation families, pets have become more popular (2) and parasitic disease levels have risen again. In an investigation of parasite infection in 1992, 297 (59%) among 503 dog stool samples contained more than one parasite, and *Toxocara canis* (*T. canis*) was present in about 11.1% (3). There are no reports of worldwide human *T. canis* infection rate. But *T. canis* infection of dogs has been reported worldwide, and canine infection rates widely vary. The environmental contamination with *T. canis* eggs in

public grounds is also widespread (4-7).

The prevalence of toxocariasis is widely known to be high in children living in developing countries, particularly in schools and apartment playgrounds where contamination with parasite eggs can be up to 87% (8). Recently, adult infection with *T. canis* or *Toxocara cati* (*T. cati*) has been increasing. The reason seems to be the increase in overseas travels and the number of pet animals.

In Korea, 68% of the cases of eosinophilia are caused by toxocariasis, which indicates that *T. canis* infection is widespread among the Korean adults (9). There are a wide variety of involved organs, and 20% of the patients infected with *T. canis* or *T. cati* have invasive lung disease (10,11).

Toxocariasis is an illness of humans caused by larvae (immature worms) of either *T. canis* or *T. cati*. Toxocariasis is known to cause visceral larva migrans. *T. canis* and *T. cati* are parasites that live in the small intestines of dogs and cats. Mature animals become infected by eating eggs from the infected soil, and it is possible to acquire infection via vertical transmission from their mother's milk or placenta. Parasitic eggs enter the soil from dog or cat feces. They enter the human intermediate host, in which the infected larvae penetrate the intestinal wall and migrate to organs including the liver, lungs, and eyes. This is known as visceral larva migrans; and if the skin is invaded, it is called cutaneous larva migrans. All of these are known as toxocariasis (12,13).

Kim *et al.* (11) characterized lung disease from toxocariasis in patients with eosinophilia, and reported an eosinophilic lung disease by toxocariasis rate of 23% (32/141 patients). Kwon *et al.* (9) reported a prevalence of 68% toxocariasis in patients with eosinophilia, and 24% had lung invasion. In a Korean study of 102 patients with toxocariasis lung invasion, only 70% were accompanied by eosinophilia (14). Therefore, we assume that 20-30% of patients with toxocariasis do not have eosinophilia. However, in the relation to the radiologic characteristics of patients without eosinophilia, no studies prior to the current study have analyzed large number of subjects and subtypes of ground glass opacity (GGO).

We studied patients who were tested positive for antibodies against Toxocara and who were diagnosed with parasitic lung diseases by chest computed tomography (CT), and the clinical and radiological features were compared between those with and without eosinophilia.

Patients and methods

Patients

From October 2009 to February 2014, we investigated patients from Chungnam National University Hospital, who were tested positive for antibodies against Toxocara by using enzyme-linked immunosorbent assay (ELISA) and who seemed to have infectious lung disease based on chest CT, during the admission or in the Outpatient Department. A total of 88 patients met eligible criteria to be included. We also measured IgG antibodies to Clonorchis sinensis, paragonimiasis, sparganosis, and cysticercosis antigens using ELISA in these patients, and the patients who had positive results were removed from the study. Therefore, we ruled out other parasitic infections. We performed retrospective analyses of the clinical outcomes, symptoms, chest CT, and initial laboratory data. We compared the radiological features in patients with toxocariasis and invasive lung disease with and without eosinophilia. Eosinophilia is defined by blood test showing greater than 500 cells/μL in the peripheral blood or 10% of total white blood cell count (15). Serum toxocara ELISA test was carried out based on the decision of the physician whether parasitic infection was suspected from clinical symptoms, history. Therefore, we tried to establish symptoms and hematological findings of toxocariasis with pulmonary invasion.

Diagnosis of toxocariasis larval infection

We measured antibodies against Toxocara using ELISA for serological testing of parasite antigens. Negative and positive serologic tests were defined as values below 0.250 and above 0.250, respectively. Serum was sent to the Institute of Infectious Disease/Department of Parasitology at College of Medicine in Seoul National University. The same samples were tested twice and the average values were derived. This method for measuring IgG antibodies against Toxocara has been reported to have 91% sensitivity and 86% specificity (16).

Data analysis methods

The blood tests were analyzed on the day of diagnosis. Many Koreans eat various forms of raw meat, and thus we also surveyed on the consumption of raw meat during the past 6 months. Chest CT findings of pulmonary involvement of toxocariasis were analyzed according to the methods of Cheon *et al.* (17) and Johkoh *et al.* (18). The findings were categorized into pulmonary infiltration pattern, anatomical distribution, and zonal distribution. The pulmonary infiltration category is shown by the plus notation if each lesions of different pattern can be seen in chest CT of a single

Table 1 Clinical characteristics of 88 patients with pulmonary toxocariasis

Characteristics	Number of patients (%)
Gender	
Male (%)	69 (78.4)
Female (%)	19 (21.6)
Age [years]	51±12.5 [18-77]
Raw food intake history[a]	57 (64.8)
Liver involvement	4 (4.5)
Number of patients with eosinophilia[b]	47 (53.4)
Hemoglobin (g/dL)[b]	14.6±1.3
White blood cell (cells/μL)[b]	8,175.5±2,861.7
Eosinophil in peripheral blood[b] (%)	11.8±10.4
Eosinophil count (cells/μL)[b]	994.6±1,093.8
ESR (mm/hr)[c]	20.5±14.6
CRP (mg/dL)[d]	1.7±4.8
Aspartate aminotransferase (U/L)[e]	20.6±10.1
Aanine aminotransferase (U/L)[e]	22.5±12.9
Ig E (IU/mL)[f]	1,287.6±1,583.5
Eosinophils in sputum of 18 patients (%)	2.4±2.4
Eosinophils in bronchoscopic washing fluid of 15 patients (%)	9.3±17.6

Data are expressed as mean ± standard deviation or as Number. [a], it was impossible to find raw food intake history of nine patients; [b], five patients had not been measured; [c], only 29 patients were measured for ESR; [d], only 19 patients were measured for CRP; [e], 72 patients were measured for AST and ALT; [f], only 12 patients were measured for IgE. ESR, erythrocyte sedimentation rate; CRP, C-reactive protein.

patient. If there is a GGO lesion, the GGO was classified based on its main subtype, according to Suzuki *et al.* (19). The study protocol was approved by the Institutional Review Board of the Chungnam National University Hospital (IRB file No. 2013-01-003). This was a retrospective study, so the informed consent was waived by the board.

Statistical analysis

Clinical data were analyzed using IBM SPSS Statistics version 19, and the mean and standard deviation (SD) of each measurement were obtained. The results of clinical signs and symptoms, chest CT according to the presence or absence of eosinophilia were analyzed using the χ^2 test with Fisher's exact test. A P value <0.05 was considered as statistically significant.

Results

Clinical characteristics (Table 1)

A total of 88 patients who were tested positive for antibodies against Toxocara were diagnosed with lung-involved toxocariasis. Out of 88 target patients, 69 (78%) were male and 19 (22%) were female. The mean age at diagnosis was 51 (range, 18-77) years. During the past 6 months, 57 patients (65%) had ingested uncooked cow liver, intestine, or meat; and 9 (10%) had no history of ingesting raw animal parts. Therefore, more than half of the patients had a history of eating raw animal products. Four patients (5%) were suspected of having liver abscess caused by *T. canis/cati*, due to the presence of hypo-dense lesions in the liver. The mean hemoglobin count was 15 g/dL, and many patients did not have accompanying anemia. The mean white blood cell count was 8,176 cells/μL (range, 4,510-18,490 cells/μL), mean eosinophil fraction in peripheral blood was 11.8% (range, 0.3-44.5%), and mean absolute eosinophil count was 995 cells/μL (range, 30-4,860 cells/μL). Mean erythrocyte sedimentation rate (ESR) and C-reactive protein (CRP) level were 21 mm/hr and 1.7 mg/dL, respectively. It seemed that toxocariasis was not accompanied by an increase in ESR. CRP was measured in 19 patients, and the level increased by more than 0.5 mg/dL in 3 of these patients. Therefore, it seemed that toxocariasis was not accompanied by an increase in CRP. Mean aspartate aminotransferase/alanine aminotransferase levels were 21/23 U/L, which was thought to be due to the small number of patients with liver involvement. Mean serum IgE level was 1,288 IU/mL. Eosinophil fraction in sputum and bronchial aspiration was 2.4% and 9.3%, respectively, which was higher than average. However, this was only measured in 18 and 15 patients, respectively.

Symptoms at admission (Table 2)

A total of 44 (50%) patients had respiratory symptoms on the day of admission, and half of the patients did not have such symptoms. Cough was the most common (26%), followed by chest pain or discomfort (15%). Gastrointestinal symptoms were seen in 3 (3%) patients, and one of these patients had abdominal discomfort, diarrhea, nausea, and vomiting. The other patients only had

Table 2 Clinical signs and symptoms of patients with pulmonary toxocariasis

Categories	Number of patients (%)			P value[b]
	Total (n=88) (%)[a]	With eosinophilia (n=47)	Without eosinophilia (n=36)	
Respiratory	44 (50.0)	23 (48.9)	19 (52.8)	0.729
Cough	23 (26.1)	12 (25.5)	9 (25.0)	0.956
Dyspnea	8 (9.1)	4 (8.5)	4 (11.1)	0.722
Chest pain/discomfort	13 (14.8)	7 (14.9)	6 (16.7)	0.826
Sputum	12 (13.6)	7 (14.9)	4 (11.1)	0.749
Rhinorrhea/nasal obstruction	6 (6.8)	3 (6.4)	3 (8.3)	1.000
Sore throat	3 (3.4)	1 (2.1)	2 (5.6)	0.576
Blood tingled sputum/hemoptysis	2 (2.3)	1 (2.1)	1 (2.8)	1.000
Gastrointestinal	3 (3.4)	2 (4.3)	1 (2.8)	1.000
Abdominal pain/discomfort	2 (2.3)	2 (4.3)	0 (0)	0.503
Diarrhea	2 (2.3)	1 (2.1)	1 (2.8)	1.000
Nausea/vomiting	1 (1.1)	1 (2.1)	0 (0)	1.000
General	4 (4.5)	3 (6.4)	1 (2.8)	0.629
Fever	2 (2.3)	1 (2.1)	1 (2.8)	1.000
Myalgia	2 (2.3)	2 (4.3)	0 (0)	0.503
Chill	1 (1.1)	1 (2.1)	0 (0)	1.000
Neurologic				
Dizziness	1 (1.1)	1 (2.1)	0 (0)	1.000
No symptom	41 (46.6)	21 (44.7)	17 (47.2)	0.818

[a], five patients were not measured of blood eosinophil level; [b], P value was calculated by χ^2 test with Fisher's exact test.

diarrhea or abdominal pain. Two patients (2%) had fever and 41 patients (47%) were asymptomatic. There was no statistical significance between patients with eosinophilia and those without.

Chest CT differences depending on eosinophilia (Table 3)

All targeted patients underwent chest CT. Among them, nodules with GGO patterns were the most common finding (25 patients; 28%), followed by nodule pattern alone (24; 27%). The pattern of GGO alone was third in group (23; 26%). In addition, two patients had cavitary lesions, and one of these patients had cavities with consolidation and the other had cavities with nodules and GGO patterns. Both of these patients did not have leukocytosis or elevation of CRP on blood test. Also, they did not have enough symptoms, such as fever on admission, to suggest of a bacterial infection. In addition, the lesions showed improvement on chest CT without any treatment, and new lesions rather appeared. Therefore, we considered these cavitary lesions to be caused by toxocariasis rather than by microbial infection. In one of the patients, decrease in the size of the cavities and thinning of the wall thickness were shown on the follow up chest CT after two weeks, even without any treatment. We started on albendazole treatment, since toxocara ELISA positivity was confirmed at that time (*Figure 1*). To the best of our knowledge, no previous studies have reported on cavitary lesions in pulmonary toxocariasis, and it is a novel suggestion that toxocariasis pulmonary involvement may also appear as cavitary lesions.

In terms of anatomical distribution, 49 patients (56%) had a peripheral distribution, 33 (38%) had a random distribution, and 6 (7%) had a central distribution. For zonal distribution, 25 patients (28%) had both upper and lower lobe involvement, 24 (27%) patients had random distribution, 17 (19%) patients had only the upper lobe involvement, and 17 (19%) patients had only the lower lobe involvement. Two patients had pleural effusion accompanied by GGO pattern in lung parenchyma, which was in the right and left lungs, respectively. Six cases had reactive enlargement of lymph nodes with infiltration of lung parenchyma.

A total of 83 patients with toxocariasis who had lung involvement underwent blood tests, and 47 (57%) had eosinophilia and 36 (43%) did not. The most common chest CT findings of patients with eosinophilia were

Table 3 Comparison of CT findings between patients with blood eosinophilia and those without eosinophilia

HRCT finding	Number of patients (%)			P value[b]
	Total (n=88)[a]	Patients with eosinophilia (n=47)	Patients without eosinophilia (n=36)	
Pattern				
GGO	23 (26.1)	10 (21.3)	10 (27.8)	0.492
GGO + nodule	25 (28.4)	16 (34.0)	9 (25.0)	0.374
GGO + consolidation	5 (5.7)	5 (10.6)	0 (0)	0.066
GGO + consolidation + nodule	3 (3.4)	3 (6.4)	0 (0)	0.254
Nodule + consolidation	4 (4.5)	2 (4.3)	1 (2.8)	1.000
Nodule	24 (27.3)	11 (23.4)	12 (33.3)	0.317
Consolidation	3 (3.4)	0 (0)	3 (8.3)	0.078
GGO predominant subtype				
Pure	18 (20.5)	13 (27.7)	4 (11.1)	0.064
Semiconsolidation	10 (11.4)	8 (17)	1 (2.8)	0.071
Halo	20 (22.7)	9 (19.1)	10 (27.8)	0.354
Mixed	10 (11.4)	6 (12.8)	4 (11.1)	1.000
Anatomic distribution				
Random	33 (37.5)	22 (46.8)	9 (25.0)	0.042
Peripheral	49 (55.7)	23 (48.9)	23 (63.9)	0.174
Central	6 (6.8)	2 (4.3)	4 (11.1)	0.396
Zonal distribution				
Random	24 (27.3)	15 (31.9)	8 (22.2)	0.328
Upper	17 (19.3)	8 (17)	8 (22.2)	0.552
Lower	17 (19.3)	7 (14.9)	9 (25.0)	0.247
Upper + lower	25 (28.4)	13 (27.7)	10 (27.8)	0.990
Middle + lower	1 (1.1)	1 (2.1)	0 (0)	1.000
Upper + middle	4 (4.5)	3 (6.4)	1 (2.8)	0.629
Pleural effusion	2 (2.3)	1 (2.1)	1 (2.8)	1.000
Migration[c]	12/50 (24.0)	11/25 (44.0)	1/23 (4.3)	0.008
Fixed[c]	39/50 (78.0)	14/25 (56.0)	22/23 (95.7)	0.004
Size reduction	10/50 (20.0)	5/25 (20.0)	4/23 (17.4)	1.000
Clearing	25/50 (50.0)	8/25 (32.0)	16/23 (69.6)	0.006
No change	4/50 (8.0)	1/25 (4.0)	3/23 (13.0)	0.312
Cavity	2 (2.3)	0 (0)	2 (5.6)	0.185
Lymph node enlargement	6 (6.8)	5 (10.6)	1 (2.8)	0.227

CT, computed tomography; GGO, ground glass opacity; [a], five patients were not measured of blood eosinophil level; [b], P value was calculated by χ^2 test with Fisher's exact test; [c], 38 patients did not take any follow up chest CT.

nodules with GGO pattern which were seen in 16 patients (34%). The most common chest CT findings in patients without eosinophilia were nodules (33%). There were no significant differences in the lesion characteristics between patients with and without eosinophilia. Depending on the predominant type, patients who have GGO lesions were reanalyzed by classifying as shown in *Table 3*. The patients with eosinophilia relatively had many pure GGO, but those without eosinophilia had more of halo GGO. But there was no statistically significant difference.

In terms of anatomical distribution, peripheral distribution was observed in 23 (49%) patients with eosinophilia and in 23 (64%) patients without eosinophilia. However, there was no significant difference (P=0.174). Random distribution was significantly different between the two groups; patients with eosinophilia were found to be distributed more randomly (P=0.042). In 22 of 47 patients who had eosinophilia, it was difficult to assess whether the

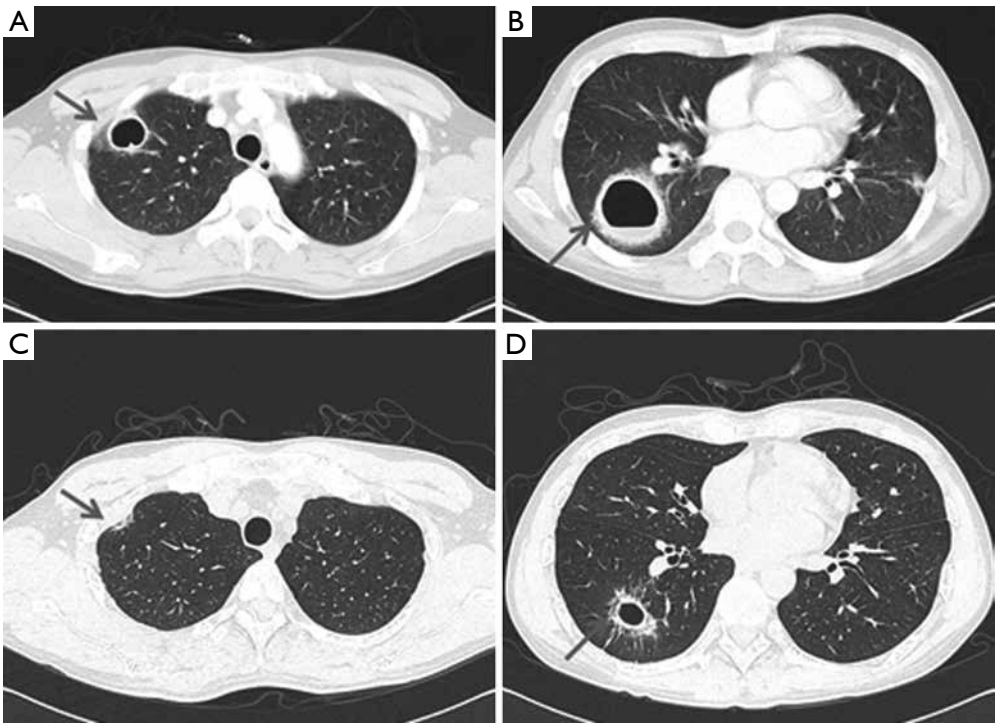

Figure 1 Computed tomography (CT) findings of a 43-year-old man. (A,B) The figures show multiple cavities (arrows) with wall thickness in right upper lobe (RUL) and right lower lobe (RLL) at diagnosis; (C,D) the figures show decrease in the size of cavity after 15 days without any treatment.

lesion was migrating or fixed, because additional chest CT was not performed within 6 months. In the remaining 25 patients, additional chest CT was performed two or three times to determine whether the lesions have improved or not. Eleven (44%) patients were identified to have migrating lesions with disappearance, improvement of existing lesions, and occurrence of new lesions elsewhere. Additional chest CTs were performed on 23 patients without eosinophilia, but only one of them had migrating lesions; there were significance differences between patients with and without eosinophilia (P=0.008). All of the lesions of these patients, except for one person without eosinophilia, were improved or fixed compared to lesions at the time of diagnosis. There was a significant difference among the lesions in patients with eosinophilia (P=0.004).

Treatment and clinical results

Twenty-seven patients diagnosed with pulmonary involvement of toxocariasis were treated with albendazole 400 mg twice daily for 5 days from the day toxocariasis was confirmed. The remaining patients did not receive any prescription. All patients showed improved symptoms within 6 months after the diagnosis regardless of albendazole treatment, and lesions decreased in size or disappeared on the last chest CT or X-ray. None of the patients had any clinical or radiological recurrence.

Discussion

Toxocariasis has become a frequent cause of eosinophilic lung disease, and its prevalence has increased. Therefore, we were interested in establishing the clinical manifestations of toxocariasis parasitic lung disease.

It is often assumed that serology, imaging, and pathological examinations are needed to diagnose toxocariasis. However, we believe that serological testing using ELISA and chest CT can be used to diagnose toxocariasis without the risk and invasiveness of biopsy (13). This type of toxocariasis serodiagnosis cross reacts with some other helminthes, such as Trichinella, Strongyloides (16), Fasciola, Ascaris, geohelminthes (20-22), and filariasis (20). Fortunately, geohelminthes have almost disappeared, filarisis has been eradicated in Korea, and it is difficult to find poly parasitism in Korea (23). Therefore, the serological test has sufficient specificity to be the best

indirect test for diagnosing this infection.

In this study, the male/female *T. canis* infection rates were 78%/22%, which was similar to previous studies reporting 82%/12% (9) and 78%/22% (11) and are due to eating habits. Some people like to eat uncooked cow liver or stomach, as they believe raw cow liver is a "health-promoting food" (24). These foods tend to be readily consumed by men but not by women, although it has not been studied. We think that these foods that produce an aversion are consumed more frequently by men than women.

Our results are not greatly different from those of other studies on eosinophilic lung disease, which have reported random GGO patterns on chest CT (2,14). A total of 64% of our cases had lesions with GGO, so the GGO pattern is a typical radiological finding in toxocariasis with lung involvement. We found cavitary lesions, which have not been reported in other studies. We suggest that pulmonary involvement of toxocariasis may manifest as cavitary lesions.

In this study, respiratory symptoms, fever, and gastrointestinal symptoms were thought to be due to a hyper-reaction caused by *T. canis* larvae systemic involvement. However, 47% of the patients were asymptomatic, and most were diagnosed by the presence of an IgG antibody against Toxocara. These examinations were performed due to abnormal findings on simple X-rays during health check-ups. All patients regardless of symptoms were treated, and lesions on CT findings resolved or improved, indicating that pulmonary involvement of toxocariasis has a good prognosis. This result is similar to a previous study (9) showing that 25 of 54 patients with toxocariasis had improved symptoms and chest radiography findings without treatment. Many authors have suggested that toxocariasis is a self-healing disease; therefore, there is no need for treatment if the symptoms are mild.

A 2009 study in Korea (14) analyzed the presence of migrating masses in 58 patients with antibodies against Toxocara. The lesions resolved or improved in 48% of cases, and migrating nodules were confirmed in 35% of cases. However, they did not analyze the coexistence of eosinophilia in the patients with migrating nodules, so the relationship between these two features was not established. Peripheral blood eosinophilia is related to the degree of tissue involvement (25). One review article reported that peak eosinophil levels occur 11-30 weeks after infection, which is consistent with differences in life cycles between parasites. The spontaneous decrease in the number of eosinophils without treatment suggests active and spontaneous modulation of eosinophilia, which generally occurs when migration of the larval form ceases and the infection becomes patent (26). For this reason, we think that a pattern of migrating lesions was shown in the patients with eosinophilia in this study.

Interleukin-5 from Th2 lymphocytes triggers formation of eosinophils, which excrete cytotoxic granules and destroy parasites directly as well as necrotize tissue (27). In contrast, parasites trapped in intact cysts or in the intestinal lumen that do not invade tissues tend not to cause eosinophilia (28). Thus, the non-migrating nodules on CT in patients without eosinophilia may not be lung nodules caused by Toxocara. However, disease course of the patients improved on chest X-ray or follow-up chest CT and was similar to those with toxocariasis. Additionally, no evidence indicated another disease. Therefore, we thought that the lesions were due to the Toxocara infection.

We included patients with toxocariasis not accompanied by eosinophilia. We also described a subtype of GGO that has not been analyzed to date. However, the retrospective nature of the study design and the lack of follow-up CT are limitations of this study. Future studies involving more patients with follow-up chest CT and more clinical and radiological characteristics should be performed for a more accurate investigation of pulmonary involvement of toxocariasis.

Conclusions

In conclusion, not all of the patients with toxocariasis had eosinophilia, and eosinophilia seemed to be related to lesion migration. The lesions of lung involved toxocariasis with eosinophilia tend to be more migrating, and those without eosinophilia tend to be fixed.

Acknowledgements

Authors' contributions: Jeong Eun Lee designed the overall study with contributions from Sun Young Kim, Ju Ock Kim, Sung Soo Jung, Hee Sun Park. Bo Mi Park and Sang Ok Jeong collected and analyzed data. Bo Mi Park wrote the paper.

Disclosure: The authors declare no conflict of interest.

References

1. Hong ST. Gungnae gisaengchung gamnyeomjeungui hyeonhwang. J Korean Med Assoc 1998;41:737-45.
2. Shin S. Parasitic zoonosis transmitted by pet animals. J

Korean Med Assoc 2004;47:527-34.
3. Yang HJ, Yoon YB, Yi H, et al. Prevalence of Intestinal Parasites Infection of Dogs in Chonbuk Province. Korean J Vet Serv 1992;15:7-16.
4. Habluetzel A, Traldi G, Ruggieri S, et al. An estimation of Toxocara canis prevalence in dogs, environmental egg contamination and risk of human infection in the Marche region of Italy. Vet Parasitol 2003;113:243-52.
5. Anaruma Filho F, Chieffi PP, Correa CR, et al. Human toxocariasis: a seroepidemiological survey in the municipality of Campinas (SP), Brazil. Rev Inst Med Trop Sao Paulo 2002;44:303-7.
6. Richards DT, Harris S, Lewis JW. Epidemiology of Toxocara canis in red foxes (Vulpes vulpes) from urban areas of Bristol. Parasitology 1993;107:167-73.
7. O'Lorcain P. Prevalence of Toxocara canis ova in public playgrounds in the Dublin area of Ireland. J Helminthol 1994;68:237-41.
8. Barriga OO. A critical look at the importance, prevalence and control of toxocariasis and the possibilities of immunological control. Vet Parasitol 1988;29:195-234.
9. Kwon NH, Oh MJ, Lee SP, et al. The prevalence and diagnostic value of toxocariasis in unknown eosinophilia. Ann Hematol 2006;85:233-8.
10. Lee SP. Pathophysiology of hypersensitivity in human by Toxocara canis larval infection. Chung-Ang University Doctoral Thesis. 2001.
11. Kim YJ, Kyung SY, An CH, et al. The characteristics of eosinophilc lung diseases cause by Toxocara canis larval infestation. Tuberc Respir Dis 2007;62:19-26.
12. Vijayan VK. Tropical parasitic lung diseases. Indian J Chest Dis Allied Sci 2008;50:49-66.
13. Despommier D. Toxocariasis: clinical aspects, epidemiology, medical ecology, and molecular aspects. Clin Microbiol Rev 2003;16:265-72.
14. Yoon YS, Lee CH, Kang YA, et al. Impact of toxocariasis in patients with unexplained patchy pulmonary infiltrate in Korea. J Korean Med Sci 2009;24:40-5.
15. van Assendelft OW. Reference values for the total and differential leukocyte count. Blood Cells 1985;11:77-96.
16. Jacquier P, Gottstein B, Stingelin Y, et al. Immunodiagnosis of toxocarosis in humans: evaluation of a new enzyme-linked immunosorbent assay kit. J Clin Microbiol 1991;29:1831-5.
17. Cheon JE, Lee KS, Jung GS, et al. Acute eosinophilic pneumonia: radiographic and CT findings in six patients. AJR Am J Roentgenol 1996;167:1195-9.
18. Johkoh T, Müller NL, Akira M, et al. Eosinophilic lung diseases: diagnostic accuracy of thin-section CT in 111 patients. Radiology 2000;216:773-80.
19. Suzuki K, Kusumoto M, Watanabe S, et al. Radiologic classification of small adenocarcinoma of the lung: radiologic-pathologic correlation and its prognostic impact. Ann Thorac Surg 2006;81:413-9.
20. Mohamad S, Azmi NC, Noordin R. Development and evaluation of a sensitive and specific assay for diagnosis of human toxocariasis by use of three recombinant antigens (TES-26, TES-30USM, and TES-120). J Clin Microbiol 2009;47:1712-7.
21. Magnaval JF, Fabre R, Maurières P, et al. Application of the western blotting procedure for the immunodiagnosis of human toxocariasis. Parasitol Res 1991;77:697-702.
22. Romasanta A, Romero JL, Arias M, et al. Diagnosis of parasitic zoonoses by immunoenzymatic assays--analysis of cross-reactivity among the excretory/secretory antigens of Fasciola hepatica, Toxocara canis, and Ascaris suum. Immunol Invest 2003;32:131-42.
23. Jin Y, Shen C, Huh S, et al. Serodiagnosis of toxocariasis by ELISA using crude antigen of Toxocara canis larvae. Korean J Parasitol 2013;51:433-9.
24. Lim JH. Foodborne eosinophilia due to visceral larva migrans: a disease abandoned. J Korean Med Sci 2012;27:1-2.
25. John TJ, Walker DH. Tropical infectious diseases, principles, pathogens, and practice. In: Guerrant RL, Walker DH, Weller PF. eds. Philadelphia: Churchill Livingstone, 1999:1123-32.
26. Klion AD, Nutman TB. The role of eosinophils in host defense against helminth parasites. J Allergy Clin Immunol 2004;113:30-7.
27. Rothenberg ME. Eosinophilia. N Engl J Med 1998;338:1592-600.
28. Leder K, Weller PF. Eosinophilia and helminthic infections. Baillieres Best Pract Res Clin Haematol 2000;13:301-17.

Cite this article as: Park BM, Jeong SO, Park HS, Jung SS, Kim SY, Kim JO, Lee JE. Differences in the clinical and radiological characteristics of lung-involved toxocariasis between toxocariasis with eosinophilia and those without eosinophilia. J Thorac Dis 2014;6(12):1757-1764. doi: 10.3978/j.issn.2072-1439.2014.12.24

Original Article

Antihypertensive therapy with nicardipine for patients with aortic disease is associated with more esmolol usage than urapidil

Kang-Song Wu[1], Jian-Cang Zhou[2], Hang-Yang Li[2], Dan-Yan Gu[2], Kong-Han Pan[2], Wei-Dong Li[3], Ying-Hong Hu[1]

[1]Department of Intensive Care Unit, The Second Affiliated Hospital, [2]Department of Critical Care Medicine, Sir Run Run Shaw Hospital, [3]Department of Cardiothoracic Surgery, The First Affiliated Hospital, Zhejiang University School of Medicine, Hangzhou 310016, China

Correspondence to: Jian-Cang Zhou. Department of Critical Care Medicine, Sir Run Run Shaw Hospital, Zhejiang University School of Medicine, Hangzhou 310016, China. Email: jiancangzhou@hotmail.com.

Background: Acute aortic disease is a common but challenging entity in clinical practice. Titration the blood pressure and heart rate to a target level is of paramount importance in the acute phase regardless of whether the patient will undergo a surgery or not eventually. In addition to the initially intravenous β-blockers, parenteral infusion of nicardipine and urapidil are the most common used antihypertensive therapy currently in mainland China. However, few empirical data was available with respect to the different effect on patients' outcome of the two antihypertensive strategies. Specifically given the deleterious reflex tachycardia of vasodilators which may increase force of ventricular contraction and potentially worsen aortic disease. Therefore, this study was aimed to evaluate the difference of the abovementioned two antihypertensive strategies on the outcome of patients with aortic disease.

Methods: All patients with new diagnosed aortic diseases presented to our hospitals from January 1, 2013 to June 30, 2014 were retrospectively reviewed. The antihypertensive strategies and their association with patients' outcomes were evaluated with logistics regression.

Results: A total of 120 patients with new diagnosed aortic disease were included in the study. Of them, 47 patients received urapidil while 73 patients received nicardipine antihypertensive therapy. Patients with nicardipine were more quickly to reach the target blood pressure level than those treated with urapidil (median, 18 *vs.* 35 min, P=0.024). After adjustment for patient demographics, co-morbidity, involved extend of aorta, interventional strategies, antihypertensive therapy with nicardipine (with urapidil as reference) for patients with aortic disease was significantly associated with high esmolol cost [odds ratio (OR): 6.2, 95% confidence interval (CI), 1.8-21.6, P=0.004] and longer ICU length of stay (LOS) (OR: 3.9, 95% CI, 1.5-10.3, P=0.006). However, there was no significant correlation between nicardipine use and ICU mortality (OR: 0.3; 95% CI, 0.1-1.4, P=0.123).

Conclusions: Although nicardipine achieved the target blood pressure level more quickly than urapidil for patients with aortic disease, it was associated with more esmolol use and longer ICU LOS.

Keywords: Aortic disease; antihypertensive therapy; nicardipine; urapidil

Submitted Sep 19, 2014. Accepted for publication Nov 13, 2014.
doi: 10.3978/j.issn.2072-1439.2014.12.22
View this article at: http://dx.doi.org/10.3978/j.issn.2072-1439.2014.12.22

Introduction

Acute aortic disease is a common and challenging emergency in clinical practice. Of them, aortic aneurysm and aortic dissection are of the most common type. The prognosis of aortic dissection is poor if untreated. Although the outcomes of patients with Stanford type A dissection improved after early repair, both the perioperative and one-year mortality remained high, with a 30-day hospital mortality varying from 9% to 30% and survival rates at five years varying from 50% to 80% (1,2). Titrate the blood

pressure and heart rate to a target level is of paramount importance in the acute phase although whether an urgent surgical therapy is necessary varies according to the classification of aortic disease (3). Hence, in addition to the prior β-blockers, intravenous vasodilators are widely used to achieve aggressive blood pressure and heart rate control. Among the vasodilators, most established agents including intravenous sodium nitroprusside, nicardipine, urapidil, nitroglycerin, fenoldopam (4). Currently, parenteral infusion of nicardipine or urapidil are the most common used strategy in mainland China. Nevertheless, few empirical data was available with respect to the different effect on patients' outcome of various antihypertensive strategies for patients with aortic disease. Especially given the potential deleterious effects of reflex tachycardia of vasodilators which may increase force of ventricular contraction and potentially worsen the diseased aorta (4). Therefore, this study was aimed to evaluate the difference of the abovementioned two antihypertensive strategies on the outcome of patients with aortic disease.

Materials and methods

Study design

This was a retrospective review of all aortic diseases admitted to our hospitals from January 1, 2013 to June 30, 2014, to examine their antihypertensive strategies and their association with patients' outcomes. The institutional review board of our hospitals approved the study protocol and waived from the need for a consent form given the observational nature of this study.

As practiced in our hospitals, vast majority patients with aortic disease are required to be admitted to ICU for aggressive control of heart rate and blood pressure and close monitoring. Generally, esmolol was infused firstly to control heart rate for patients with tachycardia, then urapidil or nicardipine was administrated continuously for antihypertensive therapy. The target systolic blood pressure and heart rate for aortic disease in our ICU were defined as 100-120 mmHg and 60-70/min respectively. All the parenteral medications were administrated according the pharmacological instruction. The infusion rate was adjusted until the target level was reached within 30-60 min. After the target level had been reached, the rate of infusion was adjusted to maintain this level of heart rate or blood pressure. Given emergency operation indication and the possible clinically instability, all patients received parenteral medications for 3-5 days to manage the heart rate and blood pressure. Thereafter, it was switched to oral antihypertensive agents and β-blockers at the discretion of the attending physicians.

All adult patients with new diagnosed aortic diseases during the study period were screened to be included in the study. However, patients with the following characteristics were excluded: (I) did not necessitate the mentioned antihypertensive therapy after admission; (II) with prior signed "Do not resuscitation" directives; (III) refractory hypertension necessitated ≥2 intravenous antihypertensive agents administrated simultaneously; (IV) patients with a contraindication to esmolol such as asthma; (V) antihypertensive therapy with other medications.

Data sources and processing

The hospital admission database and the ICU database were queried to extract all the patients with aortic diseases during the study period. For each patient, the following data were extracted: (I) date and time of hospital and ICU admission; (II) demographic characteristics (age, gender); (III) CT images; (IV) clinical symptom on admission; (V) co-morbidity; (VI) management strategy and whether the patient underwent an urgent surgical intervention, what were the concomitant procedures, and the operation time; (VII) the start and end time for the administration of urapidil, nicardipine, or esmolol; (VIII) the time from the start of antihypertensive therapy to target level; (IX) cost of the above parenteral medications and the total ICU and hospital costs; (X) whether the patient underwent reoperation for postoperative bleeding or pericardial effusion, prolonged intubation >48 hours, renal replacement therapy, or stroke; (XI) ICU and hospital length of stay (LOS); (XII) patient's ICU outcome.

Primary data analysis

Descriptive data were reported as either mean ± SD, median (interquartile range) or number and percentage. With respect to the differences between urapidil and nicardipine therapy groups, categorical variables were compared using chi-square analysis. Continuous variables were compared using Independent Sample *t*-test for normally distributed data and Mann-Whitney U test for non-normally distributed data. To evaluate whether various antihypertensive strategies associated with different outcomes for patients with aortic diseases, the median

Table 1 Patient characteristics of two groups

Variables	Urapidil group (n=47)	Nicardipine group (n=73)	P value
Age (yrs)	58.2±16.1	54.6±14.7	0.216
Gender (male)	34 (72.3%)	47 (64.4%)	0.364
Classification of aortic disease			0.174
Thoracic aortic aneurysm	7	5	
Abdominal aortic aneurysm	4	2	
Penetrating atherosclerotic ulcer	5	3	
Intramural hematoma	1	3	
Traumatic rupture of the thoracic aorta	2	2	
Aortic dissection	28	58	0.081
DeBakey I	5	22	
DeBakey II	6	5	
DeBakey III	17	31	
Aortic disease involved with			0.056
Isolated ascending aorta	10	8	
Arch and supra-aortic vessels	7	8	
Descending thoracic aorta	7	3	
Abdominal aorta	15	34	
Iliac arteries	8	20	
Severe clinical presentation on admission			0.270
Cardiac tamponade	4	2	
Hemiparesis	1	1	
Unconsciousness	0	3	
Co-morbidity*			0.103
Coronary heart disease	4	2	
COPD	3	2	
Diabetes mellitus	26	40	
Hypertension	3	1	
Chronic kidney disease	1	0	

*, patients may have more than one condition.

values of the ICU/esmolol cost and ICU LOS were used as cutoffs to transform the data into categorical variables (high/low ICU/esmolol cost, and long/short ICU LOS respectively) for regression analysis.

To clarify potential association between nicardipine antihypertensive therapy and ICU outcomes, binary logistic regression analysis was performed using ICU outcomes [high ICU/esmolol cost (yes/no), long ICU LOS (yes/no), necessitate renal replacement therapy (yes/no), and died in ICU (yes/no), respectively] as the dependent variable and nicardipine antihypertensive therapy (with urapidil as reference), patient demographics, co-morbidity, involved extend of aorta, interventional strategies were used as variables. Odds ratios (ORs) and their 95% confidence intervals (95% CIs) were calculated. Statistical analysis was performed by using SPSS 16.0 (Chicago, Ill, USA). Statistical significance was defined as a P value <0.05.

Results

A total of 120 patients with new diagnosed aortic disease were included in the study. Of them, 47 patients received urapidil while 73 patients received nicardipine antihypertensive therapy. The patients' characteristics were shown in *Table 1*. There was no significant difference of age, male percent, classification of aortic disease, severe

Table 2 Treatments for the two groups

Treatments	Urapidil group (n=47)	Nicardipine group (n=73)	P value
Time to target blood pressure (min)	35 [15-75]	18 [5-45]	0.024
Concomitant esmolol administration	41	66	0.585
Duration of intravenous antihypertensive administration (d)	4.0 [1.0-5.0]	4.0 [1.0-6.0]	0.261
Duration of esmolol administration (d)	6.5±5.7	13.4±9.2	0.001
Total dose of intravenous esmolol (g)	4.0 [2.2-11.2]	7.4 [2.4-21.6]	0.002
Management strategy			0.833
Conservative management†	8	14	
Percutaneous aortic fenestration††	25	36	
Surgical procedures	16	29	
Ascending aortic replacement	11	14	
Proximal aortic replacement + hemi arch replacement	3	8	
Proximal aortic replacement + total arch replacement	2	7	
Concomitant procedures*	14	28	0.292
Coronary artery bypass graft	3	7	
Aortic valve replacement	5	16	
Mitral valve replacement	3	1	
Subclavian artery bypass	3	4	
Operation time (min)	285 [85-455]	293 [88-475]	0.411
Cardiopulmonary bypass time (min)**	164 [109-221]	162 [114-198]	0.481
Cross-clamp time (min)**	109 [80-150]	108 [72-154]	0.417

†, including 1 and 3 patients who suffered suddenly devastating rupture before intervention respectively; ††, including 2 and 6 patients underwent surgical procedures and concomitant percutaneous aortic fenestration respectively; *, some patients may undergo more than one concomitant procedure; **, for 16 and 29 patients who underwent cardiopulmonary bypass in each group respectively.

presentation on admission, and co-morbidity between two groups. However, it seemed that more patients in nicardipine group had aortic dissection of Debakey type I, and therefore a more extensive portion of aorta was involved (P=0.081 and P=0.056, respectively) (*Table 2*). As expected, patients with nicardipine were more quickly to reach the target blood pressure level (median, 18 *vs.* 35 min, P=0.024). The median duration of intravenous antihypertensive therapy was similar within the two groups. Moreover, the percent of patients who necessitated esmolol for heart rate control was comparable between the two groups (66/73 *vs.* 41/47, P=0.585). Surprisingly, patients of nicardipine group received a significant longer duration of esmolol administration and higher total dose of esmolol (P=0.001 and P=0.002, respectively) (*Table 2*). With respect to the management strategy, concomitant procedures, operation time and cardiopulmonary time, there was no significant difference between the two groups (*Table 2*).

When it comes to the outcomes, there were no difference of percentage of patients with devastating rupture before intervention, reoperation for bleeding/effusion, prolonged intubation >48 h, stroke and renal replacement therapy among the two groups (*Table 3*). The ICU mortality was 11.0% (8/73) in nicardipine group and 14.9% (7/47) in urpidil group respectively (P=0.525, *Table 3*). Meanwhile, the total cost for urapidil or nicardipine, hospital LOS and total hospital cost were similar between the two groups (*Table 3*). Interestingly, the patients in the nicardipine group stayed a median 2.6 days longer in ICU than urapidil treated patients. Moreover, patients with nicardipine antihypertensive therapy spent more median money for intravenous esmolol and ICU stay ($487 *vs.* $263, P=0.002, and $19,516 *vs.* $10,677, P=0.029 respectively, *Table 3*).

The median esmolol cost, ICU cost and ICU LOS was $374, $15,115, and 4.7 days respectively. Hence, the esmolol/ICU cost and ICU LOS were dichotomized into high (≥ median) and low cost, and long (≥ median) and short ICU LOS respectively. Thereafter, the association

Table 3 Outcomes for patients treated with the two regimens

Treatments	Urapidil group (n=47)	Nicardipine group (n=73)	P value
Devastating rupture before intervention	1	3	0.555
Reoperation for bleeding/effusion	4	6	0.955
Prolonged intubation >48 h	9	11	0.558
Stroke	0	5	0.067
Renal replacement therapy	8	9	0.472
ICU mortality	7 (14.9%)	8 (11.0%)	0.525
ICU LOS (d)	3.1 [2.4-5.8]	5.7 [2.9-10.1]	0.014
Hospital LOS (d)	18.0 [10.5-25.5]	16.0 [11.5-23.0]	0.298
Total cost of intravenous antihypertensive agents ($)	263 [72-789]	240 [118-613]	0.600
Total cost of intravenous esmolol ($)	263 [145-737]	487 [158-1,421]	0.002
Total ICU cost ($)	10,677 [2,806-19,839]	19,516 [4,339-29,032]	0.029
Total hospital cost ($)	21,129 [13,419-27,581]	24,194 [19,677-32,419]	0.236

LOS, length of stay.

Table 4 Association between antihypertensive strategy and ICU outcomes

ICU outcomes	Antihypertensive strategy	OR	95% CI	P
Renal replacement treatment	Urapidil	Reference	–	–
	Nicardipine	0.6	0.1-3.0	0.490
High esmolol cost	Urapidil	Reference	–	–
	Nicardipine	6.2	1.8-21.6	0.004
High ICU cost	Urapidil	Reference	–	–
	Nicardipine	2.7	0.9-8.2	0.083
Long ICU LOS	Urapidil	Reference	–	–
	Nicardipine	3.9	1.5-10.3	0.006
ICU mortality	Urapidil	Reference	–	–
	Nicardipine	0.3	0.1-1.4	0.123

OR, odds ratio, CI, confidence interval; LOS, length of stay.

between antihypertensive strategy and patients' outcomes were further assessed by regression analysis with adjustment for age, patient gender, co-morbidity, involved extend of aorta and interventional strategies (*Table 4*). As a result, antihypertensive therapy with nicardipine in acute phase was significantly associated with high esmolol cost (OR: 6.2, 95% CI, 1.8-21.6, P=0.004) and longer ICU LOS (OR: 3.9, 95% CI, 1.5-10.3, P=0.006) (*Table 4*). However, there was no significant correlation between nicardipine use and ICU mortality (OR: 0.3, 95% CI, 0.1-1.4, P=0.123).

Discussion

This study demonstrated that although antihypertensive therapy with nicardipine for patient with aortic disease reached the target blood pressure level more quickly than urapidil, nicardipine was associated with more esmolol use and longer ICU LOS.

Treatment varies greatly according to the location and severity of the aortic disease. Surgery is generally indicated for those involving the ascending aorta, while medical management and subsequently endovascular stent is usually reserved for stable descending aortic disease. Despite contemporary surgical advances, aortic diseases are still a clinical challenge and are associated with high mortality and morbidity. Once the diagnosis of aortic aneurysm or dissection is made, initial management by controlling aortic shear stress while simultaneously determining which patients will

benefit from surgical or endovascular repair is essential (4). Given that aortic wall stress is mainly correlated with the velocity of ventricular contraction (dP/dt), blood pressure and heart rate, using β-blockers to reduce heart rate and blood pressure is of top priority. Reasonable initial targets are a heart rate less than 60 bpm and a systolic blood pressure between 100 and 120 mmHg (4). Tight heart rate control was associated with a significantly reduction in aortic events compared to conventional heart rate control group (OR: 0.25, P<0.01) (5). Moreover, patients who started and maintained on β-blockers throughout their hospital course were associated with a significant reduction in postoperative adverse cardiac events (6). This may be because postoperative hemodynamic stability was help to maintain aortic stability and prevent aortic expansion with possible rupture and recurrent dissection.

Given arterial hypertension is the most important predisposing factor for aortic aneurysm or dissection, prompt anti-hypertensive therapy and maintenance of an optimal systolic blood pressure level is of paramount importance. Therefore, if beta-blockade alone does not control hypertension, combination with intravenous antihypertensive agents may be required for more severe hypertension. In acute aortic dissection, goals of anti-hypertensive therapy are the prevention of both the propagation of the dissection and early thrombus formation within the false lumen. The preferred method of antihypertensive therapy is the continuous infusion of parenteral anti-hypertensive drugs (4). An ideal antihypertensive agent should have a rapid onset of action and a predictable dose response, would be easily titratable to the desired blood pressure (7). Although sodium nitroprusside is a potent and short acting vasodilator and had been widely used hypertension emergency, it is photosensitive and requires time-consuming foil wrapping of the administration set to safeguard its potency. Furthermore, it may cause reflex tachycardia which is extraordinary hazardous for patients with aortic dissection (4). As a result, the nicardipine and urapidil had been the most widely used agents for antihypertensive therapy in patients with aortic disease. Urapidil is a competitive and selective short acting blocker of post-synaptic α1-receptor, which inhibits the vasoconstrictive action of catecholamines and consequently decreases blood pressure (8). On the other hand, nicardipine is an effective antihypertensive agent that decreases afterload by reducing total peripheral resistance without reducing cardiac output. Although nicardipine has been widely used in peri- or intra-operative hypertension, recent trials of urapidil in patients with phaeochromocytoma and pre-eclampsia had demonstrated the urapidil is efficient and also well tolerated in control of hypertension (8,9). Nevertheless, few study has compared the effect of this two different antihypertensive agents on the outcomes of patients with aortic disease. In this study, we demonstrated that although patients with nicardipine were more quickly to reach the target blood pressure level (median, 18 *vs.* 35 min, P=0.024), antihypertensive therapy with nicardipine was significantly associated with high esmolol cost (OR: 6.2, P=0.004). This may be because urapidil had additional central serotonin receptor-mediated antihypertensive activity, this mechanism could explain the lack of reflex tachycardia associated with urapidil use (10). In contrast, nicardipine may be associated with somewhat reflex tachycardia because of its significantly vasodilatation effect. Surprisingly, we also found the nicardipine use was associated with longer ICU LOS (OR: 3.9, P=0.006). This may be because patients in nicardipine group were more severe with more complicated aortic disease and more extensive aorta involved. Thus, some patients may prefer to stay in ICU a bit longer for close monitoring while discharged shortly after transfer from ICU to wards. This was consistent with that the median hospital LOS is comparable in the two groups.

Of note, the postoperative blood pressure level is also associated with the patients' long-term prognosis. Tsai and colleagues found that patients who died within 3 years of surgery had higher systolic blood pressure compared with those who survived (130 *vs.* 122 mmHg, P<0.01) (11). In a recent study of 10 years follow-up demonstrated patients who maintained systolic blood pressure <120 mmHg had improved freedom from reoperation compared with those with blood pressure 120-140 or >140 mmHg (92%±5% *vs.* 74%±7% and 49%±14% respectively, P<0.001) (12). Thus, both the preoperative and postoperative heart rate and blood pressure control for patients with aortic disease play an important role in preventing the continuing damage to the already diseased aorta.

Conclusions

In summary, our finding demonstrated that although nicardipine tends to achieve the target blood pressure level more quickly than urapidil for patients with aortic disease, it was associated with more esmolol use and longer ICU LOS.

Acknowledgements

Disclosure: The authors declare no conflict of interest.

References

1. Pagni S, Ganzel BL, Trivedi JR, et al. Early and midterm outcomes following surgery for acute type A aortic dissection. J Card Surg 2013;28:543-9.
2. Kim KH, Moon IS, Park JS, et al. Nicardipine hydrochloride injectable phase IV open-label clinical trial: study on the anti-hypertensive effect and safety of nicardipine for acute aortic dissection. J Int Med Res 2002;30:337-45.
3. Boodhwani M, Andelfinger G, Leipsic J, et al. Canadian Cardiovascular Society position statement on the management of thoracic aortic disease. Can J Cardiol 2014;30:577-89.
4. Hiratzka LF, Bakris GL, Beckman JA, et al. 2010 ACCF/AHA/AATS/ACR/ASA/SCA/SCAI/SIR/STS/SVM guidelines for the diagnosis and management of patients with Thoracic Aortic Disease: a report of the American College of Cardiology Foundation/American Heart Association Task Force on Practice Guidelines, American Association for Thoracic Surgery, American College of Radiology, American Stroke Association, Society of Cardiovascular Anesthesiologists, Society for Cardiovascular Angiography and Interventions, Society of Interventional Radiology, Society of Thoracic Surgeons, and Society for Vascular Medicine. Circulation 2010;121:e266-369.
5. Kodama K, Nishigami K, Sakamoto T, et al. Tight heart rate control reduces secondary adverse events in patients with type B acute aortic dissection. Circulation 2008;118:S167-70.
6. Brooke BS, Dominici F, Makary MA, et al. Use of beta-blockers during aortic aneurysm repair: bridging the gap between evidence and effective practice. Health Aff (Millwood) 2009;28:1199-209.
7. Khoynezhad A, Plestis KA. Managing emergency hypertension in aortic dissection and aortic aneurysm surgery. J Card Surg 2006;21:S3-7.
8. Wacker JR, Wagner BK, Briese V, et al. Antihypertensive therapy in patients with pre-eclampsia: A prospective randomised multicentre study comparing dihydralazine with urapidil. Eur J Obstet Gynecol Reprod Biol 2006;127:160-5.
9. Tauzin-Fin P, Sesay M, Gosse P, et al. Effects of perioperative alpha1 block on haemodynamic control during laparoscopic surgery for phaeochromocytoma. Br J Anaesth 2004;92:512-7.
10. Alijotas-Reig J, Bove-Farre I, de Cabo-Frances F, et al. Effectiveness and safety of prehospital urapidil for hypertensive emergencies. Am J Emerg Med 2001;19:130-3.
11. Tsai TT, Evangelista A, Nienaber CA, et al. Long-term survival in patients presenting with type A acute aortic dissection: insights from the International Registry of Acute Aortic Dissection (IRAD). Circulation 2006;114:I350-6.
12. Melby SJ, Zierer A, Damiano RJ Jr, et al. Importance of blood pressure control after repair of acute type a aortic dissection: 25-year follow-up in 252 patients. J Clin Hypertens (Greenwich) 2013;15:63-8.

Cite this article as: Wu KS, Zhou JC, Li HY, Gu DY, Pan KH, Li WD, Hu YH. Antihypertensive therapy with nicardipine for patients with aortic disease is associated with more esmolol usage than urapidil. J Thorac Dis 2014;6(12):1765-1771. doi: 10.3978/j.issn.2072-1439.2014.12.22

Original Article

In vitro study of coronary flow occlusion in transcatheter aortic valve implantation

Zheng-Fu He[1], Wei-Ming Zhang[1], George Lutter[2], Rene Quaden[2], Jochen Cremer[2], Xiu-Jun Cai[3]

[1]Department of Cardiothoracic Surgery, Sir Run Run Shaw Hospital, Zhejiang University School of Medicine, Hangzhou 310016, China; [2]Department of Cardiovascular Surgery, School of Medicine, University Of Kiel, Kiel, Germany; [3]Department of General Surgery, Sir Run Run Shaw Hospital, Zhejiang University School of Medicine, Hangzhou 310016, China

Correspondence to: Dr. Xiu-Jun Cai. Department of General surgery, Sir Run Run Shaw Hospital, Zhejiang University School of Medicine, Hangzhou 310016, China. Email: srrshe@gmail.com.

Background: Transcatheter aortic valve implantation (TAVI) has been developed recently for patients with high morbidities and who are believed to be not tolerate standard surgical aortic valve replacement. Nevertheless, the TAVI is associated with complications such as potential obstruction of coronary ostia, mitral valve insufficiency, and stent migration although it seems promising. Impairment of the coronary blood flow after TAVI is catastrophic and it was believed to be associated with the close position of the coronary orifice and the aortic leaflets and valve stent. However, few data was available as to the anatomic relationship between valve stent and aortic root anatomic structures including the coronary arterial ostia, aortic leaflets.

Methods: The aortic roots were observed in 40 hearts specimens. The width of aortic leaflet, height of aortic sinus annulus to the sinutubular junction (STJ), distance between aortic sinus annulus to its corresponding coronary ostia, and coronary arterial ostia to its corresponding STJ level were measured. Moreover, the relationships of valve stent, aortic leaflets and coronary ostia before/post stent implantation and after the open of aorta were evaluated respectively.

Results: Approximate three quarters of the coronary ostia were located below the STJ level. The mean distances from left, right and posterior aortic sinus annulus to the related STJ level was comparable, which was 18.5±2.7, 18.9±2.6, 18.7±2.6 mm, respectively. Meanwhile, the height of left and right aortic sinus annulus to its corresponding coronary ostia was 16.6±2.8 and 17.2±3.1 mm for left and right side respectively.

Conclusions: Most of the coronary ostia were located below the STJ level and could be covered by the leaflets. This highlights the need of modified stents to prevent occlusion of coronary flow after TAVI.

Keywords: Aortic valve; coronary ostia; transcatheter aortic valve implantation (TAVI); stent

Submitted Sep 29, 2014. Accepted for publication Nov 13, 2014.
doi: 10.3978/j.issn.2072-1439.2014.12.19
View this article at: http://dx.doi.org/10.3978/j.issn.2072-1439.2014.12.19

Introduction

Surgical aortic valve replacement has been proven to be an effective treatment of symptomatic aortic valve disease with low operative morbidity and mortality in selected patient groups. Traditional surgical approaches require a midline sternotomy and cardiopulmonary bypass with or without cardioplegic arrest. To minimize the invasiveness of operations, a broad spectrum of techniques, including endoscopic and robotic surgery, has been developed and optimized (1-3).

Of note, an increasing number of patients are poor surgical candidates due to advanced age, co-morbidities and previous cardiac surgery. Thus, transcatheter aortic valve implantation (TAVI) was developed and it has been shown to be an effective and feasible procedure in selected patients (4-6), which is believed to benefit a large patient population in the future. Despite the TAVI holds great promise, many technological difficulties and limitations still exist, including potential restriction of coronary ostia, mitral valve insufficiency, and stent migration. Most

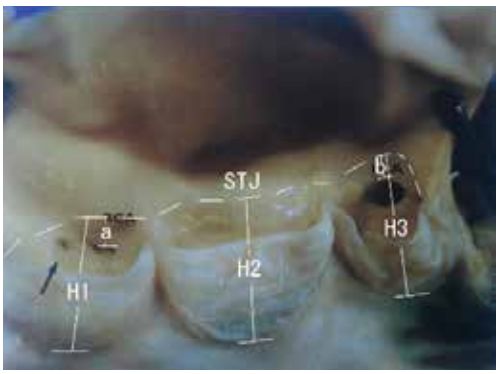

Figure 1 Distance between aortic sinus annulus to the sinutubular junction level (H1, H2, H3) and coronary arterial ostia (a and b) to its corresponding sinutubular junction level.

investigators (7,8) reported the impairment of the coronary blood flow was mainly due to the position of the coronary orifice and the close relationship with the aortic leaflets, valve stent and anterior mitral leaflet during the TAVI. To avoid the impairment of the coronary flow during TAVI, a basic research concerning the relation between valve stent and aortic root anatomic structures including the coronary arterial ostia, aortic leaflets is of paramount importance. Therefore, in current study, we measured the structures of aortic root in 40 fresh adult heart specimens. Through the post mortem aortic valved stent implantation, we investigated the relation of coronary ostia, aortic leaflets, and valved stents, so as to disclose the mechanism of TAVI influence on the coronary blood flow.

Materials and methods

Between March 2007 and August 2007, 40 post mortem hearts were enrolled and dissected in our study, collected at autopsy in the Department of Pathology of University Hospital of Schleswig-Holstein, German. All the cadavers were white adults of both genders. The cadavers were kept in cool place until it was used for autopsy. All the hearts were dissected according to the previously described methods (9). The aorta was opened between the attachment of left and right aortic leaflet. The aortic root including ascending aorta was sectioned sequentially for evaluations as below: first, the ascending aorta was transversally sectioned approximately 1 cm below the arch of aorta and measured the valve size. Second, we removed the aorta at level of the proximal aorta, just approximate 1 cm above the level of sinutubular junction (STJ) of the aorta, and measured the diameter of the proximal aorta, STJ and aortic sinus annulus respectively. Meanwhile, width of aortic leaflet, height of aortic sinus annulus to the STJ level (from the lowest point of aortic sinus annulus to STJ), distance between aortic sinus annulus to its corresponding coronary ostia, and coronary arterial ostia (from the superior margin of the ostia) to its corresponding STJ level were measured (*Figure 1*). After above measurement was performed, a cut across the aorta above the aortic annulus (approximate 0.5 cm above the STJ) was made to exposure the valve architecture so as to determine the relation of valve stent, aortic leaflets and coronary ostia. Meanwhile, the relationships of valve stent, aortic leaflets and coronary ostia before/post stent implantation and after the open of aorta were evaluated respectively. To illustrate the relation of coronary ostia, aortic leaflets and valve stent, the relation between coronary ostia and leaflets were firstly measured before the stent implantation. Thereafter, we observed the relation among the coronary ostia, leaflets and stents after the stent implantation in the aortic annulus position. Finally, when the aorta was opened, we inspected the aortic leaflets would or not cover the coronary ostia.

Statistical analysis

Descriptive data were reported as either mean ± Standard Deviation, or number and percentage. Continuous variables were compared using Independent Sample *T* test for normally distributed data. Statistical analysis was performed by using SPSS 16.0 (Chicago, Ill, USA). Statistical significance was defined as a P value <0.05.

Results

There were 19 men and 21 women cadavers were collected in this study. The average age, height, body weight, and heart weight were 69.7 years old, 168.6 cm, 80.6 kg, and 453.1 g respectively.

All 40 hearts possessed three semi-lunar aortic valves and two main coronary ostia. Vast majority coronary arteries originated from the appropriated aortic sinuses, with 34 (85%) left coronary ostia originated from left aortic sinus and 33 (82.5%) right coronary ostia originated from right aortic sinus. The mean diameter of the proximal ascending aorta, STJ, and aortic sinus annulus were 31, 30 and 24 mm respectively. Average size of left and right coronary ostia was 5.3 mm and 4.7 mm respectively.

The mean widths of left, right and posterior aortic leaflet were comparable at 28.92±5.10, 31.22±6.02, and 30.88±5.06 mm respectively. The mean height of left, right and posterior aortic sinus annulus to the related STJ level (from the lowest point of aortic sinus annulus to STJ) was comparable, which was 18.5±2.7, 18.9±2.6, 18.7±2.6 mm, respectively. Likewise, the height of left and right aortic sinus annulus to its corresponding coronary ostia, it was 16.6±2.8 and 17.2±3.1 mm for left and right side respectively. Meanwhile, mean height of left, right and posterior aortic leaflet (from the bottom of aortic valve to the free ridge of the cusp) was 16.1±2.0, 16.4±2.1 and 16.8±1.7 mm respectively. Thus, the height of left and right coronary arterial ostia (from the superior margin of the ostia) to its corresponding STJ level was 1.8±1.1 and 1.8±1.3 mm for two sides respectively.

The location of the coronary arterial ostia was measured in relation to the STJ and described as being below, above and at the level of STJ (*Table 1*). Theoretically, if the height of the aortic leaflet is higher than that of the aortic annulus to its corresponding STJ, this may cause coronary ostia be covered by the aortic leaflet. Of them, both ostia of 17.5% patients were cover by leaflets, while both ostia of 45.0% patients were not covered by leaflets. However, in 12.5% patients, the left ostia was covered while the right ostia was not. Conversely, right ostia of one quarter patients was covered but with left was not (*Figure 2*). When both ostia lay in the valsalva sinus (below the STJ level), the mean height of the left ostia to STJ line measured 1.9±0.6 mm, and the right was 2.2±0.9 mm. Thus, the right ostia was located lower (deeper) position than the left coronary ostia in the sinus of valsalva.

Table 1 Location of the coronary ostia with respect to the STJ level (n=40)

Coronary ostia	Cases (%)
Both below	29 (72.5)
Both above	1 (2.5)
Left above, right below	2 (5.0)
Left above, right at level	1 (2.5)
Left below, right above	2 (5.0)
Left below, right at level	3 (7.5)
Left at level, right below	2 (5.0)

STJ, sinutubular junction.

Discussion

In this study, we demonstrated that nearly three quarters of the coronary ostia were located below the STJ level and could be covered by the leaflets. This indicated an advanced valve may be necessary to avoid occlusion of coronary blood flow during TAVI.

In certain patients, especially elderly patients with declining overall health status or life-threatening co-morbidities, aortic valve replacement is considered either too risky or contraindicate, because of the significant risk of morbidity and mortality. Furthermore, symptomatic patients with severe aortic stenosis managed medically have a poor prognosis. As an alternative, the transcatheter balloon aortic valvuloplasty is palliative and with an incidence of restenosis, although it may result in temporary improvement of valvular function and relief of symptoms. Given the limited

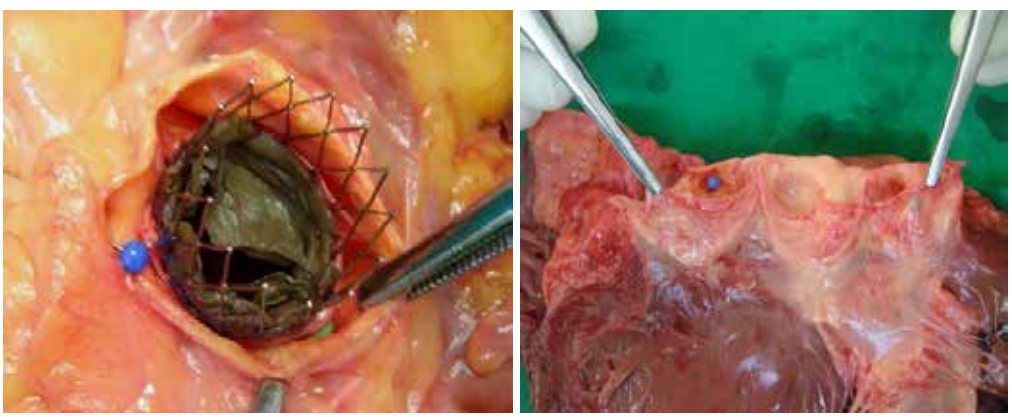

Figure 2 The diagram illustrated the left coronary ostia (green marker) was covered by the aortic leaflet post stent implantation, while the right ostia (blue marker) was not covered.

therapeutic options in this subset of patients, TAVI has been an increasingly available therapy for the management of aortic stenosis in high-risk patients (10).

Coronary flow impairment, as a major issue encountered in TAVI, might be caused by the obstruction of coronary ostia by the native leaflets, which was firstly reported by Andersen in 1992. Another *in vitro* study showed that the deployment of a cylindrical, stented aortic valve can severely affect coronary flow by obstructing the coronary ostia with the native leaflets (11). During orthotopic TAVI, obstruction of coronary ostia, result in coronary flow restriction can occur either by direct blocking from the implanted stent, or from the native aortic leaflets immobilized against the coronary orifices (7,12). Based on this, we observed and investigated the anatomy of aortic root structures, to elucidate the relation of aortic root structures and valved stent, and the influence of valved stents on these anatomic structures by postmortem aortic valve stent implantation.

With respect to the position of coronary ostia in relation to STJ in our study, 29 of 40 (72.5%) hearts analyzed had both ostia located in the aortic sinus, and 11(27.5%) hearts had one or both ostia above or at the STJ level. Of the 80 ostia analyzed in our 40 postmortem hearts, 83.7% (67/80) ostia were located below the sinotubular junctional level, only 7.5% (6/80) ostia were at its level, and 8.8% (7/80) above it. These results are similar to the study by Muriago *et al.* (13), in which they reported 13% of the ostia at or above that level. On the other hand, our results were different from those of Cavalcanti JS *et al.* (14) which indicated that 34 of the 50 (68%) hearts studied had one or both ostia above or at the STJ level, while both ostia located below the level only in 32% of cases. Moreover, our study are also different from the study by Waller *et al.* (15), who have noted up to three-tenths of coronary orifices arising above the STJ. Moreover, the typical vertical and centrically positioning of the ostia in some patients, particularly when both coronary ostia lying above the STJ level, might confer functional advantages for coronary flow during ventricular systole and also prevent the obstruction of the ostia when the aortic valve was opened.

When the valved stents were properly implanted in the postmortem aortic annulus, we found the native aortic leaflets were obviously folded upwards, pushed by valved stents, and immobilized against the leaflets close to the aorta wall. Most of the coronary ostia were partially or fully covered by its native leaflets. In 22 of 40 (55%) of our postmortem study (both covered in seven cases, left in five cases, and right in ten cases), one or both coronary ostia were covered by the aortic leaflets after stents implantation. Among them, 72.4% (21 of 29) cases, which the coronary ostia were located below the STJ, had ostia fully covered by the aortic leaflets. However, only one case (1/11, 9.1%) which the right ostia were located at the STJ level was covered , and the remaining 10 cases which one or both ostia were located at or above the sinutubular level did not have ostia covered. Regarding to the respective ostia, there were 28 of 67 (41.8%) ostia below the STJ were covered, whereas only 1of 13 (7.7%) ostia located at or above the STJ level was covered. Thus, if the coronary ostia lays below the STJ or in the aortic sinus, there is higher frequency they would be covered by their leaflets than ostia located at or above the STJ level. Nevertheless, coronary obstruction after TAVI is rarely observed in the real clinical practice. Coronary obstruction occurred only in 0.72% (3/418) and 0.82% (2/244) of cases after TAVI (16,17). The great discrepancy of incidence of coronary obstruction after TAVI between our study and clinical practice may be because anatomical cover of the coronary ostia shown in our postmortem study is not equal to physiological obstruction of coronary flow on angiography because coronary ostia may be lateral to the stent frame or there may be flow laterally from the open sinuses. Thus, we may overestimate the rate of coronary occlusion in our study. Moreover, different material used in prostheses and their implantation mechanisms may have some influence on the chance of coronary flow impairment. For example, a new-generation SAPIEN 3 valve could prevent the occurrence of this severe complication than earlier generation of balloon-expandable valve (18,19). The cylindrical stent used in out study was prepared by mounting a special material into a self-expandable nitinol stent by means of a suture technique, which was different from more advanced stents currently used for TAVI. A shorter stent placed as low as possible in the aortic annulus has obvious theoretical advantages (11).

Therefore, a good pre-procedural evaluation of the patients in order to avoid this severe complication through measuring the aortic root structure including the height of aortic leaflets, the distance from aortic annulus to its corresponding coronary ostia, or the distance of aortic annulus to STJ by echocardiography (20), CT scan (21) or MRI techniques before the orthotopic TAVI. Moreover, these techniques could accurately assess the calcification of aorta and aortic annulus area (22). Likewise, knowledge of the coronary arteries orifice in relation to the valve plane is critical to prevent inadvertent coronary artery occlusion, and would clearly be beneficial when planning future valve

designs (23).

There were several limitations in our study. Firstly, average age of our specimen was 69.7 years old while the reported age for patients underwent TAVI was around 82. Most of the aortic leaflets and annulus tissue of our specimens were normal or mild calcification, which may be different from clinical candidates of TAVI were believed to have severe aortic stenosis and calcification. Secondary, *in vitro* postmortem aortic valve implantation was performed in our study. It will be more physiological related if we could study in a dynamic and physiological environment *in vivo*. Lastly, performing such study by using a different style valved stent will be further required. Then, we can compare the options of design a new style valved stent.

In summary, current study demonstrated that most of the coronary ostia were located below the STJ level. This fundamental anatomy may explain potential obstruction of coronary ostia in postmortem orthotopic aortic valved stents implantation. Therefore, new stents should be designed so as to avoid occlusion of coronary blood flow during orthotopic TAVI.

Acknowledgements

This paper was partial supported by Zhejiang Qianjiang Talent Plan (2013R10030) and Zhejiang Province Education Department Project (Y201223135).
Disclosure: The authors declare no conflict of interest.

References

1. Rozeik MM, Wheatley DJ, Gourlay T. Percutaneous heart valves; past, present and future. Perfusion 2014;29:397-410.
2. Hawkey MC, Lauck SB, Perpetua EM, et al. Transcatheter aortic valve replacement program development: Recommendations for best practice. Catheter Cardiovasc Interv 2014;84:859-67.
3. Meredith Am IT, Walters DL, Dumonteil N, et al. Transcatheter aortic valve replacement for severe symptomatic aortic stenosis using a repositionable valve system: 30-day primary endpoint results from the REPRISE II study. J Am Coll Cardiol 2014;64:1339-48.
4. Leon MB, Smith CR, Mack M, et al. Transcatheter aortic-valve implantation for aortic stenosis in patients who cannot undergo surgery. N Engl J Med 2010;363:1597-607.
5. Smith CR, Leon MB, Mack MJ, et al. Transcatheter versus surgical aortic-valve replacement in high-risk patients. N Engl J Med 2011;364:2187-98.
6. Varela-Lema L, Queiro-Verdes T, Baz-Alonso JA, et al. Post-introduction observation of transcatheter aortic valve implantation in Galicia (Spain). J Eval Clin Pract 2014. [Epub ahead of print].
7. Ben-Dor I, Goldstein SA, Waksman R, et al. Effects of percutaneous aortic valve replacement on coronary blood flow assessed with transesophageal Doppler echocardiography in patients with severe aortic stenosis. Am J Cardiol 2009;104:850-5.
8. Bourantas CV, Serruys PW. Evolution of transcatheter aortic valve replacement. Circ Res 2014;114:1037-51.
9. Chapman CB. On the study of the heart: a comment on autopsy techniques. Arch Intern Med 1964;113:318-22.
10. Cribier A, Eltchaninoff H, Tron C, et al. Early experience with percutaneous transcatheter implantation of heart valve prosthesis for the treatment of end-stage inoperable patients with calcific aortic stenosis. J Am Coll Cardiol 2004;43:698-703.
11. Flecher EM, Curry JW, Joudinaud TM, et al. Coronary flow obstruction in percutaneous aortic valve replacement. An in vitro study. Eur J Cardiothorac Surg 2007;32:291-4; discussion 295.
12. Holmes DR Jr, Mack MJ, Kaul S, et al. 2012 ACCF/AATS/SCAI/STS expert consensus document on transcatheter aortic valve replacement: developed in collabration with the American Heart Association, American Society of Echocardiography, European Association for Cardio-Thoracic Surgery, Heart Failure Society of America, Mended Hearts, Society of Cardiovascular Anesthesiologists, Society of Cardiovascular Computed Tomography, and Society for Cardiovascular Magnetic Resonance. J Thorac Cardiovasc Surg 2012;144:e29-84.
13. Muriago M, Sheppard MN, Ho SY, et al. Location of the coronary arterial orifices in the normal heart. Clin Anat 1997;10:297-302.
14. Cavalcanti JS, de Melo NC, de Vasconcelos RS. Morphometric and topographic study of coronary ostia. Arq Bras Cardiol 2003;81:359-62, 355-8.
15. Waller BF, Orr CM, Slack JD, et al. Anatomy, histology, and pathology of coronary arteries: a review relevant to new interventional and imaging techniques--Part I. Clin Cardiol 1992;15:451-7.
16. Ribeiro HB, Sarmento-Leite R, Siqueira DA, et al. Coronary obstruction following transcatheter aortic valve implantation. Arq Bras Cardiol 2014;102:93-6.
17. Kapadia SR, Svensson LG, Roselli E, et al. Single center TAVR experience with a focus on the prevention and management of catastrophic complications. Catheter

Cardiovasc Interv 2014;84:834-42.
18. Amat-Santos IJ, Dahou A, Webb J, et al. Comparison of hemodynamic performance of the balloon-expandable SAPIEN 3 versus SAPIEN XT transcatheter valve. Am J Cardiol 2014;114:1075-82.
19. Ribeiro HB, Nombela-Franco L, Urena M, et al. Coronary obstruction following transcatheter aortic valve implantation: a systematic review. JACC Cardiovasc Interv 2013;6:452-61.
20. Islam MN, Khan ZI, Khan SR, et al. Morphometry of the intercommissural distances and other structures of the aortic valve of bovine heart. Mymensingh Med J 2006;15:153-8.
21. Krishnaswamy A, Parashar A, Agarwal S, et al. Predicting vascular complications during transfemoral transcatheter aortic valve replacement using computed tomography: a novel area-based index. Catheter Cardiovasc Interv 2014;84:844-51.
22. Hawkey MC, Lauck SB, Perpetua EM, et al. Transcatheter aortic valve replacement program development: Recommendations for best practice. Catheter Cardiovasc Interv 2014;84:859-67.
23. Rivard AL, Bartel T, Bianco RW, et al. Evaluation of aortic root and valve calcifications by multi-detector computed tomography. J Heart Valve Dis 2009;18:662-70.

Cite this article as: He ZF, Zhang WM, Lutter G, Quaden R, Cremer J, Cai XJ. *In vitro* study of coronary flow occlusion in transcatheter aortic valve implantation. J Thorac Dis 2014;6(12):1772-1777. doi: 10.3978/j.issn.2072-1439.2014.12.19

Original Article

Adrenergic regulation of the rapid component of delayed rectifier K+ currents in guinea pig cardiomyocytes

Sen Wang, Xiao-Yan Min, Si-Si Pang, Jin Qian, Di Xu, Yan Guo

Department of Geriatric Cardiology, First Affiliated Hospital of Nanjing Medical University, Nanjing, 210029, China

Correspondence to: Yan Guo, PhD. Department of Geriatric Cardiology, First Affiliated Hospital of Nanjing Medical University, Nanjing, 210029, China. Email: lnxxgk@163.com.

Background: Guinea pig ventricular cardiomyocytes display the rapid component of the delayed rectifier potassium current (I_{kr}) that contributes to ventricular repolarization and promotes stress-induced arrhythmias. Adrenergic stimulation favors ventricular arrhythmogenesis but its effects on I_{kr} are poorly understood.

Methods: Adrenergic modulation of I_{kr} was studied in isolated guinea pig ventricular cardiomyocytes using whole-cell patch clamping.

Results: We found that the I_{kr} amplitude was reduced to 0.66±0.02 and 0.62±0.03 in response to 0.1 μM phenylephrine (PE), an α_1AR agonist, and 10 μM isoproterenol (ISO), a βAR agonist, respectively. The effect of PE can be blocked by the selective α_1A-adrenoceptor antagonist 5-methylurapidil, but not by the α_1B-adrenoceptor antagonist chloroethylclonidine or α_1D-adrenoceptor antagonist BMY7378. Additionally, the effect of ISO can be blocked by the β_1-selective AR antagonist CGP-20712A, but not by the β_2-selective AR antagonist ICI-118551. Although PE and ISO was continuously added to cells, ISO did not decrease the current to a greater extent when cells were first given PE. In addition, PE's effect on I_{kr} was suppressed by β1AR stimulation.

Conclusions: I_{kr} can by regulated by both the α_1 and β ARs system, and that in addition to direct regulation by each receptor system, crosstalk may exist between the two systems.

Keywords: Adrenergic receptors (ARs); potassium current; crosstalk; cardiomyocytes

Submitted Aug 12, 2014. Accepted for publication Nov 13, 2014.
doi: 10.3978/j.issn.2072-1439.2014.12.27
View this article at: http://dx.doi.org/10.3978/j.issn.2072-1439.2014.12.27

Introduction

Cardiac action potential repolarization is carried out by different potassium currents. The rapid component of the delayed rectifier potassium current (I_{kr}) is the most important component for phase 3 repolarization and is required to control orderly repolarization at the end of each cardiac action potential, particularly near the threshold potential of early afterdepolarizations that can trigger tachyarrhythmias (1). The human ether-a-go-go-related gene (*hERG*) encodes the alpha subunit of I_{kr} current (2-5). HERG channels are a primary target for the pharmacological management of cardiac arrhythmias using class III antiarrhythmic agents, such as dofetilide and amiodarone (6-8). Reduced hERG currents due to hERG mutations or excessive blockade of hERG channels by antiarrhythmic or non-antiarrhythmic drugs may lead to congenital or acquired long QT syndrome (9,10). The sympathetic nervous system modulates the I_{kr} current though both α1 and β-adrenoceptors (ARs) (11-14). Separate stimulation of α_1-ARs or β-ARs decreased I_{kr} current and prolonged action potential. In recent years, considerable progress has been made toward a detailed understanding of these two signaling pathways. Bian and colleagues revealed that hERG potassium channels or the I_{kr} current of rabbit cardiomyocytes can be regulated by the α_1-adrenoreceptor agonist phenylephrine (PE), which is consistent with our previous work in guinea pig (12,15). In an early report by Heath and Terrar, a concentration-independent increase

in I_{kr} currents was observed at low concentrations of the β-adrenergic agonist isoprenaline (16), whereas Karle found activation of β-adrenoceptors elicits an inhibitory effect on I_{kr} or hERG via a cAMP/PKA-dependent pathway (17). Morever, at least three α_1 adrenoceptor subtypes (α_{1A}, α_{1B}, and α_{1D}) and three β adrenoceptor subtypes (β_1, β_2, and β_3) have been pharmacologically identified, it is unclear which AR subtypes primarily regulate I_{kr}. In addition, the interaction between the α_1 and β-adrenergic components during sympathetic regulation of the cardiac I_{kr} current were not examined, and their functional importance was not determined.

Methods

Cardiomyocyte preparation and whole-cell patch clamp

Guinea pigs (male, weighing 300±50 g) were purchased from Nanjing Medical University Institutional Animal Care. Single left ventricular myocytes were isolated from the heart of guinea pigs using the Langendorff apparatus as described previously (12). All experiments were performed in accordance with animal care protocols approved by the Nanjing Medical University Institutional Animal Care and Use Committee.

Cells were transferred to a recording chamber that was continuously perfused with bath solution. Whole-cell patch-clamp recordings were performed with an EPC-9 amplifier (HEKA, Germany) at 37±0.5 ℃. Pipettes, filled with the pipette solution, had resistances of 3-6 MΩ. The flow rate of bath solution through the chamber was maintained at 2-3 mL/min.

Data analyses

Currents were acquired with Pulse + Pulsefit V8.53 and analyzed using SPSS 13.0 software. Statistical data are expressed as the mean ± standard error of the mean (S.E.M). Paired-sample *t*-tests were used to determine significant differences before and after PE or ISO intervention. One-way analyses of variance (ANOVA), with post-hoc comparisons using Newman-Keuls tests, were performed to compare differences among groups. Differences were considered significant if $P<0.05$.

Solutions and drug administration

For I_{kr} recordings, the solution was prepared as described by Wang *et al.* (12). The pipette solution contained 140 mM KCl, 1 mM $CaCl_2$, 2 mM $MgCl_2$, 10 mM HEPES, 11 mM EGTA, 5 mM Na_2-ATP, and 5 mM creatine phosphate (disodium salt). The pH was adjusted to 7.4 using 8 M KOH. The bath solution contained 140 mM NaCl, 3.5 mM KCl, 1.5 mM $CaCl_2$, 1.4 mM $MgSO_4$, and 10 mM HEPES. The pH was adjusted to 7.4 using 10 M NaOH. Nifedipine (10 μM) was added to the bath solution to block calcium currents and 10 μM chromanol 293B was added to ablate the slow component of delayed rectifier potassium currents (I_{Ks}). Na_2-ATP, EGTA, creatine phosphate, *L*-glutamic acid, HEPES, taurine, bovine serum albumin (BSA), nifedipine, chromanol 293B, dofetilide, PE, and ISO were purchased from Sigma (St. Louis, MO). Collagenase II was purchased from Worthington (Lakewood, NJ). All other reagents were obtained from Amresco.

For stock solutions, nifedipine and chromanol 293B were dissolved in dimethyl sulfoxide (DMSO) to a concentration of 10 mM. ISO was dissolved in distilled water to 10 mM, and PE and dofetilide were dissolved in distilled water to 1 mM. All stock solutions were stored at –20 ℃, except nifedipine, which was stored at 4 ℃.

Results (*Figures 1-3*)

I_{kr} tail currents are inhibited by PE and α_{1A} subtype mediates this effect

When cell chambers were perfused with a bath solution containing 0.1 μM of the specific α_1-adrenereceptor agonist PE, the tail current amplitude significantly decreased (*Figure 1A,B*). The mean I_{kr} current density-voltage relations before and after PE are shown in *Figure 1C*. I_{kr} tail current density at +40 mV decreased to 0.66±0.02 upon the addition of 0.1 μM PE (first column of *Figure 1H*). When cells were pretreated with the non-selective α_1-adrenergic antagonist prazosin (1 μM), PE does not decrease I_{kr} current (*Figure 1D*, second column of *Figure 1H*). To further evaluate the α_1-adrenergic receptor (AR) subtype involved, selective α_1-AR blockers, α_{1A}-selective 5-methylurapidil (5-MU; 1μM), α_{1B}-selective chloroethylclonidine (CEC; 10 μM), or α_{1D}-selective BMY7378 (BMY; 1 nM) were applied together with PE (0.1 μM). When 5-MU, CEC, or BMY7378 was applied together with PE, the I_{kr} amplitudes decreased to 0.99±0.07, 0.62±0.03, and 0.70±0.04, respectively, indicating the α_{1A}-receptor antagonist 5-MU prevented PE-induced suppression of I_{kr}, whereas the α_{1B} and α_{1D}-receptor blockers did not (*Figure 1E-H*). These results suggested that stimulation of the α_1 adrenereceptor may

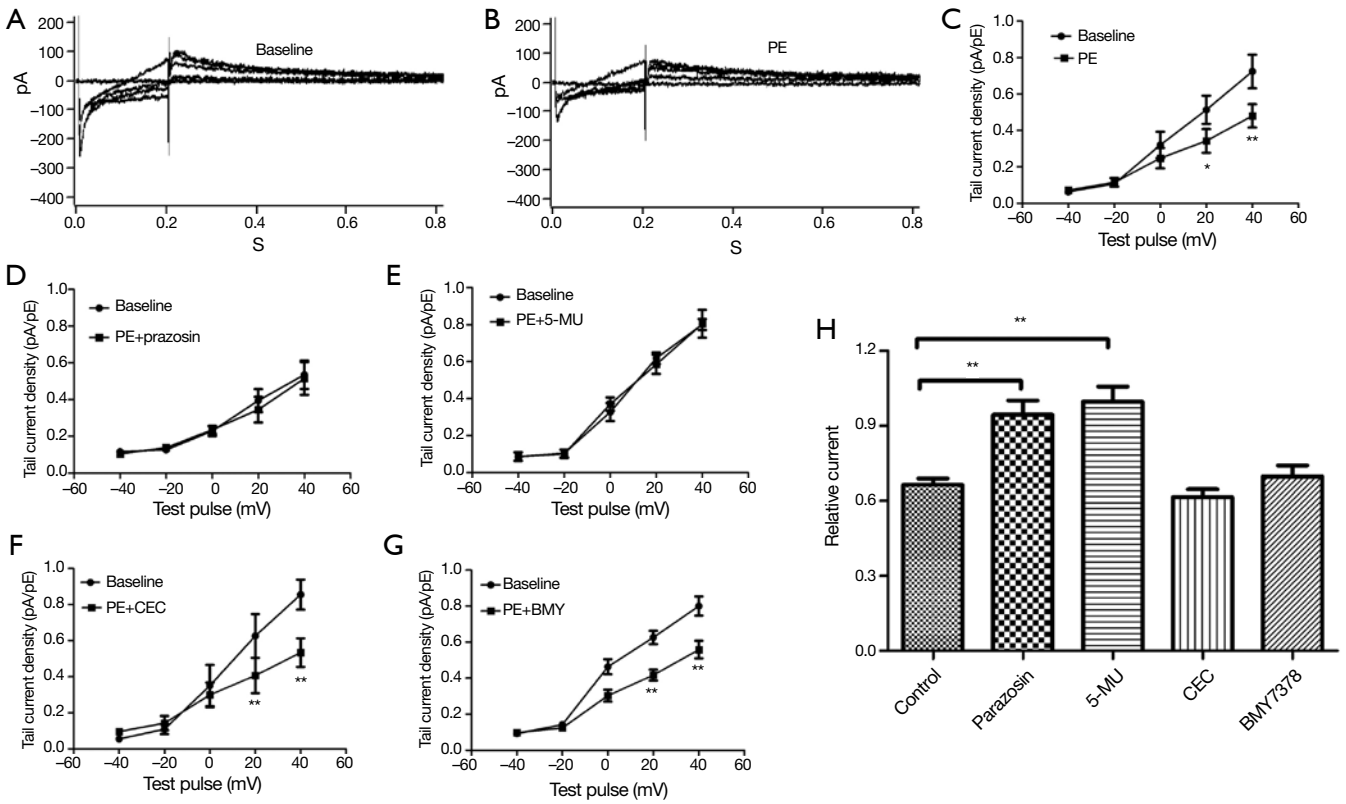

Figure 1 Effect of α-adrenoceptor and subtype on I_{kr}. (A,B) Representative I_{kr} current trace before and after PE application; (C) I_{kr} density-voltage relations (mean ± S.E.M) from five cells under control conditions (baseline) or in the presence of PE; (D-G) I_{kr} density-voltage relations (mean ± S.E.M) under control conditions and after the addition of 0.1 μM PE plus the α_1 antagonist prazosin (1 μM), α_{1A}-selective antagonist 5-MU (1 μM), α_{1B}-selective antagonist CEC (10 μM), or α_{1D}-selective antagonist BMY (1 nM); (H) current amplitudes were measured at +40 mV and amplitudes were normalized to the values before PE perfusion in the control, prazosin, 5-MU, CEC, and BMY groups (n=5, **P<0.01).

reduce I_{kr} tail current, and that α_{1A}, rather than the α_{1B} or α_{1D} receptor subtypes, is involved in this effect.

I_{kr} tail currents are inhibited by isoproterenol and β_1 subtype mediates this effect

When cell chambers were perfused with a bath solution containing 10 μM of the non-specific β-adrenereceptor agonist isoproterenol (ISO), the tail current amplitude significantly decreased (*Figure 2A*). The mean I_{kr} current density-voltage relations before and after ISO are shown in *Figure 2B*. I_{kr} tail current density at +40 mV decreased to 0.62±0.03 upon the addition of ISO (first column of *Figure 2F*). Propranolol blocked this effect because when cells were pretreated with the non-specific β-adrenereceptor blocker propranolol (10 μM), ISO no longer decreased the I_{kr} tail current (*Figure 2C*, second column of *Figure 2F*). To evaluate the β-AR subtype involved, we added selective β-AR blockers along with ISO: β_1-selective CGP-20712A (10 μM) and β_2-selective ICI-118551 (10 μM). The β_1-receptor blocker CGP completely prevented the ISO-induced reduction in I_{kr} (the I_{kr} tail current density at +40 mV decreased to 0.97±0.08), whereas the β_2-receptor blocker ICI did not alter the action of ISO (the I_{kr} tail current density at +40 mV decreased to 0.55±0.06) (*Figure 2D,E*; first, third, and fourth columns of *Figure 2F*). These results suggested that stimulation of the β-adrenereceptor reduced I_{kr} tail current, and that the β_1 rather than β2 receptor subtype is involved in the regulation of I_{kr}.

PE prevents the inhibitory effect of ISO on I_{kr}

We evaluated the effects of ISO in the presence of PE (0.1 μM). ISO (10 μM) was applied after the PE-induced changes

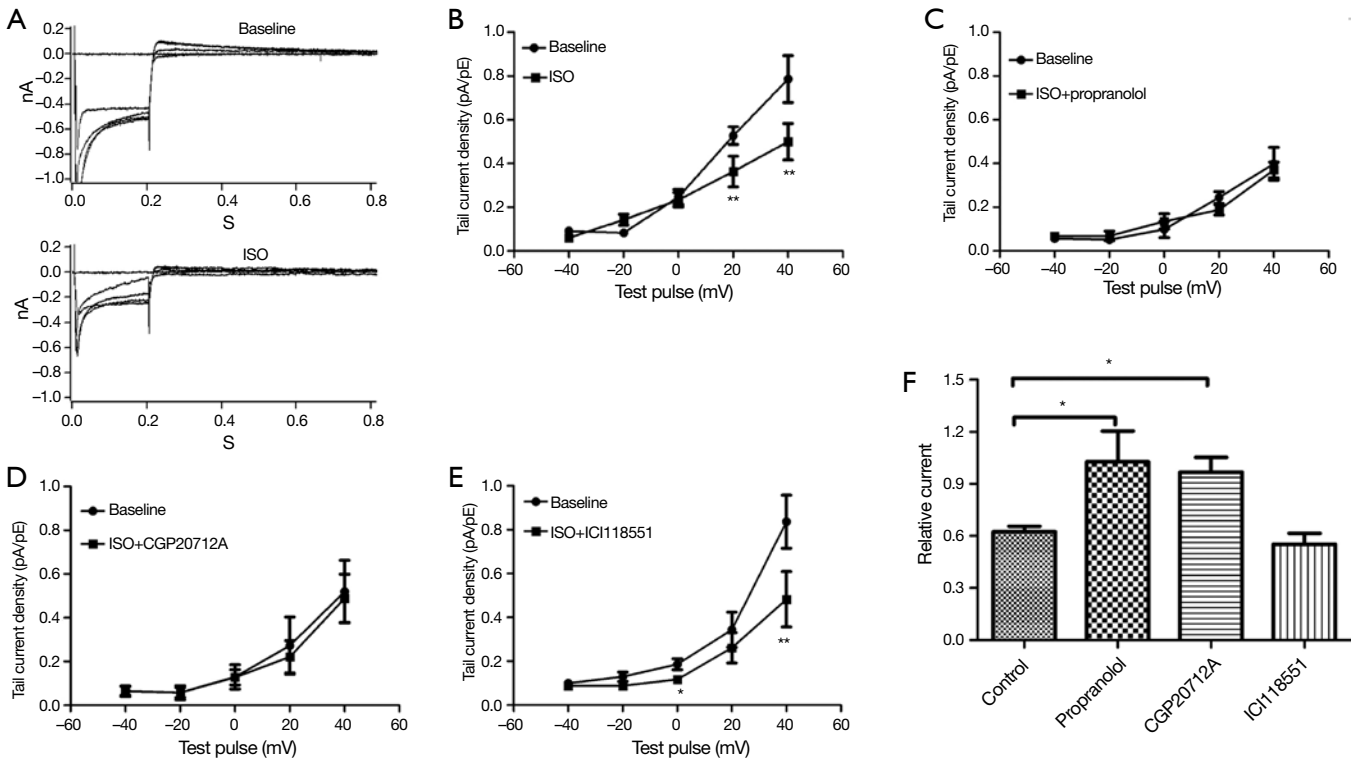

Figure 2 Effect of β-adrenoceptor and subtype on I_{kr}. (A) Representative I_{kr} current trace before and after ISO application; (B) I_{kr} density-voltage relations (mean ± S.E.M) from four cells under control conditions (baseline) and in the presence of ISO; (C-E) I_{kr} density-voltage relations (mean ± S.E.M) under control conditions and after the addition of 10 μM ISO plus the β_1 antagonist propranolol (10 μM), the β_{1A}-selective antagonist CGP-20712A (10 μM), or the β_{1B}-selective antagonist ICI-118551 (10 μM); (F) current amplitudes were measured at +40 mV and amplitudes were normalized to the value before ISO perfusion in control, propranolol, CGP-20712A, and ICI-118551 groups (n=4, *P<0.05).

stabilized (approximately 8-10 min after PE application). Changes in current amplitude are expressed relative to the amplitude before application of any drug (PE or ISO). *Figure 3A* shows a typical current trace of cells without drugs, then followed by PE and the last ISO. *Figure 3B* shows the relative current at test pulse +40 mV in each group. When cells were acutely stimulated with PE, the I_{kr} tail currents did not decrease with ISO addition (10 μM ISO after 0.1 μM PE). The relative current amplitudes were 1.01±0.12, which was significantly different from the ISO effect on I_{kr} without PE (third and fourth columns of *Figure 3E*). Thus, ISO does not reduce I_{kr} tail currents in cardiomyocytes pretreated with PE, which significantly differed from cardiomyocytes not acutely stimulated by PE. These results suggested that the PE prevents the current reduction effects of ISO on I_{kr}.

ISO attenuates the inhibitory effect of PE on I_{kr}

We also evaluated the effects of PE in the presence of ISO. PE (10 μM) was applied after the ISO-induced changes had stabilized. A typical current trace and the relative current at +40 mV test pulse in each group are shown in *Figure 3C,D*. When cardiomyocytes were acutely stimulated with ISO, the I_{kr} tail currents only decreased to 0.80±0.02 upon PE addition. This result significantly differed from cardiomyocytes that were not acutely stimulated by ISO (0.58±0.04, P<0.05) (first and second columns of *Figure 3E*). These data suggested that the inhibitory effects of PE on I_{kr} can be attenuated by ISO.

Discussion

In the present study, we report that the β_1 and α_{1A}-AR systems modulate I_{kr}. The current reduction effects of ISO can be prevented by preactivation of α_1-adrenoceptors whereas the inhibitory effects of PE can be attenuated by preactivation of β-adrenoceptors. Signaling crosstalk between the α_{1A}- and β_1-adrenergic cascades might be involved in I_{kr} tail current

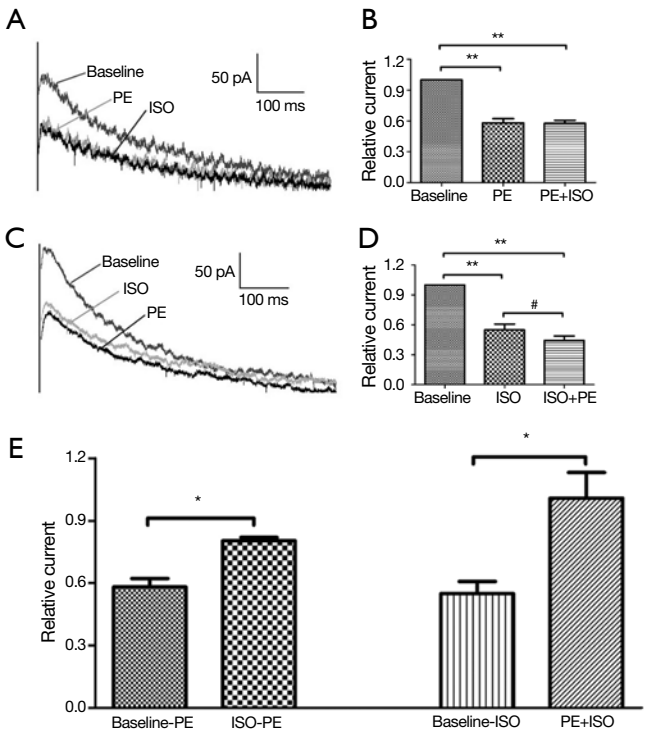

Figure 3 Interaction of α- and β-adrenoceptors on I_{kr}. (A) Representative current changes in the amplitude of peak I_{kr} tail current (test pulse at +40 mV) following exposure to PE and PE plus ISO; (B) the relative current at test pulse +40 mV in relative groups of *Figure 3A*; (C) representative current changes in the amplitude of peak I_{kr} tail current (test pulse at +40 mV) following exposure to ISO and ISO plus PE; (D) the relative current at test pulse +40 mV in relative groups of *Figure 3C*; (E) comparison of decreased I_{Kr} tail currents after application of different adrenergic agonists. Column baseline-PE represents the relative I_{Kr} tail current upon application of α_1-adrenergic agonist alone, column ISO-PE represents the α_1-AR activation-induced percentage of I_{Kr} after preactivation of β_1-AR, column baseline-ISO indicates the β_1-AR alone stimulation-induced inhibition percentage, and column PE-ISO shows the β_1-AR stimulation-induced inhibition percentage after pre-stimulation with α_1-AR (n=3; *P<0.05).

regulation in guinea pig ventricular myocytes.

ARs bind and are activated by the endogenous catecholamine hormones epinephrine and norepinephrine (NE). Epinephrine is primarily produced and released into circulation from the adrenal gland. However, NE is synthesized and released by sympathetic nerve terminals in the peripheral nervous system and brain. In the heart, the two main ARs are the β-ARs, which comprise roughly 90% of total cardiac ARs, and α_1-ARs, which account for approximately 10% (18). In this study, α_1-adrenergic activation reduced I_{kr} in guinea pig ventricular cardiomyocytes, which are similar results to those reported by Thomas *et al.* (19) and Wang *et al.* (12). At least three α_1-AR subtypes (α_{1A}, α_{1B}, α_{1D}) have been described using molecular and pharmacological techniques (20,21). The ventricular α1-adrenoceptor densities did not significantly differ between guinea pig and human (22). A previous study found that different adrenoceptor subtypes have different effects on I_{to} (23) and $I_{ca\text{-}L}$ (24). We found that α_1 adrenergic action on I_{kr} was via α_{1A}. Currently, there are no data regarding the effects of α_{1B} or α_{1D} on I_{kr}. Moreover, we also found that in addition to α_1, β-adrenergic activation also reduced I_{kr}, which is consistent with the study by Karle *et al.* (17). These results differ from the data of Heath and Terrar who reported that isoprenaline increased I_{kr} (16). This discrepancy could be related to ISO concentrations, different techniques inherent to whole-cell perforated patch clamp and switched electrode voltage clamp (SEVC), and/or different effects of β adreneoceptor subtypes on I_{kr}. The β_1 and β_2 adreneoceptor subtypes have different effects in regulating Ica-L (25) and cardiac function (26,27). Our study found that β-adrenoceptor action is mediated by the β_1-adrenoceptor subtype rather than the β_2-adrenoceptor subtype.

It is noteworthy that α_1-AR activation-induced inhibition of I_{kr} tail current in the presence of β-AR activation differs significantly from α_1-AR activation alone-induced inhibition of I_{kr} tail current. These data suggests that pre-activation of β-ARs suppresses the effect of α_1-AR activation on I_{kr} tail current, and pre-activation of α_1-ARs inhibits the effect of β-AR activation on I_{kr} tail current. Thus, pre-activation of one subtype adrenoceptor restrains the effect of another adrenoceptor subtype on I_{kr} tail current. That is, crosstalk exists in regulating I_{kr} current via acute adrenergic stimulation in physical circumstances. We propose that this is a protective regulatory mechanism against severe inhibition of I_{kr} tail current that occurs during excessive release of catecholamines in pathological circumstances.

Conclusions

I_{kr} in guinea pig cardiomyocyte can be regulated by both the α_1 adrenergic system through the α_{1A} subtype and the β adrenergic system through the β_1 subtype. The absence of an inhibitory effect on I_{kr} by ISO was noted in cells pretreated with PE. The PE effect on I_{kr} was also attenuated in cells

pretreated with ISO. Our results suggest a negative feedback loop intrinsic to norepinephrine stimulation in the heart and signaling crosstalk between α_{1A}- and β_1-adrenergic cascades, which might be involved in I_{kr} regulation in guinea pig ventricular myocytes. Signaling crosstalk may have a crucial role when plasma levels of both endogenous regulators are elevated.

Limitations

Our study found that crosstalk between α_{1A}-ARs and β_1-ARs in I_{kr} regulation exists. However, the precise adrenergic effects require further study to elucidate the molecular mechanisms that underlie the functional crosstalk as well as to identify putative intermediate proteins in the signal transduction pathways involved in modulation of I_{kr} current via adrenergic activation.

Acknowledgements

We thank Xiang-Jian Chen, Yang-Di, and Dao-Wu Wang for their assistance, and the Research Institute of Cardiovascular Disease of the First Affiliated Hospital of Nanjing Medical University.
Funding: This study was supported by the National Scientific Foundation of China (NSFC No. 81100123).
Disclosure: The authors declare no conflict of interest.

References

1. Sanguinetti MC, Tristani-Firouzi M. hERG potassium channels and cardiac arrhythmia. Nature 2006;440:463-9.
2. Keating MT, Sanguinetti MC. Molecular and cellular mechanisms of cardiac arrhythmias. Cell 2001;104:569-80.
3. Sanguinetti MC, Jiang C, Curran ME, et al. A mechanistic link between an inherited and an acquired cardiac arrhythmia: HERG encodes the IKr potassium channel. Cell 1995;81:299-307.
4. Tseng GN. I(Kr): the hERG channel. J Mol Cell Cardiol 2001;33:835-49.
5. Charpentier F, Mérot J, Loussouarn G, et al. Delayed rectifier K(+) currents and cardiac repolarization. J Mol Cell Cardiol 2010;48:37-44.
6. Spector PS, Curran ME, Keating MT, et al. Class III antiarrhythmic drugs block HERG, a human cardiac delayed rectifier K+ channel. Open-channel block by methanesulfonanilides. Circ Res 1996;78:499-503.
7. Busch AE, Eigenberger B, Jurkiewicz NK, et al. Blockade of HERG channels by the class III antiarrhythmic azimilide: mode of action. Br J Pharmacol 1998;123:23-30.
8. Kiehn J, Lacerda AE, Wible B, et al. Molecular physiology and pharmacology of HERG. Single-channel currents and block by dofetilide. Circulation 1996;94:2572-9.
9. van Noord C, Sturkenboom MC, Straus SM, et al. Non-cardiovascular drugs that inhibit hERG-encoded potassium channels and risk of sudden cardiac death. Heart 2011;97:215-20.
10. Vandenberg JI, Perry MD, Perrin MJ, et al. hERG K(+) channels: structure, function, and clinical significance. Physiol Rev 2012;92:1393-478.
11. Thomas D, Karle CA, Kiehn J. The cardiac hERG/IKr potassium channel as pharmacological target: structure, function, regulation, and clinical applications. Curr Pharm Des 2006;12:2271-83.
12. Wang S, Xu DJ, Cai JB, et al. Rapid component I(Kr) of cardiac delayed rectifier potassium currents in guinea-pig is inhibited by alpha(1)-adrenoreceptor activation via protein kinase A and protein kinase C-dependent pathways. Eur J Pharmacol 2009;608:1-6.
13. Tutor AS, Delpón E, Caballero R, et al. Association of 14-3-3 proteins to beta1-adrenergic receptors modulates Kv11.1 K+ channel activity in recombinant systems. Mol Biol Cell 2006;17:4666-74.
14. Wang H, Chen Y, Zhu H, et al. Increased response to β_2-adrenoreceptor stimulation augments inhibition of IKr in heart failure ventricular myocytes. PLoS One 2012;7:e46186.
15. Bian JS, Kagan A, McDonald TV. Molecular analysis of PIP2 regulation of HERG and IKr. Am J Physiol Heart Circ Physiol 2004;287:H2154-63.
16. Heath BM, Terrar DA. Protein kinase C enhances the rapidly activating delayed rectifier potassium current, IKr, through a reduction in C-type inactivation in guinea-pig ventricular myocytes. J Physiol 2000;522 Pt 3:391-402.
17. Karle CA, Zitron E, Zhang W, et al. Rapid component I(Kr) of the guinea-pig cardiac delayed rectifier K(+) current is inhibited by beta(1)-adrenoreceptor activation, via cAMP/protein kinase A-dependent pathways. Cardiovasc Res 2002;53:355-62.
18. Brodde OE, Michel MC. Adrenergic and muscarinic receptors in the human heart. Pharmacol Rev 1999;51:651-90.
19. Thomas D, Wu K, Wimmer AB, et al. Activation of cardiac human ether-a-go-go related gene potassium currents is regulated by alpha(1A)-adrenoceptors. J Mol Med (Berl) 2004;82:826-37.

20. Price DT, Lefkowitz RJ, Caron MG, et al. Localization of mRNA for three distinct alpha 1-adrenergic receptor subtypes in human tissues: implications for human alpha-adrenergic physiology. Mol Pharmacol 1994;45:171-5.
21. Jensen BC, Swigart PM, De Marco T, et al. {alpha}1-Adrenergic receptor subtypes in nonfailing and failing human myocardium. Circ Heart Fail 2009;2:654-63.
22. Steinfath M, Chen YY, Lavický J, et al. Cardiac alpha 1-adrenoceptor densities in different mammalian species. Br J Pharmacol 1992;107:185-8.
23. Martínez ML, Delgado C. Methoxamine inhibits transient outward potassium current through alpha1A-adrenoceptors in rat ventricular myocytes. J Cardiovasc Pharmacol 2000;35:212-8.
24. O-Uchi, Sasaki H, Morimoto S, et al. Interaction of alpha1-adrenoceptor subtypes with different G proteins induces opposite effects on cardiac L-type Ca2+ channel. Circ Res 2008;102:1378-88.
25. Nagykaldi Z, Kem D, Lazzara R, et al. Conditioning of beta(1)-adrenoceptor effect via beta(2)-subtype on L-type Ca(2+) current in canine ventricular myocytes. Am J Physiol Heart Circ Physiol 2000;279:H1329-37.
26. Devic E, Xiang Y, Gould D, et al. β-Adrenergic Receptor Subtype-Specific Signaling in Cardiac Myocytes from β1 and β2 Adrenoceptor Knockout Mice. Mol Pharmacol 2001;60:577-83.
27. Ecker PM, Lin CC, Powers J, et al. Effect of targeted deletions of beta1- and beta2-adrenergic-receptor subtypes on heart rate variability. Am J Physiol Heart Circ Physiol 2006;290:H192-9.

Cite this article as: Wang S, Min XY, Pang SS, Qian J, Xu D, Guo Y. Adrenergic regulation of the rapid component of delayed rectifier K+ currents in guinea pig cardiomyocytes. J Thorac Dis 2014;6(12):1778-1784. doi: 10.3978/j.issn.2072-1439.2014.12.27

Original Article

Epidemiological and viral genome characteristics of the first human H7N9 influenza infection in Guangdong Province, China

Zi-Feng Yang[1,2*], Jian-Feng He[3*], Xiao-Bo Li[4*], Wen-Da Guan[1,2], Chang-Wen Ke[3], Shi-Guan Wu[1,2], Si-Hua Pan[1,2], Run-Feng Li[1,2], Min Kang[3], Jie Wu[3], Jin-Yan Lin[3], Guo-Yun Ding[4], Ji-Cheng Huang[4], Wei-Qi Pan[1,2], Rong Zhou[1,2], Yong-Ping Lin[5], Rong-Chang Chen[1,2], Yi-Min Li[1,2], Ling Chen[1,2], Wen-Long Xiao[6], Yong-Hui Zhang[3], Nan-Shan Zhong[1,2]

[1]State Key Laboratory of Respiratory Disease (Guangzhou Medical University), [2]National Clinical Research Center for Respiratory Disease, The First Affiliated Hospital of Guangzhou Medical University, Guangzhou 510120, China; [3]Guangdong Center for Disease Control and Prevention, Guangzhou 511430, China; [4]Health quarantine (BSL-3) Lab, Guangdong Inspection and Quarantine Technology Center, Guangzhou 510623, China; [5]Clinical Laboratory, The First Affiliated Hospital of Guangzhou Medical University, Guangzhou 510120, China; [6]Huizhou Center for Disease Control and Prevention, Huizhou 516001, China

*These authors contributed equally to this work.

Correspondence to: Yong-Hui Zhang. Guangdong Center for Disease Control and Prevention, Qunxian Road, Guangzhou 511430, China. Email: zyh@cdcp.org.cn; Nan-Shan Zhong. State Key Laboratory of Respiratory Disease (Guangzhou Medical University), The First Affiliated Hospital of Guangzhou Medical University, Yanjiang Road, Guangzhou 510120, China. Email: nanshan@vip.163.com.

Background: The first H7N9 human case in south of China was confirmed in Guangdong Province on August 2013, outside of the typical influenza season. For investigating the H7N9 virus source and transmission in the local community, we analyze the epidemiology and genome features of the virus isolated from the first human infection detected in Guangdong Province.

Methods: The data including medical records, exposure history and time line of events for the H7N9 patient and close contacts was collected. Variation and genetic signatures of H7N9 virus in Guangdong was analyzed using ClustalW algorithm and comparison with mutations associated with changes in biological characteristics of the virus.

Results: The female patient had a history of poultry exposure, and she was transferred from a local primary hospital to an intensive care unit (ICU) upon deterioration. No additional cases were reported. Similar to previous infections with avian influenza A (H7N9) virus, the patient presented with both upper and lower respiratory tract symptoms. Respiratory failure progressed quickly, and the patient recovered 4 weeks after the onset of symptoms. Genome analysis of the virus indicated that the predicted antigen city and internal genes of the virus are similar to previously reported H7N9 viruses. The isolated virus is susceptible to neuraminidase (NA) inhibitors but resistant to adamantine. Although this virus contains some unique mutations that were only detected in avian or environment-origin avian influenza A (H7N9) viruses, it is still quite similar to other human H7N9 isolates.

Conclusions: The epidemiological features and genome of the first H7N9 virus in Guangdong Province are similar to other human H7N9 infections. This virus may have existed in the environment and live poultry locally; therefore, it is important to be alert of the risk of H7N9 re-emergence in China, including emergence outside the typical influenza season.

Keywords: Avian influenza virus; epidemiology; H7N9; viral genome

Submitted Feb 02, 2014. Accepted for publication Dec 05, 2014.
doi: 10.3978/j.issn.2072-1439.2014.12.09
View this article at: http://dx.doi.org/10.3978/j.issn.2072-1439.2014.12.09

Background

On 19 February 2013, the first avian influenza A (H7N9) virus was identified in humans, initiating an influenza outbreak in Eastern and Northern China in domestic birds and humans. As of 27 July, the case-fatality rate in 135 laboratory confirmed human cases was reported to be 32.6% (1). Phylogenetic analysis revealed that the gene segments of H7N9 virus stemmed from three reassortment events: the H7 gene segment are closest to hemagglutinin (HA) of the H7N3 of wild ducks, the six internal genes clustered with those of poultry H9N2 viruses of China (2), and the N9 gene segment shared the highest similarity with wild ducks in South Korea (3) and Baikal teal from Jiangsu Province in China (4). Because the poultry markets are possible locations for the emergence of new influenza viruses by mutations and/or reassortments (5), more monitoring of poultry markets has occurred recently. As a result, many control policies for prevention and response to H7N9 outbreaks have been reinforced, and surveillance has been increased to find people with symptoms early, even in provinces in China that have not had a human H7N9 case before, such as Guangdong Province.

To date, there have been three stages of the H7N9 epidemic in humans. The first stage consisted of sporadic isolations of virus in February and March, followed by an epidemic in April and May in Eastern and Northern China (6). The third stage is currently ongoing, with sporadic H7N9 virus isolations in China. Avian influenza A (H5N1) and seasonal influenza viruses have shown a seasonal pattern whereby human cases are much more common in winter and autumn than in summer. However, two H7N9 human avian influenza cases recently occurred in the summer; these cases have again attracted global concerns of H7N9 influenza. The first of these summer cases was a 61-year-old female from Hebei Province on July 27, 2013. The second case, from Guangdong Province, where had no reported human H7N9 cases prior to this isolation, was a previously healthy 51-year-old female worker with a long history of contact with live poultry.

Here, we analyze the epidemiology and genome features of the first human infected H7N9 virus in Southern China (Guangdong Province), to investigate the H7N9 virus source and transmission in the local community.

Methods

Epidemiological data collection

Collection of data from the H7N9 patient and her close contacts was required by the National Health and Family Planning Commission and conducted by Guangdong Center for Disease Control and Prevention; it was exempt from ethical review by an institutional review board. The information collected included medical records, exposure history and time line of events for the H7N9 patient and close contacts. All close contacts, as well as the environment in which the patient may have been exposed, were sampled to investigate transmission of H7N9 virus.

RNA extraction, genome sequencing, and phylogenetic analysis

The full genome of the virus was amplified by 12 primer sets (designed by our lab basing on the H7N9 sequences published on Genbank) using OneStep RT-PCR Kit (Qiagen, Hilden, Germany) for sequencing. PCR products were gel purified using QIAquick Gel Extraction Kit (Qiagen, Hilden, Germany) and sequenced by ABI 3130xl automatic DNA analyzer (Life Technologies, Carlsbad, USA). The full genome of the virus was deposited into the GenBank database on 13 September 2013 (GenBank: KF662943-KF66295). Multiple alignments of HA and neuraminidase (NA) genes were conducted using the ClustalW algorithm. Phylogenetic trees were constructed by the maximum likelihood method with 1,000 bootstrap replications in ClustalW. Accession numbers for reference sequences used in the phylogenetic analysis are listed in *Table S1*.

Genetic signatures of A/Guangdong/1/2013(H7N9) (H7N9 Guangdong strain)

To identify the genetic signatures of virus, the full genome of the H7N9 Guangdong strain was compared with sequences of H7N9 viruses previously isolated from humans, birds, and the environment. In addition, key amino acid sequences that have been previously associated with viral characteristics were identified in the H7N9 Guangdong strain.

Results

Epidemiological features

The seasonal distribution of influenza viruses in Guangdong province in 2012-2013 is shown in *Figure 1*. Before epidemic week (EW) 8 the influenza activity was

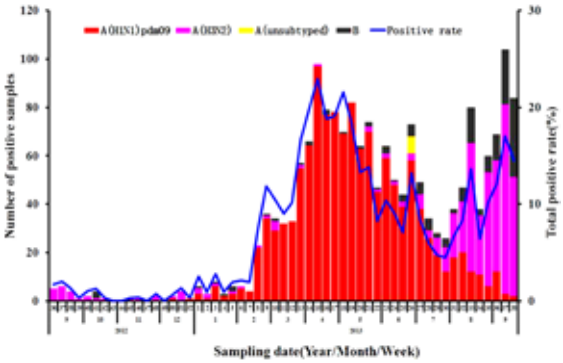

Figure 1 Influenza virus activity in Guangdong Province from September 2012 to September 2013.

Figure 2 Geographic distribution of H7N9 viruses identified in poultry and humans in Guangdong Province. Blue circles denote identification of H7N9 virus in poultry. The red star represents the confirmed human case of H7N9 virus infection in Huizhou.

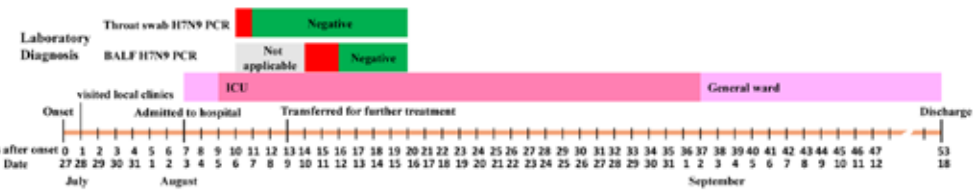

Figure 3 Timeline of disease and treatment of first human infected in Guangdong Province. Positive results of PCR were showed in red.

low. However, after EW8, A (H1N1) pdm09 dramatically increased and predominated until EW30. Prior to August 2013, influenza B and H3N2 viruses were rarely detected, but both became more common in August, with H3N2 predominating. It is particularly intriguing that at EW17 and EW20 two samples from live poultry were found positive for avian influenza A (H7N9) virus in Dongguan and Zengcheng cities both of which located in Guangdong Province (7,8). Despite the fact that human H7N9 cases were distributed across most regions of Eastern or Northern China before July, the most recent animal and human cases detected were concentrated in the cities of the Pearl River delta in Southern China (*Figure 2*).

The H7N9 patient from Guangdong province did not have any recent travel history and lived in a two-story building, of which the ground floor for was used for selling poultry and the second floor for living. This building was located in a wet poultry market of Boluo (a county in Huizhou city). Because of H7N9 outbreaks reported in other regions in China, Guangdong performed emergency surveillance for avian influenza A (H7N9) in wet poultry markets throughout all 21 prefectures from 15 April to 31 May 2013. A total of 3,235 samples were collected from wet market environments, including 120 samples from Huizhou. No sample was found to be H7N9 positive in this surveillance. We tested 65 throat swabs and 125 blood samples from the case's close contacts, including her husbands, son, and daughter, but none tested positive for the A (H7N9) virus, suggesting that this patient did not spread the virus to other humans.

At the onset of disease, the patient developed fever, headache and chills. After receiving medical care in a private clinic for three days without improvement, she visited an outpatient department of a county hospital on day 4, and had watery stools and fatigue on day 6. She was hospitalized at Huizhou central hospital on day 7, her condition became more severe, and she was transferred to the intensive care unit (ICU) because of an infection in the right lung on chest radiograph on day 9. Although an influenza test was negative on day 9, the patient became critically ill and was started on a ventilator. A sample from the patient on day 10 was positive for avian influenza A (H7N9) virus, detected by Huizhou Centers for Disease Control and Prevention (CDC) and confirmed by China CDC. On day 13, the patient was transferred to the Guangzhou Institute of Respiratory Diseases for further treatment. The patient recovered and was discharged uneventfully on day 53 (*Figure 3*).

Table 1 The nucleotide percent identities between A/Guangdong/1/2013, its closest relative and the first three H7N9 human isolates

A/Guangdong/1/2013	Identity (closest relative)	A/Shanghai/1/2013	A/Shanghai/2/2013	A/Anhui/1/2013
PA	99 [A/chicken/Hong Kong/TC18/2011(H9N2)]	99	99	99
PB1	99 [A/duck/QuanhNinh/21/2013(H5N1)]	97	97	97
PB2	99 [A/chicken/Jiangsu/S002/2013(H7N9)]	96	96	96
HA	99 [A/environment/Hangzhou/34/2013(H7N9)]	99	99	99
NP	99 [A/chicken/Hong Kong/TC8/2012(H9N2)]	97	97	97
NA	100 [A/environment/Hangzhou/34/2013(H7N9), A/Hangzhou/2/2013(H7N9)]	99	99	99
M	100 [A/Shanghai/02/2013(H7N9)]	99	100	100
NS	99 [A/chicken/Jiangsu/Q3/2010(H9N2)]	97	97	97

Phylogenetic analysis of A/Guangdong/1/2013 (H7N9)

An H7N9 virus, named A/Guangdong/1/2013 (H7N9), was isolated from day 14 sample (BALF) of the patient using 9-11-day-old embrocated chicken eggs in a BSL-3 laboratory. Multiple sequence alignment showed that the Guangdong strain was 96-100% identical to the first three reported avian influenza A (H7N9) viruses in all eight genes (*Table 1*), including 99% identical in the HA and NA genes. Blast analysis of the viral genome showed that each gene was from avian origin, and no evidence of genetic reassortment with human viruses was found (*Table 1*). Phylogenetic analysis suggested that A/Guangdong/1/2013 (H7N9) has similar antigen city to previous avian influenza A (H7N9) viruses reported in China (*Figure 4*). The HA gene shared the highest identity with A/environment/Hangzhou/34/2013 (H7N9), while the NA gene was most closely related to A/environment/Hangzhou/34/2013 (H7N9) and A/Hangzhou/2/2013 (H7N9) (*Table 1*). The HA and NA genes were 99.6% and 99.9% identical, respectively, with genes of H7N9 viruses detected in the local environment.

Genetic signatures of A/Guangdong/1/2013 (H7N9)

The genome signatures of Guangdong strain were identified, including T160A, V186G, and Q266L in HA, N30D in M1, and E627K in PB2 (*Table 2*). These mutations were observed in most of the avian influenza A (H7N9) viruses isolated from humans in the epidemic of 2013, and appear to have allowed the virus to adapt to humans by increasing binding to the human receptor as well as increasing virus virulence. Although the genome of A/Guangdong/1/2013 (H7N9) was similar to previously isolated H7N9 viruses in China, some unique mutations existed in the PA, PB1, PB2, HA and NS1 genes when compared with other H7N9 viral genes. However, there is a lack of published evidence that these mutations affect the biological properties of H7N9 viruses. Interestingly, 191E in PB2, 65K in HA and 27L, 111V, and 212P in NS1 were observed in A/Guangdong/1/2013 (H7N9) and the viruses from birds and the environment, but were not seen in other H7N9 viruses isolated from humans. This finding implies that the Guangdong H7N9 patient may have been infected from birds or the environment, due to her working in a poultry market.

Discussion

In the 20th century, three of four influenza pandemics were thought to have originated in Southern China (23,24). Guangdong Province has often been the focus of attention in influenza epidemiology. In this study, we analyzed the epidemiology and genetic signatures of the H7N9 virus from the first human H7N9 case in Guangdong Province, and compared the virus to those isolated from birds, the environment, and humans in Eastern and Northern China.

Live poultry markets bring together bird and poultry species from different sources in a concentrated environment, providing an environment for reassortment among avian influenza viruses of different subtypes (25,26). Most human H7N9 infections were diagnosed in poultry workers or visitors to poultry markets, implying that the market environment plays a critical role in the epidemic (27). In this study, the patient who is a poultry worker has been involved in this field for over 10 years. That supports the notion that avian influenza A (H7N9) virus-infected poultry are a transmission source.

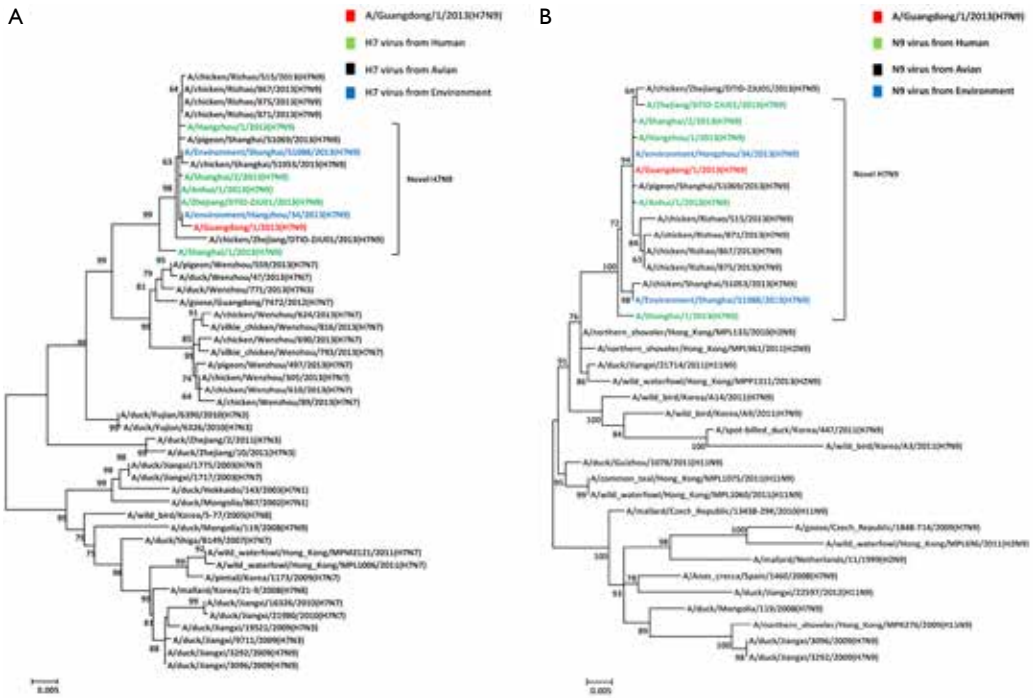

Figure 4 Phylogenetic analysis of antigens in H7N9 virus, (A) hemagglutinin; (B) neuraminidase.

Table 2 Mutations of A/Guangdong/1/2013 compared with H7N9 viruses previously reported in 2013

Viral gene	Amino acid position	A/ Guangdong/1/2013	H7N9 from patients [2013]	H7N9 from birds [2013]	H7N9 from the environment [2013]	Biological feature altered by mutations
PA	343	T	A	A	A	Unknown
	519	T	N	N	N	Unknown
PB1	171	V	M	M	M	Unknown
	368	V	V	V	V	I368V enables droplet transmission in ferrets (9)
	374	V	A	A/T	A	Unknown
	397	M	I	I	I	Unknown
	694	S	N	N	N	Unknown
PB2	89	V	V	V	V	L89V increases polymerase activity (9)
	139	I	V	V	V	Unknown
	191	E	K	K/E/T	K/E	Unknown
	570	I	M	M/I	M/I	M570I may affect RNA cap-binding (10,11)
	627	K	K/E	E	E	E627K increases adaptation to mammals (12)
	676	V	M	M	M	Unknown
	701	D	D/N	D	D	D701N increases adaptation to mammals (9)

Table 2 (*continued*)

Table 2 (*continued*)

Viral gene	Amino acid position	A/ Guangdong/1/2013	H7N9 from patients [2013]	H7N9 from birds [2013]	H7N9 from the environment [2013]	Biological feature altered by mutations
HA	65	K	R/M	R/M/K	R/M/K	Unknown
	138a	A	A/S	A	A	S138A increases virus binding to α-2,6-linked sialic acid receptor (human receptor) (13)
	140	A	T	T	T	Unknown
	160[a]	A	A	A	A	T160A Increases binding to α-2,6-linked sialic acid receptor (human receptor) (14)
	186[a]	V	V/G	V	V	G186V Increases binding to α-2,6-linked sialic acid receptor (human receptor) (15)
	226[a]	L	Q/L	Q/L	Q/L	Q226L increases binding to α-2,6-linked sialic acid receptor (human receptor) (16)
	PEIPKGR*GLF	PEIPKGR*GLF	PEIPKGR*GLF	PEIPKGR*GLF	PEIPKGR*GLF	Cleavage site (9)
NA	294	R	R/K	R	R	R294K is known to confer resistance to oseltamivir and zanamivir (17)
	69-73[b]	deleted	deleted	deleted	deleted	Stalk deletion increases virulence in mammals (18)
M1	30	D	D	D	D	N30D increases virulence in mice (19)
	215	A	A	A	A	T215A increases virulence in mice (19)
M2	31	N	N	N	N	S31N is known to confer resistance to amantadine and rimantadine (20)
NS1	27	L	M/K	M/L/K	M/K	Unknown
	42	S	S	S	S	P42S increases virulence in mice (21)
	80	T	S	S	S	Unknown
	111	V	I	I/V	I/V	Unknown
	152	D	E	E	G	Unknown
	212	P	S	S/Y	S/P	Unknown
	218-230	Deleted	Deleted	Deleted	Deleted	Lack of PDZ-binding motif decrease virulence in mice (22)

[a], H3 numbering; [b], N9 numbering.

Many studies based on retrospective investigations have stated that poultry market exposure is a key risk factor for H7N9 infection. Notably, before the isolation of A/Guangdong/1/2013 (H7N9), avian influenza A (H7N9) viruses were isolated from chickens in live poultry markets of the nearby cities of Dongguan and Zengcheng in Guangdong Province. This finding provides chronological evidence for poultry markets as a source of H7N9 infection. Therefore, it is thought that those who have close contact to live poultry in Southern China have a high risk of infection with avian influenza A (H7N9) virus. Vigilance is needed to continue surveillance of live poultry markets and those who frequent them.

Guangdong Province, located in a subtropical area, has multiple peaks of seasonal influenza activity annually, and the highest peak tends to occur in warmer months (June and July) (28). The activity of avian influenza A (H5N1) is similar to that of seasonal influenza, in that in tropical areas of Asia, avian influenza A (H5N1) has been more common during the warmer months (29). Therefore, this human H7N9 case in Guangdong province occurring in summer season followed the expected seasonality. However, no further positive detection of avian influenza A (H7N9) virus in local live poultry markets and no additional human case has been identified within one month after this isolation in Guangdong or adjacent southern provinces in China. Hence, it does not appear that H7N9 virus is currently moving south.

The avian influenza A (H7N9) virus we identified from the first human case in Guangdong was closely related to A/environment/Hangzhou/34/2013(H7N9) in its surface glycoprotein's (HA and NA), and also has internal genes similar to other N7N9 viruses detected from birds and the environment. We compared the sequences of A/Guangdong/1/2013 (H7N9) with those of previously reported avian influenza A (H7N9) viruses. In the HA protein, A/Guangdong/1/2013 (H7N9) had a Q226L substitution, which increases virus binding to the human receptor; other previous avian influenza A (H7N9) viruses isolated from humans had the same mutation (12,30). In the PB2 protein, A/Guangdong/1/2013 (H7N9) had an E627K mutation; this change is thought to increase the virulence of avian viruses in mice. Avian influenza A (H7N9) viruses from birds and the environment typically have 627E. Interestingly, four previously reported human isolates of H7N9 viruses also had 627E in PB2, while two of them had D701N, which is thought to play a key role in viral adaption to mammals and take the place of the E627K mutation (31). This implies that there is more than one possible PB2 mutation for H7N9 viruses to adapt to mammalian hosts. However, it is worth noting that 191E in PB1, 570I in PB2, 65K in HA, and 27L, 111V, and 212P in NS1 were only observed in A/Guangdong/1/2013 (H7N9) and in H7N9 virus isolates from birds and the environment. Among these mutations, M570I is located in the binding region of PB2 and is reported to possibly alter the secondary structure from a strand to a helix, and may affect RNA cap-binding (10,11). Several unique substitutions were observed in A/Guangdong/1/2013 (H7N9) compared with other avian influenza A (H7N9) viruses, including T343A in PA, which also has been found in A (H1N1) pdm09 viruses (32,33). Whereas effects of them on the fitness of viruses need to be studied further due to unknown biological function. Based on the findings above, to study the virus's virulence more accurately and objectively, it is important that the sequence and virological analyses are considered in combination with the epidemiological findings.

Conclusions

Overall, the epidemiology and genome characteristics of A/Guangdong/1/2013 (H7N9) seemed to be similar with previously reported H7N9 viruses isolated from humans. However, several unique substitutions never reported before need to be investigated, and may already exist in the environment and live poultry locally. Although their impact on the pathogenesis of viruses is unclear, it is necessary to emphasize that agriculture and forestry departments should continue monitoring and sharing animal surveillance information, which can facilitate early warning and intervention.

Acknowledgements

This study was financially supported by Municipal Science and Technology Bureau Foundation of Guangzhou, the Science and Technology Planning Project of Guangdong Province, China (Guangdong–Macau Joint Research Centre for New Drug Discovery Against Respiratory Pathogens, Grant No. 2010B091000018), Emergency Response Project of Ministry of Science and Technology of China (Grant No. KJYJ-2013-01-05), National Science and Technology Major Project of the Ministry of Science and Technology of China (Grant No. 2014ZX10004006), and the National Key Technology R&D Program of the 12th National Five-year Development Plan of China (Grant No. 2012BAI05B01).
Authors' contributions: Nan-shan Zhong and Yong-hui

Zhang designed the study. Shi-guan Wu, Xiao-bo Li, Guo-yun Ding and Ji-cheng Huang conducted H7N9 nucleic acid detection and virus isolation in P3 lab. Wen-da Guan and Si-hua Pan sequenced the full genome of virus, did phylogenetic analysis. Run-feng Li, Min Kang, Jie Wu and Yong-ping Li did analysis of genetic features. Wei-qi Pan, Rong Zhou, Ling Chen, Rong-chang Chen, Yi-min Li collected clinical data. Jianfeng He, Chang-wen Ke, Jin-yan Lin and Wen-long Xiao collected and analyzed epidemiological data. Zi-feng Yang wrote the first draft, and all authors contributed to review and revision and have seen and approved the final version.

Disclosure: The authors declare no conflict of interest.

References

1. World Health Organization. Human infection with avian influenza A(H7N9) virus – update. Available online: http://www.who.int/csr/don/2013_08_11/en/index.html
2. Gao R, Cao B, Hu Y, et al. Human infection with a novel avian-origin influenza A (H7N9) virus. N Engl J Med 2013;368:1888-97.
3. Liu D, Shi W, Shi Y, et al. Origin and diversity of novel avian influenza A H7N9 viruses causing human infection: phylogenetic, structural, and coalescent analyses. Lancet 2013;381:1926-32.
4. Xiong C, Zhang Z, Jiang Q, et al. Evolutionary characteristics of A/Hangzhou/1/2013 and source of avian influenza virus H7N9 subtype in China. Clin Infect Dis 2013;57:622-4.
5. Lai KY, Wing YNG, Wong KF, et al. Human H7N9 avian influenza virus infection: a review and pandemic risk assessment. Emerging Microbes & Infections 2013;2:e48.
6. Li Q, Zhou L, Zhou M, et al. Epidemiology of Human Infections with Avian Influenza A(H7N9) Virus in China. N Engl J Med 2014;370:520-32.
7. Ministry of Agriculture of China. Avian influenza A(H7N9) virus–update 2013-05-05. Available online: http://www.moa.gov.cn/zwllm/zwdt/201305/t20130505_3450918.htm
8. Ministry of Agriculture of China. Avian influenza A(H7N9) virus–update 2013-05-20. Available online: http://www.moa.gov.cn/zwllm/zwdt/201305/t20130520_3467279.htm
9. To KK, Chan JF, Chen H, et al. The emergence of influenza A H7N9 in human beings 16 years after influenza A H5N1: a tale of two cities. Lancet Infect Dis 2013;13:809-21.
10. Honda A, Mizumoto K, Ishihama A. Two separate sequences of PB2 subunit constitute the RNA cap-binding site of influenza virus RNA polymerase. Genes Cells 1999;4:475-85.
11. Danishuddin, Khan AU. Analysis of PB2 protein from H9N2 and H5N1 avian flu virus. Bioinformation 2008;3:41-6.
12. Hatta M, Gao P, Halfmann P, et al. Molecular basis for high virulence of Hong Kong H5N1 influenza A viruses. Science 2001;293:1840-2.
13. Nidom CA, Takano R, Yamada S, et al. Influenza A (H5N1) viruses from pigs, Indonesia. Emerg Infect Dis 2010;16:1515-23.
14. Wang W, Lu B, Zhou H, et al. Glycosylation at 158N of the hemagglutinin protein and receptor binding specificity synergistically affect the antigenicity and immunogenicity of a live attenuated H5N1 A/Vietnam/1203/2004 vaccine virus in ferrets. J Virol 2010;84:6570-7.
15. Yang H, Chen LM, Carney PJ, et al. Structures of receptor complexes of a North American H7N2 influenza hemagglutinin with a loop deletion in the receptor binding site. PLoS Pathog 2010;6:e1001081.
16. Srinivasan K, Raman R, Jayaraman A, et al. Quantitative description of glycan-receptor binding of influenza A virus H7 hemagglutinin. PLoS One 2013;8:e49597.
17. McKimm-Breschkin JL, Sahasrabudhe A, Blick TJ, et al. Mutations in a conserved residue in the influenza virus neuraminidase active site decreases sensitivity to Neu5Ac2en-derived inhibitors. J Virol 1998;72:2456-62.
18. Matsuoka Y, Swayne DE, Thomas C, et al. Neuraminidase stalk length and additional glycosylation of the hemagglutinin influence the virulence of influenza H5N1 viruses for mice. J Virol 2009;83:4704-8.
19. Fan S, Deng G, Song J, et al. Two amino acid residues in the matrix protein M1 contribute to the virulence difference of H5N1 avian influenza viruses in mice. Virology 2009;384:28-32.
20. Hay AJ, Wolstenholme AJ, Skehel JJ, et al. The molecular basis of the specific anti-influenza action of amantadine. EMBO J 1985;4:3021-4.
21. Jiao P, Tian G, Li Y, et al. A single-amino-acid substitution in the NS1 protein changes the pathogenicity of H5N1 avian influenza viruses in mice. J Virol 2008;82:1146-54.
22. Jackson D, Hossain MJ, Hickman D,et al. A new influenza virus virulence determinant: the NS1 protein four C-terminal residues modulate pathogenicity. Proc Natl Acad Sci U S A 2008;105:4381-6.
23. Shortridge KF, Stuart-Harris CH. An influenza epicentre? Lancet 1982;2:812-3.
24. Neumann G, Noda T, Kawaoka Y. Emergence and

pandemic potential of swine-origin H1N1 influenza virus. Nature 2009;459:931-9.
25. Correa P, Haenszel W, Cuello C, et al. Gastric precancerous process in a high risk population: cross-sectional studies. Cancer Res 1990;50:4731-6.
26. Lam TT, Wang J, Shen Y, et al. The genesis and source of the H7N9 influenza viruses causing human infections in China. Nature 2013;502:241-4.
27. Han J, Jin M, Zhang P, et al. Epidemiological link between exposure to poultry and all influenza A(H7N9) confirmed cases in Huzhou city, China, March to May 2013.Euro Surveill 2013;18. pii: 20481.
28. Deng A, He J, Kang M. Epidemiologic characteristics of influenza in Guangdong Province, 2005–2007. South China J Prev Med 2008;34:14-7.
29. Webster RG, Govorkova EA. H5N1 influenza--continuing evolution and spread. N Engl J Med 2006;355:2174-7.
30. Li J, Yu X, Pu X, et al. Environmental connections of novel avian-origin H7N9 influenza virus infection and virus adaptation to the human. Sci China Life Sci 2013;56:485-92.
31. de Jong MD, Simmons CP, Thanh TT, et al. Fatal outcome of human influenza A (H5N1) is associated with high viral load and hypercytokinemia. Nat Med 2006;12:1203-7.
32. Yang JR, Huang YP, Chang FY, et al. New variants and age shift to high fatality groups contribute to severe successive waves in the 2009 influenza pandemic in Taiwan. PLoS One 2011;6:e28288.
33. Xu L, Bao L, Zhou J, et al. Genomic polymorphism of the pandemic A (H1N1) influenza viruses correlates with viral replication, virulence, and pathogenicity in vitro and in vivo. PLoS One 2011;6:e20698.

Cite this article as: Yang ZF, He JF, Li XB, Guan WD, Ke CW, Wu SG, Pan SH, Li RF, Kang M, Wu J, Lin JY, Ding GY, Huang JC, Pan WQ, Zhou R, Lin YP, Chen RC, Li YM, Chen L, Xiao WL, Zhang YH, Zhong NS. Epidemiological and viral genome characteristics of the first human H7N9 influenza infection in Guangdong Province, China. J Thorac Dis 2014;6(12):1785-1793. doi: 10.3978/j.issn.2072-1439.2014.12.09

Supplement

Table S1 Accession numbers of sequences used in phylogenetic analysis

Hemagglutinin (HA)
KF259019.1; KF259013.1; KF259010.1; KF259033.1; KF259024.1; KF259022.1; KF259041.1; KF259036.1; KF259015.1; KF259040.1; KF259009.1; KF258995.1; KF258994.1; JQ906573.1; JQ906574.1; KF258981.1; KF258984.1; KF258971.1; KF258968.1; KF258998.1; KF258996.1; KF258992.1; KF258951.1; JX444843.1; JN244229.1; KF259006.1; KF259007.1; AB481212.1; AB473543.1; AB269694.2; AB558257.1; KF258958.1; KF001519.1; JX444827; EPI439486; EPI439502; EPI439507; CY147124.1; KC853766.1; CY147172.1; KC885956.1; KC899669.1; CY146956.1; KF259044.1; KF259042.1; KF259045.1; KF259043.1; KF259043.1
Neuraminidase (NA)
KF259720.1; KF259688.1; AB481213.1; KF259728.1; KF259698.1; KF259701.1; KF259695.1; JN244224.1; JN244223.2; JN244225.1; JN244222.1; KF259727.1; KF259725.1; KF259726.1; KF259715.1; KF259703.1; KF259704.1; JF789604.1; HQ244417.1; KF001520.1; CY122246.1; HQ244409.1; EPI439487; EPI439500; EPI439509; CY146958.1; KF259732.1; KF259730.1; KF259733.1; KF259731.1; KC899671.1; KC885958.1; KC853765.1; CY147174.1; CY147126.1

Original Article

Sodium tanshinone IIA silate as an add-on therapy in patients with unstable angina pectoris

Haiyan Zhang, Mingzhi Long, Zhiwen Wu, Xu Han, Yichao Yu

Department of Cardiology, The Second Affiliated Hospital of Nanjing Medical University, Nanjing 210011, China

Correspondence to: Professor Mingzhi Long. Department of Cardiology, The Second Affiliated Hospital of Nanjing Medical University, Nanjing 210011, China. Email: longmingzhi88@126.com.

Objective: To investigate whether sodium tanshinone IIA silate (STS) as an add-on therapy to conventional treatment may provide additional benefits for patients with unstable angina pectoris (UAP) and is associated with changes in profiles of serum inflammatory factors.

Methods: Eighty patients diagnosed with UAP were randomly divided into two groups for the 2-week treatment. The control group received conventional therapy, while the treatment group was given intravenous STS (0.06 mg in 250 mL, once daily) as an add-on therapy to the conventional medications. The therapeutic efficacy and changes in serum levels of several inflammatory cytokines, including monocyte chemotactic protein 1 (MCP-1), tumor necrosis factor alpha (TNF-α), peroxisome proliferator-activated receptor (PPAR-γ), and high-sensitivity C-reactive protein (hs-CRP) from baseline were determined and compared between the two group.

Results: The clinical symptoms of all patients in both groups were improved after treatment. The overall rate of effectiveness was 97.5% in the treatment group *vs*. 80.0% in the control group. Serum levels of MCP-1, TNF-α, and hs-CRP levels were significantly reduced in both groups ($P<0.01$), whereas the reduction was greater in patients receiving additional STS ($P<0.05$). PPAR-γ was significantly elevated in both groups ($P<0.01$).

Conclusions: STS in combination with conventional treatment may be associated with better outcomes in patients with UAP.

Keywords: Unstable angina pectoris (UAP); sodium tanshinone IIA silate (STS); monocyte chemotactic protein 1 (MCP-1); tumor necrosis factor alpha (TNF-α); peroxisome proliferator-activated receptor (PPAR-γ); high-sensitivity C-reactive protein (hs-CRP)

Submitted Oct 20, 2014. Accepted for publication Dec 11, 2014.

doi: 10.3978/j.issn.2072-1439.2014.12.37

View this article at: http://dx.doi.org/10.3978/j.issn.2072-1439.2014.12.37

Introduction

Unstable angina pectoris (UAP) as a subclass of acute coronary syndrome (ACS), is one of important causes of death in cardiovascular diseases (1-3). A common occurrence in ACS patients may be the cardiac instability and rupture of atherosclerotic plaques (4,5). Several studies have demonstrated the involvement of inflammatory response in these events and the subsequent thrombus formation (6-9).

Sodium tanshinone IIA silate (STS), a tanshinone IIA (Tan IIA) derivative, is an active, lipid-soluble component isolated from *Salvia miltiorrhiza* (10) which has been shown to improve blood circulation, dilate coronary arteries, reduce heart rate, increase myocardial contractility, and relieve hypoxia-induced myocardial disorders (11,12). STS exhibits a range of favorable cardiovascular actions like anticoagulation, tissue repair, and blood lipid-lowering (13,14). In addition, studies also suggested the role of STS in modulating inflammatory response associated with the process of myocardial infarction (MI), endothelium injury, atherosclerosis, and cardiovascular hypertrophy (2-5,15). However, so far the data remain limited regarding the

profiles of inflammatory factors in ACS patients receiving STS. We hypothesized that STS could relieve inflammation response and thus improve the clinical efficacy in patients with UAP.

This study was conducted to investigate whether STS as an add-on treatment to conventional treatment may provide additional benefits for UAP patients and is associated with changes in profiles of serum inflammatory factors, such as monocyte chemotactic protein 1 (MCP-1), tumor necrosis factor alpha (TNF-α), peroxisome proliferator-activated receptor (PPAR-γ), high-sensitivity C-reactive protein (hs-CRP), thereby improving the clinical curative effect in this subset of patients.

Patients and methods

Study population

Between August 2012 and April 2014, a cohort of consecutive patients with UAP hospitalized at Department of Cardiology, The Second Affiliated Hospital of Nanjing Medical University, were included in this study. The diagnosis of UAP was based on conventional coronary angiography or computed tomographic angiography, following the diagnostic criteria jointly established by American Heart Association/American College of Cardiology (ACCF/AHA) (16). Exclusion criteria were as follows: (I) a history of cerebral hemorrhage or acute cerebral infarction in the previous 3 months; (II) a history of surgery and trauma in the previous 6 months; (III) severe left ventricular dysfunction (EF <30%); (IV) severe hepatic and renal dysfunctions; (V) deep vein thrombosis of the lower extremity or pulmonary embolism; and (VI) signs of acute or chronic infections. The patients were randomized into the treatment group and the control group based on a computer-generated program. Baseline characteristics of these patients, including blood pressure, blood glucose, serum lipids, smoking history, co-morbidities, and other general demographics were recorded. This study was approved by the Ethics Committee of The Second Affiliated Hospital of Nanjing Medical University. All patients who participated in the study gave informed consent.

Treatments

After admission, all patients were given conventional treatment, which included oxygen inhalation, bed rest, ECG monitoring and oral aspirin or clopidogrel, as well as administration of angiotensin converting enzyme inhibitors (ACEI) or angiotensin receptor blockers (ARB), lipid-lowering agents, β-blockers, and calcium ion antagonists, according to patients' conditions. The treatment group was given additional intravenous STS (0.06 mg in 250 mL normal saline, once daily). The duration of treatment was 2 weeks. Throughout the study, all patients were allowed to take oral nitroglycerin for relieving agina attacks as needed. Blood and urine samples were analyzed, and liver and kidney function, electrocardiogram (ECG), dynamic ECG, fasting blood glucose, blood lipids were measured at baseline and at the end of the 2-week treatment. The clinical events (such as ST segment changes), the frequency and duration of angina pectoris attacks, and the dosage of nitroglycerin were also recorded. Adverse reactions related to use of STS were observed and noted, if any.

Measurements of blood sample

Fasting blood samples (3 mL) were collected in anticoagulant tubes from both groups of patients at baseline and after 2 weeks of treatments. The samples were centrifuged at 3,000 r/min for 15 min, allowed to sit for 3 h, and then the serum was isolated and stored at –70 ℃. Serum levels of MCP-1, TNF-α, and PPAR-γ were measured by enzyme-linked immunosorbent (ELISA), according to the manufacturer's instructions (R&D Systems, Minneapolis, USA). Serum hs-CRP was detected by using the immune turbidity method (Orion Diagnostica, Uusimaa, Finland).

Evaluation of therapeutic efficacy

At the end of 2-week treatment, we evaluated the therapeutic efficacy in all patients, which was categorized as: (I) significantly effective—no angina attacks or up to 80% reduction in the duration of angina attacks; ST segment returned to normal or nearly normal; >80% reduction in the total time of myocardial ischemia as indicated by dynamic ECG; (II) effective—50% to 80% reduction in the frequency or duration of angina attacks; ST depression reduced by more than 0.1 mV; 50% to 80% reduction in the total time of myocardial ischemia; and (III) ineffective—less than 50% reduction in the frequency or duration of angina attack; ST depression did not obviously improved; <50% reduction in total time of myocardial ischemia on ECG.

Table 1 Patient demography and clinical characteristics at baseline

Variables	Control group	Treatment group	P value
Baseline data			
Number of patients	40	40	
Age (year)	66.3±9.2	63.5±12.3	0.736
Sex (M/F)	25/15	22/18	0.431
SBP (mmHg)	137.0±18.6	132.3±20.5	0.654
DBP (mmHg)	76.7±12.0	79.8±16.9	0.476
FBS (mmol/L)	5.8±1.70	6.01±2.7	0.806
Lipid profile			
TG (mmol/L)	1.53±1.2	1.91±0.3	0.734
TC (mmol/L)	3.96±1.02	3.96±0.60	0.996
HDL (mmol/L)	1.02±0.23	0.97±0.30	0.630
LDL (mmol/L)	2.31±0.86	2.42±0.56	0.718
Risk factors			
Cigarette smoking, %	17.5	22.5	0.793
Hypertension, %	57.5	82.5	0.202
Diabetes mellitus, %	15.0	17.5	0.845
Hyperlipemia, %	52.5	57.5	0.791
Medical treatment			
Statin, %	85.0	87.5	0.891
CCB, %	32.5	37.5	0.634
Beta-blocker, %	37.5	67.5	0.116
Aspirin, %	60.0	61.5	0.839
Clopidogrel, %	50.0	57.5	0.420
ACEI, %	25.0	22.5	0.901
ARB, %	17.5	17.5	>0.99

SBP, systolic blood pressure; DBP, diastolic blood pressure; FBS, fasting blood sugar; TG, triglycerides; TC, total cholesterol; HDL, high-density lipids; LDL, low-density lipids; CCB, calcium channel blockers; ACEI, angiotensin converting enzyme inhibitor; ARB, angiotensin receptor blocker.

Table 2 The nitroglycerin dosage in the patients before and after treatment (tablets/week)

Group	N	Before treatment	After treatment
Control group	40	7.7±1.1	3.6±2.5*
Treatment group	40	7.8±1.3	1.9±1.8*#

*, *vs*. before treatment P<0.01; #, *vs*. controls P<0.01.

Statistical analysis

Statistical analyses were performed by using the Statistical Package for the Social Sciences Ver. 16.0 for Windows (SPSS, Chicago, IL, USA). Numerical values were expressed as means ± standard deviation. Between-group comparison was performed by ANOVA or Chi-square tests where applicable. P<0.05 was considered statistically significant.

Results

Demographics and clinical characteristics of the patients

A total of 80 UAP patients who fulfilled the inclusion criteria and passed the exclusion criteria were included in this study, comprising 22 males and 18 females in the treatment group (n=40; aged, 39 to 74 years old; mean, 63.5±12.3 years old) versus 25 males and 15 females in the control group (n=40; aged, 41 to 75 years old; mean, 66.3±9.2 years old). The clinical characteristics of the patients were shown in *Table 1*. There were no significant differences in age, sex, blood pressure, fasting blood glucose, smoking history, high-risk factors and use of conventional medications between the two groups (P>0.05).

Treatment outcomes

Evaluation of the therapeutic efficacy identified 20 cases with significant effective response and 19 with effective response contributing to an overall effectiveness rate of 97.5% in the treatment group, compared with 12 cases with significant effective response and 20 with effective response contributing to an overall effectiveness rate of 80.0% in the control group (P<0.05). The nitroglycerin dosages after the 2-week treatment in both groups were significantly reduced from baseline. Noticeably, the reduction in nitroglycerin dosage was greater in the treatment group (P<0.01; *Table 2*). Moreover, there were no adverse events related to use of STS in the treatment group.

Changes in serum inflammatory cytokines

At the end of 2-week study, the serum levels of MCP-1, TNF-α, and hs-CRP in all subjects were significantly

Table 3 Serum cytokine levels before and after treatment

Groups	MCP-1 (ng/mL)	TNF-α (ng/mL)	hs-CRP (mg/L)	PPAR-γ (pg/mL)
Control				
Before	197.4±33.4	45.0±4.1	8.7±1.9	185.5±37.4
After	128.5±16.6*	32.9±2.2*	5.5±1.8*	512.4±48.7*
Treatment				
Before	210.8±53.0	43.7±3.8	8.7±2.3	195.3±51.3
After	112.8±23.0*#	27.1±2.0*#	4.0±1.4*#	520.1±50.0*

*, compared with before treatment P<0.01; #, compared with after treatment P<0.05. MCP-1, monocyte chemotactic protein 1; TNF-α, tumor necrosis factor alpha; hs-CRP, high-sensitivity C-reactive protein; PPAR-γ, peroxisome proliferator-activated receptor.

reduced from baseline (P<0.01), and the reduction in all these inflammatory factors was more evident in the treatment group than in the control group (P<0.05). In contrast, the serum level of PPAR-γ was elevated in both groups after treatment compared with baseline (P<0.01). The increase in PPAR-γ seemed slightly greater in patients who received additional STS than the controls, though, the difference did not reach a level of significance (P=0.231) (*Table 3*).

Discussion

Over the past decade, UAP has become an important subtype of ACS contributing to high morbidity and mortality, and therefore attracting more research attention. A growing body of evidence suggests that UAP is associated with local and systemic activation of the immune system (17,18). Studies show that UAP is a complicated pathological progression involving the interaction of many factors. Plasma levels of several inflammation markers have been found to be associated with future cardiovascular risk in patients with UAP. Recently, multi-target and multi-link agents derived from herbal Chinese medicine are widely discussed as to their significant role in the systematic intervention of UAP. Hence, it would be a topic of research interest whether STS with favorable inflammation modulating actions used as additional treatment could provide clinical benefits and thus improve the therapeutic efficacy in patients with UAP.

In this study, 80 patients with UAP were recruited to investigate the efficacy of STS on several inflammatory cytokines in order to provide evidence for its clinical use in this disease. Our results showed that STS, in combination with conventional treatment, may reduce the serum levels of MCP-1, TNF-α and hs-CRP, and elevate the level of PPAR-γ in patients with UAP.

Previous research has found that STS may exhibit myocardial protection against ischemia/reperfusion by inhibiting TNF-α through a positive feedback of the NF-κB/TNF-α pathways, suggesting an anti-inflammatory activity of STS (19,20). Furthermore, STS has also been shown to exert some anti-inflammatory effects by inhibiting inducible NOS (iNOS) gene expression and NO production, as well as inhibiting inflammatory cytokine (IL-1β, IL-6, and TNF-α) expression (21). These findings might be responsible for the mechanisms underlying the anti-inflammatory activity of STS. We also found that the levels of several serum biomarkers, including TNF-α, MCP-1 and hs-CRP, were decreased to a greater magnitude in the STS group as compared to controls (P<0.05). PPAR-γ is a type II nuclear receptor that helps decrease the inflammatory cytokine response in many cardiovascular cells (22-25). Elevation of serum PPAR-γ is therefore inhibitory against TNF-α, MCP-1 and hs-CRP, and may help further relieve of systemic inflammation. Our findings suggested that there was also a slightly greater increase in the serum PPAR-γ levels among patients given additional STS, although the difference did not reach level of significance, possibly owing to insufficient sample size. Further studies with inclusion of large patient series are warranted to validate our results.

Our results also showed that STS combined with conventional medications can improve the symptoms of UAP and lead to less use of nitroglycerin compared with the conventional treatment alone. The difference may result from the anti-inflammatory effects of STS. In addition, the add-on STS therapy was tolerable and safe in all patients given the treatment.

Several limitations in this study should be acknowledged. Firstly, this was a single-center study. Robust evidence with the benefits of STS in UAP patients would require on-going collaboration between multiple institutions in the future. Secondly, STS was used as an add-on therapy rather than a monotherapy in this study. The unique efficacy of STS could not be addressed with our observation, and would warrant subsequent research. Thirdly, the sample size in this study may not be fully adequate to shed light on

the clinical benefits of STS.

Nevertheless, the present study may be an early attempt to explore the therapeutic value of STS as a derivative of herbal Chinese medicine drug in clinical practices. Although future validation needed, our results showed that STS in combination with conventional treatment may be associated with better outcomes in patients with UAP.

Acknowledgements

Disclosure: The authors declare no conflict of interest.

References

1. Kubková L, Spinar J, Pávková Goldbergová M, et al. Inflammatory response and C-reactive protein value in patient with acute coronary syndrome. Vnitr Lek 2013;59:981-8.
2. Napoleão P, Santos MC, Selas M, et al. Variations in inflammatory markers in acute myocardial infarction: a longitudinal study. Rev Port Cardiol 2007;26:1357-63.
3. Garg A, Bansal A, Bhuyan S, et al. Paraplegia during coronary artery bypass graft surgery caused by bilateral anterior cerebral artery territory infarction. Ann Transl Med 2014;2:49.
4. Pomianowski P, Elefteriades JA. The genetics and genomics of thoracic aortic disease. Ann Cardiothorac Surg 2013;2:271-9.
5. Cerrato E, D'Ascenzo F, Biondi-Zoccai G, et al. Acute coronary syndrome in HIV patients: from pathophysiology to clinical practice. Cardiovasc Diagn Ther 2012;2:50-5.
6. Searle J, Danne O, Müller C, et al. Biomarkers in acute coronary syndrome and percutaneous coronary intervention. Minerva Cardioangiol 2011;59:203-23.
7. Yang GJ. Antiplatelet therapy in patients with hypertension. J Transl Intern Med 2013;1:28-31.
8. Shang Q, Xu H, Huang L. Tanshinone IIA: A Promising Natural Cardioprotective Agent. Evid Based Complement Alternat Med 2012;2012:716459.
9. Wang J, Lu W, Wang W, et al. Promising therapeutic effects of sodium tanshinone IIA sulfonate towards pulmonary arterial hypertension in patients. J Thorac Dis 2013;5:169-72.
10. Raja SG. Sodium tanshinone IIA sulfonate for pulmonary arterial hypertension: emerging therapeutic option. J Thorac Dis 2013;5:114-5.
11. He WF, Lu Z, Zhang QB. Research progress on Tanshinone in pharmacological mechanism of cardiovascular protection. China Medical Herald 2013;10:34-8.
12. Cheng F, Yang LF. Clinical Observation on Sulfotanshinone Sodium Injection treating angina pectoris. Northern Pharmacology 2013;10:56-7.
13. Jin UH, Suh SJ, Chang HW, et al. Tanshinone IIA from Salvia miltiorrhiza BUNGE inhibits human aortic smooth muscle cell migration and MMP-9 activity through AKT signaling pathway. J Cell Biochem 2008;104:15-26.
14. Fang ZY, Lin R, Yuan BX, et al. Tanshinone IIA downregulates the CD40 expression and decreases MMP-2 activity on atherosclerosis induced by high fatty diet in rabbit. J Ethnopharmacol 2008;115:217-22.
15. Fang ZY, Lin R, Yuan BX, et al. Tanshinone IIA inhibits atherosclerotic plaque formation by down-regulating MMP-2 and MMP-9 expression in rabbits fed a high-fat diet. Life Sci 2007;81:1339-45.
16. Ren ZH, Tong YH, Xu W, et al. Tanshinone II A attenuates inflammatory responses of rats with myocardial infarction by reducing MCP-1 expression. Phytomedicine 2010;17:212-8.
17. Feng Y, Zhang JC, Xi RX. Clinical significance of inflammation factors in acute coronary syndrome from pathogenic toxin. Chin J Integr Med 2009;15:307-12.
18. Jneid H, Anderson JL, Wright RS, et al. 2012 ACCF/AHA focused update of the guideline for the management of patients with unstable angina/non-ST-elevation myocardial infarction (updating the 2007 guideline and replacing the 2011 focused update): a report of the American College of Cardiology Foundation/American Heart Association Task Force on Practice Guidelines. J Am Coll Cardiol 2012;60:645-81.
19. Lu Y, Li L, Yan H, et al. Endothelial microparticles exert differential effects on functions of Th1 in patients with acute coronary syndrome. Int J Cardiol 2013;168:5396-404.
20. Gökçe M, Erdöl C, Orem C, et al. Inflammation and immune system response against unstable angina and its relationship with coronary angiographic findings. Jpn Heart J 2002;43:593-605.
21. Honoré PM, Spapen H. Embracing western and Chinese research and clinical knowledge: We take up the translational gauntlet! J Transl Intern Med 2013;1:1-2.
22. Wu WY, Wang WY, Ma YL, et al. Sodium tanshinone IIA silate inhibits oxygen-glucose deprivation/recovery-induced cardiomyocyte apoptosis via suppression of the NF-κB/TNF-α pathway. Br J Pharmacol 2013;169:1058-71.
23. Ripley DP, Motwani M, Plein S, et al. Established and emerging cardiovascular magnetic resonance techniques

for the assessment of stable coronary heart disease and acute coronary syndromes. Quant Imaging Med Surg 2014;4:330-44.
24. Fan GW, Gao XM, Wang H, et al. The anti-inflammatory activities of Tanshinone IIA, an active component of TCM, are mediated by estrogen receptor activation and inhibition of iNOS. J Steroid Biochem Mol Biol 2009;113:275-80.
25. Ding Y, Yang KD, Yang Q. The role of PPARδ signaling in the cardiovascular system. Prog Mol Biol Transl Sci 2014;121:451-73.

Cite this article as: Zhang H, Long M, Wu Z, Han X, Yu Y. Sodium tanshinone IIA silate as an add-on therapy in patients with unstable angina pectoris. J Thorac Dis 2014;6(12):1794-1799. doi: 10.3978/j.issn.2072-1439.2014.12.37

Original Article

Lung protective effects of budesonide nebulization during perioperative period of thoracolumbar fusion

Wenjing Li, Yu Zhao, Zhijian Sun, Xu Yang, Lijuan Zhao, Jianxiong Shen

Department of Orthopaedics, Peking Union Medical College Hospital, Chinese Academy of Medical Sciences and Peking Union Medical College, Beijing 100730, China

Correspondence to: Professor Yu Zhao. Department of Orthopaedics, Peking Union Medical College Hospital, Chinese Academy of Medical Sciences & Peking Union Medical College, No. 1 Shuaifuyuan, Dongcheng District, Beijing 100730, China. Email: zhaoyupumch@163.com.

Objective: To determine the pulmonary protective effect of budesonide nebulization in patients undergoing spinal fusion for thoracolumbar degenerative disorders.

Methods: Forty patients who underwent spinal fusion at our hospital from January 2013 to December 2013 for the treatment of thoracolumbar degenerative disorders were randomly allocated into a budesonide intervention group (budesonide group) and a control group. The control group received routine supportive therapy including rehydration, analgesia, and neurotrophic drug treatment; in addition to these, the budesonide group was administered with budesonide nebulization (1-mg budesonide/2-mL saline, twice daily) from 1 day preoperatively through 3 days postoperatively. Respiratory symptoms, arterial blood gas, and pulmonary complication before and after the operations were observed and compared between the two groups.

Results: The patients ranged in age from 46 to 81 years old (mean, 62.4±9.4 years), and comprised 20 men and 20 women. There were no significant differences in postoperative body temperature, heart rate, and respiratory rate between the groups (P>0.05). The change in arterial partial pressure of oxygen (PaO_2) from baseline was significantly lower in the budesonide group than in the control group (at 2.4±12.4 *vs.* 16.0±11.3 mmHg) (P=0.002), so was the findings for oxygen saturation (SpO_2) (0.2%±2.3% *vs.* 2.6%±3.3%), respectively (P=0.047). The incidence of postoperative pulmonary symptoms and complications, such as coughing, shortness of breath, and dyspnea, was 0% in the budesonide group and 15% in the control group; overall, the budesonide group performed better than control group in all pulmonary parameters. None of the patients in the budesonide group experienced severe events associated with glucocorticoid therapy.

Conclusions: Perioperative budesonide nebulization may reduce the postoperative pulmonary complications in middle-aged and elderly patients undergoing thoracolumbar fusion to treat thoracolumbar degeneration, with favorable efficacy and safety.

Keywords: Nebulization; budesonide; thoracolumbar degenerative disease; perioperative period; lung protection

Submitted Oct 25, 2014. Accepted for publication Dec 16, 2014.
doi: 10.3978/j.issn.2072-1439.2014.12.36
View this article at: http://dx.doi.org/10.3978/j.issn.2072-1439.2014.12.36

Introduction

Indications for orthopaedic surgeries are expanding along with the advance of medical sciences and techniques. As China evolves into an aging society, a significant percentage of middle-aged and elderly patients undergo surgery for degenerative thoracolumbar disorders each year. Compared with younger age groups, elder patients usually present with multiple pulmonary and cardiovascular co-morbidities, weakened airway defense, and in males, a long history of cigarette smoking (1,2). Several perioperative factors have been shown to affect the airway and reduce postoperative pulmonary function, resulting in a variety of respiratory complications such as pulmonary atelectasis, pneumonia, bronchospasm, respiratory failure, and acute respiratory distress syndrome (3-6). Pulmonary conditions are among the most common complications following thoracolumbar

fusion (5,7), with the perioperative incidence being 5.5% and 7%, respectively, in patients with thoracic and lumbar spinal stenosis. In addition, the incidence of respiratory complication is closely related to the 2-year mortality (relative risk: 10.76) (6). Proactive prevention against pulmonary complications is therefore essential to improve the surgical outcomes and facilitate postoperative recovery in the elderly.

Budesonide is a glucocorticoid typically administered through nebulization. In addition to its powerful anti-inflammatory actions, budesonide may also reduce airway edema, inhibit airway remodeling, and is widely used in treating chronic obstructive pulmonary disease, asthma and many other pulmonary disorders (8-10). During the recent years, perioperative use of budesonide in selected patients for cardiac surgery, thoracic surgery and other procedures has yielded satisfactory pulmonary protective effects (11-15). Pulmonary protection associated with perioperative budesonide nebulization has not been reported in middle-aged or elderly patients undergoing spinal fusion for treatment of thoracolumbar degenerative diseases. We set out to investigate whether budesonide inhaled perioperatively protects against occurrence of pulmonary complications in this subset of patients.

Patients and methods

Patient selection

Between January 2013 and December 2013, forty middle-aged or elderly subjects were randomly selected from all patients undergoing thoracolumbar fusion at the Orthopaedics Department of Peking Union Medical College Hospital. The inclusion criteria were: (I) a confirmed diagnosis of degenerative thoracolumbar disease based on clinical findings and imaging studies; (II) age above 45 years old; (III) risk factors for perioperative pulmonary complications (such as advanced aged >65; BMI ≥28.0; preoperative bedridden time ≥3 days; smoking index ≥400; previous cardiac events; diabetes; cerebrovascular disease; COPD; hypertension; anemia; ASA classification >2; FEV1 ratio ≤65%; operation time ≥3 hours); (IV) with surgical indications for posterior spinal fusion; (V) use of general anesthesia; and (VI) no difficulty in verbal and written communication in Chinese. The exclusion criteria were: (I) use of systemic glucocorticoids within the four weeks prior to surgery; (II) any contraindication for the medication with budesonide, such as drug-related hypersensitivity; (III) necessity of perioperative mechanical ventilation; and (IV) severe co-morbidities of the heart, lung, liver or other vital organs. Those with concomitant trauma of the chest, abdomen or the head, or signs of adrenocortical dysfunction, pregnant or lactating women, and patients who refused to participate in the study were also excluded.

This study was approved by the Ethics Committee of Peking Union Medical College Hospital. All enrolled patients gave informed written consent before entering the study.

Study design and patient treatments

The 40 patients were divided into the control and budesonide groups comprising 20 individuals each using a random number table. All patients underwent general anesthesia with endotracheal intubation before total laminectomy and spinal fusion. All surgeries were performed by the same orthopaedic surgical team. All patients received routine supportive care such as rehydration, analgesia, and neurotrophic drug treatment postoperatively. Antibiotics were discontinued 24 h postoperatively. Non-steroidal anti-inflammatory drugs were administered perioperatively to relieve pain.

In addition, the budesonide group was given 1 mg Pulmicort Respules (budesonide inhalation suspension, AstraZeneca Plc., Sweden) dissolved in 2 mL of normal saline delivered by nebulization (PARI LC Disposable Nebulizer, PARI GmbH., Germany) from days 1 through 3 postoperatively. Instructions to these patients to ensure proper use of budesonide nebulization were given and enhanced before and after the surgical operations. The nebulization lasted 20 min for each session and was performed twice daily (at 9 am and 3 pm).

The investigators of this study were blinded to group assignment; thus, all perioperative data were evaluated in a single-blinded manner.

Data collection

Pulmonary function parameters were measured using spirometry (Master Screen IOS, JAEGER, Germany) 1 day before nebulization: forced expiratory volume in 1 second (FEV_1), forced vital capacity (FVC), and FEV_1/FVC. Arterial blood gas analysis was performed when the patients were breathing room air at 1 day before nebulization and at 3 days postoperatively after discontinuing nebulization (4 pm) to estimate pulmonary ventilation and air exchange functions.

Table 1 Patient demographics and pulmonary function at baseline in control and budesonide groups ($\bar{x}\pm s$)

Characteristic	Budesonide group	Control group	P value
Sample size (n)	20	20	
General information			
Gender (male/female)	11/9	9/11	0.527
Age (years)	59.9±10.3	60.1±13.5	0.949
Height (cm)	166.5±7.2	162.3±8.3	0.087
Body weight (kg)	71.7±9.1	70.3±12.4	0.680
BMI	25.7±3.1	26.8±4.8	0.399
Smoking history-persistent smokers (n)	5	6	0.723
Indexes of preoperative lung function examination			
FEV_1 (%)	100.1±13.9	98.0±13.2	0.651
FVC (L)	3.4±0.8	3.1±0.8	0.253
FEV_1/FVC (%)	77.4±6.3	74.4±14.4	0.782

FEV_1, forced expiratory volume in one second; FVC, forced vital capacity.

Table 2 Intraoperative clinical data in the control and budesonide groups ($\bar{x}\pm s$)

Group	Difficult airway, N [%]	Endotracheal intubation time (min)	Blood loss (mL)
Budesonide group	3 [15]	248.3±85.5	740.4±472.7
Control group	3 [15]	231.1±56.5	550.0±266.6
P value		0.744	0.221

Intraoperatively, presence of a difficult airway (16), endotracheal intubation time, and blood loss were recorded.

Clinical data were observed and recorded daily as follows: (I) general vital signs including body temperature, heart rate, and respiratory rate; (II) pulmonary complications including atelectasis, pneumonia, respiratory failure, bronchospasm, pulmonary embolism, and pulmonary edema, which were diagnosed based on clinical symptoms (coughing, sputum, wheezing, dyspnea), physical checkup, imaging and pathological studies; and (III) nebulization-related adverse reactions: symptoms and clinical signs attributable to glucocorticoids or drug administration (nausea or vomiting) during observation (from the beginning of nebulization to hospital discharge), apart from allergic reactions secondary to other drugs. Adverse reactions were classified into three categories according to severity: mild, with tolerable symptoms or vital signs; moderate, modest interference with normal activities; and severe, noted by severe adverse reactions and inability for normal activities (17).

Statistical analysis

All numerical data were expressed as mean ± standard deviation (SD). Normally distributed data were compared using the independent sample t test, and non-normally distributed data using the rank sum test. Enumeration data were expressed as sample size and percentage, and analyzed using the Chi-square test or Fisher's exact test. A P value less than 0.05 was considered statistically significant. All data were processed using PASW Statistics for Windows (Version 18.0, SPSS Inc., Chicago, USA).

Results

Patient demographics at baseline

In total, there were 40 patients included in this study, comprising 20 men (50%) and 20 women (50%) aged 46-81 years (mean: 62.4±9.4 years). Before the operations (baseline), there were no statistically significant differences between the two groups with respect to age, height, body weight, BMI, and gender ratio (all P>0.05), as shown in *Table 1*. Five patients in the budesonide group and six in the control group had a smoking history (P=0.723). The three pulmonary function indices, FEV_1, FVC, and FEV_1/FVC, were not significantly different between the two groups (all P>0.05), as shown in *Table 1*.

Intraoperative data

Three patients (15%) each in the budesonide and control groups had a combined difficult airway due to previous cervical vertebral surgery. The both groups did not differ statistically in intraoperative endotracheal intubation time or blood loss, as shown in *Table 2*.

Arterial blood gas

There were no significant differences in the preoperative

Table 3 Pre- and postoperative arterial blood gas analysis in the budesonide and control groups ($\bar{x}\pm s$)

Arterial blood gas analysis	Budesonide group	Control group	P value
PaO_2 (mmHg)			
Preoperative	79.2±10.9	82.7±10.6	0.304
Postoperative	76.6±9.4	72.0±11.7	
Difference (preoperative-postoperative)	2.4±12.4	16.0±11.3	0.002*
$PaCO_2$ (mmHg)			
Preoperative	39.2±3.8	40.4±3.6	0.314
Postoperative	35.5±4.5	39.2±3.2	
Difference (preoperative-postoperative)	3.8±4.2	1.1±3.7	0.063
SpO_2 (%)			
Preoperative	95.6±1.8	96.2±1.8	0.292
Postoperative	95.3±2.1	94.3±3.3	
Difference (preoperative-postoperative)	0.2±2.3	2.6±3.3	0.047*

*Compared to the control group P<0.05.

arterial blood gas analyses (PaO_2, $PaCO_2$, SpO_2) between the two groups (P>0.05); however, the reduction in levels of postoperative PaO_2 and SpO_2 from pre-operation was significantly less in the budesonide group than the findings in the control group (P<0.05), as summarized in *Table 3*.

Postoperative vital signs

General vital signs including body temperature, heart rate, and respiratory rate during preoperative days 1 through 3 days did not show significant differences between the groups (P>0.05), as shown in *Table 4*, suggesting that budesonide nebulization perioperatively did not significantly influence the general postoperative vital signs.

Pulmonary symptoms and complications

No patients in the budesonide group experienced respiratory symptoms such as coughing, expectoration, or wheezing. Three patients (15%) in the control group experienced respiratory symptoms during the study period: two patients (10%) reported coughing and expectoration on the postoperative day 2, and one (5%) reported wheezing and dyspnea on postoperative day 3. All symptoms resolved after symptomatic and supportive treatment, and there were no significant findings in imaging and pathological studies. The budesonide group did not experience any pulmonary complications, compared with one patient in the control group diagnosed with pneumonia based on imaging study and clinical signs including fever, coughing, and expectoration. The patient was given medical treatment and recovered uneventfully.

Table 4 Vital sign compared between the budesonide and control groups ($\bar{x}\pm s$)

Time	Group		P value
	Budesonide group	Control group	
Pre			
T (℃)	36.5±0.3	36.6±0.3	0.584
HR (bpm)	78.4±11.5	80.4±13.3	0.597
RR (breaths/min)	18.5±1.3	19.0±1.4	0.367
Day 1			
T (℃)	37.0±0.45	37.0±0.38	0.576
HR (bpm)	80.0±6.0	77.2±6.5	0.149
RR (breaths/min)	18.8±1.0	18.7±0.9	0.681
Day 2			
T (℃)	36.9±0.4	37.0±0.5	0.444
HR (bpm)	79.5±5.8	78.6±4.4	0.618
RR (breaths/min)	18.8±1.0	18.8±0.6	0.892
Day 3			
T (℃)	36.8±0.39	36.8±0.39	0.455
HR (bpm)	78.7±5.5	78.0±4.5	0.407
RR (breaths/min)	18.8±0.7	18.7±0.7	0.458

Pre, before operation; Day 1, 1st day postoperatively; Day 2, 2nd day postoperatively; Day 3, 3rd day postoperatively; T, temperature; HR, heart rate; RR, respiratory rate.

None patients of the budesonide group experienced events associated with glucocorticoid administration such as allergic reactions, oropharyngeal disease, and systemic reactions. One patient (5%) had a local discomfort related to nebulization, manifesting as nausea during nebulization on the first postoperative day. The patient's vital signs were stable; the adverse event was deemed attributed to the nebulization procedure, and classified as a mild adverse reaction according to the described classification standards. He recovered with bed-rest and did not require additional treatment.

Discussion

This randomized controlled study indicated that perioperative budesonide nebulization reduced fluctuations in PaO_2 and SpO_2, and was associated with lower incidence of pulmonary symptoms such as coughing, wheezing, and dyspnea, and pulmonary complications in middle-aged and elderly patients after thoracolumbar fusion. None patients of the budesonide group experienced complications associated with glucocorticoids such as allergic reactions, oropharyngeal disease, and systemic reactions. Moreover, nebulization as administered in this study (1-mg budesonide in 2-mL saline given twice daily from 1 day preoperatively to 3 days postoperatively) was safe and effective for perioperative clinical care.

During thoracolumbar fusion, perioperative pulmonary complications associated with patient age warrant consideration (4,18,19). In degenerative thoracolumbar spinal diseases, a variety of factors can affect occurrence of perioperative pulmonary complications. Preoperative factors include advanced age, cardiopulmonary disease, and a long history of smoking, impaired airway defensive capacity; intraoperative factors such as placement in a prone position, long surgical duration, large surgical incision, endotracheal intubation, anesthetic drugs, and mechanical ventilation, can in many ways stimulate the airway by destroying the respiratory barrier, damaging the tracheal mucosa, and reducing the lung compliance. Postoperative factors such as pain and immobilization limit coughing, prevents discharge of airway secretions. These numerous factors can result in a series of perioperative pulmonary complications such as atelectasis, pneumonia, and bronchospasm. In the 40 middle-aged and elderly patients included in this study, the incidence of pulmonary complications was 2.5% and 5% in the control group. In a clinical study with large sample sizs, He *et al*. (7) reported a 5.5% perioperative incidence rate of pulmonary complication in thoracic spinal stenosis patients; Lee *et al*. reported a 7% incidence after lumbar surgery and 13% after spinal surgery (6). The pulmonary complication rate in this study was slightly lower than that reported previously, most probably as a result of rigorous criteria for patient inclusion. In order to control for potential confounders and more objectively evaluate the pulmonary protective effect of budesonide nebulization, patients requiring perioperative mechanical ventilation, concurrent severe or uncontrolled systemic disease such as vital organ failure, concurrent thoracic, abdominal, and head trauma, and those at high risk of severe pulmonary complications were excluded.

Pulmonary protection refers to proactive prevention and treatment of imminent pulmonary injury of various etiologies (20). An appropriate protective strategy during the perioperative period of thoracolumbar fusion can effectively maintain pulmonary function and prevent related complications. This ensures that the patient safely survives the perioperative period and strongly supports the effectiveness of the operation to help patients recover faster.

Budesonide as an inhaled glucocorticoid may effectively inhibit a variety of inflammatory cells, reduces the generation of inflammatory mediators, and exhibits significant anti-inflammatory effect; in the airway, it also induces vessel contraction, inhibits mucosal edema, reduces cell exudation, mitigates edema, and prevents airway remodeling (21-24). Compared to systemic glucocorticoids, such as dexamethasone and hydrocortisone, budesonide nebulization offers the following unique benefits: (I) high concentration primarily in the lungs; (II) high hepatic clearance; and (III) high glucocorticoid receptor affinity. During nebulization, the nebulizer unit breaks the liquid into micro-particles, which are directly inhaled into the lower respiratory tract and rapidly absorbed by the pulmonary mucosa, thus increasing the local drug concentration. It also hydrates the airways, which dilutes airway secretions and facilitates their discharge.

For patients undergoing thoracolumbar fusion, the pharmacologic and pharmacokinetics characteristics of budesonide, combined with local administration using nebulization effectively prevents airway inflammation, alleviates edema, inhibits airway remodeling, and promotes expectoration, which maintains pulmonary function and reduces adverse events associated with glucocorticoid accumulation, such as hypothalamic-pituitary-adrenal axis suppression, bone demineralization, and growth inhibition (25,26). Budesonide nebulization could function as a pulmonary protectant during the perioperative period of thoracolumbar fusion.

This randomized controlled study is the first attempt to evaluate the pulmonary protective effect of budesonide nebulization during perioperative thoracolumbar fusion in middle-aged and elderly patients. Preoperative factors such as age, general health, pulmonary function, and smoking history, which are associated with perioperative pulmonary complications, were consistent between the budesonide and control patients. Reportedly, the presence of a difficult airway affects respiratory function during the perioperative period (16); endotracheal intubation time and the surgical

trauma severity also influence the pulmonary complication rate after spinal surgery (6). In this study, the intraoperative blood loss was an indicator for severity of surgical trauma. There were no statistically significant differences intraoperatively between the two groups. Postoperatively, the budesonide group showed remarkably less reduction from baseline in PaO_2 and SpO_2 as compared with the control group ($P<0.05$). In addition, incidence of respiratory symptoms such as coughing, asthma, and dyspnea was 15% in the control group, and one (5%) postoperative pneumonia case was observed; the incidences of pulmonary symptoms and complications were higher in the control group than in the budesonide group. These findings indicate that budesonide nebulization perioperatively has a pulmonary protective effect in middle-aged and elderly patients with degenerative thoracolumbar disease, and specifically, nebulization administered as presently described (1-mg budesonide/2-mL saline, twice daily, from 1 day preoperatively to 3 days postoperatively) is clinically effective.

Recently, budesonide has been used more widely perioperatively in several surgical fields including cardiac, thoracic, and abdominal surgeries, and the treatment has achieved good effects (12,14,27-29). Fang *et al*. (12) evaluated the effect of budesonide nebulization on pulmonary function in a study of 22 elderly patients undergoing abdominal surgery and found that pre- and intraoperative budesonide inhalation improved pulmonary ventilation with no impact on respiratory mechanics. In a randomized controlled study, Ju *et al*. (14) evaluated the effect of preoperative budesonide nebulization on inflammation in thoracotomy patients receiving single-lung ventilation and revealed that preoperative budesonide nebulization reduced the peak airway pressure and plateau pressure, increased pulmonary compliance, inhibited inflammation, and ultimately improved pulmonary function. A study conducted by Sawada *et al*. (28) also confirmed the effectiveness of preoperative budesonide nebulization in thoracic surgery patients. Collectively, the results of these prior studies and the current study show that perioperative budesonide nebulization can provide effective pulmonary protection in numerous procedures.

In this study, inhaled corticosteroids in the budesonide group were given in a short duration and low dose. General vital signs such as body temperature, heart rate, and respiratory rate during this period were similar between the groups, and none of the patients experienced allergic reactions, oropharyngeal disease secondary to glucocorticoid nebulization, or systemic adverse reactions; only one patient reported transient nausea following nebulization, which resolved after a short period of rest. These results indicate that in the targeted patient population, short-course perioperative budesonide nebulization as administered in the present study protocol was safe. Presumably, the local administration of budesonide restricted its effect on the lung; this, combined with a higher hepatic clearance, causes fewer systemic adverse reactions compared to intravenous glucocorticoid administration. Previous reports indicate that systemic reactions and oropharyngeal complications caused by budesonide depended on the dosage and treatment duration and occurred solely in patients receiving long-term and large-dosages. Otherwise, adverse reactions were mostly mild, and the complication rate of short-course budesonide treatment was low (8,30,31). Both the present study and previous studies confirm that short-course low-dose budesonide treatment during perioperative thoracolumbar fusion is clinically safe. Budesonide was well tolerated and had a low rate of allergic reactions; however, there are individual reports of delayed allergic reactions following budesonide nebulization (32,33). Although none of the patients experienced an allergic reaction, this complication should be considered in future clinical application of budesonide.

There were several potential limitations in this study. The sample size was small, and patients were not stratified according to factors such as age and smoking history. Correlation factors analysis of pulmonary complications was not performed due to the small sample size. In addition, postoperative follow-up with pulmonary function test was not performed due to potential pain and inconvenience to the patient, and other factors. These limitations may introduce bias in evaluating the clinical effectiveness of budesonide nebulization. Therefore our findings need further validation in future large-sample studies.

In conclusion, perioperative budesonide nebulization may reduce the incidence of pulmonary complications and improved clinical symptoms in middle-aged and elderly patients with thoracolumbar degeneration undergoing spinal fusion. Perioperative budesonide inhalation in this patient population is also tolerable.

Acknowledgements

Disclosure: The authors declare no conflict of interest.

References

1. Wang Ld. Tobacco or Health? J Transl Intern Med 2014;2:7-10.
2. Filippidou EC, Liolios E, Ioannidi V, et al. The smoking habits in rural population and its effects on the lung. J Thorac Dis 2012;4:AB38.
3. Schoenfeld AJ, Carey PA, Cleveland AW 3rd, et al. Patient factors, comorbidities, and surgical characteristics that increase mortality and complication risk after spinal arthrodesis: a prognostic study based on 5,887 patients. Spine J 2013;13:1171-9.
4. Wider J, Przyklenk K. Ischemic conditioning: the challenge of protecting the diabetic heart. Cardiovasc Diagn Ther 2014;4:383-96.
5. Franchitto A, Onori P, Renzi A, et al. Recent advances on the mechanisms regulating cholangiocyte proliferation and the significance of the neuroendocrine regulation of cholangiocyte pathophysiology. Ann Transl Med 2013;1:27.
6. Lee MJ, Konodi MA, Cizik AM, et al. Risk factors for medical complication after spine surgery: a multivariate analysis of 1,591 patients. Spine J 2012;12:197-206.
7. He B, Yan L, Xu Z, et al. Treatment strategies for the surgical complications of thoracic spinal stenosis: a retrospective analysis of two hundred and eighty three cases. Int Orthop 2014;38:117-22.
8. Hernando R, Drobnic ME, Cruz MJ, et al. Budesonide efficacy and safety in patients with bronchiectasis not due to cystic fibrosis. Int J Clin Pharm 2012;34:644-50.
9. Jorens PG. Glucocorticoids: Basic in depth. J Transl Intern Med 2014;2:98-9.
10. Han D, Wang GZ, Xie XM, et al. Effect and safety of budesonide nebulization on acute and exacerbated chronic obstruction pulmonary disease by Meta analysis. Chin J Intern Med 2013;52:975-7.
11. Verborgh C. Corticosteroids in cardiac anesthesia. J Transl Intern Med 2014;2:76-7.
12. Fang JY, Huang WQ, Xu KQ, et al. Changes in preoperative and intraoperative abdominal surgeries by budesonide nebulization in elderly patients during the perioperative period. Chin J of Anesthesiol 2005;25:714-5.
13. Cheng AB, Shang XJ. Airway protective effect of budesonide suspension for patients undergoing general anesthesia. J Pract Med 2013;29:675-6.
14. Ju NY, Gao H, Huang W, et al. Therapeutic effect of inhaled budesonide (Pulmicort® Turbuhaler) on the inflammatory response to one-lung ventilation. Anaesthesia 2014;69:14-23.
15. Zhang JP, Zhang RD, Bai J, et al. Lung effect of budesonide nebulization for children with congenital heart disease during the perioperative period. J Clin Res 2011;28:1043-5.
16. Apfelbaum JL, Hagberg CA, Caplan RA, et al. Practice guidelines for management of the difficult airway: an updated report by the American Society of Anesthesiologists Task Force on Management of the Difficult Airway. Anesthesiology 2013;118:251-70.
17. Pohunek P, Kuna P, Jorup C, et al. Budesonide/formoterol improves lung function compared with budesonide alone in children with asthma. Pediatr Allergy Immunol 2006;17:458-65.
18. Cloyd JM, Acosta FL Jr, Cloyd C, et al. Effects of age on perioperative complications of extensive multilevel thoracolumbar spinal fusion surgery. J Neurosurg Spine 2010;12:402-8.
19. Kalanithi PS, Patil CG, Boakye M. National complication rates and disposition after posterior lumbar fusion for acquired spondylolisthesis. Spine (Phila Pa 1976) 2009;34:1963-9.
20. Wang TY. Expert consensus on lung protection of thoracic surgery during the perioperative period. Chin J Surg 2009;47:1361-4.
21. Perng DW, Su KC, Chou KT, et al. Long-acting β2 agonists and corticosteroids restore the reduction of histone deacetylase activity and inhibit H2O2-induced mediator release from alveolar macrophages. Pulm Pharmacol Ther 2012;25:312-8.
22. Bos IS, Gosens R, Zuidhof AB, et al. Inhibition of allergen-induced airway remodelling by tiotropium and budesonide: a comparison. Eur Respir J 2007;30:653-61.
23. Boorsma M, Lutter R, van de Pol MA, et al. Long-term effects of budesonide on inflammatory status in COPD. COPD 2008;5:97-104.
24. Fang Q, Schulte NA, Kim H, et al. Effect of budesonide on fibroblast-mediated collagen gel contraction and degradation. J Inflamm Res 2013;6:25-33.
25. Chung KF, Caramori G, Adcock IM. Inhaled corticosteroids as combination therapy with beta-adrenergic agonists in airways disease: present and future. Eur J Clin Pharmacol 2009;65:853-71.
26. Fahim A, Faruqi S, Wright CE, et al. Comparison of the effect of high-dose inhaled budesonide and fluticasone on adrenal function in patients with severe chronic obstructive pulmonary disease. Ann Thorac Med 2012;7:140-4.
27. Ocalan K, Solak O, Esme H, et al. Efficacy of budesonide

and interleukin-10 in an experimental rat model with isolated bilateral pulmonary contusion created by blunt thoracic trauma. Eur J Cardiothorac Surg 2013;43:163-7.
28. Sawada S, Suehisa H, Yamashita M. Inhalation of corticosteroid and β-agonist for persistent cough following pulmonary resection. Gen Thorac Cardiovasc Surg 2012;60:285-8.
29. Ju YN, Gao H, Huang W, et al. Effects of preoperative budesonide nebulization on inflammatory responses in patients undergoing thoracic surgery during one-lung ventilation. Chin J Anesthesiol 2013;33:714-7.
30. Sin DD, Tashkin D, Zhang X, et al. Budesonide and the risk of pneumonia: a meta-analysis of individual patient data. Lancet 2009;374:712-9.
31. Melamies M, Vainio O, Spillmann T, et al. Endocrine effects of inhaled budesonide compared with inhaled fluticasone propionate and oral prednisolone in healthy Beagle dogs. Vet J 2012;194:349-53.
32. Salava A, Alanko K, Hyry H. A case of systemic allergic dermatitis caused by inhaled budesonide: cross-reactivity in patch tests with the novel inhaled corticosteroid ciclesonide. Contact Dermatitis 2012;67:244-6.
33. Baeck M, Pilette C, Drieghe J, et al. Allergic contact dermatitis to inhalation corticosteroids. Eur J Dermatol 2010;20:102-8.

Cite this article as: Li W, Zhao Y, Sun Z, Yang X, Zhao L, Shen J. Lung protective effects of budesonide nebulization during perioperative period of thoracolumbar fusion. J Thorac Dis 2014;6(12):1800-1807. doi: 10.3978/j.issn.2072-1439.2014.12.36

Brief Report

Chemotherapy with paclitaxel plus carboplatin for relapsed advanced thymic carcinoma

Zhengbo Song[1,2]

[1]Department of Chemotherapy, Zhejiang Cancer Hospital, Hangzhou 310022, China; [2]Key Laboratory Diagnosis and Treatment Technology on Thoracic Oncology, Hangzhou 310022, China

Correspondence to: Zhengbo Song, MD. Department of Chemotherapy, Zhejiang Cancer Hospital, 38 Guangji Road, Hangzhou 310022, China. Email: songzhengbo83@163.com.

Objective: For rarity of thymic carcinoma, no definitive chemotherapeutic regimen has been established in second- or further-line settings. The aim of this study was to evaluate the feasibility and safety of paclitaxel plus carboplatin in advanced thymic carcinoma as second- or further-line treatment in our institute.

Methods: We evaluated the efficacy and toxicity of paclitaxel plus carboplatin as salvage therapy in 12 patients with previously treated advanced thymic carcinoma from 2005 to 2012 in Zhejiang Cancer Hospital. Survival analysis was evaluated by Kaplan-Meier method.

Results: Twelve patients were included in current study. Four patients achieved stable disease (SD), and three achieved partial response (PR), representing a response rate of 25.0% and disease control rate (DCR) of 58.3%. Median progression-free survival (PFS) and overall survival (OS) were 3.5 and 24.0 months, respectively. The toxicities associated with the paclitaxel plus carboplatin was generally acceptable.

Conclusions: Paclitaxel plus carboplatin appears to have some activity against thymic carcinoma as second-line or later chemotherapy in advanced thymic carcinoma.

Keywords: Thymic carcinoma; paclitaxel; salvage chemotherapy; efficacy

Submitted Jul 01, 2014. Accepted for publication Sep 12, 2014.
doi: 10.3978/j.issn.2072-1439.2014.11.18
View this article at: http://dx.doi.org/10.3978/j.issn.2072-1439.2014.11.18

Introduction

Thymic carcinoma is a rare and invasive mediastinal neoplasm (1). The role of systemic chemotherapy is important for advanced thymic carcinoma (2). For rarity of this tumor, no definitive chemotherapeutic regimen has been established. Several reports have indicated a well efficacy of different regimens, such as cisplatin + vincristine + doxorubicin + etoposide (CODE), cisplatin + doxorubicin + vincristine + cyclophosphamide (ADOC), and etoposide + ifosfamide + cisplatin (VIP) against thymic carcinoma in first-line treatment (3-5).

Paclitaxel has a mechanism of action that differs from older agents and the relatively less toxic profile of combination with platinum enables it to be used most widely in the treatment of many solid tumors (6). For the same epithelial origin of thymic tumors with other solid tumors, several studies detected the efficacy of paclitaxel plus carboplatin in thymic carcinoma, and some patients yielded a well response in first-line treatment (7,8). However, the efficacy data evaluation of paclitaxel plus carboplatin in second- or further-line treatment of thymic carcinoma is lacking.

We conducted a retrospective study to evaluate the efficacy and safety of paclitaxel plus carboplatin against advanced thymic carcinoma as second- or further-line chemotherapy.

Materials and methods

Patient eligibility

This retrospective study was conducted through a review of medical records of patients with advanced thymic

Table 1 Characteristics of 12 patients

Characteristics	Data
Gender	
Male	8
Female	4
Age	
Range	20-67
Median	47
<50	8
≥50	4
Which line	
Second-line	7
Third-line	5
Histology	
Squamous cell carcinoma	8
Undifferentiated carcinoma	4
Clinical stage	
IVa	2
IVb	10
Performance status	
0	6
1	6
Surgery history	
Yes	4
No	8

carcinoma who received paclitaxel plus carboplatin as second- or further-line treatment between 2005 and 2012. Inclusion criteria were: (I) histological or cytological diagnosis of thymic carcinoma according to the histopathological criteria proposed by the WHO 2004 version; (II) Masaoka criteria stage IVa or IVb; (III) all patients received prior chemotherapy regimens; (IV) without any local treatment such as radiotherapy or interventional therapy during the paclitaxel plus carboplatin therapy time; (V) the recurrence or metastases performed with chest CT scans, abdominal, brain CT and bone scans.

Treatment methods

Paclitaxel was administered at a dose of 175 mg/m^2 intravenously over 1 h, with the treatment cycle repeated every 3 weeks. Carboplatin (AUC =5) on day 1 was administered synchronous.

Responses and toxicity

Tumor responses were assessed every two cycles, or were evaluated early when significant signs of progression appeared. Objective tumor responses were according to the Response Evaluation Criteria in Solid Tumors (RECIST 1.1). Objective tumor responses included complete response (CR), partial response (PR), stable disease (SD), and progressive disease (PD). The disease control rate (DCR) was defined as the addition of objective response and stabilization rates (CR + PR + SD). Toxicities were evaluated according to the National Cancer Institute Common Toxicity Criteria version 3.0 (CTC3.0).

Follow-up

All the patients that were evaluated for tumor response had a progression-free survival (PFS). Follow-up rate was 100%. Overall survival (OS) was defined as the time from the first day of diagnosis to death or last follow-up. PFS encompassed the time from the first cycle of paclitaxel plus carboplatin treatment to documented progression or death from any cause. The median follow-up period was 25.0 months (range, 5.5-65 months). The last follow-up time was Jan 31, 2014.

Statistical analysis

The survival curves were calculated according to the method of Kaplan-Meier. Statistical analysis was performed using SPSS version 16.0 (SPSS Inc., Chicago, IL, USA).

Results

Characteristics of the treatment patients

A total of 12 patients were included in the study. Among the 12 patients, resection was performed in four cases (three with median sternotomy and one with anterolateral thoracotomy). The first-line regimens of all the 12 patients contained CAP (cyclophosphamide + doxorubicin + cisplatin, n=7), VIP (n=3) and EP (etoposide+ cisplatin, n=2). Seven patients received paclitaxel plus carboplatin regimen as second-line and five as third-line chemotherapy. The median (range) number of paclitaxel plus carboplatin chemotherapy cycles was 3 (range, 1-4). Patients' characteristics are shown in *Table 1*.

Table 2 Clinical characteristics of 12 patients with advanced thymic carcinoma

Case	Gender/age	Histology	Metastasis site	Which line	Response	PFS (month)	OS (month)
1	M/36	Undifferentiated	Lung	Second	PD	1.5	20.5
2	F/45	SCC	Supraclavicular LN	Third	SD	4.0	26.5
3	M/54	SCC	Liver	Second	PR	5.0	30.5
4	F/48	Undifferentiated	Pleura	Second	PR	6.0	27.0
5	M/46	SCC	Supraclavicular LN	Third	PD	1.0	15.0
6	F/50	SCC	Liver	Second	PR	4.0	25.0
7	M/55	Undifferentiated	Bone	Third	PD	1.4	18.0
8	M/20	Undifferentiated	Bone	Third	SD	7.0	35.5+
9	M/59	SCC	Pleura	Second	SD	3.5	24.0
10	M/67	SCC	Bone	Second	SD	4.0	25.0
11	F/44	SCC	Liver	Second	PD	1.4	20.0
12	M/28	SCC	Supraclavicular LN	Third	PD	1.0	15.0

M, man; F, female; PFS, progression-free survival; OS, overall survival; PD, progressive disease; SCC, squamous cell carcinoma; LN, lymph node; SD, stable disease; PR, partial response.

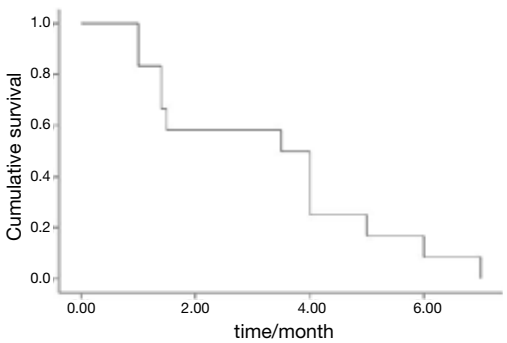

Figure 1 Progression-free survival of 12 patients.

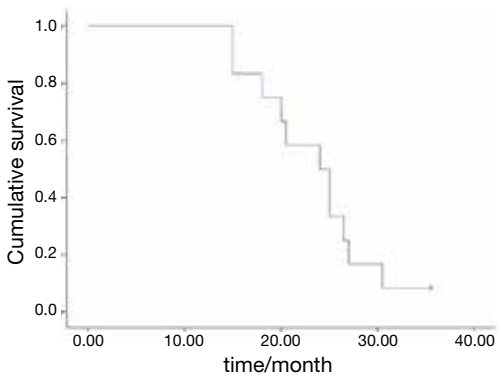

Figure 2 Survival curves of 12 patients.

Response data and survival analysis

Response data for paclitaxel plus carboplatin therapy are shown in *Table 2*. Among the 12 patients, PR was confirmed in 3 patients and 4 showed SR, representing a response rate of 25.0% and DCR of 58.3%. There was no significant difference between the response (PR + CR) and no-response (SD + PD) patients among the gender (P=0.89), age (P=0.74), pathological subtype (P=0.81) and metastatic sites (P=1.0).

The median PFS was 3.5 months (95% CI, 1.4-5.6) (*Figure 1*). The median OS was 24.0 months (95% CI, 8.9-29.1) (*Figure 2*). There was no significant association for the PFS among the gender (P=0.68), age (P=0.21), stage (P=0.64) and pathological subtype (P=0.68). No difference was found in PFS between the second- and further-line chemotherapy (4.0 *vs.* 3.5 months, P=0.86).

Toxicity evaluation

All patients were assessed for toxicity. Grade 3/4 hematological toxicities were observed in three patients (one anemia, two neutropenia), and grade 3/4 non-hematological toxicities were seen in four patients (one fatigue, one hepatic injure, one neurotoxicity, one nausea). Two patients reduced

Table 3 Articles published about chemotherapy as a salvage treatment in thymic carcinoma

First author	Number	Gender (M/F)	Which line	Regimen	PR/SD/PD	Median PFS (month)	Median OS (month)
Kanda (11)	7	4/3	Second	CPT-11 + platinum	2/3/2	4	17
Koizumi (12)	1	0/1	Sixth	S-1	1/0/0	18	Unknown
Komatsu (13)	3	2/1	Second [1]; third [2]	Carboplatin + paclitaxel	2/1/0	Unknown	Unknown
Koizumi (14)	6	4/2	Second [1]; third [4]; fifth [1]	Amrubicin + platinum	2/3/1	4.5	Unknown
Watanabe (15)	3	Unknown	Second	Carboplatin + paclitaxel	1/2/0	6.7	36
Oguri (9)	1	0/1	Second	Docetaxel	1/0/0	4	Unknown
Palmieri (16)	3	Unknown	Second	Capecitabine + gemcitabine	1/1/1	Unknown	Unknown
Okuma (10)	4	2/2	Second [2]; third [4]; fifth [1]	S-1	2/2/0	8.1	Unknown

M, man; F, female; PR, partial response; SD, stable disease; PD, progressive disease; PFS, progression-free survival; OS, overall survival.

the dosage for the grade 4 toxicity (one anemia and one nausea). No febrile neutropenia or toxic death occurred.

Discussion

To the best of our knowledge, our represents the largest data to assess whether paclitaxel plus carboplatin as second- or further-line chemotherapy confers any clinical benefit in patients with advanced thymic carcinoma. The outcome showed that paclitaxel plus carboplatin was useful as an alternative chemotherapy regimen for advanced thymic carcinoma in second or later-line treatment.

Standard systemic chemotherapy for advanced thymic carcinoma has not been determined because of its rarity. Anthracycline-based regimens such as CAP and ADOC were widely used in clinic. However, the toxicity of anthracycline-based regimens is a big question in clinical practice. Platinum-based chemotherapy such as TC (paclitaxel plus carboplatin) and EP is another choice for advanced thymic carcinoma and showed a well efficacy in several reports. A phase II study included 19 patients with thymic carcinoma showed a promising result with carboplatin and paclitaxel regimen as first-line chemotherapy (7). Followed this report, several retrospective studies have shown that carboplatin and paclitaxel regimen had a well efficacy and acceptable toxicity (7,8). Previous case series of second-line chemotherapy for advanced thymic carcinoma were based on regimens that were originally used for advanced thymoma or other solid tumors. Published case reports and series include treatment with S-1, irinotecan and docetaxel (9-11) (*Table 3*). The median PFS was ranged from 4 to 18 months. Only two studies totally included 6 patients showed a well efficacy of paclitaxel plus carboplatin regimen for advanced thymic carcinoma as second-line therapy (13,15). Our analysis indicated that the regimen of paclitaxel plus carboplatin was active for advanced thymic carcinoma patients as salvage chemotherapy with a response rate of 25.0% and median PFS of 3.5 months. The adverse events occurred at a similar incidence as previous reports in other solid tumors (6). Neutropenia is the most frequently reported ones and no patients refused further treatment for the toxicity.

The major limitation of the present study is its retrospective nature and small number of patients. However, with no cases in prospective clinical studies, our retrospective study can also be considered to be meaningful.

Our results suggest that paclitaxel plus carboplatin is a promising regimen as salvage chemotherapy for pretreated advanced thymic carcinoma, but further studies are required to fully quantify the efficacy of this regimen.

Acknowledgements

Disclosure: The author declares no conflict of interest.

References

1. Gubens MA. Treatment updates in advanced thymoma and thymic carcinoma. Curr Treat Options Oncol 2012;13:527-34.
2. Wei ML, Kang D, Gu L, et al. Chemotherapy for thymic carcinoma and advanced thymoma in adults. Cochrane Database Syst Rev 2013;8:CD008588.
3. Rea F, Marulli G, Di Chiara F, et al. Multidisciplinary approach for advanced stage thymic tumors: long-term outcome. Lung Cancer 2011;72:68-72.
4. Loehrer PJ Sr, Jiroutek M, Aisner S, et al. Combined etoposide, ifosfamide, and cisplatin in the treatment of patients with advanced thymoma and thymic carcinoma: an intergroup trial. Cancer 2001;91:2010-5.
5. Kunitoh H, Tamura T, Shibata T, et al. A phase-II trial of dose-dense chemotherapy in patients with disseminated thymoma: report of a Japan Clinical Oncology Group trial (JCOG 9605). Br J Cancer 2009;101:1549-54.
6. Schiller JH, Harrington D, Belani CP, et al. Comparison of four chemotherapy regimens for advanced non-small-cell lung cancer. N Engl J Med 2002;346:92-8.
7. Lemma GL, Lee JW, Aisner SC, et al. Phase II study of carboplatin and paclitaxel in advanced thymoma and thymic carcinoma. J Clin Oncol 2011;29:2060-5.
8. Igawa S, Murakami H, Takahashi T, et al. Efficacy of chemotherapy with carboplatin and paclitaxel for unresectable thymic carcinoma. Lung Cancer 2010;67:194-7.
9. Oguri T, Achiwa H, Kato D, et al. Efficacy of docetaxel as a second-line chemotherapy for thymic carcinoma. Chemotherapy 2004;50:279-82.
10. Okuma Y, Shimokawa T, Takagi Y, et al. S-1 is an active anticancer agent for advanced thymic carcinoma. Lung Cancer 2010;70:357-63.
11. Kanda S, Koizumi T, Komatsu Y, et al. Second-line chemotherapy of platinum compound plus CPT-11 following ADOC chemotherapy in advanced thymic carcinoma: analysis of seven cases. Anticancer Res 2007;27:3005-8.
12. Koizumi T, Agatsuma T, Komatsu Y, et al. Successful S-1 monotherapy for chemorefractory thymic carcinoma. Anticancer Res 2011;31:299-301.
13. Komatsu Y, Koizumi T, Tanabe T, et al. Salvage chemotherapy with carboplatin and paclitaxel for cisplatin-resistant thymic carcinoma—three cases. Anticancer Res 2006;26:4851-5.
14. Koizumi T, Agatsuma T, Ichiyama T, et al. Salvage chemotherapy with amrubicin and platinum for relapsed thymic carcinoma: experience in six cases. Med Oncol 2010;27:392-6.
15. Watanabe K, Shinkai M, Goto H, et al. Chemotherapy with carboplatin and paclitaxel after failure of primary chemotherapy for advanced thymic carcinoma. A report of three cases and review of the literature. Tumori 2013;99:e172-6.
16. Palmieri G, Merola G, Federico P, et al. Preliminary results of phase II study of capecitabine and gemcitabine (CAP-GEM) in patients with metastatic pretreated thymic epithelial tumors (TETs). Ann Oncol 2010;21:1168-72.

Cite this article as: Song Z. Chemotherapy with paclitaxel plus carboplatin for relapsed advanced thymic carcinoma. J Thorac Dis 2014;6(12):1808-1812. doi: 10.3978/j.issn.2072-1439.2014.11.18

Video-assisted thoracoscopic left upper lobe sleeve lobectomy combined with pulmonary arterioplasty via two-port approach

Wenjie Jiao, Yandong Zhao, Xiaofei Wang, Jinpeng Zhao

Department of Thoracic Surgery, The Affiliated Hospital of Qingdao University, Qingdao 266003, China

Correspondence to: Wenjie Jiao. Department of Thoracic Surgery, The Affiliated Hospital of Qingdao University, 16 Jiangsu Road, Qingdao 266003, China. Email: xwkjiao@126.com.

Abstract: Here we report a case of left upper lobe sleeve lobectomy with pulmonary arterioplasty via video-assisted thoracoscopy surgery (VATS) two-port approach. A squamous cell carcinoma with stage T3N1M0 was identified on pathological examination. The bronchial anastomosis was performed using running suture with a 3-0 prolene. Two bulldog clamps were used to gain adequate vascular control. Partial pulmonary artery resection was achieved tangentially with a stapler. The postoperative course was uneventful.

Keywords: Lung cancer; thoracoscopic; lobectomy

Submitted Jul 09, 2014. Accepted for publication Sep 27, 2014.
doi: 10.3978/j.issn.2072-1439.2014.11.09
View this article at: http://dx.doi.org/10.3978/j.issn.2072-1439.2014.11.09

Introduction

Locally advanced lung cancer, even with major artery involvement, has been adapted for thoracoscopic lung resection and obtained worldwide acceptance (1). In some patients, a resection and reconstruction of the pulmonary artery has been increasingly accepted as an alternative to total pneumonectomy as being less invasive. This technique allows patients to preserve more pulmonary function similar to the effect of bronchial sleeve lobectomy. However, vascular arterioplasty is considered a contraindication for the video-assisted thoracoscopy surgery (VATS) approach, even for experienced thoracoscopic surgeons for the high operative risk. This report describes a minimally invasive technique for VATS left upper sleeve lobectomy with pulmonary arterioplasty via the two-port approach.

Operative techniques

A 64-year-old male, nonsmoker with a 4 cm mass located in the left upper lobe was diagnosed with squamous cell carcinoma with clinical stage IIIa. He had no other comorbidities. The bronchus and the arterial branches of the upper lobe were involved. Before the operation, the pulmonary function test, blood gas analysis, cardiac evaluation and basic examinations were within normal limits.

The patient received general anesthesia with dual-lumen endotracheal intubation. He was positioned in the lateral decubitus position with the bed flexed to increase the intercostal spacing. A 1.5-cm-long incision at the 7th intercostal space of the mid-axillary line was placed as camera port; the other incision, 4 cm long, was made in the 4th intercostal space in the anterior position between latissimus dorsi and pectoralis major for utility access. The mass was confirmed in the upper lobe and the arterial branches for the apical segment were involved. The surgical procedure of arterioplasty is described below. Bronchial sleeve lobectomy and anastomosis was then carried out (*Figure 1*).

According to our practice, we released the inferior pulmonary ligament to allow sufficient mobility, retracted the lung superiorly with orbicular-ovate grasping forceps, followed by dissection of the posterior and anterior wall of the hilum. Dissection of lymph nodes in the stations of 7, 10, 4, 5 and 11 was undertaken. The anterior fissure was divided and the posterior fissure was stapled and divided. The branche of the artery for lingular segment were dissected and ligated with silk and divided with ultrasonic scalpel, and then followed by mobilization and transection of the left superior pulmonary vein using a 2 mm stapler (EndoGIA™ 30 mm, Covidien, USA).

Figure 1 Video-assisted thoracoscopic left upper lobe sleeve lobectomy combined with pulmonary arterioplasty via two-port approach (2). Available online: http://www.asvide.com/articles/394

The mass was confirmed in the upper lobe and several ascending arterial branches for the apical segment were involved. Before the surgical procedure for the pulmonary vessels, the bronchus was encircled and then divided. The long scissors were used to transect the bronchus proximal and distal to the tumor over a length about 3 cm.

For the sake of security, the main pulmonary artery and the interlobar artery were dissected to gain adequate vascular control, and then two bulldog clamps (45 mm) were used to occlude them. Single 1-0 silk suture was used around the pulmonary artery trunk (encircled twice) and then the suture was tightened to control the proximal pulmonary artery, followed by application of the bulldog clamps to occlude the main pulmonary artery and the interlobar artery respectively. The instrumentation was inserted through the utility port. Both clamps were placed by orbicular-ovate forceps parallel to the mediastinum to facilitate instrumentation and observation.

Next, long scissors were used to carefully dissect the interspace between pulmonary artery and tumor and the arterial branch was ligated and divided with the ultrasonic scalpel. After further dissection, the branches were deemed impossible to divide directly due to insufficient space. We utilized a 30 mm stapler through the utility port to occlude the branches at their origin with part of the pulmonary artery wall. The thoracoscope was adjusted to confirm an adequate. The lobe was completely disconnected. The sutures and the bulldog clamps were removed to ensure hemostasis of the stapled pulmonary artery sidewall. The specimen was then removed in a glove.

Bronchial reconstruction with the anastomosis between the left main bronchus and lower lobe bronchus was performed subsequently, and long curved suction apparatus and long needle holder were used mainly to finish exposure and suture. The main and lower bronchus were then joined together using complete continuous suture with single 3/0 prolene (Ethicon, Johnson & Johnson, USA). First we used a 1-0 silk suture to retract the pulmonary artery up and forward to get a good visual field, and maneuvered the ends of the bronchus by long curved suction apparatus to facilitate the suture running. We started from the anterior wall of the pars cartilaginea with continuous suture. The knot was made at the posterior wall of the bronchus. Leak testing was conducted following the anastomosis. No leakage was detected up to an airway pressure of 25 cm H_2O. The bronchial anastomosis was covered with an anterior mediastinal fat flap.

Total surgery time was 230 min; the pulmonary artery clamping time was 20 min and estimated blood loss was 200 mL. Postoperative chest X-rays showed no signs of atelectasis. The chest tube was removed on the 5th postoperative day. The patient was discharged on the 7th postoperative day with no complication. A 4 cm squamous cell carcinoma with pathological stage IIb was identified on pathological examination with single bronchial lymph node involvement, while a total of 18 nodes from stations 4, 5, 7, 9, 10 and 11 were clear of tumor.

Discussion

Sleeve resection by VATS has been viewed as an absolute contraindication and few studies have been reported (3). This kind of procedure was increasingly accepted after the first report of a VATS sleeve lobectomy was described by Santambrogio *et al*. in 2002 (4). Nevertheless, in our review, we have found few reports of sleeve lobectomy combined with pulmonary artery arterioplasty performed through a two-port approach. Most of the cases of pulmonary arterioplasty published were performed by using 3-4 incisions, with the vascular clamps inserted through additional incisions (5). Two-port or even single-port VATS for advanced procedures such as vascular arterioplasty can be performed (6). Surgeons and more patients may be more willing to accept the minimally invasive surgery rather than open.

The methods of pulmonary arterioplasty were different. According to the literature, typically the main pulmonary artery and interlobar artery were occluded followed by artery repair using continuous non-absorbable sutures (7). As for this case report, the use of a stapler has not previously been

reviewed and further studies and experience are required.

VATS artery reconstruction and bronchial sleeve lobectomy are all minimally invasive approaches for thorough removal of tumor lesions while sparing normal lung tissue. However, the combined procedure of the two high-risk and technically demanding procedures should be performed only by experienced VATS surgeons.

Acknowledgements

Disclosure: The authors declare no conflict of interest.

References

1. Hennon M, Sahai RK, Yendamuri S, et al. Safety of thoracoscopic lobectomy in locally advanced lung cancer. Ann Surg Oncol 2011;18:3732-6.
2. Jiao W, Zhao Y, Wang X, et al. Video-assisted thoracoscopic left upper lobe sleeve lobectomy combined with pulmonary arterioplasty via two-port approach. Asvide 2014;1:360. Available online: http://www.asvide.com/articles/394
3. Predina JD, Kunkala M, Aliperti LA, et al. Sleeve lobectomy: current indications and future directions. Ann Thorac Cardiovasc Surg 2010;16:310-8.
4. Santambrogio L, Cioffi U, De Simone M, et al. Video-assisted sleeve lobectomy for mucoepidermoid carcinoma of the left lower lobar bronchus: a case report. Chest 2002;121:635-6.
5. Nakanishi R, Yamashita T, Oka S. Initial experience of video-assisted thoracic surgery lobectomy with partial removal of the pulmonary artery. Interact Cardiovasc Thorac Surg 2008;7:996-1000.
6. Gonzalez-Rivas D, Delgado M, Fieira E, et al. Single-port video-assisted thoracoscopic lobectomy with pulmonary artery reconstruction. Interact Cardiovasc Thorac Surg 2013;17:889-91.
7. Alifano M, Cusumano G, Strano S, et al. Lobectomy with pulmonary artery resection: morbidity, mortality, and long-term survival. J Thorac Cardiovasc Surg 2009;137:1400-5.

Cite this article as: Jiao W, Zhao Y, Wang X, Zhao J. Video-assisted thoracoscopic left upper lobe sleeve lobectomy combined with pulmonary arterioplasty via two-port approach. J Thorac Dis 2014;6(12):1813-1815. doi: 10.3978/j.issn.2072-1439.2014.11.09

Total thoracoscopic combined lingulectomy and pericardial cystectomy

Yi Zhang, Yong Lin, Guoyi Shen, Guilong Li

Department of Cardiothoracic Surgery, Zhangzhou Affiliated Hospital of Fujian Medical University, Zhangzhou 363000, China
Correspondence to: Yi Zhang. Department of Cardiothoracic Surgery, Zhangzhou Affiliated Hospital of Fujian Medical University, Zhangzhou 363000, China. Email: 13906969033@163.com.

Abstract: Thoracoscopic anatomic segmentectomy is usually more complex than lobectomy. This video shows a 58-year-old female who suffered from limited bronchiectasis of the lingular segment of the left upper lung and a pericardial cyst on the same side. Both of these benign thoracic diseases can cause pleural adhesions. Repeated chronic inflammation contributes to hypervascularity and lymph node enlargement, making surgery more difficult. We used single-direction thoracoscopic segmentectomy via a three-port approach and successfully removed the lingula and pericardial cyst.

Keywords: Pulmonary segmental resection; bronchiectasis; pericardial cyst; total thoracoscopy

Submitted Sep 07, 2014. Accepted for publication Oct 24, 2014.
doi: 10.3978/j.issn.2072-1439.2014.11.42
View this article at: http://dx.doi.org/10.3978/j.issn.2072-1439.2014.11.42

Introduction

Segmentectomy is an effective treatment for certain lung diseases. In principle, for some benign lesions, lung resection should be sufficient for complete removal without risk of recurrence, but the procedure should conserve a maximum amount of normal lung tissue in order to maintain better lung function. Compared to segmentectomy a lobectomy results in removal of more normal lung tissue, with the potential for worse post-operative lung function. Pulmonary wedge resection also conserves lung tissue, but because it is a non-anatomic resection, it is unsuitable for deep lung tissue resection. In this instance, segmentectomy is a good choice. The increased use of low-dose spiral CT for screening will result in more lung cancer being diagnosed early, including in an older population, therefore thoracoscopic segmentectomy is becoming a topic of much interest and research.

Surgical technology (*Figure 1*)

Triple-port approach by thoracoscopy; the 7th intercostal space on the axillary line for an observation port, the fifth intercostal space on the anterior axillary line for the operating port, and the 8th intercostal on the posterior axillary line for the secondary operations port (*Figure 2*).

Step 1: removal of the pericardial cyst (01:15-01:42)

We used a diathermy hook and an ultrasonic scalpel dissection to divide intrathoracic adhesions. The boundary of pericardial cyst was clear, so we removed it first. We removed the pericardial cyst from the edge, while trying to maintain the integrity of the cyst wall in order to obtain better exposure. The assistant pulled the cyst in the opposite direction to form tension in favor of removal. Neovascularization may exist in the base of the cyst, so we used the ultrasonic scalpel to avoid hemorrhage.

Step 2: release the left inferior pulmonary ligament and mediastinal pleura (03:21-03:50)

The left inferior pulmonary ligament and mediastinal pleura were released, improving lung exposure and retraction in all directions. For the triple-port approach, we place the suction and diathermy hook through the utility port in the 5th intercostal space to divide the anterior mediastinal pleura then use the access through the posterior working

Figure 1 Total thoracoscopic combined lingulectomy and pericardial cystectomy (1).
Available online: http://www.asvide.com/articles/395

Figure 2 Incision position.

port in the 8th intercostal to divide the posterior mediastinal pleura. We have found this to be the simplest.

Step 3: division of the lingular vein (10:27-11:09, 14:20-14:35)

We dissected the left superior pulmonary vein from proximal to distal, isolated three tributaries, confirmed the anatomy, and divided the lingular vein. Vascular variation in lung segments is common, and therefore it is sometimes difficult to separate the independent segment vein. When the segment venous anatomy is difficult to judge, our principle is to divide the most distal vein, to avoid affecting the venous return to the remaining lung segment, which may cause pulmonary congestion. When the left superior pulmonary vein was trifurcated, we would cut only the lowest tributary to the lingula.

Step 4: division of the lingular segmental bronchi (15:45-16:35)

We cleared the bronchus circumferentially then isolated and divided the lingular bronchus. The lingular bronchus can be divided directly without lung expansion if the bronchial anatomy can be clearly demonstrated. We attempt to thoroughly free up the distal bronchi in order to avoid dividing the entire upper lobe bronchi. When we cannot confidently confirm the anatomy, lung expansion, while clamping the presumed lingular bronchus, can be used to avoid accidental lobectomy.

Step 5: complete interlobar fissure and divide the lingular segmental artery (22:50-25:19)

The anterior part of the oblique fissure can be dealt with safely without injuring the pulmonary artery. We next open the pulmonary vascular sheath, making it easier to separate the interlobar fissure. By retracting the left upper lobe superiorly after dividing the interlobar fissure, the lingular artery can be more easily identified, dissected, and divided.

Step 6: completion of the intersegmental fissure (25:55-26:58, 27:40-28:12)

The posterior interlobar fissure does not require division. As the lingular bronchus has been divided, when the left lung is inflated, the intersegmental fissure will be clearly demonstrated. The lingulectomy is completed by dividing the line where the lung tissue fails to inflate.

Surgical evaluation

(I) VATS access can be by single, double, triple or four ports in contemporary practice. Single-port surgery promises minimal trauma and best cosmesis, but may result in more difficult operating conditions. By increasing the number of operating ports, the surgery is easier, surgical speed is improved and we can save more time. Different port access approaches each have their advantages and disadvantages, and should be based on the surgeon's skill and operating practices, as well as the equipment used. We routinely use triple-port surgery, in this way we can place the suction and electrical hook through the utility port in the 5th intercostal space to divide the anterior mediastinal pleura, and through the posterior working port in the 8th intercostal space to divide the posterior mediastinal pleura. During division of the vein and bronchus, when using the stapler from the posterior working port, it is possible to get a better operating perspective, especially using non-roticulating stapler

instruments;

(II) This patient suffered from bronchiectasis in the lingular segment and a pericardial cyst in the ipsilateral hemithorax. Therefore, using triple-port thoracoscopic resection to deal with two lesions in the same incision at the same time was appropriate. The pericardial cyst was mobilized and easily removed, providing much improved space for the VATS approach;

(III) The instruments included suction, diathermy hook, ultrasonic scalpel, and energy platform to dissect tissue in the chest. The diathermy hook is flexible and accurate. The ultrasonic scalpel and energy platform provides good hemostasis;

(IV) Lymph node dissection is unnecessary with benign lesions, but removal of hilar lymph nodes can help reveal blood vessels, trachea and other important structures, improve the speed of surgery and make the surgery safe;

(V) We adhere to the concept of single-direction total thoracoscopic lobectomy (2). We reveal the bronchi and pulmonary artery from front to back after the pulmonary vein is dealt with;

(VI) The difficulties of segmentectomy are the judgment of the target segment and the intersegmental fissure. There are several ways of resolving these. Firstly, the target lung segment remains collapsed, while the surrounding lung segment is inflated (3). Secondly, the target lung segment can be inflated while the surrounding lung segment remains collapsed (4). To achieve this, Okada *et al.* (5) used selective jet ventilation of the target segments via fiberoptic bronchoscopy to determine the boundaries of the segment. A third method is lung segment chromogenic technology. In order to determine the boundary between the lung segments, Misaki *et al.* injected intravenous dye following pulmonary vessel division, so that adjacent lung segments stained, but the target segment did not (6). In keeping with single-direction surgery, the lingular segmental bronchus should be divided first, so we used the first method to determine the target lung segment. This method is relatively simple and easy to teach, and the result is satisfactory.

Cite this article as: Zhang Y, Lin Y, Shen G, Li G. Total thoracoscopic combined lingulectomy and pericardial cystectomy. J Thorac Dis 2014;6(12):1816-1818. doi: 10.3978/j.issn.2072-1439.2014.11.42

Acknowledgements

Disclosure: The authors declare no conflict of interest.

References

1. Zhang Y, Lin Y, Shen G, et al. Total thoracoscopic combined lingulectomy and pericardial cystectomy. Asvide 2014;1:361. Available online: http://www.asvide.com/articles/395
2. Liu L, Che G, Pu Q, et al. A new concept of endoscopic lung cancer resection: Single-direction thoracoscopic lobectomy. Surg Oncol 2010;19:e71-7.
3. Gossot D, Ramos R, Brian E, et al. A totally thoracoscopic approach for pulmonary anatomic segmentectomies. Interact Cardiovasc Thorac Surg 2011;12:529-32.
4. Watanabe A, Ohori S, Nakashima S, et al. Feasibility of video-assisted thoracoscopic surgery segmentectomy for selected peripheral lung carcinomas. Eur J Cardiothorac Surg 2009;35:775-80.
5. Okada M, Mimura T, Ikegaki J, et al. A novel video-assisted anatomic segmentectomy technique: selective segmental inflation via bronchofiberoptic jet followed by cautery cutting. J Thorac Cardiovasc Surg 2007;133:753-8.
6. Misaki N, Chang SS, Igai H, et al. New clinically applicable method for visualizing adjacent lung segments using an infrared thoracoscopy system. J Thorac Cardiovasc Surg 2010;140:752-6.

Visualized Surgery

Video-assisted thoracoscopic surgery right upper posterior segmentectomywith systemic mediastinal lymph node dissection

Lin Ma, Chengwu Liu, Lunxu Liu

Department of Thoracic Surgery, West China Hospital, Sichuan University, Chengdu 610041, China
Correspondence to: Lunxu Liu, MD, PhD. No. 37, Guoxue Alley, Chengdu 610041, China. Email: lunxu_liu@aliyun.com.

Abstract: Video-assisted thoracoscopic surgery (VATS) segmentectomy is a promising treatment option for rigorously selected patients with earlystage non-small cell lung cancer. In the presented video, a 66-year-old male with a 1.6 cm suspicious nodule located at the posterior segment of the right upper lobe was treated with anatomic segmentectomy and systemic mediastinal lymph node (LN) dissection successfully.

Keywords: Video-assisted thoracoscopic surgery (VATS); segmentectomy; lung cancer

Submitted Sep 14, 2014. Accepted for publication Oct 24, 2014.
doi: 10.3978/j.issn.2072-1439.2014.11.43
View this article at: http://dx.doi.org/10.3978/j.issn.2072-1439.2014.11.43

Introduction

Lobectomy is the established procedure for earlystage non-small cell lung cancer (1). However, anatomic segmentectomy has been an optimized choicefor elderly patients and for patients with a compromised cardiopulmonary function (2). In addition, data in medical Literature have demonstrated an equivalent perioperative morbidity and mortality, as well as long-term outcomes of anatomic segmentectomy in patients with smaller tumors (especially ≤2 cm) compared with standard lobectomy (2). Video-assisted thoracoscopic surgery (VATS) approach to anatomic segmentectomy has become widely accepted, achieving similar oncological outcomes compared with the open techniques (3,4). Experienced hands and rigorous patient selection concerning individualized assessment of each patient and tumor characteristics will aid in benefiting more patients. In this video, we will present our operative techniques of VATS right upper posterior segmentectomy with systemic mediastinal lymph node (LN) dissection for the treatment of a 66-year-old male patient with a 1.6 cm suspicious lung nodule. The histology of the nodule was well differentiated adenocarcinoma, the post operative staging was T1aN0M0.

Operative techniques (*Figure 1*)

Port strategy (Figure 2)

First thoracoport (1 cm) was placed in the seventh intercostal space (ICS) at the mid-axillary line (MAL). The main utility incision (2.5 cm) was made at the anterior axillary line (AAL) in the third ICS. The assistant incision (1 cm) was placed in the ninth ICS [between the posterior axillary line (PAL) and subscapular line (SSL)].

Anatomic segmentectomy

The approach to thoracoscopic right upper posterior segmentectomy began with opening the oblique fissure. Incomplete oblique fissure could be divided via endoscopic stapler (Covidien Endo GIA stapler, blue staples). Any LNs encountered would be resected to facilitate further dissection of the posterior segmental artery and drainage vein, which would be encircled and transected together (Covidien Endo GIA stapler, white vascular staples). The next step was the dissection of the posterior segmental bronchus. Before closing the bronchus with the stapler, differential ventilation should be performed to confirm the target bronchus, and to define the correct intersegmental

Figure 1 VATS right upper lobe posterior segmentectomy and lymphadenectomy (5).
Available online: http://www.asvide.com/articles/396

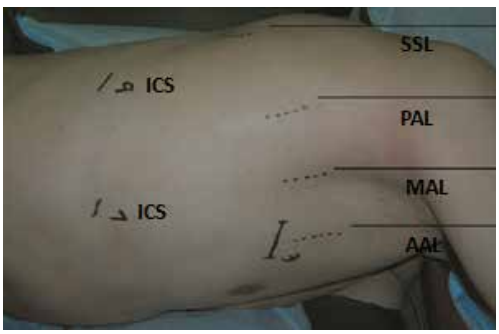

Figure 2 Port strategy. ICS, intercostal space; MAL, mid-axillary line; AAl, anterior axillary line; PAL, posterior axillary line; SSL, subscapular line.

parenchymal plane. Then, the posterior segmental bronchus was transected (Covidien Endo GIA stapler, green staples) followed by division of the parenchyma (Covidien Endo GIA stapler, green and blue staples). The specimen would be retrieved in a self-made bag using a surgical glove.

Lymph nodes (LNs) dissection

Hilar LNs dissection and systemic mediastinal LNs dissection were routinely performed for an adequate staging according to the current oncological guidelines.

2R and 4R stations

Using the electrocoagulation hook (ECH), the dissection was initiated by opening the mediastinal pleura along the caudal border of the azygos vein and detaching the LNs block from the arch of azygos vein. Then, the mediastinal pleura was opened by the ECH along the upper border of the azygos vein and along the posterior border of the superior vena cava (SVC) to the caudal border of the innominate artery. With help of the metal endoscopic suction, the block would be hollowed out using the ultrasound scalpel (US) from the interspace surrounded by the arch of azygos, SVC, lower trachea, and ascending aorta. After the lower part of the block was free, it would be flipped over the arch of azygos vein. Next, the block was dissected off the posterior border of the SVC, the lateral border of the ascending aorta and the anterior border of the trachea sequentially from the upper border of the azygos vein to the caudal border of the innominate artery. At last, the block would be dissected longitudinally and anterior to the vagus nerve en bloc.

7 station

Dissection of the subcarinal LNs block was initiated by opening the mediastinal pleura using the ECH along the posterior border of the right intermediate and main-stem bronchi until approaching the arch of azygos vein. Small bronchial arteries and/or pulmonary branches of the vagus nerve were cut by the US. Then the subcarinal block would be dissected off the right intermediate and main-stem bronchi, pericardium, carina, esophagus, and the left main-stem bronchus.

Comments

In our experience executing VATS segmentectomy there are some tips and pitfalls.

The port strategy is constant with that we used for the single-direction thoracoscopic lobectomy (6) and it will aid the introduction of endoscopic stapler and straight metal endoscopic suction.

To accurately locate the target nodule buried in the parenchyma, we provide two modalities according to different situations: (I) if the chest CT scan shows that the tumor is ≥0.7 cm in diameter and ≤2 cm distant from the visceral pleura, digital palpation will be performed focusing on the target area containing the nodule. After the nodule been palpated, a marking suture is placed in the featureless pulmonary parenchyma on top of the nodule, guided by the surgeon's finger; (II) preoperative CT-guided location by

hook wire will be performed to the nodules ≥2 cm distant from the visceral pleura.

To find the correct artery and vein to posterior segment, opening the borderline between the oblique fissure and the horizontal fissure, and exposing the pulmonary artery is the fist step. After dissected the oblique fissure with the endoscopic stapler, the artery to posterior segment will be exposed and the corresponding vein will be found nearby in most instances. Differential ventilation is used to aid confirming the border of the target segment. The target segment of which the bronchus is clamped will keep collapsing. If the tumor does not conform to discrete segmental boundaries, extended segmentectomy might be worth to obtain an adequate margin especially for a patient who has compromised pulmonary function and cannot bear a lobectomy.

The procedure of mediastinal LN dissection showed a non-grasping en bloc mediastinal LN dissection. When dissecting the subcarinal LNs, meticulousness should be retained to avoid injury to the membraneous portion of the right and left main-stem bronchi. Negative intersegmental LNs should be confirmed by frozen-section pathological examination. Otherwise, this approach should be converted to a VATS lobectomy.

Cite this article as: Ma L, Liu C, Liu L. Video-assisted thoracoscopic surgery right upper posterior segmentectomywith systemic mediastinal lymph node dissection. J Thorac Dis 2014;6(12):1819-1821. doi: 10.3978/j.issn.2072-1439.2014.11.43

Acknowledgements

Disclosure: The authors declare no conflict of interest.

References

1. Vansteenkiste J, Crinò L, Dooms C, et al. 2nd ESMO Consensus Conference on Lung Cancer: early-stage non-small-cell lung cancer consensus on diagnosis, treatment and follow-up. Ann Oncol 2014;25:1462-74.
2. Schuchert MJ, Abbas G, Pennathur A, et al. Sublobar resection for early-stage lung cancer. Semin Thorac Cardiovasc Surg 2010;22:22-31.
3. Swanson SJ. Video-assisted thoracic surgery segmentectomy: the future of surgery for lung cancer? Ann Thorac Surg 2010;89:S2096-7.
4. D'Amico TA. Thoracoscopic segmentectomy: technical considerations and outcomes. Ann Thorac Surg 2008;85:S716-8.
5. Ma L, Liu C, Liu L. VATS right upper lobe posterior segmentectomy and lymphadenectomy. Asvide 2014;1:362. Available online: http://www.asvide.com/articles/396
6. Liu L, Che G, Pu Q, et al. A new concept of endoscopic lung cancer resection: Single-direction thoracoscopic lobectomy. Surg Oncol 2010;19:e71-7.

Visualized Surgery

Video-assisted thoracoscopic left upper lobe apical trisegmentectomy with the Harmonic scalpel

Jun Peng[1], Xin-Long Chen[1], Xin Mao[1], Hui-Ping Wang[2], Jun Liu[1], Xian-Gu Ning[1]

[1]Department of Thoracic Surgery, The First People's Hospital of Yunnan Province, Kunming University of Science and Technology, Kunming 650032, China; [2]Children's Hospital Affiliated to Kunming Medical University, Kunming 650034, China

Correspondence to: Jun Peng. Department of Thoracic Surgery, The First People's Hospital of Yunnan Province, Kunming University of Science and Technology, No. 157 Jinbi Road, Kunming 650032, China. Email: 389647518@qq.com.

Abstract: Segmental resection is a useful procedure to preserve respiratory function. A 56-year-old woman presented with a finding of a left upper lobe lesion on CT scanning. She was performed video-assisted thoracoscopic left upper lobe apical trisegmentectomy with the Harmonic scalpel. Video-assisted thoracoscopy surgery (VATS) segmentectomy is associated with safe and feasible procedure. With the Harmonic scalpel dissection, blood loss is minimal and this speeds patient recovery.

Keywords: Video-assisted thoracoscopy surgery (VATS); segmentectomy; Harmonic scalpel

Submitted Sep 09, 2014. Accepted for publication Oct 28, 2014.
doi: 10.3978/j.issn.2072-1439.2014.11.40
View this article at: http://dx.doi.org/10.3978/j.issn.2072-1439.2014.11.40

Introduction

Segmental resection is a useful procedure to preserve respiratory function. During the past decade, thoracoscopic lobectomy for lung cancer has been widely accepted, but video-assisted thoracoscopic surgery (VATS) segmentectomies are usually more complex procedures than lobectomies. With the gained experience in the field of thoracoscopic surgery, A few thoracic surgeons have progressively adopted VATS segmentectomy to preserve lung parenchyma. Several papers have reported the benefits of thoracoscopic segmentectomy compared with open segmentectomy. Multiple studies of the Harmonic scalpel scalpel have shown it to be safe and to minimize blood loss in various surgeries, such as vaginal hysterectomies and laparoscopic nephrectomies. The purpose of this video was to show our institution's techniques and experience with the Harmonic scalpel scalpel during VATS segmentectomy (*Figure 1*).

The technique of VATS segmentectomy described here is that which is currently employed in the unit of thoracic surgery at The First People's Hospital of Yunnan Province, Kunming University of Science and Technology.

Clinical summary other section

A 56-year-old woman felt chest pain with tenderness before half a year. She presented with a finding of a left upper lobe lesion on CT scanning. Past medical history included a high blood pressure 4 years. CT imaging revealed a 9.7 mm AP × 9.3 mm TR, lesion in the left upper lobe (LUL) which may be adherent to the aorto (*Figures 2,3*). Bronchoscopy and brushings did not show any bronchial abnormal. Lung function was assessed via formal spirometry with a FEV1 of 1.97 (89% predicted), a FVC of 2.04 (81% predicted) and an FEV1/FVC ratio of 96.5%. The patient was proposed for VATS. She was performed video-assisted thoracoscopic left upper lobe apical trisegmentectomy. The frozen pathological examination revealed a hamartoma during opration. The surgical time was 70 min. Postoperative hospital stay was 4 days.

Technique other section

Positioning and incisions

The patient is placed in the right lateral decubitus position with a slight posterior tilt under single-lung ventilation. The surgeon stands on the anterior side of the patient. The 10-mm camera port is made at the seventh intercostal space between the anterior and mid-axillary line. The utility incision (3.0 cm in length) is placed at the third intercostal space in the anterior axillary line. The utility incision is

Figure 1 VATS segmentectomy: the First People's Hospital of Yunnan Province, Kunming University of Science and Technology (1). Available online: http://www.asvide.com/articles/397

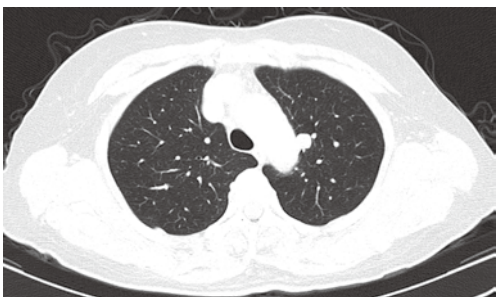

Figure 2 Axial chest CT shows a left upper lobe lesion on lung window.

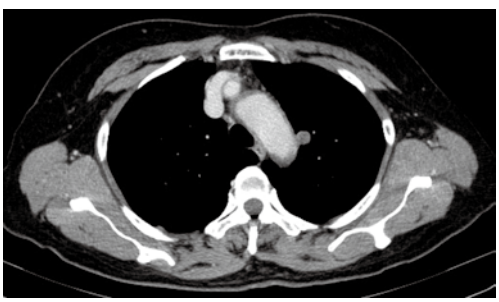

Figure 3 Axial contrast-enhanced chest CT shows a left upper lobe lesion on mediastinal window.

located directly over the superior pulmonary vein for a left upper lobe apical trisegmentectomy. An additional 10-mm posterior port is made at the ninth intercostal space left below the tip of the scapula.

The first step in the procedure is to confirm resectability and identify invasion of the chest wall, pleurae and hilar structures including the aorta, pulmonary artery and bronchus.

The order of the steps of the operation is as follows: posterior, anterior, and superior pleurae over the hilum; upper division vein; anterior trunk; posterior artery; bronchus; and the fissure.

Step 1: tumor palpation

Exposure: move the lung toward the access port with a ringed forceps placed through the posterior port.

Place the thoracoscope in the camera port with the side arm straight up.

Carefully palpate and examine the tumor to be certain a sublobar resection constitutes optimal cancer treatment. This is done by corroborating the tumor size and confirming that tumor is far enough away from the lingula so that the margins will be adequate if a trisegmentectomy is performed.

Step 2: takedown inferior pulmonary ligament and posterior mediastinal pleura

Exposure: hold the left lower lobe superiorly with a ring clamp through the posterior incision.

The thoracoscope is aimed anteriorly with the 30-degree lens pointed posteriorly. The suction catheter introduced from the utility incision. Transect the inferior pulmonary ligament with Harmonic scalpel, which is brought through the posterior incision. The tip of the suction catheter should be held close to the Harmonic scalpel tip to aid in blunt dissection and remove the smoke created. Harmonic scalpel transects the ligament up to the level of the right inferior pulmonary vein. Retract the left lower lobe lung anteriorly to show posterior mediastinal pleura. Continue opening the pleural superiorly until the apical hilum.

Step 3: open anterior hilum and aortopulmonary window

Exposure: retract the left upper lobe posteriorly with a ring clamp through the posterior port.

Place the thoracoscope in the camera port with the side arm to the left to look at anterior hilar structures. Aim the thoracoscope slightly anteromedially and the lens slightly posteriorly. Open the mediastinal pleura over the anterior hilum with the Harmonic scalpel and the suction catheter. This defines the venous drainage from the upper division of the left upper lobe (LUL). Dissect superiorly to the level of the aortopulmonary window. Removal of the level 5 nodes facilitates exposure of the vessels and prepares the superior

and posterior aspect of the anterior trunk for subsequent transection.

Step 4: upper division pulmonary vein division

Exposure: retract the left upper lobe posteriorly with a ring clamp through the posterior port.

The thoracoscope is aimed anteriorly and slightly medially, and the lens is pointed toward the mediastinum and slightly posteriorly.

Bring the suction catheter through the utility incision while passing the Harmonic scalpel through the posterior incision. With the Harmonic scalpel and suction catheter, dissect the inferior border of the Superior pulmonary vein. Carefully identify and preserve the lingular veins. Mobilize the upper division pulmonary vein. Extension between the vein and the bronchus with right-angle clamp farther than the anvil is performed, since this approach ensures that the stapler completely crosses the vein before stapling. Divide the upper division pulmonary vein using an endovascular stapler placed through the posterior port while retracting the lung with a ring forceps placed through the utility incision. The stapler is closed and fired. After transecting the vein, the left upper lobe bronchus and anterior trunk can be seen.

Step 5: anterior trunk

Exposure: the lung is retracted laterally and inferiorly through the posterior incision.

The thoracoscope is aimed anteriorly, and the lens is pointed slightly posteriorly. After stapling the superior pulmonary vein, the anterior trunk of the pulmonary artery (PA) is readily visualized. Incise the lymphatics on the superior aspect of the LUL bronchus, and remove lymph nodes to better expose the PA. Remove the lymph node between the bifurcation of the anterior trunk and the main PA for easier isolation of the anterior trunk.

A right-angle clamp introduced through the utility incision passes around the anterior trunk of the PA. Adjust the angle of the camera to allow complete visualization of the right-angle clamp as it encircles the anterior trunk. There should be little or no resistance to the passage of the right-angle clamp after prior dissection of the superior aspect of the hilum. The right-angle clamp is spread widely to create an adequate tunnel for subsequent stapler placement.

The vascular stapler is brought through the posterior incision and placed across the anterior trunk. The anvil of the stapler should be placed in the tunnel between the PA and the anterior trunk. The anterior trunk was transected.

Step 6: posterior artery division

Exposure: a ring clamp through the posterior incision lifts the upper lobe to expose the posterior segmental artery to the left upper lobe.

The thoracoscope is positioned with the 30-degree lens pointing medially, and the lens pointing posteriorly. Begin a combination of blunt and sharp dissection on the surface of the main PA to expose the posterior segmental artery to the left upper lobe. The right-angle clamp is spread widely to create an adequate tunnel for subsequent stapler placement. Divide the posterior segmental artery with an endovascular stapler introduced through the posterior port.

Step 7: bronchus division

Exposure: retract the lung toward posteriorly with a ringed forceps through the posterior incision to gain as much length on the bronchus as possible, and put it under some mild tension in the vertical plane.

Dissect the anterior aspect of the bronchus. Identify the upper division bronchus in the fissure, and sweep all peribronchial tissue up onto the bronchus with the Harmonic scalpel and suction catheter. This helps to identify the carina between the upper division bronchus and the lingular bronchus.

Dissect the anterior aspect of the upper division bronchus. The right-angle clamp is spread widely to create an adequate tunnel. Introduce a silk thread across the upper division bronchus and pull toward the utility incision for subsequent stapler placement. Use an endobronchial stapler placed through the posterior port to divide the upper division bronchus. Reinflation of the lung after closed stapler helps to ensure that the correct bronchus is occluded and that there is no impingement on lingual bronchi. It must be ensured that there are no devices within the airway, and fire the stapler.

Step 8: complete the fissure between the upper division and the lingula

The anesthesiologist should inflate the left lung. The lingula inflates adequately. The bronchus for the upper division can be divided and the lingula ventilated to determine where

to place the staples to separate the upper division. At the same time the vessels help to determine the separation between the upper division and the lingual. Divide the lung anteriorly between the stump of the upper division vein and lingular vein by placing the stapler through the utility incision while retracting the lung toward the anterior chest wall with a ring forceps placed through the posterior port. Finish the fissure between the upper division and the lingual from anterior to posterior with staplers through the utility incision.

Step 9: specimen retrieval

The left upper lobe apical trisegmentectomy is placed into an open bag for removal through the utility incision.

Comments

VATS segmentectomy is safe and feasible procedure in experienced VATS centres. The difficulty of thoracoscopic segmentectomies is mainly based on the division of the segmental plane and the distal dissection of hilar structures. Our technique is dissection of hilar structures go forward one by one from anterior to posterior. We found the procedure was performed smoothly and easily. With Harmonic scalpel dissection, blood loss is minimal and this speeds patient recovery. The technique of VATS lobectomy with Harmonic scalpel is outlined in a previously published report (2). It does not leave behind foreign materials, such as sutures or clips, and there is therefore more rapid wound healing and less chance of delayed complications.

Cite this article as: Peng J, Chen XL, Mao X, Wang HP, Liu J, Ning XG. Video-assisted thoracoscopic left upper lobe apical trisegmentectomy with the Harmonic scalpel. J Thorac Dis 2014;6(12):1822-1825. doi: 10.3978/j.issn.2072-1439.2014.11.40

Acknowledgements

Funding: The Fund of Application Basis Research of Yunnan Province (2010ZC216).
Disclosure: The authors declare no conflict of interest.

References

1. Peng J, Chen XL, Mao X, et al. VATS segmentectomy: the First People's Hospital of Yunnan Province, Kunming University of Science and Technology. Asvide 2014;1:363. Available online: http://www.asvide.com/articles/397
2. Peng J, Chen XL, Mao X, et al. Video-assisted thoracoscopic right lower lobectomy for lung cancer using the Harmonic scalpel. J Thorac Dis 2013;5:864-7.

Visualized Surgery

Left lower sleeve lobectomy and systematic lymph node dissection by complete video-assisted thoracic surgery

Jun-Qiang Fan, Jie Yao, Zhi-Bo Chang, Qi Wang, Bai-Qin Zhao

Department of Thoracic Surgery, the Second Affiliated Hospital of Zhejiang University College of Medicine, Hangzhou 310009, China
Correspondence to: Jie Yao, MD. Department of Thoracic Surgery, the Second Affiliated Hospital of Zhejiang University College of Medicine, 88 Jiefang Road, Hangzhou 31009, China. Email: fanfun@126.com.

Abstract: Sleeve lobectomy for selected cases of central lung cancer has better functional outcomes comparing to pneumonectomy. With improved technology and increased experiences in complete video-assisted thoracic surgery (VATS) lobectomy, complete VATS sleeve lobectomy has been applied in major medical centers recently. A 64-year-old male patient with left lower central lung cancer underwent thoracoscopic sleeve lobectomy and systemic mediastinal lymph node dissection. The major incision, of four incisions in total, was a 4 cm mini-incision in the 4th intercostal space of anterior axillary line. The patient had recovered uneventfully after the surgery.

Keywords: Sleeve resection; lobectomy; lung cancer; mediastinal lymph node dissection; video-assisted thoracic surgery (VATS)

Submitted Aug 16, 2014. Accepted for publication Oct 28, 2014.
doi: 10.3978/j.issn.2072-1439.2014.12.01
View this article at: http://dx.doi.org/10.3978/j.issn.2072-1439.2014.12.01

Introduction

In 1947, Price Thomas pioneered a circumferential resection of the right bronchus in a patient with bronchial adenoma (1). A decade later, in 1956, Allison reported the first case of non-small-cell lung carcinoma (NSCLC) treated by sleeve lobectomy (2). Sleeve lobectomy adequately preserves the lung function and achieves complete resection of the neoplasm, recently developed in selected cases of lung cancer patients. Various studies have shown that the long-term survival after sleeve resection is similar or sometimes better than pneumonectomy, but results in the lower perioperative risk and better quality of life (3-6).

Video-assisted thoracic surgery (VATS) lobectomy, first reported in 1992 (7), had developed an established approach for lung cancer management after 20 years of technique improvement. Due to the surgical difficultly, VATS sleeve lobectomy used to be a contraindication in lung cancer surgical treatment (8). Nowadays with improved technology and increased experiences in VATS lobectomy, thoracic surgeons have gradually mastered the techniques of sleeve lobectomy by VATS. Left lower lobectomy with sleeve bronchial resection is one of the most difficult thoracic surgical procedures (9), and approach to left bronchial anastomosis is also limited and unclear. Here we present a technical procedure for left lower sleeve lobectomy by complete VATS.

Case presentation

A 64-year-old male was presented with cough for 2 months. He had a history of subtotal gastrectomy, cholecystectomy and hypertension. He had smoked about 20 cigarettes per day for 40 years. A preoperative chest computed tomography (CT) revealed a mass in the left hilum of the lung, with complete left low pulmonary atelectasis (*Figure 1*), and fiberoptic bronchoscopy showed a neoplasm at the orifice of the left lower lobar bronchus (*Figure 2*). Preoperative pathological examination of the lung lesion indicated a poorly differentiated squamous cell carcinoma. Left lower Sleeve lobectomy was performed. The operation takes 200 minutes. During the operation, the estimated blood loss was 100 mL. On postoperative day (POD) 1, the amount of fluid drainage was 350 mL, and chest X-ray showed left lung inflation satisfactory (*Figure 3*). The chest

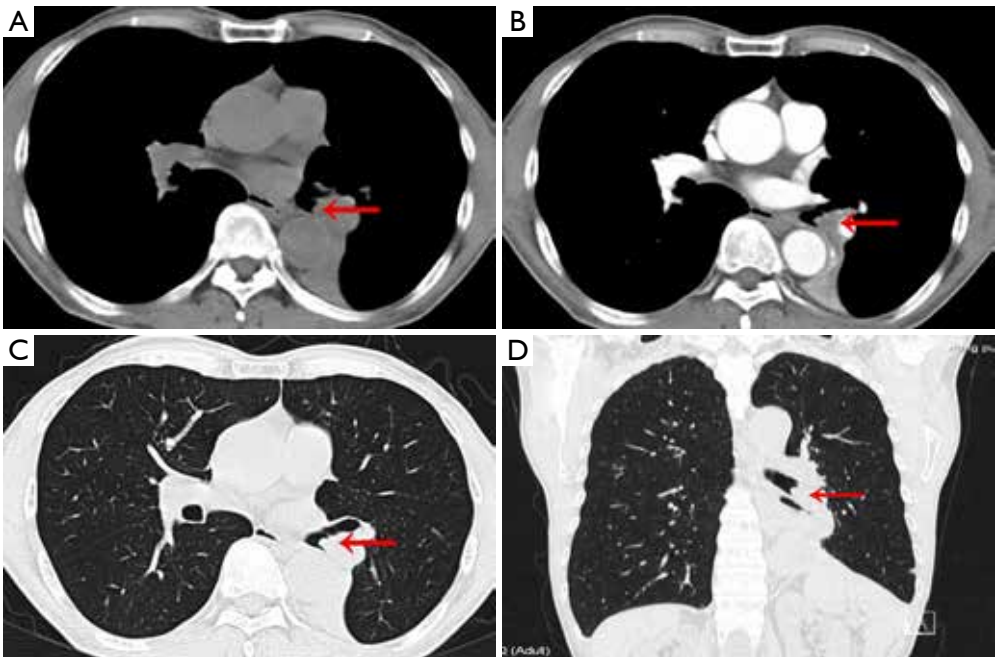

Figure 1 A chest CT scan revealed left lower lobe atelectasis, and a mass (red arrowheads) in the left hilum (lung cancer). CT, computed tomography.

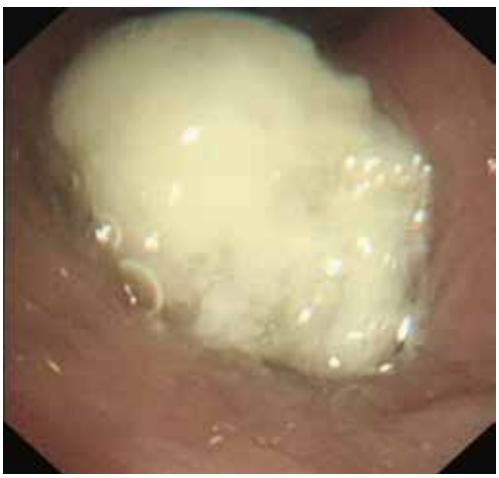

Figure 2 Fiberoptic bronchoscopy demostrated the neoplasm located at the orifice of left lower lobe bronchus.

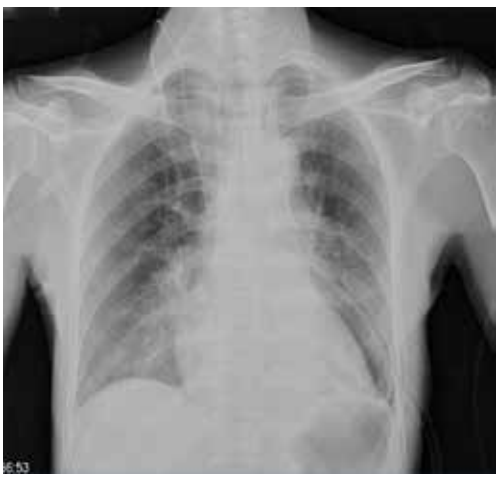

Figure 3 Chest X-ray showed left lung inflation satisfactory on POD 1. POD, postoperative day.

tube was removed on POD 4. The patient was discharged on POD 6 with no complications. The tumor size was 3 cm in diameter, and the pathology confirmed lymph metastasis in station 9 while the other lymph stations were negative pathological results. Three months later, a chest CT showed no obvious locoregional recurrence (*Figure 4*). Six months later, fiberoptic bronchoscopy showed the intact anastomosis site and no sign of stenosis (*Figure 5*).

Operative techniques

(I) Operative insicion: four insicions were performed (*Figure 6*), the initial camera port (1.5-cm-long incision) was made in the 7th intercostal space in the midaxillary line, the utility incision (4-cm-long incision) was placed at the level of 4th intercostal space in anterior axillary line. Another two 0.5-cm-

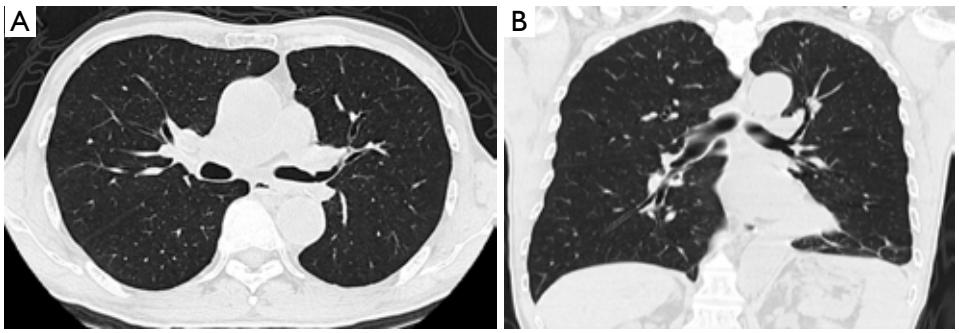

Figure 4 Postoperative chest CT showed no locoregional recurrence after 3 months of surgery. CT, computed tomography.

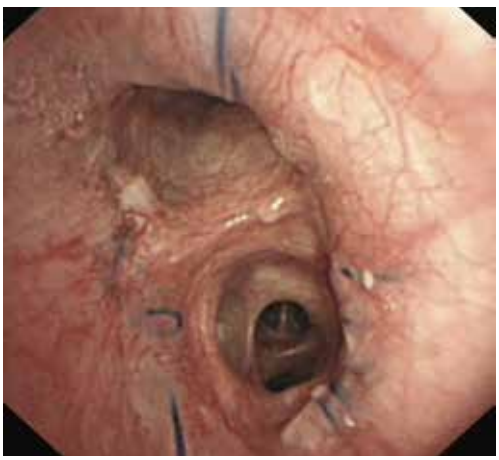

Figure 5 Postoperative fiberoptic bronchoscopy showed the intact anastomosis site and no sign of stenosis at 6 months after surgery.

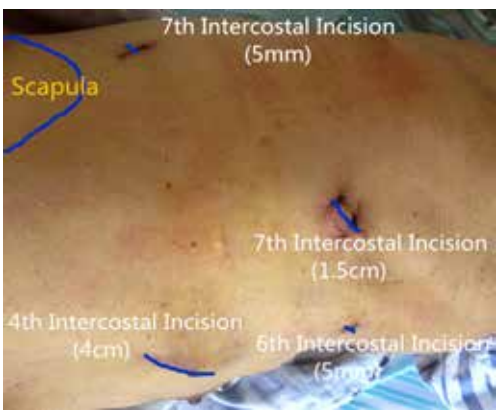

Figure 6 Operative incisions.

long additional insicions were performed in the 7th intercostal space in the posterior axillary and in the 6th intercostal space in the anterior axillary line respectively. A 0.5 cm incisional length may reduce the impairment and compression of intercostal nerves and vessels, and increase the conveniency of operation. No rib spreader was used;

Figure 7 Video-assisted thoracic surgery, left lower sleeve lobectomy (10).
Available online: http://www.asvide.com/articles/398

(II) Operative key points and procedure (*Figure 7*).
- (i) After division of the inferior pulmonary ligament the lymph nodes from stations 8 and 9 were excised. The dissection continued by division of the mediastinal pleura around the pulmonary hilum;
- (ii) Mobilization of pulmonary vessels. The pulmonary artery was identified and dissected at the fissure. The oblique fissure was dissected by ultrasonic scalpel. The pulmonary artery sheath was dissected by electrocautery hook, and the lower lobe branches of pulmonary artery were mobilized. The basal and dorsal segmental artery was stapled with a vascular (white cartridge, 45-mm-long) endostapler (Endo GIA, Covidien, USA). The fissure was completed by a stapler firing. The lymph nodes of station 11 was then dissected;
- (iii) Dissection of mediastinal lymph nodes. The ring forceps was applied to pull the left lower lung

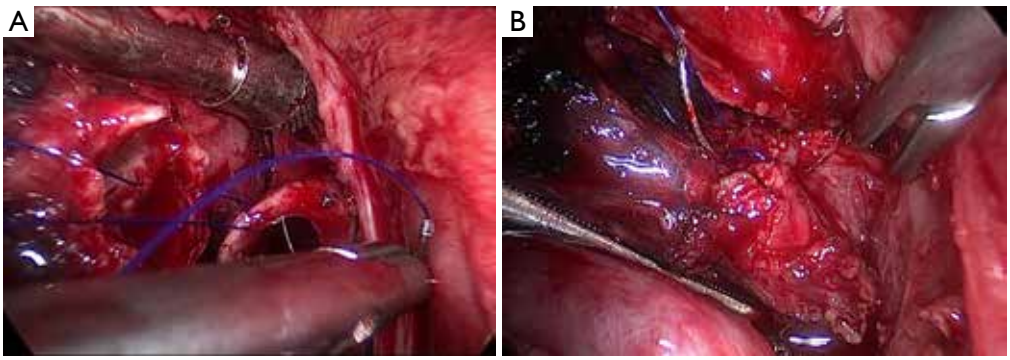

Figure 8 (A) Anastomosis of the posterior bronchus; (B) anastomosis of the anterior bronchus.

forwards to expose the posterior mediastinum. We dissected along the posterior aspect of subcarinal lymph nodes (station 7), and the small vessels between esophagus and lymph nodes were cauterized with electrocautery hook to reduce bleeding. The lymph nodes of station 7 were completely removed. The station 4 lymph nodes were dissected using a combination of blunt and sharp dissection technique, with special care to expose and to preserve the left recurrent laryngeal nerve. The stations 5 and 6 lymph nodes were dissected with avoidance of the phrenic nerve and the left innominate vein damage;

(iv) Bronchial anastomosis. The secondary carina and left main bronchus were completely dissected. The left main bronchus and upper bronchus was transected through the utility incision. The lobe was placed in a specimen bag and was then removed from the thoracic cavity. The specimen was sent for pathological frozen section, and bronchial margins were confirmed negative. A 4-0 prolene was used in continuous suture for anastomosis from posterior to anterior. The knots were made outside the bronchial lumen (*Figure 8*). When anastomosis proceeding, needle holder was placed through a 5 mm incision at the 6th intercostal space in the anterior axillary line or the 7th intercostal space in the posterior axillary;

(v) Check the anastomosis. The bronchus anastomosis was tested with lavage with distilled water, and the lung was inflated to rule out the air leak.

Comments

Sleeve lobectomy was an approach option only for thoracotomy before because of its difficulty. Patients undergoing traditional thoracotomy suffered problems like slow recovery, serious trauma, and postoperative pain. However, comparing to thoracotomy, VATS lobectomy has various potential advantages like less postoperative pain, faster recover, fewer complications, and shorter hospital stay (11). Thanks to the rapid improvement and development of thoracoscopic techniques in recent decades, VATS sleeve lobectomy gradually became a feasible, attractive and challenging procedure for selected patients.

Bronchial anastomosis in VATS sleeve lobectomy used to be difficult. The key points of this procedure are removal of subcarinal lymph nodes (station 7) and station 11 lymph nodes, and completely dissection of the secondary carina and left main bronchus. Continuous or interrupted suture can be applied to anastomosis after bronchus transection. According to our experience, the method of continuous suture takes less time. The "difficult-to-easy" principle should be followed while placing sutures from posterior to anterior along the membranous portion with 4-0 prolene. Meanwhile, suturing order should be properly arranged to prevent twisting. Single continues suture could reduce the probability of twining (9).

Proper incision placement is critical in bronchial anastomosis of VATS sleeve lobectomy. We chose three routine incisions for the most of VATS lobectomies. We also added a port in the left lower sleeve lobectomy. During bronchial anastomosis procedure, the needle holder was put through the 5-mm-long incision at the 6th intercostal space in the anterior axillary line and the 7th intercostal space in the posterior axillary. A 0.5 cm of incisional length may reduce the impairment of chest wall and the adjacent tissues, especially the intercostal nerves, and could increase the conveniency of operation (12).

VATS sleeve lobectomy is feasible and safe. However,

VATS sleeve lobectomy, like all other procedures, has its learning curve for surgeons and assistants. According to our own experience, we suggest that a surgeon needs to perform at least 100 cases of VATS lobectomy and 20 cases of open sleeve resection procedures before beginning to perform VATS sleeve lobectomy. In addition, the cases for VATS sleeve lobectomy should be highly selected, limited to a few conditions especially like small central tumors.

In conclusion, VATS sleeve lobectomy should be an ideal option in patients with specific surgical indications. Development of VATS techniques may gradually make VATS sleeve lobectomy a more common procedure in thoracic surgery.

Acknowledgements

Disclosure: The authors declare no conflict of interest.

References

1. Thomas CP. Conservative resection of the bronchial tree. J R Coll Surg Edinb 1956;1:169-86.
2. Allison PR, Course of thoracic surgery in Groningen. Ann R Coll Surg 1954;25:20-22.
3. Okada M, Yamagishi H, Satake S, et al. Survival related to lymph node involvement in lung cancer after sleeve lobectomy compared with pneumonectomy. J Thorac Cardiovasc Surg 2000;119:814-9.
4. Terzi A, Lonardoni A, Falezza G, et al. Sleeve lobectomy for non-small cell lung cancer and carcinoids: results in 160 cases. Eur J Cardiothorac Surg 2002;21:888-93.
5. Merritt RE, Mathisen DJ, Wain JC, et al. Long-term results of sleeve lobectomy in the management of non-small cell lung carcinoma and low-grade neoplasms. Ann Thorac Surg 2009;88:1574-81; discussion 1581-2.
6. Ma Z, Dong A, Fan J, et al. Does sleeve lobectomy concomitant with or without pulmonary artery reconstruction (double sleeve) have favorable results for non-small cell lung cancer compared with pneumonectomy? A meta-analysis. Eur J Cardiothorac Surg 2007;32:20-8.
7. Roviaro G, Rebuffat C, Varoli F, et al. Videoendoscopic pulmonary lobectomy for cancer. Surg Laparosc Endosc 1992;2:244-7.
8. McKenna RJ Jr, Houck W, Fuller CB. Video-assisted thoracic surgery lobectomy: experience with 1,100 cases. Ann Thorac Surg 2006;81:421-5; discussion 425-6.
9. Gonzalez-Rivas D, Delgadoa M, Fieira E. Left lower sleeve lobectomy by uniportal video-assisted thoracoscopic approach. Interact. CardioVasc Thorac Surg 2014;18:237-9.
10. Fan JQ, Yao J, Chang ZB, et al. Video-assisted thoracic surgery, left lower sleeve lobectomy. Asvide 2014;1:364. Available online: http://www.asvide.com/articles/398.
11. Shaw JP, Dembitzer FR, Wisnivesky JP, et al. Video-assisted thoracoscopic lobectomy: state of the art and future directions. Ann Thorac Surg 2008;85:S705-9.
12. Fan J, Chang Z, Ye C, et al. Video-assisted thoracoscopic superior segmentectomy of the right lower lobe. J Thorac Dis 2013;5:S287-8.

Cite this article as: Fan JQ, Yao J, Chang ZB, Wang Q, Zhao BQ. Left lower sleeve lobectomy and systematic lymph node dissection by complete video-assisted thoracic surgery. J Thorac Dis 2014;6(12):1826-1830. doi: 10.3978/j.issn.2072-1439.2014.12.01

Visualized Surgery

Video-assisted thoracic surgery right sleeve lobectomy

Fei Xiong, Sheng Wang, Jindan Kai

Department of Thoracic Surgery, Hubei Cancer Hospital, Wuhan 430000, China

Correspondence to: Fei Xiong. Department of Thoracic Surgery, Hubei Cancer Hospital, No. 116 Zhuodaoquan South Load, Hongshan District, Wuhan 430000, China. Email: xiongf66@sohu.com.

Abstract: A 50-year-old active male with a smoking history of 30 years (20 cigarettes per day) was admitted to hospital because of more than one month's cough without sputum. No comorbidity was present. The preoperative examination showed: blood test normal, ECG normal, cardio-pulmonary function normal, chest computed tomography (CT) display right upper lobe (RUL) mass of 5 cm diameter. Bronchoscopy examination and biopsy indicated large cell neuroendocrine carcinoma (LCNEC) in the take-off of RUL bronchus. No metastatic focus was found after emission computed tomography (ECT) scan of whole body bone, abdominal US scanning and brain MR. After initial evaluation, the clinical stage before operation was cT2bN0M0 (IIA stage). A selective video-assisted thoracic surgery (VATS) operation was arranged after 9 days of smoking cessation. Lateral position, one 10 mm trocar for camera in the 7th intercostals space in the mid-auxiliary line, 4 cm trocar for operation in the 4th intercostal space in the anterior axillary line, 15 mm trocar for auxiliary operation in the 8th intercostal space in the scapula line, the patient received VATS RUL lobectomy, plus systemic mediastinal lymph nodes dissection. The procedure of 200 minutes operation was smooth with blood loss of about 150 mL. Chest tube was removed 6 days after operation, and the patient discharged 11 days after the operation; The post-operation pathological examination showed RUL LCNEC, and the pathological stage was pT2bN0M0R0 (IIA stage). The patient has received four cycles of EP adjuvant chemotherapy per 21 days and is still alive without disease recurrence and metastasis after re-examination.

Keywords: Carcinoma; non-small-cell lung; thoracic surgery; video-assisted; pneumonectomy; thoracic surgical procedures

Submitted Aug 13, 2014. Accepted for publication Oct 31, 2014.
doi: 10.3978/j.issn.2072-1439.2014.12.03
View this article at: http://dx.doi.org/10.3978/j.issn.2072-1439.2014.12.03

Introduction

In recent years, lung cancer has become the leading malignant tumor in terms of morbidity and mortality in many countries around the world (1). The pneumonectomy plus systemic mediastinal lymph nodes dissection is one of the major lung cancer treatments which contribute to survival benefit for many lung cancer patients (2). In selective patients, either intentional or compromised sleeve lobectomy, instead of pneumonectomy, could obtain better quality of life and adjuvant treatment compliance after radical tumor dissection, which has been widely recognized by thoracic surgeon (3). Many multiple-institutional trials have already reported that video-assisted thoracic surgery (VATS) pulmonary lobectomy plus systemic mediastinal lymph nodes dissection could obtain comparable and even more satisfactory immediate and long-term therapeutic results than traditional thoracotomy. Therefore, VATS has already been accepted by National Comprehensive Cancer Network (NCCN) as one of surgery candidates for lung cancer since 2006. With increasing and improving experience, more VATS lung-sparing lobotomy with bronchoplasty and/or angioplasty has be performed in selected patients, but there is still no standard and widely accepted surgical procedure.

Operative techniques (*Figure 1*)

Patient and trocar position (Figure 2)

The patient was set in the lateral position with the arm hanging down. The surgeon stood at the abdominal of the patient. After single lung ventilation, three trocars were inserted:

Figure 1 Video-assisted thoracic surgery right sleeve lobectomy (4). Available online: http://www.asvide.com/articles/399

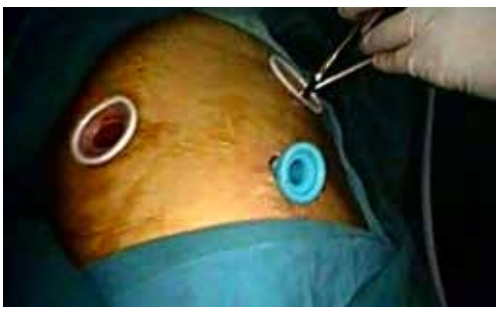

Figure 2 Trocars position.

(I) Ten mm trocar in the 7th intercostal space in the mid-axillary line for the scope camera (Storz, 30 degree);
(II) A total of 15 mm trocar in the 8th intercostal space in the scapula line, for the endostaple (Covidien, Mansfield, MA, USA) and other instruments such as grasping forceps, Harmonic scalpel and suction;
(III) Four cm length trocar was inserted in the 4th intercostal space in the anterior axillary line, and this port for the main operation, such as grasping, dissection, suction, specimen extraction, and suturing.

Mobilization and dissection of the upper lobe branch of the right superior pulmonary vein

The upper lobe branch of the right superior pulmonary vein was dissected after dividing of the parietal pleura anterior to the phrenic nerve; the adjacent middle lobe vein must be carefully preserved. When the upper, lower, and anterior borders were dissected out, the vein was encircled with a right-angled clamp and transected with an endoscopic vascular stapler (Covidien, 2.5 mm). The ongoing pulmonary artery that lies directly posterior to the vein must be carefully avoided.

Mobilization and dissection of the truncus anterior branch of the right pulmonary artery

Grasping the divided vein end, the ongoing pulmonary artery was dissected out. Dividing the pulmonary artery adventitial, the superior and inferior border of the truncus anterior branch was dissected. The plane between the right upper bronchus and the truncus anterior branch artery was then carefully developed. This is a difficult area to repair if injured. Once the plane developed, the artery was encircled with a right-angled clamp and transected with an endoscopic vascular staple (Covidien, 2.5 mm) through the 8th intercostal space trocar in the scapula line.

Dissection of the horizontal fissure with harmonic scalpel

We divided the minor fissure between the right upper and middle lobe that were almost complete with harmonic scalpel.

Mobilization and dissection of the superior segmental anterior of the right lower lobe

After dividing the minor fissure, the posterior ascending branch arising from the superior segmental artery of the right lower lobe was dissected. The posterior ascending branch could not be freely mobilized because the take-off of the artery was entirely invaded by the tumor. Then the superior segmental artery of the right lower lobe was carefully dissected out. Being retracted with 1-0 silk, the artery was then divided with an endoscopic vascular stapler (Covidien, 2.5 mm) through the 8th intercostal space trocar in the scapula line.

Dissection of the #7 and #8 stations of mediastinal lymph nodes

Grasping upwards the right lower lobe gently, the right inferior pulmonary ligament up to the inferior pulmonary vein and parietal pleura anterior to the esophagus was divided with electrocautery. When the esophagus was kept retracted posteriorly and the lung anteriorly, the #7 and #8 stations of mediastinal lymph nodes were entirely dissected with Harmonic. The dissection was carried out along the border of the left and right main stem bronchus, pericardium, and esophagus, which should be carefully reserved to avoid inadvertent injury. Bronchial and esophageal arterial branches were carefully clipped with Harmonic. The posterior aspect of the major fissure were thick and incomplete, it was divided with endoscopic stapler (Covidien, 4.8 mm) through the 4th intercostal space trocar in the anterior axillary line.

Extraction of the specimen

The 11th lymph nodes adjacent to the intermediate bronchus were dissected with Harmonic. When all the lymph nodes was swept off the bronchus or up into the specimen, the right main bronchus and intermediate bronchus was mobilized and cut off respectively with scissor. The specimen was packed into a 7.5 size glove and then extracted through the 4th intercostal space incision in the anterior axillary line. The proximal and distal bronchus resection margins were checked to be pathology negative in the intraoperative frozen section analysis.

Anastomosis of the bronchus ends

The anastomosis between the right main bronchus and intermediate bronchus ends (end-to-end anastomosis) were performed carefully by running and circumferential suture technique with one 3-0 non-absorbable prolene suture (BRAUN). The first suture was begun at the membranous and cartilaginous junction portion. The suture was tightened by nerve hook when the posterior wall of the anastomosis was completed. Then the suture of the anterior wall was performed. When the whole anastomosis was completed, we tightened and tied the suture. Finally, the right middle and lower lobes were inflated to ensure that the anastomosis and airway were air leaks free.

Dissection of the #2 and #4 stations of mediastinal lymph nodes

After dividing the parietal pleura posterior to the superior vena cava and superior to the azygos vein with electrocautery, the #2 and #4 stations of mediastinal lymph nodes were entirely dissected with Harmonic. The right recurrent nerve should be carefully preserved to avoid injury and the small venous branches off the superior vena cava were carefully clipped with harmonic.

Completion of the procedure

When the sleeve lobectomy and radical lymphadenectomy were completed, the right middle lobe and lower lobe received reventilation. The chest tube (24F) was administrated through the camera port in the 7th intercostal space and the tip of the tube was kept in the cavity of the removed right upper lobe (RUL).

Comments

Compared to pneumonectomy, sleeve lobectomy (more technically demanding) can obtained lower associated morbidity and mortality together with more satisfactory cardiopulmonary function and comparable long-term outcome (1,5). VATS sleeve lobectomy developed in recent years for lung cancer in selected patients is proven technically feasible and safe. Various suture material and technique for the bronchus anastomosis are proven feasible. The running and circumferential suture technique for end-to-end bronchus anastomosis with the material of one 3-0 non-absorbable prolene suture which could be easily tightened by nerve hook is proven to be ease, feasible, safe and time-saving, and the kinking of the suture which should be especially carefully avoided in VATS is the main pitfall of the procedure. We do not consider the encirclement of the anastomosis in sleeve lobectomy is necessary even after the skeletonizing of the bronchus. The suture technique performed in the video could simplify the procedure. With increasing experiences, more VATS lung-sparing surgeries should be encouraged to be performed in selected patients in high volume lung cancer centers.

Acknowledgements

Disclosure: The authors declare no conflict of interest.

References

1. Siegel R, Ma J, Zou Z, et al. Cancer statistics, 2014. CA Cancer J Clin 2014;64:9-29.
2. Ginsberg RJ, Rubinstein LV. Randomized trial of lobectomy versus limited resection for T1 N0 non-small cell lung cancer. Lung Cancer Study Group. Ann Thorac Surg 1995;60:615-22; discussion 622-3.
3. Parissis H, Leotsinidis M, Hughes A, et al. Comparative analysis and outcomes of sleeve resection versus pneumonectomy. Asian Cardiovasc Thorac Ann 2009;17:175-82.
4. Xiong F, Wang S, Kai J. Video-assisted thoracic surgery right sleeve lobectomy. Asvide 2014;1:365. Available online: http://www.asvide.com/articles/399
5. Stallard J, Loberg A, Dunning J, et al. Is a sleeve lobectomy significantly better than a pneumonectomy? Interact Cardiovasc Thorac Surg 2010;11:660-6.

Cite this article as: Xiong F, Wang S, Kai J. Video-assisted thoracic surgery right sleeve lobectomy. J Thorac Dis 2014;6(12):1831-1833. doi: 10.3978/j.issn.2072-1439.2014.12.03

Uniportal video-assisted thoracoscopic left basilar segmentectomy

Lei Jiang, Yi Bao, Ming Liu, Lei Lin, Lei Zhang, Gening Jiang

Department of Thoracic Surgery, Shanghai Pulmonary Hospital, Tongji University of Medicine, Shanghai 200433, China

Correspondence to: Lei Jiang, MD. Department of Thoracic Surgery, Shanghai Pulmonary Hospital, Tongji University of Medicine, No. 507 Zhengming Road, Shanghai 200433, China. Email: jiangleiem@aliyun.com.

Abstract: Uniportal video-assisted thoracoscopic surgery (VATS) has recently been introduced as an acceptable alternative to the traditional three-port VATS. Uniportal VATS lobectomy and segmentectomy actually gained increasing popularity. Until now there have been few reports about uniportal VATS basilar segmentectomy; we herein reported our experience with a patient who suffered from recurrent hemoptysis with 1-cm nodule in the basilar segment of the left lower lobe. A left basilar segmentectomy was performed through a single port. Operating time was 90 minutes, and postoperative course was uneventful. Pathology revealed cryptococcosis. Follow-up at 6 months after surgery demonstrated a normal chest computed tomographic (CT) scan and complete recovery without complications.

Keywords: Lobectomy; segmentectomy; wedge resection; postoperative complications; surgery/incisions/exposure/techniques; thoracoscopy/video-assisted thoracoscopic surgery (VATS)

Submitted Sep 03, 2014. Accepted for publication Nov 14, 2014.
doi: 10.3978/j.issn.2072-1439.2014.12.18
View this article at: http://dx.doi.org/10.3978/j.issn.2072-1439.2014.12.18

Introduction

Uniportal video-assisted thoracoscopic surgery (VATS) has recently been introduced as an alternative to the traditional three-port VATS. Uniportal VATS lobectomy and segmentectomy actually gained increasing popularity (1-4). Until now there have been few reports about uniportal VATS basilar segmentectomy. Herein we reported our experience with a patient who suffered from recurrent hemoptysis with a 1-cm nodule in the basilar segment of the left lower lobe, and received VATS basilar segmentectomy of the left lower lobe through a single port.

Clinical summary

A 48-year-old male patient was referred to our department because of recurrent hemoptysis for 3 months, refractory to medications. Past history and physical examination were unremarkable. Chest computed tomographic (CT) scan revealed a poorly demarcated nodule with a diameter of 1 cm (*Figure 1*); a low-grade malignancy could not be excluded. Bronchoscopy did not show visible lesions. Pulmonary function tests and other systemic examinations were unremarkable. The patient underwent a left basilar segmentectomy through a single port. Postoperative pathologic examination revealed cryptococcosis. He was well at 6-month follow-up, and chest CT scan revealed excellent healing without any complications.

Surgical technique (*Figure 2*)

In December 2013, a 4-cm incision was made in the fourth intercostal anterior axillary line, after achievement of general anesthesia with a double-lumen endobronchial tube. After placement of a wound protector, a 30-degree video scope provided visualization. There were no pleural adhesions and no evidence of pleural metastasis in the left thoracic cavity. The nodule was located by palpation in the basilar segment of the left lower lobe, and marked with electrocautery. We first opened the oblique fissure to isolate the superior and basilar branches of the lower lobe artery, and transected the basilar branches using 3-cm EndoGIA linear white stapler (Covidien, Mansfield, MA, USA). The basilar bronchus of the left lower lobe was mobilized, and several station 11 lymph nodes were dissected. After division of inferior pulmonary ligament, basilar tributary of

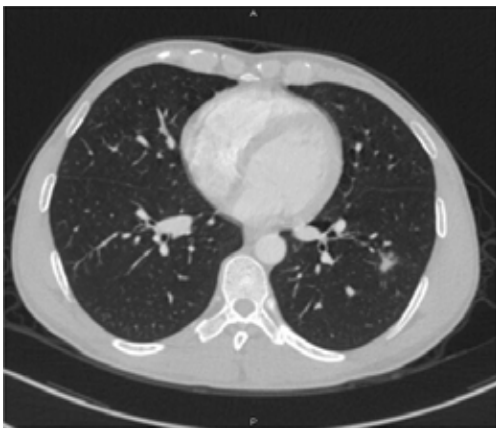

Figure 1 Chest CT scan showed one 1-cm spiculated nodule in the basilar segment of the left lower lobe. CT, computed tomographic.

Figure 2 Uniportal VATS basilar segmentectomy of the left lower lobe (5). Available online: http://www.asvide.com/articles/400

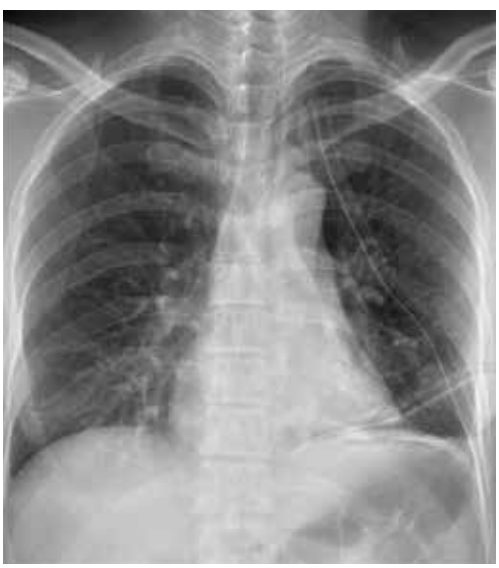

Figure 3 Chest X-ray examination showed the left lung was fully expanded and two chest tubes properly positioned.

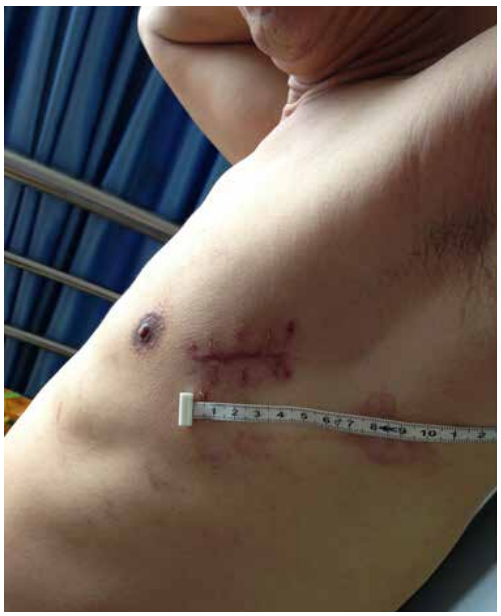

Figure 4 Postoperative examinations revealed satisfactory healing of the chest incision.

the inferior pulmonary vein was isolated and divided with 3-cm white stapler, sparing the superior tributary. Then, the basilar bronchus was divided with 4.5-cm green stapler. After inflating the residual superior segment of the lower lobe to demarcate the intersegmental plane, the basilar segment was divided along the plane, and removed in a specimen bag, sent for frozen section, which confirmed a benign lesion. Two chest tubes were routinely placed in the chest (*Figure 3*). Operation time was 90 minutes, and operative blood loss 50 mL. After an uncomplicated recovery, the patient was discharged home 3 days after operation (*Figure 4*).

Discussion

Operative uniportal VATS is an interesting approach to malignant and benign lung diseases, with both a diagnostic and therapeutic intention, especially in patients with borderline cardiorespiratory function or advanced age. According to our clinical experiences, uniportal VATS patients had a shorter hospital stay and generated lower postoperative costs and a better aesthetic result than conventional VATS, and the technique might suffice for most situations treated by conventional VATS. Herein we reported our experience with a uniportal VATS left basilar segmentectomy of the

left lower lobe.

Uniportal VATS segmentectomy is technically demanding operation whose difficulties are compounded by the inherent disadvantages of VATS though single port, including the limited maneuverability, unsatisfactory ergonomic characteristic of the instruments, poor visualization, and instrument-videothoracoscope interference. The placement of the incision in the fourth intercostal anterior axillary line depends on the location of the nodule in the chest, bearing in mind that an adequate distance between the single port and the target area. During the surgical procedure, it was easier to divide the basilar artery and vein branches firstly, which provided enough space to pass the straight anvil of an endoscopic stapler for division of the bronchus. Finally, because we sometimes find one of these tubes being obstructed, we routinely place two chest tubes through the same incision as video shows, to provide best chest drainage, with one tube directing upward for removal of air, the other downward for evacuation of fluid.

Cite this article as: Jiang L, Bao Y, Liu M, Lin L, Zhang L, Jiang G. Uniportal video-assisted thoracoscopic left basilar segmentectomy. J Thorac Dis 2014;6(12):1834-1836. doi: 10.3978/j.issn.2072-1439.2014.12.18

Acknowledgements

Disclosure: The authors declare no conflict of interest.

References

1. Gonzalez-Rivas D, Fernandez R, Fieira E, et al. Uniportal video-assisted thoracoscopic bronchial sleeve lobectomy: first report. J Thorac Cardiovasc Surg 2013;145:1676-7.
2. Gonzalez-Rivas D, Paradela M, Fernandez R, et al. Uniportal video-assisted thoracoscopic lobectomy: two years of experience. Ann Thorac Surg 2013;95:426-32.
3. Gonzalez-Rivas D, Fieira E, Mendez L, et al. Single-port video-assisted thoracoscopic anatomic segmentectomy and right upper lobectomy. Eur J Cardiothorac Surg 2012;42:e169-71.
4. Gonzalez-Rivas D, Fieira E, Delgado M, et al. Uniportal video-assisted thoracoscopic lobectomy. J Thorac Dis 2013;5:S234-45.
5. Jiang L, Bao Y, Liu M, et al. Uniportal VATS basilar segmentectomy of the left lower lobe. Asvide 2014;1:366. Available online: http://www.asvide.com/articles/400

Video-assisted thoracic surgery left S1+2+3 segmentectomy for lung cancer

Jinshi Liu, Weishan Lu, Xinming Zhou

Department of Thoracic Surgery, Zhejiang Cancer Hospital, Hangzhou 310022, China

Correspondence to: Jinshi Liu, MD. Department of Thoracic Surgery, Zhejiang Cancer Hospital, Hangzhou 310022, China. Email: yefeng9725boy@163.com.

Abstract: A 49-year-old female presented with a solitary pulmonary nodule on the chest screening computed tomography (CT) scan. The nodule was 1.3 cm in diameter and located in the apical segment of left upper lobe. The lesion was considered to be cT1aN0M0 non-small cell lung cancer (NSCLC) and a 3-port video-assisted thoracic surgery (VATS) wedge resection was performed. Intraoperative frozen sections revealed a lung adenocarcinoma. Therefore, sequential S1+2+3 segmentectomy of the left upper lobe was performed, also systematic lymph node dissection was carried out. The final pathological stage was pT1aN0M0 (Ia).

Keywords: Video-assisted thoracic surgery (VATS); segmentectomy; systematic lymph node dissection; lung cancer

Submitted Sep 09, 2014. Accepted for publication Nov 21, 2014.
doi: 10.3978/j.issn.2072-1439.2014.12.39
View this article at: http://dx.doi.org/10.3978/j.issn.2072-1439.2014.12.39

Introduction

Although the use of segmentectomy for early lung cancer is still controversial, it has recently been accepted as a radical surgery for cT1aN0M0 non-small cell lung cancer (NSCLC). This surgery can be performed safely as open procedure (1,2). According to several recent reports, the clinical outcomes of segmentectomy are equal to lobectomy (1-4).

A 49-year-old female presented with a solitary pulmonary nodule on the chest screening computed tomography (CT) scan. The nodule was 1.3 cm in diameter and located in the apical segment of left upper lobe. The lesion was considered to be cT1aN0M0 NSCLC. There were no remarkable enlarged lymph nodes in pulmonary hilum and mediastinum on CT scan. No distal metastasis was found according to preoperative examinations including abdominal CT scan, enhanced head MRI and bone scanning. Pulmonary function was normal. Video-assisted thoracic surgery (VATS) wedge resection was thus performed and intraoperative frozen sections revealed a lung adenocarcinoma. Therefore, sequential S1+2+3 segmentectomy of the left upper lobe was performed, also systematic lymph node dissection was carried out. The final pathological stage was pT1aN0M0 (Ia). The patient was well recovered and discharged on postoperative day 4.

Operative techniques (*Figure 1*)

The patient was positioned in the right lateral decubitus position and intubated with a dual lumen endotracheal tube. The surgeon stood in front of the patient, and the assistant stood behind the patient. Three-port approach was applied. The observation port was in the 8th intercostal space at the middle axillary line about 1 cm in length. The main operation incision was in the 4th intercostal space at anterior axillary line about 3 cm in length.The assisted operation port was located in the 8th intercostal space at the posterior axillary line about 0.5 cm in length.

The nodule was in the apical segment of left upper lobe and palpable. Wedge resection was performed first and intraoperative frozen sections revealed a lung adenocarcinoma. Therefore, sequential S1+2+3 segmentectomy of the left upper lobe was decided to perform.

The upper lobe was gently retracted backward, the pleura covering the surface of superior pulmonary vein was opened with an electric hook. Combination of electric hook and blunt dissection, the S1+2+3 segmental pulmonary vein was dissociated, but the vein was not cut off yet. At the same time, the lingular vein should be identified and be preserved. Then pulled the upper lobe forward, opened the mediastinal pleura around the hilum and dissected

Figure 1 Video-assisted thoracic surgery left S1+2+3 segmentectomy for lung cancer (5).
Available online: http://www.asvide.com/articles/401

the anterior trunk of the pulmonary artery. Devided the posterior part of the fissure with endo-GIA (blue stapler) and continued to dissected the S3 segmental pulmonary artery, then the artery was devided with endo-GIA (white stapler). There was bleeding at the anterior trunk when the artery was dissected, and the artery was pressed with a gauze to stop the bleeding and to be dissected later. Therefor we retracted the upper lobe backward and cut off the S1+2+3 segmental pulmonary vein with endo-GIA (white stapler). The anterior trunk was visualized clearly when the vein was separated and the bleeding had already stopped, then the artery was devided with endo-GIA (white stapler). Now the S1+2+3 bronchus was dissected easily and the linguar bronchus could be identified clearly, then the S1+2+3 bronchus was devided with endo-GIA (green stapler). Lymph nodes around the bronchus were dissected at the same time. At last, the lung was re-inflated and the segmental boundary was identified, and endo-GIA (green stapler) was used to devide the parenchyma. The specimen was removed in a glove.

Systematic lymph node (include station 5, 7, 8 lymph nodes) dissection was carried out subsequently. Station 4L lymph node was invisible in this patient. At last, the inferior pulmonary ligament was divided.

To avoid damaging left recurrent nerve, the nerve shoule be dissected carefully. Also, the vagus should be preserved. Electric hook and ultrasonic scalpel was used in the procedure of lymphadenectomy. Aspirator also acts as an important role in this surgery.

Comments

With the advances in radiographic devices such as high-resolution computed tomography (CT) and the widespread practice of low-dose helical CT for screening, more and more early NSCLCs are detected (6). For some patients in high risk, there is a decreased likelihood of having a second or even a third NSCLC. So, segmentectomy is more often performed and it can be applied to complicated operation such as bilateral segmentectomy (7).

Because the assisted operation port is only 0.5 cm in length, the endo-GIA should be introduced into the thoracic cavity through the main operation port. Therefore, the artery should be divided first for VATS left upper lobectomy or S1+2+3 segmentectomy, then the vein and bronchus could be divided easily.

To avoid damaging more intercostal nerves, the observation port and the assisted operation port is always located in the same intercostal space. Postoperative chest pain could be reduced with a 0.5 cm assisted operation port.

Combination of electric hook and ultrasonic scalpel, and cooperated with aspirator can make the surgery smoothly.

Acknowledgements

Disclosure: The corresponding author has received a signed release form from the patient recorded on the video. The authors declare no conflict of interest.

References

1. Soukiasian HJ, Hong E, McKenna RJ Jr. Video-assisted thoracoscopic trisegmentectomy and left upper lobectomy provide equivalent survivals for stage IA and IB lung cancer. J Thorac Cardiovasc Surg 2012;144:S23-6.
2. Zhao X, Qian L, Luo Q, et al. Segmentectomy as a safe and equally effective surgical option under complete video-assisted thoracic surgery for patients of stage I non-small cell lung cancer. J Cardiothorac Surg 2013;8:116.
3. Tsutani Y, Miyata Y, Nakayama H, et al. Oncologic outcomes of segmentectomy compared with lobectomy for clinical stage IA lung adenocarcinoma: propensity score-matched analysis in a multicenter study. J Thorac Cardiovasc Surg 2013;146:358-64.
4. Tsutani Y, Miyata Y, Nakayama H, et al. Segmentectomy

for clinical stage IA lung adenocarcinoma showing solid dominance on radiology. Eur J Cardiothorac Surg 2014;46:637-42.
5. Liu J, Lu W, Zhou X. Video-assisted thoracic surgery left S1+2+3 segmentectomy for lung cancer. Asvide 2014;1:367. Available online: http://www.asvide.com/articles/401
6. National Lung Screening Trial Research Team, Aberle DR, Adams AM, et al. Reduced lung-cancer mortality with low-dose computed tomographic screening. N Engl J Med 2011;365:395-409.
7. Witte B, Wolf M, Hillebrand H, et al. Complete video-assisted thoracoscopic surgery anatomic segmentectomy for clinical stage I lung carcinoma - technique and feasibility. Interact Cardiovasc Thorac Surg 2011;13:148-52.

Cite this article as: Liu J, Lu W, Zhou X. Video-assisted thoracic surgery left S1+2+3 segmentectomy for lung cancer. J Thorac Dis 2014;6(12):1837-1839. doi: 10.3978/j.issn.2072-1439.2014.12.39

Visualized Surgery

Uniportal video-assisted thoracoscopic surgery right upper lobectomy with systematic lymphadenectomy in a semiprone position

Zongwu Lin, Songtao Xu, Qun Wang

Department of Thoracic Surgery, Fudan University, Zhongshan Hospital, Shanghai 200032, China

Correspondence to: Songtao Xu. Department of Thoracic Surgery, Fudan University, Zhongshan Hospital, Shanghai 200032, China. Email: xu.songtao@zs-hospital.sh.cn.

Abstract: A 53-year-old male smoker was referred to our hospital with an enlarged lesion in the right upper lung. Computed tomography (CT) showed a 1.5 cm solid lesion with pleural indentation in the right upper lobe adjacent to the oblique fissure. The preoperative clinical diagnosis was stage I primary lung cancer. Uniportal video-assisted thoracoscopic surgery (VATS) right upper lobectomy in a semiprone position was performed in this case. Frozen section examination confirmed the diagnosis of lung adenocarcinoma, and systematic lymphadenectomy was then performed. A chest tube was placed at the posterior part of the incision through the dorsal thoracic cavity to the apex. The postoperative pathologic diagnosis was T2aN0M0 adenocarcinoma.

Keywords: Video-assisted thoracoscopic surgery (VATS); uniportal; lobectomy; lung cancer; lymphadenectomy

Submitted Sep 16, 2014. Accepted for publication Nov 18, 2014.
doi: 10.3978/j.issn.2072-1439.2014.11.22
View this article at: http://dx.doi.org/10.3978/j.issn.2072-1439.2014.11.22

Introduction

With the development of thoracoscopic instruments and techniques, video-assisted thoracoscopic surgery (VATS) lobectomy has become the first choice for early stage non-small-cell lung carcinoma. Most surgeons prefer three-port or four-port VATS lobectomy, because multiple ports provide different angles facilitating better dissection and division of the bronchus and vessels. We performed our first uniportal VATS lobectomy in November 2013, and both the surgeon and the assistant felt very fatigued after the operation. In an effort to achieve better ergonomics, we performed our first uniportal VATS lobectomy in a semiprone position in May 2014.

Clinical data

A 53-year-old male smoker was referred to our hospital due to an enlarged lesion in his right upper lung. Computed tomography (CT) showed a 1.5 cm solid lesion with pleural indentation in the right upper lobe adjacent to the oblique fissure. No metastases or contraindications were found in the preoperative evaluation. The clinical diagnosis was stage I primary lung cancer. Uniportal VATS right upper lobectomy in a semiprone position was performed (*Figure 1*). Intraoperative frozen section examination confirmed lung adenocarcinoma, and systematic lymphadenectomy was then performed.

Operative techniques

The patient was placed in a semiprone position under general anaesthesia, with single-lung ventilation provided by a double-lumen endotracheal tube. Thoracic paravertebral block was used. The surgeon and the sole assistant participating in the operation both stood on the ventral side of the patient. A single incision was employed, which was 3.5 cm long and positioned at the fifth intercostal space on the anterior axillary line. A plastic wound protector was used to prevent the lung from expanding when suction was applied. A high definition 30° 10 mm thoracoscope was

Figure 1 Uniportal video-assisted thoracoscopic surgery right upper lobectomy with systematic lymphadenectomy in a semiprone position (1). Available online: http://www.asvide.com/articles/402

Figure 2 The operation room setup for uniportal video-assisted thoracoscopic surgery lobectomy in a semiprone position.

placed at the posterior part of the incision.

The instruments used were a harmonic scalpel, curved suction device, endoscopic grasper, double-jointed forceps and endoscopic linear cutter. An endoscopic grasper containing a small gauze was used to push the lung to promote exposure.

The surgeon stood caudally, while the assistant stood cranially. The surgeon held the suction in the left hand, and the harmonic scalpel (or sometimes the double-jointed forceps or the endoscopic linear cutter) in the right hand. The assistant held the thoracoscope in one hand and the endoscopic grasper in the other hand (*Figure 2*).

We began the procedure with exploration to find the lesion, locating it in the right upper lobe with pleural indentation, no metastases in the pleurae, complete oblique fissure and poor horizontal fissure. The oblique fissure was divided with a harmonic scalpel, and the ascending A2 pulmonary artery was exposed. The ascending A2 was closed proximally with two 5-mm vascular clips and then cut with a harmonic scalpel. The posterior mediastinal pleura was opened until the upper edge of the right upper bronchus was visible. The 12th group lymph nodes were dissected to the distal lung.

The right upper lobe was pushed down to expose the apico-anterior pulmonary arterial trunk. The apical artery and anterior artery branched from the right pulmonary arterial trunk separately in this case. The apical artery was mobilised, and cut with an endoscopic linear stapler, whereas the anterior artery was hard to expose at this angle. The 12th group lymph nodes between the upper right bronchus and apical artery were dissected to the distal lung at this angle. The right upper bronchus was mobilised with double-jointed forceps from the dorsal aspect, then transected with an endoscopic linear stapler. The anterior artery was then exposed dorsally, and cut with an endoscopic linear stapler.

The right upper lobe was pushed backwards. The right upper pulmonary vein was mobilised, and then cut with an endoscopic linear stapler. The 11th group lymph nodes were dissected before the horizontal fissure was cut with an endoscopic linear stapler. The specimen was put into a protected bag, and removed for frozen section examination. Lung adenocarcinoma was confirmed, and systematic lymphadenectomy was performed.

The lung was pushed downwards by the assistant. The surgeon lifted the azygos vein via suction, and dissected the 4th group lymph nodes with a harmonic scalpel. After an approximately 1 cm length of the pericardium was exposed, the mediastinal pleura above the azygos vein was opened. The 2nd and 4th lymph nodes were dissected en bloc, with the right vagus nerve left untouched.

The lung was pushed forwards by the assistant. The posterior mediastinal pleura was opened in front of the right vagus nerve, from the right inferior pulmonary vein to the azygos vein. The oesophagus was separated from the 7th group lymph nodes, and the bilateral main bronchus was exposed. The 7th group lymph nodes were then dissected en bloc. The inferior pulmonary ligament was mobilised, and the 9th group lymph nodes were dissected. A chest tube was placed at the posterior part of the incision through the posterior thoracic cavity to the apex.

Comments

Uniportal VATS lobectomy was first reported by Gonzalez-Rivas *et al.* (2) in 2011. Gonzalez-Rivas *et al.* (2) proved the practical feasibility and safety of uniportal VATS lobectomy, and utilised the technique in more complex cases, including double sleeve lobectomy. The patient was placed in the lateral decubitus position in previous reports. Under such conditions, the cameraman is required to raise their arm to hold the thoracoscope, which easily leads to arm fatigue.

A prone position was utilised in thoracoscopic mobilisation of the oesophagus (3), and subsequently a semiprone position was investigated, due to the convenience of relatively uncomplicated conversion to thoracotomy, where required. A semiprone position is now widely utilised in thoracoscopic mobilisation of the oesophagus, because it reduces workload and facilitates better ergonomics (4). However, it is seldom utilised for VATS lobectomy (5).

We first performed uniportal VATS lobectomy in a semiprone position in May 2014, and achieved great success. Not only does a semiprone position relieve arm fatigue in the surgeon and assistant, but it also provides more angles for the surgeon. In this operation, only three instruments are inserted into the thoracic cavity at the same time, and they rarely interfere with each other because they are all slim. More than 20 patients have now successfully received uniportal VATS lobectomy in a semiprone position.

The most difficult manipulation during uniportal VATS right upper lobectomy is the division of the right upper pulmonary vein. Initial division of the anterior trunk can facilitate the insertion of a stapler to divide the right upper pulmonary vein. The anterior pulmonary artery could be divided apically or dorsally after cutting the right upper bronchus.

The oblique fissure is divided first, if the interlobar pulmonary is visible in the fissure. Otherwise, the oblique fissure is divided last. The horizontal fissure is divided last, unless it is completely developed. We did not grasp the lung or the lymph nodes throughout the operation, in order to reduce the possibility of trauma to the lung, and avoid crushing the lymph nodes. The lung was pushed to the appropriate angle using an endoscopic grasper containing a gauze, and a curved suction instrument. The lymph nodes were pushed to the appropriate angle via a curved suction instrument only. In uniportal VATS lobectomy, a semiprone position facilitates pushing of the lung, and facilitates more manipulation angles, less workload and better ergonomics for both the surgeon and the assistant.

Cite this article as: Lin Z, Xu S, Wang Q. Uniportal video-assisted thoracoscopic surgery right upper lobectomy with systematic lymphadenectomy in a semiprone position. J Thorac Dis 2014;6(12):1840-1842. doi: 10.3978/j.issn.2072-1439.2014.11.22

Acknowledgements

Disclosure: The authors declare no conflicts of interest.

References

1. Lin Z, Xu S, Wang Q. Uniportal video-assisted thoracoscopic surgery right upper lobectomy with systematic lymphadenectomy in a semiprone position. Asvide 2014;1:368. Available online: http://www.asvide.com/articles/402
2. Gonzalez-Rivas D, Delgado M, Fieira E, et al. Double sleeve uniportal video-assisted thoracoscopic lobectomy for non-small cell lung cancer. Ann Cardiothorac Surg 2014;3:E2.
3. Palanivelu C, Prakash A, Senthilkumar R, et al. Minimally invasive esophagectomy: thoracoscopic mobilization of the esophagus and mediastinal lymphadenectomy in prone position--experience of 130 patients. J Am Coll Surg 2006;203:7-16.
4. Shen Y, Feng M, Tan L, et al. Thoracoscopic esophagectomy in prone versus decubitus position: ergonomic evaluation from a randomized and controlled study. Ann Thorac Surg 2014;98:1072-8.
5. Agasthian T. Revisiting the prone position in video-assisted thoracoscopic surgery. Asian Cardiovasc Thorac Ann 2010;18:364-7.

Visualized Surgery

Unidirectionally progressive resection of left upper pulmonary lobe under video-assisted thoracoscopy

Kaican Cai, Hancheng Zhao, Hua Wu, Siyang Feng, Pengfei Ren, Ruijun Cai, Gang Xiong

Department of Thoracic Surgery, Nanfang Hospital, Southern Medical University, Guangzhou 510515, China

Correspondence to: Kaican Cai. Department of Thoracic Surgery, Nanfang Hospital, Southern Medical University, Guangzhou 510515, China. Email: doc_cai@163.com.

Abstract: The case is a nodule in the upper left lobe, and intraoperative frozen section pathological diagnosis on the removed nodule confirmed well differentiated mucinous adenocarcinoma. Unidirectionally progressive resection of the left upper pulmonary lobe under video-assisted thoracoscopy is selected as the surgical method. Right below the operation hole, surgeons gradually advanced in one direction, and dissociated and divided in such order: the upper left pulmonary vein, the upper left lobe bronchus, the upper left pulmonary arterial branches and the fissures. Endoscopic linear cutters and hem-o-lok clip applicator were used to deal with the blood vessels, bronchus, and under-differentiated fissures. At last, the removed upper left lobe was put into a size eight sterile glove and taken out through the main operation hole. General anesthesia with double-lumen endotracheal intubation is used. The patient took a 90 degree decubitus on his contralateral side. The surgeons were on the ventral side of the patient, and operated with endoscope apparatus under the monitor.

Keywords: Video-assisted thoracic surgery (VATS); lung adenocarcinoma; upper left lobe lobectomy

Submitted Oct 13, 2014. Accepted for publication Dec 01, 2014.
doi: 10.3978/j.issn.2072-1439.2014.12.26
View this article at: http://dx.doi.org/10.3978/j.issn.2072-1439.2014.12.26

Introduction

Lung cancer is the leading cause of cancer related morbidity and mortality worldwide, more than 85% of which is non-small-cell lung carcinoma (NSCLC) (1). Adenocarcinoma is a common type of NSCLC, and there are big differences among different tissue subtypes in terms of clinical features, imaging results, pathology, genetics, therapies, and prognosis. In the past two decades, video-assisted thoracic surgery (VATS) is one of the most impressive new technologies in the chest surgery area. Using this technology, there would be smaller incisions, convenient operation, and less damage. Surgeons do not have to cut off rib(s), and could open up and close the chest rapidly, and patients lose less blood during operation, experiences less post-operational incision pain, and face less risk of venous thromboembolism (2). VATS has been widely applied to wedge resection of pulmonary masses, radical cure of lung cancers, mediastinal tumor resection, radical cure of esophagus cancer, removal of esophageal leiomyoma, and many other thoracic operations. National Comprehensive Cancer Network (NCCN) recommended pulmonary lobectomy with VATS as the standard procedure of lung cancer treatment in 2006. VATS pulmonary lobectomy is usually carried out through the traditional procedure or the unidirectional procedure. In 1994, Prof. Jianxing He carried out VATS pulmonary lobectomy through the traditional procedure, which is one of the early cases of radical cure of lung cancer with VATS. In the traditional procedure, the lobe is removed in the order of fissures-pulmonary artery-pulmonary vein-bronchus, and the lobe is overturned multiple times in the operation. Comparing to traditional thoracotomy, this surgical method could better handle the pulmonary hilar vessels and pulmonary bronchus and clean the lymph nodes (3).

In this operation, we advanced in a single direction from the front to the back, and we dissociated and divided in the order of the upper left pulmonary vein, the upper left

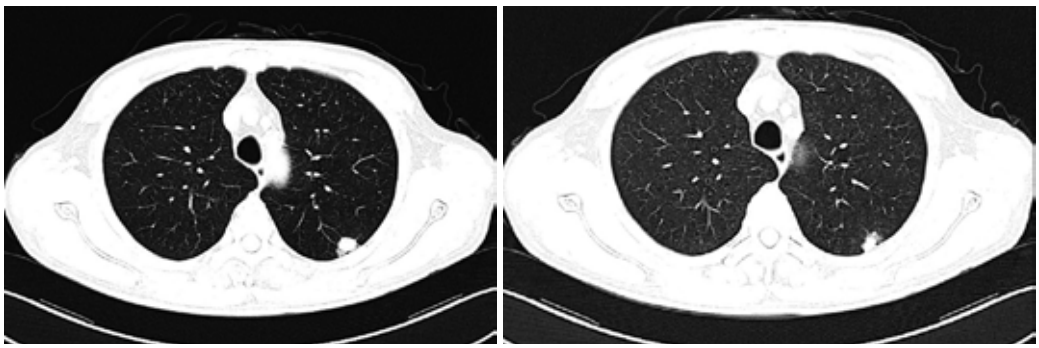

Figure 1 Chest CT.

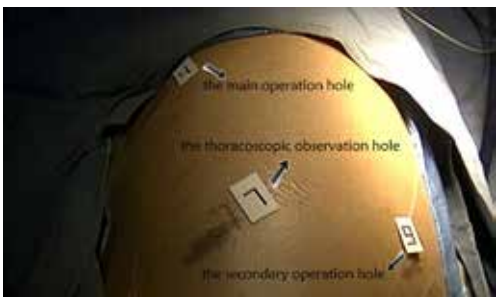

Figure 2 The thoracoscopic incision.

lobe bronchus, the upper left lobe arterial branches and the fissures.

Case report

The case is about a 74-year-old male. Before being admitted, a nodule in the upper left lobe was detected via chest radiographs in regular physical examination, and enhanced CT of the chest was carried out then (*Figure 1*). The results reveal a nodule in the upper left lobe, and there is a considerable possibility of peripheral lung cancer. Past medical history: smoking for over 40 years. After being admitted to hospital, brain MRI, general ECT bone imaging, abdominal ultrasound, and other auxiliary examinations were carried out, in which distant metastasis were not found. As the nodule in the upper left lobe is ill-defined, we decided to carry out wedge resection on the upper left lobe nodule, and intraoperative frozen section pathological diagnosis on the removed nodule confirmed well differentiated mucinous adenocarcinoma. Then we decided to carry out unidirectionally progressive resection of left upper pulmonary lobe under video-assisted thoracoscopy and mediastinal lymph node dissection. During the operation, we dissociated and divided in order the upper left pulmonary vein-upper left lobe bronchus-upper left lobe arterial branches-fissures. The pathological stage of this patient was $T_{1b}N_0M_0$, IA.

Video descriptions

General anesthesia is adopted through double-lumen endotracheal intubation, one-lung ventilation on the contralateral, and intravenous injection. Double-lumen endotracheal intubation is essential to the VATS, and lung tissue on the operated side should be collapsed completely, or the operation could not proceed smoothly.

The patient took a 90 degree decubitus on his contralateral side.

As for surgical incisions, an 1.5 cm incision is made as the thoracoscopic observation hole at the 7th intercostal space between the midaxillary line and the anterior axillary line, a second horizontal incision of 3.5 cm as the main operation hole at the 4th intercostal space between the anterior axillary line and the midclavicular line, and a third incision of 1.5 cm as the secondary operation hole at the 9th intercostal space between the axillary line and the bottom scapular line (*Figure 2*). The surgeons were on the ventral side of the patient, and operated with endoscope apparatus under the monitor.

Unidirectionally progressive resection under video-assisted thoracoscopy is adopted in the operation, i.e., operate right below the operation hole, and dissect the tissue to be removed from the surface. Follow a single direction to advance, and expose, dissociate, and divide in the order of upper left pulmonary vein-upper left lobe bronchus-upper left pulmonary artery and branches-fissures. Use mainly the coagulation hook to dissociate tissues, with the support of suction apparatus. Endoscopic linear cutters and hem-o-lok

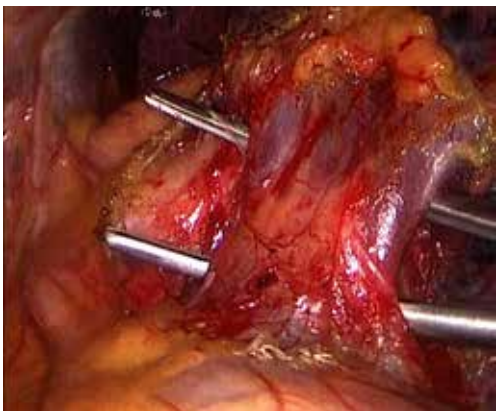

Figure 3 Dissociate the upper left pulmonary vein.

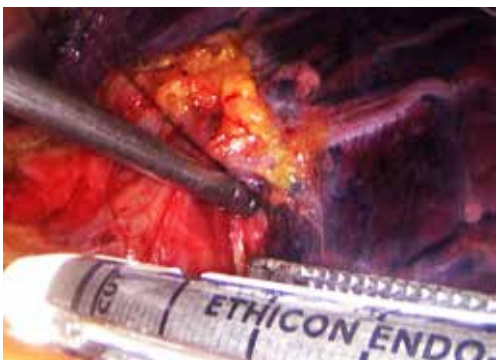

Figure 4 Draw the dissociated upper left pulmonary vein with No. 7 silk suture, and divide it with an endoscopic linear cutter.

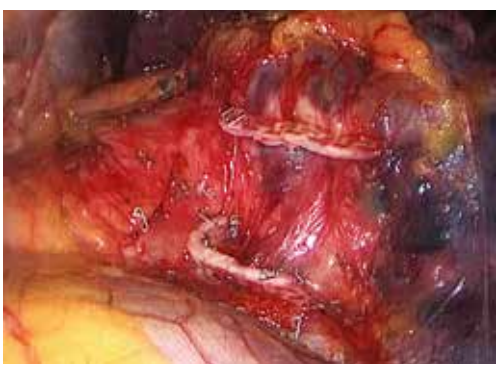

Figure 5 Divided stump of upper left pulmonary vein.

clip applicator are used to deal with blood vessels, bronchus, and pulmonary parenchyma

Procedure of key surgical positions:

(I) Step 1: amputate the upper left pulmonary vein (*Figures 3-5*). Draw the upper left lobe rightward and outward to expose the upper left pulmonary vein, which is below the left pulmonary trunk and front of the upper left pulmonary bronchus. Dissociate and expose the upper left pulmonary vein with a coagulation hook, draw it with No. 7 silk suture, and divide it with an endoscopic linear cutter.

(II) Step 2: amputate the upper left lobe bronchus (*Figures 6,7*). The upper left lobe bronchus would be exposed when the upper left pulmonary vein is divided. Dissociate and divide the bronchus exposed.

(III) Step 3: amputate the upper left pulmonary artery (*Figures 8-10*). Cut the upper left lobe bronchus and the upper left pulmonary arteries will be exposed. Dissociate the superior lingular segment and the inferior lingular segment, draw them with a No. 7 silk suture, and divide them with an endoscopic linear cutter. Then dissociate arteries in the apical segment and the apicoposterior segment of the upper left lobe in order. Use absorbable clip to close both ends of the arteries and ligate them with No. 7 silk suture before dividing.

(IV) Step 4: resect the interlobar fissure of the left pulmonary (*Figure 11*). Use an endoscopic linear cutter to clip the fissure tissue, and ventilate to see if the lower left lobe upswells. If yes, divide the fissure. Put the removed upper left lobe in a size 8 sterile glove and take it out (*Figure 12*).

Conclusions

VATS is one of the most impressive new technologies in the field of thoracic surgery and was recommended as the standard procedure for lung cancer treatment by NCCN (1). Thoracoscopic resection of lung cancer just makes small incisions, which are only 3-4 cm wide, thus avoid big cuttings into the chest flesh and damage on tissue caused by the chest opening apparatus. Comparing to the traditional thoracotomy and video assisted minithoracotomy, this approach causes less post-operative pain, and reduces the possibilities of intraoperative bleeding and postoperative complications significantly. The unidirectionally progressive resection under video-assisted thoracoscopy was first adopted by Prof. Liu *et al.* in China. During this resection, surgeries do not need to turn over the lobe back and forth or up and down, nor dissect the pulmonary lobe blood vessel and bronchus among underdeveloped fissures (4), so the damage to the lung tissue could be avoided even more.

From the technical perspective, resection of the left upper pulmonary lobe is considered as the most difficult

Figure 6 Dissociate the upper left lobe bronchus, and draw it with a No. 7 silk suture. Clip it with an endoscopic linear cutter, ventilate both lungs to confirm that the clipped tissue is the upper left lobe bronchus, and then cut it.

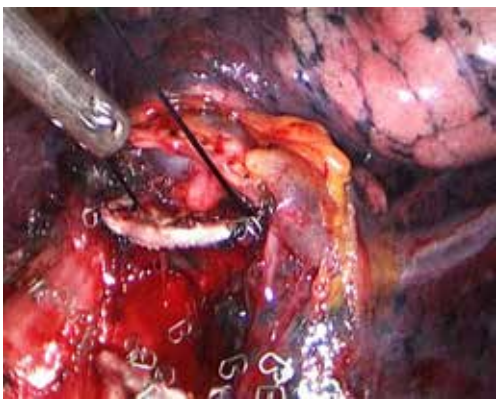

Figure 7 Divided stump of upper left pulmonary bronchus.

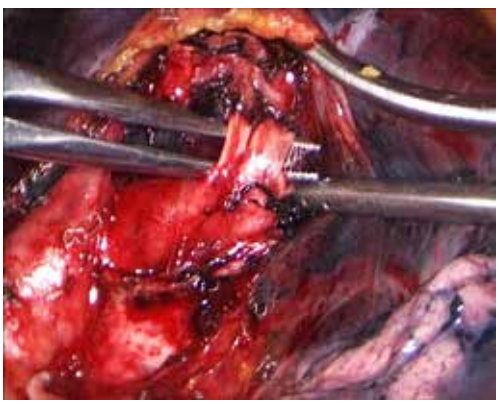

Figure 8 Dissociate the superior lingular segment and the inferior lingular segment of the upper left pulmonary artery.

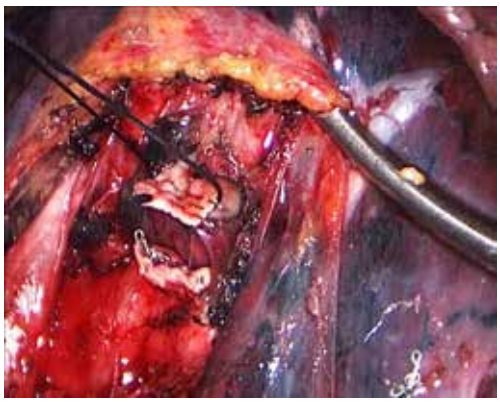

Figure 9 Divided stump of the superior lingular segment and the inferior lingular segment of the upper left pulmonary artery.

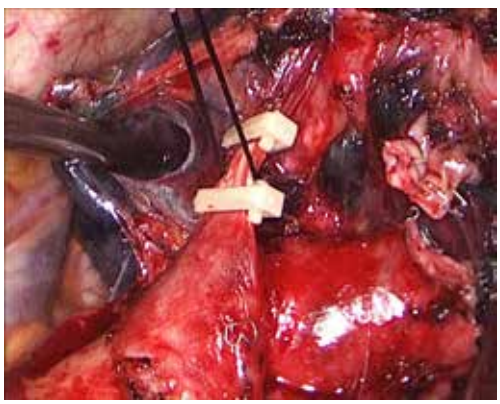

Figure 10 Use an absorbable clip to close both ends of the apical segment and the apicoposterior segment of the upper left pulmonary artery, ligate them with No. 7 silk suture, and divide it.

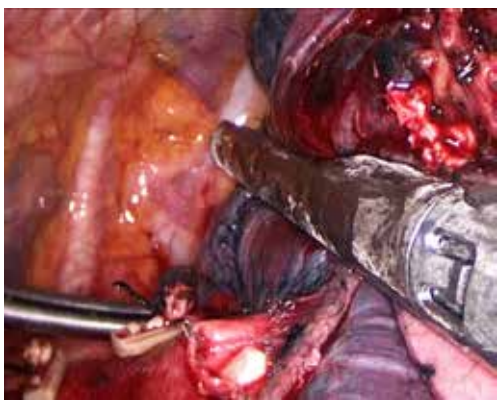

Figure 11 Clip the fissure with an endoscopic linear cutter, and ventilate both lungs. If the lower left lob upswells, remove the upper left lobe.

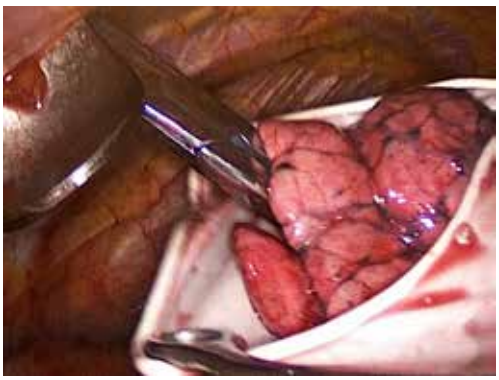

Figure 12 Put the removed upper left lobe in a size eight sterile glove and take it out through the main operation hole. Clean the lymph nodes, and end the operation.

Figure 13 Unidirectionally progressive resection of left upper pulmonary lobe under video-assisted thoracoscopy (5). Available online: http://www.asvide.com/articles/403

pulmonary lobectomy because of the different kinds of anatomic variations of the left upper lobe artery (*Figure 13*). There are 4-7 branches of the left upper lobe artery generally, which may cause massive bleeding by an incorrect operation (6). By video-assisted thoracoscopy surgery, the risk of bleeding occurs when handling the pulmonary hilar vessels and bronchus could be reduced, which is the most common reason why a traditional thoracoscopic pulmonary lobectomy is changed into an opening chest operation (7).

Unidirectionally progressive resection of pulmonary lobectomy has its special incision and operating procedure which has been adopted in different pulmonary lobectomy resection successfully (8,9). We would suggest that the very kind of surgery be worth of applying in pulmonary lobectomy and other minimally invasive lung surgeries.

Acknowledgements

Funding: Sub-subject of nationally supportive subject—Research and Application of Appropriate Technology in Control and Prevention of Common Diseases in Xinjiang Autonomous Region (No. 2013BAI05B02); "Twelfth Five Year" major drug discovery projects of China (No. 2012zx09101103).
Disclosure: The authors declare no conflict of interest.

References

1. NCCN clinical practice guidelines in oncology: non-small cell lung cancer. 3th edition. Fort Washington, PA: NCCN, 2014.
2. Pu JT, Dai TY, Tang XJ, et al. VATS Thoracic Small Incision and Conventional Surgery for Lung Cancer: Comparison of Therapy Effect and Impact on Blood Coagulation. Chinese Modern Doctor 2010;48:5-7.
3. Zhou HY, Ye X, Chen G, et al. Primary outcome of completely thoracoscopic pneumonectomy for non-smaU cell lung cancer. Chinese Journal of Thoracic and Cardiovascular Surgery 2013;29:1-3.
4. Liu LX, Che WG, Pu Q, et al. Single-direction VATS lobectomy. Chinese Journal of Clinical Thoracic and Cardiovascular Surgery 2008;24:156-8.
5. Cai K, Zhao H, Wu H, et al. Unidirectionally progressive resection of left upper pulmonary lobe under video-assisted thoracoscopy. Asvide 2014;1:369. Available online: http://www.asvide.com/articles/403
6. Zhang GL. eds. Practical Chest Surgery. Beijing: Chinese Medical Science and Technology Press, 2007:1317.
7. Sugi K, Sudoh M, Hirazawa K, et al. Intrathoracic bleeding during video-assisted thoracoscopic lobectomy and segmentectomy. Kyobu Geka 2003;56:928-31.
8. Cai K, Ren P, Feng S, et al. Unidirectionally progressive left pneumonectomy & mediastinal lymph node dissection. J Thorac Dis 2013;5:886-91.
9. Cai K, Wu H, Ren P, et al. Unidirectionally progressive resection of lower right lung cancer under video-assisted thoracoscopy. J Thorac Dis 2013;5:S310-4.

Cite this article as: Cai K, Zhao H, Wu H, Feng S, Ren P, Cai R, Xiong G. Unidirectionally progressive resection of left upper pulmonary lobe under video-assisted thoracoscopy. J Thorac Dis 2014;6(12):1843-1847. doi: 10.3978/j.issn.2072-1439.2014.12.26

GCTAB Column

Video-assisted thoracic surgery left upper lobectomy with systematic lymphadenectomy

Zongwu Lin[1], Songtao Xu[1], Junjie Zhao[2], Qun Wang[1]

[1]Department of Thoracic Surgery, Zhongshan Hospital, Fudan University, Shanghai 200032, China; [2]Department of Thoracic Surgery, Jiaxing First Hospital, Jiaxing 314001, China

Correspondence to: Songtao Xu, Department of Thoracic Surgery, Zhongshan Hospital, Fudan University, Shanghai 200032, China.
Email: xu.songtao@zs-hospital.sh.cn.

Abstract: A 43-year-old man was referred to our hospital after chest computed tomography revealed a 2.5-cm mixed ground-glass opacity peripherally in the left upper lobe of the lung. No metastasis or contraindication for surgery was found. Video-assisted thoracic surgery (VATS) left upper lobectomy was performed, and analysis of the intraoperative frozen section confirmed the diagnosis of adenocarcinoma. Subsequently, systematic lymphadenectomy was performed. By using this method, suction and harmonic scalpel were the only two major instruments needed throughout the operation. The use of suction ensures a clear view, and the harmonic scalpel functions as a combined dissector, grasper, and cutter, which helps avoid changing instruments during the surgery and saves time. Moreover, the use of this technique for three-port VATS lobectomy facilitates the conversion into single-port VATS if needed.

Keywords: Video-assisted thoracic surgery (VATS); lobectomy; lung cancer; harmonic scalpel

Submitted Sep 23, 2014. Accepted for publication Nov 03, 2014.
doi: 10.3978/j.issn.2072-1439.2014.11.38
View this article at: http://dx.doi.org/10.3978/j.issn.2072-1439.2014.11.38

Introduction

Over the last two decades, the utility of video-assisted thoracic surgery (VATS) has been greatly expanded, and VATS lobectomy with systematic lymphadenectomy has become the first choice of treatment for early-stage non-small-cell lung carcinoma. Three-port VATS lobectomy, which has now evolved into single-port VATS lobectomy, was once the first choice of treatment in our department. Here, we describe our unique technique for three-port VATS lobectomy, in which suction and harmonic scalpel are the only two major instruments needed. The use of this technique for three-port VATS lobectomy facilitates the conversion into single-port VATS if needed.

Clinical data

A 43-year-old man was referred to our hospital after computed tomography revealed a 2.5-cm mixed ground-glass opacity peripherally in the left upper lobe with spicular formation during his routine medical examination. No metastasis was found by positron emission tomography/computed tomography or brain magnetic resonance imaging preoperatively. His heart and lung functions were normal, and there was no contraindication for surgery. VATS left upper lobectomy was performed (*Figure 1*), and the intraoperative frozen section confirmed the diagnosis of adenocarcinoma. Subsequently, systematic lymphadenectomy was performed.

Operative techniques

The patient was placed in the lateral decubitus position under general anesthesia with single lung ventilation provided by a double-lumen endotracheal tube. Thoracic epidural anesthesia was used. The surgeon and assistant stood on the dorsal and ventral sides of the patient respectively. Three ports were employed. The first port for the thoracoscope was located at the eighth intercostal

Figure 1 Video-assisted thoracic surgery left upper lobectomy with systematic lymphadenectomy (1).
Available online: http://www.asvide.com/articles/404

space (ICS) on the midaxillary line, the second port was positioned on the triangle of auscultation regardless of the ICS, and the third port (3.5-cm long) was positioned on the fifth ICS between the anterior axillary line and midclavicular line.

First, the thoracic cavity was explored. There were no adhesions, pleural effusion, or pleural nodules observed. The lesion was located in the left upper lobe peripherally, with obvious pleural indentation. The posterior part of the oblique fissure was well developed, while the anterior part was not completed. The interlobar pulmonary artery could be seen from the oblique fissure.

The inferior pulmonary ligament was dissected, with the group 9 lymph nodes left at the mediastinum. The mediastinal pleura in front of the hilum was opened using a harmonic scalpel until the left pulmonary trunk was exposed, whereas and the mediastinal pleura behind the hilum was opened until the incision of the anterior mediastinal pleura was exposed. The tissue covering the left pulmonary artery trunk and anterior trunk was dissected. The posterior part of the oblique fissure was dissected to expose the interlobar pulmonary artery trunk and lingual pulmonary artery. A tunnel was made on the surface of the intralobar pulmonary artery, after which the uncompleted oblique fissure was divided by an endoscopic stapler.

Subsequently, the superior pulmonary vein and left upper bronchus were dissected and cut by an endoscopic stapler. All of the pulmonary artery branches of the left upper lobe were dissected and cut together using only an endoscopic stapler. Next, the left upper lobe was placed into a protective bag and removed from the thoracic cavity for subsequent frozen section examination. Based on the frozen specimen, lung adenocarcinoma with pleural involvement was confirmed, with no involvement of the edge of the bronchus observed.

Further, the group 10 lymph nodes were dissected, and the left phrenic nerve, left vagus nerve, and recurrent nerve were exposed to facilitate the dissection of the group 5 and 6 lymph nodes. The left lower lobe was retracted forward and the left vagus nerve and esophagus were dissociated from the group 7 lymph nodes to expose the bilateral main bronchus. These lymph nodes were dissected from the junction of the inferior pulmonary vein and the right main bronchus to the carina, after which they were dissociated from the left main bronchus and removed. Moreover, the recurrent laryngeal nerve was exposed to facilitate dissection of the group 4 lymph nodes; and, finally, the group 9 lymph nodes were also dissected.

Comments

Suction and harmonic scalpel were the only two major instruments used during the operation, while a cautery was conversely not used. The use of suction ensures a clear view, and the harmonic scalpel functions as a dissector, grasper, as well as a cutter, which helps avoid changing instruments during the surgery and saves time.

If the interlobar pulmonary artery can be easily seen from the fissure, the fissure is cut first; otherwise, the fissure is cut last. The key structures can be exposed more easily after the fissure is cut, and the procedure is subsequently performed in a single direction (anterior to posterior).

In most cases, one of the bronchial arteries is located between the left upper bronchus and the pulmonary artery trunk, and this bronchial artery should be dealt with before the left upper bronchus is cut to avoid bleeding. In this case, the bronchial artery could not be exposed until the left upper bronchus was cut, although the use of a harmonic scalpel with suction could easily treat this kind of bleeding.

Finally, when the fissure is completed and the lingual artery is adjacent to the anterior trunk, the branches of the left upper pulmonary artery can be cut together using an endoscopic stapler. If the branches are located far away from the same line, they can be treated separately. When dissecting the mediastinal lymph nodes, care should be taken to avoid clamping the lymph nodes as much as

possible in order to avoid crushing them.

Acknowledgements

Disclosure: The authors declare no conflict of interest.

Cite this article as: Lin Z, Xu S, Zhao J, Wang Q. Video-assisted thoracic surgery left upper lobectomy with systematic lymphadenectomy. J Thorac Dis 2014;6(12):1848-1850. doi: 10.3978/j.issn.2072-1439.2014.11.38

References

1. Lin Z, Xu S, Zhao J, et al. Video-assisted thoracic surgery left upper lobectomy with systematic lymphadenectomy. Asvide 2014;1:370. Available online: http://www.asvide.com/articles/404

GCTAB Column

Autogenous rib graft for reconstruction of sternal defects

Wenshan Li, Guofei Zhang, Chenyang Ye, Degang Yin, Gang Shen, Ying Chai

Department of Thoracic Surgery, The Second Affiliated Hospital, Zhejiang University School of Medicine, Hangzhou 310009, China

Correspondence to: Ying Chai, MD. Department of Thoracic Surgery, The Second Affiliated Hospital Zhejiang University School of Medicine, 88 Jiefang Road, Hangzhou 310009, China. Email: chai_y@126.com.

Abstract: Those who have undergone sternum resection need graft to stabilize the sternum with steel wire, titanium mesh or polypropylene mesh. The current study reports a case of using autogenous rib graft to reconstruct the sternum after resection. A 53-year-old man, whose chest computed tomography (CT) identified expansive lesions and the presence of osteocytes lesions in the sternum, with no apparent involvement of the mediastina structures, come to our medical center due to pain and a lump of the anterior chest wall. The patient underwent tumor radical resection and sternal reconstruction with autogenous rib graft, and the histopathological examination of the surgical specimen determined the diagnosis of osteosarcoma. The patient has recovered well after the surgery.

Keywords: Autogenous rib graft; sternal defects; sternum tumor

Submitted Nov 11, 2014. Accepted for publication Nov 14, 2014.
doi: 10.3978/j.issn.2072-1439.2014.11.37
View this article at: http://dx.doi.org/10.3978/j.issn.2072-1439.2014.11.37

Introduction

The resection of a large portion of the sternum requires a careful reconstruction to avoid secondary complications. The requirements of an ideal replacement for reconstruction of the sternum are availability, durability, non-reactivity, and resistance to infection. There is steel wire, titanium mesh or polypropylene mesh that can be used for reconstructing the sternum after resection; however, we describe our use of autogenous rib graft to reconstruct the segment defect of the sternum in a patient who had undergone partial resection.

A 53-year-old male, with no notable medical history, was admitted to our hospital due to pain and a lump of the anterior chest wall. Before the operation, a chest computed tomography (CT) scan reconstruction identified the abnormal mass on the manubrium sterni (size, 6 cm × 4 cm in diameter). An aspiration needle biopsy was not conducted; however, the patient underwent tumor radical resection and sternal reconstruction using autogenous rib (*Figure 1*). With the final histopathology showing osteosarcoma, negative margin. Postoperative courses are uneventful, clinical and radiologic follow-up 2 months after surgery showed excellent morphological and functional outcome.

Figure 1 Radical resection of sternal tumor and reconstruction with autogenous rib graft (1).
Available online: http://www.asvide.com/articles/405

Operative techniques

In the operating theatre, two incisions were made, which one was made over the anterior portion of the sternum, another made through the left anterior lateral. We detected the specific position of the tumor, and confirmed the target lesion based on the preoperative chest CT. After being dissected skin and soft tissue, then the sternal lesion

dissection was performed. After being dissected and isolated in the bilateral sternocostal joints, the lower edge of the sternal lesion was dissected and cut off by fret-saw, and then the tumor was removed from the sternum, which resulted in a vertical defect of 5.0 to 6.0 cm.

The rib graft that was designed to reconstruct the sternal defects were obtained from the sixth rib after it was stripped of its periosteal and divided into two parts. The two rib grafts were then placed vertical to one another with sternal wires, which the size and shape of the implant were designed to reconstruct the sternum after the resection. Then the implant was placed in situ and fixed to the ribs and sternum with sterna wires. The chest wall was then closed.

Comments

The reconstruction of sternum defects is a challenging problem for thoracic surgeons. The location and the size of the defect play a major role when selecting the method of reconstruction, while acceptable morphological and functional results remain the primary goal. Currently, titanium mesh or polypropylene mesh is widely used in the reconstruction of sternum defects. In our case, the autogenous rib graft was successfully used to reconstruct sternal defects after partial resection. With the advantages, such as biocompatibility, stabilization, strength, and lack of risk of disease associated with prosthetic materials and myoplasties, autogenous rib graft could be very suitable for reconstruction in sternal defects, we consider that the autogenous rib grafts could be a viable alternative for patients who had sternal defects due to infection, tumor, or trauma need graft to stabilize the sternum.

Cite this article as: Li W, Zhang G, Ye C, Yin D, Shen G, Chai Y. Autogenous rib graft for reconstruction of sternal defects. J Thorac Dis 2014;6(12):1851-1852. doi: 10.3978/j.issn.2072-1439.2014.11.37

Acknowledgements

Disclosure: The authors declare no conflict of interest.

References

1. Li W, Zhang G, Ye C, et al. Radical resection of sternal tumor and reconstruction with autogenous rib graft. Asvide 2014;1:371. Available online: http://www.asvide.com/articles/405

GCTAB Column

VATS right upper lobectomy

Xinyu Mei, Tian Li, Mingran Xie, Dongchun Ma

Department of Thoracic Surgery, The Anhui Affiliated Provincial Hospital, Anhui Medical University, Hefei 230001, China

Correspondence to: Dongchun Ma. Department of Thoracic Surgery, The Anhui Affiliated Provincial Hospital, Anhui Medical University, Hefei 230001, China. Email: madongchun126@126.com.

Abstract: A 56-year-old male patient was admitted due to one small pulmonary nodule in the apicoposterior segment of the right upper lobe, which was found on his health screening one month ago. Preoperative examinations showed no distant metastasis, and his heart and lung functions could tolerate the lobectomy. Chest computed tomography (CT) showed one small pulmonary nodules on the apicoposterior segment of the right upper lobe, which was considered to be malignant lesions. No remarkably swollen lymph node was visible in the mediastinum. Therefore, VATS right upper lobectomy was performed and intraoperative frozen section confirmed the diagnosis of adenocarcinoma.

Keywords: VATS; right upper lobectomy; sequential dissection

Submitted Nov 11, 2014. Accepted for publication Nov 14, 2014.
doi: 10.3978/j.issn.2072-1439.2014.12.15
View this article at: http://dx.doi.org/10.3978/j.issn.2072-1439.2014.12.15

Case report

Introduction

A 56-year-old male patient was admitted due to one small pulmonary nodule in the apicoposterior segment of the right upper lobe, which was found on his health screening 1 month ago. Preoperative examinations showed no distant metastasis, and his heart and lung functions could tolerate the lobectomy. Chest computed tomography (CT) showed one small pulmonary nodules on the apicoposterior segment of the right upper lobe, which was considered to be malignant lesions. No remarkably swollen lymph node was visible in the mediastinum. Therefore, VATS right upper lobectomy was performed and intraoperative frozen section confirmed the diagnosis of adenocarcinoma.

Procedure (*Figure 1*)

Operative techniques

The three-port method was applied: the observation port was made in the 7th intercostal space at the middle axillary line, the main working port was in the 3th intercostal space at the anterior axillary line, and the remaining one auxiliary port was located in the 9th intercostal space at the posterior axillary line. Sequential dissection (right superior pulmonary vein-right pulmonary truncus anterior artery-right pulmonary posterior ascending artery-right upper lobe bronchus) was applied.

The main device used in the surgery was electric hook, which is featured by clear operation field, easy to operate and good hemostatic effect. The device used in lymph node dissection was ultrasonic scalpel, which had the advantage of good hemostatic effect and multiple procedures including clamping and propping using its different parts.

Firstly, a VATS lung clamp was applied to lift the right upper lobe to expose the hilum of the lung. Electric hook was then applied to open the pleura covering the surface of superior pulmonary vein and continued downwards to identify the presence of inferior pulmonary vein. Then, the spaces between the superior pulmonary vein and its deep pulmonary artery trunk were separated; the right superior pulmonary vein was dissociated. An Ethicon Endo-Surgery endoscopic cutter (EC-60) and white staple cartridge were applied.

The right pulmonary truncus anterior artery was exposure and dissociated, an Ethicon Endo-Surgery endoscopic cutter and white staple cartridge was applied. Then the right pulmonary posterior ascending artery was separated and the lymph nodes in the pulmonary hilum

Figure 1 VATS right upper lobectomy (1).
Available online: http://www.asvide.com/articles/406

(station 10, near the root of right lung artery and right main bronchus) were dissociated. The right pulmonary posterior ascending artery was ligatured by surgical suture and dissected by ultrasonic scalpel.

The right main bronchus was exposed; an Ethicon Endo-Surgery endoscopic cutter and green staple cartridge was applied. After the right main bronchus was dissociated, the pulmonary fissure was then dissociated by Ethicon Endo-Surgery endoscopic cutter and blue staple cartridges. Then, the right upper lobe was placed in an endobag and extracted.

Cite this article as: Mei X, Li T, Xie M, Ma D. ATS right upper lobectomy. J Thorac Dis 2014;6(12):1853-1854. doi: 10.3978/j.issn.2072-1439.2014.12.15

Ultrasonic scalpel was used to dissect the interlobar, pulmonary hilum and mediastinum (station 2, 3, 4, 7, 9) lymph nodes. The nervi vagus and pulmonary plexus of the right pulmonary were protected during the dissection of the station 2, 4 and 7 lymph nodes.

Comments

Sequential dissection (or, single-direction approach) was applied in this surgery to avoid frequent turn-over of the lung lobes and shift of visual angle during the procedures. The electric hook and ultrasonic scalpel were used in this surgery enables rapid dissection and dissociation, with clear visual field and small blood loss. It is feasible and beneficial to protect the nervi vagus and pulmonary plexus during the dissection of the mediastinum lymph nodes.

Acknowledgements

Disclosure: The authors declare no conflict of interest.

References

1. Mei X, Li T, Xie M, et al. VATS right upper lobectomy. Asvide 2014;1:372. Available online: http://www.asvide.com/articles/406

GCTAB Column

Thoracoscopic left upper lobectomy with systematic lymph nodes dissection under left pulmonary artery clamping

Yi-Nan Dong, Nan Sun, Yi Ren, Liang Zhang, Ji-Jia Li, Yong-Yu Liu

Department of Thoracic Surgery, Liaoning Province Cancer Hospital, Shenyang 110042, China

Correspondence to: Prof. Yong-Yu Liu. Department of Thoracic Surgery, Liaoning Province Cancer Hospital, 44 Xiao He Yan Road, Shenyang 110042, China. Email: profyongyuliu@163.com.

Abstract: Video-assisted thoracoscopic surgery (VATS) has become a routine procedure for stage I and II lung cancers. However, in the presence of multiple metastasized lymph nodes invading the pulmonary artery or its major branches, the pulmonary artery have to be resected partially or sleeve resected, which could be extremely risky under thoracoscopic conditions. In order to reduce the risk of bleeding, an experienced thoracic surgeon would occlude the inflow and outflow of the pulmonary artery before anatomically dissecting the area of the pulmonary artery with tumor invasion. Different centers may use different clamping techniques and devices. Here, we report our technique of totally thoracoscopic left upper lobectomy with systematic lymph nodes dissection under pulmonary artery clamping for a 49-year-old woman with left upper lobe carcinoma. The video demonstrates our thinking and surgical process.

Keywords: Video-assisted thoracoscopic surgery (VATS); left pulmonary artery clamping; left lower lobe pulmonary artery; left upper lobectomy; systematic lymph node dissection

Submitted Nov 11, 2014. Accepted for publication Nov 14, 2014.
doi: 10.3978/j.issn.2072-1439.2014.11.23
View this article at: http://dx.doi.org/10.3978/j.issn.2072-1439.2014.11.23

Introduction

A stage I or II lung cancer without or with mild lymph node metastasis can be easily operated using an anatomical resection or the single-direction approach. However, multiple hilar and mediastinal lymph nodes metastasis increases the difficulty of a VATS procedure. This is particularly the case, where the pulmonary artery or its major branches are suspected to be invaded by metastasized lymph nodes, which significantly increases the risk of arterial bleeding. Pulmonary artery clamping following an anatomical lobectomy can reduce the risk of an uncontrollable bleeding from a pulmonary artery, and allow the thoracoscope procedure to proceed. There is no doubt that, before the pulmonary artery clamping, it is critical to conduct a surgical exploration, removing the metastatic lymph nodes and fibrofatty tissues surrounding the artery to be clamped, and determine the feasibility of the clamping and the necessity of an open conversion. With a successful upstream and downstream control, we would be able to confidently manage the pulmonary artery or its major branches with suspected tumor invasion.

Summary of clinical case

The patient was a 49-year-old woman, who was found to have a left upper lobe mass during a health check (*Figure 1A,B*). A chest CT with enhancement revealed multiple enlarged hilar and mediastinal lymph nodes. The nature of the mass was confirmed to be adenocarcinoma by transpercutaneous lung biopsy. There was no evidence of any distant metastasis or surgical contraindication judging from the preoperative workups. We decided to operate the patient using VATS left upper lobectomy with systematic lymph node dissection. The challenge of our preoperative patient evaluation came from the fact that, around the apical branch of the left upper pulmonary artery, there were enlarged lymph nodes with potential tumor metastasis (*Figure 2*), which would bring difficulty to the dissection of the apical segmental artery. Thoracoscopic pulmonary artery clamping might be needed

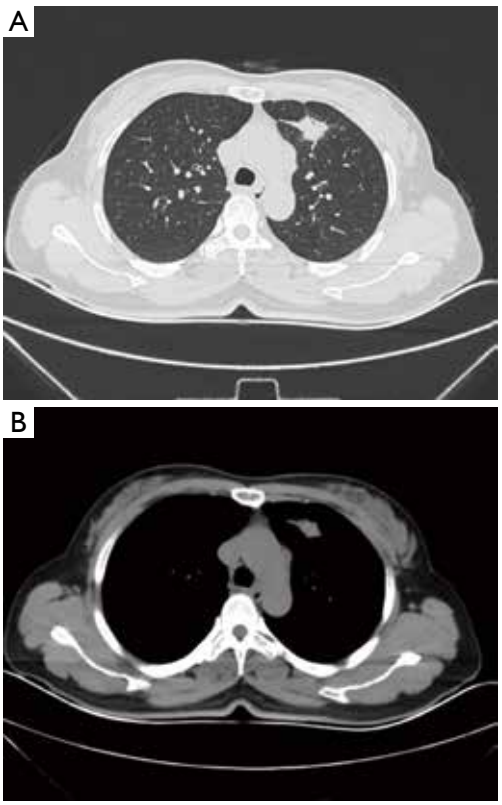

Figure 1 The left upper lobe tumor with multiple enlarged hilar and mediastinal lymph nodes.

during the procedure.

Surgical techniques

The patient was placed on her right lateral decubitus position. The operation was conducted under general anesthesia with double-lumen endotracheal intubation. The camera port (1 cm in diameter) was placed in the seventh intercostal space (ICS) on the left posterior axillary line. The utility port (3 cm) was placed in the fourth ICS on the left anterior axillary line. The first auxiliary port (1 cm in length) was placed in the sixth ICS on the left anterior axillary line. The second auxiliary port (0.5 cm) was placed in the fifth ICS below the subscapular angle (*Figure 3*).

Step 1: dissecting the station 5 lymph nodes

The mediastinal pleura on the surface of the left superior pulmonary vein was opened using a hook-shaped electrocautery. The station 5 lymph nodes were dissected,

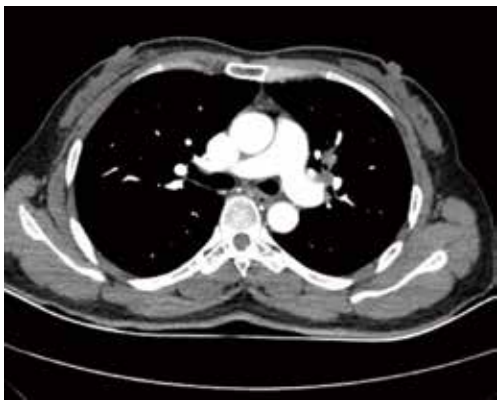

Figure 2 The enlarged lymph nodes covered the apical artery.

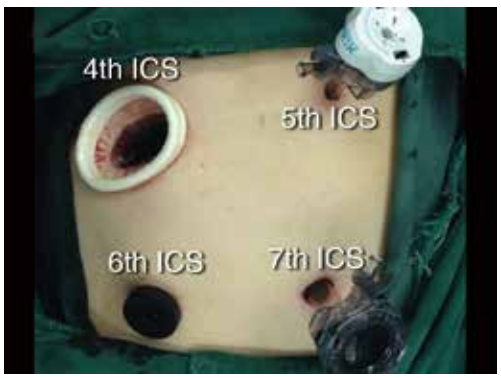

Figure 3 The thoracoscopic port was made on the posterior axillary line in the seventh intercostal space (ICS). The utility port was on the anterior axillary line in the forth ICS. The first auxiliary port was on the anterior axillary line in the sixth ICS. The second auxiliary port was placed in the fifth ICS below the subscapular angle.

along the space superior to the left pulmonary vein, using dissecting forceps and a Harmonic scalpel (*Figure 4*). During the dissection process, attention and precaution were given to protect the phrenic nerve and recurrent laryngeal nerve. Attention was given to determine the relationship between the enlarged lymph nodes and the anterior wall of the left main pulmonary artery. In the event the enlarged lymph nodes tightly adhere to the left main pulmonary artery, subsequent thoracoscopic mobilization of the artery would carry a fairly high risk of an uncontrollable major bleeding, if this artery were injured. This procedure started with the dissection of the station 5 lymph nodes, with the objective to explore and assess whether the proximal left pulmonary artery could dissected and exposed for subsequent arterial clamping. The second objective was to assess whether the

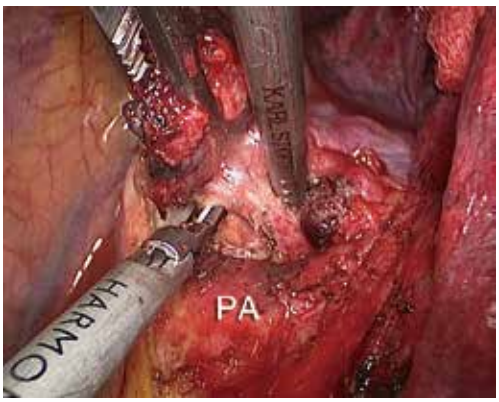

Figure 4 Dissecting the station 5 lymph nodes.

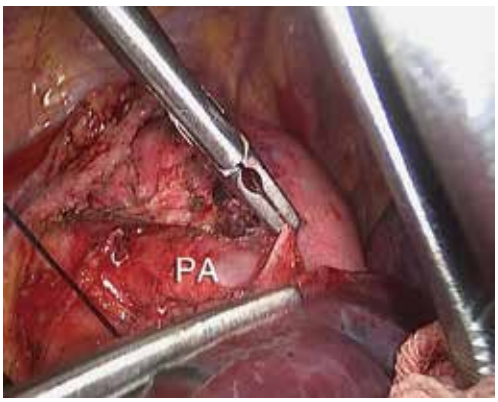

Figure 5 The enlarged station 4 lymph nodes did not invade the left pulmonary artery.

aortic arch had been invaded. It would be very difficult to clamp the left pulmonary artery, if its anterior wall could not be exposed by dissection.

Step 2: opening the posterior mediastinal pleura and exploring the tissues posterior to the hilum

The posterior mediastinal pleura were opened towards superiorly, to determine whether there were any significantly enlarged hilar or mediastinal lymph nodes, and whether major tissues behind the hilum were immobilized due to the invasion and adhesion by metastasized lymph nodes. In this procedure, the tissues anterior to the hilum were found to be fairly mobile, although the lymph nodes were enlarged.

Step 3: dissecting the left superior pulmonary vein

We returned to the area anterior to the hilum, where we mobilized the left superior pulmonary vein sufficiently using dissecting forceps. As we were mobilizing the posterior wall, the dissecting forceps were placed as much as closer to the left upper lobe bronchus, to avoid potential injury to the left superior pulmonary vein. Afterwards, a double 7-0 suture was placed across the vein for traction purposes.

Step 4: probing the proximal left main pulmonary artery

The superior pulmonary vein was pulled downwards. The sheath of the left main pulmonary artery was dissected bluntly using dissecting forceps, and it was opened using a Harmonic scalpel. The proximal trunk of the left main pulmonary artery was found to be fairly mobile, although posteriorly there were station 4 lymph nodes, which, however, did not invade the left pulmonary artery (*Figure 5*). Therefore, we were confident that the proximal trunk of the left main pulmonary artery could be released and mobilized.

Step 5: managing the fissure and mobilizing left upper lobe arterial branches

After confirming that the proximal pulmonary artery trunk could be mobilized, we proceed to manage the oblique fissure. The objective was to know whether there were enlarged lymph nodes surrounding the trunk of the left lower lobe pulmonary artery, which might preventing us from freeing the artery. In addition, the left upper lobe lingual segmental artery and the posterior segmental artery could be managed, after the oblique fissure was separated. The apical artery with suspected tumor invasion would be divided, after the left pulmonary artery clamping. In this patient, the fissure was well developed, and we open the fissure using an electrocautery and a Harmonic scalpel. The lymph nodes in front of the lingual artery were also dissected, and the lingual artery and posterior segmental artery were subsequently divided in an anterior-to-posterior direction. While dissecting the apical artery, we found stiff lymph nodes adhering to the apical artery (*Figure 6*), and we therefore chose to mobilize this artery after the clamping the left main pulmonary artery and left lower lobe pulmonary artery.

Step 6: dividing the left upper pulmonary vein

Following the surgical exploration, we confirmed that the left upper lobe and its tumor tissues could be completely

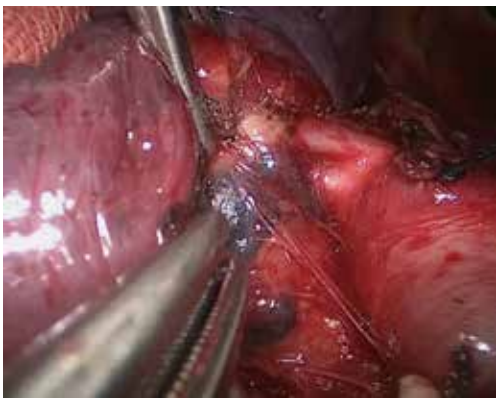

Figure 6 There were stiff lymph nodes adhering to the apical artery.

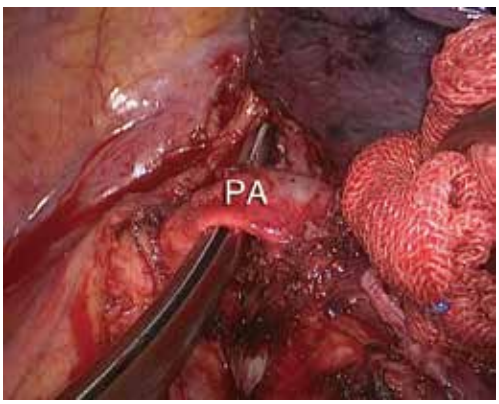

Figure 7 Complete mobilization of the proximal left main pulmonary.

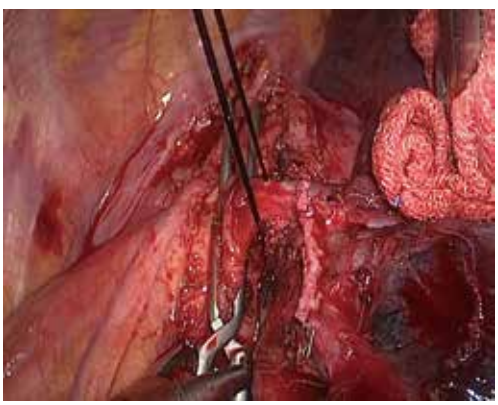

Figure 8 The left pulmonary artery were clamped using an endoscopic bulldog clamp.

resected under left pulmonary artery clamping. We divided the left superior pulmonary vein using an Ethicon 45 linear stapler with a white cartridge. The anterior wall of the left main pulmonary artery could now be accessed without any barrier.

Step 7: complete mobilization of the proximal left main pulmonary and the dissection of station 4 lymph nodes

The sheath of the proximal trunk of the left main pulmonary artery was further opened using dissecting forceps and a Harmonic scalpel. The space between this artery and the left upper lobe bronchus was further dissected and expanded. The left upper lobe was pulled anteriorly, exposing the posterior wall of the left main pulmonary artery. The station 4 lymph nodes were removed, and the posterior wall of the left main pulmonary artery was able to be fully mobilized. A pair of ring forceps was then placed across this artery to lay down the traction suture (*Figure 7*), finishing the preparation for the proximal clamping of the left main pulmonary artery.

Step 8: mobilizing the left main lower pulmonary artery

The left lower lobe artery was dissected bluntly, and a double 7-0 traction suture was placed across the artery, to facilitate subsequent vascular clamping.

Step 9: simultaneous clamping of the proximal left main pulmonary artery and the main left inferior pulmonary artery

The left pulmonary artery (*Figure 8*) and left inferior pulmonary artery (*Figure 9*) were clamped using an endoscopic bulldog clamp.

Step 10: blunt mobilization of the apical artery of the left upper lobe

The left pulmonary artery and left lower lobe pulmonary artery were clamped, and the apical artery with possible tumor invasion was then dissected bluntly. While there were enlarged lymph nodes surrounding the apical artery;

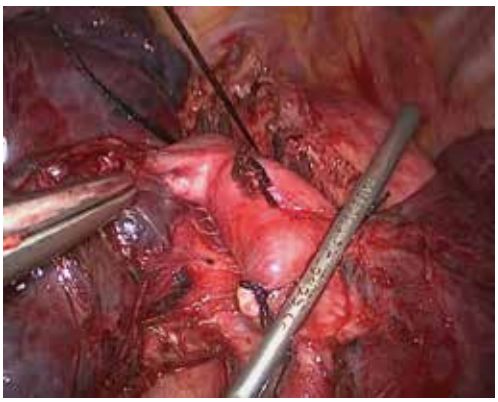

Figure 9 The left inferior pulmonary artery were clamped using another endoscopic bulldog clamp.

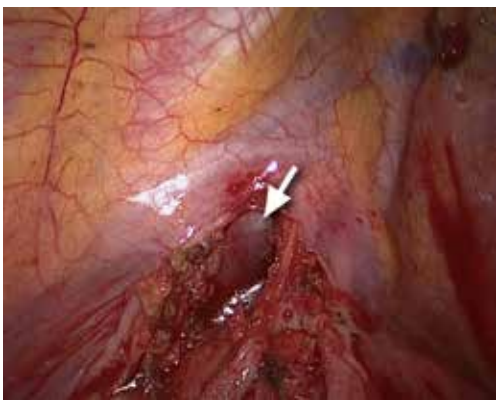

Figure 10 The inferior wall of the left innominate vein must be revealed, following a successful dissection of the station 6 lymph nodes and associated fatty tissues.

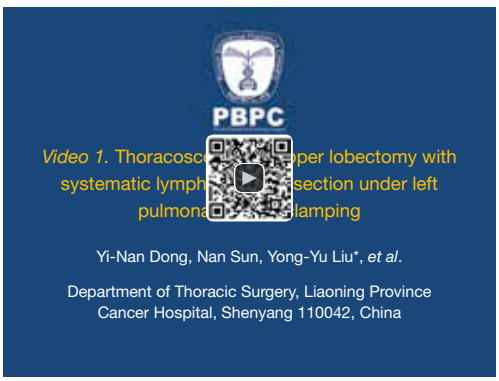

Figure 11 Thoracoscopic left upper lobectomy with systematic lymph nodes dissection under left pulmonary artery clamping (1). Available online: http://www.asvide.com/articles/407

however, the lymph nodes did not fully cover the artery. Instead, there was a short free space, which allowed us to divide the artery using an Ethicon 45 linear stapler loaded with a white cartridge. All high risk steps of this procedure were now completed.

Step 11: transection of the left upper lobe bronchus

The left upper lobe bronchus was mobilized from its surrounding tissues, and was then divided using an Ethicon 45 linear stapler loaded with a green cartridge. The left upper lobe specimen was subsequently retrieved through the utility port.

Step 12: further mediastinal lymph nodes dissection

After the left upper lobe resection, we proceeded with the dissection of station 6 and 7 lymph nodes. We followed the principle of regional lymph nodes dissection. By definition, station 7 lymph nodes refer to those below the trachea bifurcation, above the lower pulmonary vein, posterior to the pericardium, and anterior to the esophageal wall. All lymph nodes and fat tissues within this range were resected in an en bloc manner. The inferior wall of the left innominate vein must be revealed, following a successful dissection of the station 6 lymph nodes and associated fatty tissues (*Figure 10*).

Comments

In thoracoscopic left upper lobectomy under left main pulmonary artery clamping, we first need to dissect the tissue anterosuperior to the left hilum, and explore the anterior wall of the left main pulmonary artery. If station 5 and 10 lymph nodes are enlarged due to metastasis, these lymph nodes need to be dissected. If these lymph nodes show significant extranodal invasion and appear to be immobilized, managing these lymph nodes thoracoscopically carries an extremely high risk of a major bleeding, and open conversion would be a better option. As demonstrated in *Figure 11*, the station 5 lymph nodes with metastasis were dissected with caution, and the anterior wall of the left main pulmonary artery was revealed. Afterwards, we shifted our focus to the posterior wall of the left main pulmonary artery, where station 4 lymph nodes were located. The removal of these nodes allowed us to dissect within the space between the left pulmonary artery and left

main bronchus, towards the anterior wall of the left main pulmonary artery. An endoscopic bulldog clamp was then placed on the left mainly pulmonary artery, in an anterior-to-posterior direction. Because the artery that we wish to manage was a branch of the left upper lobe pulmonary artery, simply clamping proximal left main pulmonary artery (upstream) would not be sufficient. The inferior pulmonary artery (downstream) would have to clamp as well, so as to prevent blood backflow. This is what we call "inflow-outlfow bidirectional occlusion", which enabled us to mobilize the apical branch of the left upper lobe with confidence. We were pleased to find that this arterial branch was not fully covered by metastasized lymph nodes. This gave us the space to manipulate an Ethicon stapler, and successfully complete the high risk steps of this left upper lobectomy.

Another challenge that we faced was how to manage the arterial branches with suspected tumor invasion. Our practice is that this branch shall be mobilized first, because transection after mobilization is the safest and most reliable approach. In the event this branch is circumferentially covered by tumor or metastatic lymph nodes, or if the main trunk at the bifurcation is also invaded, the only option would be left pulmonary artery wall resection or sleeve resection. However, this approach is very challenging, and is better completed by a thoracic surgeon with extensive experiences. Another safe option is open conversion.

Thoracoscopic pulmonary artery clamping is not a routine surgery. It demands a surgeon with extensive thoracoscopic surgery experiences and accurate and objective intra-operative judgment. What we advocate is a safe and effective surgery, not a minimally invasive procedure for the sake of minimally invasiveness.

Cite this article as: Dong YN, Sun N, Ren Y, Zhang L, Li JJ, Liu YY. Thoracoscopic left upper lobectomy with systematic lymph nodes dissection under left pulmonary artery clamping. J Thorac Dis 2014;6(12):1855-1860. doi: 10.3978/j.issn.2072-1439.2014.11.23

Acknowledgements

Disclosure: The authors declare no conflict of interest.

References

1. Dong YN, Sun N, Ren Y, et al. Thoracoscopic left upper lobectomy with systematic lymph nodes dissection under left pulmonary artery clamping. Asvide 2014;1:373. Available online: http://www.asvide.com/articles/407

GCTAB Column

Thoracoscopic resection of functional posterior mediastinal paraganglioma: a case report

Lin Ma, Jianong Mei, Lunxu Liu

Department of Thoracic Surgery, West China Hospital of Sichuan University, Chengdu 610041, China
Correspondence to: Lunxu Liu. Department of Thoracic Surgery, West China Hospital of Sichuan University, No. 37, Guoxue Alley, Chengdu 610041, China. Email: lunxu_liu@aliyun.com.

Abstract: A 48-year-old man with posterior mediastinal mass was diagnosed as functional mediastinal paraganglioma during surgical exploration via open thoracotomy in another hospital. The operation was terminated because of severe hypertension when touching the tumor. He was transferred to our center later. After systemic evaluation, the patient was medicated with oral alpha- and beta-blockades, as well as intravenous fluid resuscitation for two weeks. His blood pressure became stable and a second operation was planned. The tumor was removed completely via the thoracoscopic approach, and was finally confirmed as functional paraganglioma by immunohistochemistry. The patient recovered uneventfully after surgery, with no recurrence during one year follow-up visit.

Keywords: Thoracoscopic resection; functional mediastinal paraganglioma; case report

Submitted Nov 11, 2014. Accepted for publication Dec 16, 2014.
doi: 10.3978/j.issn.2072-1439.2014.12.30
View this article at: http://dx.doi.org/10.3978/j.issn.2072-1439.2014.12.30

Case presentation (*Figure 1*)

A 48-year-old man was admitted to our center for a functional posterior mediastinal paraganglioma on the left side of the vertebrae. He suffered from hypertension for nine years with intermittent palpitation and headaches without significant family history. The tumor was found incidentally on abdominal computed tomography (CT) scan two months before admission. He underwent surgical exploration via open thoracotomy in another hospital previously. However, his blood pressure increased to 302/165 mmHg when touching the tumor and the operation was terminated. After previous surgery, plasma test of catecholamines showed that norepinephrine was 839 ng/L (ref range, less than 559 ng/L) and epinephrine was 2,340 ng/L (ref range, less than 122 ng/L). He was diagnosed as functional mediastinal paraganglioma and transmitted to our department later. Chest magnetic resonance imaging (MRI) scan was performed and revealed a 2 cm × 3 cm paravertebral mass centered at T11-T12 without vertebrae destruction (*Figure 2*). Abdominal contrast CT scan showed no abnormalities of the adrenal glands or the retroperitoneum. The patient was medicated with oral alpha- and beta-blockades, as well as intravenous Ringer's solution (40 mL/kg/day) for two weeks. His hypertension was stabilized and a complete resection of the tumor was planned, using the thoracoscopic approach.

The patient was placed in the right lateral decubitus position after general anesthesia with double-lumen endotracheal intubation. Both arterial blood pressure and central venous pressure were monitored carefully during the operation. A 1-cm thoracoscopic port was made in the seventh intercostal space (ICS) on the midaxillary line. After thoracoscopic exploration, the other two 2-cm incisions were made in the fifth ICS on the anterior axillary line and in the ninth ICS between the posterior axillary line and the scapular line, respectively (*Figure 3A*). Pleural adhesiolysis was performed first. A 2 cm × 3 cm mass was found in the left side, adjoining the T11-T12 vertebral body. The patient's blood pressure varied between 125/75 and 165/95 mmHg when cutting the pleura along the basement of the mass. After ligating the vein of the tumor, his blood pressure decreased to 90/50 mmHg, and intravenous norepinephrine was administered to maintain hemodynamic stability.

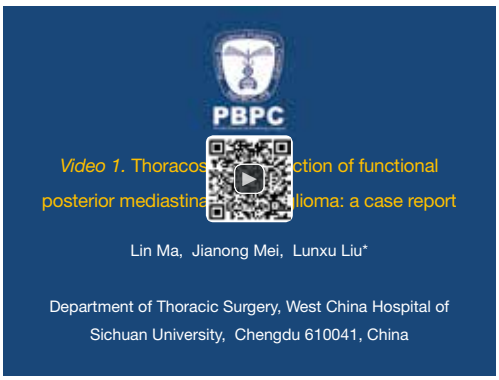

Figure 1 Thoracoscopic resection of functional posterior mediastinal paraganglioma: a case report (1).
Available online: http://www.asvide.com/articles/408

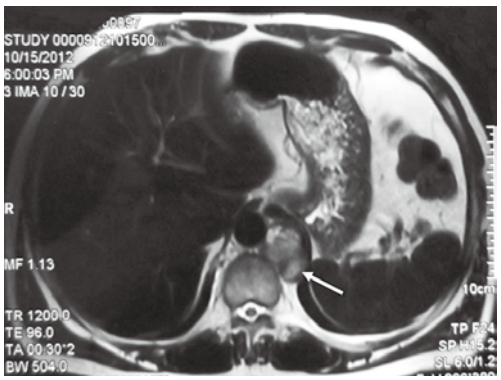

Figure 2 MRI scan revealed a 2 cm × 3 cm paravertebral mass in the posterior mediastinum centered at T11-T12 without vertebrae destruction. MRI, magnetic resonance imaging.

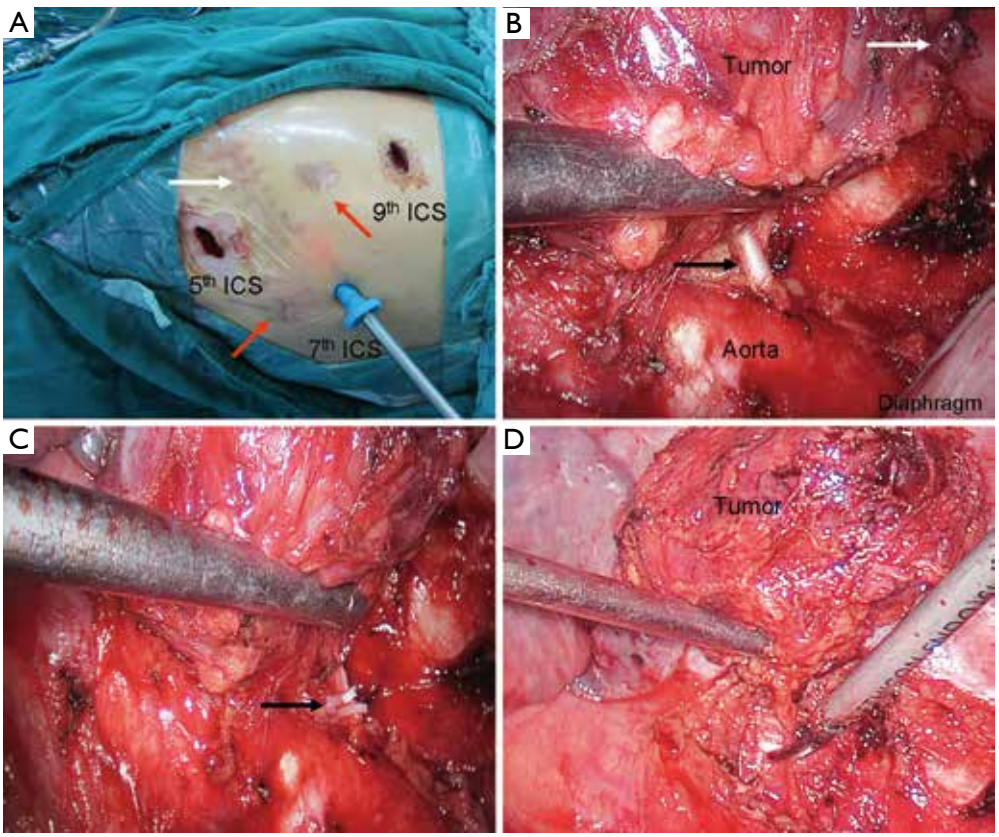

Figure 3 (A) Thoracoscopic incisions of the operation; (B) nutrient artery of the tumor was derived from the descending aorta; (C) proximal artery was double ligated with two hemolock clips; (D) en-block resection of the tumor. ICS, seventh intercostal space.

En bloc resection of the tumor was achieved after transecting the nutrient artery derived from the descending aorta (*Figure 3B-D*). The tumor was removed using a bag made from a rubber glove.

Immunohistochemistry analysis revealed that chromogranin (CgA), synaptophysin (Syn) and S-100 protein were highly expressed in the tumor. The patient was finally confirmed as functional mediastinal paraganglioma. Intravenous medication of norepinephrine was gradually withdrawn on the operative day. His serum

catecholamines recovered to normal level on postoperative day 3. The patient recovered uneventfully and stopped using antihypertensive drugs after surgery. He was discharged home on postoperative day 6, and had neither hypertension nor local recurrence during 18 months follow-up.

Discussion

Paragangliomas refer to a set of tumors arising from the chromaffin cells of the autonomic ganglia. Most of these tumors occur in the adrenal medulla and are commonly known as pheochromocytomas. Extra-adrenal pheochromocytomas account for about 15% of all the pheochromocytomas in adult patients (2), and can be classified as functional or non-functional paragangliomas based on the ability of synthesizing and releasing catecholamines (3). More than 75% of the extra-adrenal functional paragangliomas derive from organ of Zuckerkandl at the bifurcation of the aorta and the para-aortic region in the retroperitoneum (2). Functional mediastinal paragangliomas are rare, and most of them origin in the posterior mediastinum (4). These tumors may cause the same physiologic changes and symptoms as those occur in the adrenal medulla, or sometimes asymptomatic (4-7). The level of plasma free or urinary fractionated metanephrines is helpful in screening patients with functional paragangliomas (8). The possibility of functional paragangliomas can be virtually ruled out in patients with negative plasma free metanephrines. Additionally, ^{123}I- or ^{131}I-metaiodobenzylguanidine (MIBG) scan would provide detailed information on the function and location of these tumors, especially for the extra-adrenal lesions and metastases (9,10).

Preoperative diagnosis of ectopic pheochromocytoma is still more or less a challenge for thoracic surgeons. Some patients may be misdiagnosed as nonfunctional tumors until surgery due to insufficient preoperative assessment (3,6). Delayed diagnosis of these tumors caused unexpected critical hypertension when starting surgical resection of the tumor and severe hypotension or even shock after removing the tumor. This may put the patient in jeopardy. In the present case, functional paraganglioma was also ignored before the first operation in such a middle-aged man with early onset of hypertension combined with a posterior mediastinal neoplasm. The patient presented with incredible high blood pressure during the first operation when touching the tumor. As Sakamaki *et al.* and our previously reports (4,6), the operation could be safely continued in asymptomatic patients with functional paragangliomas diagnosed during the operation after preparation with antihypertensive drugs as well as sufficient fluid resuscitation. However, symptomatic patients with functional paragangliomas diagnosed during the operation have been rarely reported to be removed successfully with one-stage operation. When concerning the high risk of removing pheochromocytoma without effective preoperative preparation, we believe that it's a wise choice to terminate the operation for this patient. When the patient was transmitted to our center, we assessed his blood catecholamines and thoracoabdominal imaging scan. The patient was clinically diagnosed as functional posterior mediastinal paraganglioma and no more lesions were identified before surgery. Though MIBG scan can help us in excluding whether there were any other lesions in this patient, we chose routine thoracoabdominal imaging techniques such as CT and MRI to evaluate the most common sites of paragangliomas. These techniques provided us more useful and detailed anatomical information for surgical decision. Postoperative decrease of plasma catecholamines and normalization of blood pressure confirmed that there no other lesions. The operation was then carried out after systemic preparation with drugs and blood volume expansion for two weeks to achieve a stable haemodynamic status.

Surgical resection is the most preferred treatment for patients with paraganglioma (9). For patients with adrenal pheochromocytoma or retroperitoneal paraganglioma, video-assisted endoscope has been increasingly adopted as a feasible and safe approach for operation (11). Intraoperative hemodynamic changes were the same in patients with adrenal pheochromocytoma who underwent video-assisted endoscopic or open operations (12). Thoracoscope has been widely applied in the treatment of thoracic diseases since last two decades, including the mediastinal neurogenic tumors (13). However, only a young girl with concomitant right adrenal pheochromocytoma and functional mediastinal paraganglioma has been reported underwent video-assisted endoscopic resection of the tumor (14). Most of the reported cases with functional mediastinal paraganglioma were removed via posterolateral thoracotomy. Even though the present case has undergone previous thoracotomy, we still planned a thoracoscopic operation for him after a careful evaluation of the chest MRI scan. When performing the operation, we tried our best to avoid squeezing the tumor in order to minimize the fluctuations of the patient's blood pressure. The tumor was dissected along the basement. Nourishing blood vessels of the tumor were ligated when identified. An obvious decrease of arterial blood pressure

was observed after ligating the drainage vein of the tumor. The anesthesiologist then medicated intravenous norepinephrine to maintain the patients' blood pressure immediately. An experienced anesthesiologist is very important for the safety of such an operation. With effective co-operation with the anesthesiologist, the operation was finished uneventfully. Though thoracoscopic approach was successfully applied in the present case, we believe that thoracotomy should be preferred for tumors with abundant blood supply. After surgery, a regular follow-up is needed for these patients because both pheochromocytoma and functional paraganglioma are potentially malignant tumors.

In conclusion, functional mediastinal paragangliomas are still easily misdiagnosed and this should be taken into account in patients with unknown mediastinal neoplasm, especially those in the posterior mediastinum. Thoracoscopic resection of a functional mediastinal paraganglioma is feasible and safe in selected patients.

Acknowledgements

Disclosure: The authors declare no conflict of interest.

References

1. Ma L, Mei J, Liu L. Thoracoscopic resection of functional posterior mediastinal paraganglioma: a case report. Asvide 2014;1:374. Available online: http://www.asvide.com/articles/408
2. Whalen RK, Althausen AF, Daniels GH. Extra-adrenal pheochromocytoma. J Urol 1992;147:1-10.
3. Soffer D, Scheithauer BW. Paraganglioma. In: Kleihues P, Cavenee WK. eds. Pathology and Genetics of Tumours of the Nervous System. Lyon, France: IARC Press, 2000:112-4.
4. Sakamaki Y, Yasukawa M, Kido T. Pheochromocytoma of the posterior mediastinum undiagnosed until the onset of intraoperative hypertension. Gen Thorac Cardiovasc Surg 2008;56:509-11.
5. Suzawa K, Yamamoto H, Ichimura K, et al. Asymptomatic but functional paraganglioma of the posterior mediastinum. Ann Thorac Surg 2014;97:1077-80.
6. Liu L, Mei J, Che G. Asymptomatic paraganglioma of the posterior mediastinum misdiagnosed until operation. Thorac Cardiovasc Surg 2010;58:302-4.
7. Paul S, Jain SH, Gallegos RP, et al. Functional paraganglioma of the middle mediastinum. Ann Thorac Surg 2007;83:e14-6.
8. Lenders JW, Pacak K, Walther MM, et al. Biochemical diagnosis of pheochromocytoma: which test is best? JAMA 2002;287:1427-34.
9. Young WF Jr. Paragangliomas: clinical overview. Ann N Y Acad Sci 2006;1073:21-9.
10. Spector JA, Willis DN, Ginsburg HB. Paraganglioma (pheochromocytoma) of the posterior mediastinum: a case report and review of the literature. J Pediatr Surg 2003;38:1114-6.
11. Walz MK, Alesina PF, Wenger FA, et al. Laparoscopic and retroperitoneoscopic treatment of pheochromocytomas and retroperitoneal paragangliomas: results of 161 tumors in 126 patients. World J Surg 2006;30:899-908.
12. Vargas HI, Kavoussi LR, Bartlett DL, et al. Laparoscopic adrenalectomy: a new standard of care. Urology 1997;49:673-8.
13. Liu HP, Yim AP, Wan J, et al. Thoracoscopic removal of intrathoracic neurogenic tumors: a combined Chinese experience. Ann Surg 2000;232:187-90.
14. Qazi A, Najmaldin A, Powis M. Combined laparoscopic and thoracoscopic excision of pheochromocytoma and functional paraganglioma. J Laparoendosc Adv Surg Tech A 2007;17:704-6.

Cite this article as: Ma L, Mei J, Liu L. Thoracoscopic resection of functional posterior mediastinal paraganglioma: a case report. J Thorac Dis 2014;6(12):1861-1864. doi: 10.3978/j.issn.2072-1439.2014.12.30

GCTAB Column

Optimization of lymph node dissection with VATS right upper lobectomy

Hui-Wen Miao, Zhou-Miao Chen

Department of Thoracic Surgery, Sir Run Run Shaw Hospital, School of Medicine, Zhejiang University, Hangzhou 310006, China
Correspondence to: Zhou-Miao Chen. Qingchun Road 3, Hangzhou 310006, China. Email: 351426012@qq.com.

Abstract: Video-assisted thoracoscopic lobectomy (VATSL) has developed rapidly. As per the requirements of tumor staging and oncotherapy, the technique of VATS mediastinal lymph node dissection plays an important role. With our experience, lymph node dissection can be performed very well on the condition that surgical process and skills be optimized.

Keywords: Video-assisted thoracoscopic (VATS); lymphadenectomy; lung cancer

Submitted Nov 11, 2014. Accepted for publication Nov 14, 2014.
doi: 10.3978/j.issn.2072-1439.2014.11.26
View this article at: http://dx.doi.org/10.3978/j.issn.2072-1439.2014.11.26

Introduction

In recent years, pulmonary lobectomy of full endoscope has developed rapidly. Lots of retrospective studies (1,2) showed safety and feasibility of Video-assisted thoracoscopic lobectomy (VATSL). On the premise of choosing incision properly, to carry out VATSL is not difficult. However, whether VATS can perform complete lymph node dissection to achieve a similar effect of thoracotomy remains a bone of contention for clinical workers (2,3). Thus, we gradually carried out a series of optimization and improvement on operation steps to achieve the aim of mediastinum lymphadenectomy.

Clinical summary

A patient, female, 61 years old, was discovered with a space-occupying lesion on the right upper lung (*Figures 1*,*2*) during the routine physical examination. She has no past medical history (PMH) of long-term chronic diseases. After knowing that this mass might be lung cancer, the patient refused aspiration biopsy and asked for a thoracoscopic exploratory surgery.

Before the surgery, the patient accepted enhanced MRI of the head and ETC for whole-body bones and B-ultrasonic examination of liver and adrenal gland routinely and no specific metastatic mass wan found. No abnormity such as neoplasm was found during bronchoscopy. Preopreative examinations such as color Doppler echocardiography and pulmonary function test didn't show any clear surgical contraindication.

Preoperative assessment

It should be noted that influenced by medical costs and concepts, most Chinese patients cannot accept examinations such as mediastinoscopy and EBUS-TBNA. At the same time, PET-CT doesn't become a preoperative routine examination to help identify clinical stages. Thus, before the surgery, there is no instructional scheme of lymphadenectomy.

Though systemic lymph node biopsy has little effects on staging diagnosis, there is a possibility to miss metastatic lymph nodes and reduce radical cure of patients' surgery (4). Thus, according to guidelines of ACOSOG (5) and IASLC (6), we conduct routine lymph node dissection on lymph nodes of group 2, 4, 7, 8, 9, 10 and 11.

Anaesthesia and positioning

The patient was put as left lateral position with 90°. In order to unfold intercostal space and get a better field of view, the operating table near ribs 5-8 needs to be blocked up as high as possible.

We apply general anesthesia and double-lumen trachea cannula routinely. In order to achieve a better analgesic Port

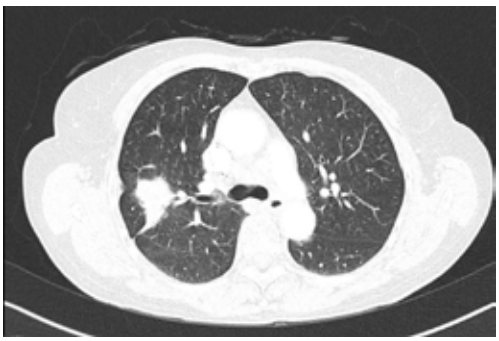

Figure 1 Relationship between the tumor and hilar.

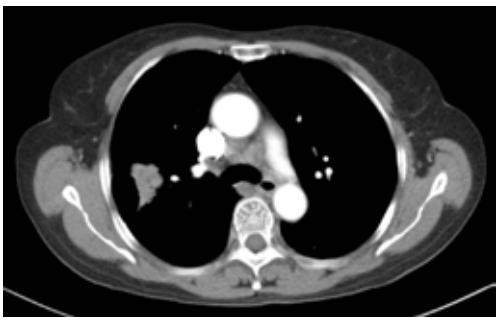

Figure 2 Relationship between the mediastinal lymph nodes and vessels.

Figure 3 Port placement.

placement effect for facilitating cough and expectoration during the perioperative period and to leave an observation hole after the surgery (leaving a postoperative drainage tube) and continuous intercostal nerve block (*Figure 3*).

Operative technique

We apply a 3-hole operation: the observation hole of thoracoscope is chosen to be located between the

Figure 4 Optimization of lymph node dissection with VATS right upper lobectomy (7).
Available online: http://www.asvide.com/articles/409

midaxillary line and the posterior axillary line of the 8th intercostal space with a length about 1.5 cm; the main operation incision is located between the anterior axillary line and the posterior axillary line of the 3rd intercostal space (limited to excision of the upper right pulmonary lobe) with a length about 3 cm. Apply protective cover of incision to protect the main operation incision during the surgery to be convenient for in-and-out of instrument and preventing tumor deposit; the auxiliary operation hole is chosen to be in the the 9th intercostal space of the scapular line with a length about 1.5 cm. After finish making incisions, first explore the chest roundly, separate the adhesion and after excluding special conditions such as metastasis in the chest, start the surgery. Decide whether to carry out pulmonary lobectomy according to results of frozen sections.

As shown in *Figure 4*, we generally use the natural angle of the single-bend attractor of the main operation incision to make the coagulation hook locate in the angle of the attractor for operation. Sponge forceps within the auxiliary operation hole are used as tools for stretching and exposing. During the operation, the dissection should be as fine as possible. Advice: (I) use HD video equipment; (II) surgical assistants of good teamwork; (III) ample view showing for the surgery; (IV) steady and patient operation habits; (V) dissociate along the natural anatomic space. Try to be exsanguine in the surgical field.

Our method of lymph node dissection tries to protect lymph nodes in adipose tissue as much as possible and avoids damage and bleeding of lymph nodesb due to holding by forceps directly. What important is that excision of the whole piece of tissue is beneficial to preventing

dissemination of tumor and accuracy of clinical staging.

Results

Pathology results of this patient indicated that 38 lymph nodes were excised. Wherein, there were 8 lymph nodes in group 2, 14 in group 7, 1 in group 8, 1 in group 9, and 5 in group 10 and 11 in total. And no metastasis was found on these lymph nodes. And it took 7 days to for drainage (we usually remove the drainage tube when the drainage is less than 200 mL/d).

Comments

Whether VATS can perform complete lymph node dissection to achieve a similar effect of thoracotomy remains a bone of contention for clinical workers (1,2). Some literature has reported that the same number of total and mediastinal LN stations could be harvested by VATS and traditional thoracotomy. The same number of N1 LNs could be harvested by VATS and traditional thoracotomy, while less total and mediastinal LNs could be harvested by VATS (8). Our experience is that thoracoscope can achieve observation in a close range with a high amplification factor, good lightning and multiple optional angles. It can expose the chest completely which cannot be matched by the traditional thoracotomy. Thus, to choose a proper operation scheme can finish lymph node dissection better.

Acknowledgements

Disclosure: The authors declare no conflict of interest.

Cite this article as: Miao HW, Chen ZM. Optimization of lymph node dissection with VATS right upper lobectomy. J Thorac Dis 2014;6(12):1865-1867. doi: 10.3978/j.issn.2072-1439.2014.11.26

References

1. Park BJ. Is surgical morbidity decreased with minimally invasive lobectomy? Cancer J 2011;17:18-22.
2. Yan TD, Black D, Bannon PG, et al. Systematic review and meta-analysis of randomized and nonrandomized trials on safety and efficacy of video-assisted thoracic surgery lobectomy for early-stage non-small-cell lung cancer. J Clin Oncol 2009;27:2553-62.
3. Topol M, Masłoń A. The problem of direct lymph drainage of the bronchopulmonary segments into the mediastinal and hilar lymph nodes. Clin Anat 2009;22:509-16.
4. Wu N, Yan S, Lv C, et al. Comparison of systematic mediastinal lymph node dissection versus systematic sampling for lung cancer staging and completeness of surgery. J Surg Res 2011;171:e169-73.
5. Darling GE, Allen MS, Decker PA, et al. Randomized trial of mediastinal lymph node sampling versus complete lymphadenectomy during pulmonary resection in the patient with N0 or N1 (less than hilar) non-small cell carcinoma: results of the American College of Surgery Oncology Group Z0030 Trial. J Thorac Cardiovasc Surg 2011;141:662-70.
6. Rusch VW, Crowley J, Giroux DJ, et al. The IASLC Lung Cancer Staging Project: proposals for the revision of the N descriptors in the forthcoming seventh edition of the TNM classification for lung cancer. J Thorac Oncol 2007;2:603-12.
7. Miao HW, Chen ZM. Optimization of lymph node dissection with VATS right upper lobectomy. Asvide 2014;1:375. Available online: http://www.asvide.com/articles/409
8. Zhang Z, Feng H, Wang X, et al. Can lymph node evaluation be performed well by video-assisted thoracic surgery? J Cancer Res Clin Oncol 2014. [Epub ahead of print].

Review Article

Nonintubated anesthesia for thoracic surgery

Bei Wang, Shengjin Ge

Department of Anesthesia, Zhongshan Hospital, Fudan University, Shanghai 200032, China
Correspondence to: Shengjin Ge. Department of Anesthesia, Zhongshan Hospital, Fudan University, Shanghai 200032, China.
Email: ge.shengjin@fudan.edu.cn.

Abstract: Nonintubated thoracic surgery has been used in procedures including pleura, lungs and mediastinum. Appropriate anesthesia techniques with or without sedation allow thoracic surgery patients to avoid the potential risks of intubated general anesthesia, particularly for the high-risk patients. However, nonintubated anesthesia for thoracic surgery has some benefits as well as problems. In this review, the background, indication, perioperative anesthetic consideration and management, and advantages and disadvantages are discussed and summarized.

Keywords: Thoracic surgery; nonintubated anesthesia; epidural block; anesthesia technique

Submitted Aug 31, 2014. Accepted for publication Nov 10, 2014.
doi: 10.3978/j.issn.2072-1439.2014.11.39
View this article at: http://dx.doi.org/10.3978/j.issn.2072-1439.2014.11.39

In recent years, with the techniques and managements of thoracic surgery increasingly improved, better lung separation and hypoxemia treatment as well as widely-used lung protective strategy have obtained proud achievement (1-3). On the other hand, to fit in with the needs of the fast track and enhanced recovery after surgery, nonintubated anesthesia for thoracic surgery has been intensively researched, reported and advocated (4-8).

Background

There are a lot of studies showing that nonintubated anesthesia for thoracic surgery is superior to the conventional general anesthesia in patients' outcomes. Nevertheless, some patients who are supposed to under nonintubated anesthesia still need intubated during the thoracic surgery (9). In 2004, Pompeo and his coworkers evaluated the feasibility of awake thoracoscopic resection of solitary pulmonary nodules in 30 patients under sole thoracic epidural anesthesia. Comparing to patients with intubated general anesthesia, their results showed that awake technique was safely feasible with better patient satisfaction, less nursing care and shorter in-hospital stay. However, it is important to note that two of the patients in the awake group were converted to intubated general anesthesia because of lung cancer requiring lobectomy via thoracotomy approach (10-12). Therefore, anesthesiologists should emphasize and balance the indication, contradiction, advantages, disadvantages, risks and benefits of nonintubated anesthesia for thoracic surgery, in order to choose better way to perform the anesthesia safely.

Indication

According to recent evidence and experience, several thoracic surgery procedures have been proved suitable for nonintubated anesthesia, such as pleural/pericardial effusion, empyema thoracis, bullous emphysema, non-resectional lung volume reduction surgery, spontaneous pneumothorax, biopsy of interstitial lung disease, wedge resection of lung nodules, segmentectomy and lobectomy for lung cancer, mediastinal biopsy and tumor excision (6,13-22).

The patients under nonintubated anesthesia should have well-evaluation and well-preparation without contraindications and should not reject to receive it. It is worth noting that Wu and colleagues had evaluated the feasibility of geriatric patients (age ranging from 65 to 87) undergoing lobectomy, which showed comparable safety profile with control group. This study opened up the possibility of nonintubated video-assisted thoracoscopic

surgery (VATS) on the old age group (23).

Contraindication

The general patients exclusion criteria includes American Society of Anesthesiologists (ASA) physical status 4 and higher, bleeding disorders, sleep apnea, unfavorable airway or spinal anatomy, strict contralateral lung isolation, clinically significant sputum production, bronchiectasis, asthma, extreme of body mass index (BMI), preoperative decompensated heart disease, severe pleural adhesion over targeted hemithorax, and noncompliance to the procedure or patient refusal (6,24).

The implement of anesthesia

Nonintubated anesthesia for thoracic surgery refers to the operation performed under regional anesthetic techniques in spontaneously breathing patients, with or without conscious sedation. Conscious sedation is safe and effective for patients using sedative or dissociative agents such as propofol, midazolam, with or without analgesics such as fentanyl to keep patient tolerate unpleasant procedures while maintaining cardiorespiratory function. That is an induced depressed level of consciousness in which a patient retains the ability to independently and continuously maintain an open airway and a regular breathing pattern, and to respond appropriately and rationally to physical stimulation and verbal commands.

Psychological preparation

Preoperative communication for reassuring the patients, intraoperative coaching, mental support, verbal communication with medical personnel, and comfortable environment with low-volume music might all contribute to calm the patients down with acceptable respiration (25,26).

Monitoring

Standard monitoring with pulse oximeter, electrocardiogram, sphygmomanometer, and end-tidal CO_2 should always be in place. In addition, invasive arterial pressure monitor is often set for its versatility on monitoring arterial blood gas, real-time hemodynamic index, and fluid status inclination. For the occasion in which sedation is part of the planning, bispectral index (BIS) is highly recommended for evaluation of sedation level and advanced judgment of the anesthesia/sedation depth.

Anesthesia techniques

The anesthetic techniques consist of local anesthesia, intercostal nerve blocks, paravertebral blocks, thoracic epidural anesthesia, and spontaneous breathing anesthesia with laryngeal mask airway (LMA). Intravenous narcotics and conscious sedation are often combined with the techniques as above. After intravenous administration of fentanyl 25 to 50 mcg, target controlled infusion of propofol and/or remifentanil is started, aiming for BIS over 50 to 70 (24). Among them, thoracic epidural anesthesia is the most popular and can be enough.

Thoracic epidural anesthesia

The use of thoracic epidural anesthesia in awake thoracic surgery was first proposed in 1950 by Buckingham *et al.* (27,28). Recent studies have reported that thoracic surgery under epidural anesthesia can be easily and safely carried out with less charges and hospital-stay (10,24,29,30). However, it is a novel field to explore and investigate the benefits, risks and disadvantages of thoracic epidural anesthesia in nonintubated thoracic surgery, although the technique has been used in other surgeries for many decades.

Thoracic paravertebral block

Paravertebral block is an alternative technique that may offer a comparable analgesic effect and a better side-effect profile, which is associated with a reduction in pulmonary complications (31). Komatsu *et al.* found that paravertebral block could greatly contribute to enhanced recovery after thoracic surgery owing to effective and fewer side effects in a retrospective observational study (32). Katayama *et al.* suggested that paravertebral block was safe in patients ineligible for epidural block and could contribute to their pain relief following pulmonary resection procedure including VATS (33). However, the study of Messina *et al.* showed that epidural analgesia was more efficient than paravertebral continuous block at reducing pain after thoracic surgery (34).

Percutaneous or thoracoscopic intercostal nerve block

Hung and his colleagues reported that nonintubated thoracoscopic surgery using internal intercostal nerve

block, vagal block and targeted sedation was technically feasible and safe in surgical treatment of lung, mediastinal and pleural tumors in selected patients (9). Wurnig *et al*. suggested that pain management by intercostal block was superior during the first 24 h after surgery whereas on the second day after surgery pain control was significantly better achieved by the epidural catheter in relaxed position. A combination of intercostal block and epidural block seems to be an ideal pain management in patients undergoing thoracic surgery (35).

Spontaneous breathing anesthesia with LMA

Cai and his colleagues found that thoracoscopic bulla resection under laryngeal mask anesthesia with low tidal volume high-frequency lung ventilation was safe and feasible and resulted in better patient satisfaction and shorter in-hospital stay than procedures performed under intubation anesthesia with one-lung ventilation (36). Ambrogi *et al*. suggested that thoracoscopic wedge resection of lung nodule was safe and feasible under spontaneous breathing anesthesia with LMA. It is a new technique permitted a confident manipulation of lung parenchyma and a safe stapler positioning without cough, pain, or panic attack described for awake epidural anesthesia, avoiding the risks of tracheal intubation and mechanical ventilation (37). However, it is influenced by surgical personal skills and patients with tenacious pleural adhesions or with nodule unsuitable for VATS resection must be excluded.

Cough control

Preoperative inhalation of aerosolized lidocaine and ipsilateral stellate ganglion block had been proposed to reach cough control in some extent (15,38). Chen and colleagues have routinely performed intraoperative thorascopic vagal block, and it has been proved effective on cough reflex suppression without causing hemodynamic instability (16). In some more cases, incremental intravenous fentanyl can be applied in place of vagal block to decrease cough suppression duration (24).

Respiration management

During the whole operation, nasopharyngeal airway and face mask are required for oxygen inhalation, with an oxygen flow of 3-5 L/min. After the pleural cavity is closed and the wound is sutured, the patients are assisted via a face mask in ventilation to inflate the lung tissue.

In sedated patients, premedication with opioid agent followed by deliberate titration had been proved to control respiratory rate effectively. Meticulous use of nasal airway can be of great benefit if upper airway obstruction raises clinical concerns. If significant hypoventilation happens, modest assisted ventilation by a mask may be required after notification of the surgical team. Oxygenation can be facilitated with O_2 supplement by nasal cannula 3-4 L/min or by Venturi Mask. Overly hypercapnia should be avoided; a good-quality end-tidal CO_2 trace and serial arterial blood sampling before/after iatrogenic open pneumothorax should suffice for close monitoring (24,28).

Postoperative analgesia

Thoracic epidural block is still the preferable standard for thoracic surgery analgesia with traumatic procedure. However, some anesthesiologists have some concern for epidural analgesia. Anticoagulant therapy with low molecular weight heparin has been increasingly used in surgical patients, which may make it difficult to safely manage the epidural analgesia. Bang and his colleagues reported a case of epidural hematoma in a 55-year-old male patient who had a thoracic epidural catheter placed under general anesthesia preceding a cardiac surgery. Epidural catheter insertion in a patient anticoagulated with heparin may increase the risk of epidural hematoma (39).

Ding and his colleagues reviewed the updated meta-analysis comparing the analgesic efficacy and side effects of paravertebral and epidural block for thoracotomy, showing that paravertebral block can provide comparable pain relief to traditional epidural block, and may have a better side-effect profile for pain relief after thoracic surgery (29). Recently, the systematic review of Steinthorsdottir *et al*. suggested that thoracic epidural block and especially paravertebral block showed some effect on pain scores for VATS in comparative studies (40). Certainly, a specified catheter for continuous paravertebral block would be more beneficial.

Ishikawa *et al*. have reported that for minimally invasive thoracoscopic surgery, intrapleural analgesia could be one of the good postoperative analgesia for its efficacy, safety, and benefit of easy placement of the catheter (41). Fibla *et al*. showed that the analgesic regimen combining paravertebral block and non-steroid anti-inflammatory drugs (NSAIDs) provided an excellent level of pain control for thoracoscopic surgery through a prospective randomized study (42).

The promising analgesia, including continuous intercostal-intrapleural analgesia or narcotic-based intravenous patient controlled analgesia combining with NSAIDs still need more attention and further study.

Advantages

Nonintubated anesthesia allows thoracic surgery patients to avoid the potential risks of tracheal intubation including the impacts from the manipulation, various anesthetic drugs and mechanical ventilation etc., particularly for the high-risk patients (43).

Liu *et al*. recently compared two groups of patients who received thoracic surgery under epidural anesthesia and those under general anesthesia with double lumen tube, the results showed significant differences in postoperative fasting time, duration of postoperative antibiotic use, and duration of postoperative hospital stay (30).

Mineo and his colleagues studied the quality of life after nonintubated versus intubated VATS talc pleurodesis using case-matched study recruited 391 patients, showing that two groups achieved similar results in pleural effusion and nonintubated VATS got earlier improvement of some quality-of-life domains as well as better mortality, morbidity, hospital stay, and costs (12).

Moreover, Vanni and his coworkers demonstrated that when compared with conventional thoracoscopic surgery under general anesthesia with single-lung ventilation, awake thoracoscopic surgery attenuated the surgical stress responses and had a smaller impact on the postoperative lymphocyte responses (44,45).

Disadvantages

Once mentioned of thoracic surgery just under epidural block, some anesthesiologists will recall the discomfort, irritation, and respiratory depression of the patients and the hustle and frustration of the anesthesiologists during upper abdominal surgery under epidural block decades years ago, even the anesthetics and monitor machines have made great developments. In addition, the thoracic epidural block has been abandoned in lots of hospitals. With heavy labor intensity and various degree of anxiety, anesthesiologists should keep monitoring without distractions and absences.

Some thoracic surgeons also disapprove with the nonintubated anesthesia, because they require that the patient should be unconscious, and are not satisfied with the surgical condition, worry about the position limitation and the possible body movement of the patient (46).

Some patients are not comfortable and even scared about being awake during the surgery, hearing the discussion and noises in the operating room, which may cause mental stress and post-traumatic stress disorder (PTSD). Although there is no related study, a normal human response to such an exceptional situation can for instance be the delayed appearance of unintentional distressing recollections of the event despite the patients' satisfaction concerning the procedure (41,47).

Inexperienced and poorly cooperative surgical team may be the difficulties in performing the nonintubated anesthesia for thoracic surgery. The coordination and cooperation between surgeons and anesthesiologists are very important in operating room. The weak teamwork and poor communication could induce lots of problems even mistakes, seriously endangering the patients' safety.

Hypercapnia can develop during nonintubated thoracic surgery and correlates with the operative time directly. Whereas it is worth noting that clinical study has shown that perioperative hypercapnia without hypoxemia rarely becomes clinically dangerous (13,48). Anyway, airway support and preparation for conversion to intubated general anesthesia should always be in hand in case of respiration depression, insufficient anesthesia and significant bleeding (15,24).

The charge of nonintubated anesthesia is quite lower than that of general anesthesia with double lumen endobronchial tube, and the anesthesiologists in some hospitals may get less economic benefits, for example, in the current bonus distribution system in China.

The advantages and disadvantages of nonintubated anesthesia for thoracic surgery are listed in the *Table 1*.

Future directions

In a modern era of minimally invasive thoracoscopic surgery, we are encouraged that tracheal intubation with double lumen tube or bronchial blocker is no longer regarded as a prerequisite for single lung ventilation in series of reported studies. Nonintubated thoracoscopic surgery is feasible and safe in a variety of thoracic procedures, including pulmonary resection, empyema, and excision of pleural and mediastinal tumors. Although the risks and benefits of this technique are not clear yet, it seems to offer an equally effective and safe alternative for those patients with high risks to intubated general

Table 1 Advantages and disadvantages of nonintubated anesthesia for thoracic surgery

Advantages
Avoiding the potential risks of tracheal intubation
Better results in postoperative fasting time, duration of postoperative antibiotic use, and duration of postoperative hospital stay
Earlier improvement of some quality-of-life domains, better mortality, morbidity, hospital stay, and costs
Attenuated the surgical stress responses and had a smaller impact on the postoperative lymphocyte responses
Disadvantages
Challenge and increased labor intensity to anesthesiologists
Disapproval from some thoracic surgeons
The risk of mental stress and post-traumatic stress disorder for some patients
Problems even mistakes induced by the weak teamwork and poor communication
Hypercapnia, airway support and preparation for conversion to intubated general anesthesia
Less economic benefits in some countries

anesthesia, and the postoperative recovery is faster with less complication rates.

Summary

The psychological preparation and physical evaluation of the patients, the applying of suitable techniques, intraoperative management and communication with surgeons are important for the safety and practicality of nonintubated anesthesia for thoracic surgery. Nevertheless, more evidence and studies are needed to ascertain the risks and benefits of this technique.

Acknowledgements

Disclosure: The authors declare no conflict of interest.

References

1. Della Rocca G, Langiano N, Baroselli A, et al. Survey of thoracic anesthetic practice in Italy. J Cardiothorac Vasc Anesth 2013;27:1321-9.
2. Ruetzler K, Grubhofer G, Schmid W, et al. Randomized clinical trial comparing double-lumen tube and EZ-Blocker for single-lung ventilation. Br J Anaesth 2011;106:896-902.
3. Campos JH. Progress in lung separation. Thorac Surg Clin 2005;15:71-83.
4. Komatsu T, Kino A, Inoue M, et al. Paravertebral block for video-assisted thoracoscopic surgery: analgesic effectiveness and role in fast-track surgery. Int J Surg 2014;12:936-9.
5. Markar SR, Karthikesalingam A, Low DE. Enhanced recovery pathways lead to an improvement in postoperative outcomes following esophagectomy: systematic review and pooled analysis. Dis Esophagus 2014. [Epub ahead of print].
6. Hung MH, Hsu HH, Cheng YJ, et al. Nonintubated thoracoscopic surgery: state of the art and future directions. J Thorac Dis 2014;6:2-9.
7. Klijian AS, Gibbs M, Andonian NT. AVATS: Awake Video Assisted Thoracic Surgery--extended series report. J Cardiothorac Surg 2014;9:149.
8. Englbrecht JS, Pogatzki-Zahn EM. Perioperative pain management for abdominal and thoracic surgery. Schmerz 2014;28:265-81.
9. Hung MH, Hsu HH, Chan KC, et al. Non-intubated thoracoscopic surgery using internal intercostal nerve block, vagal block and targeted sedation. Eur J Cardiothorac Surg 2014;46:620-5.
10. Pompeo E, Mineo D, Rogliani P, et al. Feasibility and results of awake thoracoscopic resection of solitary pulmonary nodules. Ann Thorac Surg 2004;78:1761-8.
11. Pompeo E, Rogliani P, Tacconi F, et al. Randomized comparison of awake nonresectional versus nonawake resectional lung volume reduction surgery. J Thorac Cardiovasc Surg 2012;143:47-54.
12. Mineo TC, Sellitri F, Tacconi F, et al. Quality of life and outcomes after nonintubated versus intubated video-thoracoscopic pleurodesis for malignant pleural effusion: comparison by a case-matched study. J Palliat Med 2014;17:761-8.

13. Mineo TC. Epidural anesthesia in awake thoracic surgery. Eur J Cardiothorac Surg 2007;32:13-9.
14. Pompeo E, Tacconi F, Mineo TC. Awake video-assisted thoracoscopic biopsy in complex anterior mediastinal masses. Thorac Surg Clin 2010;20:225-33.
15. Pompeo E, Mineo TC. Awake operative videothoracoscopic pulmonary resections. Thorac Surg Clin 2008;18:311-20.
16. Chen JS, Cheng YJ, Hung MH, et al. Nonintubated thoracoscopic lobectomy for lung cancer. Ann Surg 2011;254:1038-43.
17. Pompeo E, Rogliani P, Cristino B, et al. Awake thoracoscopic biopsy of interstitial lung disease. Ann Thorac Surg 2013;95:445-52.
18. Pompeo E, Tacconi F, Mineo D, et al. The role of awake video-assisted thoracoscopic surgery in spontaneous pneumothorax. J Thorac Cardiovasc Surg 2007;133:786-90.
19. Pompeo E, Mineo TC. Awake pulmonary metastasectomy. J Thorac Cardiovasc Surg 2007;133:960-6.
20. Rocco G, Romano V, Accardo R, et al. Awake single-access (uniportal) video-assisted thoracoscopic surgery for peripheral pulmonary nodules in a complete ambulatory setting. Ann Thorac Surg 2010;89:1625-7.
21. Rocco G, La Rocca A, Martucci N, et al. Awake single-access (uniportal) video-assisted thoracoscopic surgery for spontaneous pneumothorax. J Thorac Cardiovasc Surg 2011;142:944-5.
22. Tseng YD, Cheng YJ, Hung MH, et al. Nonintubated needlescopic video-assisted thoracic surgery for management of peripheral lung nodules. Ann Thorac Surg 2012;93:1049-54.
23. Wu CY, Chen JS, Lin YS, et al. Feasibility and safety of nonintubated thoracoscopic lobectomy for geriatric lung cancer patients. Ann Thorac Surg 2013;95:405-11.
24. Yang JT, Hung MH, Chen JS, et al. Anesthetic consideration for nonintubated VATS. J Thorac Dis 2014;6:10-3.
25. Lepage C, Drolet P, Girard M, et al. Music decreases sedative requirements during spinal anesthesia. Anesth Analg 2001;93:912-6.
26. Bradt J, Dileo C, Shim M. Music interventions for preoperative anxiety. Cochrane Database Syst Rev 2013;6:CD006908.
27. Buckingham WW, Beatty AJ, Brasher CA, et al. An analysis of 607 surgical procedures done under epidural anesthesia. Mo Med 1950;47:485-7.
28. Pompeo E. Awake thoracic surgery--is it worth the trouble? Semin Thorac Cardiovasc Surg 2012;24:106-14.
29. Ding X, Jin S, Niu X, et al. A comparison of the analgesia efficacy and side effects of paravertebral compared with epidural blockade for thoracotomy: an updated meta-analysis. PLoS One 2014;9:e96233.
30. Liu J, Cui F, Li S, et al. Nonintubated Video-Assisted Thoracoscopic Surgery Under Epidural Anesthesia Compared With Conventional Anesthetic Option: A Randomized Control Study. Surg Innov 2014. [Epub ahead of print].
31. Wenk M, Schug SA. Perioperative pain management after thoracotomy. Curr Opin Anaesthesiol 2011;24:8-12.
32. Komatsu T, Kino A, Inoue M, et al. Paravertebral block for video-assisted thoracoscopic surgery: analgesic effectiveness and role in fast-track surgery. Int J Surg 2014;12:936-9.
33. Katayama T, Hirai S, Kobayashi R, et al. Safety of the paravertebral block in patients ineligible for epidural block undergoing pulmonary resection. Gen Thorac Cardiovasc Surg 2012;60:811-4.
34. Messina M, Borol i F, Landoni G, et al. A comparison of epidural vs. paravertebral blockade in thoracic surgery. Minerva Anestesiol 2009;75:616-21.
35. Wurnig PN, Lackner H, Teiner C, et al. Is intercostal block for pain management in thoracic surgery more successful than epidural anaesthesia? Eur J Cardiothorac Surg 2002;21:1115-9.
36. Cai K, Wang X, Ye J, et al. Laryngeal mask anesthesia in video-assisted thoracoscopic surgery for pulmonary bulla: comparison with intubation anesthesia. Nan Fang Yi Ke Da Xue Xue Bao 2013;33:756-60.
37. Ambrogi MC, Fanucchi O, Korasidis S, et al. Nonintubated thoracoscopic pulmonary nodule resection under spontaneous breathing anesthesia with laryngeal mask. Innovations (Phila) 2014;9:276-80.
38. Guarracino F, Gemignani R, Pratesi G, et al. Awake palliative thoracic surgery in a high-risk patient: one-lung, non-invasive ventilation combined with epidural blockade. Anaesthesia 2008;63:761-3.
39. Bang J, Kim JU, Lee YM, et al. Spinal epidural hematoma related to an epidural catheter in a cardiac surgery patient -A case report-. Korean J Anesthesiol 2011;61:524-7.
40. Steinthorsdottir KJ, Wildgaard L, Hansen HJ, et al. Regional analgesia for video-assisted thoracic surgery: a systematic review. Eur J Cardiothorac Surg 2014;45:959-66.
41. Ishikawa Y, Maehara T, Nishii T, et al. Intrapleural

analgesia using ropivacaine for postoperative pain relief after minimally invasive thoracoscopic surgery. Ann Thorac Cardiovasc Surg 2012;18:429-33.
42. Fibla JJ, Molins L, Mier JM, et al. The efficacy of paravertebral block using a catheter technique for postoperative analgesia in thoracoscopic surgery: a randomized trial. Eur J Cardiothorac Surg 2011;40:907-11.
43. Kiss G, Claret A, Desbordes J, et al. Thoracic epidural anaesthesia for awake thoracic surgery in severely dyspnoeic patients excluded from general anaesthesia†. Interact Cardiovasc Thorac Surg 2014;19:816-23.
44. Vanni G, Tacconi F, Sellitri F, et al. Impact of awake videothoracoscopic surgery on postoperative lymphocyte responses. Ann Thorac Surg 2010;90:973-8.
45. Tacconi F, Pompeo E, Sellitri F, et al. Surgical stress hormones response is reduced after awake videothoracoscopy. Interact Cardiovasc Thorac Surg 2010;10:666-71.
46. Nakanishi R, Yasuda M. Awake thoracoscopic surgery under epidural anesthesia: is it really safe? Chin J Cancer Res 2014;26:368-70.
47. Milian M, Tatagiba M, Feigl GC. Patient response to awake craniotomy - a summary overview. Acta Neurochir (Wien) 2014;156:1063-70.
48. Laffey JG, O'Croinin D, McLoughlin P, et al. Permissive hypercapnia--role in protective lung ventilatory strategies. Intensive Care Med 2004;30:347-56.

Cite this article as: Wang B, Ge S. Nonintubated anesthesia for thoracic surgery. J Thorac Dis 2014;6(12):1868-1874. doi: 10.3978/j.issn.2072-1439.2014.11.39

Basic statistics (the fundamental concepts)

Eric Lim

Consultant Thoracic Surgeon, Imperial College and the Academic Division of Thoracic Surgery, Royal Brompton Hospital, London, UK
Correspondence to: Mr Eric Lim. Imperial College and The Academic Division of Thoracic Surgery, The Royal Brompton Hospital, Sydney Street, London SW3 6NP, UK. Email: e.lim@rbht.nhs.uk.

Abstract: An appreciation and understanding of statistics is import to all practising clinicians, not simply researchers. This is because mathematics is the fundamental basis to which we base clinical decisions, usually with reference to the benefit in relation to risk. Unless a clinician has a basic understanding of statistics, he or she will never be in a position to question healthcare management decisions that have been handed down from generation to generation, will not be able to conduct research effectively nor evaluate the validity of published evidence (usually making an assumption that most published work is either all good or all bad). This article provides a brief introduction to basic statistical methods and illustrates its use in common clinical scenarios. In addition, pitfalls of incorrect usage have been highlighted. However, it is not meant to be a substitute for formal training or consultation with a qualified and experienced medical statistician prior to starting any research project.

Keywords: Statistics; research; thoracic surgery

Submitted Aug 03, 2014. Accepted for publication Aug 10, 2014.
doi: 10.3978/j.issn.2072-1439.2014.08.36
View this article at: http://dx.doi.org/10.3978/j.issn.2072-1439.2014.08.36

Introduction

An appreciation and understanding of statistics is import to all practising clinicians, not simply researchers. This is because mathematics is the fundamental basis to which we base clinical decisions, usually with reference to the benefit in relation to risk. Unless a clinician has a basic understanding of statistics, he or she will never be in a position to question healthcare management decisions that have been handed down from generation to generation, will not be able to conduct research effectively nor evaluate the validity of published evidence (usually making an assumption that most published work is either all good or all bad).

Summarising and presenting data

Why is it important?

Summarising data is usually the fundamental basis to which the background data on a cohort is described. Often it is too cumbersome to describe all the features of each individual that is studied and becomes impossible to do so with large numbers.

How is it done?

In general data are summarised with two measures, a statement of "central tendency" followed by a statement of "variation". In general data are divided into continuous (normal and non-normally distributed) or categorical (binary or multiple categories).

It is important to separate continuous data in normal and non-normally distributed because the summary measures used are different. When data is normally distributed (e.g., age, *Figure 1*) we can use summary measures such as the mean and standard deviation. Because of the distribution of the data, we can use "shortcuts" to calculate the spread, for example we know that 95.45% of the observations will lie between two standard deviations of the mean. This is not the same for non-normally distributed data (e.g., length of follow up, *Figure 2*), which is summarised as median and interquartile range.

Categorical data can be more straightforward. It can be a binary category (e.g., gender with only two outcomes, male

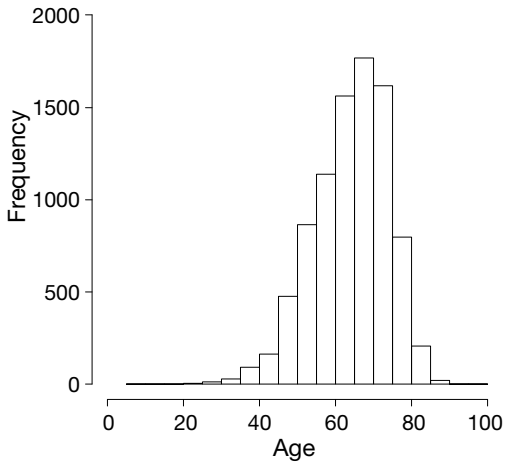

Figure 1 Normally distributed data—patients age.

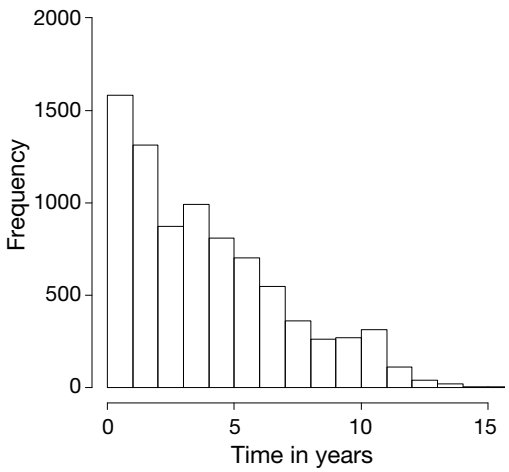

Figure 2 Non-normally distributed data—follow up time in years.

or female) or multiple categories (e.g., colour). Categorical data is summarised as frequency and percentage e.g., 32 (34%).

What is the relevance?

If you apply the mean and standard deviation wrongly to describe the data that is not normally distributed, for example mean length of follow up of 4 years, standard deviation of 3 years, and then the data is interpreted as 95.45% of the observations will lie between –2 and 10 years. It is impossible to have a length of follow up of –2 years!
It is important to appreciate outcomes such as cancer stage (I-IV) should be treated as categorical and not continuous, because a cancer stage of III does not imply that the outcome is 3-fold worse than a cancer stage of I.

Comparing single outcomes and single variables

Why is it important?

One of the most basic aspects evaluating improvements in healthcare or surgical techniques is by comparing the outcomes of two (or more) different procedures.

How is it done?

Like summary measures, statistical tests used to compare outcomes are based on calculations that make assumptions on the data distributions. Therefore it is important that the correct test is applied to the corresponding data distributions. In general, when comparing two different and independent outcomes, a *t*-test is used to compare normally distributed continuous data, the Mann-Whitney or a Wilcoxon rank sum test is used to compare continuous non-normally distributed data and the Chi-square test (or Fisher's exact test if the numbers are very small) is used to compare categorical data.

The statistical test generates a P value for example 0.05, which correctly interpreted means that if the test was done (over and over) many times, the likelihood of observing the difference (or more extreme value) due to chance is 5%.

What is the relevance?

It is important to use the correct test to each distribution, for example if a Chi-square test is used when the observed (more correctly predicted) values are very low (e.g., 1/25) then the chances of achieving a statistically significance result is (incorrectly) easier.

Many clinicians do not understand how to interpret a P value. Firstly, it implies that the "test" will be performed over and over again many time (long run frequency), and this is clearly not the case in clinical practice. Secondly, many take it as an absolute value in that a P value of 0.04 is significant but a P value of 0.06 is not. To appreciate that attitude is saying that a 4% and 6% chance of rain tomorrow is extremely and completely different, clearly for all intents and purposed there is no difference between 4-6%. In fact, my own opinion is that there really is not

much difference between 5% or 10% (i.e., P=0.10). Another lesser known fact is that the P value is driven by the size of the data, therefore differences between 9/10 versus 7/10 may not be significant (P=0.582), but the P value for the difference between 9,000/10,000 versus 7,000/10,000 is (P<0.001), this becomes more important to appreciate when numbers are large—all differences (whether clinically important or not) become significant.

Comparing single outcomes with multiple variables

Why is it important?

So far, we have only discussed comparing one outcomes and one variable (e.g., death versus surgical group), however outcomes can be influenced by multiple variables. Regression analyses are multivariable methods that allow us to compare an outcome adjusting for multiple different variables (e.g., death versus surgical group, age and lung function).

How is it done?

There are a family of regression methods appropriate to the type and distribution of the outcome of interest. Linear regression is the basic model that is applied to a continuous normally distributed outcome (e.g., serum potassium) and the measures of association are usually given in the same units as the outcome measure (e.g., each year of age increases serum potassium by 0.011 mmol/L). For binary outcomes, logistic regression is used and the measure of association is given as an odds ratio (the odds of an event happening versus the odds of an event not happening). The odds ratio is a difficult ratio for most to interpret (unless you are an experienced gambler) and often it is (incorrectly) interpreted as a relative risk. The discussion is out of the scope of this article, but as an illustration the two ratios of 2/4 and 1/4 is expressed as a relative risk of 2/4÷1/4=2 and an odds ratio of 2/2÷1/3=3. Therefore the output of a measure of association in a logistic regression model is interpreted for example in men, the odds ratio of developing ischaemic heart disease is 4.3 compared to women.

What is the relevance?

It is important to be able to appreciate the correct regression method for the correct type and distribution of outcomes. Often clinicians who are less experienced try to convert outcomes from continuous to binary simply to apply a different method of analyses for example, instead of using a linear regression for serum potassium, they would convert it into high *versus* low serum potassium (above or below 4.5 mmol/L) and apply logistic regression methods.

Advanced statistical methods

Why is it important?

As data become more complex, correct handling and analyses is important to be able to get valid results.

How is it done?

So far, we have discussed comparing one outcome with one variable and with multiple variables that does not take time or missing data into account. The commonly used data in medical literature that includes missing data and time is survival analyses. This is when patients are followed up to a time point and are alive (censored) or died. The most common regression method in this circumstance is the use of the Cox proportional hazards regression where time and censoring is taken into account. The measure of association is a hazard ratio that refers to the relative risk of death.

As data becomes more complicated, more sophisticated methods are applied, such as longitudinal data analyses when multiple time points of interest are analysed, the most common thoracic surgical example is the longitudinal lung function outcomes after lung volume reduction surgery. The analysis needs to take into account, time, irregular time intervals, correlation within each patient, and correlation with time before comparison can be made with another group.

What is the relevance?

If proper statistical methods are not used to account for time and missing data, erroneous conclusions can occur. For example, if a new surgical intervention is introduced and the follow up time is only 1 month compared to the old technique used for over 30 years, with follow up time of 30 years, few deaths will occurs in the new technique group with a follow up time of 1 month compared to the old technique group of 30 years, and a researcher could make the false conclusion that there we statistically significantly less deaths on follow up with the new technique.

Conclusions

This article provides a brief introduction to basic statistical methods and illustrates its use in common clinical scenarios. In addition, pitfalls of incorrect usage have been highlighted. It is not meant to be a substitute for formal training or consultation with a qualified and experienced medical statistician prior to starting any research project.

Cite this article as: Lim E. Basic statistics (the fundamental concepts). J Thorac Dis 2014;6(12):1875-1878. doi: 10.3978/j.issn.2072-1439.2014.08.36

Acknowledgements

Disclosure: The author declares no conflict of interest.

Statistic Corner

A synopsis of resampling techniques

Alessandro Brunelli

Department of Thoracic Surgery, St. James's University Hospital, Leeds, LS9 7TF, UK

Correspondence to: Dr. Alessandro Brunelli, MD, Consultant Thoracic Surgeon LTHT, Honorary Senior Lecturer University of Leeds. Department of Thoracic Surgery, St. James's University Hospital, Bexley Wing, Beckett Street, Leeds, LS9 7TF, UK. Email: brunellialex@gmail.com.

Abstract: Bootstrap is a computer intensive technique of resampling with replacement, which can be applied in many statistical analytical tests. The article describes the most frequent situations where bootstrap resampling can be applied in thoracic surgical research: variable selection for multivariable regression analysis, internal validation of regression equations, model validation. Practical examples for programming bootstrap in commercially available statistical software are finally reported.

Keywords: Resampling statistics; bootstrap; risk modelling; thoracic surgery

Submitted Aug 25, 2014. Accepted for publication Sep 04, 2014.
doi: 10.3978/j.issn.2072-1439.2014.09.09
View this article at: http://dx.doi.org/10.3978/j.issn.2072-1439.2014.09.09

Introduction

Re-sampling statistics has been only recently popularized in biomedical science owing to the availability of statistical programs and computing capability.

Bootstrap is perhaps the most popular of these computer intensive methods in our specialty.

Bootstrap refers to a simulation technique proposed by Efron and colleagues more than 30 years ago (1,2). It consists of generating observations from the distribution of the original sample of patients at hand.

Each simulation results in a new sample typically of the same size (number of individuals) as the original. The simulated sample is generated through a process of random selection (with replacement) of individuals from the original sample.

Sampling with replacement means that at each step of the simulation every individual from the original sample (or dataset) is again eligible to be selected, irrespective of whether he has already been selected.

Therefore, in each bootstrap sample some of the original individuals may not be represented and others may be represented more than once. Hypothetically, a bootstrap sample can be composed by a population represented by the same individual randomly sampled n times.

This random sampling with replacement is repeated to generate hundreds or thousands (typically 1,000) new simulated populations (samples) ensuring accurate statistics without assumptions by combining and analyzing the information generated from these many datasets.

The name "bootstrap" derives from the expression "pulling yourself up by your own bootstraps," reflecting the fact that one could develop all the statistical testing necessary directly from the actual data at hand.

These techniques have been applied to all analytical processes. However, there are situations when bootstrap resampling has been utilized more often in our field of scientific research.

When do I apply bootstrap in my research?

Selection of variables for multivariable analysis

Linear or non-linear regression analyses require the selection of variables to be entered in the model. One of the most used methods to screen variables of interest for multivariable regression analysis is univariable testing.

Usually those variables with a pre-determined P value (typically $P<0.05$ or $P<0.1$) are selected and used as independent variables in the multivariable analysis. However, one has to pay attention to the correlation of the numeric variables to be entered in the regression model. Highly correlated variables should not be entered simultaneously in the same regression iterations as they

will cause a problem of multicollinearity that will affect the results of the analysis. To obviate this problem one can perform multiple regression iteration using one or the other correlated variable at each time and then select the best performing model. Another method is to select the independent variable among those with a high correlation (r>0.5) using bootstrap resampling simulation. This is the method I prefer when facing this problem.

Basically, the univariable comparative analysis (unpaired *t* Student or Mann Whitney test) is repeated in the 1,000 simulated samples generated with bootstrap bagging. The variable that will result associated with outcome (P<0.05) in more samples will be the one to be selected and entered in to the multivariable analysis.

A practical example is the selection of variables such as forced expiratory volume in 1 second (FEV1), forced vital capacity (FVC), FEV1/FVC ratio or predicted postoperative forced expiratory volumes in 1 second (ppoFEV1) for a logistic regression analysis to build a predictive model of in-hospital mortality after lung resection. All these variables are highly correlated each other (r>0.5) and often associated with mortality at univariable analysis. They cannot be used together in the same regression iteration. Bootstrap is my method of choice to verify which one of those variables is most frequently associated with outcome when tested in 1,000 simulated samples.

To this purpose I use the following programming syntax in the Stata 12 statistical software (Stata Corp., College Station, TX) and repeat it for every variable I want to test:

a. *Bootstrap "t test ppoFEV1, by(mortality)" r(P), reps(1,000) sav(name) replace*
   Where ppoFEV1 is the variable I want to test for the association with mortality and name is a name of your choice to save the bootstrap file. The t test can be replaced by any other test. For instance in case of non normal distribution of the numeric variable of interest a Wilcoxon rank-sum (or Mann Whitney test) can be used (command rank-sum instead of t test).
   The program saves the P values as _bs1_1
b. *Use name, clear*
c. *Count if _bs1_1<0.05*

This final command will return the number of times P value is less than 0.05 in 1,000 samples.

Internal validation of regression models

One of the most common use of bootstrap is regression model validation.

If applied to regression analysis, bootstrap can provide variables that have a high degree of reliability as independent risk factors (3).

We recently demonstrated that internal validation using resampling technique is superior to the traditional training and testing method (4). In this latter method, the original sample is randomly split in two sets, a development and a validation set. Most commonly 60% of the data at hand are used to develop the model and the other 40% to test the performance and validate the regression model.

This approach may be affected by selection bias and results may greatly vary owing to pure chance.

We compared the performance of a risk adjusted mortality model developed from the entire dataset of patients submitted to major lung resection and validated by bootstrap with that of ten different mortality models developed by using the traditional training-and-test method from the same dataset.

The performance of these eleven mortality models was tested by using the c-statistics in an external population of patients operated in another center.

Seventy percent of the models derived by the training and test method included different combinations of variables.

Their performances were extremely variable from one model to another, and in general, only modest compared to the model derived by using the entire sample validated by bootstrap. The latter method appears therefore much superior and reliable to develop reproducible and stable risk models to be applied in external populations.

One of the great advantages of using bootstrap to validate a regression model is that the entire original dataset can be utilized to develop more robust regression equations. This appears particularly important in moderate-size databases and for rare outcomes (i.e., mortality after major lung resection).

In practice, after a careful variables screening, a selected set of independent variables is entered in a regression analysis.

Then, a random sample of cases is selected with replacement, most commonly of the same size as the original sample. Regression is performed using this random simulated sample. This process is completely automated and the results of the analysis are stored. Then, another random sample of the same size is drawn from the original dataset with replacement (bootstrap) and regression is performed again in this new simulated sample of patients. This resampling of the original data

set followed by analysis continues most typically hundreds of times (typically 1,000 times). Finally, the frequency of occurrence of risk factors among these many models is summarized. Interestingly, each regression analysis performed in different simulated samples of observations usually generates different models containing different predictors. However, some predictors never turn out significant and others do so more frequently.

Usually predictors that result significant in more than 50% of bootstrap samples can be considered reliable and can be included in the final regression model.

The entire process is completely computer-automated and relies on specific statistical software and programs.

Bootstrap resampling allows to removing much of the human biases associated with regression analysis. It is a reliability test, which is able to eliminate or minimize the risks of selecting unreliable variables (type I error) and excluding reliable ones (type II error) (3).

To this purpose I use the following programming syntax in the Stata 12 statistical software (Stata Corp., College Station, TX):

Suppose I want to develop a risk model to identify risk factors associated with in-hospital mortality after lung resection. After a careful univariable screening of variables the following factors resulted associated with mortality: age, ppoFEV1, body mass index (BMI), pneumonectomy, predicted postoperative carbon monoxide lung diffusion capacity (ppoDLCO), induction chemotherapy.

I start with programming my logistic regression as follows:

a. *Program myreg, eclass*
b. *Logit mortality age ppoFEV1 BMI pneumonectomy ppoDLCO induction chemotherapy*
c. *Test age=0*
d. *Eret scalar Page=r(p)*
e. *Test ppoFEV1=0*
f. *Eret scalar ppoFEV1=r(p)*

……

q. end

Then I call myreg and verify the regression results. Subsequently I run the bootstrap command as follows:

a. *Bootstrap myreg _b Page=e(Page) ppoFEV1=e(ppoFEV1) ….., reps(1,000) sav(name)*
b. *Use name, clear*
c. *Count if Page<0.05*

This last command return the number of times age results significantly associated (P<0.05) with mortality in 1,000 bootstrap samples.

Model validation

Resampling with replacement can be also used to test a model on an external population not just once but hundreds of times.

One example is to verify performance of a risk score. In a recent paper, we developed an aggregate risk score to predict prolonged air leak (PAL) after lobectomy (5). We used a population of over 600 patients to develop the risk score, which was created by proportionally weighting the regression coefficients of the significant variables. According to their scores, patients were grouped in four risk classes with an incremental risk of developing PAL. The aggregate score was then validated in an external population of 230 patients operated on in another center. Instead of testing the score in one validation set, the latter one was bootstrapped to obtain 1,000 simulated external samples of patients of the same number of patients as the original validation set [230] and obviously different from the ones used to derive the model (derivation set). The frequency of occurrence of PAL in each class of risk was then tested in each of these 1,000 bootstrapped samples. For instance we found that in class A (the class with the lowest risk of PAL) 98% of samples had a risk of PAL less than 5%, whereas in class D (the highest class of risk) 99% of samples showed a PAL incidence of greater than 20%. This process showed that the score performed reliably across multiple populations and it is well suited to be used outside the set of patients from which it was derived.

Conclusions

Bootstrap resampling procedure is a computer intensive simulation technique that is capable to minimize much of the human arbitrariness from multivariable analysis and other analytical statistical techniques. It provides another important statistic: a measure of reliability of a risk factor that should complement the traditional calibration and discrimination measures of performance of a multivariable model. This measure should always be reported along with the magnitude of effect, its variance and P value in a regression table.

Acknowledgements

Disclosure: The author declares no conflict of interest.

References

1. Efron B. Bootstrap methods: another look at the jackknife. Ann Statist 1979;7:1-26.

2. Efron B, Tibshirani RJ. eds. An introduction to the bootstrap. New York: Chapman and Hall/CRC, 1993.
3. Blackstone EH. Breaking down barriers: helpful breakthrough statistical methods you need to understand better. J Thorac Cardiovasc Surg 2001;122:430-9.
4. Brunelli A, Rocco G. Internal validation of risk models in lung resection surgery: bootstrap versus training-and-test sampling. J Thorac Cardiovasc Surg 2006;131:1243-7.
5. Brunelli A, Varela G, Refai M, et al. A scoring system to predict the risk of prolonged air leak after lobectomy. Ann Thorac Surg 2010;90:204-9.

Cite this article as: Brunelli A. A synopsis of resampling techniques. J Thorac Dis 2014;6(12):1879-1882. doi: 10.3978/j.issn.2072-1439.2014.09.09

Professor I-wen Wang: better life supported through mechanical circulatory devices-a dream within reach

Submitted Oct 11, 2014. Accepted for publication Oct 28, 2014.
doi: 10.3978/j.issn.2072-1439.2014.12.08
View this article at: http://dx.doi.org/10.3978/j.issn.2072-1439.2014.12.08

Professor I-wen Wang (*Figure 1*) received his medical degree from Case Western Reserve University School of Medicine, after that he has 17 years of experience and practices in thoracic surgery and cardiovascular surgery. With his rich experience, he was elected one of nine doctors at Indiana University Health Methodist Hospital of Indianapolis who specialize in Thoracic & Cardiac Surgery. *Journal of Thoracic Disease* (*JTD*) had the honor to conduct an in-depth interview with him concerning his studies in left assisted ventricular device (LVAD) and extracorporeal membrane oxygenation (ECMO) at the 2014 Chinese Heart Congress.

Figure 1 Professor I-wen Wang.

JTD: As you are an expert in the field of mechanical circulatory support, what device do you think is clinically preferable in terms of Impella, LVAD, totally artificial heart?

Prof. Wang: It depends on the patient because the three devices connote very different types of patient's scenario. The Impella is primarily a short-term device and used for patients in acute cardiogenic shock. It can be implanted without sternotomy and via axillary artery, so patients can be supported sometimes for up to several weeks and the patient can be up and moving. The patient can be bridged to recovery, to transplant or to durable LVAD. It is a first and initial device. Typically we try not to put the durable LVADs into patients who are in acute cardiogenic shock because the data clearly shows that the survival based on Intermacs profile is variable. The one-year survival tend to be worse for Intermacs I patients versus Intermacs II and III patients and so on. So the more stable the patient who is going to have surgery for LVAD, the better the outcome. Sometimes, we do implant durable LVADs into the Intermacs I patients but the majority of patients we put in to LVAD turned out to be Intemacs II or III. The LVADs such as HeartMate-II and HearWare are durable devices so they are intended as bridge to recovery, bridge to transplant or destination therapy, which means they can be used for periods of months and even years, especially if they are used as destination therapy. The total artificial heart is used for patients who need biventricular support and other specific indications. In the US, it is approved to be only as bridge to transplant. The total artificial heart operation is much more complicated than the LVAD. There is not one single device that's suitable for every patient, but every patient should be assessed individually to see which device will best benefit him.

JTD: Given the high cost of these devices, it seems that they are somewhat reserved for the wealthy. How does the patient cover the cost in America? How in your opinion can we better balance the high price of these devices and the true need from patients?

Prof. Wang: In the United States, these devices are

implanted in patients regardless of their income because they have coverage from insurance. Some patients who have limited or no income have government insurance that can cover the costs. So income level is less of a barrier to getting LVADs. In China I think it's a different because the insurance coverage is different. Government provides insurance coverage for everyone, but the extent of coverage is more limited. The initial access for LVADs will likely be very limited number, as part of clinical trials. The cost of the devices in clinical trials is often absorbed by the LVAD companies and hospitals. But this technology, like any other medical technological advances, will be available to those who have the economic ability to pay for it. But as these technologies will become more common and even better technology comes on board, the current generation of LVADs will hopefully become less and less expensive and more and more affordable to everyone. Also advances in manufacturing may allow great efficiency and lower costs in production.

JTD: In America, which type of LVAD is applied more widely?

Prof. Wang: I think the most widely used LVAD in America is Thoratec's HeartMate-II and then the second is the HeartWare HVAD. There are two reasons accounting for this. One is because the HeartMate-II has been in the heart device market longer than the HeartWare device. Another reason is that HeartMate II is approved by United States FDA for bridge to transplantation and for destination therapy. HeartWare, on the other hand, currently has FDA's approval for bridge to transplant but it is still awaiting FDA's approval for destination therapy. Some insurance companies will only cover the FDA approved device. Therefore there are some constraints on what device you can implant for patients.

JTD: What are the features of the common types of LVAD and what is the difference? Based on your experience in China, where do you see the future of LVAD is leading in China?

Prof. Wang: I think the number one is to understand that the LVAD is only the part of the overall care of the end-stage heart failure patients. It's not the ultimate answer, because the device itself is not the final solution. Current devices still have potential risk of complications. The other thing that should be realized is that the successful use of LVAD is not just the surgery to implant a LVAD. The surgery is actually a very simple operation for most surgeons. What is complicated is how to take care of these very sick patients. Taking care of them before the surgery to make them in the best condition for the surgery; taking care of them during the surgery to make sure they survive the operation and taking care of them after the surgery so that they can live and enjoy their life and avoid complications. So for China the next step is to understand and acquire the teamwork necessary to take care of these patients. Once the technology become available, it will undergo very fast adaptation by the surgical and medical community.

JTD: Would you like to introduce the status quo of heart transplantation (the five- or ten-year survival specifically) in America?

Prof. Wang: The current five-year heart transplantation survival in the US is somewhere near 70%, and the one-year survival is around 85%. Approximately 50% of the heart transplantation patients are still alive eleven years after the surgery. For certain, the current generation of patient data is probably better than earlier cohorts as the process of total patient care is constantly improving. I think it's fairly kind of mature medicine and surgery compared to LVADs as much experience has been gained in heart transplantation.

JTD: Indiana University Health Methodist Hospital is world-famous in the field of heart and lung transplantation. Would you like to share with us your experience?

Prof. Wang: Unfortunately, I am only a relatively recent participant in their success. I joined the Indiana University Health Methodist Hospital in September 2011 so I have only been there for three years. This year was actually the 25th anniversary of the first lung transplant performed at IUH Methodist Hospital. It also has a longstanding history of a heart transplant program. They were actually the first private hospital in the United States to do heart transplantation surgery at the very beginning. So we have a very successful heart and lung transplant program. Each year, we are doing approximately 25 heart transplants per year, 35 to 40 LVADs, and nearly 60 lung transplants. The other component is the ECMO program and again it is a very important part of the successful heart and lung transplant program. We formally started the ECMO program in 2011 and in the past three years we have rapidly increased the number of cases we've performed. In 2013,

we supported 37 patients on ECMO; by this June, we have already done 47 cases. We are expecting over 70 cases this year, which nearly double last year's volume. So the ECMO is a fast growing part of our program-supporting both our heart and lung transplant programs as well as our other critical cardiac and respiratory patients.

JTD: As one of the emerging trends in recent years, ECMO attracts more and more attention. Could you give us more detailed information about it?

Prof. Wang: ECMO is a relatively new technology, basically developed by Dr. Robert Bartlett at the University of Michigan. Initially, it is often used in salvage or as the last ditch effort to save a patient. The outcomes were not as good as today. Nowadays we have better timing of using ECMO as well as better critical care. So the survival could almost reach 90% for veno-venous ECMO patients. Our survival for cardiac support is probably close to 60%. It's really a very simple technology to use but it may need to be used earlier in the course for treatment. We need to do very careful patient selection as we don't want to put it into patients where it would be futile.

JTD: In terms of the criteria of selecting patients, will the age be included?

Prof. Wang: The answer is no. We do not have an absolute cut-off for patients who need heart and lung transplant, LVAD or ECMO. Doctor Dong from Wuhan Union Hospital present today their oldest heart transplant patient is 76. Actually we do the same thing. We transplant patients in seventies for both heart and lung. We have put an implant device in a woman in 72 and conducted the transplant a year later in 73. I think age is a part of patient selection but other characteristics must be assessed. There are some patients who are over seventy years of age, but are in a very good cardiac surgery condition; but there are patients in thirties who are not a good heart surgical candidate. So we don't have an absolute cut-off, we take a look at the patients individually. It's reasonable to think that patients who are seventies are probably frailer than some who are 35. But that's not always true. It's the same thing with ECMO. We do not have age as the definitive selection criteria. We take into consideration that whether the patient is suitable for ECMO, whether they have other limiting diseases that prevent them from surviving and recovering from whatever the current status is. That's important what matter is often more than the age. And I should say it's not the chronological age but the physiologic age that's important.

JTD: Thank you very much for sharing you insights!

Cite this article as: Li GS. Professor I-wen Wang: better life supported through mechanical circulatory devices-a dream within reach. J Thorac Dis 2014;6(12):1883-1885. doi: 10.3978/j.issn.2072-1439.2014.12.08

Acknowledgements

Disclosure: The author declares no conflict of interest.

(Senior Editor: Grace S. Li, JTD, jtd@thepbpc.org)

Professor Mario Cazzola: prospect of the COPD medicine

Submitted Dec 15, 2014. Accepted for publication Dec 18, 2014.
doi: 10.3978/j.issn.2072-1439.2014.12.38
View this article at: http://dx.doi.org/10.3978/j.issn.2072-1439.2014.12.38

Mario Cazzola (*Figure 1*) is a Professor of Respiratory Medicine and Director of the Postgraduate School of Respiratory Medicine at the University of Rome 'Tor Vergata', Rome, Italy, where he is also Chief of the Respiratory Clinical Pharmacology Unit. He is Honorary Professor at the Sackler Institute of Pulmonary Pharmacology, GKT School of Biomedical Sciences, London, UK. He is the author or co-author of almost 500 scientific papers.

He founded Therapeutic Advances in Respiratory Diseases and served as its first Editor-in-Chief. He is serving as the Editor-in-Chief for Pulmonary Pharmacology & Therapeutics, an Associate Editor for Respiratory Medicine, for Respiratory Research, and for Clinical Investigation, and a Section Editor for The Open Respiratory Medicine Journal.

He was the Chairman of the Airway Pharmacology and Treatment Group, the Secretary of the Inflammatory Airway Diseases and Clinical Allergy Assembly and the Postgraduate Courses Director at the European Respiratory Society. He was the co-chairman of the European Respiratory Society/American Thoracic Society Task Force "Outcomes for COPD pharmacological trials: from lung function to biomarkers". He is a member of the steering committee of the Airway Disorders Network and is serving as Governor of the Italian Chapter at the American College of Chest Physicians. He is the Chairman of the Southern Europe Chapter at Interasma, and the Chair of the Med COPD Forum.

In 2014, Prof. Mario Cazzola's outstanding article "The role of indacaterol for chronic obstructive pulmonary disease (COPD)" published on *Journal of Thoracic Disease* (*JTD*) has been globally well-received. To meet the large demand of its international readers, this article has come out in three languages: English, Italian and Chinese. Beginning with the successful article, JTD has a special interview with Prof. Mario Cazzola.

Figure 1 Professor Mario Cazzola.

JTD: What do you think has made "The role of indacaterol for chronic obstructive pulmonary disease (COPD)" so popular?

Prof. Cazzola: I honestly do not know the answer to this question. In writing this article, we simply included all the information we hold and we illustrated and commented it in the most unbiased manner. Probably, colleagues acknowledge that our group has a good credibility in the field of bronchodilators and, consequently, they trust our opinion.

JTD: As a leading expert on COPD, would you like to retrospectively comment on the content of your own article?

Prof. Cazzola: I do not think there is anything more to add except to suggest colleagues to read the paper critically and to compare their experience with what has been described on it. However, I hope that all will agree that the duration of bronchodilation seems to determine the clinical efficacy of bronchodilators in COPD, although agents with a rapid onset of action could be more effective on nocturnal and morning symptoms than those with a relatively slow onset of action. The need for a rapid onset of action and a long duration of the broncholytic effect is the likely reason for the development of new LABAs that are fast acting and have true 24 h duration of action. Indacaterol is the archetype of once-daily LABAs, which I prefer to call ultra-LABAs

to differentiate them from traditional LABAs that have a duration of action of 12 hours.

JTD: What are the major limitations in the medicine for COPD at present? What do you think is the main trend in the future development of COPD medicine?

Prof. Cazzola: International guidelines try to simplify the diagnosis and treatment of patients affected by COPD. However, there is an enormous variability in the response to drugs between patients suffering from this morbid condition. For this reason, it is fundamental to identify the characteristics of patients that predict response to drugs used to manage COPD. Individualized therapy allows administration of the right treatment to the right patient, increasing, in this way, the subject's response to therapy, avoiding treatments not indicated and reducing the onset of adverse effects.

JTD: I've found the last part of your article on "positioning indacaterol in the therapeutic scheme of COPD" to be both original and fascinating. How will this affect the current treatment option for COPD?

Prof. Cazzola: We thought it was important to highlight where we place indacaterol, and probably where we will place the new ultra-LABAs such as olodaterol and vilanterol, in the therapeutic scheme proposed by GOLD. In truth, this is a simplification because the evidence that emerged in recent years makes us think properly that the choice of bronchodilator to start treatment with in a patient with COPD mainly depends on the outcome of interest. LABAs are more effective than LAMAs if we consider symptoms or health-related quality of life as the primary outcome, whereas in frequent exacerbators, it seems preferable to use a LAMA. In any case, a critical evaluation of the most recent literature let us to confirm our opinion that it is preferable to initiate the treatment of the patient with mild/moderate stable COPD, at least those who are not frequent exacerbators, choosing indacaterol.

JTD: The studies have well proved the positive effectiveness of indacaterol on COPD. Is there anything that the patients or doctors should pay attention to when they are using indacaterol for the treatment of COPD?

Prof. Cazzola: I do not think there is a specific problem related to the use of indacaterol in COPD patients. Rather, there are still fundamental questions regarding bronchodilators in general that require clarification to optimise their utilisation. I still wonder if it is appropriate to treat all COPD patients with long-acting bronchodilators, it is better to start with a β_2-agonist or with an anti-muscarinic agent, it is useful to use a bronchodilator with a rapid onset of action, and also if once- or twice-daily dosing is preferable. Moreover, it is important to understand when we can add a second bronchodilator with a different mechanism of action, and when we must add an ICS.

JTD: What do you think of the drug resistance of indacaterol in the future? What should be done to better avoid its drug resistance? Otherwise, how many years will it take to develop the drug resistance?

Prof. Cazzola: Tolerance to the bronchodilator effects of LABAs may occur with their prolonged use in COPD. In particular, high-efficacy β_2-agonists may cause a greater loss of receptors and it is likely that relevant tolerance to rescue salbutamol treatment could be more likely with β_2-agonists that are able of a really long residency at the β_2-adrenoceptor. In effect, in many stable COPD patients under regular treatment with a conventional dose of indacaterol 150 μg, an additional dose of indacaterol 150 μg, which is allowed in Europe, does not induce any substantial improvement in lung function, but I think this is more related to a ceiling broncholytic effect rather than to the appearance of tolerance. In fact, it has been shown that a regular treatment with indacaterol does not alter bronchodilator response to repeated doses of salbutamol. In any case, it seems reasonable and safe to increase the dose of indacaterol in those stable COPD patients who are under regular therapy with indacaterol 150 μg from which they do not draw the maximum benefit because they are unable to perceive bronchodilation.

Acknowledgements

Disclosure: The author declares no conflict of interest.

(Science Editor: Melanie C. He, JTD, jtd@thepbpc.org)

Cite this article as: He MC. Professor Mario Cazzola: prospect of the COPD medicine. J Thorac Dis 2014;6(12):1886-1887. doi: 10.3978/j.issn.2072-1439.2014.12.38

Opinion

Buyer beware: understanding the assumptions behind health economic assessments in personalized cancer care

D. Ross Camidge[1], Adam J. Atherly[2]

[1]University of Colorado Cancer Center, Anschutz Medical Campus, Aurora, Colorado, USA; [2]Colorado School of Public Health, University of Colorado Anschutz Medical Campus, Aurora, Colorado, USA

Correspondence to: D. Ross Camidge. University of Colorado Comprehensive Cancer Center, Aurora, CO 80045, USA. Email: ross.camidge@ucdenver.edu.

Submitted Dec 10, 2014. Accepted for publication Dec 15, 2014.
doi: 10.3978/j.issn.2072-1439.2014.12.41
View this article at: http://dx.doi.org/10.3978/j.issn.2072-1439.2014.12.41

After 'lies, damn lies and statistics' (a quote widely attributed to the 19th century British Prime Minister Benjamin Disraeli), health economics may represent the next most complex kind of analyses offered up to physicians in order to influence their practice. On the one hand, basic cost effectiveness calculations are straightforward. The extra benefit from the new approach (beyond that of the existing standard) divided by the extra cost for the new approach (beyond that of the existing standard) generates the incremental cost effectiveness ratio (ICER). The ICER is then normalized to present an incremental cost per unit of health, usually either the cost per life years gained or quality-adjusted life years gained (QALYs), and measured against a perceived acceptability threshold. However, the complexity and controversy of most health economics lies not in the calculation but in the assumptions made to generate the costs and the benefits used in these analyses in the first place.

In the 2014 paper by Djalalov *et al*., a Markov model was used to assess the cost effectiveness of finding and treating ALK positive lung cancer with crizotinib from the perspective of the Ontario Health Care System in Canada (1). To put this into context, the discovery and exploitation of ALK rearranged non-small cell lung cancer (NSCLC) arguably represents one of the key advances that has helped to shape our modern treatment philosophy in advanced lung cancer. When patients were preselected from the start for the presence of an ALK gene rearrangement, the benefit from crizotinib was remarkable. Treatment was routinely associated with objective response rates of 60-70%, median progression free-survival (PFS) times of 8-10 months and a very reasonable side effect profile (2,3). In the USA, the drug was heralded as a breakthrough and rapidly licensed on the basis of single arm trial results. Later phase III trials confirmed the superiority of the targeted approach in this molecularly defined population compared to both 1st and 2nd line standard chemotherapies (3,4).

Yet this breakthrough may not be implemented in some countries, simply because it is not considered cost effective. With multiple other examples of giving specific targeted drugs to specific molecular subtypes of disease occurring, it is becoming vitally important to accurately address the health economics of these personalized medicine scenarios. For if we don't address the feasibility of actually delivering these breakthroughs to patients in the real world they will not be breakthroughs at all.

Early on, we had raised the idea that in the era of increasingly personalized cancer care, health economic assessments would also now have to take into account the cost of the biomarker screening in addition to the cost and benefit of the drug. When the predictive biomarker is either very cheap and/or present in a large proportion of the population, the cost per QALY is primarily influenced by the cost, benefit and side effects of the new drug in the target population; however the cost of the screening can become dominant at very low biomarker positivity rates, with the point of inflection occurring at higher frequencies as the screening test becomes more expensive (5). In the Canadian study, immunohistochemistry (IHC) for ALK was utilized as the primary screening assay (estimated at 40 Canadian dollars per patient) with FISH (estimated at 388 dollars/patient) reserved as a confirmatory assay in IHC positive cases. Benefit from comparator use (i.e., without crizotinib) and subsequent use (i.e., post-crizotinib) of 1st line cisplatin-gemcitabine chemotherapy, 2nd line pemetrexed chemotherapy and 3rd line erlotinib was based

on efficacy within a large, but molecularly unselected registry of Ontario patients from 2005-2009. The quality of life on crizotinib was estimated to be only 6% better than the quality of life on platinum doublet chemotherapy, and 18% worse than life on erlotinib.

In their analyses, the dominant contributor to the cost per QALY was the cost of the crizotinib. Crizotinib use cost an additional $255,970 per QALY including the screening costs and $250,632 per QALY assuming no costs from the screening. Both of these values would be above commonly considered acceptability thresholds in Canada. But what if we change some of the assumptions used in their model?

For example, we now know that crizotinib is, in general, very well tolerated. In addition, due to the dramatic effects of the crizotinib on the underlying ALK positive cancer, the quality of these patients' lives is far better than other advanced disease patients even in the absence of treatment related side effects. Multiple news stories of ALK positive patients returning to normal lives, pursuing active sports, even running for public office and winning have been aired. What if we assume that the utility of time on crizotinib approaches perfect quality of life, say 90% of perfect quality of life?

In that circumstance, recalculating based on the methodology described in the Djalalov paper, the cost effectiveness ratio reduces dramatically from 255,970 per quality adjusted life year gained to $143,421 per quality adjusted life year gained. Although this still will not meet most accepted cost effectiveness thresholds, it demonstrates the sensitivity of their results to one of the key underlying assumptions.

The results may also be sensitive to the particular clinical treatment options selected. For example, what if pemetrexed was used as part of a platinum doublet in the 1st line setting, as opposed to as monotherapy in the 2nd line setting? While the Canadian study used cisplatin-gemcitabine as their assumed 1st line platinum doublet, increasingly platinum-pemetrexed is the 1st line doublet of choice in non-squamous patients in many countries, often with continuation maintenance of the pemetrexed after 4-6 cycles of the doublet have been completed (6,7). Platinum-pemetrexed is both more expensive than platinum-gemcitabine, but also potentially more efficacious in the ALK positive population. Within the Phase III 1007 study quoted by Djalalov, which compared crizotinib to either docetaxel or pemetrexed in the 2nd line setting, while these two chemotherapies were perceived to be equivalent in terms of efficacy in an unselected population, this was clearly not the case in the ALK positive population (4,8). Several retrospective studies had already suggested that ALK positive patients may do particularly well with pemetrexed, which was then confirmed within the 2nd line 1007 study with the pemetrexed arm having almost twice the PFS (crizotinib: 7.7 months, pemetrexed: 4.2 months, docetaxel: 2.6 months) and nearly four times the response rate of the docetaxel arm (29% *vs.* 7%) (3,9,10). Subsequent data from the 1st line PROFILE 1014 Phase III study of crizotinib versus up to six cycles of platinum-p xemetrexed, which was not available at the time of the Djalalov modeling, showed that although crizotinib was again superior to the chemotherapy in the ALK positive population, the proportional increase in PFS in the 1st line setting (55%; 7 *vs.* 10.9 months) was less than in the 2nd line setting (83%) even without the use of continuation maintenance pemetrexed (4).

How these different factors would interplay in the ICER calculation is unclear without explicit modeling. Markov models, such as the one used by the Djalalov paper, first assume a beginning health condition (known as a 'state') and then estimate what would happen to a typical population, given what we know about likely health outcomes from treatment. The key to economic analyses of this type are 'transition probabilities' which represent the probability of transitioning from one health 'state' to another at a defined time point. The table in the Djalalov paper provides the 'transition' probabilities from one line of treatment to the next line of treatment (e.g., from crizotinib to platinum doublet), or to other outcomes (e.g., post-treatment but stable, to supportive care or to death). If the treatment line changes, this creates a cascade effect through the model. As pemetrexed is more expensive than gemcitabine, *in isolation* this would reduce the incremental cost of using crizotinib and the ICER of crizotinib would decrease. Yet, on the other hand, *in isolation*, the potential increased clinical effectiveness of the chemotherapy in the 1st line setting would reduce the relative gain in efficacy from using crizotinib and the ICER would increase. The net effect would depend on many factors, ranging from the absolute costs and clinical effectiveness already mentioned to the transition probabilities and quality of life estimates used in each state.

With regard to the impact of molecular testing on the ICER, it should be recognized that IHC for ALK is still not nationally validated and no standardized test yet exists. Usually, if and when such an official test is developed, the cost of the assay will be significantly higher than a home-grown assay as described in the Canadian study. So what if we assume that the IHC test doesn't cost $40 but actually

$400 dollars? If, as assumed, 95% of eligible patients take the IHC test, this increases the cost per patient to $3,105 which increases the cost effectiveness ratio by around $24,000 to approximately $280,000 per quality adjusted life year gained when screening costs are included. This still shows that the dominant contributor to the ICER is the cost of the drug, but illustrates the impact of the screening assumptions in their model.

One of the key things to recognize in the Canadian model is that the incremental gain assessed for their ICER is minuscule as it is calculated on a population level—0.011 QALYs gained. Consequently, even relatively small changes in baseline assumptions can alter the cost effectiveness ratio dramatically. For example, doubling the frequency of the ALK fusion genes from 3.4% to 6.8% effectively halves the cost effectiveness ratio. We have previously modelled how using clinical enrichment strategies to determine who to test based on histology, smoking status and absence of other known driver oncogenes can dramatically increase the frequency of ALK positive disease in the tested population (for example, to over 30% in the most enriched scenario) while also reducing the absolute costs as the total population tested diminishes (5). On a medical basis, we have argued against this approach, as enrichment is not perfect and many ALK positive cases will be left behind who do not meet the classical picture of the disease. However, if a breakthrough treatment is potentially being denied to all patients in a health system because of the perceived health economics of an all-inclusive approach, accepting clinical enrichment as a necessary evil to allow at least some to benefit may be the most pragmatic approach in these difficult situations.

The purpose of all of the above remodeling of the Djalalov paper is not to argue whether crizotinib is or is not cost effective, but simply to illustrate that what seems like an unequivocal fact (cost per QALY of X or Y) is actually highly equivocal and subject to considerable local, national and international variation as the assumptions and costs within the analysis are customized to specific health system factors and emerging factors in relation to efficacy and tolerability. While the Djalalov paper is very balanced in its views, it has to be recognized that the data for standard therapeutic practices and the expert opinions used to generate information on the expected quality of life and transition probabilities of each state will, inevitably, have had specific viewpoints associated with them. Certainly, no one would deny that Ontario is part of the real-world, but is it any more representative of the whole real world than say, California, or Japan or France?

Finally, when assessing health economics, the impact of time also needs to be considered. ICERs often depend critically on data drawn from clinical trials in relation to medications that are on patent protection. The extent that the results of the trials reflect the later effectiveness in a broader population, or of the treatment being delivered by a more or less experienced group of physicians and the extent to which current prices reflect ultimate prices, will all influence how robust these ICERs will be over time. If, for example, screening becomes cheaper or a higher frequency of the abnormality becomes detectable due to advances in technology or understanding of the underlying biology; or treatment costs decline; or treatment effectiveness and tolerability increase as clinicians gain more experience with the new treatments, then ICERs will improve. The case of treatment of childhood acute lymphoblastic leukemia is instructive in this regard (11). Today, survival rates for childhood acute lymphoblastic leukemia have reached 80-90% and ICERs are in the range of $8,215 per quality adjusted life year gained—clearly meeting the usual cost effectiveness thresholds. Yet, many of the incremental advances in treatment over the past half century did not initially meet these thresholds.

So, while cost effectiveness is undeniably becoming an increasingly important hurdle to clear in order for modern breakthroughs to see the light of day, the consumers of these data should continue to recall the ancient principle of *caveat emptor*—buyer beware. To make sense of health economic data we must always strive to understand and at times question or update the assumptions about both cost and effectiveness that have been used in the calculations in order to determine their true applicability in whatever version of the real world we are living in at the time.

Acknowledgements

Disclosure: The authors declare no conflict of interest.

References

1. Djalalov S, Beca J, Hoch JS, et al. Cost effectiveness of EML4-ALK fusion testing and first-line crizotinib treatment for patients with advanced ALK-positive non-small-cell lung cancer. J Clin Oncol 2014;32:1012-9.
2. Camidge DR, Bang YJ, Kwak EL, et al. Activity and safety of crizotinib in patients with ALK-positive non-small-cell lung cancer: updated results from a phase 1 study. Lancet Oncol 2012;13:1011-9.

3. Shaw AT, Kim DW, Nakagawa K, et al. Crizotinib versus chemotherapy in advanced ALK-positive lung cancer. N Engl J Med 2013;368:2385-94.
4. Solomon BJ, Mok T, Kim DW, et al. First-line crizotinib versus chemotherapy in ALK-positive lung cancer. N Engl J Med 2014;371:2167-77.
5. Atherly AJ, Camidge DR. The cost-effectiveness of screening lung cancer patients for targeted drug sensitivity markers. Br J Cancer 2012;106:1100-6.
6. Scagliotti GV, Parikh P, von Pawel J, et al. Phase III study comparing cisplatin plus gemcitabine with cisplatin plus pemetrexed in chemotherapy-naive patients with advanced-stage non-small-cell lung cancer. J Clin Oncol 2008;26:3543-51.
7. Paz-Ares L, de Marinis F, Dediu M, et al. Maintenance therapy with pemetrexed plus best supportive care versus placebo plus best supportive care after induction therapy with pemetrexed plus cisplatin for advanced non-squamous non-small-cell lung cancer (PARAMOUNT): a double-blind, phase 3, randomised controlled trial. Lancet Oncol 2012;13:247-55.
8. Hanna N, Shepherd FA, Fossella FV, et al. Randomized phase III trial of pemetrexed versus docetaxel in patients with non-small-cell lung cancer previously treated with chemotherapy. J Clin Oncol 2004;22:1589-97.
9. Camidge DR, Kono SA, Lu X, et al. Anaplastic lymphoma kinase gene rearrangements in non-small cell lung cancer are associated with prolonged progression-free survival on pemetrexed. J Thorac Oncol 2011;6:774-80.
10. Lee JO, Kim TM, Lee SH, et al. Anaplastic lymphoma kinase translocation: a predictive biomarker of pemetrexed in patients with non-small cell lung cancer. J Thorac Oncol 2011;6:1474-80.
11. van Litsenburg RR, Uyl-de Groot CA, Raat H, et al. Cost-effectiveness of treatment of childhood acute lymphoblastic leukemia with chemotherapy only: the influence of new medication and diagnostic technology. Pediatr Blood Cancer 2011;57:1005-10.

Cite this article as: Camidge DR, Atherly AJ. Buyer beware: understanding the assumptions behind health economic assessments in personalized cancer care. J Thorac Dis 2014;6(12):1888-1891. doi: 10.3978/j.issn.2072-1439.2014.12.41

Case Report

Pyrexia in patients with uncontrolled systemic hypertension: could they have an aortic dissection?

Vasileios Patris[1], Jennifer Whiteley[1], Orestis Argiriou[2], Niki Lama[3], Haris Georgiou[3], Charalampos Constantinou[1], Mihalis Argiriou[4], Christos Charitos[4]

[1]Department of Cardiac Surgery, Heart and Chest Hospital, Liverpool, UK; [2]Medical School, University of Ioannina, Ioannina, Greece; [3]Department of Radiology, Agia Olga General Hospital, Athens, Greece; [4]Department of Cardiac Surgery, "Evangelismos" General Hospital of Athens, Athens, Greece
Correspondence to: Orestis Argiriou, MD. Medical School, University of Ioannina, 41, Aetideon str. 15561 Athens , Greece. Email: orestisargiriou@yahoo.gr.

Abstract: Aortic dissection can present in a variety of ways and one of the most documented risk factors includes systemic hypertension. Occasionally aortic dissection can be diagnosed late due to an insidious presentation. Fever has been described in people with aortic dissection but rarely as the main presenting feature. We present the cases of two patients with type B aortic dissections who shared three pertinent features which could have alerted the clinicians of the potential diagnosis; systemic hypertension, small left sided pleural effusion and a fever of unknown origin.

Keywords: Type B aortic dissection; unknown fever; pyrexia; hypertension; stent graft

Submitted Apr 15, 2014. Accepted for publication Sep 01, 2014.
doi: 10.3978/j.issn.2072-1439.2014.11.13
View this article at: http://dx.doi.org/10.3978/j.issn.2072-1439.2014.11.13

Introduction

Aortic dissection is a potentially life threatening disease, consequently, obtaining a diagnosis quickly is vital and can affect the patients mortality and morbidity. The exact cause of aortic dissection is unknown but uncontrolled hypertension is among one of the most common risk factors (1). It classically presents with severe chest pain, which radiates to the back but there has been a diverse set of clinical features documented and can present painlessly (2). There have been some reports of fever being a feature of an acute aortic dissection but it is rarely the main presenting complaint (3).

We describe two cases of delayed diagnosis of type B aortic dissection where fever was the presenting feature in patients who had uncontrolled hypertension. In both cases there was also an incidental finding of a small, left sided pleural effusion.

Case reports

Case 1

Case 1 is of a 42-year-old female, 6 months post-partum, with a past medical history of hypertension. This patient was taking a once daily dose of amlodipine (10 mg) at the time of presentation, however, her hypertension remained uncontrolled with a systolic blood pressure of more than 170 mmHg. She presented to a general hospital with symptoms of epigastric pain, vomiting and pyrexia, and was admitted to a medical ward. Investigations included abdominal ultrasound, echocardiogram, upper gastro-intestinal (GI) endoscopy, urine and blood cultures; no abnormalities were detected. Inflammatory markers were raised [white cell count (WCC) 12.5×10^9 g/dL, C-reactive protein (CRP) 126 mg/L and erythrocyte sedimentation rate (ESR) 36 units] and she had persistent pyrexia of around 38.5 ℃. The coagulation function was also normal [platelets (PLT) 255000, international normalized ratio (INR) 1.18, activated partial thromboplastin time (APTT) 34 s, prothrombin time (Pt) 12 s, Fibrinogen 240 mg/dL). After 12 days with persistent symptoms, not changing from presentation, a CT of the chest, abdomen and pelvis was done. This demonstrated a type B aortic dissection extending from the origin of the left subclavian artery to the left iliac artery, there was no evidence of mal-perfusion. Additionally, there was a small left sided pleural effusion (*Figure 1*). The patient was then transferred to a

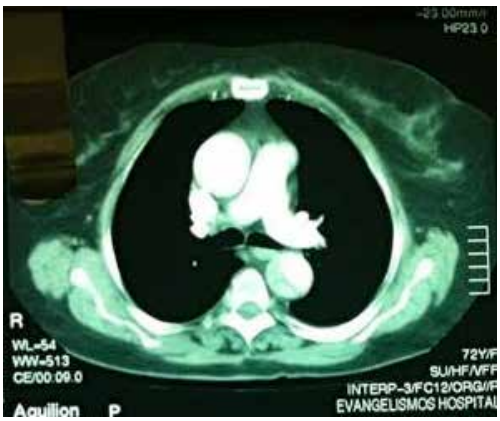

Figure 1 CT scan demonstrating aortic dissection and intraluminal haematoma.

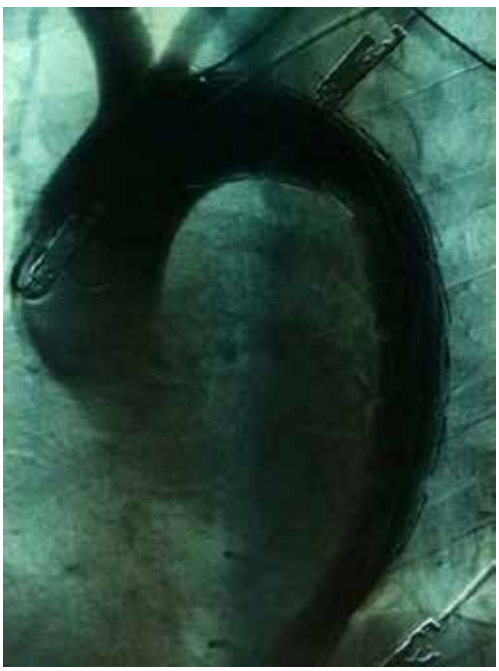

Figure 2 Angiogram showing position of the stent immediately after insertion- demonstrating no endo-leak.

cardiothoracic unit on the same day; her hypertension was treated with intravenous glyceryl trinitrate and esmolol. Raised inflammatory markers were thought to be due to an inflammatory process originating from the aortic haematoma. The next day a stent graft was inserted through the right femoral artery and was placed between the origin of the left subclavian artery and the aorta at the level of the seventh thoracic vertebra. Angiogram immediately after insertion showed correct position with no endo-leak (*Figure 2*).

Post procedure she remained haemodynamically stable (blood pressure around 110/80 mmHg). Hypertension postoperatively was treated with Exforge® (a combination drug of amlodipine and valsartan). Follow up CT scan at day 4 and 3 months post procedure both showed good placement of the stent without any endo-leaks. The 3-month scan showed minimal haematoma.

Case 2

Case 2 is of a 48-year-old male, overweight, smoker with uncontrolled hypertension (not medicated). He presented to the A&E department with a 5-day history of epigastric pain, vomiting and pyrexia. At presentation his systolic blood pressure was more than 170 mmHg. He was admitted to a medical ward and underwent blood and urine cultures, abdominal ultrasound scan which showed no abnormalities. Upper GI endoscopy demonstrated an area of mild gastritis in the pyloric antrum which was biopsied at the time but this was not thought to be contributing to the on-going symptoms. Similarly to the first case, the patient remained pyrexic throughout admission and WCC and CRP were raised (13.2×10^9 and 126 respectively). The coagulation function was normal (PLT 315,000, INR 1.25, APTT 33 s, Pt 13 s, Fibrinogen 270 mg/dL), too. After 12 days, a CT scan of the abdomen demonstrated dissection at the level of the diaphragm, and therefore the radiologist progressed to scan the remaining thorax which demonstrated a type B aortic dissection with the presence of haematoma, a small left sided pleural effusion and small pericardial collection. This patient underwent the same procedure and follow up as case 1, his hypertension was also controlled with intravenous GTN and esmolol preoperatively and Exforge®, post operatively. The fever resolved in the post-operative period and the inflammatory makers normalised. CT scan at day 4 and 3 months showed reducing size of haematoma and no leaks.

Discussion

The two cases described above demonstrate that pyrexia, in the absence of an obvious source with negative investigations, in a patient with a background of uncontrolled hypertension, could be a presenting feature of an aortic dissection. In both cases there was a considerable time delay between presentation and diagnosis which could have potentially been avoided had dissection been included in the original differential diagnosis and subsequent appropriate investigations been done in a timely manner.

A retrospective case series from Spain in 2010 also describes fever as a feature of aortic dissection, most frequently in type B dissections (3). Fever tended to be low grade and the patient was generally well when compared with a patient who has a fever caused by infection. This case series looked at patients with a diagnosis of aortic dissection and then identified those who had a fever as part of the acute episode. They determined the difference between a fever due to the inflammatory process as a result of a dissection and fever due to an intercurrent infection, they do not however suggest that fever can be the prominent presenting feature of an acute aortic dissection, as with two cases previously described.

In both cases described, the CT scan which diagnosed the aortic dissection also revealed a small left sided pleural effusion. Similar presentations have been described before, a retrospective review published in 2012 of 71 patients presenting with fever and a pleural effusion of unknown aetiology described three cases which had large thoracic vessel pathology. One of these patients had an aortic dissection (the two other patients had giant cell arteritis and Takayasu arteritis). In all three of these cases the pleural effusion was left sided, small-moderate in size and non-diagnostic on thoracocentesis. The effusions resolved following treatment (4). All patients presenting with fever would have a chest X-ray as part of a septic screen as an early investigation. Identification of a pleural effusion at this early stage in the absence of any other positive investigations could provide a clue that there may be aortic pathology and prompt appropriate investigation.

An inflammatory reaction to the aortic dissection can explain the pyrexia and raised inflammatory markers in these patients. As the left pleura are in contact with the aorta this may explain why the pleural effusions were always left sided. Inflammation of the aorta from a dissection could irritate the pleura leading to a reactionary effusion (5).

The right pleura is away from the aorta and in contact with the major veins in the thorax. Sato *et al.* analyzed 66 patients with aortic dissection, there were 16 pleural effusion cases found (3 type A and 13 type B classification). The result also suggested that transient rupture or leakage in descending aortic dissection was the possibly mechanism of pleural effusion (6).

Conclusions

Physicians should remember the association of pyrexia and left sided pleural effusion with aortic dissection when investigating patients with similar presentations, especially if they are known to have uncontrolled hypertension. Although it is a rare cause of these symptoms, it is important and missing the diagnosis could lead to catastrophic consequences to the patient.

Acknowledgements

Disclosure: The authors declare no conflict of interest.

References

1. Larson EW, Edwards WD. Risk factors for aortic dissection: a necropsy study of 161 cases. Am J Cardiol 1984;53:849-55.
2. Yamada S, Tokumoto M, Ohkuma T, et al. Slowly progressive and painless thoracic aortic dissection presenting with a persistent Fever in an elderly patient: the usefulness of combined measurement of biochemical parameters. Case Rep Med 2013;2013:498129.
3. García-Romo E, López-Medrano F, Llovet A, et al. Fever due to inflammation in acute aortic dissection: Description and proposals for diagnostic and therapeutic management. Rev Esp Cardiol 2010;63:602-6.
4. Schattner A, Klepfish A. Left pleural effusion and fever of unknown origin--a clue to thoracic arterial pathology. J Gen Intern Med 2012;27:1084-7.
5. Yamada S, Tokumoto M, Ohkuma T, et al. Slowly progressive and painless thoracic aortic dissection presenting with a persistent Fever in an elderly patient: the usefulness of combined measurement of biochemical parameters. Case Rep Med 2013;2013:498129.
6. Sato F, Kitamura T, Kongo M, et al. Newly diagnosed acute aortic dissection: characteristics, treatment modifications, and outcomes. Int Heart J 2005;46:1083-98.

Cite this article as: Patris V, Whiteley J, Argiriou O, Lama N, Georgiou H, Constantinou C, Argiriou M, Charitos C. Pyrexia in patients with uncontrolled systemic Hypertension: could they have an Aortic Dissection? A discussion with two examples. J Thorac Dis 2014;6(12):E246-E248. doi: 10.3978/j.issn.2072-1439.2014.11.13

Case Report

Primary synovial sarcoma of the lung: can haemothorax be the first manifestation?

Wen Ling Woo[1], Nikolaos Panagiotopoulos[1], Lasha Gvinianidze[1], Sadeer Fhadil[1], Elaine Borg[2], Mary Falzon[2], David Lawrence[1]

[1]Department of Cardiothoracic Surgery, [2]Department of Histopathology, University College London Hospitals (UCLH), London, UK

Correspondence to: Wen Ling Woo. Department of Cardiothoracic Surgery, University College London Hospitals (UCLH), London, UK. Email: wenling.woo@uclh.nhs.uk.

Abstract: Primary pulmonary synovial sarcomas represent a rare clinical entity and account for approximately 0.5% of lung malignancies. We report the case of a 30-year-old male who presented clinically with haemothorax. Imaging revealed a complex collection obscuring a multi-lobulated mass in the right lower lobe of the lung. He underwent a right thoracotomy for evacuation of collection and surgical resection of his pulmonary mass. Histological analysis confirmed a grade 3 monophasic fibrous synovial sarcoma of the lung with infiltration to adjacent pleura, causing his initial haemothorax. Postoperative period was uneventful and patient was referred to the oncology team for further management. Primary pulmonary synovial sarcoma, though rare, should remain an important differential when considering lung malignancies, as complete surgical resection is the mainstay of treatment.

Keywords: Primary pulmonary synovial sarcoma; haemothorax

Submitted Jul 02, 2014. Accepted for publication Sep 09, 2014.
doi: 10.3978/j.issn.2072-1439.2014.11.01
View this article at: http://dx.doi.org/10.3978/j.issn.2072-1439.2014.11.01

Background

Primary pulmonary synovial sarcoma of the lung is exceedingly rare and accounts for 0.5% of primary lung malignancies. We report the case of a 30-year-old man who presented clinically with haemothorax, who was subsequently diagnosed with primary synovial sarcoma of the lung following complete surgical resection of the lesion.

Case report

A 30-year-old male presented with 3-week history of fever, cough, and chest pain. He had no medical history of note and was a non-smoker. Clinical examination showed reduced breath sounds and dullness to percussion in the right mid to lower zones. Systemic examination was otherwise unremarkable. Chest radiograph confirmed a large right-sided pleural effusion (*Figure 1*). A chest drain was inserted which drained blood, revealing that the effusion was in fact a haemothorax. A computer tomography (CT) scan of the chest was performed, which established a complex large effusion obscuring a possible multi-lobulated mass lying posteriorly (*Figure 2*). A right posterolateral thoracotomy was performed for evacuation of the collection and resection of the right lower lobe, as the lung tissue was necrotic macroscopically. Intra-operative specimens were negative for microbiology. Histological analysis showed pulmonary parenchyma and pleural tissue infiltration by high grade monomorphous spindle cells (*Figure 3*). High mitotic activity is present and there are diffuse areas of necrosis. Immunohistochemistry of the tumour was positive for EMA (*Figure 4*) and Bc12 (*Figure 5*) diffusely and focally for MCK. There was also diffuse dot-like positivity for CD99 (*Figure 6*). CD34 was negative. Interphase fluorescence in situ hybridisation (FISH) gene rearrangement was positive. These findings are consistent with grade 3 monophasic fibrous synovial sarcoma (pT2b N0 M0 G3).

Post-operatively the course was uneventful and he was discharged on the seventh day and remained well clinically. He has been referred to the oncologist for chemotherapy and further management.

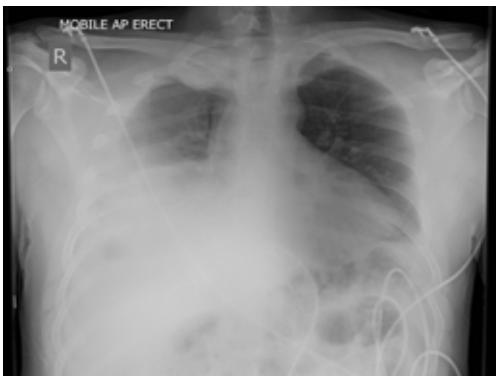

Figure 1 Chest radiograph demonstrating a large right sided pleural effusion.

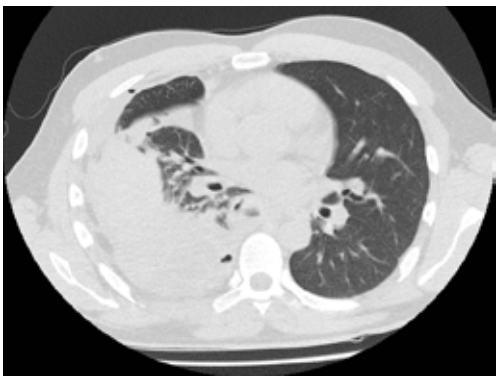

Figure 2 Computed tomography (CT) scan of the chest confirming right sided pleural effusion and a multi-lobulated mass in the right lower lobe.

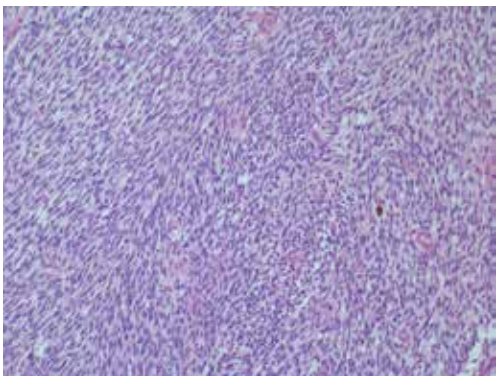

Figure 3 Monophasic high grade synovial sarcoma infiltrating lung and pleura. The tumour is composed of dense cellular sheets and fascicles of bland spindle cells (H&E ×40).

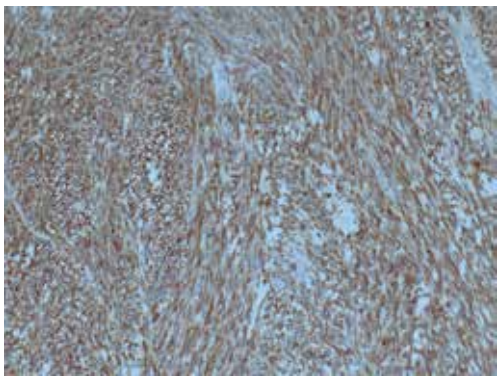

Figure 4 Immunohistochemistry shows EMA expression by tumour cells (×100).

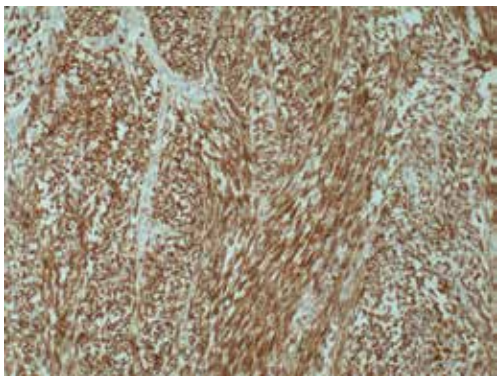

Figure 5 Immunohistochemistry shows Bc12 expression by tumour cells (×200).

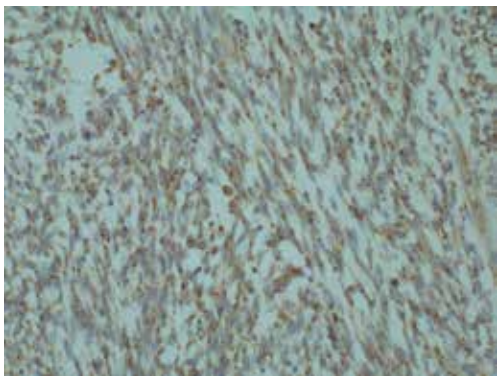

Figure 6 Immunohistochemistry shows CD99 expression by tumour cells (×200).

Discussion

Synovial sarcomas are rare mesenchymal tumours accounting for only 8% of soft tissue tumours. They commonly present in soft tissue of extremities in adolescents and young adults, however other sites have been reported including lung, heart, head and neck (1). There are four histological classifications: monophasic fibrous, monophasic epithelial, biphasic (contains both spindle and epithelial cells), and poorly differentiated subtypes.

Primary pulmonary synovial sarcomas are rare and account for approximately 0.5% of lung malignancies. Important differentials of primary pulmonary neoplasm include adenocarcinoma, malignant fibrous histiocytoma, and malignant mesothelioma. Extra-thoracic primary sources should also be excluded as lung metastases from distant synovial sarcomas can also occur (2).

Tumours are often centrally located, with patients frequently presenting with respiratory symptoms including chest pain, cough and haemoptysis. Peripheral tumours are less common. Patients can be asymptomatic initially, present with a pleural effusion when there is invasion of the adjacent pleura (3), or in the case of our patient, with a haemothorax where the tumour has likely infiltrated and bled into the pleural space.

Imaging like chest radiograph and chest CT scans are often carried out as primary investigations, providing information on location and size of lesions, and further information regarding infiltration to adjacent sites. Imaging is non-specific and diagnosis is achieved through histological and immunohistochemistry analysis and can also include cytogenetic testing. Cytogenetic testing is helpful as t(X;18)(p11.2;q11.2) is characteristic of synovial sarcoma, distinguishing it from other soft tissue tumours. There is a range of tests that can be carried out including reverse transcriptase polymerase chain reaction (RT-PCR) to detect gene fusion and product expression, or interphase FISH gene arrangement.

Surgical resection with clear resection margins is the main treatment modality. Prognosis is variable depending on tumour grade; 5-year survival is estimated to be approximately 50%. Adverse prognostic factors include disease stage, increasing age (>20 years old), male gender, large tumour size (>5 cm) and high mitotic activity (>9 mitoses per 10 HPF) (4).

Radiotherapy has no apparent effect on control of local disease or overall survival. Patients may benefit from adjuvant or neoadjuvant chemotherapy, though there is no specific recommended therapy, as studies carried out remain largely inconclusive. This is due to small sample sizes and differing treatments administered in each case (4). Systemic chemotherapy is often administered in palliative cases where surgical resection is not possible (5). In view of high tumour grade and multiple adverse prognostic markers, our patient has been referred for palliative chemotherapy using doxorubicin and ifosfamide, as per local oncology advice.

Given the rapid disease progression and prognostic outcomes, primary pulmonary synovial sarcoma, though rare, should remain an important differential when considering lung malignancies, as complete surgical resection is the mainstay of treatment. Patients may benefit from post-operative adjuvant or neoadjuvant chemotherapy, although evidence remains largely inconclusive till date.

Conclusions

Primary pulmonary synovial sarcoma, though rare, should be considered as one of the differential diagnoses in patients with pulmonary lesions with a variety of clinical presentation as disease progression is rapid, prognostic outcomes are generally unfavourable, and the mainstay of treatment is complete surgical resection, which can only be achieved if diagnosed early.

Acknowledgements

Disclosure: The authors declare no conflict of interest.

References

1. Dennison S, Weppler E, Giacoppe G. Primary pulmonary synovial sarcoma: a case report and review of current diagnostic and therapeutic standards. Oncologist 2004;9:339-42.
2. Aydogdu K, Sahin F, Findik G, et al. Pulmonary synovial sarcoma. Asian Cardiovasc Thorac Ann 2014;22:92-4.
3. Roy P, Das A, Sarkar A, et al. A primary synovial sarcoma of lung. N Am J Med Sci 2012;4:241-3.
4. Trassard M, Le Doussal V, Hacène K, et al. Prognostic factors in localized primary synovial sarcoma: a multicenter study of 128 adult patients. J Clin Oncol 2001;19:525-34.
5. Falkenstern-Ge RF, Kimmich M, Grabner A, et al. Primary pulmonary synovial sarcoma: a rare primary pulmonary tumor. Lung 2014;192:211-4.

Cite this article as: Woo WL, Panagiotopoulos N, Gvinianidze L, Fhadil S, Borg E, Falzon M, Lawrence D. Primary synovial sarcoma of the lung: can haemothorax be the first manifestation? J Thorac Dis 2014;6(12):E249-E251. doi: 10.3978/j.issn.2072-1439.2014.11.01

Case Report

Palliative stent graft placement combined with subsequent open surgery for retrograde ascending dissection intra-thoracic endovascular aortic repair

Kai Zhu, Hao Lai, Changfa Guo, Jun Li, Chunsheng Wang

Department of Cardiac Surgery, Zhongshan Hospital, Fudan University & Shanghai Institute of Cardiovascular Disease, Shanghai 200032, China
Correspondence to: Hao Lai; Chunsheng Wang. No. 180, Fenglin Road, Xuhui District, Shanghai 200032, China. Email: lai.hao@zs-hospital.sh.cn; cswang@medmail.com.cn.

Abstract: Thoracic endovascular aortic repair (TEVAR) is an effective strategy for type B dissection. Retrograde ascending dissection (RAD) intra-TEVAR is a rare complication on clinic. In this case, a 48-year-old Chinese man with Stanford type B aortic dissection suffered acute RAD during the TEVAR. And palliative stent grafts placement was performed in a local hospital, which earned the time for transfer and subsequent total arch replacement surgery in Zhongshan Hospital Fudan University. This report suggests that the palliative strategy may be an option for RAD in some specific situation.

Keywords: Thoracic endovascular aortic repair (TEVAR); retrograde ascending dissection (RAD); surgery

Submitted Jul 23, 2014. Accepted for publication Sep 17, 2014.
doi: 10.3978/j.issn.2072-1439.2014.11.02
View this article at: http://dx.doi.org/10.3978/j.issn.2072-1439.2014.11.02

Introduction

Thoracic endovascular aortic repair (TEVAR) is a safe and effective alternative to traditional open surgery for uncomplicated type B dissections (1). Retrograde ascending dissection (RAD) is a life-threatening complication that may occur on intra- or post-TEVAR. And RAD intra-TEVAR is extremely rare on clinic (2,3). In this case, we report a case management for a patient with RAD intra-TEVAR.

Case report

A 48-year-old Chinese man presented an acute severe chest pain with back irradiation and was sent to the local hospital at the onset of symptoms. He had a history of severe hypertension for four years. And no other positive medical history was reviewed. Computed tomography angiography (CTA) revealed Stanford type B aortic dissection with a site of entry tear at 2 cm upon the origin of renal artery. TEVAR was chosen to perform for this patient on emergency. However, acute RAD occurred before stent grafts placement. The retrograde dissection expanded to the middle of ascending aorta, with a new entry tear near the origin of left subclavian artery (LSCA).

Given that the local hospital lacked cardiac surgery department, a distal bare stent restraint combined with proximal covered stent was then palliatively placed to cover the new entry tear, which kept from further retrograde dissection. After TEVAR, the patient felt symptom alleviation, but a little bit dizzy and amaurosis. CTA revealed that proximal part of stent graft covered the origins of LSCA and left common carotid (LCC) (*Figure 1*). He was then transferred to Zhongshan Hospital Fudan University for an open surgery on emergency. After induction of general anesthesia, the right axillary artery is exposed through a right subclavian incision as routinely used for cardiopulmonary bypass (CPB) and antegrade selective cerebral perfusion. And the femoral artery was cannulated in addition to the axillary artery cannulation. An arterial cannula is inserted into the right axillary artery, and a dual-stage caval cannula is inserted into the right atrium. The CPB flow is maintained between 2.2 and 2.4 L/min/m^2, and the patient was cooled to a rectal temperature of 20 ℃. During the cooling period, the ascending aorta is cross-clamped and the heart is arrested with cold blood cardioplegia. The brain is perfused through

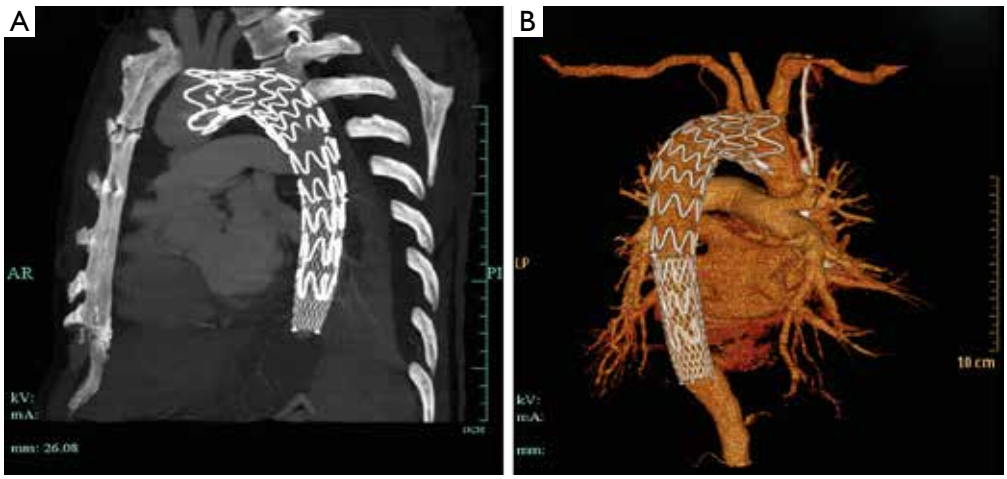

Figure 1 Computed tomography angiography demonstrating that proximal part of the palliative stent graft covered the origins of left subclavian artery and left common carotid as seen on sagittal (A) and three-dimensional reconstruction (B) views.

the right axillary artery at a flow rate of 5 to 10 mL/kg/min. Through the transverse incision of the ascending aorta, we found the ascending aorta dissection with a diameter of 55 mm, and confirmed that the proximal part of stent graft covered the new entry tears, as well as origins of LSCA and LCC. We cut off the dissection part of ascending aorta, aorta arch and proximal part of stent graft. A triple-branched artificial vessel was one by one sutured to the stent graft, aortic branches and ascending aorta. The CPB time was 189 minutes with aortic cross-clamp time of 117 minutes and cerebral perfusion of 30 minutes. The patient recovered well, and was discharged after 2 weeks.

Discussion

Published literatures have identified RAD as a lethal complication of TEVAR for all indications with an estimate of 1.3% to 6.8% (1-3). Given the recent evidence, this complication may be associated with the procedure or device, or as a result of natural progression of aorta disease. Potential risk factors for RAD include the following: (I) proximal stent graft with a free-flow bare spring; (II) endoleak at the proximal fixation site leading to retrograde enlargement of the false lumen; (III) passive bending of TEVAR at the arch with over-stenting of the LSCA leading to spring-back strength, which could yield stress on the greater curve of arch; (IV) wire and sheath handling or balloon dilatation during the endovascular procedure might trigger the intimal damage in the extremely fragile aortic wall; and (V) patients with connective tissue disorders such as Marfan, Ehlers-Danlos, and Loeys-Dietz syndromes (4-7).

The median interval between TEVAR and repair of retrograde dissection was 6 months. RAD intra-TEVAR is extremely rare on clinic (8). In our case, RAD occurred acutely before stent graft placement. The new entry tear led to the expansion of retrograde dissection with ascending aorta involved. We assumed that the introduction of guide wire and sheath handling during the endovascular procedure might injury the fragile and vulnerable aortic wall and result in acute RAD.

RAD is an emergency that requires surgical repair. And expanded dissection may result in the subsequently lethal aortic rupture (9). In the present case, cardiac surgery was unable to be done in the local hospital. Therefore, palliative TEVAR was performed alternatively, which aimed to cover the new entry tear and blocked further expansion of ascending dissection before the open surgery. The strategy earned time for transfer and reduced risk of death. And it could be applied in this specific situation. However, this strategy may result in the risk of coverage for branched artery origins, which may subsequently lead to cerebral ischemia. Therefore, lack of cardiac surgery department in a hospital posed difficulties for the management of a RAD patient. All contingency plans should be arranged before TEVAR, including standby of cardiac surgeons and operation room.

The operative strategies regarding the rescue of RAD are similar to those for acute type A dissection. The reverse frozen elephant trunk procedure or total arch replacement were the preferred choices for patients with a dissection

tear involving the arch, and ascending and hemi-arch repair was sufficient in patients with the dissection limited to the proximal aorta (8-10). In this case, we chose to perform total arch replacement during the open surgery. We cut off proximal part of the stent graft and sutured the distal end of artificial vessel to the remaining stent graft, which could work as reverse elephant trunk technique.

Conclusions

In conclusion, we consider palliative TEVAR associated with open surgery may enable a novel strategy for acute RAD during endovascular procedure for hospital that is lack of cardiac surgery department. And emergency surgical repair is still the best choice for all patients.

Acknowledgements

This work was supported by a grant from the National Key Technologies R & D Program of China during the Twelfth Five-Year Plan Period (No. 2011BA11B20).
Disclosure: The authors declare no conflict of interest.

References

1. Dake MD, Kato N, Mitchell RS, et al. Endovascular stent-graft placement for the treatment of acute aortic dissection. N Engl J Med 1999;340:1546-52.
2. Dong ZH, Fu WG, Wang YQ, et al. Retrograde type A aortic dissection after endovascular stent graft placement for treatment of type B dissection. Circulation 2009;119:735-41.
3. Eggebrecht H, Thompson M, Rousseau H, et al. Retrograde ascending aortic dissection during or after thoracic aortic stent graft placement: insight from the European registry on endovascular aortic repair complications. Circulation 2009;120:S276-81.
4. Kische S, Ehrlich MP, Nienaber CA, et al. Endovascular treatment of acute and chronic aortic dissection: midterm results from the Talent Thoracic Retrospective Registry. J Thorac Cardiovasc Surg 2009;138:115-24.
5. Williams JB, Andersen ND, Bhattacharya SD, et al. Retrograde ascending aortic dissection as an early complication of thoracic endovascular aortic repair. J Vasc Surg 2012;55:1255-62.
6. Neuhauser B, Greiner A, Jaschke W, et al. Serious complications following endovascular thoracic aortic stent-graft repair for type B dissection. Eur J Cardiothorac Surg 2008;33:58-63.
7. Svensson LG, Kouchoukos NT, Miller DC, et al. Expert consensus document on the treatment of descending thoracic aortic disease using endovascular stent-grafts. Ann Thorac Surg 2008;85:S1-41.
8. Idrees J, Arafat A, Johnston DR, et al. Repair of retrograde ascending dissection after descending stent grafting. J Thorac Cardiovasc Surg 2014;147:151-4.
9. Li B, Pan XD, Ma WG, et al. Stented elephant trunk technique for retrograde type A aortic dissection after endovascular stent graft repair. Ann Thorac Surg 2014;97:596-602.
10. Lu S, Lai H, Wang C, et al. Surgical treatment for retrograde type A aortic dissection after endovascular stent graft placement for type B dissection. Interact Cardiovasc Thorac Surg 2012;14:538-42.

Cite this article as: Zhu K, Lai H, Guo C, Li J, Wang C. Palliative stent graft placement combined with subsequent open surgery for retrograde ascending dissection intra-thoracic endovascular aortic repair. J Thorac Dis 2014;6(12):E252-E254. doi: 10.3978/j.issn.2072-1439.2014.11.02

Case Report

Induced airway obstruction under extracorporeal membrane oxygenation during treatment of life-threatening massive hemoptysis due to severe blunt chest trauma

Jong Myung Park[1], Chang Wan Kim[2], Hyun Min Cho[2], Bong Soo Son[1], Do Hyung Kim[1]

[1]Department of Thoracic and Cardiovascular Surgery, Pusan National University Yangsan Hospital, Yangsan, South Korea; [2]Department of Thoracic and Cardiovascular Surgery, Trauma Center of Pusan National University Hospital, Pusan, South Korea

Correspondence to: Do Hyung Kim, MD. Department of Thoracic and Cardiovascular Surgery, Pusan National University Yangsan Hospital, Beomeo-ri, Mulgeum-eup, Yangsan, Gyeongsangnam-do, 626-770, South Korea. Email: yumccs@nate.com.

Abstract: Simultaneous improvement in respiratory maintenance and bleeding control increases survival of patients with life-threatening hemoptysis. Endobronchial blockade is an effective method and is preferred for emergency hemostasis. However, when the volume of hemoptysis is high, emergency hemostasis and airway maintenance are impossible due to flooding of blood into the airway. We used extracorporeal membrane oxygenation (ECMO) to overcome these limitations in a patient with massive hemoptysis due to severe blunt trauma and succeeded in saving the life by inducing a near-total airway obstruction.

Keywords: Hemoptysis; extracorporeal membrane oxygenation (ECMO); hemostasis; trauma

Submitted May 30, 2014. Accepted for publication Sep 23, 2014.
doi: 10.3978/j.issn.2072-1439.2014.10.22
View this article at: http://dx.doi.org/10.3978/j.issn.2072-1439.2014.10.22

Introduction

It is challenging to evaluate hemorrhage and selective hemostasis in many patients with life-threatening hemoptysis in which respiratory maintenance is difficult due to airway obstruction from blood aspiration. Once life-threatening hemoptysis occurs, patients can die due to hypovolemic shock from uncontrolled bleeding or airway obstruction due to failure to remove blood clots. Thus, simultaneously improving respiratory maintenance and bleeding control increases survival of patients with life-threatening hemoptysis (1).

Extracorporeal membrane oxygenation (ECMO) has been used widely to treat acute respiratory failure in patients who are struggling to survive using a ventilator alone. Thus, ECMO can be used for respiration in patients with life-threatening massive hemoptysis in which the bleeding focus cannot be identified, and even in conditions with near-total airway obstruction. The trachea or main bronchus can be simultaneously blocked to control bleeding.

Case report

A 40-year-old female was admitted to the emergency department due to blunt trauma sustained in a traffic accident. The patient was diagnosed with intracerebral hemorrhage, severe contusion in both lungs, multiple rib fractures, right hemothorax, femur fracture, and liver laceration (*Figure 1*). The Glascow Coma Scale score of the patient was seven. Normal respiration was not maintained because of life-threatening massive hemoptysis; thus, venovenous (VV) ECMO (PLS System, MAQUET, Rastatt, Germany) was initiated. Emergency surgery to control left hemothorax bleeding and a wedge resection of the multiple lung laceration sites were performed under VV ECMO. Despite the surgery, the bleeding could not be controlled, and the patient was eventually transferred to the intensive care unit after gauze packing (*Figure 2*). However, the hemoptysis remained, so we applied endobronchial ballooning (Arndt endobronchial blocker, Cook Medical

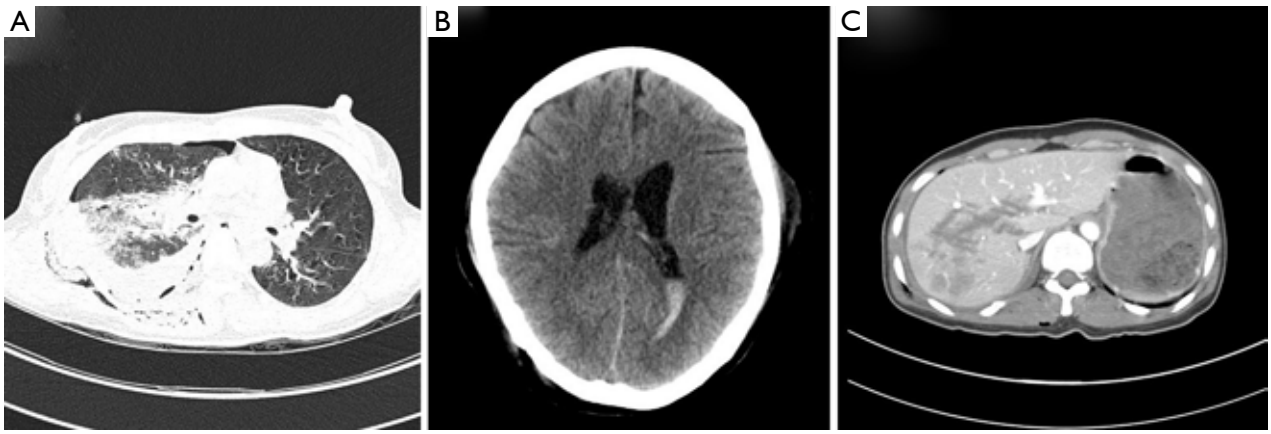

Figure 1 (A) Chest; (B) brain; (C) abdominal computed tomography scans of a patient admitted to the emergency department due to blunt trauma sustained in a traffic accident.

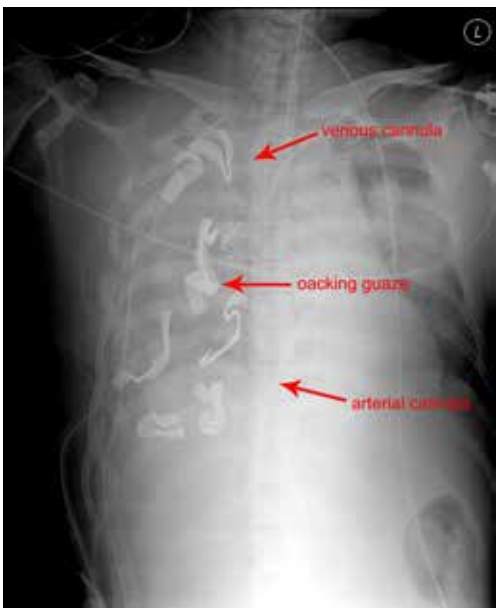

Figure 2 Chest radiograph obtained when the patient was transferred to the intensive care unit after gauze packing.

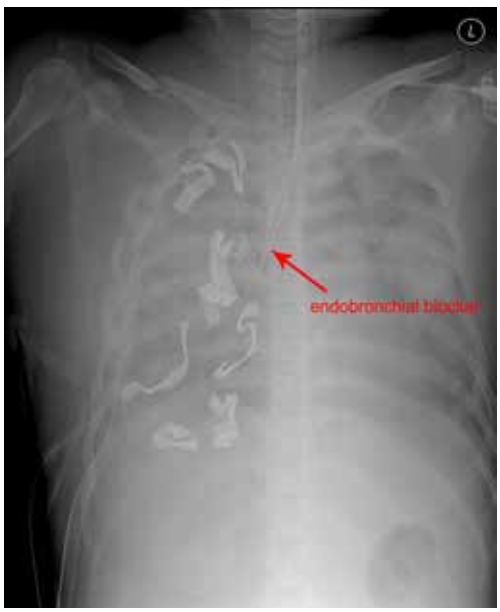

Figure 3 Chest radiograph obtained after endobronchial ballooning was applied to the right main bronchus and oxidized regenerated cellulose packing was performed on both sides of the bronchus for hemostasis.

Supply, Morton, MS, USA) for hemostasis in the right main bronchus under fibrobronchoscopy. However, the tracheal bleeding did not stop, and massive hemoptysis from the left lung was also detected. Severe hemorrhage necessitated oxidized regenerated cellulose (ORC) (Surgicel, Ethicon, Somerville, NJ, USA) packing on both sides of the bronchus (*Figure 3*). Respiratory support was employed with ECMO but without ventilator support. The packed ORC on the left bronchus, which had less of an injury as determined by chest computed tomography, was removed on the first day of ECMO support. PaO_2 and PCO_2 were 70-130 and 24-32 mmHg, respectively, in ECMO blood flow of 4-5 L/min with gas flow of 3-4 L/min. The packed ORC on the right bronchus was removed on the second day. Additional hemoptysis did not occur. VV ECMO was maintained for 11 days due to

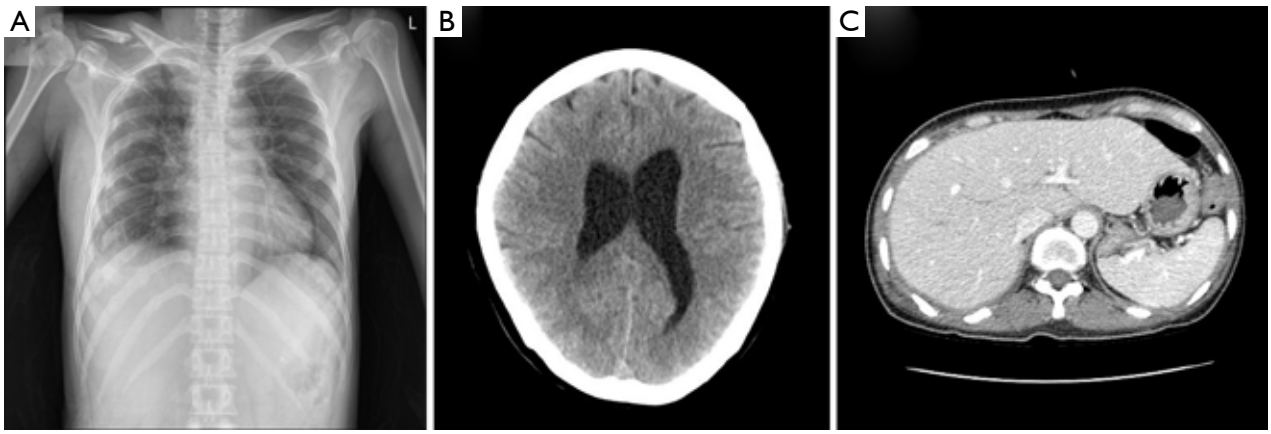

Figure 4 (A) Chest X-ray; (B) brain; (C) abdominal computed tomography scans of the improved patient during hospitalization.

acute respiratory distress syndrome. We weaned the patient from mechanical ventilation and then weaned her from ECMO. She was transfused with 50 units of red blood cells, 40 units of platelets, and 32 units of fresh frozen plasma before being removed from ECMO. We did not use anticoagulation agents until the bleeding stopped and vital signs were stable. Instead, we used a heparin-coated ECMO circuit. The femoral fracture and liver laceration were treated conservatively during ECMO. The patient received reduction surgery for the femoral fracture on day 19 after admission. The patient was discharged from the hospital on day 85. The intracranial hemorrhage and liver laceration improved spontaneously (*Figure 4*). The clinical progress of the patient was observed for 12 months in an outpatient clinic setting, and no further respiratory symptoms were observed. No physical or neurological deficits were detected, except for a gait disturbance due to the femoral fracture.

Discussion

Maintenance of airway patency and bleeding control should be performed simultaneously to rescue life in cases of massive hemoptysis. Then, definitive treatment such as bronchial arterial embolization (BAE) and surgery should be undertaken. However, when the volume of hemoptysis is so high that emergency hemostasis and airway maintenance are impossible due to flooding of blood into the airway, the patient dies from hypovolemia or airway obstruction without having a chance to undergo BAE or surgery. Therefore, a new life-saving rescue method needs to be developed to maintain life until definitive treatment, such as BAE and surgery, can be applied.

We thought that ECMO was ideal. ECMO is not used widely for massive hemoptysis but has been suggested in some case reports to be useful for life saving and as a bridge to treatment. Bianchini *et al.* (2) used ECMO as a life-saving technique in a patient with massive hemoptysis due to pulmonary artery rupture caused by a Swan-Ganz catheter and reported successful pulmonary arterial embolization. Bédard *et al.* (3) used ECMO as a bridge to lobectomy in patients with hypoxemia and repetitive hemoptysis due to an aortopulmonary collateral artery that occurred after a Fontan operation. Yuan *et al.* (4) reported the use of conservative treatment by applying ECMO in patients with massive hemoptysis due to blunt trauma.

As these reports show, sufficient blood oxygenation is possible without ventilation during maintenance with ECMO. Thus, hemostatic treatment under a non-respiratory condition is possible. We used these advantages of ECMO and actually used ECMO to execute both respiratory support and bleeding control at the same time in a patient with difficulty maintaining vital signs. Priority care in a case of respiratory failure should be focused on life rescue, and upon recovery of respiratory function, hemostasis should be performed.

Endobronchial blockade is an effective method and is preferred for emergency hemostasis. Freitag *et al.* (5) reported that balloon tamponade showed a 96% success rate for hemostasis in 27 patients, except one patient with short-term recurrence of hemoptysis. Valipour *et al.* (6) reported that ORC packing of a bleeding bronchus controlled bleeding immediately in 98% of cases, suggesting its effectiveness as a hemostasis method. However, hemostasis

using endobronchial blockade requires contralateral lung protection from bleeding. This is difficult to execute in patients with massive hemoptysis and blood aspiration in both lungs. Applying ECMO can overcome these limitations.

We would have selectively packed only at the bleeding site, if it were possible to identify the site, but identifying the bleeding site was difficult because of the filled blood that made selective blocking impossible. Immediate hemostasis was needed when the exact bleeding site could not be identified. Thus, endotracheal packing using ORC was performed. In a situation where mechanical ventilation was not performed due to flooding of blood before tracheal packing, maintenance of optimal blood oxygen and carbon dioxide concentrations was possible. Thus, the patient's vital signs remained stable even when a near total airway obstruction was induced. We rescued a life and controlled bleeding through endotracheal tamponade using ECMO in a case of life-threatening hemoptysis.

The most important factor to consider when treating massive bleeding is anticoagulation. Anticoagulation is generally necessary when using ECMO, so we thought that ECMO was not appropriate during thoracic surgery of bleeding patients despite its respiratory support advantages. However, the limitation was resolved by the introduction of the heparin-coated circuit. This circuit allows ECMO to be maintained at a lower anticoagulation level or without anticoagulation. Ried *et al*. reported applying only a heparin-coated circuit and avoided heparin in patients with a high risk for bleeding complications (7). We thought that strict anticoagulation was not essential. We would not use heparin in a patient who has ongoing massive bleeding because a mild coagulation defect is induced by blood loss, and hemodilution occurs due to massive crystaloid volume replacement.

Cite this article as: Park JM, Kim CW, Cho HM, Son BS, Kim DH. Induced airway obstruction under extracorporeal membrane oxygenation during treatment of life-threatening massive hemoptysis due to severe blunt chest trauma. J Thorac Dis 2014;6(12):E255-E258. doi: 10.3978/j.issn.2072-1439.2014.10.22

In conclusion, applying ECMO could be an alternative and effective treatment in patients with respiratory failure and hypovolemic shock due to massive hemoptysis.

Acknowledgements

This study was supported by the Research Institute for Convergence of Biomedical Science and Technology, Pusan National University Yangsan Hospital.
Disclosure: The authors declare no conflict of interest.

References

1. Crocco JA, Rooney JJ, Fankushen DS, et al. Massive hemoptysis. Arch Intern Med 1968;121:495-8.
2. Bianchini R, Melina G, Benedetto U, et al. Extracorporeal membrane oxygenation for Swan-Ganz induced intraoperative hemorrhage. Ann Thorac Surg 2007;83:2213-4.
3. Bédard E, Lopez S, Perron J, et al. Life-threatening hemoptysis following the Fontan procedure. Can J Cardiol 2008;24:145-7.
4. Yuan KC, Fang JF, Chen MF. Treatment of endobronchial hemorrhage after blunt chest trauma with extracorporeal membrane oxygenation (ECMO). J Trauma 2008;65:1151-4.
5. Freitag L, Tekolf E, Stamatis G, et al. Three years experience with a new balloon catheter for the management of haemoptysis. Eur Respir J 1994;7:2033-7.
6. Valipour A, Kreuzer A, Koller H, et al. Bronchoscopy-guided topical hemostatic tamponade therapy for the management of life-threatening hemoptysis. Chest 2005;127:2113-8.
7. Ried M, Bein T, Philipp A, et al. Extracorporeal lung support in trauma patients with severe chest injury and acute lung failure: a 10-year institutional experience. Crit Care 2013;17:R110.

Case Report

Unexpectedly long intravenous and intracardiac extension of a small-sized pulmonary pleomorphic carcinoma

Aya Ishii[1], Tokuhiro Kimura[1], Koshiro Moritani[2], Dan Cui[1], Shinsuke Tanaka[3], Hiroo Kawano[4], Eiji Ikeda[1]

[1]Department of Pathology, Yamaguchi University Graduate School of Medicine, Ube, Japan; [2]Department of Internal Medicine, Ube Industries, Ltd. Central Hospital, Ube, Japan; [3]Division of Surgical Pathology, Yamaguchi University Hospital, Ube, Japan; [4]Department of Basic Laboratory Sciences, Yamaguchi University Graduate School of Medicine, Ube, Japan

Correspondence to: Eiji Ikeda, MD, PhD. Department of Pathology, Yamaguchi University Graduate School of Medicine, 1-1-1 Minami-Kogushi, Ube, Yamaguchi 755-8505, Japan. Email: ikedae@yamaguchi-u.ac.jp.

Abstract: Pleomorphic carcinoma of the lung is one of the uncommon histological types of lung cancers, which shows an aggressive behavior. Intravenous extension (not metastasis or direct invasion) of the tumor into the heart is a rare complication of lung cancers. We present a case of a 64-year-old man, who was admitted to hospital due to severe dyspnea. Chest CT scan revealed a 2-cm nodule in the upper lobe of the right lung. Echocardiography demonstrated a giant mass in the left atrium. Because of a considerable distance between the lung nodule and heart, the relation of these two lesions was unclear. He died four days after the admission. At autopsy, the lung nodule was pleomorphic carcinoma composed of spindle and giant cells, which invaded the pulmonary vein and extended intravenously to the left atrium. The intravenous component of the tumor measured approximately ten cm in length. At the tip of the extension, an 8 cm × 5 cm × 3 cm mass was formed in the left atrium, which obstructed the mitral valve. This case highlights a possibility that even a small-sized, peripherally located pleomorphic carcinoma of the lung could extend for an unexpectedly long distance to the heart, causing cardiac complications.

Keywords: Lung cancer; pleomorphic carcinoma; intracardiac extension; mitral valve; secondary cardiac tumor

Submitted Jun 02, 2014. Accepted for publication Aug 07, 2014.
doi: 10.3978/j.issn.2072-1439.2014.10.25
View this article at: http://dx.doi.org/10.3978/j.issn.2072-1439.2014.10.25

Introduction

Secondary cardiac malignancies, especially symptomatic ones, are uncommon, serious conditions. The routes by which neoplasms spread to the heart include direct invasion, hematogenous metastasis, lymphatic metastasis and transvenous extension. As for transvenous extension, renal cell carcinoma and hepatocellular carcinoma sometimes extend into the inferior vena cava and grow into the right atrium (1,2), but intracardiac extension of lung cancers via the pulmonary vein is rare, particularly when the lung tumor is small-sized and distant from the heart.

According to the 2004 World Health Organization (WHO) classification of the lung tumors (3), sarcomatoid carcinoma group of the lung are classified into five types: pleomorphic carcinoma, spindle cell carcinoma, giant cell carcinoma, carcinosarcoma and pulmonary blastoma. These neoplasms are uncommon histological types of lung carcinomas, comprising 0.3-1.3% of all pulmonary malignancies (3). Pleomorphic carcinoma is defined as squamous cell carcinoma, adenocarcinoma or large cell carcinoma containing spindle cells and/or giant cells, or carcinoma consisting only of spindle and giant cells. On the other hand, non-small cell carcinoma consisting only of spindle cells is called spindle cell carcinoma, and non-small cell carcinoma composed only of giant cells is named giant cell carcinoma. The behavior of tumors of this group is reported to be more aggressive than conventional non-small cell lung carcinomas (4-6).

Here we report a case of a pulmonary pleomorphic carcinoma of small size which showed unexpectedly long intravenous extension to the left atrium, resulting in fatal obstruction of the mitral valve.

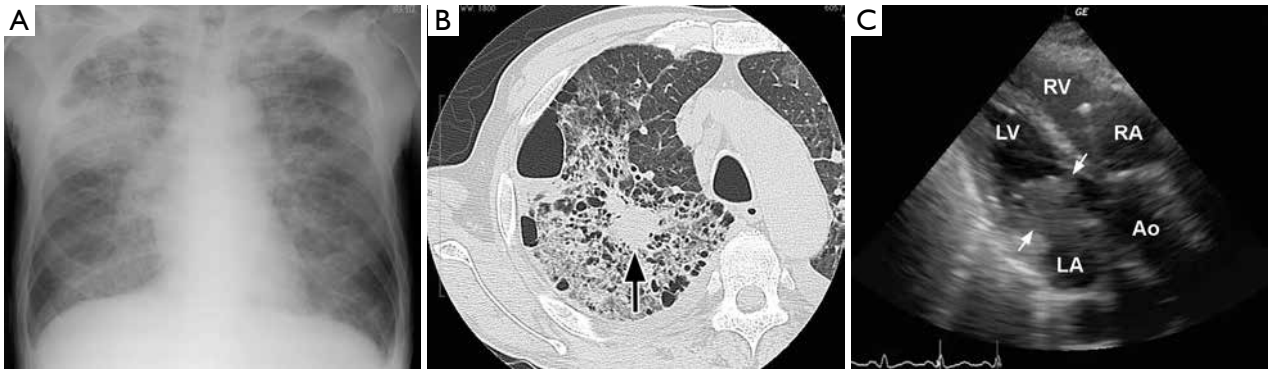

Figure 1 (A) Chest radiograph showed congestion of the bilateral lungs and opacity in the right upper lung; (B) chest CT scan revealed a nodule (arrow) of approximately two cm in diameter with opacity in the upper lobe of the right lung; (C) echocardiography showed a large mass (arrows) in the left atrium, causing obstruction of the mitral valve. Ao, aorta; LA, left atrium; LV, left ventricle; RA, right atrium; RV, right ventricle.

Case report

A 64-year-old male was admitted to the hospital because of dyspnea at rest and fever. He reported a history of 10-kg weight loss for six months, cough for two weeks, and fatigue, dysphagia and muscle weakness for one week. He smoked three packs of cigarettes per day for over 40 years. On admission, the height was 167 cm and the weight 55 kg, the blood pressure 97/70 mmHg, the pulse 115 beats per minute, the temperature 37.1 degree C and SpO_2 92%. Chest radiograph showed pulmonary congestion and opacity in the right upper lung (*Figure 1A*). Chest CT scan revealed opacity in the right upper lung with a tumor of approximately two cm in diameter in it (*Figure 1B*). Electrocardiogram showed no specific abnormality. Treatment with antibiotics and oxygen were started but his condition and respiration was progressively worsened next four days. Echocardiogram on third hospital day showed a large mass in the left atrium that caused obstruction of the mitral inflow of left ventricle (*Figure 1C*). Surgical removal of the mass was not selected because of his condition. He died of cardiac inflow obstruction four days after the admission. An autopsy was performed.

Grossly, a white, well-circumscribed nodule of 22 mm in diameter was found in the peripheral region of the upper lobe of the right lung (*Figure 2A*). The tumor showed direct invasion to the pulmonary vein branch (*Figure 2B*), and the tumor tissue extended intravenously and continuously from the lung nodule to the left atrium through the superior right pulmonary vein (*Figure 2C,D*). The distance between the lung nodule and the left atrium was approximately ten cm, and therefore the tumor tissue was elongated for this distance intravenously. In the lumen of the left atrium, the tumor tissue formed a mass of 8 cm × 5 cm × 3 cm (*Figure 2E*). The surface of the mass facing the mitral valve was indented as a mold of the shape of the mitral cusps (*Figure 2F*), suggesting that the mass obstructed the mitral valve. The morphology of the mitral valve itself was almost normal. Neither distant metastasis nor nodal involvement was observed. Systemic embolism of the tumor fragments was not found.

Histologically, the lung nodule as well as the intravenous and intraatrial portion of the tumor was composed of atypical spindle cells and giant cells (*Figure 3A,B*). Neutrophil infiltration was observed. Component of conventional non-small cell lung carcinoma (squamous cell, adeno-, or large cell carcinoma) was not found. Immunohistochemically, the spindle and giant cells were positive for cytokeratin AE1/AE3 (*Figure 3C*) and cytokeratin 7, and a small number of these cells were positive for TTF-1 (*Figure 3D*). These cells were negative for cytokeratin 20. Mallory-azan stain (which stains fibrous tissue blue) (*Figure 3E*) and CD34 immunostain (an endothelial marker) (*Figure 3F*) revealed that the tumor tissue had scant fibrous stroma and abundant small blood vessels, respectively. These findings indicate that the tumor was pleomorphic carcinoma of the lung with marked intravenous extension to the left atrium, resulting in fatal obstruction of the mitral valve. The non-neoplastic lung tissue around the nodule of the right upper lobe showed congestion and edema with marked intra-alveolar fibrin and organization. Mild emphysema was also found.

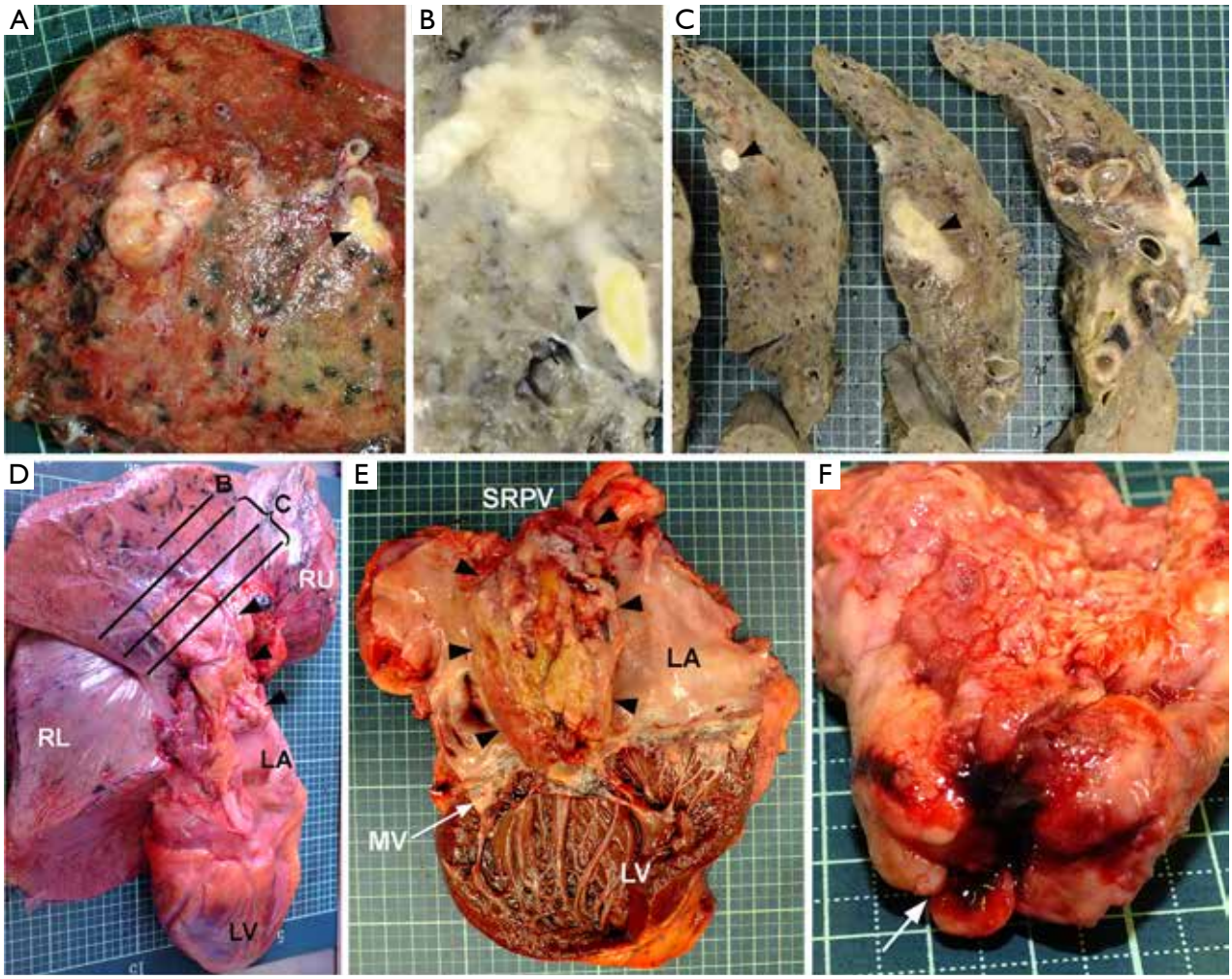

Figure 2 Gross findings of the lung tumor (A-D) and intracardiac tumor (E,F). A white, well-circumscribed nodule of 22 mm in diameter was found in the upper lobe of the right lung (A). The neighboring section (B) showed direct invasion of the tumor to the pulmonary vein branch. The intravenous component of the tumor extended from the nodule (B) to the pulmonary hilum (C), and finally into the left atrium (D). Arrowheads (A-D) indicate intravenous extension of the tumor. B and C in (D) correspond to the sections of (B) and (C), respectively. (E) A mass of 8 cm × 5 cm × 3 cm (arrowheads) was found in the left atrium, which was continuous with the intravenous component of the lung tumor in the superior right pulmonary vein. (F) The surface of the intraatrial mass facing the mitral valve (arrow) was indented as a mold of the shape of the mitral cusps. LA, left atrium; LV, left ventricle; MV, mitral valve; RL, lower lobe of right lung; RU, upper lobe of right lung; SRPV, junction of superior right pulmonary vein and left atrium.

Discussion

In the present case, one of the clinical problems was the relation between the intracardiac mass and lung nodule detected by echocardiography and chest CT, respectively. Several hypotheses were considered: these tumors might be independent primaries; the former might be metastasis of the latter, and vice versa; both of them might be metastasis of an unknown primary neoplasm. At autopsy, the continuity of these two tumors via the pulmonary vein, and immunoreactivity to TTF-1 (a specific marker for primary lung carcinoma) and cytokeratin clearly indicated that the lung nodule was the primary site and the intracardiac mass was the leading edge of endovascular extension of the carcinoma.

Pleomorphic carcinoma is a rare histological type of lung carcinoma. Patients of pleomorphic carcinoma are reported to be predominantly male smokers with a mean

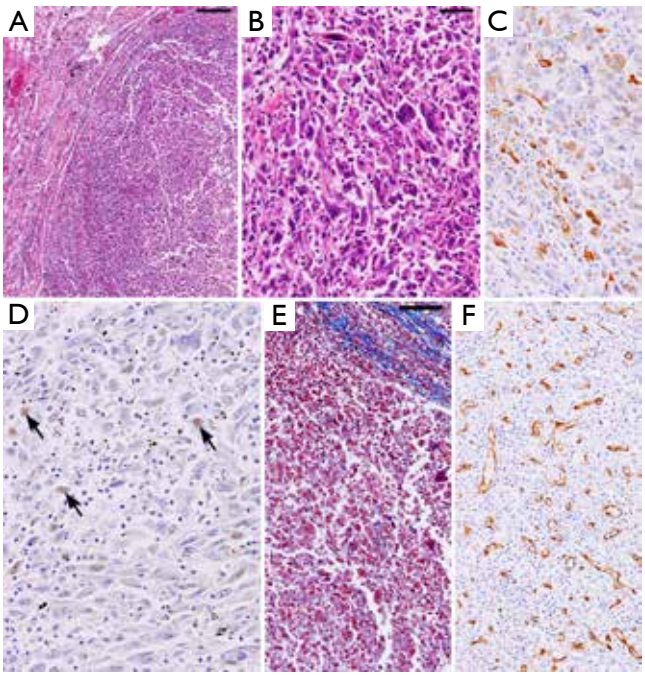

Figure 3 Histological findings of the lung tumor. Microscopically, low-power (A) and high-power (B) views of the lung nodule revealed that it was composed of atypical spindle and giant cells with neutrophil infiltration (hematoxylin-eosin stain). Immunohistochemically, the tumor cells were positive for cytokeratin AE1/AE3 (C) and TTF-1 (D, arrows). Mallory-azan stain showed that the tumor tissue had scant fibrous stroma (E), and immunostain for CD34 demonstrated numerous blood vessels in the tumor tissue (F). Scale bars for A, 250 μm; for B-D, 50 μm; for E and F, 100 μm.

age of 66 years (4-7). It tends to arise as a peripheral mass with a predilection for the upper lobes (5,7). The clinical course of this tumor is reported to be aggressive, compared to conventional non-small cell lung carcinomas (4-6). Histologically, pleomorphic carcinoma can be divided into two subgroups: (I) a conventional non-small cell carcinoma admixed with malignant spindle cells and/or giant cells; and (II) a carcinoma composed only of malignant spindle and giant cells. The present case corresponds to the subgroup (II), and the patient's age, smoking habit and location of the lung tumor are thought to be typical of pleomorphic carcinoma.

Intravenous extension to the left atrium is a rare complication of lung carcinomas, and several cases including small cell carcinoma (8,9) and conventional non-small cell carcinomas (10-14) were reported previously. Among them, intracardiac extension of sarcomatoid carcinoma group is extremely rare, and only one case of giant cell carcinoma (10) and one case of pleomorphic carcinoma composed of adenocarcinoma and spindle-cell components [subgroup (I), see above] (15) were described (*Table 1*). Thus, our paper is the second report of pulmonary pleomorphic carcinoma extending intravenously to the left atrium.

As shown in *Table 1*, common symptoms of these patients include weight loss and cough, which probably resulted from the lung tumor itself. Dyspnea, palpitations and arrhythmia might represent signs caused by an intracardiac tumor. The present case showed these common symptoms including dyspnea while muscle weakness, the pathophysiology of which was not clear, was a peculiar symptom to this case.

In the previously reported cases of sarcomatoid carcinomas (*Table 1*) and other histological types (8-14), the primary tumors in the lungs were advanced, large masses and therefore invaded near the heart. However, one of the remarkable findings of the present case is disproportionately long intravenous extension compared to the small size of the lung tumor. In fact, the lung tumor of the present case is much smaller than the previous cases (*Table 1*), and the intravenous component of the present tumor running from the lung nodule to the left atrium is markedly long (approximately 10 cm in length). This made clinical diagnosis difficult because the lung tumor was so distant from the heart that the intracardiac extension of the lung tumor seemed very unlikely. The histological features of the present tumor might explain this unexpectedly long extension in the pulmonary vein. First, the histological type of the lung cancer is pleomorphic carcinoma, which is biologically more aggressive than ordinary non-small cell carcinomas. Secondly, the tumor tissue had abundant blood vessels and lacked desmoplasia, which might facilitate smooth elongation in the venous lumen without necrotic collapse of the tumor tissue or hard adhesion to the surrounding structure. Hypervascularity and scant fibroplasia are shared features of other cancers with high propensity for intravenous extension, for example, hepatocellular carcinoma and renal cell carcinoma.

In summary, the present case teaches us that when a patient with a lung carcinoma even of a small size and located distantly from the heart presents with dyspnea, we should consider the possibility of intracardiac extension of the pulmonary neoplasm.

Table 1 Reported cases of sarcomatoid carcinoma group of the lung with intravenous extension to the left atrium

Case No.	Reference	Age/sex	Smoking	Primary site			Symptoms	Treatment	Follow-up
				Location	Size	Histological type			
1	(10)	67/M	+	LL	9.5 cm	Giant cell carcinoma	Dyspnea, palpitations, weight loss, hemoptysis	Surgery	DOD, 2 days
2	(15)	53/M	+	RL	"large"	Pleomorphic carcinoma (adenocarcinoma + spindle cells)	Arrhythmia, weight loss, fever, cough	Surgery	ND
The present case		64/M	+	RU	2.2 cm	Pleomorphic carcinoma (spindle cells + giant cells)	Dyspnea, weight loss, fever, cough, dysphagia, muscle weakness	–	DOD, 4 days

LL, left lower lobe; RL, right lower lobe; RU, right upper lobe; DOD, die of disease; ND, not described.

Acknowledgements

Disclosure: The authors declare no conflict of interest.

References

1. Amano J, Nakayama J, Yoshimura Y, et al. Clinical classification of cardiovascular tumors and tumor-like lesions, and its incidences. Gen Thorac Cardiovasc Surg 2013;61:435-47.
2. Goldberg AD, Blankstein R, Padera RF. Tumors metastatic to the heart. Circulation 2013;128:1790-4.
3. Travis WD, Brambilla E, Mueller-Hermelink HK, et al. eds. World Health Organization Classification of tumours, pathology and genetics of tumours of the lung, pleura, thymus and heart. Lyon, France: IARC Press, 2004.
4. Rossi G, Cavazza A, Sturm N, et al. Pulmonary carcinomas with pleomorphic, sarcomatoid, or sarcomatous elements: a clinicopathologic and immunohistochemical study of 75 cases. Am J Surg Pathol 2003;27:311-24.
5. Yuki T, Sakuma T, Ohbayashi C, et al. Pleomorphic carcinoma of the lung: a surgical outcome. J Thorac Cardiovasc Surg 2007;134:399-404.
6. Mochizuki T, Ishii G, Nagai K, et al. Pleomorphic carcinoma of the lung: clinicopathologic characteristics of 70 cases. Am J Surg Pathol 2008;32:1727-35.
7. Ito K, Oizumi S, Fukumoto S, et al. Clinical characteristics of pleomorphic carcinoma of the lung. Lung Cancer. 2010;68:204-10.
8. Brandt RR, Rubin J, Reeder GS, et al. Intracardiac extension of a lung tumor causing left ventricular inflow obstruction. J Am Soc Echocardiogr 1995;8:930-3.
9. Lin MT, Ku SC, Wu MZ, et al. Intracardiac extension of lung cancer via the pulmonary vein. Thorax 2008;63:1122.
10. Kodama K, Doi O, Tatsuta M. Unusual extension of lung cancer into the left atrium via the pulmonary vein. Int Surg 1990;75:22-6.
11. Mehan VK, Deshpande J, Dalvi BV, et al. Direct extension of bronchogenic carcinoma through pulmonary veins into the left atrium mimicking left atrial myxoma. Chest 1992;101:1722-3.
12. Watanabe N, Kubo K. Images in cardiology: Intra-left atrial invasive mass extended via the pulmonary vein. Heart 2001;85:271.
13. Khan N, Golzar J, Smith NL, et al. Intracardiac extension of a large cell undifferentiated carcinoma of lung. Heart 2005;91:512.
14. Costache VS, Lantuejoul S, Stoica S, et al. Giant intracardiac neoplasic thrombus of a large cell neuroendocrine carcinoma of the lung. Cardiovasc Pathol 2010;19:e85-7.
15. Ng SW, Lim CH, Wang CW, et al. Primary pulmonary sarcomatoid carcinoma with intracardiac extension. Jpn J Thorac Cardiovasc Surg 2006;54:416-9.

Cite this article as: Ishii A, Kimura T, Moritani K, Cui D, Tanaka S, Kawano H, Ikeda E. Unexpectedly long intravenous and intracardiac extension of a small-sized pulmonary pleomorphic carcinoma. J Thorac Dis 2014;6(12):E259-E263. doi: 10.3978/j.issn.2072-1439.2014.10.25

Case Report

Beware of arteria lusoria during lymph node dissection of the right paratracheal fossa for lung cancer surgery

Daniel Pan, Maria Elena Cufari, Eric Lim

Imperial College and Academic Division of Thoracic Surgery, London, UK

Correspondence to: Mr Eric Lim. Academic Division of Thoracic Surgery, Royal Brompton Hospital, Sydney Street, London, SW3 6NP, UK. Email: e.lim@rbht.nhs.uk.

Abstract: An asymptomatic elderly woman presented with a solitary right upper lobe mass revealed to be non-small cell lung cancer following routine surveillance post mastectomy. Upon review of CT with contrast in preparation for rigid bronchoscopy and right upper lobectomy, we noticed that the patient had a rare case of *arteria lusoria*. This is the presence of an aberrant right subclavian artery extending from the left side of the aortic arch, crossing posteriorly across the midline to supply the upper limb. We suggest that with a documented 100% diagnostic sensitivity on 64 multislice computed tomography, the presence of *arteria lusoria* within the posterior paratracheal fossa may cause life-threatening complications in the unaware during systematic lymph node dissection for non-small cell lung cancer (NSCLC).

Keywords: Arteria lusoria; lobectomy; lymph node

Submitted Sep 12, 2014. Accepted for publication Oct 15, 2014.
doi: 10.3978/j.issn.2072-1439.2014.11.12
View this article at: http://dx.doi.org/10.3978/j.issn.2072-1439.2014.11.12

Case report

A 76-year-old woman who was an ex-smoker (13 pack years) presented with a solitary right upper lobe mass shadowing following routine CT surveillance post mastectomy for past breast cancer. Biopsy subsequently confirmed non-small cell lung cancer (NSCLC) with a PET staging of T1N2M0. The patient had exposure to asbestos from her previous work as a glass cutter and has a family history of aggressive metastatic cancer in multiple family members. She reported no bone pain, shortness of breath/chest pain or dysphagia, and physical examination was unremarkable at time of pre-operation.

After multidisciplinary review and patient input, the recommend course of action was right upper lobectomy and systematic nodal dissection.

Upon review of CT with contrast we (M.E.C) noticed that the patient had four branches of the aortic arch with absence of the brachiocephalic trunk (*Figure 1*). The most distal left sided origin artery passed posteriorly to the oesophagus as it crossed the midline of the body to supply the right arm. This is consistent with what is known as an abberant right subclavian artery or *arteria lusoria*. The unusual course of the artery was noted pre-operation due to its proximity with the right upper lobe tumour.

We proceeded to rigid bronchoscopy and right upper lobectomy. The aberrant vessel was noted in the right paratracheal fossa (*Figure 2*) and was carefully avoided during lymph node dissection.

Discussion

Aberrant right subclavian artery, clinically known as *arteria lusoria* is the most common embryologic abnormality of the aortic arch (1). It arises as the last branch of the aortic arch or from the proximal descending aorta, on the left side of the thorax. 80-84% crosses upwards and to the right behind the oesophagus, whilst 12.7-15% between the oesophagus and trachea and 4.2-5% in front of the trachea (2). In 60% of patients, the artery's origin arises from an aortic arch diverticulum as first described by Kommerell (3). It is thought that this aberrant origin is caused by involution of the right fourth vascular arch and proximal right dorsal aorta and the persistence of the seventh intersegmental

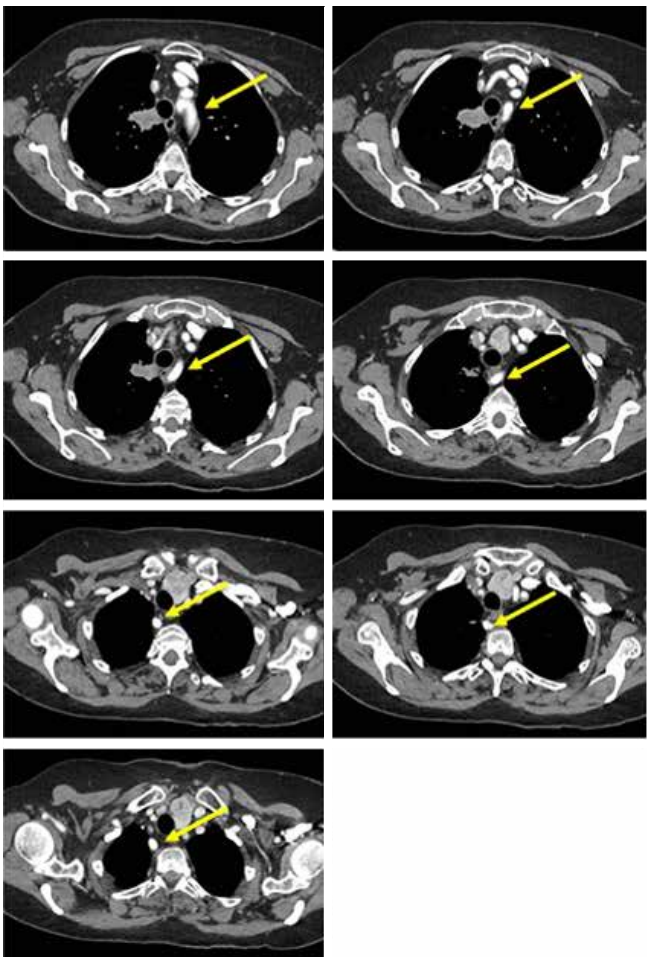

Figure 1 CT of the mediastinal window, showing the course of the right aberrant brachiocephalic artery as it branches off the aorta from the left side, crossing the midline posterior to the oesophagus to supply the right upper limb (yellow arrow).

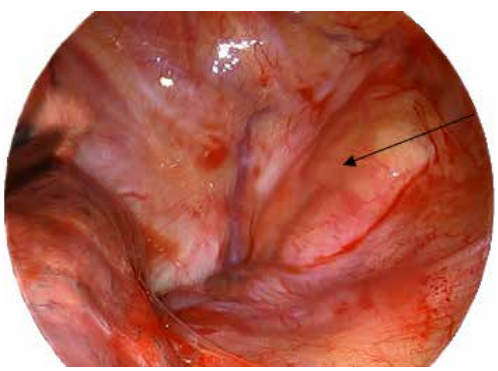

Figure 2 Photo taken during video assisted thoracotomy of the aberrant right subclavian artery (black arrow) is shown in the right paratracheal fossa.

artery originating from the proximal descending aorta (4). *Arteria lusoria* is commonly associated with a right sided nonrecurrent laryngeal nerve, where during embryonic development, the vessel fails to drag the right recurrent laryngeal nerve caudally when the heart descends and the neck elongates (5).

The vast majority of documented cases of *arteria lusoria* are clinically silent, due to the fact that the aberrant artery does not form a complete vascular ring around the oesophagus and trachea and is most often discovered by chance. Associated anomalies include a higher incidence of *truncus bicaroticus* (the presence of a common carotid trunk), aortic coarctation and a replaced right or left vertebral artery. More rarely, an aberrant left subclavian artery may also arise from a right aortic arch. *Arteria lusoria* is also associated with cardiac anomalies in 91% of patients as well as Downs', Edwards' and DiGeorge (6).

There are three possible situations in which the condition can become symptomatic in adults. These all result in compression upon the oesophagus, resulting *in dysphagia lusoria*:

- The presence of a truncus bicaroticus;
- Aberrant subclavian aneurysm;
- Atherosclerotic hardening/fibromuscular dysplasia of arteries with increasing age.

Other symptoms include breathlessness, chronic coughing and dyspnoea from compression of the trachea. This is less likely to occur because of tracheal rigidity compared with the oesophagus. A much rarer but life threatening condition is due to aneurysmal dilatation of the artery, causing right arm ischemia from embolization, oesophageal fistula formation, superior vena cava syndrome and haemorrhagic shock from rupture.

With a documented 100% diagnostic sensitivity on 64 multislice computed tomography and 97.6% on Doppler sonography, clinicians should be aware of *arteria lusoria* as it may have adverse effects on surgery in multiple disciplines (7). The presence of ARSA along with the absence of the right recurrent laryngeal nerve on the lower pole of the thyroid may cause injury to the nerve if it is not found in the aberrant area. Only 60% of transradial coronary procedures are successful in the presence of an arteria lusoria. Furthermore the possibility of fistulous connection between the oesophagus and trachea means that an abberant right subclavian artery is an added potential risk factor for haemorrhage in the presence of prolonged nasogastric, endotracheal intubation or tracheotomy as well

as transhiatal oesophagectomy for cancer (8).

In this case report, we suggest that it is important to consider arteria lusoria as a potential risk factor for operation morbidity during systematic nodal dissection for non-small cell lung cancers. The pulmonary artery vasculture lies inferior to the aortic arch and anterior to the descending aorta, making it one of the closest structures in proximity to a potential ARSA. Uniportal video-assisted thoracoscopic surgery (VATS) for lobectomy is a comparatively new procedure with greater difficulty than a traditional thoracotomy approach, since the surgeon's tactile input is compromised and the procedure relies on a thorough understanding of pulmonary anatomy in order for individual ligation and division of the pulmonary artery, pulmonary vein and bronchus where they enter the lung. Furthermore, the additional requirement of aggressive removal of mediastinal lymph nodes in non-small cell lung cancer means that there may be an increased possibility of unforeseen problems leading to possible conversion to thoracotomy and increase operation morbidity if the surgeon is unaware of this aortic vascular anomaly. The current International Association for the Study of Lung Cancer (IASLC) guidelines recommend undertaking at least three mediastinal stations. The aberrant right subclavian artery lies directly in the posterior bed of the para-tracheal fossa, which could lead to catastrophic injury in the unaware.

Conclusions/learning points

- ❖ *Arteria lusoria*/ARSA is the most common embryologic abnormality of the aortic arch.
- ❖ Although commonly asymptomatic, it can lead to dysphagia (*dysphagia lusoria)*, respiratory symptoms as well as more severe symptoms such as right arm ischaemic and haemorrhagic shock from aneurysmal rupture.
- ❖ Diagnostic sensitivity of ARSA is 100% on 64 multisplice computed tomography, allowing surgeons to be aware of this condition as it may complicate surgery to the mediastinum.
- ❖ ARSA should be taken into consideration as a possible risk factor for increased complications in VATS lobectomies.

Cite this article as: Pan D, Cufari ME, Lim E. Beware of arteria lusoria during lymph node dissection of the right paratracheal fossa for lung cancer surgery. J Thorac Dis 2014;6(12):E264-E266. doi: 10.3978/j.issn.2072-1439.2014.11.12

Acknowledgements

Disclosure: The authors declare no conflict of interest.

References

1. Polguj M, Chrzanowski Ł, Kasprzak JD, et al. The aberrant right subclavian artery (arteria lusoria): the morphological and clinical aspects of one of the most important variations--a systematic study of 141 reports. ScientificWorldJournal 2014;2014:292734.Polguj M, Chrzanowski Ł, Kasprzak JD, et al. The aberrant right subclavian artery (Arteria Lusoria)–the morphological and clinical aspects of the one of the most important variations: a systematic study of 141 reports.
2. Arteria lusoria: Developmental anatomy, clinical, radiological and surgical aspects. Annales de cardiologie et d'angeiologie: Elsevier, 2010.
3. Kommerell B. Verlagerung des Ösophagus durch eine abnorm verlaufende Arteria subclavia dextra (Arteria lusoria). Fortschr Geb Roentgenstrahlen 1936;54:590-5.
4. Kopp R, Wizgall I, Kreuzer E, et al. Surgical and endovascular treatment of symptomatic aberrant right subclavian artery (arteria lusoria). Vascular 2007;15:84-91.
5. Schneider J, Baier R, Dinges C, et al. Retroesophageal right subclavian artery (lusoria) as origin of traumatic aortic rupture. Eur J Cardiothorac Surg 2007;32:385-7.
6. Singh S, Grewal PD, Symons J, et al. Adult-onset dysphagia lusoria secondary to a dissecting aberrant right subclavian artery associated with type B acute aortic dissection. Can J Cardiol 2008;24:63-5.
7. Sun Z, Lin C, Davidson R, et al. Diagnostic value of 64-slice CT angiography in coronary artery disease: a systematic review. Eur J Radiol 2008;67:78-84.
8. Pop D, Venissac N, Nadeemy AS, et al. Lesson to be learned: beware of lusoria artery during transhiatal esophagectomy. Ann Thorac Surg 2012;94:1010-1.

Case Report

Fatal interstitial lung disease associated with icotinib

Jiexia Zhang*, Yangqing Zhan*, Ming Ouyang, Yinyin Qin, Chengzhi Zhou, Rongchang Chen

Department of Respiratory Medicine, The First Affiliated Hospital of Guangzhou Medical University, State Key Laboratory of Respiratory Disease (Guangzhou Medical University, China), Guangzhou Institute of Respiratory disease, Guangzhou 510120, China

*These authors contributed equally to this work.

Correspondence to: Rongchang Chen, MD, Professor, FCCP. No.151 Yanjiang Road, Guangzhou Ct, 510120 China. Email: chenrc@vip.163.com.

Abstract: The most serious, and maybe fatal, yet rare, adverse reaction of gefitinib and erlotinib is drug-associated interstitial lung disease (ILD), which has been often described. However, it has been less well described for icotinib, a similar orally small-molecule tyrosine kinase inhibitor (TKI). The case of a 25-year-old female patient with stage IV lung adenocarcinoma who developed fatal ILD is reported here. She denied chemotherapy, and received palliative treatment with icotinib (125 mg po, three times daily) on March 1, 2013. One month after treatment initiation, the patient complained of continuous dry cough and rapid progressive dyspnea. Forty one days after icotinib treatment, icotinib associated ILD was suspected when the patient became increasingly dyspnoeic despite of treatment of pericardial effusion, left pleural effusion and lower respiratory tract infection, and X-ray computed tomography (CT) of chest revealed multiple effusion shadows and ground-glass opacities in bilateral lungs. Then, icotinib was discontinued and intravenous corticosteroid was started (methylprednisolone 40 mg once daily, about 1 mg per kilogram) respectively. Forty three days after icotinib treatment, the patient died of hypoxic respiratory failure. ILD should be considered as a rare, but often fatal side effect associated with icotinib treatment.

Keywords: Icotinib; interstitial lung disease (ILD); lung cancer; pulmonary toxicity; epidermal growth factor receptor (EGFR); tyrosine kinase inhibitor (TKI)

Submitted Aug 18, 2014. Accepted for publication Sep 24, 2014.
doi: 10.3978/j.issn.2072-1439.2014.10.24
View this article at: http://dx.doi.org/10.3978/j.issn.2072-1439.2014.10.24

Introduction

In June 2011, icotinib (Conmana®, Zhejiang Beta pharmaceutical Co., Ltd., Hangzhou, China), a new Chinese made, orally active, small-molecule tyrosine kinase inhibitor (TKI) targeting the epidermal growth factor receptor (EGFR), was approved by China Food and Drug Administration (CFDA) and added to the treatment of non small cell lung cancer (NSCLC) in China. Similar to gefitinib and erlotinib, icotinib is an effective drug in recommended dose (125 mg, 3 times daily). However, its recommended dose is far from its tolerated dose. It shows potential superiority to erlotinib in a case report, in which a patient with lung adenocarcinoma after erlotinib failure responded to high dose icotinib (1). Additionally, it is a relatively safer drug compared with erlotinib (2). The most common adverse effects associated with icotinib are rash and diarrhea (3-8). The most serious, and maybe fatal, yet rare, adverse reaction of gefitinib and erlotinib is drug-associated interstitial lung disease (ILD), which has been often described (9-11). However, it has only been few documented in the clinical trials of icotinib. We present a fatal case of icotinib-associated ILD in a patient with lung adenocarcinoma and discuss it in the context of icotinib-associated ILD.

Case report

A 25-year-old female Chinese was diagnosed with stage IV lung adenocarcinoma with lymphangitis carcinomatosa and hydropericardium. Icotinib treatment was initiated once diagnosis of lung adenocarcinoma was made. Forty three days later, the patient died of hypoxic respiratory failure. Written consent was obtained from the patient's parents for publication of this case report and any accompanying images.

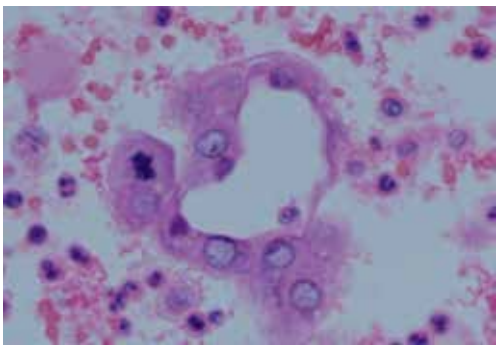

Figure 1 Pathological images of pericardial fluid sediment, showing heterogenic gland (Hematoxylin-eosin, original ×400).

The patient was healthy before the onset of illness. She had no history of smoking. She was admitted to other hospital for a complaint of dry cough and dyspnea. X-ray computed tomography (CT) of chest revealed multiple thickened bronchial wall and bronchiarctia in segment bronchus of left lung, mass shadows in apicoposterior segment and left posterior basal segment and diffuse nodular shadows in both lungs, with evidence for enlarged mediastinal, bilateral hilar and axillary lymph nodes (images were discarded by her parents after the patient was dead and were not available). There was irregular thickening of interlobular septal in bilateral lungs too. Diagnosis of stage IV lung adenocarcinoma with lymphangitis carcinomatosa was made when tranbronchial lung biopsy revealed adenocarcinoma. EGFR mutation in biopsy of lung tissue was tested negative by sequencing polymerase chain reaction. However, she had a poor World Health Organization (WHO) performance status (score 3). Chemotherapy was not reasonable and palliative treatment with icotinib (125 mg po, 3 times daily) was initiated. Ten days after treatment initiation, the patient developed a rash, a common adverse reaction of icotinib. Follow-up radiographs in our hospital 3 weeks after treatment initiation showed stable disease (SD) with no enlargement in the size of mass shadows and no increase in the number of nodular shadows.

One month after icotinib treatment, while still on icotinib therapy, the patient was admitted to our hospital with continuous dry cough and rapid progressive dyspnea, denying lying down. Chest pain and haemoptysis was denied. Physical examination revealed decreased breath sounds in left lower lobe, some inspiratory crackles in right lower lobe and distant heart sounds. Oxygen saturation was 85% in room air and supplemental oxygen was given via nasal cannula. Leukocyte count was elevated with 15.92×10^9 cells/L. Blood cultures and sputum analysis initially was tested negative. Precursor of B-type natriuretic peptide was normal. Arterial blood gas analysis indicated presence of hypoxemic respiratory failure. Hence, pericardial effusion, left pleural effusion and lower respiratory tract infection was suspected. Ultrasound revealed massive pericardial effusion and left pleural effusion. Percutaneous pericardial drainage and chest catheter closed drainage was conducted. Pathological examination of pericardial fluid sediment revealed metastatic adenocarcinoma from lung (*Figure 1*). Intracavitary chemotherapy with etoposide (0.3 g) and cisplatin (100 mg) was administrated in the treatment of pericardial effusions. Antimicrobial therapy was pragmatically initiated with intravenous levofloxacin (500 mg once daily). Other medications included furosemide 20 mg, asmeton 2 tablets and selenious yeast tablets 100 μg (3 times daily).

However, clinical symptoms (including cough, dyspnea) and oxygen saturation was only partially improved and accompanied by fever 5 days after hospital admission. D-dimers were elevated with 5,467 ng/mL. Leukocyte count recovered to normal with 8.53×10^9 cells/L and procalcitonin was elevated with 0.81 ng/mL 1 week after admission. Multi-layer spiral CT angiography of pulmonary artery confirmed suspection of pulmonary artery embolism (*Figure 2A*). Multiple effusion shadows and ground-glass opacities were also found in bilateral lungs (*Figure 2B*). Hence, nadroparin (3,075 anti-Xa units twice daily) was initiated and warfarin was added later. Antibiotic was empirically changed to piperacillin-sulbactam (2,000/1,000 mg three times daily), and changed to meropenem (500 mg 3 times daily) together with intravenous voriconazole (200 mg twice daily) later.

Forty days after icotinib treatment, ILD was suspected when the patient still became increasingly dyspnoeic, despite of treatment of pericardial effusion, left pleural effusion and lower respiratory tract infection. The onset of continuous cough and dyspnea and characteristic newly emerged diffuse ground-glass opacities in bilateral lobe both supported the diagnosis of ILD (*Figure 2B,C*). The case scored 5 by using the Naranjo scale (12). Hence, it is probable that ILD was associated to icotinib. Icotinib was discontinued and intravenous corticosteroid was started (methylprednisolone 40 mg once daily, about 1 mg per kilogram) respectively. The condition of patient went worse even under the above medication. Forty-three days later, the patient died of hypoxic respiratory failure. Autopsy was not performed due to lack of permission from her parents.

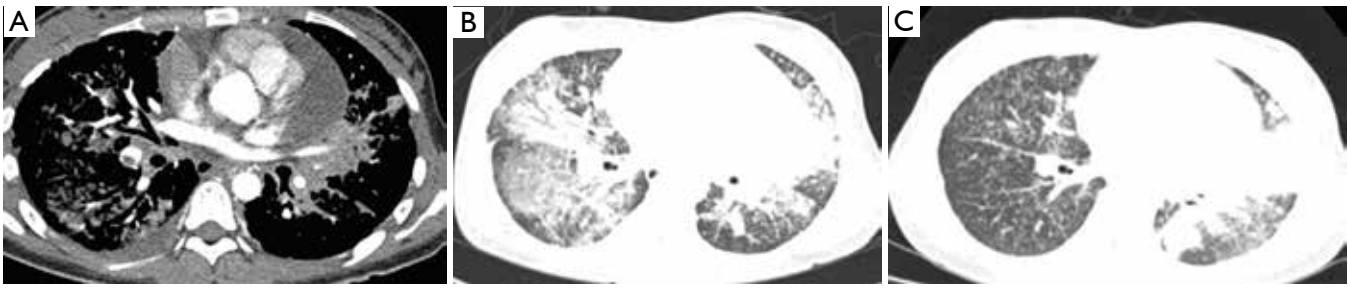

Figure 2 Newly emerged diffuse ground-glass opacities in bilateral lungs and pulmonary embolism after the onset of continuous cough and dyspnea. (A) Image of CT angiography of pulmonary artery 5 weeks after initiation of icotinib, showing pulmonary embolism in basal stem right lower lobe pulmonary artery. CT, computed tomography; (B) CT image of chest five weeks after initiation of icotinib, showing newly emerged diffuse ground-grass opacities in bilateral lungs; (C) CT image of chest three weeks after initiation of icotinib, showing mass shadow and obstructive pneumonia in left lower lobe, diffuse nodular shadows and irregular thickening of interlobular septal in bilateral lungs.

Table 1 Summary of ILD characteristics in clinical trails

Case number	Sex	Age	Stage	Dose	Onset of ILD	ILD symptoms	CT findings	Disease progression	Treatment	ILD outcome (time after onset)	Reference
1	NR	NR	NR, NSCLC	150 mg bid	9 days	Dyspnea	Pneumonitis	Yes	ID	Fatal [31]	(2)
2	NR	NR	NR, NSCLC	200 mg bid	7 days	Dyspnea	NR	Yes	ID, CS	Fatal [30]	(2)
3	Male	49	IV, Lung Adenocarcinoma	125 mg tid	4 months	Deteriorated cough, dyspnea	Ground-grass opacities and interstitial fibrosis in bilateral lungs	NR	ID, CS	Cure	(6)

ILD, interstitial lung disease; NR, not reported; ID, icotinib discontinuation; CS, corticosteroids.

A PubMed and Google Scholar search was conducted using the keywords "pulmonary toxicity", "ILD", "icotinib" and "conmana®". Similar Search was also conducted in a Chinese data-Wangfang Data. Relevant case reports and case-series were included and references of retrieved publications were screened for relevant literature. Until now, except for our case, a total of three cases of icotinib-associated ILD were reported in the clinical trial (*Table 1*). Two cases of ILD occurred within one month of icotinib treatment. Pathological examination showed that two cases of icotinib-associated ILD in phase I study of icotinib were accompanied with disease progression (4). One was considered disease-related and the other was considered both drug-related and disease-related. The third case appeared in phase IV study and diagnose of ILD was made based on ground-grass opacities and pulmonary fibrosis in CT scan, without evidence of biopsy (8). Other initial studies of icotinib leading to its approval and retrospective studies did not report pulmonary toxicity (3,6,7,13-15). There was no case report.

Discussion

The present case showed that icotinib may be associated with fatal ILD. To our knowledge, this is the first case report of fatal ILD associated with icotinib. Similar to other orally small molecule EGFR-TKIs, such as gefitinib and erlotinib, icotinib can cause or contribute significantly to the pulmonary toxicity, and thus this drug also must be considered among the EGFR-TKIs drugs which can cause fatal ILD. Respiratory symptoms should be carefully monitored for the first month period of icotinib treatment.

Severe ILD, including fatalities had been reported in clinical studies and case series with other EGFR-TKIs (16-18). For gefitinib-treated patients, FDA reported that incidence of ILD was 1% worldwide, of which more than

30% were fatal (10). The incidence of ILD varied with countries. It was higher in Japan (2%) than in the United States (0.3%) (19). In the FDA approval report, overall incidence of ILD in erlotinib-treated patients was about 0.8%, which was similar to patients in the placebo group (11). Overall incidence of ILD in icotinib treated patients was still unknown. However, results of another phase IV study in which more than 10,000 patients were enrolled are round the corner.

Thus far, no risk factors for the development of icotinib-associated ILD have been described. However, several risk factors were considered to be related to gefitinib-associated ILD, including older age, poor World Health Organization (WHO) performance status (≥2), smoking, recent NSCLC diagnosis, reduced normal lung on CT scan, preexisting chronic ILD, concurrent cardiac disease and Japanese ethnicity (20). The higher incidence of ILD in Japanese patients was considered to be contributed to the larger percentage of patients with EGFR mutations and clinical responses to gefitinib (21). Other studies have suggested recent radiation therapy and chemotherapy as risk factors for ILD (22). Most of ILD occur within 3-7 weeks after initiation of gefitinib and one third of cases are fatal. Risk factors of erlotinib-associated ILD were similar to gefitinib, with a median of 47 days after initiation therapy (11,17,23). Several of these risk factors were present in our case, including recent NSCLC diagnosis (1 month), poor WHO performance status, reduced normal lung on CT scan (diffuse nodular shadows in bilateral lungs, left pleural effusion, multiple pulmonary artery embolisms) and concurrent cardiac disease (massive pericardial effusion). Including our cases, disease progression was confirmed by pathological examination in three out of four cases of icotinib-associated ILD and it maybe consider as one of the risk factors of icotinib-associated ILD. Overall, three out of four cases of ILD occurred within one month of initiation of icotinib. Two cases of ILD reported in clinical trials of icotinib were treated with chemotherapy before initiation of icotinib. Whether risk factors of icotinib-associated ILD have its uniqueness or are similar to gefitinib and erlotinib, it remains to be investigated.

However, the mechanism for developing icotinib-associated ILD is still unknown. Phase I study of icotinib demonstrated that there was no obvious relationship between advert effects/severe advert effects and dose (3,4,24). Pharmocology and clinical evaluation revealed that the therapeutic window for icotinib-defined as the tolerable and effective dose range was 100-625 mg three times per day (24). Dose of icotinib in all of four cases of icotinib-associated ILD ranged 300-400 mg per day, which was lower than highest tolerable and effective dose. Hence, icotinib-associated ILD may seem unlikely to be dose dependent. Considering the similarities of EGFR-TKIs in chemical structure and pharmacological effects, it is likely that the mechanism for development of icotinib-associated ILD is comparable with gefitinib and erlotinib. However, whether icotinib can induce pulmonary toxicity by a mechanism related to its unique properties or similar to other EGFR-TKIs (gefitinib and erlotinib), it remains to be studied.

It is worth to note that, three out of four cases of icotinib-associated ILD were fatal. Fatality of ILD induced by icotinib was higher than that of gefitinib and erlotinib, although all three fatal cases were accompanied by disease progression. In view of poor information concerning risk factors and mechanism of icotinib-associated ILD, prevention and treatment of icotinib-associated ILD should borrow from gefitinib and erlotinib associated ILD. Medical history, including respiratory symptoms, signs, chemotherapy or radiation, etc., should be well reviewed prior to the prescription of medication. Icotinib-associated ILD should be highly suspected once respiratory symptoms (especially dry cough and dyspnea) worsen. Discontinuation of medication, initiation of high dose corticosteroids and supportive therapy with oxygen therapy or mechanical ventilation was reported in case series as the only useful interventions in the treatment of gefitinib and erlotinib associated ILD (9,25,26).

Limitation of our report was that cytomegalovirus CMV infection and pneumocystis jiroveci pneumonia could not be ruled out. Serological test for CMV infection was not performed. Because the condition of the patient was going bad rapidly, bronchoscopy could not be performed and sputum from deep position or bronchoalveolar lavage was not available for bacterial and fungal culture or detection of CMV and *pneumocystis jiroveci*. Additionally, biopsy of lung also could not be done to confirm pathology of ILD.

Acknowledgements

The authors thank Jin Zhao, Pathological Department of the First Affiliated Hospital of Guangzhou Medical University, Guangzhou Institute of Respiratory Medicine, the State Key Laboratory of Respiratory Disease (Guangzhou Medical College) for supply of pathological images.

Authors Z.YQ and Z. JX participated in the PubMed and Google Scholar search for cases of icotinib associated ILD.

All authors participated in the discussion of the data and contributed to the drafting of the manuscript.
Disclosure: The authors declare no conflict of interest.

References

1. Guan Y, Zhao H, Meng J, et al. Dramatic response to high-dose icotinib in a lung adenocarcinoma patient after erlotinib failure. Lung Cancer 2014;83:305-7.
2. Liang W, Wu X, Fang W, et al. Network meta-analysis of erlotinib, gefitinib, afatinib and icotinib in patients with advanced non-small-cell lung cancer harboring EGFR mutations. PLoS One 2014;9:e85245.
3. Zhao Q, Shentu J, Xu N, et al. Phase I study of icotinib hydrochloride (BPI-2009H), an oral EGFR tyrosine kinase inhibitor, in patients with advanced NSCLC and other solid tumors. Lung Cancer 2011;73:195-202.
4. Wang HP, Zhang L, Wang YX, et al. Phase I trial of icotinib, a novel epidermal growth factor receptor tyrosine kinase inhibitor, in Chinese patients with non-small cell lung cancer. Chin Med J (Engl) 2011;124:1933.
5. Zhao Q, Zhou J, Shentu J, et al. A phase I/IIa study of icotinib hydrochloride, a novel oral EGFR-TKI, to evaluate its safety, tolerance, and preliminary efficacy in advanced NSCLC patients in China. J Clin Oncol 2010;28:abstract 7574.
6. Lv C, Ma Y, Feng Q, et al. A pilot study: sequential gemcitabine/cisplatin and icotinib as induction therapy for stage IIB to IIIA non-small-cell lung adenocarcinoma. World J Surg Oncol 2013;11:96.
7. Shi Y, Zhang L, Liu X, et al. Icotinib versus gefitinib in previously treated advanced non-small-cell lung cancer (ICOGEN): a randomised, double-blind phase 3 non-inferiority trial. Lancet Oncol 2013;14:953-61.
8. Tan FL, Wang YX, Ding LM, et al. Safety and Efficacy of Icotinib Hydrochloride for Non-small Cell Lung Cancer (NSCLC) Patient in A Large Population. Chinese Journal of Drug Evaluation 2012;29:30-4.
9. Barber NA, Ganti AK. Pulmonary toxicities from targeted therapies: a review. Target Oncol 2011;6:235-43.
10. Cohen MH, Williams GA, Sridhara R, et al. FDA drug approval summary: gefitinib (ZD1839) (Iressa) tablets. Oncologist 2003;8:303-6.
11. Cohen MH, Johnson JR, Chen YF, et al. FDA drug approval summary: erlotinib (Tarceva) tablets. Oncologist 2005;10:461-6.
12. Naranjo CA, Busto U, Sellers EM, et al. A method for estimating the probability of adverse drug reactions. Clin Pharmacol Ther 1981;30:239-45.
13. Gu A, Shi C, Xiong L, et al. Efficacy and safety evaluation of icotinib in patients with advanced non-small cell lung cancer. Chin J Cancer Res 2013;25:90-4.
14. Nong J, Qin N, Wang J, et al. Clinical effects for patients with recurrent advanced non-small cell lung cancer treated with icotinib hydrochloride. Zhongguo Fei Ai Za Zhi 2013;16:240-5.
15. Li X, Yang XJ, Sun YF, et al. Clinical observation of icotinib hydrochloride for patients with advanced non-small cell lung cancer. Zhonghua Zhong Liu Za Zhi 2012;34:627-31.
16. Jackman DM, Yeap BY, Lindeman NI, et al. Phase II clinical trial of chemotherapy-naive patients > or = 70 years of age treated with erlotinib for advanced non-small-cell lung cancer. J Clin Oncol 2007;25:760-6.
17. Makris D, Scherpereel A, Copin MC, et al. Fatal interstitial lung disease associated with oral erlotinib therapy for lung cancer. BMC Cancer 2007;7:150.
18. Peerzada MM, Spiro TP, Daw HA. Pulmonary toxicities of tyrosine kinase inhibitors. Clin Adv Hematol Oncol 2011;9:824-36.
19. Camus P, Kudoh S, Ebina M. Interstitial lung disease associated with drug therapy. Br J Cancer 2004;91:S18-23.
20. Kudoh S, Kato H, Nishiwaki Y, et al. Interstitial lung disease in Japanese patients with lung cancer: a cohort and nested case-control study. Am J Respir Crit Care Med 2008;177:1348-57.
21. Paez JG, Jänne PA, Lee JC, et al. EGFR mutations in lung cancer: correlation with clinical response to gefitinib therapy. Science 2004;304:1497-500.
22. Inoue A, Saijo Y, Maemondo M, et al. Severe acute interstitial pneumonia and gefitinib. Lancet 2003;361:137-9.
23. Liu V, White DA, Zakowski MF, et al. Pulmonary toxicity associated with erlotinib. Chest 2007;132:1042-4.
24. Tan F, Zhang L, Zhao Q. Pharmocology and clinical evaluation of icotinib hydrochloride. Chin J New Drugs 2009;18:1-4.
25. Kuo LC, Lin PC, Wang KF, et al. Successful treatment of gefitinib-induced acute interstitial pneumonitis with high-dose corticosteroid: a case report and literature review. Med Oncol 2011;28:79-82.
26. ter Heine R, van den Bosch RT, Schaefer-Prokop CM, et al. Fatal interstitial lung disease associated with high erlotinib and metabolite levels. A case report and a review of the literature. Lung Cancer 2012;75:391-7.

Cite this article as: Zhang J, Zhan Y, Ouyang M, Qin Y, Zhou C, Chen R. Fatal interstitial lung disease associated with icotinib. J Thorac Dis 2014;6(12):E267-E271. doi: 10.3978/j.issn.2072-1439.2014.10.24

Case Report

Primary malignant pericardial mesothelioma—a rare cause of superior vena cava thrombosis and constrictive pericarditis

Wenhui Gong[1,2], Xiaofeng Ye[1], Kaihu Shi[2], Qiang Zhao[1]

[1]Department of Cardiac Surgery, Ruijin Hospital of Shanghai Jiaotong University School of Medicine, Shanghai 200025, China; [2]Department of Cardio-thoracic Surgery, the Second Affiliated Hospital of Anhui Medical University, Hefei 230601, China

Correspondence to: Qiang Zhao. Department of Cardiac Surgery, Ruijin Hospital of Shanghai Jiaotong University School of Medicine, Shanghai 200025, China. Email: zq11607@rjh.com.cn.

Abstract: Primary malignant pericardial mesothelioma (PMPM) is an extremely rare, highly lethal and often misdiagnosed tumor. We report a 60-year-old woman complaining of dry cough, shortness of breath and exertional dyspnea due to a large pericardial effusion. The pericardial fluid volume declined after pericardiocentesis; analysis of the fluid revealed malignant cells and was negative for tuberculosis. Subsequently, the patient developed a compression of the superior vena cava and pericardial constriction. The patient's symptoms marginally improved after partial pericardiectomy, and a diagnosis of pericardial mesothelioma was made on pathology. However, her symptoms continued to aggravate, and she died 8 months after presentation. Pericardial mesothelioma should be discovered earlier to treat patients who develop repeatedly pericardial effusion after pericardiocentesis and pericardial tamponade or those develop constrictive pericarditis.

Keywords: Pericardial mesothelioma; constrictive pericarditis; superior vena cava thrombosis

Submitted Jun 05, 2014. Accepted for publication Sep 23, 2014.
doi: 10.3978/j.issn.2072-1439.2014.11.36
View this article at: http://dx.doi.org/10.3978/j.issn.2072-1439.2014.11.36

Introduction

Primary malignant pericardial mesothelioma (PMPM) morbidity is rare, with high lethality. The treatment options of the tumor are limited, and the prognosis is poor.

Case report

A 60-year-old woman who was admitted to our hospital in April 2009 complained of repeatedly dry cough and shortness of breath. Transthoracic echocardiography demonstrated profuse pleural effusion and pericardial effusion. The symptoms were markedly relieved by 2 times of pericardiocentesis and 3 times of thoracentesis. Cytological analysis of the clear fluid showed no malignant cells, except for a small increase in eosinophilic cells, and PCR for tuberculosis was negative. The woman had no apparent history of occupational or incidental exposure to asbestos or history of smoking or tuberculosis. The patient was then examined by an F-18 fluorodeoxyglucose positron emission tomography/computed tomography (FDG- PET/CT) scan in another hospital, showing a recurrent large pericardial effusion and pleural effusion with a thickened pericardium (*Figure 1A*). In July 2009, the patient was re-admitted to our hospital, and transthoracic echocardiography on July 22 demonstrated copious pericardial effusion with a thickened pericardium (*Figure 1B*). The patient was misdiagnosed for tuberculosis clinically, but an experimental anti-TB treatment was ineffective. On August 14, transthoracic echocardiography and inferior vena cava ultrasound showed thrombosis of the proximal end of the right internal jugular vein and left subclavian vein (*Figure 1C*). On August 15, a chest CT scan demonstrated that she suffered from pericardial tumors (suspected malignant), bilateral pleural effusion, lung inflammation, and breast swelling (*Figure 1D*).

Digital subtraction angiography (DSA) was performed to insert a thrombosis filter in the superior vena cava but

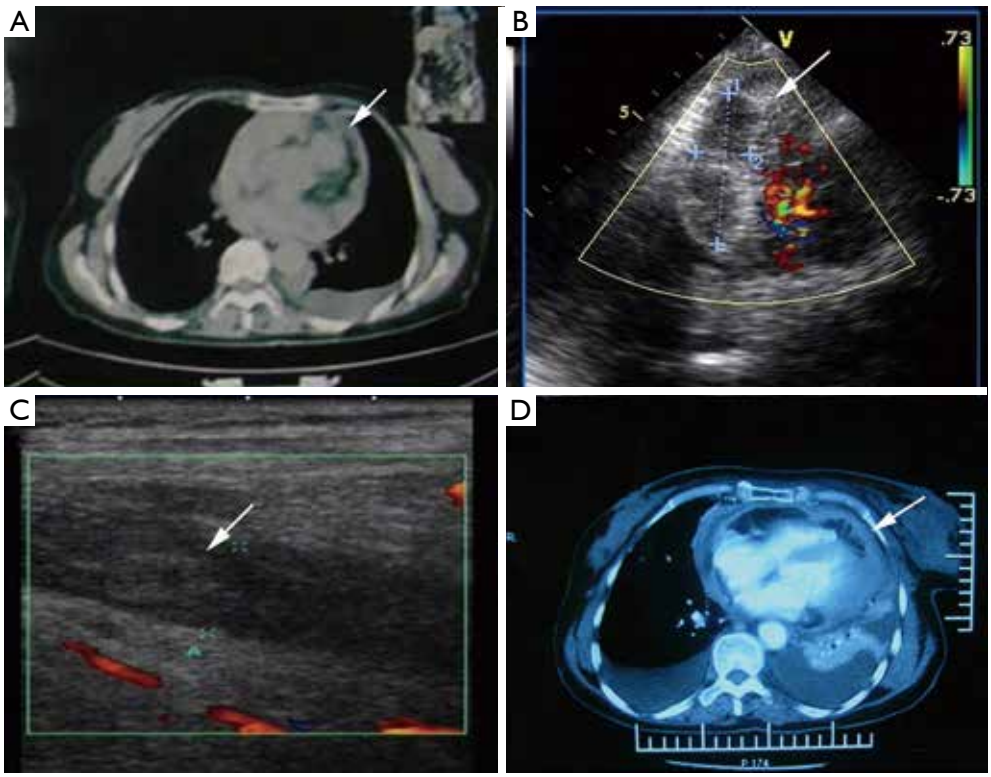

Figure 1 (A) F-18 fluorodeoxyglucose positron emission tomography/computed tomography (FDG-PET/CT) scan in June demonstrating an intrapericardial accumulation of the tracer; (B) transthoracic echocardiography demonstrating a large pericardial effusion and a thickened pericardium; (C) two-dimensional ultrasound of the inferior vena cava showing thrombosis in the right internal jugular vein; (D) CT-scan in August demonstrating pericardial tumors and bilateral pleural effusion.

failed. On the same day, the patient underwent a partial pericardiectomy, revealing a tumor 11 cm × 9 cm × 2 cm in size. However, a complete resection could not be performed due to tumor adherence to the right ventricular, right atrium and superior vena cava, and part of the inferior vena cava. Histological examination revealed diffuse infiltration of the pericardium by epithelial cells (*Figure 2A*). An evaluation of immunohistochemical markers showed a strongly positive reaction to epithelial membrane antigen (EMA) (*Figure 2B*), vimentin (*Figure 2C*) and cytokeratin (CK) (*Figure 2D*).

Some of the patients' symptoms, i.e., dyspnea and chest congestion, had been relieved after surgical resection of the mesothelioma because the compression of the tumor was reduced to a certain extent. Subsequently, two cycles of chemotherapy with cisplatin and etoposide (dosage according to recently published trials) were administered during four months (1-4), but little remission was achieved. The patient remained symptomatic and unfortunately died in December 2009 because of multiorgan dysfunction syndrome.

Discussion

Malignant mesothelioma is a malignant tumor derived from mesenchymal tissue, usually occurring in the peritoneum or pleura and rarely occurring in the pericardium. The incidence of PMPM was found to be below 0.0022% in a large autopsy study (1). Malignant pericardial mesothelioma is characterized by unrepresentative solid growth of the mesothelium, with a structure of atypical cavities environed by fibrous stroma (2).

Although PMPM is infrequent, it is the third most common tumor around the heart/pericardium, after angiosarcoma (33%) and rhabdomyosarcoma (20%) (3). A review of 29 cases presented in the recent literature indicates a higher incidence of malignant pericardial mesothelioma among men than women, with a male-female ratio of 3:1.

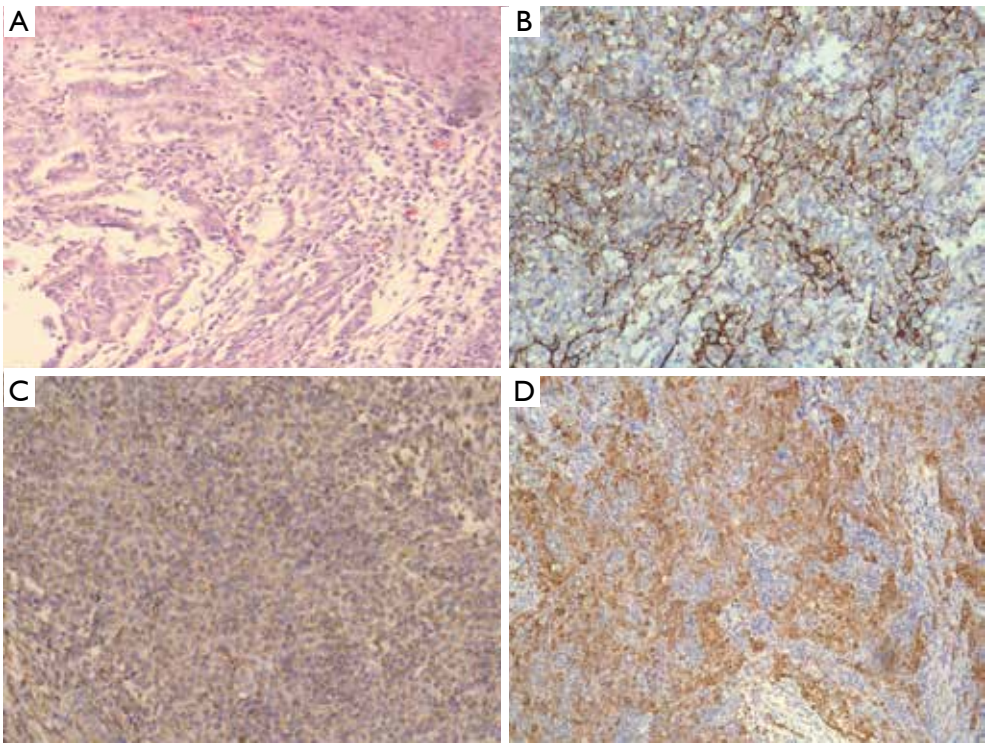

Figure 2 Tumor histology, hematoxylin-eosin staining (A) and immunohistochemical staining (B-D) (100×). (A) Diffuse infiltration of the pericardium by epithelioid cells (×100); (B) EMA (+); (C) vimentin (+); (D) CK(+). EMA, epithelial membrane antigen. CK, cytokeratin.

PMPM occurs more commonly in the elderly, and the median age is 46 (range, 19-76). No obvious relationship between asbestos exposure and the development of pericardial mesothelioma has been established (4).

PMPM is often misdiagnosed after a patient's first clinical signs because of its asymptomatic symptoms in the early course. The symptoms of PMPM usually range from dyspnea, cough and dysphagia to chest pain (5) and even superior vena cava thrombosis, as in this case. The clinical misdiagnosis rate is extremely high because the symptoms of PMPM are atypical and often confused with conditions such as tuberculous pericarditis, coronary heart disease, atrial myxoma, heart failure, and cardiomyopathy. In this case, the patient was tentatively treated with an antituberculotic due to misdiagnosis by low-grade fever and thickened pericardium.

Single or partial pericardial mesothelioma is rare, and a precise diagnosis is made prior to the patient's death in only 10-20% of all cases (6). Indeed, the challenging diagnosis of pericardial diseases often requires a combination of multimodal imaging methods including echocardiography, CT, magnetic resonance imaging and FDG-PET scans (7). Cytologic examination of pericardial fluid is seldom conclusive (malignant cells demonstrated in 4/17 cases) (4). Although clinical data and imaging are very helpful for the diagnosis of pericardial mesothelioma, a definite diagnosis still relies on pericardial biopsy or pathology (8). Immunohistochemical studies could provide a diagnosis of mesothelioma and rule out the diagnosis of other tumors, and we used the same diagnosing methods as previously used (4,6,9). The patient was finally diagnosed with PMPM because there was no evidence of primary cancer origin in other organs.

At present, the optimal therapeutic tool is surgical resection in the early clinical course combined with radiotherapy and chemotherapy (9). Partial resection of the tumor in this case merely resulted in a short period of partial symptom reduction. The newer medical treatments, i.e., genetic testing therapies, cytokines therapies, and neoadjuvant chemotherapy, are popular therapies for most mesotheliomas (8-11). In malignant pleural mesothelioma (PMP), researchers found that low EMX2 expression was a negative prognostic factor for mesothelioma, which may serve as an important prognostic and predictive molecular

biomarker of a progression-free survival (10). Komiya *et al.* indicated that CD26-expressing MPM cells upregulate the production of periostin, which enhances the migration and invasion of MPM cells (11). However, these approaches have not yet been applied for pericardial mesothelioma, perhaps due to the low incidence of PMPM and the relatively small number of cases.

The prognosis depends on tumor stage, pathology and genetics. Some 60% of patients die within 6 months after diagnosis due to complications that include heart failure or pericardial constriction, sudden invasion of the tumor into coronary thrombosis and myocardial infarction (12). Prognosis of this disease is dismal, and the median survival of patients with pericardial mesothelioma is approximately 6 months (1,4,12).

Conclusions

Primary pericardial mesotheliomas are extremely rare tumors. PMPM should be considered and appropriately managed in repeated pericardial effusion or pericardial constriction, non-responders to pericardiocentesis and even superior vena cava thrombosis of unknown etiology. Our case report shows that treatment options are limited and that the prognosis is poor.

Acknowledgements

Disclosure: The authors declare no conflict of interest.

References

1. De Rosa AF, Cecchin GV, Kujaruk MR, et al. Malignant mesothelioma of the pericardium. Medicina (B Aires) 1994;54:49-52.
2. Butz T, Faber L, Langer C, et al. Primary malignant pericardial mesothelioma - a rare cause of pericardial effusion and consecutive constrictive pericarditis: a case report. J Med Case Rep 2009;3:9256.
3. Karadzic R, Kostic-Banovic L, Antovic A, et al. Primary pericardial mesothelioma presenting as constrictive pericarditis. Arch Oncol 2005;13:150-2.
4. Nilsson A, Rasmuson T. Primary Pericardial Mesothelioma: Report of a Patient and Literature Review. Case Rep Oncol 2009;2:125-32.
5. Reardon KA, Reardon MA, Moskaluk CA, et al. Primary pericardial malignant mesothelioma and response to radiation therapy. Rare Tumors 2010;2:e51.
6. Papi M, Genestreti G, Tassinari D, et al. Malignant pericardial mesothelioma. Report of two cases, review of the literature and differential diagnosis. Tumori 2005;91:276-9.
7. Langer C, Butz T, Horstkotte D. Multimodality in imaging calcific constrictive pericarditis. Heart 2006;92:1289.
8. Sardar MR, Kuntz C, Patel T, et al. Primary pericardial mesothelioma unique case and literature review. Tex Heart Inst J 2012;39:261-4.
9. Maruyama R, Sakai M, Nakamura T, et al. Triplet chemotherapy for malignant pericardial mesothelioma: a case report. Jpn J Clin Oncol 2006;36:245-8.
10. Giroux Leprieur E, Hirata T, Mo M, et al. The homeobox gene EMX2 is a prognostic and predictive marker in malignant pleural mesothelioma. Lung Cancer 2014;85:465-71.
11. Komiya E, Ohnuma K, Yamazaki H, et al. CD26-mediated regulation of periostin expression contributes to migration and invasion of malignant pleural mesothelioma cells. Biochem Biophys Res Commun 2014;447:609-15.
12. Luk A, Ahn E, Vaideeswar P, et al. Pericardial tumors. Semin Diagn Pathol 2008;25:47-53.

Cite this article as: Gong W, Ye X, Shi K, Zhao Q. Primary malignant pericardial mesothelioma—a rare cause of superior vena cava thrombosis and constrictive pericarditis. J Thorac Dis 2014;6(12):E272-E275. doi: 10.3978/j.issn.2072-1439.2014.11.36

Case Report

IgG4-related lung disease with atypical CT imaging: a case report

Jiaxuan Zhou*, Xian Li*, Qingsi Zeng

Department of Radiology, The First Affiliated Hospital of Guangzhou Medical University, Guangzhou 510120, China

*These authors contributed equally to this work.

Correspondence to: Qingsi Zeng. Department of Radiology, The First Affiliated Hospital of Guangzhou Medical University, Yanjiang Street, Guangzhou 510120, China. Email: 1531030894@qq.com.

Abstract: IgG4-related lung disease is a rare disease, diagnosed when typical pathologic features are seen in the context of increased serum levels of IgG4 and the elevated tissue's IgG4-positive plasma cells. Here we reported the case of a 24-year-old woman with IgG4-related lung disease. This patient presented with fever, cough and shortness of breath. Thoracic computed tomography (CT) images demonstrated multiple nodules or masses with high density in both lungs, and thickened interlobular septa. The 'halo sign' was observed around the high-density lesions of the upper lobes. This range of CT images' characteristics is atypical, which differs from previous reports of this condition.

Keywords: IgG4-related lung disease; atypical computed tomography (CT) features

Submitted Aug 12, 2014. Accepted for publication Oct 29, 2014.

doi: 10.3978/j.issn.2072-1439.2014.12.11

View this article at: http://dx.doi.org/10.3978/j.issn.2072-1439.2014.12.11

Introduction

IgG4-related disease is a systemic disease, and can involve multiple organs. It is characterized by increased serum level of IgG4, infiltration of IgG4-positive lymphocytes in multiple tissues, and tissue fibrosis (1). There are various organ-specific manifestations such as IgG4-related lung disease, autoimmune pancreatitis, sclerosing cholangitis, sclerosing salivary gland inflammation, inflammatory pseudotumor, interstitial nephritis and retroperitoneal fibrosis (2,3). The incidence of IgG4-related lung disease is 15-54% (4).

Okazaki *et al.* suggests the following diagnostic criteria of IgG4-related disease: single or multiple organs showing diffuse or limited swelling; an IgG4 level in serum >1.35 g/L; and significant lymphoplasmacytic infiltration on histological assessment (5). Fibrosis and obliterans could also be observed. To make the diagnosis, IgG4-positive plasma cells need to be present at >10 per high power field (HPF), or the ratio of IgG4-positive plasma cells to all IgG plasma cell subtypes needs to be >0.4. While the pathological features of this disorder can vary between patients, the main feature is lymphoplasmacytic infiltration or fibrosis. This in turn leads to a variety of radiological features.

Case report

A 24-year-old woman was hospitalized with recurring cough and fever over a 2 month period, along with shortness of breath for 2 weeks. Physical examination demonstrated no significant abnormalities. Laboratory examination revealed an elevated ESR (105 mm/h) and CRP (28.74 mg/L); the total count of white blood cell (WBC) was increased (11.47×10^9/L), but the ratio of neutrophilia (70.1%) was increased slightly (close to the normal proportion). Total IgG levels were increased (18.60 g/L), including serum IgG4. Tumour markers including CEA, CA-125, CA-153 and CA-199 were all normal. And autoimmune markers including anti-nuclear antibodies, rheumatoid factor and anti-neutrophil cytoplasmic antibodies were negative, too.

Computed tomography (CT) images demonstrated multiple nodules or masses in both lungs, principally located in the upper lobes (*Figure 1A*). These varied in size from 0.3 cm × 0.4 cm to 3 cm × 2.7 cm, and had homogeneous density with significant enhancement (33 Hounsfield units for the plain scan compared with 102 HU for the enhanced scan). Importantly, thickened interlobular septa were also observed in the upper lobes (*Figure 1B*).

Additional radiological features included the 'halo sign' evident around some high-density lesions (*Figure 1C*),

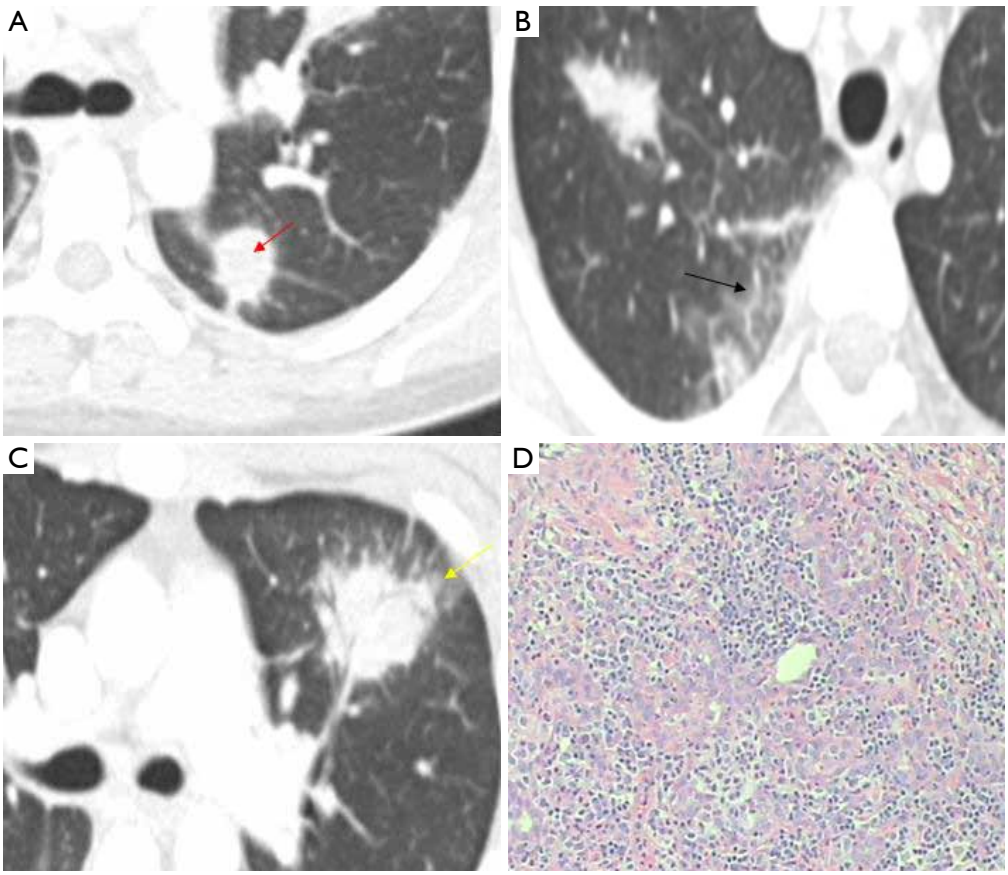

Figure 1 (A) Red arrow—nodule; (B) balck arrow—thickend interlobular septa; (C) yellow arrow—the halo sign around nodule; (D) pathologic picture (×40).

along with irregular edges, massive spiculation and the presence of the vessel convergence sign. Furthermore, some lesions were located peripleurally, with thickened and tractive adjacent pleura. The effusion was observed in the left pleural cavity. Bilateral hilar and mediastinal lymphadenopathy was also evident and enlarged.

Tissue for pathologic examination was obtained by fiber-optic bronchoscopy. In inspective lung tissue, many inflammatory cells (principally lymphocytes and plasma cells) were observed in pulmonary parenchyma (*Figure 1D*), accompanied by significant fibrosis. The lymphoplasmacytic infiltration was also observed in the interlobular interstitium, the peribronchiolar region and the alveolar interstitium. Moreover, IgG4-positive plasma cells were present on immunohistochemical staining. In *Figure 2A*,*B*, the deep cells were on behalf of IgG4-positive plasma cells (>50/HPF). Immunostaining for CD20, CD3, CD138, CD38, mum-1, CD21FDC and CD23 were all positive; stains for desmin, ALK, SMA and EBER were negative. A histological diagnosis of IgG4-related lung disease was made by the increased serum IgG4 and the tissue's infiltration of IgG4-positive lymphocytes,

On admission, this case was misdiagnosed as infection, possibly due to atypical bacteria. After anti-inflammatory treatment for 2 weeks, no improvement was evident. Then voriconazole was also used for antifungal therapy. However, the radiological picture worsened with an increase in size of several nodules. Following histological diagnosis, the management was converted to hormonal therapy, with a significant improvement in clinical and radiological abnormalities being observed over a 2-month period.

Discussion

CT findings

The CT findings in this case are various and atypical, and

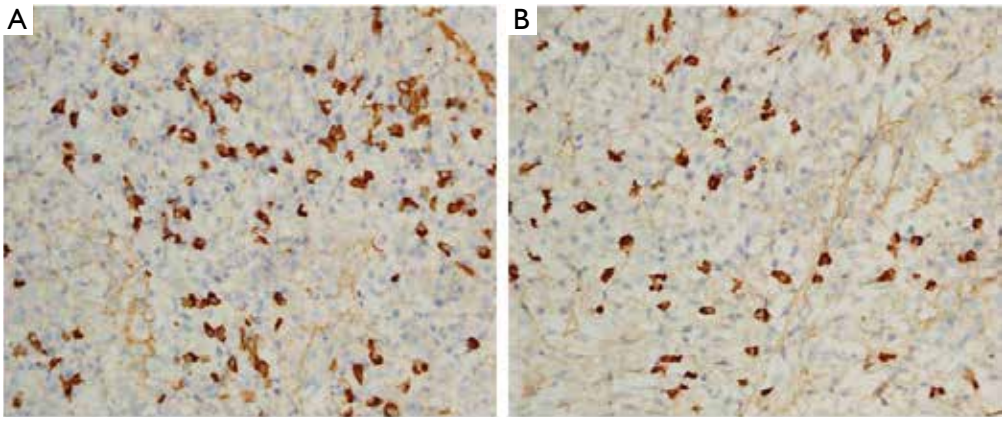

Figure 2 (A,B) Immunohistological images, the deep cells-lgG4-positive plasma cells (>50/HPF) (×400). HPF, high power field.

some findings differ from those reported in the current literature. Inoue *et al.* (6) collected 13 cases of IgG4-related lung disease, and reported that it could be categorized into four major subtypes: (I) the solid nodular type, where a solitary nodular mass lesion was present (four cases); (II) the round ground-glass opacity (GGO) type, characterized by multiple round GGOs (two cases); (III) the alveolar interstitial type, with honeycombing, bronchiectasis, and diffuse GGO (two cases); and (IV) the bronchovascular type, where there was thickening of bronchovascular bundles and interlobular septa (five cases). Histological review demonstrated that the solitary nodular lesions consisted of diffuse lymphoplasmacytic infiltration and fibrosis in pulmonary parenchyma. Thickened bronchovascular bundles or interlobular septa and GGO on CT images corresponded at a histological level to lymphoplasmacytic infiltration and fibrosis in peribronchiolar or interlobular interstitium and alveolar interstitium, respectively. In the late stages, the radiological finding of honeycombing corresponded to disrupted alveolar structures and dilated peripleural air spaces.

Importantly, nodules or masses, and thickened interlobular septa are observed concurrently in our case described above. Our case, with its various radiological features, is different from the previously reported cases and could be defined as a hybrid type of IgG4-related lung disease. We could anticipate that these features would be accompanied at the histological level by fibrosis and abundant lymphoplasmacytic infiltration in the pulmonary parenchyma, peribronchiolar, interlobular interstitium and alveolar interstitium.

Matsui *et al.* reported 18 cases with IgG4-related lung disease, in which the major CT features included thickening of the bronchial wall, bronchovascular bundles and interlobular septa (7). Soft tissue masses were observed only in two cases, suggesting that the majority of these cases belonged to the bronchovascular interstitial type. But in our case, the nodules or masses are more than simply thickened interlobular septa, requiring the creation of a hybrid class of IgG4-related lung disease.

Additional radiological features of this case include the 'halo sign' around high-density nodules or masses. The radiologic density of the halo sign is similar to that of GGO, but the distribution of these two features is quite distinct. The haloes surround nodules or masses, while GGO are observed independent of these lesions. Furthermore, the nodules or masses of IgG4-related lung disease always locate in a peripleural position. The adjacent pleura around such lesions may show mild bilateral pleural thickening (8), consistent with the findings in this case.

The bilateral hilar and mediastinal lymphadenopathy in our case is similar to that observed by Matsui. Matsui *et al.* reported the lymphadenopathy in all 18 patients of their series, using the mediastinal window setting (7). Indeed, mediastinal and/or hilar lymphadenopathy may be the most common intrathoracic manifestation of IgG4-related lung disease, being described in 40-90% of patients (9-11).

The existence of pleural effusions in IgG4-related lung disease is more contentious. Inoue *et al.* reported no pleural effusions in their 13 cases (6). But the left pleural effusion was observed in our case. The pleural effusion had also been reported by Choi *et al.* in a patient with IgG4-related lung disease (12). To clarify the significance of effusions in IgG4-related lung disease, a larger case series is required.

Clinical findings

According to the presented references, IgG4 related disease could be common in men of middle and old age. However, as a newly recognized disease, IgG4-related lung disease has not yet been well understood. Up to now, only limited cases have been reported in literature and there are not enough cases to show its all characteristics. Furthermore, Deshpande *et al*. also reported that young patient and female patient could have IgG4 related disease (13). Moreover, we observe the symptoms of fever in our case, with the increased WBC, CPR and ESR. This situation could exist in IgG4-related disease, as some references reported the similar discoveries (14-16).

On admission, this case was misdiagnosed as infection. At first, the patient accepted anti-inflammatory therapy, which included mezlocillin/sulbactam, azithromycin, moxalactam and imipenem/cilastatin. Then voriconazole was also used for antifungal therapy. However, the radiological picture worsened with an increase in size of several nodules. According to the histological diagnosis of IgG4-related lung disease, the management was converted to corticosteroid therapy. Although experience with treatment regimens in IgG4-related disease was growing, glucocorticoids still appeared to be effective (17). So methylprednisolone (40 mg qd) was used and then the symptoms of fever reduced gradually. The lesions of CT images were absorbed gradually, too. This indicated that the hormone therapy was effective.

Differential diagnosis

IgG4-related lung disease need be identified with Castleman's disease (plasma cell type) and pulmonary hyalinizing granulomas. These diseases both could have perilymphatic involvement and show abundant IgG4 positive plasma cell infiltration. CT images and clinical findings are important, as they could provide some differential points.

To patients with Castleman's disease (plasma cell type), the thoracic CT images usually show the enlargement of mediastinal and hilar lymph nodes. Only few study reported that Castleman's disease (plasma cell type) had perilymphatic involvement and thickened interlobular septa (18,19). This situation is common in IgG4-related lung disease, which is different from Castleman's disease. Furthermore, multicentric Castleman's disease could also have elevated serum IgG4 levels. But laboratory findings of anemia, hypoalbuminemia, polyclonal gammaglobulinemia, high C-reactive protein level, and elevated serum interleukin-6 level were all consistent with the multicentric Castleman's disease (20).

Pulmonary hyalinizing granuloma is a rare and benign disease. Although this disease had various degrees of lymphocytic infiltration within the lesions, its CT images presented as a solitary or, more frequently, multiple pulmonary nodular lesions (21). But IgG4-related lung disease could have different lesions, including the solid nodular mass, the round GGO and the thickened interlobular septa. Moreover, some investigation demonstrated both elevated serum IgG4 and elevated tissue IgG4-positive plasma cells in the pulmonary hyalinizing granuloma (22,23). The morphologic features of pulmonary hyalinizing granuloma overlapped those characteristics in IgG4-related lung disease, which suggested that pulmonary hyalinizing granuloma may be a form of IgG4-related disease.

Conclusions

IgG4-related disease is an uncommon but increasingly reported disease. The lung is well described as a target organ of IgG4-related disease, and the radiologic and pathologic features are varied. This report highlights the need for consideration of this condition even in the context of diverse and atypical features on CT imaging.

Acknowledgements

Disclosure: The authors declare no conflict of interest.

References

1. Stone JH, Zen Y, Deshpande V. IgG4-related disease. N Engl J Med 2012;366:539-51.
2. Takahashi H, Yamamoto M, Suzuki C, et al. The birthday of a new syndrome: IgG4-related diseases constitute a clinical entity. Autoimmun Rev 2010;9:591-4.
3. Takahashi H, Yamamoto M, Tabeya T, et al. The immunobiology and clinical characteristics of IgG4 related diseases. J Autoimmun 2012;39:93-6.
4. Ryu JH, Sekiguchi H, Yi ES. Pulmonary manifestations of immunoglobulin G4-related sclerosing disease. Eur Respir J 2012;39:180-6.
5. Okazaki K, Uchida K, Koyabu M, et al. Recent advances in the concept and diagnosis of autoimmune pancreatitis

and IgG4-related disease. J Gastroenterol 2011;46:277-88.
6. Inoue D, Zen Y, Abo H, et al. Immunoglobulin G4-related lung disease: CT findings with pathologic correlations. Radiology 2009;251:260-70.
7. Matsui S, Hebisawa A, Sakai F, et al. Immunoglobulin G4-related lung disease: clinicoradiological and pathological features. Respirology 2013;18:480-7.
8. Ryu JH, Sekiguchi H, Yi ES. Pulmonary manifestations of immunoglobulin G4-related sclerosing disease. Eur Respir J 2012;39:180-6.
9. Fujinaga Y, Kadoya M, Kawa S, et al. Characteristic findings in images of extra-pancreatic lesions associated with autoimmune pancreatitis. Eur J Radiol 2010;76:228-38.
10. Cheuk W, Yuen HK, Chu SY, et al. Lymphadenopathy of IgG4-related sclerosing disease. Am J Surg Pathol 2008;32:671-81.
11. Zen Y, Inoue D, Kitao A, et al. IgG4-related lung and pleural disease: a clinicopathologic study of 21 cases. Am J Surg Pathol 2009;33:1886-93.
12. Choi JH, Sim JK, Oh JY, et al. A Case of IgG4-Related Disease Presenting as Massive Pleural Effusion and Thrombophlebitis. Tuberc Respir Dis (Seoul) 2014;76:179-83.
13. Deshpande V, Khosroshahi A, Nielsen GP, et al. Eosinophilic angiocentric fibrosis is a form of IgG4-related systemic disease. Am J Surg Pathol 2011;35:701-6.
14. Sun X, Peng M, Hou X, et al. Refractory IgG4-related lung disease with constitutional symptoms and severe inflammation. Am J Respir Crit Care Med 2014;189:374-5.
15. Kobayashi H, Shimokawaji T, Kanoh S, et al. IgG4-positive pulmonary disease. J Thorac Imaging 2007;22:360-2.
16. Tsuboi H, Inokuma S, Setoguchi K, et al. Inflammatory pseudotumors in multiple organs associated with elevated serum IgG4 level: recovery by only a small replacement dose of steroid. Intern Med 2008;47:1139-42.
17. Stone JH. IgG4-related disease: nomenclature, clinical features, and treatment. Semin Diagn Pathol 2012;29:177-90.
18. Iyonaga K, Ichikado K, Muranaka H, et al. Multicentric Castleman's disease manifesting in the lung: clinical, radiographic, and pathologic findings and successful treatment with corticosteroid and cyclophosphamide. Intern Med 2003;42:182-6.
19. Murinello N, Matos C, Nogueira F. Castleman's disease: an unusual presentation. J Bras Pneumol 2011;37:129-32.
20. Takeuchi M, Sato Y, Takata K, et al. Cutaneous multicentric Castleman's disease mimicking IgG4-related disease. Pathol Res Pract 2012;208:746-9.
21. Shibata Y, Kobayashi T, Hattori Y, et al. High-resolution CT findings in pulmonary hyalinizing granuloma. J Thorac Imaging 2007;22:374-7.
22. Chapman EM, Gown A, Mazziotta R, et al. Pulmonary hyalinizing granuloma with associated elevation in serum and tissue IgG4 occurring in a patient with a history of sarcoidosis. Am J Surg Pathol 2012;36:774-8.
23. Shinohara T, Kaneko T, Miyazawa N, et al. Pulmonary hyalinizing granuloma with laryngeal and subcutaneous involvement: report of a case successfully treated with glucocorticoids. Intern Med 2004;43:69-73.

Cite this article as: Zhou J, Li X, Zeng Q. IgG4-related lung disease with atypical CT imaging: a case report. J Thorac Dis 2014;6(12):E276-E280. doi: 10.3978/j.issn.2072-1439.2014.12.11

Case Report

Rare and persistent Rhodococcus equi infection in a diffuse large B cell lymphoma patient: case report and review of the literature

Junli Zhang[1], Jing Xu[2], Xiaoxing Du[1], Yunsong Yu[1], Fangfang Lv[1]

[1]Department of Infectious Disease, [2]Department of Pathology, Sir Run Run Shaw Hospital, Zhejiang University School of Medicine, Hangzhou 310016, China

Correspondence to: Fangfang Lv. Department of Infectious Disease, Sir Run Run Shaw Hospital, Zhejiang University School of Medicine, 3 East Qingchun Road, Hangzhou 310016, China. Email: lvff@srrsh.com.

Abstract: Rhodococcus equi (R. equi) is an uncommon gram positive organism. It is a rare but recognized pathogen in humans and has emerged as an important cause of morbidity and mortality among immunocompromised patients. Generally, R. equi infection needs combined treatment with effective antibiotics, and often requires the immune adjuvant therapy. Here we reported a 49-year-old man presented dyspnea with fever, skin ulcer for 5 months, and the final diagnosis was diffuse large B cell lymphoma with R. equi septicemia and pneumonia, the treatment was failure, the blood culture was always positive during the course of disease, though he was given combined treatment with effective antibiotics, perhaps the immune reconstitution or immune supportive treatment was more important.

Keywords: Rhodococcus equi (R. equi); diffuse large B cell lymphoma; immunologic reconstitution; combined treatment

Submitted Sep 28, 2014. Accepted for publication Nov 13, 2014.
doi: 10.3978/j.issn.2072-1439.2014.12.17
View this article at: http://dx.doi.org/10.3978/j.issn.2072-1439.2014.12.17

Introduction

Rhodococcus equi (R. equi) formerly corynebacterium equi (C. equi), is an uncommon gram positive organism. It has been collected from soil, water, horses, cattle, swines and wild birds. R. equi is a rare but recognized pathogen in humans and has emerged as an important cause of morbidity and mortality among immunocompromised patients. It need combined treatment with effective antibiotics, and often requires the immune adjuvant therapy, due to survival inside histiocytes, immunocompromised, the site(s) and extent of infection, the duration of treatment is uncertain. A minimum of 6 months of antibiotic therapy is typically required for immunocompromised patients. Here we reported a 49-year-old man presented dyspnea with fever, skin ulcer for 5 months and the final diagnosis was diffuse large B cell lymphoma with R. equi septicemia and pneumonia, the treatment was failure, the blood culture was always positive during the course of disease, though he was given combined treatment with effective antibiotics. Perhaps the immune reconstitution or immune supportive treatment is more important.

Case report

In this article, the patient's history was divided into four parts to describe according to the treatment course and the change of disease.

The local hospital—February

A 49-year-old man presented dyspnea with fever, skin ulcer for 5 months. He had hewed out the stones for 8 years and then operated "meat pie shop" to now more than 10 years, denying that smoking and the history of tuberculosis. About 5 months ago, he had a temperature of almost 39 degrees, accompanied by shortness of breath, left cape side skin itching (a thumb nail sized red lesions with 4-5 gibbous red papules, no damage, and purulent), no

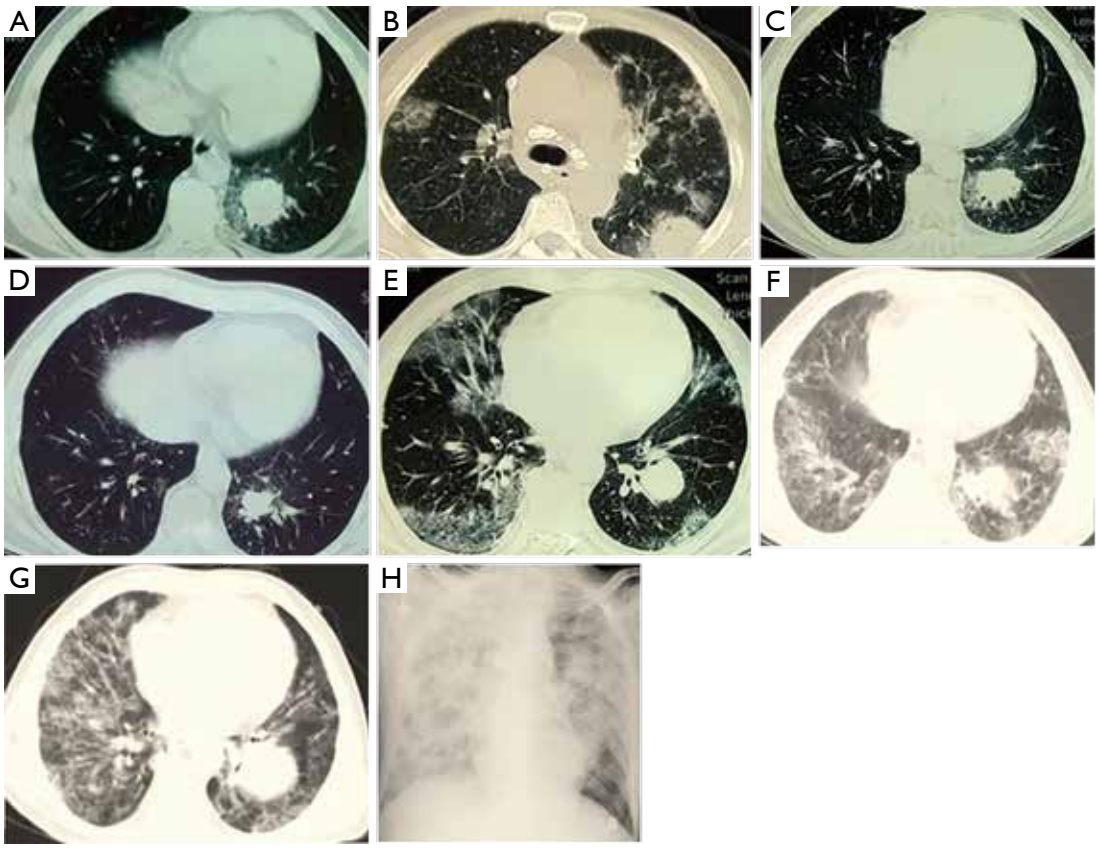

Figure 1 (A) Lung CT at the onset of the first (multiple lesions in both sides of the lung; lung mass in left lower lobe); (B) lung CT after 2 weeks treatment in local hospital; (C) after 43 days treatment in The First Hospital of Zhejiang Province, better than before treatment; (D) 2 weeks after the treatments of methylprednisolone and immunoglobulin, further improvement than (C); (E) a week after the discontinuation of hormone and immunoglobulin, pulmonary lesions deteriorated again; (F-H) lung imaging showed pulmonary lesions progressive deterioration in SRRSH. SRRSH, Sir Run Run Shaw Hospital.

cough and expectoration. White blood cell, neutrophils were normal, but lymphocytes decreased significantly: 0.2-0.7 (1.1×10^9-3.2×10^9/L), T-SPOT.TB and cryptococcal latex agglutination test, LDH were negative. Left lip pathology: ulcer with hyperplasia of squamous epithelium. Lung CT (*Figure 1*): multiple lesions in both sides with left lower lobe mass, cancer with two multiple pulmonary metastases may be; two pulmonary diffuse military and small nodules. Pathology of the left lower mass (the local hospital): suppurative granulomatous inflammation; pathology consultation of The First Hospital of Zhejiang Province: suppurative granulomatous inflammation, morphology of fungal infection was first considered. Twice-positive blood cultures were corynebacterium jeikeium: sensitive to vancomycin, imipenem, cefepime, ciprofloxacin, SMZ-TMP, cefotaxime, linezolid, and erythromycin. The patient's condition did not improve after two weeks' treatment of vancomycin, levofloxacin and voriconazole, and review the lung CT (*Figure 1B*): lung lesions progress than before.

The First Affiliated Hospital of Zhejiang University—March-May

Then to The First Hospital of Zhejiang Province for further diagnosis. Pathology of bronchoscopy (*Figure 2*): (lower left dorsal segment) mucosa of chronic inflammation with granuloma formation. Bone marrow routine: granulocyte increased active. It did not improve after two weeks' empirical anti-infective therapy of moxifloxacin and voriconazole. After that, many times of culture were R. equi: blood culture (twice), bone marrow culture (once),

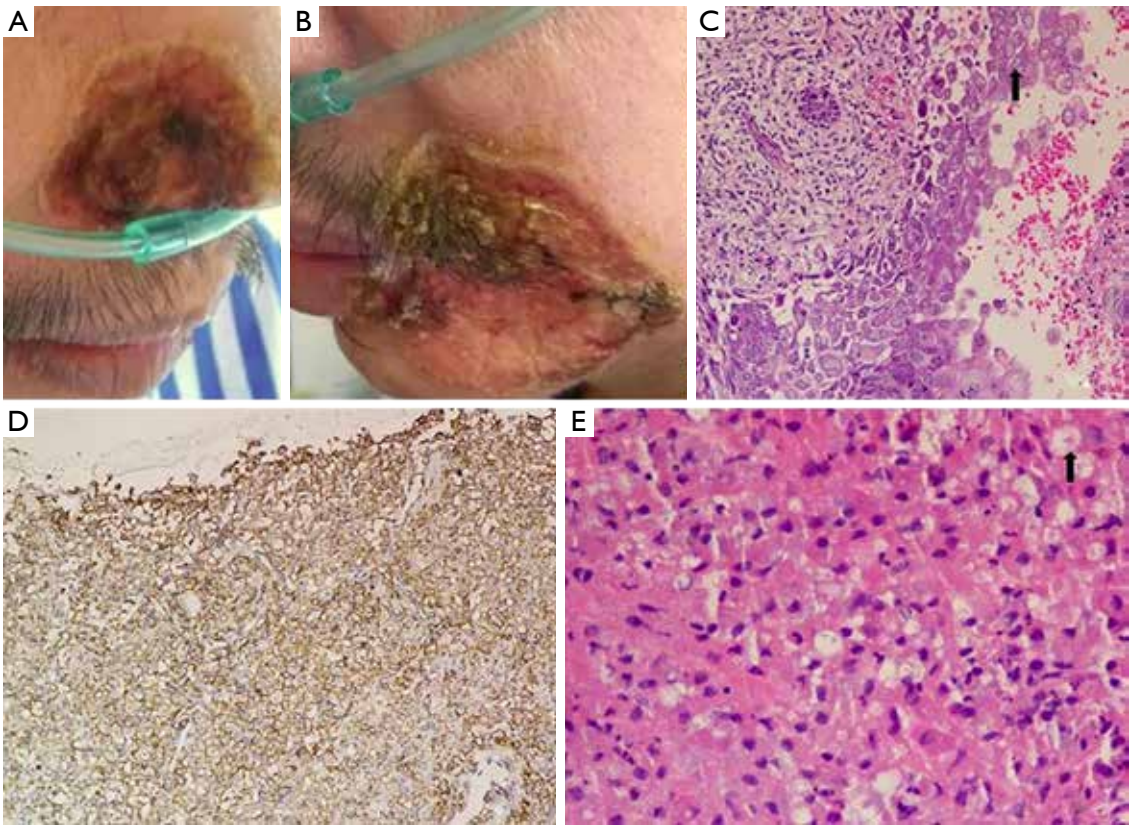

Figure 2 (A,B) Skin ulcer: left lip (d =4-5 cm), the right wing of the nose (d =2 cm); (C) pathology of the left lip (40×): chronic inflammation with necrosis of skin, with virus infection (black arrow: purple blue viral inclusion body in the cytoplasm of epidermal cells); (D) immunohistochemistry (100×): CD20+, consistent with this diagnosis diffuse large B cell lymphoma; (E) pathology of bronchoscopy (20 Mar, The First Hospital of Zhejiang Province) (HE 400×): the cytoplasm is full of purple dot (black arrow: gram positive cocci, R. equi), but were described only mucosa of chronic inflammation with granuloma formation by the front hospitals. R. equi, Rhodococcus equi.

sputum culture (once), sensitive to ceftriaxone, vancomycin, moxifloxacin, clindamycin, and erythromycin. He was then treated with moxifloxacin and vancomycin, the patient's condition improved after 5 days' treatment: no fever; breath better; but left lip skin ulcer did not improve, and after 43 days' treatment, lung CT (*Figure 1C*): better than before. However, blood cultures remained positive during the treatment: after 2 weeks and 43 days respectively.

The local hospital—June

They disable all medication because he appeared serious systemic rash after 43 days' therapy of "moxifloxacin and vancomycin". Rash slightly, but symptoms of fever and dyspnea began from 1 week after discontinuance, and he got a new ulcer in the right alar (2 cm in diameter). Hence to treated with moxifloxacin, rifampicin and SMZ-TMP. Symptoms ibid, rash worsened, so removed all drugs, then gave methylprednisolone and immunoglobulin for 3 days, sequential oral methylprednisolone and loratadine for 10 days, rash subsided, lung CT (*Figure 1D*) improved, but still have a fever, shortness of breath with skin ulcer (*Figure 2A,B*), blood culture was also R. equi. Then treated with caspofungin 3 days, moxifloxacin and rifampicin 3 days, sulperazone 2 days, but symptoms ibid, and review the lung CT (*Figure 1E*): pulmonary lesions progress.

Sir Run Run Shaw Hospital (SRRSH)—July

Department of respiration: lung CT (*Figure 1F*) showed pulmonary lesions progress obviously: the left lower pulmonary mass, tumor? The fuzzy patch scattered in both sides of the lung. Pathology of the left corner of the mouth (*Figure 2C*): chronic inflammation with necrosis

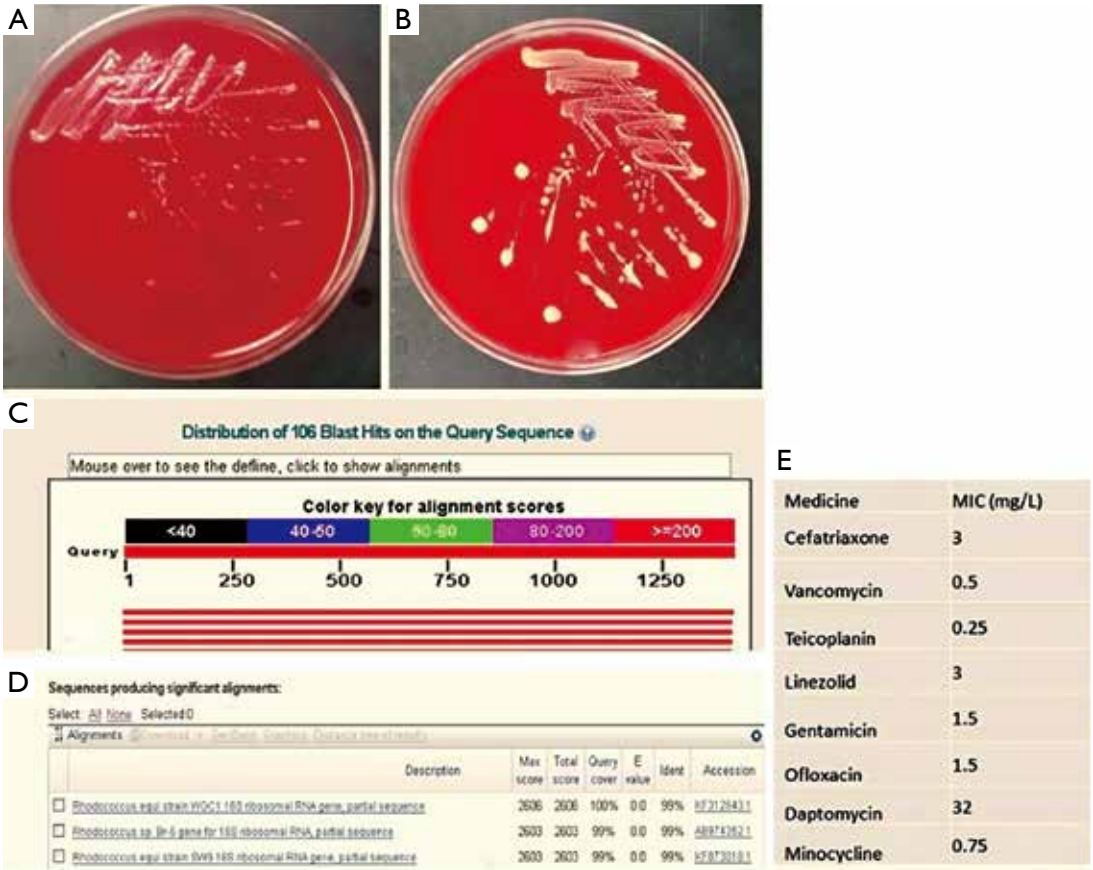

Figure 3 (A,B) Colonies on blood plate, incubation for 24 and 48 hours respectively; (C,D) we confirmed the isolate was R. equi by 16S RNA sequencing; (E) MIC of R. equi. R. equi, Rhodococcus equi.

of skin, with virus infection. Treated with moxifloxacin and teicoplanin for 2 days; cefoperazone sulbactam, ciprofloxacin and fluconazole for 4 days, levofloxacin combined with methylprednisolone for 10 days, because the patient's condition did not improve, and the family refused to continue the current treatment, so to department of infectious disease for further treatment. Combined with the local data, we can't exclude that histoplasmosis infection and R. equi infection, but had no malignant basis at least. He was given 10 days treatment with amphotericin B, imipenem, linezolid, methylprednisolone, and lung biopsy again. However, in the 10 days' treatment of our department, patients with progressive dyspnea and fever, lung CT (*Figure 1G*) and X-ray (*Figure 1H*) showed pulmonary diffuse lesions progress obviously and finally died of respiratory failure. To our surprised, the final pathology result was diffuse large B cell lymphoma (*Figure 2D*), the last 3 times blood cultures were all positive, and the isolate was identified as corynebacterium by BioMérieux Vitek2 (*Figure 3A,B*), 16S RNA sequencing was further performed and finally confirmed the isolate was R. equi (*Figure 3C,D*). We borrow patient's pathology slices outside the hospital, the full field of vision were plenty of gram positive cocci (*Figure 2E*), but were not described by the front two hospitals. The summary of main clinical, laboratory and imaging findings from patient was shown in *Tables 1,2*.

Discussion

R. equi, formerly C. equi, is an uncommon gram positive organism belonging to the group of mycolata (mycolic acid containing bacteria), that also incorporates the genera nocardia, corynebacterium and so on, it's hard to treat mostly owing to the establishment of intracellular niches (1,2). Colonies form on solid media appears irregularly round,

Table 1 Summary of main clinical, laboratory and imaging findings from patient

Date	Hospital	Symptoms	Blood culture	Lung imaging CT/X	Pathology	Treatment
Feb 14	The local hospital	Fever, dyspnea, left lip skin ulcer (d =2 cm)	Corynebacterium jeikeium × twice	Before the treatment: lung CT (*Figure 1A*), after 2 weeks treatment: lung CT (*Figure 1B*)	The left lower lung: the local hospital, suppurative granulomatous inflammation; The First Hospital of Zhejiang Province pathology consultation, suppurative granulomatous inflammation (PAS+, methenamine silver staining+), morphology of fungal infection was first considered	2 weeks: vancomycin + levofloxacin + voriconazole
Mar 2014-May 2014	The First Hospital of Zhejiang Province	No fever; breath better; left lip skin ulcer (d =3 cm); after 43 days of therapy, appear serious systemic rash, disable all medication	R. equi: before this treatment, blood culture ×2, bone marrow culture ×1, sputum culture ×1; treatment for 2 weeks ×1; treatment for 43 days ×1	Treatment for 43 days: lung CT (*Figure 1C*)	Bronchoscopy (*Figure 2E*): (lower left dorsal segment) mucosa of chronic inflammation with granuloma formation	2 weeks: moxifloxacin + voriconazole; 43 days: moxifloxacin + vancomycin
Jun 14	The local hospital	Fever dyspnea skin ulcer: left lip (d =4 cm), the right wing of the nose (d =2 cm), rash: whole body	–	–	–	2 weeks: moxifloxacin + rifampicin+ SMZ-TMP
		Symptoms ibid, rash worsened	–	Lung CT (*Figure 1D*) improve	–	Methylprednisolone + immunoglobulin (3 days); methylprednisolone (oral) + loratadine (10 days)
		Symptoms ibid, rash subsided	–	Lung CT (*Figure 1E*): pulmonary lesions progress	–	Caspofungin 3 days; moxifloxacin + rifampicin 3 days; sulperazone 2 days
Jul 14	SRRSH: Department of Respiration	Fever, dyspnea, skin ulcer: left lip (d =4 cm) (*Figure 2B*), the right wing of the nose (d =2 cm) (*Figure 2A*)	–	Lung CT (*Figure 1F*): the left lower pulmonary mass, tumor? patchy exudation: progress	The left Lip (*Figure 2C*): chronic inflammation with necrosis of skin, with virus infection	Moxifloxacin + teicoplanin: 2 days; cefoperazone sulbactam + ciprofloxacin + fluconazole: 4 days; the family refused to continue the current treatment
	Department of Infectious Disease	Symptoms ibid	R. equi: blood culture ×3 (*Figure 3A-E*)	Lung CT (*Figure 1G*): pulmonary lesions progress; lung X-ray (*Figure 1H*): pulmonary lesions progress	Left lung puncture (*Figure 2D*): diffuse large B cell lymphoma	10 days: amphotericin B + imipenem + linezolid + methylprednisolone

C. equi, corynebacterium equi; R. equi, Rhodococcus equi; SRRSH, Sir Run Run Shaw Hospital.

Table 2 T-lymphocyte subsets

Date	Hospital	Total T lymphocyte (50-84%)	T Helper/inducer cell (27-51%)	T suppressor/cytotoxic cell (15-44%)	CD4/CD8 (1.4-2.5)
Feb	Local hospital	19.2	1.8	13.2	0.14
Mar	The First Hospital	20.4	2.9	14.6	0.2
Jul	SRRSH	86.79	24.32	21.99	1.11

SRRSH, Sir Run Run Shaw Hospital.

smooth, semitransparent, glistening and mucoid (3) after incubation for 24 and 48 hours respectively (*Figure 3A,B*). R. equi has been collected from soil, water, horses, cattle, swines and wild birds, and concentrations are high in horse feces (1,2). However, the transmission of R. equi is not entirely clear; the patient of this case had no history of exposure to livestock obvious. It can cause dangerous opportunistic infections.

R. equi was first reported in 1923 in foals with pyogranulomatous pneumonia (4), with the first human infection being diagnosed in 1967 (5). The vast majority of patients infected with R. equi are immunocompromised, and more than 60% have human immunodeficiency virus infection (1,6,7), some have transplant recipient (8,9), only a few suffering from lymphoma, and most of them are Hodgkin's lymphoma, there are no reports of R. equi infection in diffuse large B cell lymphoma patients. Unlike the case, they were all secondary infection after chemotherapy in many of these lymphoma patients, most can be cured after treated by antibiotic plus chemotherapy, immune supportive treatment such as IVIG.

Clinical manifestation of R. equi infection are protean, includes fever, chills, nonproductive cough, dyspnea, weight loss, hemoptysis, and pleuritic pain etc. (3,8,10), although pulmonary infection is present up to 80% and bacteremia occurs in >80% cases (11). May be associated with invasion of the mononuclear phagocyte system, perhaps the ability of continued destruction of alveolar macrophages is the foundation of its pathogenicity, often accompanied by granuloma formation (1,11,12), caused sub-acute pneumonia with cavity and bacteremia. The mortality rate as high as 60% in immunocompromised people, infection serious degree and scavenging ability were closely associated with CD4 lymphocyte count, that is, you can improve the therapeutic effect by inducing immune reconstitution (2,6,11,13). Combination antibiotic therapy is the mainstay of treatment; R. equi is usually susceptible to erythromycin, rifampin, fluoroquinolones, aminoglycosides, glycopeptides and imipenem. Susceptibility to cotrimoxazole, tetracycline and clindamycin is variable (1,2,11), some studies such as tygecycline, vancomycin and linezolid have also successfully been used in patients (2,14-16). Like most have reported cases, due to survival inside histiocytes, immunocompromised, the site(s) and extent of infection, diseases are commonly chronic and recurrent (2), and the duration of treatment is uncertain. A minimum of 6 months of antibiotic therapy is typically required for immunocompromised patients with pulmonary, bone or multi-system infection (1,2,11,13,17).

In our study, the patients had been successively applied vancomycin, rifampin, moxifloxacin, cotrimoxazole, and when to our department, we give patient with linezolid, vancomycin, imipenem, levofloxacin, but there still were positive blood cultures during and after the whole combined treatment. The total T lymphocyte and T helper/inducer cell of the patients were very low at the onset of the first, but improved obviously after the application of methylprednisolone and immunoglobulin because of rashes, and at the same time we also found the pulmonary lesions improved than before, perhaps the immune reconstitution or immune supportive treatment more important. On the other hand, if we noticed a change of these, and further to look for the underlying diseases more actively, then given the long-term immune supportive treatment or chemotherapy, perhaps these aggressive treatment strategies can cure or significantly prolong the life of patient.

In addition, the patient of this case suffered from repeated puncture, however, we should know the positive rate of percutaneous lung biopsy is closely related with operator level of experience, distance of the lesion from the pleural surface, target lesion size, needle type, guide positioning map, pathology expert's experience (18,19). I hope we should do what we can as far as possible to improve the positive rate of puncture, which can provide the basis for clinical diagnosis as early as possible, and increase the survival rate of the patients.

Conclusions

In areas of the world where laboratory facilities are lacking, and for immunocompromised patients, R. equi infection should be considered in the differential diagnosis of a "mycobacterium-like" illness with negative smear results. And R. equi should always be considered as a potential pathogen in any immunocompromised patient and especially with cavitary pneumonia (10), like the first reaction when saw pneumocystis carinii, we need to learn what causes the immune-suppression, and further studies and procedures are often required, including CT, BAL, and transbronchial or percutaneous biopsy.

In addition, when the treatment effect is not good in immunocompromised patients, we must clearly know the importance of an effective immune recovery. Most importantly, Isolation of any of rare pathogens in practice should require a thorough search for possible malignant diseases, for example, the association between group bovis bacteremia and colon carcinoma (20,21).

Because the experience of pathology and microbiology doctors is very different, incompetent physicians will cause a high rate of misdiagnosis. We would increase clinicians' awareness of this pathogen's morbidity in compromised people and to improve the likelihood of its accurate and timely diagnosis. Further clinical and laboratory research is needed to better define the routes of acquisition and the mechanisms of pathogenesis of R. equi infection and the appropriate treatments for it.

Acknowledgements

Disclosure: The authors declare no conflict of interest.

References

1. Weinstock DM, Brown AE. Rhodococcus equi: an emerging pathogen. Clin Infect Dis 2002;34:1379-85.
2. Savini V, Salutari P, Sborgia M, et al. Brief Tale of a Bacteraemia by Rhodococcus equi, With Concomitant Lung Mass: What Came First, the Chicken or The Egg? Mediterr J Hematol Infect Dis 2011;3:e2011006.
3. Yamshchikov AV, Schuetz A, Lyon GM. Rhodococcus equi infection. Lancet Infect Dis 2010;10:350-9.
4. Magnusson H. Spezifische infektiose pneumonie beim fohlen: ein neuer eitererreger beim pferd. Arch Wiss Prakt Tierheilkd 1923;50:22-38.
5. Golub B, Falk G, Spink WW. Lung abscess due to Corynebacterium equi. Report of first human infection. Ann Intern Med 1967;66:1174-7.
6. Ferretti F, Boschini A, Iabichino C, et al. Disseminated Rhodococcus equi infection in HIV infection despite highly active antiretroviral therapy. BMC Infect Dis 2011;11:343.
7. Topino S, Galati V, Grilli E, et al. Rhodococcus equi infection in HIV-infected individuals: case reports and review of the literature. AIDS Patient Care STDS 2010;24:211-22.
8. Hayes D Jr, Diaz-Guzman E, Hoopes CW. Rhodococcus equi infection after lung transplantation. Respir Care 2011;56:1605-7.
9. Behnes CL, Neumann S, Schweyer S, et al. Pleural malakoplakia caused by Rhodococcus equi infection in a patient after stem cell transplantation. Diagn Pathol 2012;7:20.
10. Gallant JE, Ko AH. Cavitary pulmonary lesions in patients infected with human immunodeficiency virus. Clin Infect Dis 1996;22:671-82.
11. Torres-Tortosa M, Arrizabalaga J, Villanueva JL, et al. Prognosis and clinical evaluation of infection caused by Rhodococcus equi in HIV-infected patients: a multicenter study of 67 cases. Chest 2003;123:1970-6.
12. Takai S, Sasaki Y, Ikeda T, et al. Virulence of Rhodococcus equi isolates from patients with and without AIDS. J Clin Microbiol 1994;32:457-60.
13. Ng S, King CS, Hang J, et al. Severe cavitary pneumonia caused by a non-equi Rhodococcus species in an immunocompetent patient. Respir Care 2013;58:e47-50.
14. Akilesh S, Cross S, Kimmelshue K, et al. Pseudotumor of the tracheal-laryngeal junction with unusual morphologic features caused by Rhodococcus equi infection. Head Neck Pathol 2011;5:395-400.
15. El-Mofty SK, Akilesh S. Infectious pseudotumors: red herrings in head and neck pathology. Head Neck Pathol 2012;6:58-63.
16. Russo G, Lichtner M, Carnevalini M, et al. Primary retroperitoneal abscesses due to Rhodococcus equi in a patient with severe nephrotic syndrome: successful antibiotic treatment with linezolid and tigecycline. Int J Infect Dis 2010;14:e533-5.
17. Denes E, Peignon-Orsoni D, Terrade FX. Nonhealing wound due to Rhodococcus equi in an apparently immunocompetent patient, revealing CD8+ T-lymphocyte deficiency. J Clin Microbiol 2010;48:4658-60.
18. Capalbo E, Peli M, Lovisatti M, et al. Trans-thoracic biopsy of lung lesions: FNAB or CNB? Our experience

and review of the literature. Radiol Med 2014;119:572-94.
19. Boskovic T, Stanic J, Pena-Karan S, et al. Pneumothorax after transthoracic needle biopsy of lung lesions under CT guidance. J Thorac Dis 2014;6:S99-107.
20. Vollmer T, Hinse D, Kleesiek K, et al. Interactions between endocarditis-derived Streptococcus gallolyticus subsp. gallolyticus isolates and human endothelial cells. BMC Microbiology 2010;10:78.
21. Boleij A, van Gelder MM, Swinkels DW, et al. Clinical Importance of Streptococcus gallolyticus infection among colorectal cancer patients: systematic review and meta-analysis. Clin Infect Dis 2011;53:870-8.

Cite this article as: Zhang J, Xu J, Du X, Yu Y, Lv F. Rare and persistent Rhodococcus equi infection in a diffuse large B cell lymphoma patient: case report and review of the literature. J Thorac Dis 2014;6(12):E281-E288. doi: 10.3978/j.issn.2072-1439.2014.12.17

Case Report

Good neurological recovery after rescue thrombolysis of presumed pulmonary embolism despite prior 100 minutes CPR

Jiang-Ping Wu[1], Dan-Yan Gu[2], Sheng Wang[1], Zhen-Jun Zhang[1], Jian-Cang Zhou[2], Rui-Feng Zhang[3]

[1]Department of Emergency Medicine, The Second People's Hospital of Yiwu City, Yiwu 322002, China; [2]Department of Critical Care Medicine, [3]Department of Respiratory Medicine, Sir Run Run Shaw Hospital, Zhejiang University School of Medicine, Hangzhou 310016, China

Correspondence to: Dr. Jian-Cang Zhou. Department of Critical Care Medicine, Sir Run Run Shaw Hospital, Zhejiang University School of Medicine, Hangzhou 310016, China. Email: jiancangzhou@hotmail.com.

Abstract: We reported the case of a 70-year-old man who was admitted to neurologic wards for recurrent syncope for 3 years. Unfortunately, just 2 hours after his admission, he suddenly collapsed and failed to return of spontaneous circulation (ROSC) after a 100-minute standard cardiopulmonary resuscitation (CPR). Fortunately, he was timely suspected to have pulmonary embolism (PE) based on his sedentary lifestyle, elevated D-dimer and markedly enlarged right ventricle chamber on bedside echocardiography. After a rescue thrombolytic alteplase therapy, he was successfully resuscitated and good neurological recovery was achieved.

Keywords: Cardiac arrest; pulmonary embolism (PE); thrombolysis

Submitted Sep 01, 2014. Accepted for publication Nov 13, 2014.
doi: 10.3978/j.issn.2072-1439.2014.12.23
View this article at: http://dx.doi.org/10.3978/j.issn.2072-1439.2014.12.23

Introduction

Pulmonary embolism (PE) causes about 5% to 10% of all cardiac arrests (1). Whenever an atraumatic cardiac arrest happened to a previously healthy adult, it is of paramount importance to search for underlying etiology besides the implement of standard cardiopulmonary resuscitation (CPR). Specifically, for cardiac arrest caused by massive PE, an earlier thrombotic therapy based on presumptive diagnosis of PE may significantly improve patients' outcomes (2). However, it is still a challenge to make the timely diagnosis of PE in clinical practice, especially under the scenario of cardiac arrest. Herein, we reported a 70-year-old man with suddenly cardiac arrest and failed to return of spontaneous circulation (ROSC) after a 100-minute CPR. Then a rescue thrombolytic alteplase saved his life since he was highly suspected to have PE.

Case report

A 70-year-old man was admitted to neurologic department for evaluation of recurrent syncope. He had no associated chest pain, fever, or respiratory symptoms. He was otherwise healthy except a prior MRI demonstrated some minor lacunar infarctions which did not affect his speaking or movement. He was in a sedentary lifestyle after retirement, sitting at least 8 hours every day. The electrocardiogram showed sinus tachycardia with right bundle branch block. On physical examination, he was alert and with mild shortness of breath. Vital signs on presentation included heart rate 105 beats/min, blood pressure 122/78 mmHg, and respiratory rate 16 breaths/min. Oxygen saturation on room air was 95%. Echocardiography demonstrated sizes of four heart chambers were normal and the right ventricular systolic pressure was 63 mmHg. Approximate 2 hours after his arrival in neurologic ward when he was enjoying his dinner, the patient suddenly fell into unconsciousness and the saturation decreased to 90% while the heart rate and respiratory rate increased to 118 beats/min and 48 breaths/min, respectively. Approximate 10 minutes later, he restored his consciousness and complained shortness of breath and the oxygen saturation on room air was 90%. Shortly afterwards, his condition rapidly deteriorated and progressed to cardiopulmonary arrest with pulseless electric

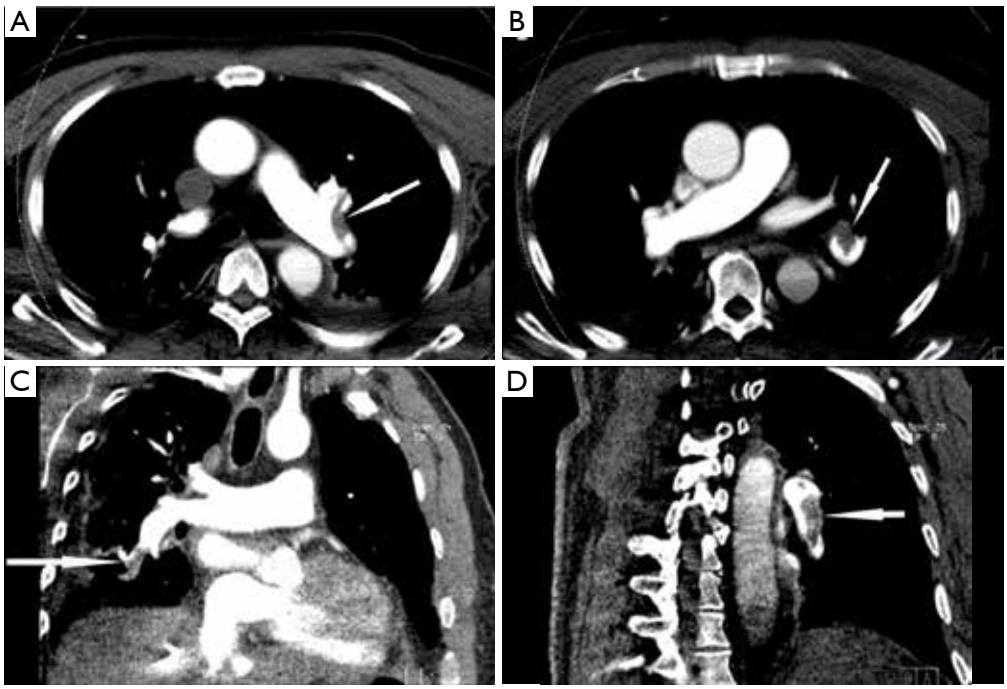

Figure 1 Computed tomographic pulmonary angiography demonstrated extensive bilateral pulmonary emboli (arrow) (A-D).

activity (PEA). Prompt CPR was initiated and epinephrine 1 mg was administered immediately. Ventricular fibrillation was demonstrated once after approximate 20 minutes CPR, therefore, electrical defibrillations were applied but failed. Thereafter, recurrent narrow QRS complex PEA at a rate around 130 beats per minute dominated the next 60 minutes of CPR, with intermittent ROSC was observed. Given the refractory PEA during the cardiac arrest, potential reversible reasons for cardiac arrest were evaluated as the CPR continued. Another bedside echocardiography demonstrated markedly dilated right ventricle deviating to the left side which significantly depressed the left ventricular systolic function. By incorporating echocardiographic findings, his sedentary lifestyle and D-dimer was 6.03 μg/mL (reference range, 0-0.05 ug/mL), the patient was deemed to have high likelihood of PE. A bolus dose of 5 mg of alteplase was administered and another 45 mg alteplase was given continuously. Approximate 2 minutes after the alteplase infusion, the refractory PEA returned into sinus rhythm and a stable spontaneous circulation was achieved under continuous dopamine support. Overall, the patient underwent approximate 100 minutes of standard CPR. Echocardiography after thrombolysis demonstrated the size of left ventricle was restored although the size of right ventricle was slightly enlarged and the right ventricular systolic pressure was decreased to 45 mmHg. After stabilization and observation for the night, the patient underwent a computed tomography pulmonary angiography which confirmed extensive bilateral pulmonary emboli and no intracranial bleeding (*Figures 1* and *2A*). The patients had a massive necrosis of intestinal mucosa after thrombolysis and acute kidney injury which necessitated renal replacement treatment for 3 months. During the following week, constant heparin infusion was administered and later was shifted to warfarin for anticoagulation. One week later, after withdrawn of sedation, the patient became awake and alert. Another head CT scan performed 6 days after thrombolysis demonstrated ischemic infarction and mild intracranial bleeding in the right occipital lobe (*Figure 2B*). However, the heparin was continued and a third head CT at 10 days post thrombolysis did not show enlarging intracranial hemorrhage (*Figure 2C*). Currently, the patient is alert and is on a physical rehabilitation program but no major neurological sequelae related to his cardiac arrest (*Figure 2D*).

Discussion

Mortality due to cardiac arrest following massive PE ranges

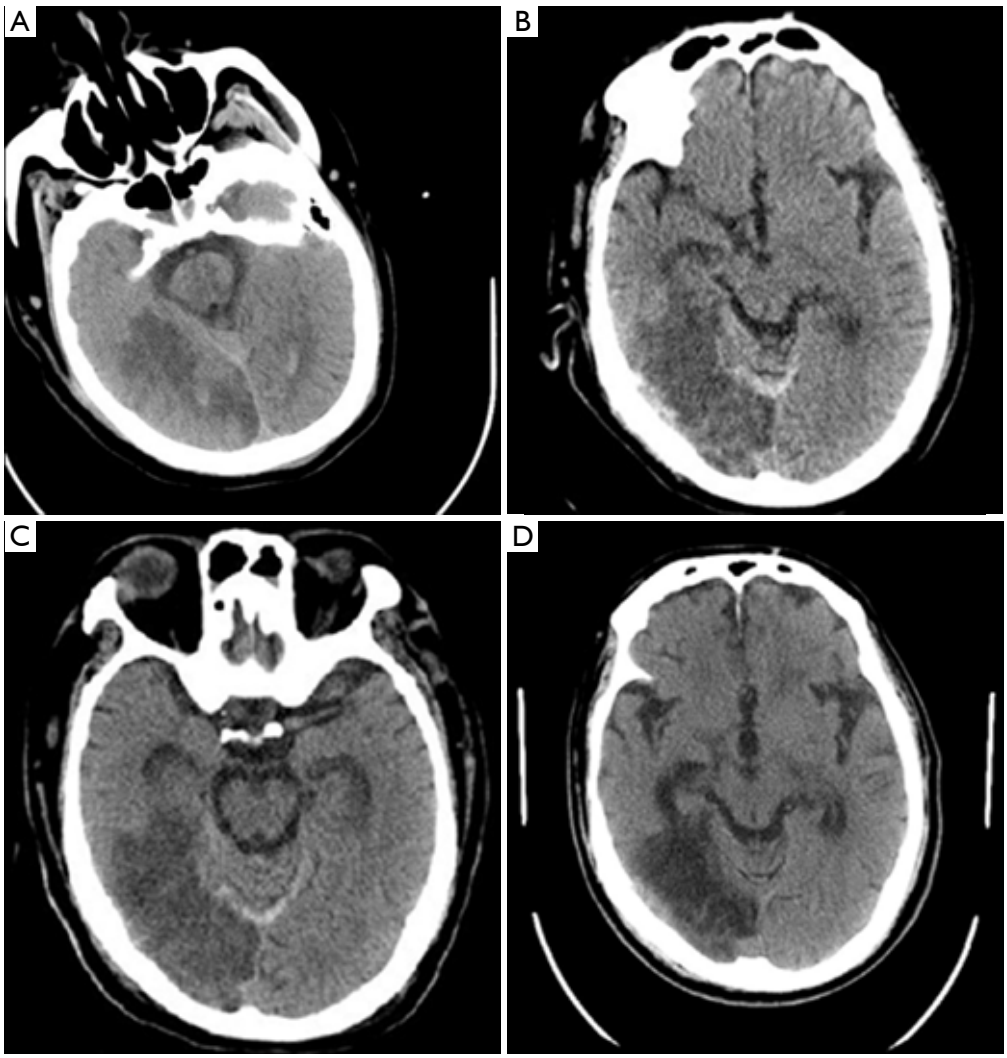

Figure 2 (A) Computed tomogram (CT) approximate 17 hours post thrombolysis demonstrated old infarction of the right occipital lobe but no intracranial bleeding; (B) six days after thrombolysis showing subarachnoid bleeding in the right occipital lobe; (C) CT of 10 days after thrombolysis did no show enlarging of the bleeding although constant infusion of heparin; (D) CT of 3 months later after the thrombolysis.

from 65% to 95% (3). As a result of persisting mechanical obstruction by PE, routine CPR is often ineffective. Given the poor outcome of prolonged unresponsive cardiac arrest and the fact that vast majority of cardiac arrest were caused by acute myocardial infarction or PE, empirical thrombolytic therapy seems to be intuitive appeal for cardiac arrests. However, a recent study from *New England Journal of Medicine* demonstrated that unselected thrombolysis for cardiac arrest patients was not all beneficial (4). Nevertheless, both the American Heart Association and European Resuscitation Council recommend "considering" use of fibrinolytic therapy when cardiac arrest is caused by proven or suspected acute PE (5,6). In patients presenting with cardiac arrest as a consequence of acute PE, thrombolytic therapy was associated with significantly higher ROSC (81% *vs.* 43%, P=0.03) (7). Overall, fibrinolysis reduced the risk of death by around 55% (8). In a recent study by Er *et al.* (9) shown that for cardiac arrests caused by PE, earlier initiated thrombosis after cardiac arrest onset (13.6 *vs.* 24.6 min) was associated with higher rate of ROSC eventually. Moreover, for those who were eventually discharged, thrombolysis was given with less delay (11.0 *vs.* 22.5 min). Therefore, the earlier rescue thrombolysis was administrated for patients

with cardiac arrest and presumptive diagnosis of PE, the better outcome it would be. In our case, however, the thrombolysis was somewhat delayed because the relative inexperience of neurologic physicians who were involved in the primary resuscitation and the CPR continued for nearly 100 minutes overall until the presumptive diagnosis was established by the consulted intensive care physician. Given an approximate 30 minutes of CPR is adopted by many physicians for cardiac arrests currently, a longer time of CPR may be associated with higher rate of ROSC, especially for patients caused by massive PE and received a timely thrombolytic therapy.

In fact, it could be extremely difficult to explore the etiology of cardiac arrest while a patient is being resuscitated, specifically for physicians outside ICU. However, certain physiologic precepts have a stronger association with PE, lending confidence to presumptive diagnosis in the absence of evident alternative etiologies (2). For example, a rapid, narrow QRS PEA rhythm with observed myocardial contraction on echocardiography may have a higher association with PE (10). A triad of witnessed cardiac arrest, age less than 65 to 70 years, and PEA as the initial rhythm was seemed to be more likely associated with massive PE (11,12). The following factors were proved to have the highest association with the diagnosis of PE: unilateral leg swelling, oxygen saturation less than 95%, active cancer, recent prolonged immobilization or orthopedic surgery (2). Importantly, a high index of suspicion for PE should be maintained especially in cardiac arrest patient who had a history or symptom profile associated with this diagnosis. In clinical practice, a rapid integration of patients' information, bedside diagnostic tools and available laboratory findings could be relied on to determine the level of suspicion of PE. With respect to the diagnostic tool, a portable echocardiography is ideal because it can differentiate shock categories and recognize the characteristics of PE even during CPR. Moreover, transesophageal echocardiography can reliably establish the cause of a circulatory arrest during CPR (13,14). However, for those who can be stabilized, a computed tomography pulmonary angiography will demonstrate filling defects in the main or lobar pulmonary arteries. As mentioned, we made the presumptive diagnosis of PE by integrating the patient's lifestyle, elevated D-dimer, and findings of bedside echocardiography.

Given the bleeding risk associated with thrombolytic therapy, this intervention should only be administrated after balancing the potential benefits of improved outcomes and bleeding risk. Of the potential bleeding risk, the intracranial hemorrhage is the most devastating complication (2). Major bleeding was reported to occur in 9.6% of patients receiving thrombolytic therapy for acute PE while intracranial hemorrhage reported to be approximate 3% (15). There was a mild bleeding after thrombolysis in our case, however, no enlargement was noticed even under constant infusion of heparin for anticoagulation for the PE. Nevertheless, risk stratification models for bleeding are warranted to identify the individuals at the highest risk of hemorrhagic complications. In the recent large Pulmonary Embolism Thrombolysis (PEITHO) trial, incidence of major bleeding and intracranial hemorrhage was 6.3% and 2% respectively (16). Interestingly, bleeding risk was lower and mortality benefit was higher in patients <75 years. This is consistent with a recent meta-analysis that although use of thrombolytics was associated with increased risks of major bleeding and intracranial hemorrhage, major bleeding was not significantly increased in patients 65 years and younger (17). Hence, attenuation of the bleeding risk in individuals 75 years and younger may suggest a stronger indication for thrombolysis in those patients. Moreover, a risk score based on six variables (age >75 years, recent bleeding, cancer, creatinine levels >1.2 mg/dL, anemia, or PE at baseline) documented at entry can identify patients with venous thromboembolism at low, intermediate, or high risk for major bleeding during the first three months of therapy (18). However, given the outcomes of cardiac arrest due to PE are uniformly poor and thrombolysis therapy is generally deemed as "last chance" under many circumstances, even for patient with contraindication such as recent intracranial hemorrhage, a good outcome could be achieved (8). Under this circumstance, contraindications of thrombolytic therapy are frequently disregarded because the potential benefit outweighs the bleeding risk.

In summary, early recognition of etiology is of paramount importance for successful resuscitation of patients with atraumatic cardiac arrest. For cardiac arrest caused by massive PE, a good neurological recovery could be achieved by rescue thrombolysis despite a prolonged 100 minutes CPR.

Acknowledgements

Disclosure: The authors declare no conflict of interest.

References

1. Adams BD, Kim JY, Jackson WO. Tenecteplase and

return of spontaneous circulation after refractory cardiopulmonary arrest. South Med J 2004;97:1015-7.
2. Logan JK, Pantle H, Huiras P, et al. Evidence-based diagnosis and thrombolytic treatment of cardiac arrest or periarrest due to suspected pulmonary embolism. Am J Emerg Med 2014;32:789-96.
3. Bailén MR, Cuadra JA, Aguayo De Hoyos E. Thrombolysis during cardiopulmonary resuscitation in fulminant pulmonary embolism: a review. Crit Care Med 2001;29:2211-9.
4. Böttiger BW, Arntz HR, Chamberlain DA, et al. Thrombolysis during resuscitation for out-of-hospital cardiac arrest. N Engl J Med 2008;359:2651-62.
5. Morrison LJ, Deakin CD, Morley PT, et al. Part 8: Advanced life support: 2010 International Consensus on Cardiopulmonary Resuscitation and Emergency Cardiovascular Care Science With Treatment Recommendations. Circulation 2010;122:S345-421.
6. Deakin CD, Nolan JP, Soar J, et al. European Resuscitation Council Guidelines for Resuscitation 2010 Section 4. Adult advanced life support. Resuscitation 2010;81:1305-52.
7. Kürkciyan I, Meron G, Sterz F, et al. Pulmonary embolism as a cause of cardiac arrest: presentation and outcome. Arch Intern Med 2000;160:1529-35.
8. Bottinor W, Turlington J, Raza S, et al. Life-saving systemic thrombolysis in a patient with massive pulmonary embolism and a recent hemorrhagic cerebrovascular accident. Tex Heart Inst J 2014;41:174-6.
9. Er F, Nia AM, Gassanov N, et al. Impact of rescue-thrombolysis during cardiopulmonary resuscitation in patients with pulmonary embolism. PLoS One 2009;4:e8323.
10. Zhu T, Pan K, Shu Q. Successful resuscitation with thrombolysis of a presumed fulminant pulmonary embolism during cardiac arrest. Am J Emerg Med 2013;31:453.e1-3.
11. Courtney DM, Sasser HC, Pincus CL, et al. Pulseless electrical activity with witnessed arrest as a predictor of sudden death from massive pulmonary embolism in outpatients. Resuscitation 2001;49:265-72.
12. Courtney DM, Kline JA. Prospective use of a clinical decision rule to identify pulmonary embolism as likely cause of outpatient cardiac arrest. Resuscitation 2005;65:57-64.
13. Dirican A, Ozkaya S, Atas AE, et al. Thrombolytic treatment (alteplase; rt-Pa) in acute massive pulmonary embolism and cardiopulmonary arrest. Drug Des Devel Ther 2014;8:759-63.
14. van der Wouw PA, Koster RW, Delemarre BJ, et al. Diagnostic accuracy of transesophageal echocardiography during cardiopulmonary resuscitation. J Am Coll Cardiol 1997;30:780-3.
15. Hefer DV, Munir A, Khouli H. Low-dose tenecteplase during cardiopulmonary resuscitation due to massive pulmonary embolism: a case report and review of previously reported cases. Blood Coagul Fibrinolysis 2007;18:691-4.
16. Meyer G, Vicaut E, Danays T, et al. Fibrinolysis for patients with intermediate-risk pulmonary embolism. N Engl J Med 2014;370:1402-11.
17. Chatterjee S, Chakraborty A, Weinberg I, et al. Thrombolysis for pulmonary embolism and risk of all-cause mortality, major bleeding, and intracranial hemorrhage: a meta-analysis. JAMA 2014;311:2414-21.
18. Ruíz-Giménez N, Suárez C, González R, et al. Predictive variables for major bleeding events in patients presenting with documented acute venous thromboembolism. Findings from the RIETE Registry. Thromb Haemost 2008;100:26-31.

Cite this article as: Wu JP, Gu DY, Wang S, Zhang ZJ, Zhou JC, Zhang RF. Good neurological recovery after rescue thrombolysis of presumed pulmonary embolism despite prior 100 minutes CPR. J Thorac Dis 2014;6(12):E289-E293. doi: 10.3978/j.issn.2072-1439.2014.12.23

Case Report

The pure distal left main bronchial sleeve resection with total lung parenchymal preservation: report of two cases and literature review

Jian Tang[1], Min Cao[1], Liqiang Qian[2], Yujie Fu[1], Jun Tang[1], Xiaojing Zhao[1]

[1]Department of Thoracic Surgery, Renji Hospital, Shanghai Jiao Tong University School of Medicine, Shanghai 200127, China; [2]Center for Lung Cancer, Chest Hospital, Shanghai Jiao Tong University, Shanghai 200030, China

Correspondence to: Xiaojing Zhao, MD. Department of Thoracic Surgery, Renji Hospital, Shanghai Jiao Tong University School of Medicine, 160 Pujian Road, Shanghai 200127, China. Email: drzhaoxiaojing@gmail.com.

Abstract: Pure bronchial sleeve resection and reconstruction is a type of rare thoracic surgery, especially for the second carina reconstruction on the left side, needs more exquisite surgical techniques, and patient selection to such surgery often requires rigorous screening. We present two cases of left main bronchial adenoid cystic carcinoma with the second carina reconstruction. The purpose of this paper is to recommend a useful supplement to conventional surgery for some very selected patients.

Keywords: Lung cancer; bronchial carcinoma; sleeve resection; bronchoplastic resection; parenchymal-sparing surgery; pulmonary preservation

Submitted Nov 05, 2014. Accepted for publication Dec 04, 2014.
doi: 10.3978/j.issn.2072-1439.2014.12.14
View this article at: http://dx.doi.org/10.3978/j.issn.2072-1439.2014.12.14

Introduction

The treatment of distal left main bronchial carcinoma usually requires a very complex surgical procedure, because of frequently involving the opening of upper and lower lobe bronchus, the vast majority of cases have to be performed sleeve lobectomy or pneumonectomy. However, under special conditions, the cases can also be strictly selected to do the pure bronchial sleeve resection with total lung parenchymal preservation (the second carina reconstruction). Compared with the right side, dependent on relationships of anatomic location, the second carina reconstruction on the left side is much more complex and difficult (1). Generally, the main indications for this surgical method include trachea-bronchial low malignant tumors (such as typical carcinoid, mucoepidermoid carcinoma and adenoid cystic carcinoma), parts of benign diseases and occasionally non-small cell lung cancer (2-4). We present the surgical results in two patients with distal left main bronchus adenoid cystic carcinoma in whom this surgical procedure were performed, and get a satisfactory therapeutic effect.

Case reports

Case 1

A 64-year-old man was referred to our hospital with irritating cough in September 2014. Chest CT scan showed a lesion in the terminal left main bronchus, bronchoscopy saw submucosal tumor at the end of the left main bronchus, from the carina 2.5 cm (seven cartilaginous rings), was pushed through to bronchial cavity and narrow the lumen. The opening of upper and lower lobe bronchus was observed free from involvement (*Figure 1A*). The diagnosis of adenoid cystic carcinoma was made on the basis of pathological findings by bronchoscopy biopsy. Surgical procedure: we used posterolateral incision through the 5th intercostal chest, breaking the 5th rib and free intercostal muscle pedicle flap. In the operative view, we first release the hilar dissect mediastinal and hilar lymph nodes. Then we fully free pulmonary vein and pulmonary artery, respectively, setting on a leash, and totally release the left main bronchus and lobar bronchus. When removing the truncus intermedius, intraoperative frozen pathological examination of tumor proximal, distal transection of the left main bronchus, and

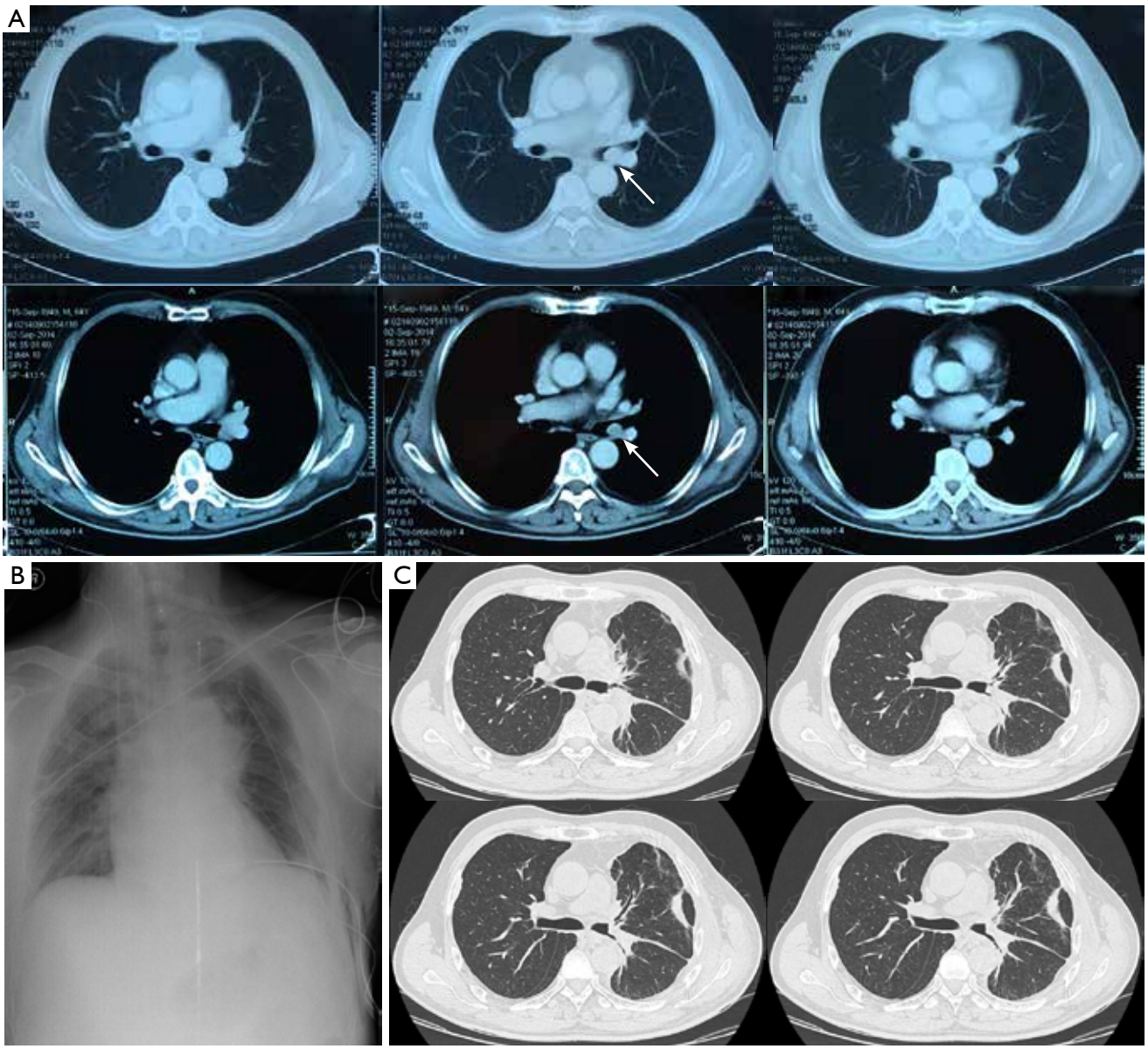

Figure 1 (A) Computed tomography scan showed the lesion located at the end of left main bronchus, between the opening of upper and lower bronchus; (B) chest radiography at the first day of postoperation showed the upper and lower lobes of left lung were both full recruitment; (C) computed tomography after 3 weeks of postoperation showed anastomotic healing well, and the opening of upper and lower lobe bronchus were smooth.

lobe bronchus showed negative. Surgical reconstruction of the second carina was performed on continuous suture upper and lower lobe bronchus side-to-side like 'B' type, and then make the left main bronchus anastomosis end-to-end with 3-0 Prolene. Intercostal muscle pedicle flap was surrounded the anastomosis and suture fixation at last (*Figure 1B,C*). Since the results of a final pathological examination showed the upper lober margin was positive, the postoperative adjuvant radiotherapy was performed 6 weeks later.

Case 2

A 67-year-old man was admitted to our hospital in July 2012 complaining of hemosputum and chest pain. The patient accepted intravenous chemotherapy 4 times with

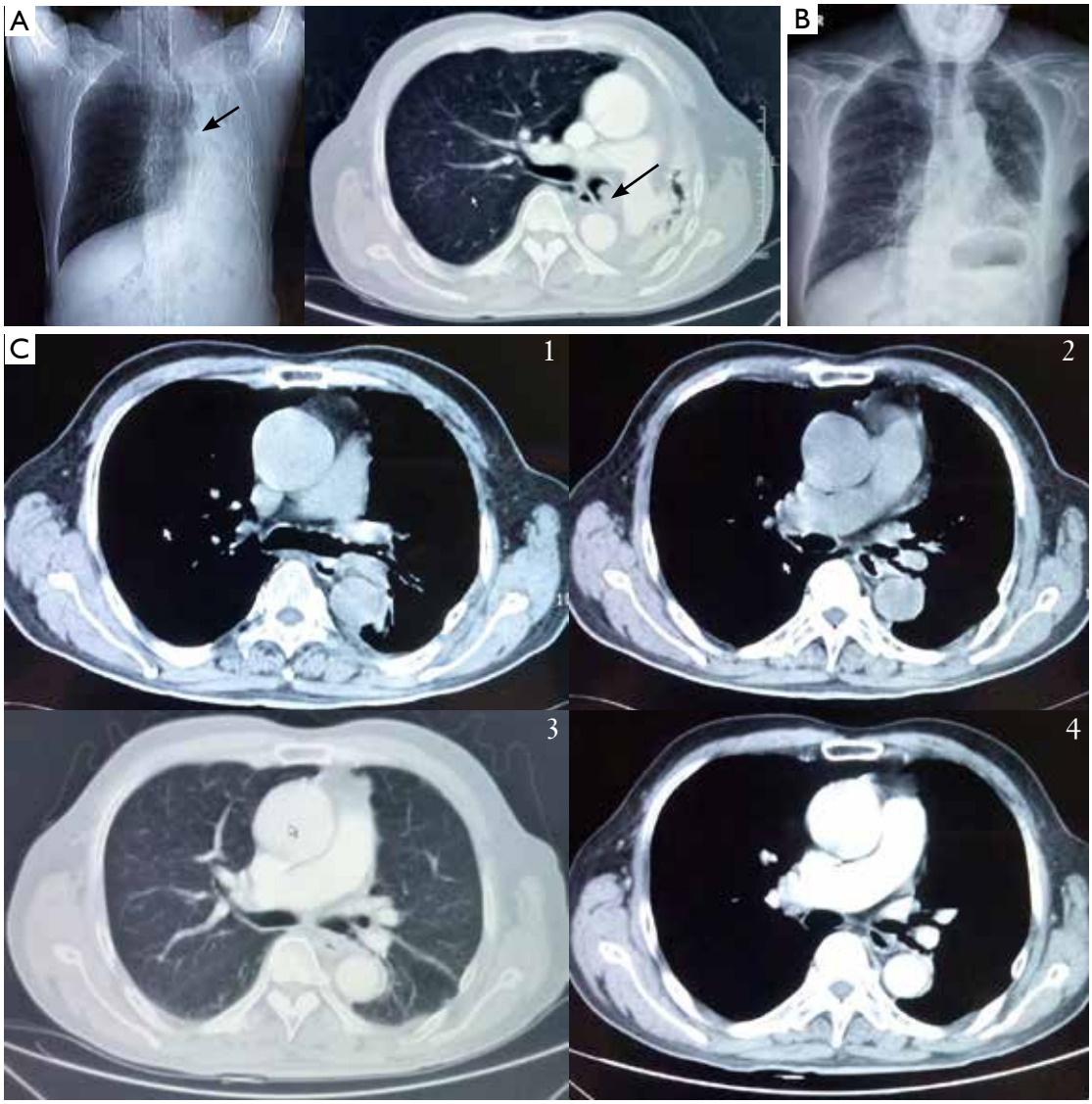

Figure 2 (A) Preoperative radiography and computed tomography show endobronchial tumor locates at the left main bronchi, the whole left lung is atelectasis, mediastinal moves to left thoracic cavity; (B) postoperative radiography showed the left lung recruit well; (C) computed tomography scan after 3 months (C_1,C_2) and 1 year (C_3,C_4) of postoperation showed anastomotic between left main bronchi and upper and lower lobe bronchial was smooth. The tumor was no recurrence sign.

paclitaxel and cisplatin before treatment in our clinic, and without any improvement in symptoms. Chest CT scan showed an intraluminal mass at the left main bronchus, the whole left lung was atelectasis (*Figure 2A*). Endobronchoscopy examination showed a papillary neoplasm bulge at the middle left main bronchial cavity in about 1 cm diameter, completely blocking the lumen. Biopsy revealed low-grade malignancy, tendency to adenoid cystic carcinoma. The basic surgical procedures in this patient were same as the first case, and the two-step anastomosis was performed between the left main bronchus and the ends of the left upper and lower bronchi, using 3-0 Vicryl sutured. The anastomosis was wrapped with the intercostal muscle pedicle flap at last. The unique procedure was that we had repeated lung lavage several times before anastomosis was performed, in order to identify the lung parenchymal was not infringed by lung abscesses and could be recruited during ventilation. The postoperative follow-up was over 2 years without recurrence of the tumor (*Figure 2B,C*).

Discussion

Pure bronchial sleeve resection and reconstruction is a type of rare thoracic surgery, especially for the second carina reconstruction on the left side, needs more exquisite surgical techniques, and patient selection to such surgery often requires rigorous screening.

Surgical indications and selection of cases

According to the literature, the same as other trachea-bronchial surgery, the indications of the pure distal main bronchial sleeve resection are the following three diseases: bronchial benign diseases (including bronchial luminal stenosis caused by inflammation, trauma and benign bronchial lesion), bronchial low-grade malignant tumor (including typical carcinoid, mucoepidermoid carcinoma and adenoid cystic carcinoma) and rare non-small cell lung cancer (1,4-6).

For bronchial stenosis caused by tuberculosis infections, whether the infection is in the active stage must be identified prior to surgery (7). The current view is that patients with active tuberculosis infection must accept anti-tuberculosis therapy for more than 6 months before surgery, and need to exclude the damage of lung parenchyma. For the rare cases of bronchial benign lesion, the growing maturity of endobronchial treatment techniques can usually replace surgery with much more invasive (8-10).

Recently, a tracheobronchial plasty mainly uses for low-grade malignant tumor. Such tumors originate in the tracheobronchial epithelium or glands, often limit in the tracheobronchial lumen, and grow slowly, few lymph node metastasis and distant metastasis are happened. Our two cases of the second carina reconstruction on the left side were both distal left main bronchial adenoid cystic carcinoma. There are literatures show that, compared to typical carcinoid and mucoepidermoid carcinoma, adenoid cystic carcinoma often grows along with submucosal, even further involves tracheal rings and violates surrounding tissues and organs outside the tracheal lumen (11). So with the highest degree of malignancy, the 5-year survival rate of ACC is only about 73% (12). The recurrence rate of endobronchial therapies is higher than 1/3 because of cartilage ring and surrounding tissue involvement. Surgical treatment can resect the tumor radically (R0 resection) and obtain a satisfactory therapeutic effect. It has been reported that even the positive bronchial margin (R1 resection), the patient can also get a long survival (13).

And pure bronchial resection is used pretty rare in the treatment of patients with non-small cell lung cancer. Previous literature points out that it must be confined to the exclusion of lung parenchyma involvement, and preoperative pathological diagnosis is required to identify no lung and mediastinal lymph node metastasis (14).

The points and difficulties of surgical techniques

Compared to the right bronchial sleeve resection, the second carina reconstruction on the left side is much more complex and difficulties. First of all, because of the aortic arch and thoracic aorta around the hilum, the relative positions are deeper when not only free of the left main bronchus and pulmonary artery, but also the reconstruction process of stitching. It has to be released more to expose enough anastomosis space, sometimes even need to free and suspend low trachea to lift stitching position. Secondly, compared to the right bronchus located at the rear side of the pulmonary artery, left pulmonary artery is through the top of the left main bronchus, across the rear of left upper lobe bronchus and traveling in the rear side of the lower lobe bronchus, the formation of 'pulmonary arch'. So when reconstructing the second carina on the left side, the anastomosis of upper-lower lobe bronchus and the left main bronchus is often hidden in the rear of the left pulmonary artery. Surgeons need to be fully free and hanging the pulmonary artery in order to successfully completing this operation. In addition, because the left main bronchus resectable length is often longer than the right side, it sometimes needs to release the hilum and even open the pericardium to avoid anastomotic tension.

Discussion of lymph node dissection (skeletonized or not)

Classic points of tracheal surgery believe the best free length for trachea-bronchial should be controlled within a distance 0.5 cm from the margin in order to avoiding weak anastomotic blood supply. But in the light of oncological surgery, we need systematic dissection of lymph nodes around bronchus, and make it 'skeletonized'. This is a contradiction. Our view is that, it should be possible to dissect the bronchial lymph node, one in favor of radical resection of the tumor, on the other hand it can help to bronchial completely release, more fully expose the surgical field. For the worry of anastomotic blood supply, we used to retain the intercostal muscle pedicle flap and surround the bronchial anastomosis to reduce tension while also promote

the growth of new blood vessels to reduce bronchial fistula occurrence. In fact, the above two cases of patients were treated with this method and did not meet bronchial fistula caused by anastomotic poor blood supply.

Preoperative evaluation and intraoperative treatment of atelectasis

We concerned that in the treatment of the second patient, the preoperative examination revealed full atelectasis of left lung. Such cases require the surgeon more adequate preoperative preparation and evaluation. Patients in the preoperative diagnosis are often difficult due to atelectasis full ventilatory defect formed after bronchial obstruction, or because of lung destruction caused by chronic inflammation of the lung. So those who plan to do the procedure need the preparation of lobectomy or pneumonectomy, while operation must clean out bronchial secretions to confirm the lung whether to recruitment or not. When we performed the pure bronchial resection, we repeated lung lavage several times and confirmed that no purulent discharge flowing out from distal lung tissue and totally recruitment the lung before reconstruction. The surgeon must not blindly reserved distal lung tissue, while ignoring the possibility of lung destruction.

Conclusions

Pure bronchial sleeve resection is better to protect lung function, and is a useful supplement to conventional surgery for some selected patients, but it can not replace the sleeve lobectomy and pneumonectomy. The second carina reconstruction needs for strict screening and preoperative evaluation of patients and also depend on higher requirements on the surgeon's surgical techniques.

Acknowledgements

Disclosure: The authors declare no conflict of interest.

References

1. Ragusa M, Vannucci J, Cagini L, et al. Left main bronchus resection and reconstruction. A single institution experience. J Cardiothorac Surg 2012;7:29.
2. Bagan P, Le Pimpec-Barthes F, Badia A, et al. Bronchial sleeve resections: lung function resurrecting procedure. Eur J Cardiothorac Surg 2008;34:484-7.
3. Cerfolio RJ, Deschamps C, Allen MS, et al. Mainstem bronchial sleeve resection with pulmonary preservation. Ann Thorac Surg 1996;61:1458-62; discussion 1462-3.
4. Bölükbas S, Schirren J. Parenchyma-sparing bronchial sleeve resections in trauma, benign and malign diseases. Thorac Cardiovasc Surg 2010;58:32-7.
5. Frist WH, Mathisen DJ, Hilgenberg AD, et al. Bronchial sleeve resection with and without pulmonary resection. J Thorac Cardiovasc Surg 1987;93:350-7.
6. Jiang X, Dong X, Zhao X, et al. Bronchial sleeve resection distal to the main bronchus with complete pulmonary preservation for benign or low-grade malignant tumors. Ann Thorac Surg 2007;84:e19-21.
7. Lei Y, Tian-Hui Z, Ming H, et al. Analysis of the surgical treatment of endobronchial tuberculosis (EBTB). Surg Today 2014;44:1434-7.
8. Dambara T. Endoscopic laser treatment of mucous gland adenoma arising in the trachea. Intern Med 1996;35:841.
9. Aggarwal A, Tewari S, Mehta AC. Successful management of adenoid cystic carcinoma of the trachea by laser and irradiation. Chest 1999;116:269-70.
10. Díaz-Jiménez JP, Canela-Cardona M, Maestre-Alcacer J. Nd:YAG laser photoresection of low-grade malignant tumors of the tracheobronchial tree. Chest 1990;97:920-2.
11. Kanematsu T, Yohena T, Uehara T, et al. Treatment outcome of resected and nonresected primary adenoid cystic carcinoma of the lung. Ann Thorac Cardiovasc Surg 2002,8:74-7.
12. Regnard JF, Fourquier P, Levasseur P. Results and prognostic factors in resections of primary tracheal tumors: a multicenter retrospective study. The French Society of Cardiovascular Surgery. J Thorac Cardiovasc Surg 1996;111:808-13; discussion 813-4.
13. Maziak DE, Todd TR, Keshavjee SH, et al. Adenoid cystic carcinoma of the airway: thirty-two-year experience. J Thorac Cardiovasc Surg 1996;112:1522-31; discussion 1531-2.
14. Ohta Y, Yachi T, Oda M, et al. Bronchial sleeve resection with complete preservation of the lung for carcinoma. Respiration 2001;68:528-32.

Cite this article as: Tang J, Cao M, Qian L, Fu Y, Tang J, Zhao X. The pure distal left main bronchial sleeve resection with total lung parenchymal preservation: report of two cases and literature review. J Thorac Dis 2014;6(12):E294-E298. doi: 10.3978/j.issn.2072-1439.2014.12.14

Letter to the Editor

Pleural fluid is surrogate for time

Pieter E. Postmus

Landauerlaan 2, 9351PP Leek, the Netherlands

Correspondence to: Pieter E. Postmus, MD, PhD, Emeritus Professor VUMC. Independent Consultant for Pulmonary Diseases, Landauerlaan 2, 9351PP Leek, the Netherlands. Email: pepostmus@gmail.com.

Submitted Oct 16, 2014. Accepted for publication Oct 17, 2014.
doi: 10.3978/j.issn.2072-1439.2014.11.24
View this article at: http://dx.doi.org/10.3978/j.issn.2072-1439.2014.11.24

I read with much interest the manuscript by Taira *et al.* (1) and like to make some comments on their results.

The authors present in their manuscript 40 patients with a primary spontaneous pneumothorax and analyse the rate of re-expansion pulmonary edema (RPE) as visible on computed tomography (CT). They describe a number of characteristics of these patients such as duration of symptoms, size of pneumothorax and radiological findings on a posteroanterior chest X-ray in erect position. They put much emphasis on presence of pleural fluid.

A common finding in patients with a pneumothorax is pleural inflammation (2,3) resulting in pleural fluid, ranging from a few millilitres to radiologically visible amounts. The authors do not discuss the reason(s) why these patients develop a pleural effusion. The by far most likely explanation is the induction of inflammation of the pleura by the presence of air in the pleural cavity. The cellular content of this fluid changes over time. After the initially influx of neutrophils and macrophages this is followed by a strong increase of eosinophils with prolonged presence of air in the pleural cavity (4). This change in differential count seems to be a reliable reflection of the duration of presence of air in the pleural cavity and therefore as a more objective proof than simply asking when symptoms started. It is well known that the moment of subjective symptoms may be many days after the first leaking of air into the pleural cavity (5).

They consider presence of pleural fluid on an erect chest X-ray as a new risk factor for the development of RPE. What the authors fail to discuss is that in about 1/3 of cases small effusions will be missed by their diagnostic approach (6). Patients who have less than 175 mL of pleural fluid, being the lower detection limit, or even much larger volumes (7), will be missed. This makes the conclusion of the authors in fact not reproducible. Although there is no proof that more fluid reflects a longer duration of air in the pleural cavity, this seems likely and this makes their risk factor in fact a reflection of duration of existence of the pneumothorax, as reported in a much larger study (8). It would have been much better if the authors had used the optimal technique for detection of pleural fluid (ultrasound) and investigated whether differential counts of the cellular content could be a supporting method for measuring time of existence of the pneumothorax and by that a reproducible risk factor.

Acknowledgements

Disclosure: The author declares no conflict of interest.

References

1. Taira N, Kawabata T, Ichi T, et al. An analysis of and new risk factors for reexpansion pulmonary edema following spontaneous pneumothorax. J Thorac Dis 2014;6:1187-92.
2. Lichter I, Gwynne JF. Spontaneous pneumothorax in young subjects. A clinical and pathological study. Thorax 1971;26:409-17.
3. Kumasaka T, Hayashi T, Mitani K, et al. Characterization of pulmonary cysts in Birt-Hogg-Dubé syndrome: histopathological and morphometric analysis of 229 pulmonary cysts from 50 unrelated patients. Histopathology 2014;65:100-10.
4. Smit HJ, van den Heuvel MM, Barbierato SB, et al. Analysis of pleural fluid in idiopathic spontaneous pneumothorax; correlation of eosinophil percentage with the duration of air in the pleural space. Respir Med 1999;93:262-7.
5. Postmus PE, Johannesma PC, Menko FH, et al. In-

flight pneumothorax: diagnosis may be missed because of symptom delay. Am J Respir Crit Care Med 2014;190:704-5.
6. Ruskin JA, Gurney JW, Thorsen MK, et al. Detection of pleural effusions on supine chest radiographs. AJR Am J Roentgenol 1987;148:681-3.
7. Woodring JH. Recognition of pleural effusion on supine radiographs: how much fluid is required? AJR Am J Roentgenol 1984;142:59-64.
8. Haga T, Kurihara M, Kataoka H. The risk for re-expansion pulmonary edema following spontaneous pneumothorax. Surg Today 2014;44:1823-7.

Cite this article as: Postmus PE. Pleural fluid is surrogate for time. J Thorac Dis 2014;6(12):E299-E300. doi: 10.3978/j.issn.2072-1439.2014.11.24

3-1-5 implementation for 2015

Lawrence Grouse

International COPD Coalition

Correspondence to: Lawrence Grouse, MD, PhD. Executive Director, International COPD Coalition. Department of Neurology, University of Washington School of Medicine, 1959 NE Pacific Ave., Rm RR650, Box 356465, Seattle, Washington 98195-6465, USA. Email: lgrouse@uw.edu.

Submitted Jul 02, 2014. Accepted for publication Jul 02, 2014.
doi: 10.3978/j.issn.2072-1439.2014.11.03
View this article at: http://dx.doi.org/10.3978/j.issn.2072-1439.2014.11.03

During 2014 and 2015, ICC will be promoting patient consumerism through the Three One Five Initiative as noted in the recent ICC column (1). As we proposed, ICC would like to make more health care professionals and patients familiar with this initiative, and we hope that many of our ICC partners and member organization will be implementing 3-1-5 activities.

ICC is in communication with the international leadership of 3-1-5, which is in China, and the SAIC governmental agency of China that works with them. We will continue to provide readers of *Journal of Thoracic Disease* (*JTD*) and our COPD patient organization partners with more information about the international plans for 3-1-5. ICC looks forward to input from its member organization, and we ask them to send us their plans for 2015 COPD patients' rights promotion, and their articles will be published in the ICC Column in *JTD*. We also look forward to *JTD* readers' thoughts about patient rights. ICC will be working with our member organizations to propose "New Laws to Protect Consumers", which is an initiative of the global 3-1-5 leadership. There are many new laws that could benefit COPD and other respiratory patients.

There are several topics for important laws and initiatives that have been suggested by ICC leaders and member organizations that could be implemented as part of 3-1-5 activities. We plan to publish reports in the March 2015 issue of *JTD* about the activities that are taking place, and after their occurrence we will have reports on the experiences and successes. Here are the ideas that have been suggested so far by ICC leaders and member organizations:

(I) The need for rules and legislation regulating the communication between pharmaceutical companies and doctors in developing countries. Such rules exist in Europe and North America, but they are needed elsewhere;

(II) The need for legislation to promote availability of health care. The lack of availability of health care services often deprives patients, particularly in developing countries and countries without universal health care, such as the USA, China, and many other countries, both developed and developing;

(III) The need for legislation that promotes cost-effective health care that identifies care that benefits patient outcomes. An example for COPD would be there are many therapies that reduce COPD exacerbations but what is the most cost-effective way to provide this patient outcome? How many of these therapies continue to provide benefits when they are used together?

(IV) The need for early COPD diagnosis to better treat and understand this disease. Delayed diagnosis of COPD harms the chances of helping the patients. Understanding the cause and mechanism of early disease may offer an opportunity to prevent or cure the disease.

The treatment of COPD has not substantially improved in 40 years, nor has its survival, although the cost of COPD care in the USA has tripled during this time even factoring in inflationary costs (2). Most COPD patients have low incomes, so they need assistance in coping with this terrible disease. Even if governments and medical organizations do not give a priority to the rights of these patients to health care, we should all realize that the steady increase of COPD and other respiratory diseases is related to the increasing global pollution and inhalation of toxic pollutants. If the cause and care of COPD is not

taken seriously now, the same fate of pollution-induced respiratory diseases awaits the entire global population as the earth's environmental compromise continues to increase (3).

Acknowledgements

Disclosure: The author declares no conflict of interest.

Cite this article as: Grouse L. 3-1-5 implementation for 2015. J Thorac Dis 2014;6(12):E301-E302. doi: 10.3978/j.issn.2072-1439.2014.11.03

References

1. Grouse L. Three One Five: a global consumer movement. J Thorac Dis 2014;6:E132.
2. Grouse L. Health or wealth? J Thorac Dis 2012;4:548-50.
3. Grouse L. The rise of a non-communicable disease epidemic. J Thorac Dis 2012;4:238-9.

News

Panhellenic Congress News: innovation in the academic world

Melanie C. He

Editorial Office, AME Publishing Company, Guangzhou 510220, China

Correspondence to: Melanie C. He. Science Editor, Journal of Thoracic Disease, Editorial Office, AME Publishing Company, Guangzhou 510220, China. Email: jtd@thepbpc.org.

Submitted Dec 14, 2014. Accepted for publication Dec 15, 2014.
doi: 10.3978/j.issn.2072-1439.2014.12.28
View this article at: http://dx.doi.org/10.3978/j.issn.2072-1439.2014.12.28

On November 20, everything on the congress site was well-organized. Under the tranquil, comfortable and pleasant atmosphere, the Panhellenic Congress on respiratory and occupational chest diseases: consensus and controversy was officially held in Thessaloniki, Greece from November 20th to 23rd, 2014. This is one of the most important congresses in northern Greece in the field of thoracic disease held by every two years since 1984 (*Figure 1*).

"Over the years, the congresses organized by the Hellenic Society of Respiratory and Occupational Chest Diseases have contributed in the formation of a unique scientific forum for the presentation of original research, diffusion of knowledge on the latest developments in respiratory medicine, and constructive networking between specialists from Greece and abroad. It also includes State-of-the-art lectures and educational workshops and seminars." the congress president addressed.

With focus on respiratory medicine, thoracic surgery and other occupational chest diseases, the congress includes, but not limited to, biopsy, screening, personalized medicine, palliative care, surgery and so on. In addition, as certified by the European Respiratory Society (ERS), the ERS postgraduate courses were also incorporated in the three days' agenda. These courses were concentrated on lung cancer, tuberculosis (TB), sleep and breathing disorder. This made the congress attract many young audiences. When we asked one of the young audiences about her view on the conference, she smiled with English that "full of innovations and information". Indeed, people were able to get access to the forefront of scientific knowledge and technology in thoracic disease by listening to various speeches from distinguished speakers (*Figure 2*).

Distinctively, this is the first time that the congress set up a special section on Chinese thoracic surgery, thanks

Figure 1 (A,B) On the site of the Panhellenic Congress on respiratory and occupational chest diseases: consensus and controversy.

to the joint efforts of the congress committee and AME Publishing Company. In cooperation with the congress and both edited by Dr. Paul Zarogoulidis (*Figure 3*), *Journal of Thoracic Disease* (*JTD*, one of the journals published by AME Publishing Company) has published a special issue on "Pneumothorax: from definition to diagnosis and treatment" before the congress, which includes fine

Figure 2 Full audiences in the conference hall.

Figure 4 Professor Jianxing He is presenting the speech on video-assisted thoracoscopic sleeve lobectomy via 2-port approach.

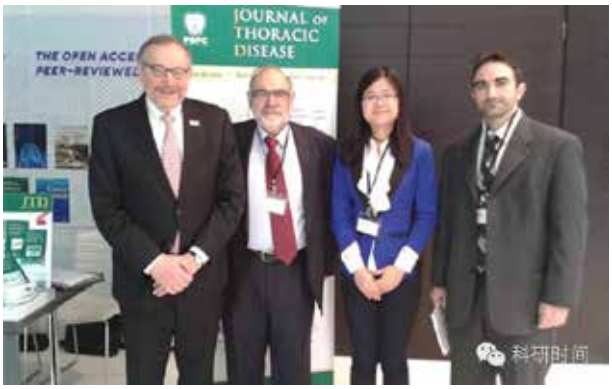

Figure 3 Dr. Fred R. Hirsch (Chief Executive Director of IASLC), Dr. Konstantinos Zarogoulidis (Congress President), Dr. Paul Zarogoulidis (Associate Editor of *Journal of Thoracic Disease*), are with AME Editor.

Figure 5 On the Chinese thoracic surgery section.

contributions from the congress president and participants. After the congress, all the original papers presented in the congress will also be published in *JTD* in early next year. Based on the solid cooperation, the editorial staffs of AME were invited to attend the congress and give a speech, which finally led to the report on this congress.

Chinese experts' surgical videos show was one of the highlights on the congress. Professor Jianxing He, the Director and Professor of the Thoracic Surgery Department, President of the First Affiliated Hospital of Guangzhou Medical College, first introduced the Chinese experience in thoracic surgery to Greek counterparts, and demonstrated the video-assisted thoracoscopic sleeve lobectomy via 2-port approach (*Figures 4*,*5*).

Following speakers were the Chinese experts who had outstanding performance in the 2014 Masters of Cardiothoracic Surgery—VATS Segmentectomy or Sleeve Lobectomy Video Contest, including Dr. Wenjie Jiao, Junjiang Fan, Liang Chen, Shidong Xu, who have displayed their surgical techniques on VATS segmentectomy or lobectomy with different ports (*Figure 6*). Their presentations with vivid surgical videos provoked active debates on the congress, especially about the question on lymph node biopsy (*Figures 7*,*8*).

Figure 6 (A-D) Outstanding Chinese experts are sharing their experience in VATS thoracic surgery.

Figure 7 (A,B) Experts from University of Novi Sad are questioning.

Figure 8 Chairs of the section are immersed in the hot discussion.

Figure 9 AME Science Editor Grace Li is speaking on the congress.

Finally, AME Science Editor Grace Li displayed a large picture of the work that AME is devoted to. Based on the 17 medical journals, AME has established novel platforms, including the AME books, AME Surgical Video Database (Asvide), Multicenter Clinical Database (e.g., ARTCH Project) (*Figure 9*). Just finished, Professor Robert Pirker (Congress President of the 14th Central European Lung Cancer Congress in 2014 and the 17th World Congress on Lung Cancer in 2016) initiatively came over to shake hands with Grace Li, "I know you are active, but did not know that you are so active!" Yes, AME is committed to providing better service and platforms for doctors, patients and investigators worldwide beyond the traditional concept of journals. As described itself as AME, academic made easy, excellent and enthusiastic (*Figure 10*)!

Figure 10 The Chinese experts and AME Science Editors on the congress.

Cite this article as: He MC. Panhellenic Congress News: innovation in the academic world. J Thorac Dis 2014;6(12):E303-E306. doi: 10.3978/j.issn.2072-1439.2014.12.28

Acknowledgements

Disclosure: The author declares no conflict of interest.

Keep calm in an emergency: an unexpected case with poisoning

Guang-Hui Liu

Department of Endocrinology, Tongji Hospital, Tongji University, Shanghai 200065, China

Correspondence to: Guang-Hui Liu. Department of Endocrinology, Tongji Hospital, Tongji University, Shanghai 200065, China. Email: lghdoctor@126.com.

Submitted Aug 19, 2014. Accepted for publication Oct 23, 2014.
doi: 10.3978/j.issn.2072-1439.2014.11.29
View this article at: http://dx.doi.org/10.3978/j.issn.2072-1439.2014.11.29

It was 11:40 pm and I was on the night shift in the emergency room when I received a call from the front desk: "Get ready; a patient with palpitations and sweating is on his way".

The call was about a 28-year-old man who was transferred in an ambulance to the Accident & Emergency department (A&E).

The patient experienced sudden episodes of palpitation and sweating without an obvious cause, 2 hours earlier. He declined other symptoms as dizziness, headache, stomach ache, diarrhea or bleeding. His family called the ambulance when they saw he was unwell.

His initial examination and observation tests including oxygen saturation and ECG monitoring were unremarkable. He was transferred to the medical assessment unit (MAU).

In such cases, doctors should respond quickly in three aspects: ask quickly, diagnose quickly, and treat quickly.

The patient developed shortness of breath and had sudden drop of his O2 saturation levels a bit later. "Tube now!" I said to the nurse by my side who quickly brought the intubation tools. I managed to advance the tracheal catheter with the help of the laryngoscope. When he was connected with a ventilator, his O2 sat levels increased to 98%.

Why did the patient progress so quickly within 5 min? His family members asked the question anxiously. Some had already been crying. This put even more pressure on me and I tried hard to seem calm.

Truth was, my heart sank!

I knew that if the family felt I had no idea about what to do, they would be upset and, to make it worse, lose trust in the team. Any attempt for diagnosis and further treatment would become even more challenging.

The rule of thumb in the emergency department is: "shoot first, ask later".

The priority was to keep the vital signs stable, and try to make a clear diagnosis later. With that in mind, I calmed myself, examined him for the second time. I noticed that his pupils were narrowed to pin size. It was exciting to find the important vital sign.

And the brainstorming started. Morphine, barbiturates, organophosphorus pesticide poisoning could be the cause. Obviously, cardiac and cerebrovascular events had to be excluded. The patient had no fever or neck stiffness, therefore I excluded CNS infection. Acute organophosphorus poisoning was my working diagnosis based on the main symptoms and findings so far. I asked his family whether he had any contact with pesticide or take pesticide by mistake. "*Certainly not*", was the answer, "*he is too busy with his job. He would have no chance to access pesticide*".

"Did he have quarrel with the family or have a bad mood?" I asked again.

The family seemed confused and said, "*No, he is cheerful and optimistic. He is the family main provider. There were no incidents between him and his family or his colleagues. It is not like him to buy pesticide to commit suicide*".

The patient was in a coma and unable to provide any history. Still, acute organophosphorus pesticide poisoning seemed the most likely diagnosis.

"Maybe his lifestyle and dietary pattern will offer a key clue," I thought to myself, "Is there any problem with his diet", I asked.

One of the family members stopped crying and said, "*Not at all. He eats at his company's restaurant during the day. And we all eat the same food at home*". This made me think about the possibility of being poisoned by others. If that was true, it would be a criminal case.

At that moment, the family member thought again and said, "*He ate a lot of longans at noon. Does it matter?*".

"Yes. Did he bite off the fruit skin or did he peel it with his hands?" I asked. "*He ate them with the skin*", he answered.

The clue for the diagnosis became apparent. Hastily,

we performed gastric lavage and catharsis, and sent gastric fluids' specimen to the poisoning identification center.

Waiting for the test result seemed like a long time. The air in MAU was stale and made us nervous. At that time, I was sure that the levels of adrenaline in my body were sky high! The family members felt helpless and cried constantly. Eventually, the patient's vital signs were stabilized. But I couldn't relax. After all, we did not have a definitive diagnosis, so the treatment remained uncertain.

After an hour the technician in the laboratory department reported the life-threatening value: the level of cholinesterase in his body was only 20% of the normal range. It was definitely organophosphorus poisoning. Which type of organophosphorus was still unknown. Two hours later the poisoning identification center reported evidence of phorate poisoning. It dawned on me that the patient may have eaten longans sprayed with pesticides just before being picked! In this case the poison was absorbed by the digestive system. It might be the only explanation. I shared the information with the family who understood and cooperated with us.

We immediately contacted with the center of hemodialysis. Pralidoxime chloride and penehyclidine were administered and he was transferred to EICU.

Author's Note: after 1 week of intensive treatment, the patient recovered and was discharged home.

I still feel stressed when I look back!

He had progressed quickly and could not provide medical history since he lost conscience. The patient was poisoned with organophosphorus pesticide via indirect contact with the fruit he ate. The diagnosis was difficult and challenging for the A&E doctors. What's noteworthy during the medical history inquiry was the way that the patient ate fruits. When he bit off the fruit skin, the pesticide residue on the fruit skin would easily be absorbed by the skin mucus.

We learned a lot from this case. When patients are stable, we need to enquire about the medical history, examine them frequently, and monitor the condition which will lead to the diagnosis. If we are stuck in a dead end, we should calm down and keep in mind that important clues may surface at a critical moment. We should believe that we will figure out a way to save patients' lives. And we will manage to do that together with the patients and their families.

Cite this article as: Liu GH. Keep calm in an emergency: an unexpected case with poisoning. J Thorac Dis 2014;6(12):E307-E308. doi: 10.3978/j.issn.2072-1439.2014.11.29

Acknowledgements

Disclosure: The author declares no conflict of interest.

Oxygen

Lawrence Grouse

Department of Neurology, University of Washington School of Medicine, Washington, USA

Correspondence to: Lawrence Grouse, MD, PhD. Department of Neurology, University of Washington School of Medicine, Washington, USA. Email: lgrouse@uw.edu.

Submitted Sep 13, 2014. Accepted for publication Sep 15, 2014.

doi: 10.3978/j.issn.2072-1439.2014.10.19

View this article at: http://dx.doi.org/10.3978/j.issn.2072-1439.2014.10.19

The end of my internship year in San Diego at UCSD approached! When it started in June of 1973, I felt certain I would never finish the stressful gauntlet of critically-ill medical patients. But as the year was coming to a close, the Stygian tunnel of internship showed signs of ending and ahead… yes!—was light, peace, and bird song! Where I had trembled with fear as emergency patients arrived when internship began, now I was confident. Did my new-found confidence result from my methodical and rational approach to sick patients? Yes, I concluded, careful attention to my patients' pathologic physiology must have done the trick! EKG's, blood gases, lab tests, X-rays—all the necessary clinical data—were the keys to my success!

On the first terrifying day of my internship I had inherited 25 sick inpatients, and I never was able to lower my patient count during the year, but as the year was ending, my service shrank rapidly, my patients were getting well, finishing their examinations, getting referred to other services, getting discharged, and heading home in droves. My current patient load was down to four patients! The medical floor had so few patients they had to close down one of the four pods!

With the luxury of time, I leisurely reviewed the charts of my four remaining patients. Only one of them was likely to have a problem in getting a discharge. His name was Billy Boyle. Billy was a 61-year-old man with end-stage chronic obstructive pulmonary disease (COPD) who had been admitted to the ICU for a serious COPD exacerbation and despite three weeks' of intubation and intense treatment, his arterial blood oxygen level (p_aO_2) remained at 45 mm of mercury even while receiving oxygen through his nasal cannulae! He was feeble and unable to eat or undertake any physical efforts without help. According to the pulmonologists, this was inconsistent with life. When I saw him in the ICU he was cyanotic, but didn't seem to be otherwise discommoded by his low oxygen level. Even after his COPD exacerbation and excess sputum production improved, his p_aO_2 remained at 45. This was a serious problem! But before I describe Billy's problem and its resolution I will try to explain how oxygen became such a vital ingredient of human survival.

Oxygen is an incredibly reactive substance, and because of its amazing ability to react chemically with almost any substance, it shouldn't be able to exist in its free state in earth's air. But somehow it does. The entire panoply of oxidation reactions in nature takes their name from this element and its voracious electrons. Teamed with its energetic electromagnetic ally, light, they drive the mechanisms that changes dross matter into life!

When life first began billions of years ago the earth's atmosphere was without oxygen, creating life required a reducing atmosphere to be present. Oxygen was initially a poison for life, and there was no oxygen in earth's atmosphere until 2.5 billion years ago when cyanobacteria (Archaea) started using the CO_2 that was present in the atmosphere and invented photosynthesis. These invisible animalcules poured out oxygen as a waste product. Bacteria and Archaea are the true heroes of evolution; they developed all the enzymes to perform essentially any chemical reaction that their little prokaryotic cells required, including harnessing oxygen for oxidative phosphorylation and energy production as well as light for photosynthesis. Bacteria were so good at this work that eukaryotic cells (like ours) engulfed them to become slave laborers known as chloroplasts and mitochondria—the main energy sources for all eukaryotic cells. After another billion years or so about 20% of the earth's atmosphere was oxygen. The existing life forms, of necessity, accommodated themselves

to the free oxygen. This atmospheric change was convenient for animal evolution since we require oxygen to survive.

Early animals evolved through stages in which oxygen had to be absorbed directly through contact with water in which it was dissolved. However, larger animals had to develop systems to bring oxygen to all the cells of their bodies. When the fish wanted to spend more time on land with ambient oxygen they had to adapt their swim bladders to become the lungs of amphibians. This permitted them to bring oxygen from the air to their cells. There, in their cells, they built themselves an interior fire and in the fire forged tissues and life. We humans do the same thing unless a disease affects the function of our lungs.

Billy Boyle's lungs suffered from just such a problem: COPD, an awful, fatal disease, but in practical terms he had a more immediate problem. The ICU staff needed his bed for acute patients, and they needed to discharge Billy from the unit, in spite of his poor prognosis. I received a call from the unit director notifying me that they were transferring Billy to my service on the medicine ward. The ICU attending sadly warned me (over the phone) that "*Mr. Boyle, unfortunately, we believe, will not be leaving the hospital alive because of his lung failure and p_aO_2 of 45, but he will be more comfortable during his last days on the ward than in the hurly burly of the unit*".

And so Billy arrived on five South of the La Jolla VA hospital, and with him came his 55-year-old sister Milly Boyle who had waited patiently each day outside the ICU, visiting Billy whenever permitted, and whispering confidently to him without any evidence that he heard her. On the ward, I would see Billy every day, while his sister Milly fed him and whispered to him about what was going on. I spoke confidently to Billy about continuing his therapy and getting him home, but he never spoke to me. I wasn't sure he heard me.

Even with his oxygen mask or nasal cannulae, his oxygen level couldn't be brought above 45. I believed what the pulmonologists told me, namely, that Billy was going to die, probably sooner rather than later. The pulmonologist instructed me to do a radial artery puncture every day to measure his blood gases in a desperate search for therapies that could raise his arterial oxygen level or perhaps just to show that we were aware of his situation. The arterial puncture was a daily ordeal for Billy. I had to wield a large-bore needle and a special heparin-rinsed glass syringe with its glass plunger that would smoothly slide back as the arterial pressure filled the syringe with blood. When the sample was adequate, I would remove the needle and put firm pressure on the artery. The syringe would be sealed and the sample would be placed in ice in an ice bucket and rushed to the lab to measure the fateful arterial blood oxygen.

No matter what we did in terms of chest physiotherapy (pounding on his chest), IPPB (pushing air into his lungs), and aerosolizing medications into his lungs, Billy's p_aO_2 remained at 45. The pulmonologists were hanging crepe and demanding that we keep assessing and documenting our vigorous efforts to salvage Billy by continuing to measure his blood gases each day. After another two weeks on the ward, his radial arteries were pretty beaten up, without providing any good news.

I can't help sending a time capsule back to 1973 to let you know that today, in 2012, putting a clip with a pulse oximeter on a patient's finger can, in most people, make the oxygen measurement in a few seconds without any invasive intervention. So don't give up on scientific progress. Back is 1973; however, things were getting a bit grim. I only had four patients on my service, but one of them was, according to my consultants, circling the drain no matter what I did.

I had to understand this fatal situation better, so I conspired to spend a half-hour each day with Billy and Milly Boyle in his hospital room. Of course, since I only had four patients, this was not difficult to arrange. With all the ward rounds and work rounds and procedure sessions we had each day, I thought that I had been seeing and communicating adequately with them (although Billy had never spoken or responded to me), but I was mistaken, and simply by sitting there in Billy's room and talking with Milly and doing my chart work and observing his interactions with Milly, I began to find out many things that I had never realized.

Billy and Milly were able to communicate quite effectively, and the information that Milly gave me about what Billy thought and felt had been accurate all along! And Billy understood what I was telling him but just didn't have the energy to respond to me and could do it with much less energy with Milly. I started looking differently at Billy; he knew that I knew that he was aware and that he could communicate his urgent messages to me by Milly. I told them about the seriousness of Billy's low arterial oxygen level and the conclusion that the experts came to about his impending death.

The next day, Milly came to me and told me that Billy had concluded that he didn't need any further care in the hospital and wanted to go home. I again summarized the situation to both of them that we had not succeeded in

improving Billy's oxygen, and we were very concerned that he would not survive at home. Milly nodded but said they were willing to take that chance. Billy, with a major effort, nodded. Yet it was clear that Milly believed the grave prognosis was the doctors' view and not her own, or Billy's view.

The medics had given up on Billy in the ICU and had sent him to me and the ward to die, which he refused to do, but now I was officially giving up on him on the ward. Milly calmly said that she would be there to feed and assist Billy at home (which she was already doing in the hospital) and would sustain him; he would be fine, she said. I agreed to discharge Billy.

This news caused the hospital to have a bureaucratic convulsion. The pulmonologists said that any person with a p_aO_2 of 45 needed to be hospitalized so that they could die while receiving medical care, and to send him home was reckless. The VA hospital director also didn't want to discharge Billy. In those days the VA hospitals would more or less let any patient stay as long as they wanted, and he thought that to discharge someone with a p_aO_2 of 45 would not look right. He told me that they had also noticed that I was discharging all my patients and they were beginning to wonder if they had really been ready to be discharged!

In responding to the hospital, I rearranged the mandate of the pulmonologists by explaining that Billy and Milly accepted the danger of discharge, and that Billy understood he was going home to die, but that he would be more comfortable at home, which is what he and Milly wanted. This was all true, except for the part about dying, but the hospital bought it, and with lots of oxygen flowing and ambulance workers taking good care of Billy and allowing Milly to ride with him in the ambulance with its sirens blaring, Billy returned home. I'd never seen an ambulance leaving in emergency mode to take a patient home from the hospital! I suppose they didn't want the morbid event to occur in transit.

Lo and behold, two weeks later at my VA medicine outpatient clinic, Billy and Milly appeared, Milly pushing Billy's wheel chair holding its oxygen canister and both of them looking pleased with themselves; Billy was as cyanotic as ever but smiling, feeling fine, and whispering back and forth with Milly. She tells me that he is afebrile and breathing better. The nurse asks if I want to do an arterial puncture for blood gases. I look at Billy and Milly, think for a moment, and then ask the nurse "Why?"

Cite this article as: Grouse L. Oxygen. J Thorac Dis 2014;6(12):E309-E311. doi: 10.3978/j.issn.2072-1439.2014.10.19

Acknowledgements

Disclosure: The author declares no conflict of interest.

Erratum

CT signs, patterns and differential diagnosis of solitary fibrous tumors of the pleura: Erratum

doi: 10.3978/j.issn.2072-1439.2014.12.43
View this article at: http://dx.doi.org/10.3978/j.issn.2072-1439.2014.12.43

Erratum to: J Thorac Dis 2010;2:21-5

In the article that appeared on Pages 21-25 of the March 2010 Issue of the *Journal of Thoracic Disease* (1), there are errors in the authors' names, that is, the first and last name of the authors are placed in the opposite way. The correct names are as follows:

Luciano Cardinale, Francesco Ardissone, Giovanni Volpicelli, Federica Solitro, Cesare Fava

Therefore, the cite information should be as follows:

Cite this article as: Cardinale L, Ardissone F, Volpicelli G, Solitro F, Fava C. CT signs, patterns and differential diagnosis of solitary fibrous tumors of the pleura. J Thorac Dis 2010;2:21-25. DOI: 10.3978/j.issn.2072-1439.2010.02.01.012

The publisher regrets these errors.

References

1. Luciano C, Francesco A, Giovanni V, et al. CT signs, patterns and differential diagnosis of solitary fibrous tumors of the pleura. J Thorac Dis 2010;2:21-5.

Cite this article as: CT signs, patterns and differential diagnosis of solitary fibrous tumors of the pleura: Erratum. J Thorac Dis 2014;6(12):E312 doi: 10.3978/j.issn.2072-1439.2014.12.43